Seven new species of *Alternaria* (Pleosporales, Pleosporaceae) associated with Chinese fir, based on morphological and molecular evidence

Jiao He[1], De-Wei Li[2], Wen-Li Cui[1], Lin Huang[1]

1 Co-Innovation Center for Sustainable Forestry in Southern China, Nanjing Forestry University, Nanjing, Jiangsu 210037, China

2 The Connecticut Agricultural Experiment Station Valley Laboratory, Windsor, CT 06095, USA

Corresponding author: Lin Huang (lhuang@njfu.edu.cn)

Abstract

Chinese fir (*Cunninghamia lanceolata*) is a special fast-growing commercial tree species in China and has significant ecological and economic value. However, it experienced damage from leaf blight caused by pathogenic fungi of the genus *Alternaria*. To determine the diversity of *Alternaria* species associated with leaf blight of Chinese fir in China, infected leaves were collected from five major cultivation provinces (Fujian, Henan, Hunan, Jiangsu and Shandong provinces). A total of 48 fungal strains of *Alternaria* were obtained. Comparison of morphology and phylogenetic analyses, based on nine loci (ITS, SSU, LSU, GAPDH, RPB2, TEF1, Alt a1, endoPG and OPA10-2) of the representative isolates as well as the pairwise homoplasy index tests, revealed that the fungal strains belonged to seven undescribed taxa of *Alternaria*, which are described here and named as *Alternaria cunninghamiicola* **sp. nov.**, *A. dongshanqiaoensis* **sp. nov.**, *A. hunanensis* **sp. nov.**, *A. kunyuensis* **sp. nov.**, *A. longqiaoensis* **sp. nov.**, *A. shandongensis* **sp. nov.** and *A. xinyangensis* **sp. nov.** In order to prove Koch's postulates, pathogenicity tests on detached Chinese fir leaves revealed significant pathogenicity amongst these species, of which *A. hunanensis* is the most pathogenic to Chinese fir. This study represents the first report of *A. cunninghamiicola*, *A. dongshanqiaoensis*, *A. hunanensis*, *A. kunyuensis*, *A. longqiaoensis*, *A. shandongensis* and *A. xinyangensis* causing leaf blight on Chinese fir. Knowledge obtained in this study enhanced our understanding of *Alternaria* species causing leaf blight on Chinese fir and was crucial for the disease management and the further studies in the future.

Key words: *Alternaria*, *Cunninghamia lanceolata*, diversity, leaf blight, new species, pathogenicity

Introduction

Alternaria is a genus (Pleosporaceae, Pleosporales, Ascomycota) (Seifert et al. 2011), which originally was described in 1816 by Nees (1816), typified with *A. tenuis* Nees. Since then, more than 900 epithets and varieties/f. spp. have been published in *Alternaria* (MycoBank 2023). At present, there are over 360 species (Wijayawardene et al. 2020). *Alternaria* is a ubiquitous fungal genus that includes saprobic, endophytic and pathogenic species (Li et al. 2023).

For example, *Alternaria* species have been recorded as endophytes in grasses, angiosperms, rice and other herbaceous plants and shrubs (Fisher and Petrini 1992; Schulz et al. 1993; Rosa et al. 2009; Polizzotto et al. 2012) and have been also isolated from soil (Hong and Pryor 2004). Many *Alternaria* species are saprobes on a variety of plant tissues in different habitats (Thomma 2003; Liu et al. 2015b; Wanasinghe et al. 2018). Some *Alternaria* species, such as *A. alternata*, produce host-specific toxins (Hyde et al. 2018). Several taxa are also important postharvest pathogens, for example, *A. alternata* and *A. solani* (El-Goorani and Sommer 1981; Reddy et al. 2000), or airborne fungal allergens/pathogens-causing upper respiratory tract infections and asthma in humans (Mitakakis et al. 2001; Woudenberg et al. 2015; Hyde et al. 2018). Due to the significant negative health effects of *Alternaria* on humans and their surroundings, a correct and rapid identification of *Alternaria* species would be of great significance to researchers, plant pathologists, medical mycologists, other biological professionals and the public alike (Woudenberg et al. 2013).

The taxonomy of *Alternaria* species especially small-spored species within the *alternata* species group are particularly challenging because few morphological characters are able to clearly differentiate taxa and these characters are strongly influenced by the environment. Morphological characteristics, such as colour, size, shape of conidia and sporulation patterns have been used for the identification and classification of *Alternaria* species (Simmons 1992). Wiltshire (1945) divided *Alternaria* into three major sections, Brevicatenatae, Longicatenatae and Noncatenatae, based on conidial catenation. However, this division is unreliable as some of these characters overlap amongst species and vary depending on the cultural conditions, such as temperature and substrate (Simmons and Roberts 1993). Simmons (1992, 1995) arranged several species groups within *Alternaria* based on the morphological similarity amongst species. Some other genera, such as *Stemphylium* (Wallroth, 1833) and *Ulocladium* (Preuss, 1852) also produce phaeodictyospores and are morphologically similar to *Alternaria*, and this has further led to taxonomic complications (Bigelow 2003). Simmons (2007) revised *Alternaria* taxonomy, based on morphology and 275 species were recognised. At the same time, Simmons (2007) proposed three new genera *Alternariaster*, *Chalastospora* and *Teretispora* for some species that were previously described in *Alternaria*.

However, molecular phylogeny has revealed polyphyletic taxa within *Alternaria* and *Alternaria* species clades, which do not always correlate with morphological species-groups (Inderbitzin et al. 2006; Runa et al. 2009; Lawrence et al. 2012). Pryor and Gilbertson (2000) elucidated relationships amongst *Alternaria*, *Stemphylium* and *Ulocladium* based on ITS and SSU sequence data and revealed that *Stemphylium* species were phylogenetically distinct from *Alternaria* and *Ulocladium* species. Most *Alternaria* and *Ulocladium* clustered together in a large *Alternaria*/*Ulocladium* clade (Pryor and Gilbertson 2000). Chou and Wu (2002) confirmed that filament-beaked *Alternaria* species constitute a monophyletic group distinct from the other members in this genus and hypothesised that this group is evolutionarily distinct, based on phylogenies of ITS sequence. Two new species groups, *A. panax* and *A. gypsophilae* were introduced by Lawrence et al. (2013) with phylogenetic evidence and they accepted eight well supported asexual species-sections within *Alternaria*, while

the taxa with known sexual morphs, the *A. infectoria* species-groups, were not given the similar rank. Woudenberg et al. (2013) delineated taxa within *Alternaria* and allied genera, based on SSU, LSU, ITS, GAPDH, RPB2 and TEF1 sequence data. The generic circumscription of *Alternaria* was emended and 24 internal clades in the *Alternaria* complex were treated as sections, together with six monotypic lineages (Woudenberg et al. 2013; Gannibal et al. 2022). Woudenberg et al. (2013) also demoted the genera *Allewia*, *Brachycladium*, *Chalastospora*, *Chmelia*, *Crivellia*, *Embellisia*, *Lewia*, *Nimbya*, *Sinomyces*, *Teretispora*, *Ulocladium*, *Undifilum* and *Ybotromyces* to synonymy with *Alternaria*. Therefore, the use of DNA sequence data is very important in resolving *Alternaria* taxonomy.

The DNA-based classification of the genus *Alternaria* has, so far, relied on over ten gene/region loci, including the nuclear small subunit (SSU) rRNA, large subunit (LSU) rRNA, internal transcribed spacer (ITS), glyceraldehyde-3-phosphate dehydrogenase (GAPDH), RNA polymerase II 2nd largest subunit (RPB2), translation elongation factor 1-α (TEF1), *Alternaria* major allergen (Alt a1), endopolygalacturonase (endoPG), anonymous gene region (OPA10-2), calmodulin (CAL) and eukaryotic orthologous group (KOG) (Lawrence et al. 2013; Woudenberg et al. 2013; Woudenberg et al. 2015; Ghafri et al. 2019; Jayawardena et al. 2019a, 2019b). Several studies have shown that multilocus phylogenetic identification can classify or segregate *Alternaria* species. For instance, Li et al. (2023) used sequences of ITS, *LSU*, *TEF1*, *RPB2*, *GAPDH* and Alt a1 loci and described 18 new species in sect. *Alternaria*, sect. *Infectoriae*, sect. *Porri* and sect. *Radicina*. Aung et al. (2020) reported the first case of small-spored *A. alternata* associated with Koerle pear (*Pyrus × sinkiangensis* T.T. Yu) in Korea, based on a multigene phylogeny of GAPDH, RPB2 and Alt a1 genes. Chen et al. (2018) used the multilocus phylogenetic analyses of ITS, GAPDH and β-tubulin genes/region to characterise *A. alternata*, a causal agent of black spots of tea plant (*Camellia sinensis* (L.) Kuntze), in the Chongqing city of China. Kgatle et al. (2018) recently showed that the multi-locus phylogeny of Alt a1, RPB2, GAPDH, TEF1 and ITS genes/region successfully identified *A. alternata* causing leaf blight on sunflower (*Helianthus annuus* L.) in South Africa. Lawrence et al. (2015) provided a comprehensive taxonomic treatment of *Alternaria* with multi-locus phylogeny and accepted 27 sections in *Alternaria*, but later revised it to 28 accepted sections (Ghafri et al. 2019; Gannibal et al. 2022; Li et al. 2023). Recently, Ghafri et al. (2019) and Gannibal et al. (2022) introduced two new sections (i.e. sects. *Helianthiinficiens* and *Omanenses*) of *Alternaria* and thus, 29 sections were accepted at present (Ghafri et al. 2019; Gannibal et al. 2022; Li et al. 2023).

Chinese fir (*Cunninghamia lanceolata* (Lamb.) Hook.) is an important fast-growing timber species in China and its afforestation area and timber volume rank first amongst forest plantations; it plays an important role in forest carbon sequestration, increasing farmers' income and rural revitalisation (Yan 2020). Average timber volume is estimated at 500−800 m^3/ha and in China, Chinese fir contributes 40% of the total commercial timber production (Zheng et al. 2016). However, Chinese fir is often damaged by many diseases and insects (Lan et al. 2015). Previous studies reported that *Alternaria* sp., *Bartalinia cunninghamiicola* Tak. Kobay. & J.Z. Zhao, *Bipolaris oryzae* (Breda de Haan) Shoemaker, *Bi. Setariae* Shoemaker, *Colletotrichum cangyuanense* Z.F. Yu,

C. fructicola Prihast., L. Cai & K.D. Hyde, *C. gloeosporioides* (Penz.) Penz. & Sacc., *C. karsti* You L. Yang, Zuo Y. Liu, K.D. Hyde & L. Cai, *C. siamense* Prihast., L. Cai & K.D. Hyde, *Curvularia spicifera* (Bainier) Boedijn, *Cur. muehlenbeckiae* Madrid, K.C. Cunha, Gené, Guarro & Crous, *Ceratocystis collisensis* F.F. Liu, M.J. Wingf. & S.F. Chen, *Diaporthe anhuiensis* H. Zhou & C.L. Hou, *Dia. citrichinensis* F. Huang, K.D. Hyde & Hong Y. Li, *Discosia pini* Heald, *Fusarium oxysporum* f. *pini* (R. Hartig) W.C. Snyder & H.N. Hansen, *Fusarium* sp., *Lophodermium uncinatum* Darker, *Nigrospora sphaerica* (Sacc.) E.W. Mason and *Rhizoctonia solani* J.G. Kühn have been identified as pathogens on Chinese fir (Anonymous 1976; Kobayashi and Zhao 1987; Wang et al. 1995; Chen 2002; Lan et al. 2015; Liu et al. 2015a; Xu and Liu 2017; Huang et al. 2018; Tian et al. 2019; Zhou and Hou 2019; Cui et al. 2020a, b; He et al. 2022). However, there is a lack of comprehensive study on *Alternaria* causing leaf blight disease on Chinese fir including diversity, occurrence and pathogenicity of the pathogens.

Surveys of fungal diseases on foliage of Chinese fir in its main cultivation regions in China were conducted from 2016 to 2020, 48 isolates of *Alternaria* spp. were collected and examined. The main aims of the present study were to determine the *Alternaria* spp. associated with leaf blight disease on Chinese fir using a polyphasic approach of fungal morphology and phylogenetic analyses, based on multi-locus sequences of ITS, SSU, LSU, GAPDH, RPB2, TEF1, Alt a1, endoPG and OPA10-2.

Materials and methods

Isolation of the potential fungal pathogen

A total of 48 isolates of *Alternaria* spp. were isolated from leaf blight samples of Chinese fir, which were collected in five provinces (Fujian, Henan, Hunan, Jiangsu and Shandong) in China (Suppl. material: table S1). Small pieces (2 × 3 mm) were cut from the margins of infected tissues and surface sterilised in 75% alcohol for 30 s, then in 1% sodium hypochlorite (NaOCl) for 90 s, followed by three rinses with sterile water (Huang et al. 2016), then blotted dry with sterilised filter paper, placed on 2% potato dextrose agar (PDA) Petri plates with 100 mg/l ampicillin and then cultured for 3 days at 25 °C in the dark. Fungal isolates were purified with the monosporic isolation method described by Li et al. (2007). Single-spore isolates were maintained on PDA plates. The obtained isolates were stored in the Forest Pathology Laboratory of Nanjing Forestry University. Holotype specimens of new species from this study were deposited at the China Forestry Culture Collection Center (**CFCC**), Chinese Academy of Forestry, Beijing, China.

DNA extraction, PCR amplification and sequencing

Genomic DNA of 48 isolates was extracted using a modified CTAB method (Damm et al. 2008). The fungal plugs of each isolate were grown on the PDA plates for 5 days and then collected in a 2 ml tube. Then, 500 μl of chloroform and 500 μl of hexadecyltrimethyl ammonium bromide (CTAB) extraction buffer (0.2 M Tris, 1.4 M NaCl, 20 mM EDTA, 0.2 g/l CTAB) were added into the tubes, which were placed in a shaker at 25 °C at 200 rpm for 2 h. The mixture was

centrifuged at 15,800 × *g* for 5 min. Three hundred µL of the supernatant was transferred into a new tube and 600 µl of 100% ethanol was added. The suspension was centrifuged at 15,800 × *g* for 5 min. Then, 600 µl of 70% ethanol was added into the precipitate. The suspension was centrifuged at 15,800 × *g* for 5 min and the supernatant was discarded. The DNA pellet was dried and resuspended in 30 µl ddH$_2$O.

Whole or partial region/genes of nine loci were amplified. ITS and SSU were amplified with primers ITS1/ITS4 and NS1/NS4 (White et al. 1990), LSU with primers LROR/LR5 (Crous et al. 2009a), GAPDH with primers gpd1/gpd2 (Berbee et al. 1999), RPB2 with primers RPB2-5f2/fRPB2-7cr (Liu et al. 1999; Sung et al. 2007), TEF1 with primers 983F/2218R (Sung et al. 2007), Alt a1 with primers Alt-for/Alt-rev (Hong et al. 2005), endoPG and OPA10-2 with primers PG3/PG2b and OPA10-2L/OPA10-2R (Andrew et al. 2009). The information on primer pairs used are listed in Suppl. material: table S2.

The polymerase chain reaction (PCR) amplification was conducted as described by Woudenberg et al. (2015). PCR was performed in a 30 µl reaction volume containing 2 µl of genomic DNA (*ca*. 200 ng/µl), 15 µl of 2× Taq Plus Master Mix (Dye Plus) (Vazyme P212-01), 1 µl of 10 µM forward primer, 1 µl of 10 µM reverse primer and 11 µl of ddH$_2$O. The PCR conditions consisted of an initial denaturation step of 4 min at 94 °C followed by 35 cycles of 30 s at 94 °C, 30 s at 55 °C and 30 s at 72 °C for ITS, GAPDH and endoPG, 35 cycles of 30 s at 94 °C, 30 s at 62 °C and 45 s at 72 °C for OPA10-2 and Alt a1, and 35 cycles of 30 s at 94 °C, 30 s at 59 °C and 60 s at 72 °C for RPB2, TEF1, LSU and SSU, and a final elongation step of 10 min at 72 °C. All DNA sequencing was performed at Shanghai Sangon Biotechnology Company (Nanjing, China). Sequences generated in this study were deposited in GenBank (Table 1).

Phylogenetic analyses

The sequences generated in this study were compared against nucleotide sequences in GenBank using BLAST to determine closely-related taxa. Alignments of different loci, including the sequences obtained from this study and the ones downloaded from GenBank, were initially performed with the MAFFT v.7 online server (https://mafft.cbrc.jp/alignment/server/) (Katoh and Standley 2013) and then manually adjusted in MEGA v. 10 (Kumar et al. 2018). The post-alignment sequences of multiple loci were concatenated in PhyloSuite software (Zhang et al. 2020). Maximum-Likelihood (ML) and Bayesian Inference (BI) were run in PhyloSuite software using IQ-TREE ver. 1.6.8 (Nguyen et al. 2015) and MrBayes v. 3.2.6 (Ronquist et al. 2012), respectively. ModelFinder was used to carry out statistical selection of best-fit models of nucleotide substitution using the corrected Akaike information criterion (AIC) (Kalyaanamoorthy et al. 2017). For ML analyses, the default parameters were used, and bootstrap support (BS) was carried out using the rapid bootstrapping algorithm with the automatic halt option. Bayesian analyses included two parallel runs of 2,000,000 generations, with the stop rule option and a sampling frequency set to each 1,000 generations. The 50% majority rule consensus trees and posterior probability (PP) values were calculated after discarding the first 25% of the samples as burn-in. Phylogenetic trees were visualised in FigTree v. 1.4.2 (http://tree.bio.ed.ac.uk/software/figtree/) (Rambaut 2014).

Table 1. Isolates used in this study and their GenBank accession numbers.

Species name and strain number[1,2]	Locality, host / substrate	GenBank accession numbers[3]								
		SSU	LSU	ITS	GAPDH	TEF1	RPB2	Alta1	endoPG	OPA10-2
Alternaria alternantherae (Outgroup) — CBS 124392; HSAUP2798	China, *Solanum melongena*	KC584251	KC584506	KC584179	KC584096	KC584633	KC584374	KP123846	–	–
A. alstroemeriae — CBS 118808; E.G.S. 50.116[R]	USA, *Alstroemeria* sp.	KP124917	KP124447	KP124296	KP124153	KP125071	KP124764	KP123845	KP123993	KP124601
A. alternata — CBS 130254	India, human sputum	KP125007	KP124537	KP124383	KP124235	KP125161	KP124853	KP123931	KP124087	KP124696
CBS 130255	India, human sputum	KP125008	KP124538	KP124384	KP124236	KP125162	KP124854	KP123932	KP124088	KP124697
CBS 130258	India, human sputum	KP125009	KP124539	KP124385	KP124237	KP125163	KP124855	KP123933	KP124089	KP124698
A. angustiovoidea — CBS 195.86, E.G.S. 36.172; DAOM 185214[T]	Canada, *Euphorbia esula*	KP124939	KP124469	KP124317	KP124173	KP125093	KP124785	JQ646398	KP124017	KP124624
A. arborescens — CBS 102605; E.G.S. 39.128[T]	USA, *Solanum lycopersicum*	KC584509	KC584253	AF347033	AY278810	KC584636	KC584377	AY563303	AY295028	KP124712
CBS 124281	Denmark, *Triticum* sp.	KP125037	KP124567	KP124414	KP124265	KP125192	KP124883	KP123961	KP124118	KP124728
CBS 124282	Denmark, *Hordeum vulgare*	KP125038	KP124568	KP124415	KP124266	KP125193	KP124884	KP123962	KP124119	KP124729
CPC 25266	Austria, *Pyrus* sp.	KP125041	KP124571	KP124418	KP124269	KP125196	KP124887	KP123965	KP124122	KP124732
A. astragali — CBS 127672; E.G.S. 52.122[T]	USA, *Astragalus bisulcatus*	KP125006	KP124536	KP124382	KP124234	KP125160	KP124852	KP123930	KP124086	KP124695
A. betae-kenyensis — CBS 118810; E.G.S. 49.159; IMI 385709[T]	Kenya, *Beta vulgaris* var. *cicla*	KP125042	KP124572	KP124419	KP124270	KP125197	KP124888	KP123966	KP124123	KP124733
A. brassicinae — CBS 118811; E.G.S. 35.158[T]	USA, *Brassica oleracea*	KP124978	KP124508	KP124356	KP124210	KP125132	KP124824	KP123904	KP124057	KP124667
A. broussonetiae — CBS 121455; E.G.S. 50.078[T]	China, *Broussonetia papyrifera*	KP124992	KP124522	KP124368	KP124220	KP125146	KP124838	KP123916	KP124072	KP124681
A. burnsii — CBS 108.27	Unknown, *Gomphrena globosa*	KC584601	KC584343	KC584236	KC584162	KC584727	KC584468	KP123850	KP123997	KP124605
CBS 107.38; E.G.S. 06.185[T]	India, *Cuminum cyminum*	KP125043	KP124573	KP124420	JQ646305	KP125198	KP124889	KP123967	KP124124	KP124734
CBS 130264	India, human sputum	KP125048	KP124578	KP124425	KP124275	KP125203	KP124894	KP123972	KP124129	KP124739
A. caudata — CBS 121544; E.G.S. 38.022[R]	USA, *Cucumis sativus*	KP124995	KP124525	KP124371	KP124223	KP125149	KP124841	KP123919	KP124075	KP124684
A. citri — CBS 107.27; ATCC 24463; QM 1736[ET]	USA, *Citrus limonium*	KP124921	KP124451	KP124300	KP124157	KP125075	KP124768	KP123849	KP123996	KP124604
A. cinerariae — CBS 612.72; DSM 62012[ET]	Germany, *Senecio cineraria*	KP124930	KP124460	KP124308	KP124165	KP125084	KP124777	KP123861	KP124008	KP124615
A. citrimacularis — CBS 102596; E.G.S. 45.090[T]	USA, *Citrus jambhiri*	KP124950	KP124480	KP124328	KP124183	KP125104	KP124796	KP123877	KP124030	KP124637
A. citriarbusti — CBS 102598; E.G.S. 46.141[T]	USA, *Minneola tangelo*	KP124951	KP124481	KP124329	KP124184	KP125105	KP124797	KP123878	KP124031	KP124638
A. citricancri — CBS 119543; E.G.S. 12.160[T]	USA, *Citrus paradisi*	KP124985	KP124515	KP124363	KP124215	KP125139	KP124831	KP123911	KP124065	KP124674
A. cunninghamiicola — DSQ3-2	**China, *Cunninghamia lanceolata* leaf**	**OR229504**	**OR229647**	**OR229442**	OR252424	OR233910	OR252520	OR252376	OR252472	OR233862
DSQ3-2-1	**China, *Cu. lanceolata* leaf**	OR229505	OR229648	OR229443	OR252425	OR233911	OR252521	OR252377	OR252473	OR233863
DSQ3-2-2	**China, *Cu. lanceolata* leaf**	OR229506	OR229649	OR229444	OR252426	OR233912	OR252522	OR252378	OR252474	OR233864
DSQ3-2-3	**China, *Cu. lanceolata* leaf**	OR229507	OR229650	OR229445	OR252427	OR233913	OR252523	OR252379	OR252475	OR233865
DSQ3-2-4	**China, *Cu. lanceolata* leaf**	OR229508	OR229651	OR229446	OR252428	OR233914	OR252524	OR252380	OR252476	OR233866
A. daucifolii — CBS 118812; E.G.S. 37.050[T]	USA, *Daucus carota*	KC584525	KC584269	KC584193	KC584112	KC584652	KC584393	KP123905	KP124058	KP124668

Species name and strain number[1,2]	Locality, host / substrate	GenBank accession numbers[3]								
		SSU	LSU	ITS	GAPDH	TEF1	RPB2	Alta1	endoPG	OPA10-2
A. destruens CBS 121454; E.G.S. 46.069^T	USA, *Cuscuta gronovii*	KP124991	KP124521	–	AY278812	KP125145	KP124837	JQ646402	KP124071	KP124680
A. dongshangjiaoensis DSQ2-2	China, *Cu. lanceolata* leaf	OR229495	OR229638	OR229433	OR252415	OR233901	OR252511	OR252367	OR252463	OR233853
DSQ2-2-1	China, *Cu. lanceolata* leaf	OR229496	OR229639	OR229434	OR252416	OR233902	OR252512	OR252368	OR252464	OR233854
DSQ2-2-2	China, *Cu. lanceolata* leaf	OR229497	OR229640	OR229435	OR252417	OR233903	OR252513	OR252369	OR252465	OR233855
DSQ2-2-3	China, *Cu. lanceolata* leaf	OR229498	OR229641	OR229436	OR252418	OR233904	OR252514	OR252370	OR252466	OR233856
HN43-6-1	China, *Cu. lanceolata* leaf	OR229499	OR229642	OR229437	OR252419	OR233905	OR252515	OR252371	OR252467	OR233857
HN43-6-1-1	China, *Cu. lanceolata* leaf	OR229500	OR229643	OR229438	OR252420	OR233906	OR252516	OR252372	OR252468	OR233858
HN43-6-1-2	China, *Cu. lanceolata* leaf	OR229501	OR229644	OR229439	OR252421	OR233907	OR252517	OR252373	OR252469	OR233859
HN43-6-1-3	China, *Cu. lanceolata* leaf	OR229502	OR229645	OR229440	OR252422	OR233908	OR252518	OR252374	OR252470	OR233860
HN43-6-1-4	China, *Cu. lanceolata* leaf	OR229503	OR229646	OR229441	OR252423	OR233909	OR252519	OR252375	OR252471	OR233861
A. dumosa CBS 102604; E.G.S. 45.007^T	Israel, *Minneola tangelo*	KP124956	KP124486	KP124334	AY562410	KP125110	KP124802	AY563305	KP124035	KP124643
A. eichhorniae CBS 489.92; ATCC 22255; ATCC 46777; IMI 121518^T	India, *Eichhornia crassipes*	KP125049	KP124579	KC146356	KP124276	KP125204	KP124895	KP123973	KP124130	KP124740
A. gaisen CBS 632.93; E.G.S. 90.512^R	Japan, *Pyrus pyrifolia*	KC584531	KC584275	KC584197	KC584116	KC584658	KC584399	KP123974	AY295033	KP124742
CBS 118488; E.G.S. 90.391^R	Japan, *Pyrus pyrifolia*	KP125051	KP124581	KP124427	KP124278	KP125206	KP124897	KP123975	KP124132	KP124743
CPC 25268	Portugal, unknown	KP125052	KP124582	KP124428	KP124279	KP125207	KP124898	KP123976	KP124133	KP124744
A. godetiae CBS 117.44; E.G.S. 06.190; VKM F-1870^T	Denmark, *Godetia* sp.	KP124925	KP124455	KP124303	KP124160	KP125079	KP124772	KP123854	KP124001	KP124609
A. gossypina CBS 104.32^T	Zimbabwe, *Gossypium* sp.	KP125054	KP124584	KP124430	JQ646312	KP125209	KP124900	JQ646395	KP124135	KP124746
A. grisea CBS 107.36^T	Indonesia, soil	KP125055	KP124585	KP124431	JQ646310	KP125210	KP124901	JQ646393	KP124136	KP124747
A. herbiphorbicola CBS 119408; E.G.S. 40.140^T	USA, *Euphorbia esula*	KP124984	KP124514	KP124362	JQ646326	KP125138	KP124830	JQ646410	KP124064	KP124673
A. hunanensis HN43-10-2	China, *Cu. lanceolata* leaf	OR229486	OR229629	OR229424	OR252406	OR233892	OR252502	OR252358	OR252454	OR233844
HN43-10-2-1	China, *Cu. lanceolata* leaf	OR229487	OR229630	OR229425	OR252407	OR233893	OR252503	OR252359	OR252455	OR233845
HN43-10-2-2	China, *Cu. lanceolata* leaf	OR229488	OR229631	OR229426	OR252408	OR233894	OR252504	OR252360	OR252456	OR233846
HN43-10-2-3	China, *Cu. lanceolata* leaf	OR229489	OR229632	OR229427	OR252409	OR233895	OR252505	OR252361	OR252457	OR233847
HN43-10-2-4	China, *Cu. lanceolata* leaf	OR229490	OR229633	OR229428	OR252410	OR233896	OR252506	OR252362	OR252458	OR233848
A. interrupta CBS 102603; E.G.S. 45.011^T	Israel, *Minneola tangelo*	KP124955	KP124485	KP124333	KP124188	KP125109	KP124801	KP123882	KP124034	KP124642
A. iridiaustralis CBS 118486; E.G.S. 43.014^T	Australia, *Iris* sp.	KP125059	KP124589	KP124435	KP124284	KP125214	KP124905	KP123981	KP124140	KP124751
CBS 118487; E.G.S. 44.147^R	Australia, *Iris* sp.	KP125060	KP124590	KP124436	KP124285	KP125215	KP124906	KP123982	KP124141	KP124752
A. jacinthicola CBS 133751; MUCL 53159^T	Mali, *Eichhornia crassipes*	KP125062	KP124592	KP124438	KP124287	KP125217	KP124908	KP123984	KP124143	KP124754
CPC 25267	Unknown, *Cucumis melo* var. *inodorus*	KP125063	KP124593	KP124439	KP124288	KP125218	KP124909	KP123985	KP124144	KP124755
A. kikuchiana CBS 107.53; DSM 3187; IFO 5778^HT	Japan, *Pyrus pyrifolia*	KP124927	KP124457	KP124305	KP124162	KP125081	KP124774	KP123858	KP124005	KP124613
A. koreana SPL2-1	Korea, *Atractylodes ovata*	–	–	LC621613	LC621647	LC621715	LC621681	LC631831	LC631844	LC631857

Species name and strain number[1,2]	Locality, host / substrate	GenBank accession numbers[3]								
		SSU	LSU	ITS	GAPDH	TEF1	RPB2	Alta1	endoPG	OPA10-2
A. koreana — SPL2-4	Korea, *Atractylodes ovata*	–	–	LC621615	LC621649	LC621717	LC621683	LC631832	LC631845	LC631858
A. kunyuensis — XXG21	China, *Cu. lanceolata* leaf	OR229515	OR229658	OR229453	OR252435	OR233921	OR252531	OR252387	OR252483	OR233873
XXG22	China, *Cu. lanceolata* leaf	OR229516	OR229659	OR229454	OR252436	OR233922	OR252532	OR252388	OR252484	OR233874
XXG26-2	China, *Cu. lanceolata* leaf	OR229517	OR229660	OR229455	OR252437	OR233923	OR252533	OR252389	OR252485	OR233875
XXG31	China, *Cu. lanceolata* leaf	OR229518	OR229661	OR229456	OR252438	OR233924	OR252534	OR252390	OR252486	OR233876
XXG30	China, *Cu. lanceolata* leaf	OR229519	OR229662	OR229457	OR252439	OR233925	OR252535	OR252391	OR252487	OR233877
XXG12-2	China, *Cu. lanceolata* leaf	OR229520	OR229663	OR229458	OR252440	OR233926	OR252536	OR252392	OR252488	OR233878
A. lini — CBS 106.34; E.G.S. 06.198; DSM 62019; MUCL 10030[T]	Unknown, *Linum usitatissimum*	KP124924	KP124454	Y17071	JQ646308	KP125078	KP124771	KP123853	KP124000	KP124608
A. limoniasperae — CBS 102595; E.G.S. 45.100[T]	USA, *Citrus jambhiri*	KC584540	KC584284	FJ266476	AY562411	KC584666	KC584408	AY563306	KP124029	KP124636
A. longipes — CBS 113.35	Unknown, *Nicotiana tabacum*	KP125064	KP124594	KP124440	KP124289	KP125219	KP124910	KP123986	KP124145	KP124756
CBS 917.96	USA, *Nicotiana tabacum*	KP125066	KP124596	KP124442	KP124291	–	KP124912	KP123988	KP124148	KP124759
A. longqiaoensis — HN43-14	China, *Cu. lanceolata* leaf	OR229491	OR229634	OR229429	OR252411	OR233897	OR252507	OR252363	OR252459	OR233849
HN43-14-1	China, *Cu. lanceolata* leaf	OR229492	OR229635	OR229430	OR252412	OR233898	OR252508	OR252364	OR252460	OR233850
HN43-14-2	China, *Cu. lanceolata* leaf	OR229493	OR229636	OR229431	OR252413	OR233899	OR252509	OR252365	OR252461	OR233851
HN43-14-3	China, *Cu. lanceolata* leaf	OR229494	OR229637	OR229432	OR252414	OR233900	OR252510	OR252366	OR252462	OR233852
A. mali — CBS 106.24; E.G.S. 38.029; ATCC 13963[T]	USA, *Malus sylvestris*	KP124919	KP124449	KP124298	KP124155	KP125073	KP124766	KP123847	AY295020	JQ800620
A. malvae — CBS 447.86	Marocco, *Malva* sp.	KP124940	KP124470	KP124318	JQ646314	KP125094	KP124786	JQ646397	KP124018	KP124625
A. palandui — CBS 121336; E.G.S. 37.005; ATCC 11680[T]	USA, *Allium* sp.	KP124987	KP124517	KJ862254	KJ862255	KP125141	KP124833	KJ862259	KP124067	KP124676
A. pellucida — CBS 479.90; E.G.S. 29.028[T]	Japan, *Citrus unshiu*	KP124941	KP124471	KP124319	KP124174	KP125095	KP124787	KP123870	KP124019	KP124626
A. perangusta — CBS 102602; E.G.S. 44.160[T]	Turkey, *Minneola tangelo*	KP124954	KP124484	KP124332	KP124187	KP125108	KP124800	KP123881	AY295023	KP124641
A. platycodonis — CBS 121348; E.G.S. 50.070[T]	China, *Platycodon grandiflorus*	KP124990	KP124520	KP124367	KP124219	KP125144	KP124836	KP123915	KP124070	KP124679
A. postmessia — CBS 119399; E.G.S. 39.189[T]	USA, *Minneola tangelo*	KP124983	KP124513	KP124361	JQ646328	KP125137	KP124829	KP123910	KP124063	KP124672
A. pulvinifungicola — CBS 194.86; E.G.S. 04.090; QM 1347[T]	USA, *Quercus* sp.	KP124938	KP124468	KP124316	KP124172	KP125092	KP124784	KP123869	KP124016	KP124623
A. rhadina — CBS 595.93[T]	Japan, *Pyrus pyrifolia*	KP124942	KP124472	KP124320	KP124175	KP125096	KP124788	JQ646399	KP124020	KP124627
A. sanguisorbae — CBS 121456; E.G.S. 50.080; HSAUP 9600197[T]	China, *Sanguisorba officinalis*	KP124993	KP124523	KP124369	KP124221	KP125147	KP124839	KP123917	KP124073	KP124682
A. seleniiphila — CBS 127671; E.G.S. 52.121[T]	USA, *Stanleya pinnata*	KP125005	KP124535	KP124381	KP124233	KP125159	KP124851	KP123929	KP124085	KP124694
A. septorioides — CBS 175.80	Italy, unknown	KP124935	KP124465	KP124313	JQ646324	KP125089	KP124781	KP123866	KP124013	KP124620
A. shandongensis — SDHG12	China, *Cu. lanceolata* leaf	OR229509	OR229652	OR229447	OR252429	OR233915	OR252525	OR252381	OR252477	OR233867
SDHG12-1	China, *Cu. lanceolata* leaf	OR229510	OR229653	OR229448	OR252430	OR233916	OR252526	OR252382	OR252478	OR233868
SDHG12-2	China, *Cu. lanceolata* leaf	OR229511	OR229654	OR229449	OR252431	OR233917	OR252527	OR252383	OR252479	OR233869

Species name and strain number[1,2]		Locality, host / substrate	GenBank accession numbers[3]									
			SSU	LSU	ITS	GAPDH	TEF1	RPB2	Alta1	endoPG	OPA10-2
A. shandongensis	**SDHG12-3**	**China, Cu. lanceolata leaf**	**OR229512**	**OR229655**	**OR229450**	**OR252432**	**OR233918**	**OR252528**	**OR252384**	**OR252480**	**OR233870**
	SDHG12-4	**China, Cu. lanceolata leaf**	**OR229513**	**OR229656**	**OR229451**	**OR252433**	**OR233919**	**OR252529**	**OR252385**	**OR252481**	**OR233871**
	LY15	**China, Cu. lanceolata leaf**	**OR229514**	**OR229657**	**OR229452**	**OR252434**	**OR233920**	**OR252530**	**OR252386**	**OR252482**	**OR233872**
A. soliaegyptiaca	CBS 103.33; E.G.S. 35.182; IHEM 3319[T]	Egypt, soil	KP124923	KP124453	KP124302	KP124159	KP125077	KP124770	KP123852	KP123999	KP124607
A. tenuis	CBS 126910	USA, soil	KP125003	KP124533	KP124379	KP124231	KP125157	KP124849	KP123927	KP124083	KP124692
A. tenuissima	CBS 620.83; ATCC 15052[ET]	USA, Nicotiana tabacum	KP124937	KP124467	KP124315	KP124171	KP125091	KP124783	KP123868	KP124015	KP124622
A. tomato	CBS 103.30	Unknown, Solanum lycopersicum	KP125069	KP124599	KP124445	KP124294	KP125224	KP124915	KP123991	KP124151	KP124762
	CBS 114.35	Unknown, Solanum lycopersicum	KP125070	KP124600	KP124446	KP124295	KP125225	KP124916	KP123992	KP124152	KP124763
A. tomaticola	CBS 118814; E.G.S. 44.048[T]	USA, Solanum lycopersicum	KP124979	KP124509	KP124357	KP124211	KP125133	KP124825	KP123906	KP124059	KP124669
A. toxicogenica	CBS 102600; E.G.S. 39.181; ATCC 38963[T]	USA, Citrus reticulata	KP124953	KP124483	KP124331	KP124186	KP125107	KP124799	KP123880	KP124033	KP124640
A. turkisafria	CBS 102599; E.G.S. 44.166[T]	Turkey, Minneola tangelo	KP124952	KP124482	KP124330	KP124185	KP125106	KP124798	KP123879	KP124032	KP124639
A. vaccinii	CBS 118818; E.G.S. 31.032[T]	USA, Vaccinium sp.	KP124981	KP124511	KP124359	KP124213	KP125135	KP124827	KP123908	KP124061	KP124671
A. xinyangensis	**ZLS1**	**China, Cu. lanceolata leaf**	**OR229521**	**OR229664**	**OR229459**	**OR252441**	**OR233927**	**OR252537**	**OR252393**	**OR252489**	**OR233879**
	ZLS1-1	**China, Cu. lanceolata leaf**	**OR229522**	**OR229665**	**OR229460**	**OR252442**	**OR233928**	**OR252538**	**OR252394**	**OR252490**	**OR233880**
	ZLS1-2	**China, Cu. lanceolata leaf**	**OR229523**	**OR229666**	**OR229461**	**OR252443**	**OR233929**	**OR252539**	**OR252395**	**OR252491**	**OR233881**
	ZLS1-3	**China, Cu. lanceolata leaf**	**OR229524**	**OR229667**	**OR229462**	**OR252444**	**OR233930**	**OR252540**	**OR252396**	**OR252492**	**OR233882**
	ZLS1-4	**China, Cu. lanceolata leaf**	**OR229525**	**OR229668**	**OR229463**	**OR252445**	**OR233931**	**OR252541**	**OR252397**	**OR252493**	**OR233883**
	XYXY06	**China, Cu. lanceolata leaf**	**OR229526**	**OR229669**	**OR229464**	**OR252446**	**OR233932**	**OR252542**	**OR252398**	**OR252494**	**OR233884**
	XYXY8-2	**China, Cu. lanceolata leaf**	**OR229527**	**OR229670**	**OR229465**	**OR252447**	**OR233933**	**OR252543**	**OR252399**	**OR252495**	**OR233885**
	XYXY16	**China, Cu. lanceolata leaf**	**OR229528**	**OR229671**	**OR229466**	**OR252448**	**OR233934**	**OR252544**	**OR252400**	**OR252496**	**OR233886**
	XYXY15	**China, Cu. lanceolata leaf**	**OR229529**	**OR229672**	**OR229467**	**OR252449**	**OR233935**	**OR252545**	**OR252401**	**OR252497**	**OR233887**
	XYXY15-1	**China, Cu. lanceolata leaf**	**OR229530**	**OR229673**	**OR229468**	**OR252450**	**OR233936**	**OR252546**	**OR252402**	**OR252498**	**OR233888**
	XYXY15-2	**China, Cu. lanceolata leaf**	**OR229531**	**OR229674**	**OR229469**	**OR252451**	**OR233937**	**OR252547**	**OR252403**	**OR252499**	**OR233889**
	XYXY15-3	**China, Cu. lanceolata leaf**	**OR229532**	**OR229675**	**OR229470**	**OR252452**	**OR233938**	**OR252548**	**OR252404**	**OR252500**	**OR233890**
	XYXY15-4	**China, Cu. lanceolata leaf**	**OR229533**	**OR229676**	**OR229471**	**OR252453**	**OR233939**	**OR252549**	**OR252405**	**OR252501**	**OR233891**
A. yali-inficiens	CBS 121547; E.G.S. 50.048[T]	China, Pyrus bretschneideri	KP124996	KP124526	KP124372	KP124224	KP125150	KP124842	KP123920	KP124076	KP124685

1 ATCC: American Type Culture Collection, Manassas, VA, USA; CBS: Culture collection of the Westerdijk Fungal Biodiversity Institute, Utrecht, The Netherlands; CPC: Personal collection of P.W. Crous, Utrecht, The Netherlands; DAOM: Canadian Collection of Fungal Cultures, Ottawa, Canada; DSM: German Collection of Microorganisms and Cell Cultures, Leibniz Institute, Braunschweig, Germany; E.G.S.: Personal collection of Dr. E.G. Simmons; HKUCC: The University of Hong Kong Culture Collection, Hong Kong, China; IFO: Institute for Fermentation Culture Collection, Osaka, Japan; IHEM: Biomedical Fungi and Yeast Collection of the Belgian Co-ordinated Collections of Micro-organisms (BCCM), Brussels, Belgium; IMI: Culture collection of CABI Europe UK Centre, Egham UK; LCP: Laboratory of Cryptogamy, National Museum of Natural History, Paris, France; MAFF: MAFF Genebank Project, Ministry of Agriculture, Forestry and Fisherie, Tsukuba, Japan; MUCL: (Agro)Industrial Fungi and Yeast Collection of the Belgian Co-ordinated Collections of Micro-organisms (BCCM), Louvain-la-Neuve, Belgium; QM: Quarter Master Culture Collection, Amherst, MA, USA; VKM: All-Russian Collection of Microorganisms, Moscow, Russia.
T: ex-type isolate; ET: ex-epitype isolate; HT: ex-holotype isolate; R: representative isolate.
3 Bold accession numbers are generated in other studies; np: no product.

Phylogenetically-related, but ambiguous species were analysed using the genealogical concordance phylogenetic species recognition (GCPSR) model by performing a pairwise homoplasy index (PHI) test as described by Quaedvlieg et al. (2014). The PHI test was performed in SplitsTree4 (Huson 1998; Huson and Bryant 2006) in order to determine the recombination level within phylogenetically closely-related species using a concatenated multi-locus dataset (ITS, SSU, LSU, GAPDH, RPB2, TEF1, Alt a1, endoPG and OPA10-2). If the pairwise-homoplasy index results were below a 0.05 threshold ($\Phi_w < 0.05$), it indicates significant recombination present in the dataset. The relationship amongst the closely-related species was visualised by constructing splits graphs.

Morphological study

One representative isolate was randomly selected from each *Alternaria* species for morphological research according to the method of Simmons (2007). Mycelial plugs (5 mm) of purified cultures were transferred from the growing edge of 5-d-old cultures to the centre of 7-mm-diameter potato carrot agar (PCA) plates (Crous et al. 2009b) in triplicate at 25 °C. Colony diameters were measured from 3 to 6 days to calculate mycelial growth rates (mm/d). Colony colour, size and density were also recorded. The morphology and size of conidial chains were studied and recorded using a Zeiss stereo microscope (SteRo Discovery v.20). The shape, colour and size of conidiophores and conidia were observed using a ZEISS Axio Imager A2m microscope (ZEISS, Germany) with differential interference contrast (DIC) optics. At least 30 measurements per structure were performed using Carl Zeiss Axio Vision software to determine their sizes, unless no or fewer individual structures were produced.

Pathogenicity tests

Seven representative isolates (ZLS1, DSQ2-2, SDHG12, XXG21, HN43-10-2, HN43-14 and DSQ3-2) of *Alternaria* species were selected for the pathogenicity test on detached leaves of Chinese fir collected from 1-year-old Chinese fir plants on the campus of Nanjing Forestry University, Jiangsu, China.

For in-vitro inoculation, detached leaves were surface-sterilised with 75% ethanol, washed three times with sterile water and air-dried on sterile filter paper. A 10 μl aliquot of conidial suspension (1.0×10^6 conidia/ml) was transferred to a sterile plastic tube (20 × 6 mm), in which a leaf was placed so that the base of the leaf was immersed in the conidial suspension. The control was treated with the same amount of double-distilled water. Leaves in the tubes were then placed in plastic trays (40 × 25 cm), covered with a piece of plastic wrap to maintain relative humidity at 99% and incubated at 25 °C in the dark for 5 days. Each treatment had twelves replicates and the experiment was conducted three times. Symptom development on each detached leaf was evaluated by determining the means of lesion lengths at 5 days post-inoculation (dpi). The data were analysed by analysis of variance (ANOVA) using SPSS v. 18 software. LSD's range test was used to determine significant differences

amongst or between different treatments. Origin v. 8.0 software was used to draw histograms (Li et al. 2020). Pathogens were re-isolated from the resulting lesions and identified as described above.

Results

Phylogenetic analyses

A total of 48 *Alternaria* isolates from Chinese fir were subjected to multi-locus phylogenetic analyses for *Alternaria* spp. with concatenated sequences of ITS, SSU, LSU, GAPDH, RPB2, TEF1, Alt a1, endoPG and OPA10-2. The data matrix contained a total of 5460 characters with gaps (Alt a1: 1–453, GAPDH: 454–952, ITS: 953–1462, LSU: 1463–2349, OPA10-2: 2350–3013, endoPG: 3014–3414, RPB2: 3415–4170, SSU: 4171–5167, TEF1: 5168–5460). *Alternaria alternantherae* Holcomb & Antonop. CBS 124392 was used as the out-group. The Maximum-likelihood (ML) and Bayesian Inference (BI) phylogenetic analyses showed that 48 isolates clustered into seven clades distantly from any known species (Fig. 1). Of these, 13 isolates clustered distantly from any known species with high support (ML-BS/BI-PP = 100/1) and closely related to *A. dongshanqiaoensis* sp. nov. (this study, DSQ2-2), *A. citri* (Penz.) Mussat (ex-epitype, CBS 107.27), *A. cinerariae* Hori & Enjoji (ex-type, CBS 612.72) and *A. kikuchiana* S. Tanaka (ex-type, CBS 107.53), are herein described as a new taxon, namely *A. xinyangensis* sp. nov. (Fig. 1). The results showed that nine isolates clustered in a distinct clade with high support (ML-BS/BI-PP = 100/1), which was distinct from all other known species and closely related to *A. xinyangensis* sp. nov. (this study, ZLS1), *A. citri* (ex-epitype, CBS 107.27), *A. cinerariae* (ex-type, CBS 612.72) and *A. kikuchiana* (ex-type, CBS 107.53), namely *A. dongshanqiaoensis* sp. nov. (Fig. 1). When applying the GCPSR concept to these isolates, the concatenated sequence dataset of nine-loci (ITS, SSU, LSU, GAPDH, RPB2, TEF1, Alt a1, endoPG and OPA10-2) was subjected to the PHI test and the result showed that no significant recombination was detected amongst these isolates/taxa (Φw = 0.1647) (Fig. 2A). It was a solid support for the proposition that these isolates belonged to six distinct taxa.

The ML/BI phylogenetic analyses also showed that *A. shandongensis* (six isolates, ML-BS/BI-PP = 98/1), *A. kunyuensis* (six isolates, ML-BS/BI-PP = 100/1), *A. hunanensis* (five isolates, ML-BS/BI-PP = 100/1) and *A. longqiaoensis* (four isolates, ML-BS/BI-PP = 100/1) clustered in four distinct clades, which were distinct from all other known species and closely related to *A. vaccinii* E.G. Simmons (ex-type, CBS 118818), *A. platycodonis* Z.Y. Zhang & H. Zhang (ex-type, CBS 121348), *A. rhadina* E.G. Simmons (ex-type, CBS 595.93), *A. citriarbusti* E.G. Simmons (ex-type, CBS 102598) and *A. tomaticola* E.G. Simmons & Chellemi (ex-type, CBS 118814) (Fig. 1). When applying the GCPSR concept to these isolates, the concatenated sequence dataset of nine-loci (ITS, SSU, LSU, GAPDH, RPB2, TEF1, Alt a1, endoPG and OPA10-2) was subjected to the PHI test and showed that no significant recombination was detected amongst these isolates/taxa (Φ_w = 0.3502) (Fig. 2B). It was a solid support for the proposition that these isolates belonged to nine distinct taxa.
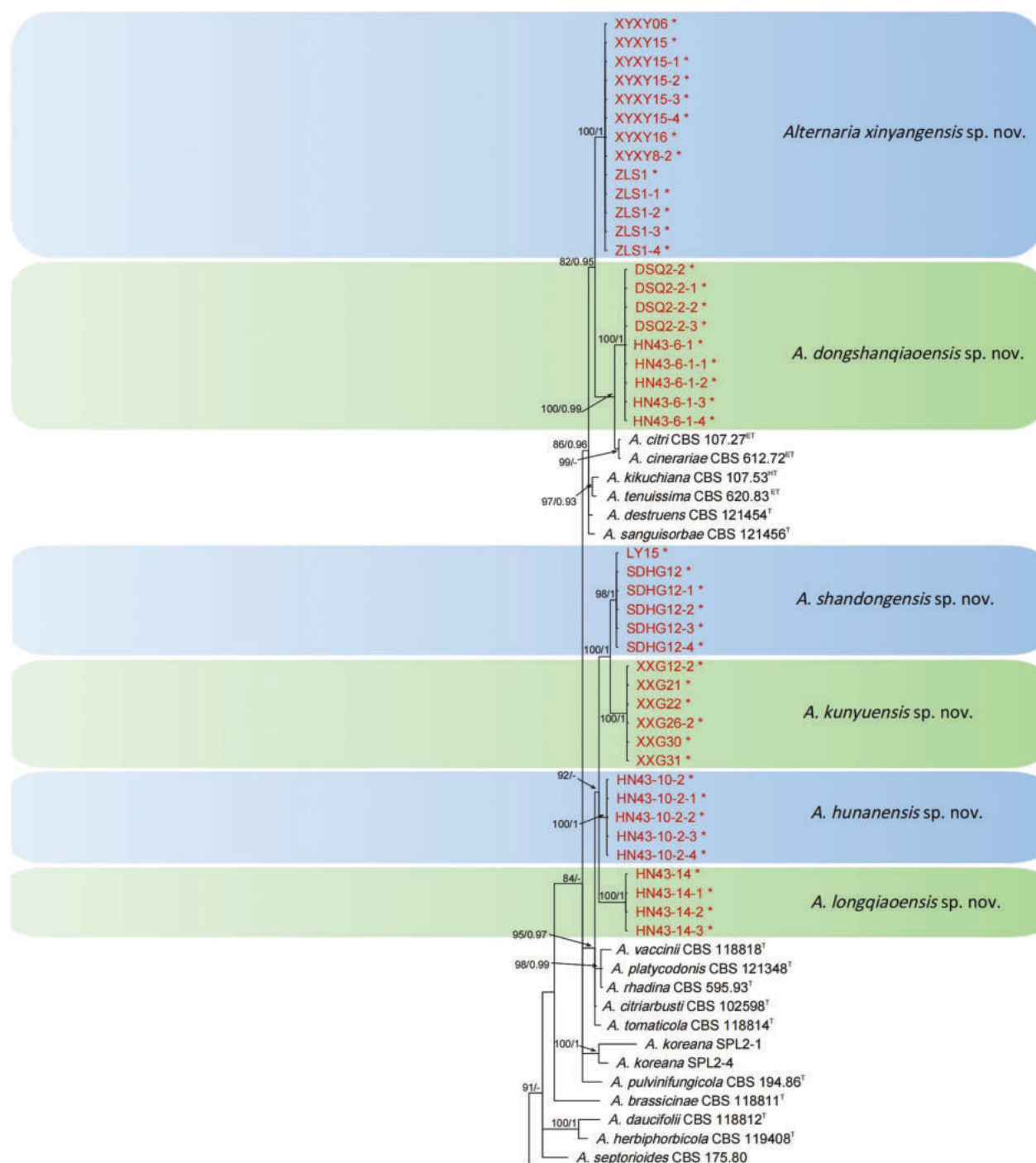
Figure 1. Phylogenetic relationships of 116 isolates of the *Alternaria* species complex with related taxa with concatenated sequences of the SSU, LSU, ITS, GAPDH, RPB2, TEF1, Alt a1, endoPG and OPA10-2 loci using Bayesian inference (BI) and Maximum-likelihood (ML) methods. Bootstrap support values from ML ≥ 70% and BI posterior values ≥ 0.9 are shown at nodes (ML/BI). *Alternaria alternantherae* CBS 124392 was the outgroup. * and red font indicates strains of this study. [T] indicates the ex-type strains, [ET] indicates the ex-epitype strains, [HT] indicates the ex-holotype strains.

Phylogenetic analyses also showed that the five isolates (DSQ3-2, DSQ3-2-1, DSQ3-2-2, DSQ3-2-3 and DSQ3-2-4) clustered in a distinct clade with high support (ML-BS/BI-PP = 100/0.99), which was distinct from all other known
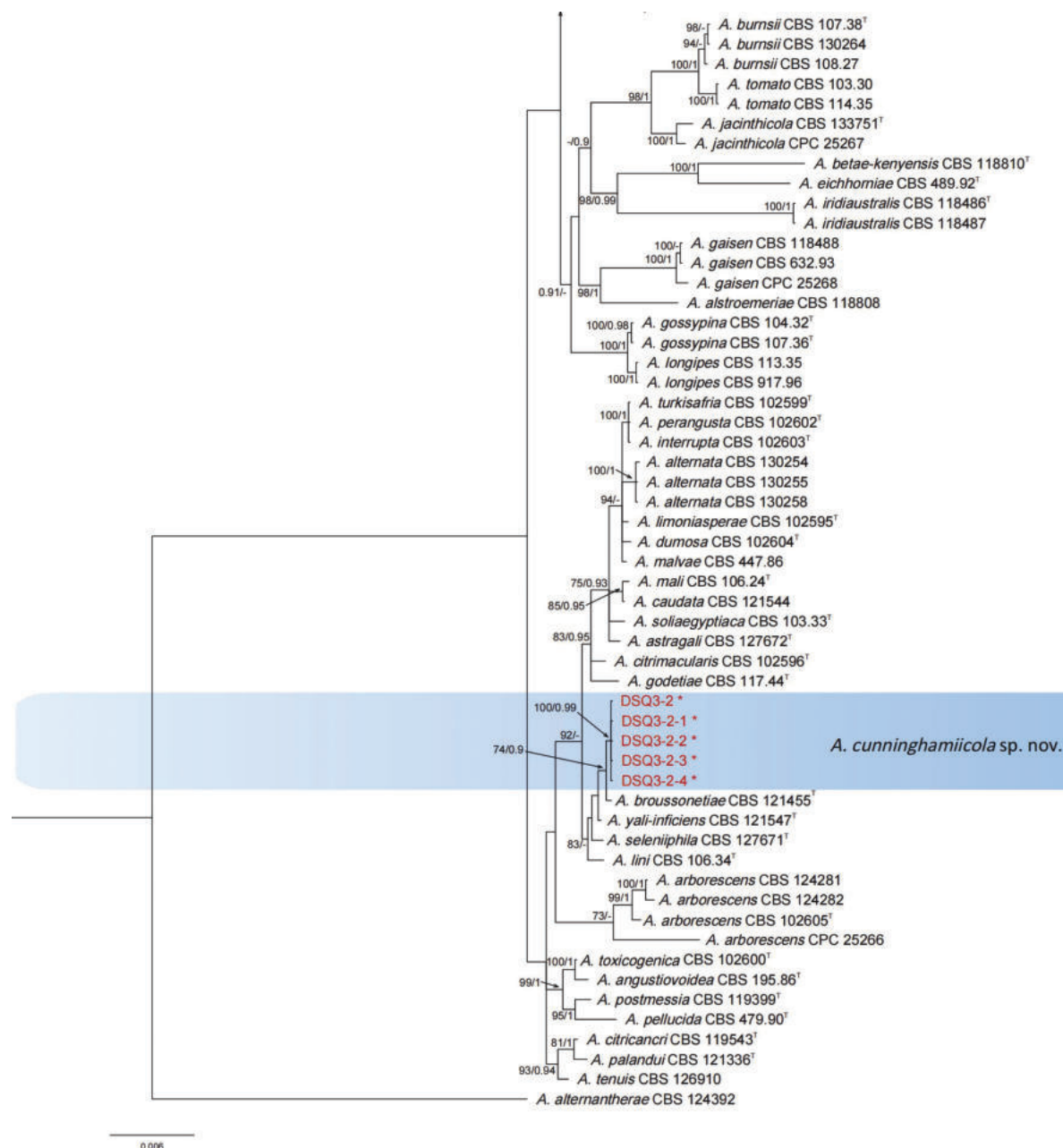
Figure 1. Continued.

species and a sister clade to the clades of *A. broussonetiae* T.Y. Zhang, W.Q. Chen & M.X. Gao (ex-type, CBS 121455), *A. yali-inficiens* R.G. Roberts (ex-type, CBS 121547), *A. seleniiphila* Wangeline & E.G. Simmons (ex-type, CBS 127671) and *A. lini* P.K. Dey (ex-type, CBS 106.34), namely *A. cunninghamiicola* sp. nov. (Fig. 1). When applying the GCPSR concept to these isolates, the concatenated sequence dataset of nine-loci (ITS, SSU, LSU, GAPDH, RPB2, TEF1, Alt a1, endoPG and OPA10-2) was subjected to the PHI test, and the result showed that no significant recombination was detected amongst these isolates/taxa (Φw = 0.2087) (Fig. 2C). It was a solid support for the proposition that these isolates belonged to five distinct taxa.
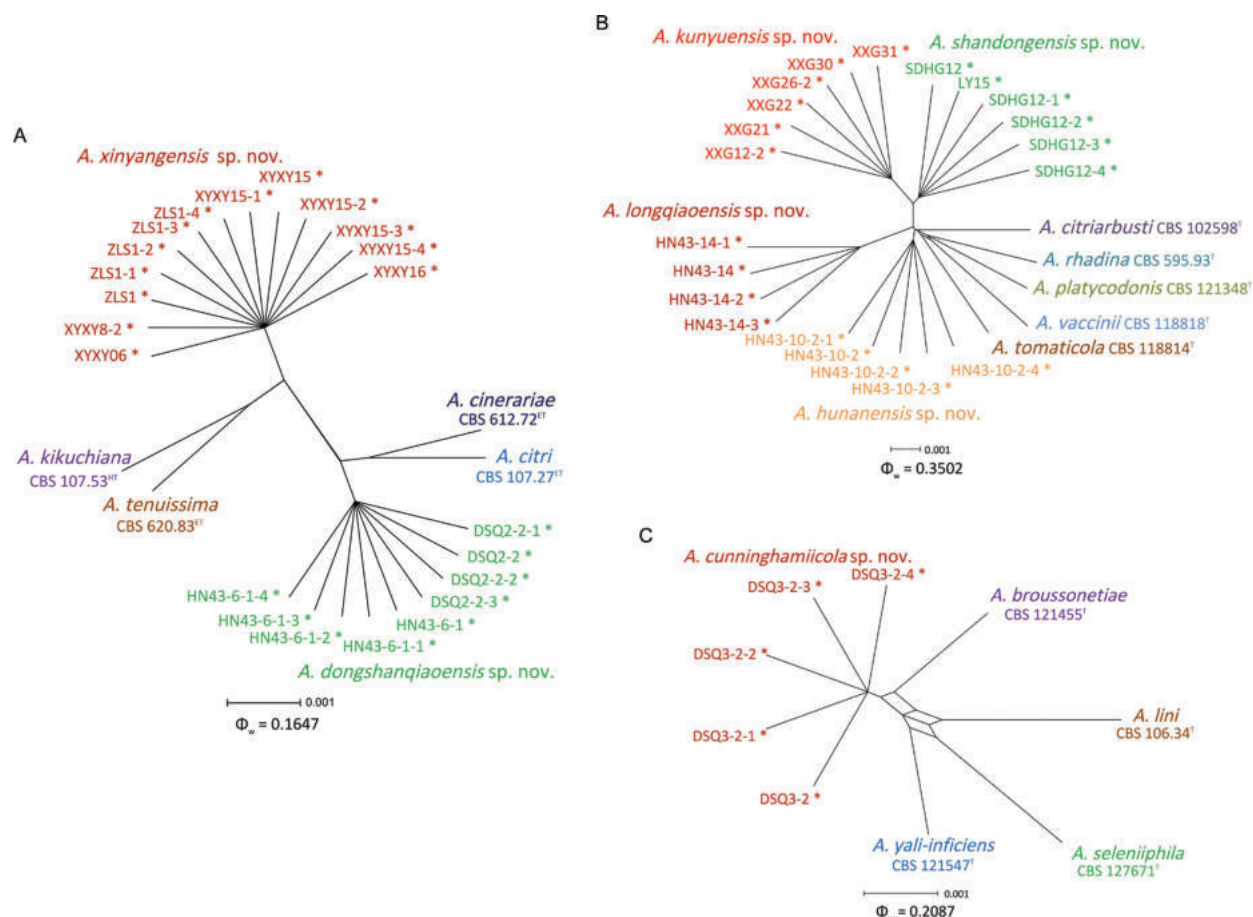
Figure 2. Splitgraphs showing the results of the pairwise homoplasy index (PHI) test of newly described taxa and closely-related species using both LogDet transformation and splits decomposition **A** the PHI of *Alternaria xinyangensis* sp. nov. and *A. dongshanqiaoensis* sp. nov. with their phylogenetically related isolates or species **B** the PHI of *A. shandongensis* sp. nov., *A. kunyuensis* sp. nov., *A. hunanensis* sp. nov. and *A. longqiaoensis* sp. nov. with their phylogenetically related isolates or species **C** the PHI of *A. cunninghamiicola* sp. nov. with their phylogenetically-related isolates or species. PHI test value (Φ_w) < 0.05 indicate significant recombination within a dataset. * indicates strains of this study. [T] indicates the ex-type strains, [ET] indicates the ex-epitype strains, [HT] indicates the ex-holotype strains.

Taxonomy

Based on morphology and multi-locus sequence data, a total of 48 obtained isolates from Chinese fir were assigned to seven species of *Alternaria*, which represented seven undescribed taxa and were described below.

Alternaria cunninghamiicola Lin Huang, Jiao He & D.W. Li, sp. nov.
Index Fungorum: IF901036
Fig. 3

Holotype. CHINA, Jiangsu Province, Nanjing City, Dongshanqiao Forest Farm, 31°51'11"N, 118°46'12"E, isolated from leaf spots of *Cunninghamia lanceolata*, May 2017, Wen-Li Cui, (holotype: CFCC 59358). Holotype specimen is a living specimen being maintained via lyophilisation at the China Forestry Culture Collection Center (CFCC). Ex-type (DSQ3-2) is maintained at the Forest Pathology Laboratory, Nanjing Forestry University.

Etymology. The specific epithet refers to the genus of the host plant (*Cunninghamia lanceolata*).

Host/distribution. From *C. lanceolata* in Dongshanqiao Forest Farm, Nanjing City, Jiangsu Province, China.

Description. Mycelium superficial on the PCA, composed of septate, branched, smooth, thin-walled, pale white to grey hyphae. Conidiophores macronematous, mononematous, solitary, subcylindrical, branched or unbranched, straight or geniculate, thin-walled, 2−10 septate, (18.3−)25.3−68.4(−93.8) × (3.0−)3.3−4.2(−4.8) μm, (mean ± SD = 46.9 ± 21.6 × 3.7 ± 0.5 μm, n = 32), arising mostly at right angles from undifferentiated hyphae, with conspicuous scars after conidia have seceded. Conidiogenous cells apical or subapical, cylindrical, light brown, smooth, (5.2−)7.3−14.0(−18.1) × (2.5−)3.0−4.2(−5.0) μm, (mean ± SD = 10.7 ± 3.3 × 3.6 ± 0.6 μm, n = 45), mono- or polytretic, with conspicuous scars at the loci of sporulating after conidia have seceded. Each conidiogenous locus bears a primary chain of 3−5 conidia with rarely lateral branches or occasionally a sole secondary conidium. Conidia pale brown to brown, shape varied, ovoid or ellipsoid, pyriform or obclavate, usually smooth; conidial bodies (12.2−)18.1−35.4(−51.6) × (7.5−)10.4−15.5(−18.7) μm, (mean ± SD = 26.6 ± 8.6 × 12.9 ± 2.6 μm, n = 53), with 1−5 transverse and 0−2 longitudinal septate. Secondary conidia directly (but rarely) produced by conidia through an inconspicuous apical conidiogenous locus or (commonly) by means of a short apical or lateral secondary conidiophore with 1−2 cells in length. Secondary conidiophores (false beaks) with one or a few conidiogenous loci, (4.5−)5.2−22.5(−32.7) × (2.7−)3.2−4.2(−4.7) μm, (mean ± SD = 13.8 ± 8.7 × 3.7 ± 0.5 μm, n = 31). Beakless conidia mostly with a conical cell at the apex. Chlamydospores not observed.

Culture characteristics. Colonies on PCA incubated at 25 °C in the dark growing at 9.3 ± 0.1 mm/d; aerial hypha cottony, white to pale grey; reverse centre dark green to black; sporulation sparse; diffusible pigment absent.

Additional materials examined. CHINA, Jiangsu Province, Nanjing City, Dongshanqiao Forest Farm, 31°51'11"N, 118°46'12"E, isolated from leaf spots of *Cunninghamia lanceolata*, May 2017, Wen-Li Cui, DSQ3-2-1, DSQ3-2-2, DSQ3-2-3, DSQ3-2-4.

Notes. The isolates of *A. cunninghamiicola* were phylogenetically close to *A. broussonetiae* (ex-type, CBS 121455), *A. yali-inficiens* (ex-type, CBS 121547), *A. seleniiphila* (ex-type, CBS 127671) and *A. lini* (ex-type, CBS 106.34) (Fig. 2). Between *A. cunninghamiicola* isolates and *A. broussonetiae* (ex-type, CBS 121455), there were 1/453 differences in Alt a1, 4/510 in ITS and 1/664 in OPA10-2. Between *A. cunninghamiicola* isolates and *A. yali-inficiens* (ex-type, CBS 121547), there were 1/453 differences in Alt a1, 2/499 in GAPDH, 3/510 in ITS and 1/401 in endoPG. Between *A. cunninghamiicola* isolates and *A. seleniiphila* (ex-type, CBS 127671), there were 1/453 differences in Alt a1, 2/499 in GAPDH, 3/510 in ITS, 1/401 in endoPG and 6/757 in RPB2. Between *A. cunninghamiicola* isolates and *A. lini* (ex-type, CBS 106.34), there were 1/453 differences in Alt a1, 2/499 in GAPDH, 4/510 in ITS, 1/887 in LSU, 1/664 in OPA10-2 and 6/757 in RPB2. The PHI analysis showed that there was no significant recombination between *A. cunninghamiicola* isolates and its related species (Φ_w = 0.2087) (Fig. 2C). Distinguishing characteristics of this new species and other related species of *Alternaria* spp. are shown in Table 2. Morphologically, conidia in chains
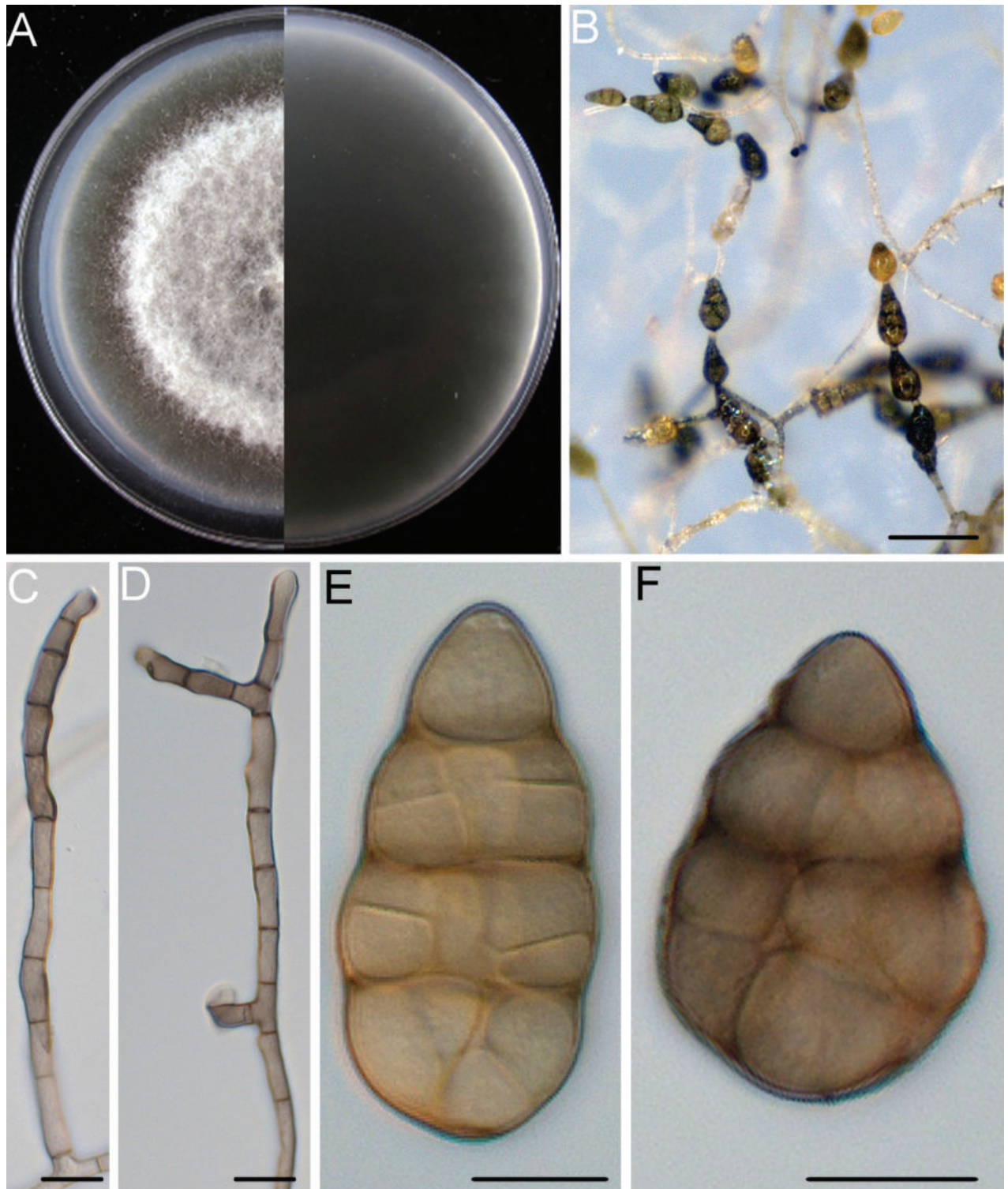
Figure 3. *Alternaria cunninghamiicola* (DSQ3-2) **A** colony on PCA after 6 days at 25 °C in the dark **B** sporulation patterns **C, D** conidiophores and conidiogenous cell **E, F** conidium. Scale bars: 50 μm (**B**); 10 μm (**C−F**).

of the *A. cunninghamiicola* isolates were less than those of *A. broussonetiae* CBS 121455 (ex-type) (3−5 vs. 8−15 conidia) (Zhang et al. 1999) and *A. yali-inficiens* CBS 121547 (ex-type) (3−5 vs. 8−18 conidia) (Roberts 2005). Conidiophores of the *A. cunninghamiicola* isolates were shorter than those of *A. seleniiphila* CBS 127671 (ex-type) (25.3−68.4 × 3.3−4.2 μm vs. 80−250 × 4−5 μm) (Wangeline and

Reeves 2007). Conidia of the *A. cunninghamiicola* isolates were shorter and wider than those of *A. lini* CBS 106.34 (ex-type) (18.1−35.4 × 10.4−15.5 µm vs. 42−60 × 3−7 µm) (Dey 1933). Thus, the phylogenetic and morphological evidence support this fungus being a new species within the *Alternaria alternata* species complex.

Alternaria dongshanqiaoensis Lin Huang, Jiao He & D.W. Li, sp. nov.

Index Fungorum: IF901037

Fig. 4

Holotype. China, Jiangsu Province, Nanjing City, Dongshanqiao Forest Farm, 31°51'11"N, 118°46'12"E, isolated from leaf spots of *Cunninghamia lanceolata*, May 2017, Wen-Li Cui, (holotype: CFCC 59353). Holotype specimen is a living specimen being maintained via lyophilisation at the China Forestry Culture Collection Center (CFCC). Ex-type (DSQ2-2) is maintained at the Forest Pathology Laboratory, Nanjing Forestry University.

Etymology. Epithet is after Dongshanqiao Forest Farm, Nanjing City, Jiangsu Province where the type specimen was collected.

Host/distribution. from *C. lanceolata* in Dongshanqiao Forest Farm, Nanjing City, Jiangsu Province, China.

Description. Mycelium superficial on the PCA, composed of septate, branched, smooth, thin-walled, white to pale brown hyphae. Conidiophores macronematous, mononematous, solitary and relatively short, pale brown, smooth, 1−3 septate, (8.1−)16.4−60.2(−100.5) × (2.4−)3.2−4.6(−5.6) µm, (mean ± SD = 38.3 ± 21.9 × 3.9 ± 0.7 µm, n = 30), arising mostly at right angles from undifferentiated hyphae. Conidiogenous cells apical or subapical, cylindrical, light brown, smooth, (3.8−)5.2−13.7(−20.2) × (2.8−)3.5−4.6(−5.2) µm, (mean ± SD = 9.4 ± 4.2 × 4.0 ± 0.5 µm, n = 36), mono- or di-tretic, with conspicuous scars at the loci of sporulating after conidia have seceded. Each conidiogenous locus bears a primary chain of 5−9 conidia; rarely with lateral branches or occasionally a sole secondary conidium. Conidial bodies brown to dark brown, ellipsoid to obclavate, smooth to verruculose, (16.4−)21.1−32.9(−40.1) × (10.2−)11.4−16.8(−22.2) µm, (mean ± SD = 27.0 ± 5.9 × 14.1 ± 2.7 µm, n = 48), with 1−4 (mostly 3) transverse and 1−4 longitudinal septate. Secondary conidia commonly produced by means of a short apical or lateral secondary conidiophore, but rarely by conidia through an inconspicuous apical conidiogenous locus. Secondary conidiophores (false beaks) at the apical end and median of conidium, short, mostly single-celled, (1.4−)2.2−9.4(−20.0) × (1.9−)2.8−4.0(−5.2) µm, (mean ± SD = 5.8 ± 3.6 × 3.4 ± 0.6 µm, n = 33). Beakless conidia mostly with a conical cell at the apex. Chlamydospores not observed.

Culture characteristics. Colonies on PCA incubated at 25 °C in the dark growing at 7.8 ± 0.2 mm/d; aerial hyphae cottony, greyish-green, with grey margins; reverse centre black, with white margins.

Additional materials examined. China, Jiangsu Province, Nanjing City, Dongshanqiao Forest Farm, 31°51'11"N, 118°46'12"E, isolated from leaf spots of *Cunninghamia lanceolata*, May 2017, Wen-Li Cui, DSQ2-2-1, DSQ2-2-2, DSQ2-2-3, DSQ2-2-4; Hunan Province, Yiyang City, Longqiao Town, 28°27'24"N, 112°29'7"E, isolated from leaf spots of *C. lanceolata*, May 2017, Wen-Li Cui, HN43-6-1, HN43-6-1-1, HN43-6-1-2, HN43-6-1-3, HN43-6-1-4.

Table 2. Distinguishing characteristics of the new species and similar known species of *Alternaria* spp. under growth conditions[a].

Species	Conidiophores (µm)[b]	Conidiogenous cells (µm)[c]	Chain	Size (µm)[d]	Conidia Transverse septa	Longitudinal or oblique septa	Beak or secondary conidiophores (false beaks) (µm)[e]	Reference
Alternaria broussonetiae (ex-type, CBS 121455)	np	np	8–15 conidia	25–38 × 9–12	5–6	0–1	beakless secondary conidiophore single hyaline cell 3–4 × 3–5 a well-differentiated up to ca 25–50 × 3–4	Zhang et al. (1999)
A. cinerariae (ex-epitype, CBS 612.72)	25–196 × 6–11	np	2–5(–9) conidia	18–295 × 8–63	1–14	up to 10	80–159 × 5–9	(Nishikawa and Nakashima 2020)
A. citri (ex-epitype, CBS 107.27)	np	np	3–6 conidia	10–22 × 8–15 (in early stages) 25–40 × 15–25 (Mature)	(3–)4–6	one or more	np	(Pierce 1902)
A. citriarbusti (ex-type, CBS 102598)	200 × 5	np	5–8 conidia	30–60 × 8–12	6–11	0–1	beakless secondary conidiophores single cell 3–5 × 4 elongate but not filiform extension up to 25–35 × 2–3	(Simmons 1999)
A. cunninghamiicola (DSQ3-2)	25.3–68.4 × 3.3–4.2	7.3–14.0 × 3.0–4.1	3–5 conidia	18.1–35.4 × 10.4–15.5	1–6	0–5	beakless secondary conidiophores (false beaks) 5.2–22.5 × 3.2–4.2	this study
A. dongshanqiaoensis (DSQ2-2)	16.4–60.2 × 3.2–4.6	5.2–13.7 × 3.5–4.6	5–9 conidia	21.1–32.9 × 11.4–16.8	1–4	1–4	beakless, secondary conidiophores (false beaks) 2.2–9.4 × 2.8–4.0	this study
A. hunanensis (HN43-10-2)	18.4–41.8 × 3.7–4.7	4.6–9.5 × 3.0–4.5	3–7 conidia; one secondary chain of 1–2 conidia.	16.7–28.8 × 8.2–12.6	1–4	0–2	beakless, secondary conidiophores (false beaks) 2.9–21.7 × 2.8–4.3	this study
A. kikuchiana (ex-holotype, CBS 107.53)	np	np	6–9 conidia	10–70 × 6–22	1–3	1–10	np	(Nishikawa and Nakashima 2019)
A. kunyuensis (XXG21)	21.4–53.5 × 3.3–4.0	5.2–11.1 × 3.2–4.2	3–8 conidia; one secondary chain of 2–4 conidia.	20.5–29.8 × 9.4–13.5	1–5	0–3	beakless, secondary conidiophores (false beaks) 2.9–20.0 × 2.8–3.9	this study
A. lini (ex-type, CBS 106.34)	26–80 × 3–7	np	np	42–60 × 3–7	2–7	1–4	beakless	(Dey 1933)
A. longqiaoensis	19.6–51.0 × 3.3–4.2	4.3–9.6 × 2.9–4.5	4–8 conidia; 1 to 3 secondary chains of 3–4	16.0–28.2 × 7.0–12.6	1–5	0–2	beakless, secondary conidiophores (false beaks) 3.3–11.6 × 2.9–3.9	this study
A. platycodonis (ex-type, CBS 121348)	np	np	8–10 conidia	25–45 × 8–12	4–7	0	beakless secondary conidiophore single hyaline cell 3–4 × 3–5 well-differentiated up to 20 × 3–4	(Zhang 2003)
A. rhadina (ex-type, CBS 595.93)	60–110 × 3–4	np	9–15 conidia 35–45 × 8–9 (narrow ovoid)	4–7	1	20–45 (tapered beak)		
A. seleniiphila (ex-type, CBS 127671)	80–250 × 4–5	np	3–6 conidia	20–40 × 8–12	1–7	0–1	beakless secondary conidiophores (false beaks) 3–30 × 3	(Wangeline and Reeves 2007)

Species	Conidiophores (μm)[b]	Conidiogenous cells (μm)[c]	Chain	Size (μm)[d]	Conidia Transverse septa	Longitudinal or oblique septa	Beak or secondary conidiophores (false beaks) (μm)[e]	Reference
A. shandongensis (SDHG12)	**23.6–51.1 × 3.4–4.3**	**4.8–9.6 × 3.2–4.3**	**9–13 conidia**	**20.1–31.2 × 9.3–14.1**	**2–7**	**0–3**	**beakless, secondary conidiophores (false beaks) 2.7–10.3 × 2.3–3.1**	**this study**
A. tenuissima (ex-epitype, CBS 620.83)	np	np	6–10 conidia	32–45 × 11–13 (only transverse septa) 32–45 × 14–18 (ovoid muriformly septate)	np	np	narrow-taper beak is near 64(–72)	(Wiltshire 1933)
A. tomaticola (ex-epitype, CBS 118814)	50–80 × 3–5	np	10–15 conidia	30–40 × 9–12 (larger conidia) 12–25 × 7–13 (smaller conidia)	6–7 (larger) 1–4 (smaller)	1–2 (larger) 0–1 (smaller)	beakless secondary conidiophores 15–50	(Simmons 2007)
A. vaccinii (ex-epitype, CBS 118818)	100–200 × 3–4	np	8–10 conidia	15–50 × 7–9	1–8	np	beakless secondary conidiophores 65–150 × 3–4	(Simmons 2007)
A. xinyangensis (ZLS1)	**15.3–54.9 × 3.7–4.8**	**5.3–9.6 × 3.3–4.9**	**2–7 conidia**	**19.9–31.8 × 8.6–12.9**	**1–6**	**1–5**	**beakless, secondary conidiophores (false beaks) 5.3–16.0 × 2.8–4.1**	**this study**
A. yali-inficiens (ex-type, CBS 121547)	80–120 × 4–5	np	8–18 conidia	20–30 × 10–12	3–4	1–2	np	(Roberts 2005)

a New species in this study are printed in bold.
bcde Dimensions of conidiophores, Conidiogenous cells, conidia, and beaks (μm, mean ± SD for length × width).
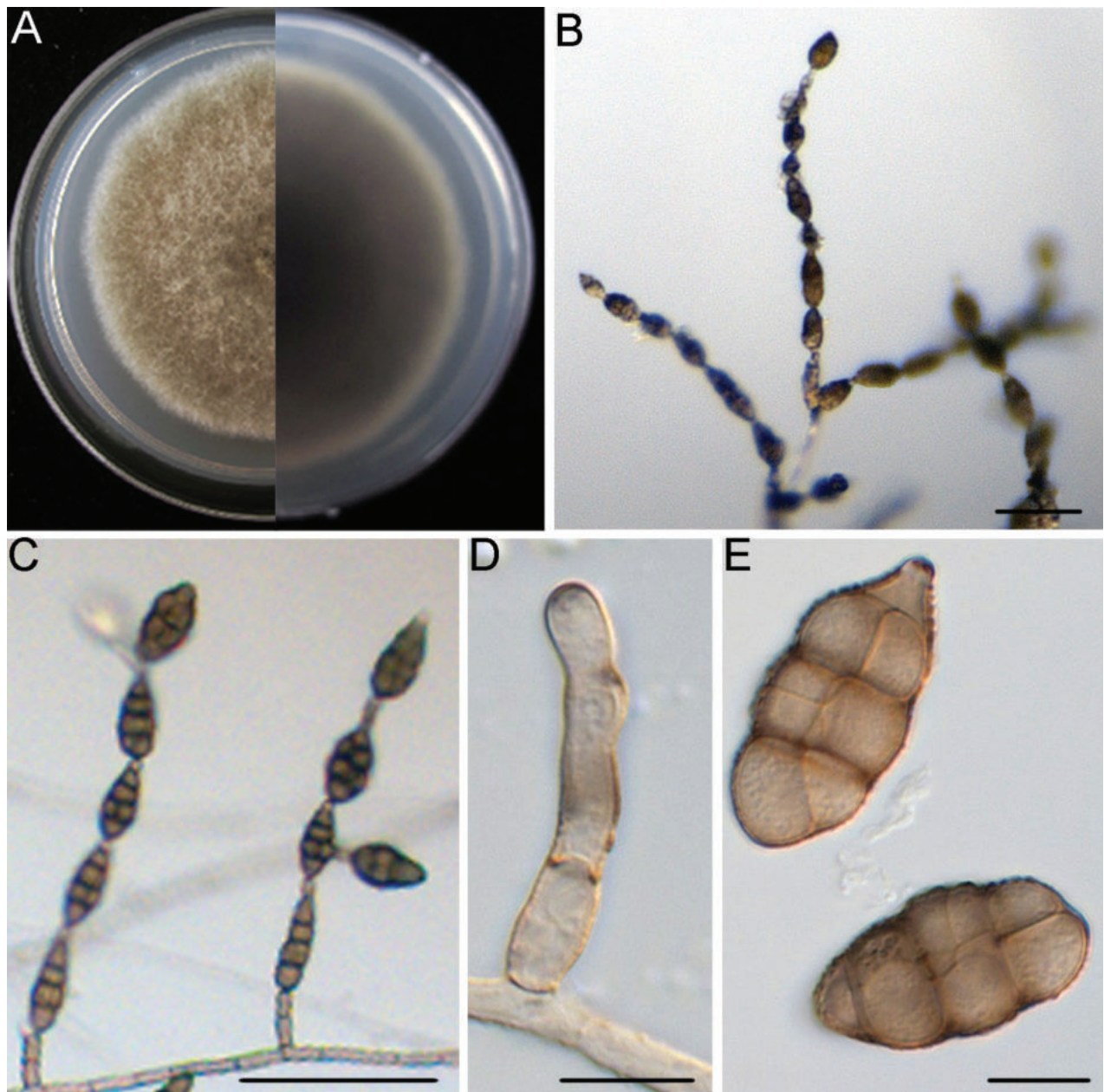np: no product.

Figure 4. *Alternaria dongshanqiaoensis* (DSQ2-2) **A** colony on PCA after 6 days at 25 °C in the dark **B, C** sporulation patterns **D** conidiophore and conidiogenous cell **E** conidia. Scale bars: 50 μm (**B, C**); 10 μm (**D, E**).

Notes. The isolates of *A. dongshanqiaoensis* were phylogenetically close to *A. citri* (ex-epitype, CBS 107.27), *A. cinerariae* (ex-epitype, CBS 612.72), *A. kikuchiana* (ex-holotype, CBS 107.53) and *A. tenuissima* (Kunze) Wiltshire (ex-epitype, CBS 620.83) (Fig. 2). Between *A. dongshanqiaoensis* isolates and *A. citri* (ex-epitype, CBS 107.27), there were 2/453 differences in Alt a1, 4/510 in ITS, 2/401 in endoPG, 1/757 in RPB2 and 2/996 in SSU. Between *A. dongshanqiaoensis* isolates and *A. cinerariae* (ex-epitype, CBS 612.72), there were 2/453 differences in Alt a1, 4/510 in ITS, 2/401 in endoPG, 1/757 in RPB2 and 2/996 in SSU. Between *A. dongshanqiaoensis* isolates and *A. kikuchiana* (ex-type, CBS 107.53), there were 2/453 differences in Alt a1, 4/510 in ITS, 8/664 in OPA10-2, 3/401 in endoPG, 2/757 in RPB2 and 2/996 in SSU. Between *A. dongshanqiaoensis* isolates and *A. tenuissima* (ex-epitype, CBS 620.83), there were 1/453 differences in Alt a1, 6/510

in ITS, 8/664 in OPA10-2, 3/401 in endoPG, 1/757 in RPB2 and 6/996 in SSU. The PHI analysis showed that there was no significant recombination between *A. dongshanqiaoensis* isolates and its related species (Φ_w = 0.1647) (Fig. 2A). Distinguishing characteristics of this new species and other related species of *Alternaria* spp. are shown in Table 2. Morphologically, conidia in chains of the *A. dongshanqiaoensis* isolates were more than those of *A. citri* CBS 107.27 (ex-epitype) (5−9 conidia vs. 3−6 conidia) (Pierce 1902). Conidia of the *A. dongshanqiaoensis* isolates were significantly different from those of *A. cinerariae* CBS 612.72 (ex-epitype) (21.1−32.9 × 11.4−16.8 μm vs. 18−295 × 8−63 μm) (Nishikawa and Nakashima 2020). Longitudinal septa of conidia of the *A. dongshanqiaoensis* isolates were less than those of *A. kikuchiana* CBS 107.53 (ex-holotype) (1−4 vs. 1−10 longitudinal or oblique septa) (Nishikawa and Nakashima 2019). Conidia of the *A. dongshanqiaoensis* isolates were different from those of *A. tenuissima* CBS 620.83 (ex-epitype) (beakless vs. with a narrow-taper beak) (Wiltshire 1933). In conclusion, the phylogenetic and morphological evidence support this fungus as being a new species within the *Alternaria alternata* species complex.

Alternaria hunanensis Lin Huang, Jiao He & D.W. Li, sp. nov.
Index Fungorum: IF901038
Fig. 5

Holotype. Chɪɴᴀ, Hunan Province, Yiyang City, Longqiao Town, 28°27'24"N, 112°29'7"E, isolated from leaf spots of *Cunninghamia lanceolata*, May 2017, Wen-Li Cui, (holotype: CFCC 59356). Holotype specimen is a living specimen being maintained via lyophilisation at the China Forestry Culture Collection Center (CFCC). Ex-type (HN43-10-2) is maintained at the Forest Pathology Laboratory, Nanjing Forestry University.

Etymology. Epithet is after Longqiao Town, Yiyang City, Hunan Province where the type specimen was collected.

Host/distribution. From *C. lanceolata* in Longqiao Town, Yiyang City, Hunan Province, China.

Description. Mycelium superficial on the PCA medium, composed of septate, branched, smooth, thin-walled, white to light brown hyphae. Conidiophores macronematous, mononematous, solitary, subcylindrical, branched or unbranched, straight or geniculate, (12.7−)18.4−41.8(−65.0) × (2.5−)3.3−4.7(−5.2) μm, (mean ± SD = 30.1 ± 11.7 × 4.0 ± 0.7 μm, n = 45). Each conidiogenous locus bears a primary chain of 3−7 conidia; each chain usually has a secondary chain of 1−2 conidia. Conidiogenous cells apical or subapical, cylindrical, light brown, smooth, (2.9−)4.6−9.5(−13.6) × (1.8−)3.0−4.5(−6.3) μm, (mean ± SD = 7.0 ± 2.5 × 3.8 ± 0.8 μm, n = 46), mono- or polytretic. Newly developed conidia subhyaline or pale greyish, ellipsoidal or subacute, thin-walled, with few or no protuberance. Mature conidia pale brown to brown, ovoid or ellipsoid to long-ellipsoid, pyriform, usually smooth. Conidial bodies (10.0−)16.7−28.8(−39.3) × (5.9−)8.2−12.6(−14.8) μm, (mean ± SD = 22.7 ± 6.0 × 10.4 ± 2.2 μm, n = 49), with 1−4 transverse and 0−2 longitudinal septa. Secondary conidia commonly produced by means of a short apical or lateral secondary conidiophore, but rarely by conidia through an inconspicuous apical conidiogenous locus. Secondary conidiophores (false beaks) at the apical end and median of conidium,
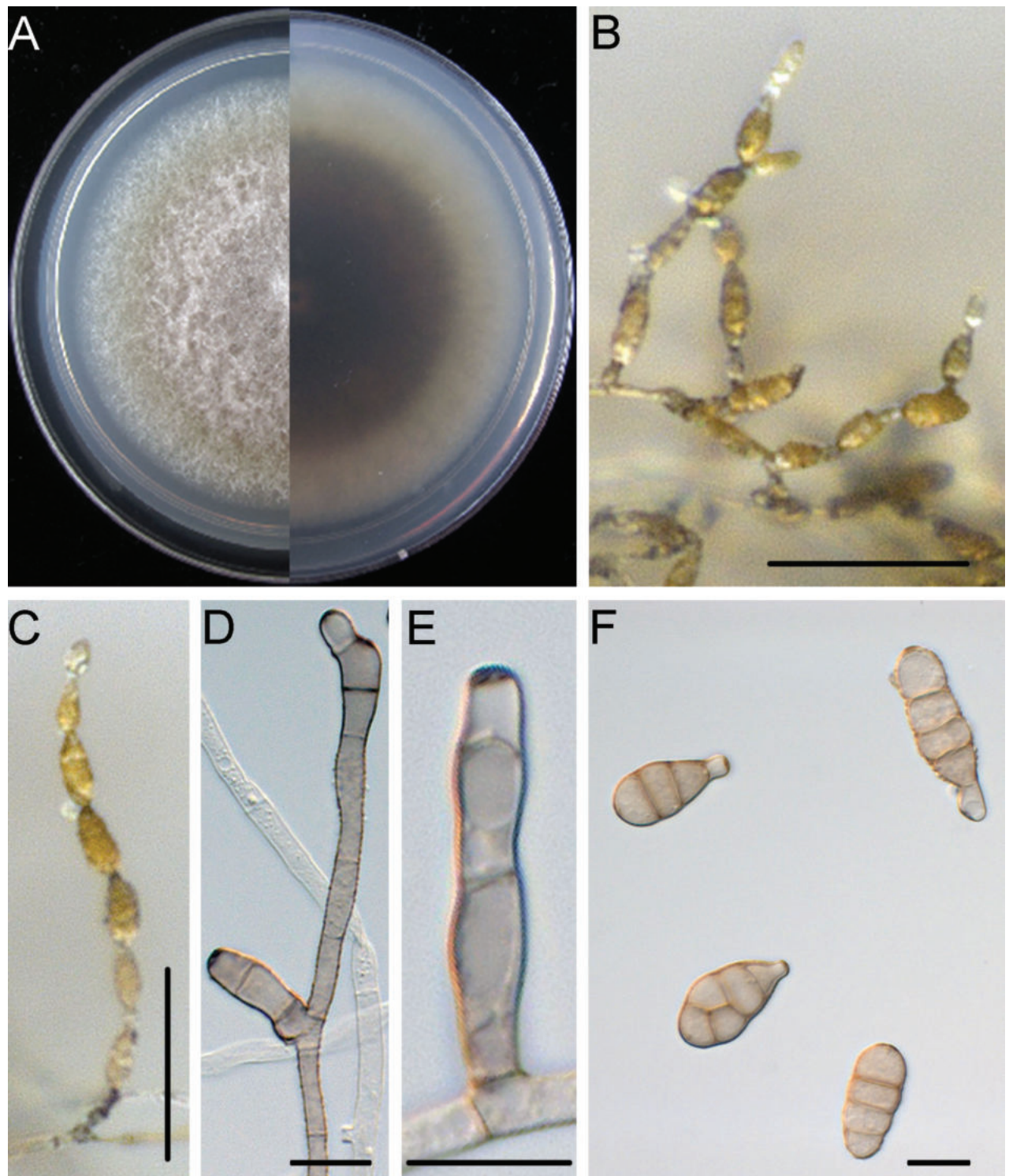
Figure 5. *Alternaria hunanensis* (HN43-10-2) **A** colony on PCA after 6 days at 25 °C in the dark **B, C** sporulation patterns **D, E** conidiophores and conidiogenous cells **F** conidia. Scale bars: 50 μm (**B, C**); 10 μm (**D–F**).

short, mostly single-celled, (2.8−)2.9−21.7(−41.7) × (2.5−)2.8−4.3(−6.2) μm, (mean ± SD = 12.3 ± 9.4 × 3.5 ± 0.7 μm, n = 37). Conidial beakless mostly with a conical cell at the apex. Chlamydospores not observed.

Culture characteristics. Colonies on PCA incubated at 25 °C in the dark growing at 7.8 ± 0.1 mm/d; aerial hypha cottony, pale gray to greyish-green,

with white to pale grey margins; reverse centre brownish to dark green with pale grey margins; sporulation sparse; diffusible pigment absent.

Additional materials examined. CHINA, Hunan Province, Yiyang City, Longqiao Town, 28°27'24"N, 112°29'7"E, isolated from leaf spots of *Cunninghamia lanceolata*, May 2017, Wen-Li Cui, HN43-10-2-1, HN43-10-2-2, HN43-10-2-3, HN43-10-2-4.

Notes. The isolates of *A. hunanensis* were phylogenetically close to *A. longqiaoensis* (this study, HN43-14), *A. vaccinii* (ex-type, CBS 118818), *A. platycodonis* (ex-type, CBS 121348), *A. rhadina* E.G. Simmons (ex-type, CBS 595.93), *A. citriarbusti* (ex-type, CBS 102598) and *A. tomaticola* (ex-type, CBS 118814) (Fig. 2). Between *A. hunanensis* isolates and *A. longqiaoensis* HN43-14, there were 2/453 differences in Alt a1, 3/510 in ITS, 2/401 in endoPG, 2/757 in RPB2 and 18/996 in SSU. Between *A. hunanensis* isolates and *A. vaccinii* (ex-type, CBS 118818), there were 4/453 differences in Alt a1, 2/499 in GAPDH, 3/510 in ITS and 3/401 in endoPG. Between *A. hunanensis* isolates and *A. platycodonis* (ex-type, CBS 121348), there were 1/453 differences in Alt a1, 2/499 in GAP-DH, 3/510 in ITS and 2/401 in endoPG. Between *A. hunanensis* isolates and *A. rhadina* (ex-type, CBS 595.93), there were 1/453 differences in Alt a1, 2/499 in GAPDH, 3/510 in ITS and 2/401 in endoPG. Between *A. hunanensis* isolates and *A. citriarbusti* (ex-type, CBS 102598), there were 1/453 differences in Alt a1, 2/499 in GAPDH, 3/510 in ITS and 2/401 in endoPG. Between *A. hunanensis* isolates and *A. tomaticola* (ex-type, CBS 118814), there were 3/453 differences in Alt a1, 2/499 in GAPDH, 3/510 in ITS and 2/401 in endoPG. The PHI analysis showed that there was no significant recombination between *A. hunanensis* isolates and its related species (Φ_w = 0.3502) (Fig. 2B). Distinguishing characteristics of this new species and other morphologically related species of *Alternaria* spp. are shown in Table 2. Morphologically, sporulation patterns of the *A. hunanensis* isolates were different from those of *A. longqiaoensis* HN43-14 (one secondary chain of 1−2 conidia vs. 1−3 further branching chains (secondary, tertiary and quaternary chains) of 3−4 conidia). Conidia in chains of the *A. hunanensis* isolates were less than those of *A. vaccinii* CBS 118818 (ex-type) (3−7 vs. 8−10 conidia) (Simmons 2007), *A. platycodonis* CBS 121348 (ex-type) (3−7 vs. 8−10 conidia) (Zhang 2003), *A. rhadina* CBS 595.93 (ex-type) (3−7 vs. 9−15 conidia) (Simmons 1993) and *A. tomaticola* CBS 118814 (ex-type) (3−7 vs. 10−15 conidia) (Simmons 2007). Transverse septa of conidia of the *A. hunanensis* isolates were less than those of *A. citriarbusti* CBS 102598 (ex-type) (1−4 vs. 6−11 transverse septa) (Simmons 1999). Thus, the phylogenetic and morphological evidence supports this fungus as being a new species within the *Alternaria alternata* species complex.

Alternaria kunyuensis Lin Huang, Jiao He & D.W. Li, sp. nov.

Index Fungorum: IF901039
Fig. 6

Holotype. CHINA, Shandong Province, Yantai City, Kunyu Mountain, 37°15'22"N, 121°46'05"E, isolated from leaf spots of *Cunninghamia lanceolata*, May 2017, Wen-Li Cui, (holotype: CFCC 59355). Holotype specimen is a living specimen being maintained via lyophilisation at the China Forestry Culture Collection
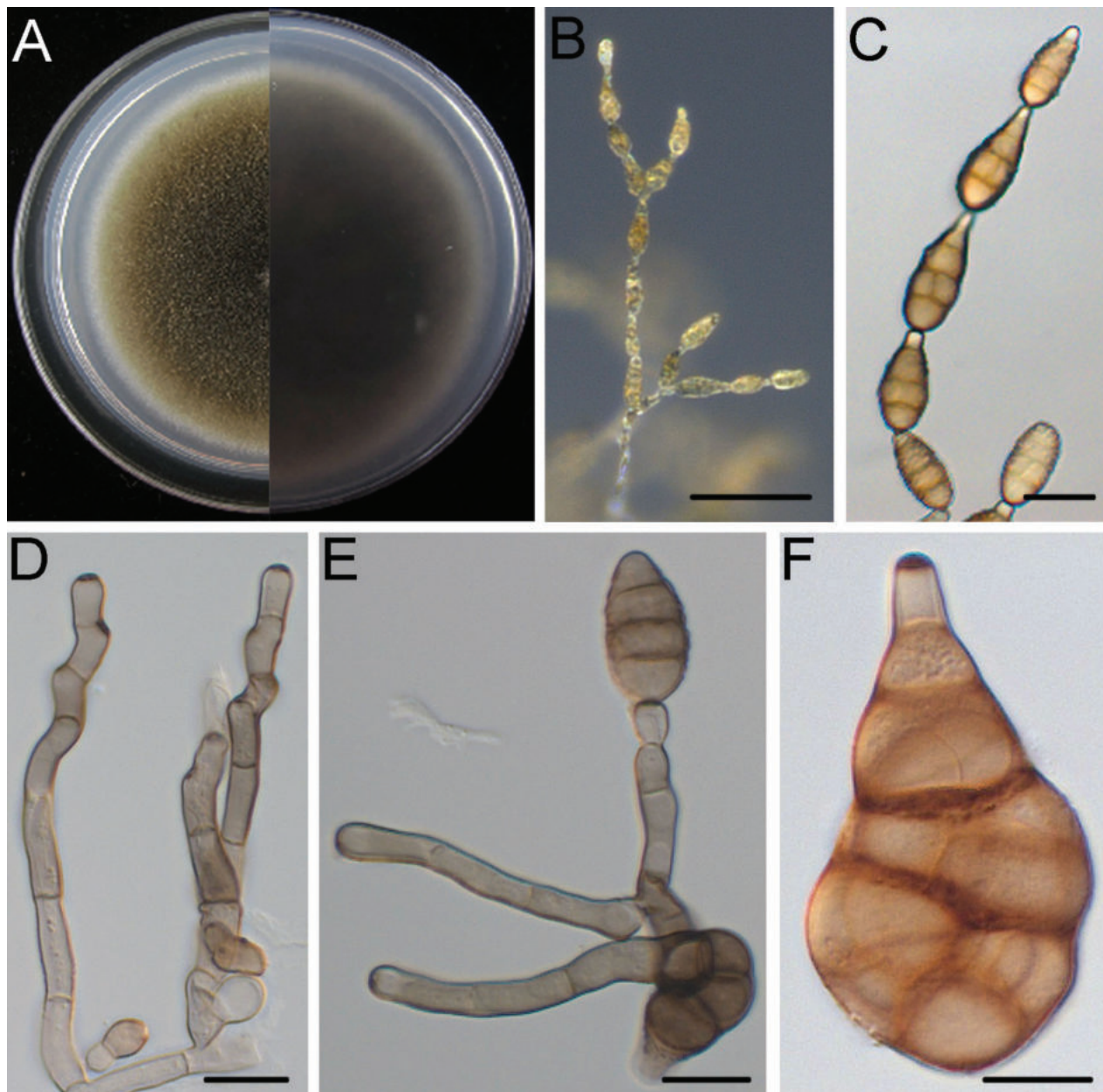
Figure 6. *Alternaria kunyuensis* (XXG21) **A** colony on PCA after 6 days at 25 °C in the dark **B, C** sporulation patterns **D** conidiophores bear conidiogenous cells **E** secondary conidiophores, conidiogenous cells and conidia **F** conidium. Scale bars: 50 μm (**B**); 10 μm (**C−F**).

Center (CFCC). Ex-type (XXG21) is maintained at the Forest Pathology Laboratory, Nanjing Forestry University.

Etymology. Epithet is after Kunyu Mountain, Yantai City, Shandong Province where the type specimen was collected.

Host/distribution. From *C. lanceolata* in Kunyu Mountain, Yantai City, Shandong Province, China.

Description. Mycelium superficial on the PCA medium, composed of septate, branched, smooth, thin-walled, colourless to pale brown hyphae. Conidiophores short to long, straight or geniculate, simple or branched, pale brown, 1−5 septate, with one or several apical conidiogenous loci, (17.0−)21.4−53.5(−79.2) × (3.0−)3.3−4.0(−4.6) μm, (mean ± SD = 37.4 ± 16.0 × 3.6 ± 0.4 μm, n = 33). Each

conidiogenous locus bears a primary chain of 3−8 conidia; each chain usually has one secondary chain of 2−4 conidia. Conidiogenous cells apical or subapical, cylindrical, light brown, smooth, (3.6−)5.2−11.1(−14.7) × (2.5−)3.2−4.2(−4.7) μm, (mean ± SD = 8.1 ± 2.9 × 3.7 ± 0.5 μm, n = 37), mono- or polytretic. Conidia ovoid to ellipsoid, pyriform, pale brown to brown, usually smooth; conidial bodies (16.1−)20.5−29.8(−36.3) × (7.7−)9.4−13.5(−15.8) μm, (mean ± SD = 25.1 ± 4.6 × 11.5 ± 2.0 μm, n = 43), 1−5 transverse and 0−3 longitudinal septate, slightly constricted at the median. Some septa darkened. Secondary conidia commonly produced via a short apical or lateral secondary conidiophore, but rarely by conidia through an inconspicuous apical conidiogenous locus. Secondary conidiophores (false beaks) at the apical end and median of conidium, short or long, multicellular or single cell, (2.9−)2.9−20.0(−37.3) × (2.3−)2.8−3.9(−4.6) μm, (mean ± SD = 11.5 ± 8.5 × 3.3 ± 0.6 μm, n = 33). Conidial beakless mostly with a conical cell at the apex. Chlamydospores not observed.

Culture characteristics. Colonies on PCA incubated at 25 °C in the dark growing at 7.5 ± 0.2 mm/d; aerial hypha sparse, olive green to dark green; reverse centre grey; sporulation abundant; diffusible pigment absent.

Additional materials examined. China, Shandong Province, Yantai City, Kunyu Mountain, 37°15'22"N, 121°46'05"E, isolated from leaf spots of *Cunninghamia lanceolata*, May 2017, Wen-Li Cui, XXG12-2, XXG22, XXG26-2, XXG30, XXG31.

Notes. The isolates of *A. kunyuensis* were phylogenetically close to *A. hunanensis* (this study, HN43-10-2), *A. longqiaoensis* (this study, HN43-14), *A. vaccinii* (ex-type, CBS 118818), *A. platycodonis* (ex-type, CBS 121348), *A. rhadina* (ex-type, CBS 595.93), *A. citriarbusti* (ex-type, CBS 102598) and *A. tomaticola* (ex-type, CBS 118814) (Fig. 2). Between *A. kunyuensis* isolates and *A. hunanensis* HN43-10-2, there were 2/453 differences in Alt a1, 1/510 in ITS, 1/664 in OPA10-2, 5/401 in endoPG, 4/757 in RPB2, 1/996 in SSU and 3/293 in TEF1. Between *A. kunyuensis* isolates and *A. longqiaoensis* HN43-14, there were 3/453 differences in Alt a1, 2/510 in ITS, 1/664 in OPA10-2, 3/401 in endoPG, 6/757 in RPB2, 19/996 in SSU and 3/293 in TEF1. Between *A. kunyuensis* isolates and *A. vaccinii* CBS 118818 (ex-type), there were 5/453 differences in Alt a1, 2/499 in GAPDH, 3/510 in ITS, 1/664 in OPA10-2, 4/401 in endoPG, 4/757 in RPB2, 1/996 in SSU and 3/293 in TEF1. Between *A. kunyuensis* isolates and *A. platycodonis* CBS 121348 (ex-type), there were 2/453 differences in Alt a1, 2/499 in GAPDH, 3/510 in ITS, 1/664 in OPA10-2, 3/401 in endoPG, 4/757 in RPB2, 1/996 in SSU and 3/293 in TEF1. Between *A. kunyuensis* isolates and *A. rhadina* CBS 595.93 (ex-type), there were 2/453 differences in Alt a1, 2/499 in GAPDH, 3/510 in ITS, 1/664 in OPA10-2, 3/401 in endoPG, 4/757 in RPB2, 1/996 in SSU and 3/293 in TEF1. Between *A. kunyuensis* isolates and *A. citriarbusti* CBS 102598 (ex-type), there were 2/453 differences in Alt a1, 3/510 in ITS, 1/664 in OPA10-2, 3/401 in endoPG, 4/757 in RPB2, 1/996 in SSU and 3/293 in TEF1. Between *A. kunyuensis* isolates and *A. tomaticola* CBS 118814 (ex-type), there were 4/453 differences in Alt a1, 3/510 in ITS, 1/664 in OPA10-2, 3/401 in endoPG, 4/757 in RPB2, 1/996 in SSU and 3/293 in TEF1. The PHI analysis showed that there was no significant recombination between *A. kunyuensis* isolates and its related species (Φ_w = 0.3502) (Fig. 2B). Distinguishing characteristics of this new species and other related species of *Alternaria* spp. are shown in Table 2. Morphologically, sporulation patterns of the *A. kunyuensis* isolates were different from those of *A. hunanensis* HN43-10-2 (one secondary

chain of 2−4 conidia vs. one secondary chain of 1−2 conidia.) and *A. longqiaoensis* HN43-14 (one secondary chain of 2−4 conidia vs. 1−3 branching chains of 3−4 conidia). Conidia in chains of the *A. kunyuensis* isolates were less than those of *A. vaccinii* CBS 118818 (ex-type) (3−8 conidia vs. 8−10 conidia) (Simmons 2007), *A. platycodonis* CBS 121348 (ex-type) (3−8 conidia vs. 8−10 conidia) (Zhang 2003) *A. rhadina* CBS 595.93 (ex-type) (3−8 conidia vs. 9−15 conidia) (Simmons 1993) and *A. tomaticola* CBS 118814 (ex-type) (3−8 conidia vs. 10−15 conidia) (Simmons 2007). Transverse septa of conidia of the *A. kunyuensis* isolates were less than those of *A. citriarbusti* CBS 102598 (ex-type) (1−5 transverse septa vs. 6−11 transverse septa) (Simmons 1999). Thus, the phylogenetic and morphological evidence supports this fungus being as a new species within the *Alternaria alternata* species complex.

Alternaria longqiaoensis Lin Huang, Jiao He & D.W. Li, sp. nov.

Index Fungorum: IF901040

Fig. 7

Holotype. CHINA, Hunan Province, Yiyang City, Longqiao Town, 28°27'24"N, 112°29'7"E, isolated from leaf spots of *Cunninghamia lanceolata*, May 2017, Wen-Li Cui, (holotype: CFCC 59357). Holotype specimen is a living specimen being maintained via lyophilisation at the China Forestry Culture Collection Center (CFCC). Ex-type (HN43-14) is maintained at the Forest Pathology Laboratory, Nanjing Forestry University.

Etymology. Epithet is after Longqiao Town, Yiyang City, Hunan Province where the type specimen was collected.

Host/distribution. from *C. lanceolata* in Longqiao Town, Yiyang City, Hunan Province, China.

Description. Mycelium superficial on the PCA medium, composed of septate, branched, smooth, thin-walled, pale brown to brown hyphae. Conidiophores macronematous, mononematous, solitary, subcylindrical, unbranched or barely branched, straight or geniculate, 2−4 septa, (4.7−) 19.6−51.0 (−66.3) × (2.9−)3.3−4.2(−4.8) μm, (mean ± SD = 35.3 ± 15.7 × 3.8 ± 0.5 μm, n = 39). Each conidiogenous locus bears a primary chain of 4−8 conidia; each chain usually has 1−3 secondary chains of 3−4 conidia. Conidiogenous cells apical or subapical, cylindrical, light brown, smooth, (2.8−)4.3−9.6(−17.4) × (2.3−)2.9−4.5(−5.8) μm, (mean ± SD = 7.0 ± 2.7 × 3.7 ± 0.8 μm, n = 45), mono- or polytretic. Conidia pale brown to brown, ovoid or ellipsoid to long-ellipsoid, pyriform, smooth or verruculose. Conidial bodies (11.0−)16.0−28.2(−40.2) × (6.1−)7.0−12.6(−20.8) μm, (mean ± SD = 22.1 ± 6.1 × 9.8 ± 2.8 μm, n = 48), with 1−5 transverse and 0−2 longitudinal septate. Secondary conidia commonly produced via a short lateral secondary conidiophore, but rarely by conidia through an inconspicuous apical conidiogenous locus. Apically or laterally formed secondary conidiophores (false beaks) with one or several conidiogenous loci, short, mostly single-celled, (3.5−)3.3−11.6(−19.7) × (2.8−)2.9−3.9(−4.8) μm, (mean ± SD = 7.5 ± 4.2 × 3.4 ± 0.5 μm, n = 33). Conidial beakless mostly with a conical cell at the apex. Chlamydospores not observed.

Culture characteristics. Colonies on PCA incubated at 25 °C in the dark growing at 8.3 ± 0.4 mm/d; aerial hypha cottony, dark green to black, with pale
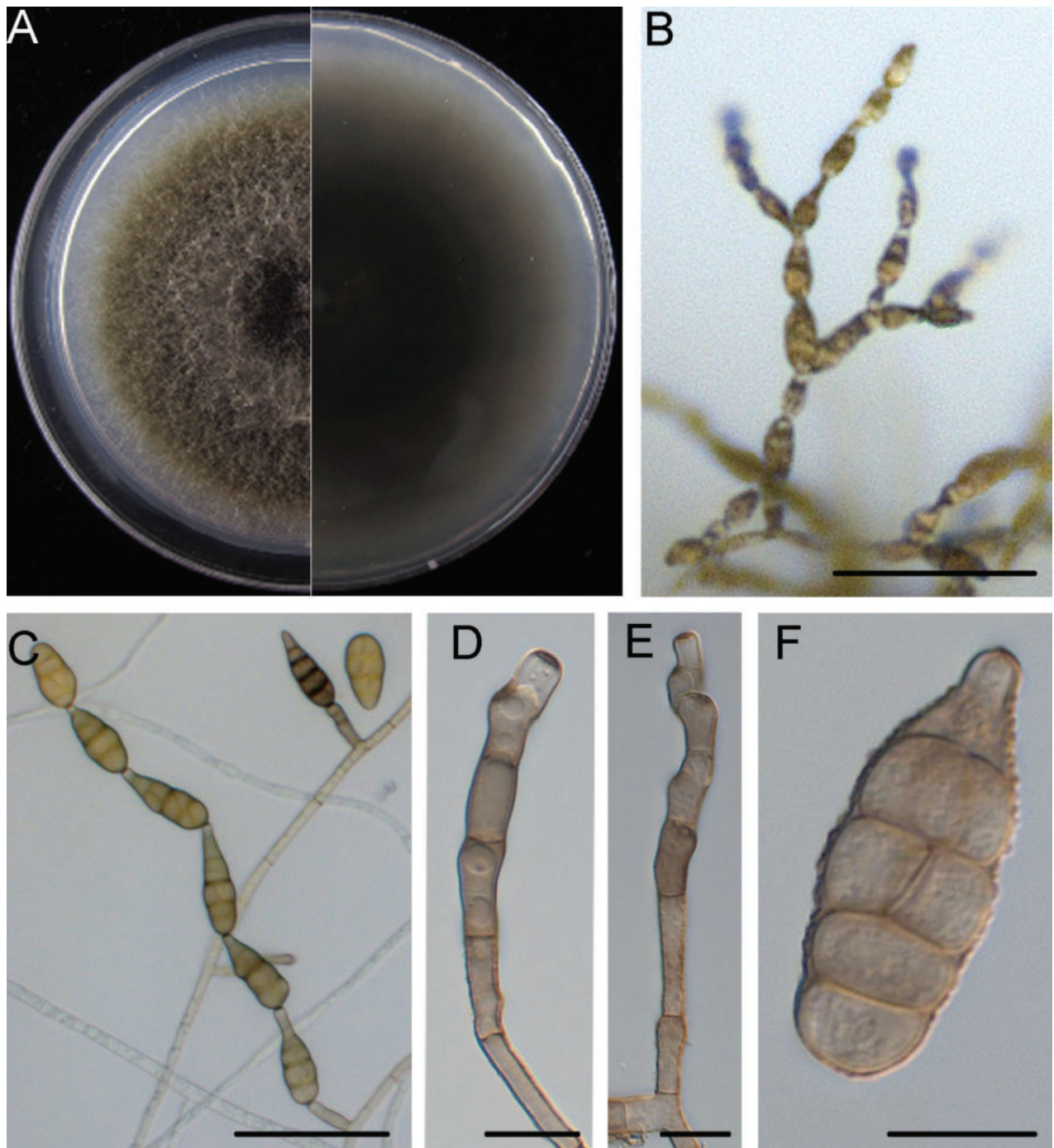
Figure 7. *Alternaria longqiaoensis* (HN43-14) **A** colony on PCA after 6 days at 25 °C in the dark **B, C** sporulation patterns **D, E** conidiophore and conidiogenous cells **F** conidium. Scale bars: 50 μm (**B, C**); 10 μm (**D–F**).

green margins; reverse centre black with pale grey margins; sporulation abundant; diffusible pigment absent.

Additional materials examined. CHINA, Hunan Province, Yiyang City, Longqiao Town, 28°27'24"N, 112°29'7"E, isolated from leaf spots of *Cunninghamia lanceolata*, May 2017, Wen-Li Cui, HN43-14-1, HN43-14-2, HN43-14-3.

Notes. The isolates of *A. longqiaoensis* were phylogenetically close to *A. vaccinii* (ex-type, CBS 118818), *A. platycodonis* (ex-type, CBS 121348), *A. rhadina* (ex-type, CBS 595.93), *A. citriarbusti* (ex-type, CBS 102598) and *A. tomaticola*

(ex-type, CBS 118814) (Fig. 2). Between *A. longqiaoensis* isolates and *A. vaccinii* CBS 118818 (ex-type), there were 4/453 differences in Alt a1, 2/499 in GAPDH, 4/510 in ITS, 1/401 in endoPG, 2/757 in RPB2 and 18/996 in SSU. Between *A. longqiaoensis* isolates and ex-type of *A. platycodonis* CBS 121348, there were 1/453 differences in Alt a1, 2/499 in GAPDH, 4/510 in ITS, 2/757 in RPB2 and 18/996 in SSU. Between *A. longqiaoensis* isolates and *A. rhadina* CBS 595.93 (ex-type), there were 1/453 differences in Alt a1, 2/499 in GAPDH, 4/510 in ITS, 2/757 in RPB2 and 18/996 in SSU. Between *A. longqiaoensis* isolates and *A. citriarbusti* CBS 102598 (ex-type), there were 1/453 differences in Alt a1, 4/510 in ITS, 2/757 in RPB2 and 18/996 in SSU. Between *A. longqiaoensis* isolates and *A. tomaticola* CBS 118814 (ex-type), there were 3/453 differences in Alt a1, 4/510 in ITS, 2/757 in RPB2 and 18/996 in SSU. The PHI analysis showed that there was no significant recombination between *A. longqiaoensis* isolates and its related species (Φ_w = 0.3502) (Fig. 2B). Distinguishing characteristics of this new species and other morphologically-related species of *Alternaria* spp. are shown in Table 2. Morphologically, conidia in chains of the *A. longqiaoensis* isolates were less than those of *A. vaccinii* CBS 118818 (ex-type) (4−8 conidia vs. 8−10 conidia) (Simmons 2007), *A. platycodonis* CBS 121348 (ex-type) (4−8 conidia vs. 8−10 conidia) (Zhang 2003) *A. rhadina* CBS 595.93 (ex-type) (4−8 conidia vs. 9−15 conidia) (Simmons 1993) and *A. tomaticola* CBS 118814 (ex-type) (4−8 conidia vs. 10−15 conidia) (Simmons 2007). Transverse septa of conidia of the *A. longqiaoensis* isolates were less than those of *A. citriarbusti* CBS 102598 (ex-type) (1−5 vs. 6−11 transverse septa) (Simmons 1999). Thus, the phylogenetic and morphological evidence supports this fungus as being a new species within the *Alternaria alternata* species complex.

Alternaria shandongensis Lin Huang, Jiao He & D.W. Li, sp. nov.
Index Fungorum: IF901041
Fig. 8

Holotype. CHINA, Shandong Province, Yantai City, Penglai District, Hougou village, 37°27'32"N, 120°46'48"E, isolated from leaf spots of *Cunninghamia lanceolata*, May 2017, Wen-Li Cui, (holotype: CFCC 59354). Holotype specimen is a living specimen being maintained via lyophilisation at the China Forestry Culture Collection Center (CFCC). Ex-type (SDHG12) is maintained at the Forest Pathology Laboratory, Nanjing Forestry University.

Etymology. Epithet is after Shandong Province where the type specimen was collected.

Host/distribution. From *C. lanceolata* in Hougou village, Penglai District, Yantai City, Shandong Province, China.

Description. Mycelium superficial on the PCA medium, composed of septate, branched, smooth, thin-walled, pale brown hyphae. Conidiophores solitary, emerging from aerial or creeping hyphae, straight or geniculate, simple or branched, with one or several apical conidiogenous loci, 1−5 septate, variable in length, (16.8−)23.6−51.1(−68.8) × (3.0−)3.4−4.3(−5.0) μm, (mean ± SD = 37.3 ± 13.8 × 3.8 ± 0.4 μm, n = 35). Each conidiogenous locus bears a primary chain of 9−13 conidia; each primary chain usually has 1−3 lateral branches (secondary chains) of 1−2 conidia. Conidiogenous cells apical or subapical,
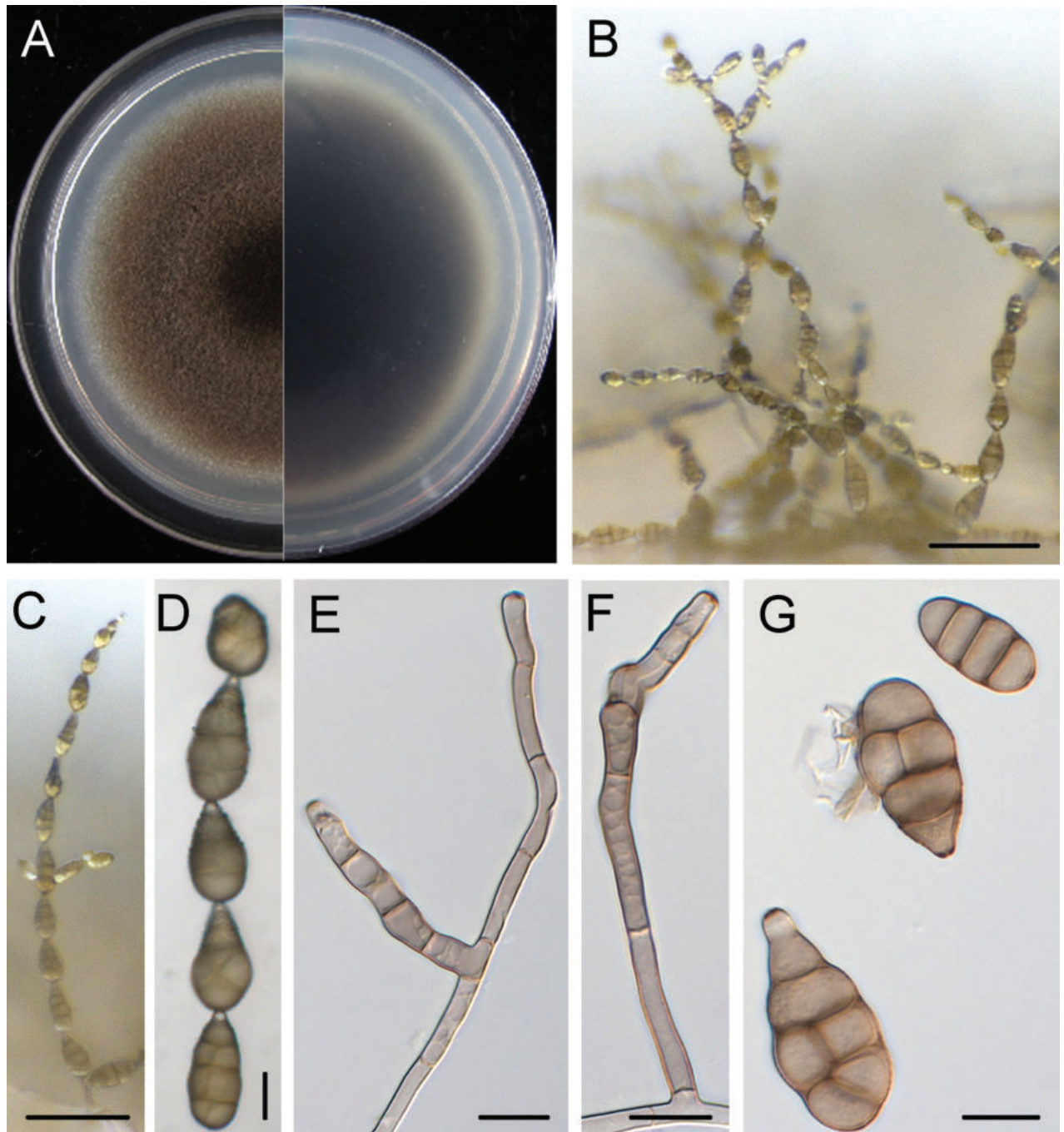
Figure 8. *Alternaria shandongensis* (SDHG12) **A** colony on PCA after 6 days at 25 °C in the dark **B–D** sporulation patterns **E, F** conidiophores and conidiogenous cells **G** conidia. Scale bars: 50 μm (**B, C**); 10 μm (**D–G**).

cylindrical, light brown, smooth, (3.9−)4.8−9.6(−17.3) × (2.5−)3.2−4.3(−4.8) μm, (mean ± SD = 7.2 ± 2.4 × 3.7 ± 0.6 μm, n = 46), mono- or polytretic. Conidial bodies ovoid to ellipsoid, brown to dark brown, (14.8−)20.1−31.2(−51.5) × (7.5−)9.3−14.1(−17.0) μm, (mean ± SD = 25.6 ± 5.6 × 11.7 ± 2.4 μm, n = 66), with 2−7 transverse and 0−3 longitudinal septa, mostly smooth to occasionally roughened. Secondary conidia commonly produced via a short lateral secondary conidiophore. Secondary conidiophores (false beaks) at the apical end and median of conidium, short, mostly single-celled, (2.9−)2.7−10.3(−23.5) μm × (2.0−)2.3−3.1(−3.7) μm, (mean ± SD = 6.5 ± 3.9 μm × 2.7 ± 0.4 μm,

n = 34). Conidial beakless mostly with a conical cell at the apex. Chlamydospores not observed.

Culture characteristics. Colonies on PCA incubated at 25 °C in the dark growing at 7.6 ± 0.7 mm/d; aerial hypha sparse, dark green to black; reverse centre grey, sporulation abundant; diffusible pigment absent.

Additional materials examined. China, Shandong Province, Yantai City, Penglai District, Hougou village, 37°27'32"N, 120°46'48"E, isolated from leaf spots of *Cunninghamia lanceolata*, May 2017, Wen-Li Cui, SDHG12-1, SDHG12-2, SDHG12-3, SDHG12-4; China, Fujian Province, Longyan City, Lianfeng Town, 25°09'27"N, 117°01'50"E, isolated from leaf spots of *C. lanceolata*, May 2017, Wen-Li Cui, LY15.

Notes. The isolates of *A. shandongensis* were phylogenetically close to *A. kunyuensis* (this study, XXG21), *A. hunanensis* (this study, HN43-10-2), *A. longqiaoensis* (this study, HN43-14), *A. vaccinii* (ex-type, CBS 118818), *A. platycodonis* (ex-type, CBS 121348), *A. rhadina* (ex-type, CBS 595.93), *A. citriarbusti* (ex-type, CBS 102598) and *A. tomaticola* (ex-type, CBS 118814) (Fig. 2). Between *A. shandongensis* isolates and *A. kunyuensis* XXG21, there were 1/453 differences in Alt a1, 2/499 in GAPDH, 1/664 in OPA10-2, 5/757 in RPB2, 1/996 in SSU and 3/293 in TEF1. Between *A. shandongensis* isolates and *A. hunanensis* HN43-10-2, there were 1/453 differences in Alt a1, 2/499 in GAPDH, 1/510 in ITS, 5/401 in endoPG and 1/757 in RPB2. Between *A. shandongensis* isolates and *A. longqiaoensis* HN43-14, there were 3/453 differences in Alt a1, 2/499 in GAPDH, 2/510 in ITS, 3/401 in endoPG, 1/757 in RPB2 and 18/996 in SSU. Between *A. shandongensis* isolates and *A. vaccinii* CBS 118818 (ex-type), there were 5/453 differences in Alt a1, 4/499 in GAPDH, 3/510 in ITS, 4/401 in endoPG and 1/757 in RPB2. Between *A. shandongensis* isolates and *A. platycodonis* CBS 121348 (ex-type), there were 2/453 differences in Alt a1, 4/499 in GAPDH, 3/510 in ITS, 3/401 in endoPG and 1/757 in RPB2. Between *A. shandongensis* isolates and *A. rhadina* CBS 595.93 (ex-type), there were 2/453 differences in Alt a1, 4/499 in GAPDH, 3/510 in ITS, 3/401 in endoPG and 1/757 in RPB2. Between *A. shandongensis* isolates and *A. citriarbusti* CBS 102598 (ex-type), there were 2/453 differences in Alt a1, 2/499 in GAPDH, 3/510 in ITS, 3/401 in endoPG and 1/757 in RPB2. Between *A. shandongensis* isolates and *A. tomaticola* CBS 118814 (ex-type), there were 4/453 differences in Alt a1, 2/499 in GAPDH, 3/510 in ITS, 3/401 in endoPG and 1/757 in RPB2. The PHI analysis showed that there was no significant recombination between *A. shandongensis* isolates and its related species (Φ_w = 0.3502) (Fig. 2B). Distinguishing characteristics of this new species and their related species of *Alternaria* are shown in Table 2. Morphologically, conidia in chains of the *A. shandongensis* isolates were more than those of *A. kunyuensis* XXG21 (9−13 conidia vs. 6−8 conidia), *A. hunanensis* HN43-10-2 (9−13 conidia vs. 3−7 conidia), *A. longqiaoensis* HN43-14 (9−13 conidia vs. 4−8 conidia), *A. citriarbusti* CBS 102598 (ex-type) (9−13 conidia vs. 5−8 conidia) (Simmons 1999) and *A. platycodonis* CBS 121348 (ex-type) (9−13 conidia vs. 8−10 conidia) (Zhang 2003). Conidiophores of the *A. shandongensis* isolates were significantly shorter than those of *A. vaccinii* CBS 118818 (ex-type) (23.6−51.1 × 3.4−4.3 μm vs. 100−200 × 3−4 μm) (Simmons 2007), *A. rhadina* CBS 595.93 (ex-type) (23.6−51.1 × 3.4−4.3 μm vs. 60−110 × 3−4 μm) (Simmons 1993), *A. citriarbusti* CBS 102598 (ex-type) (23.6−51.1 × 3.4−4.3 μm vs. 200 × 5 μm) (Simmons 1999) and *A. tomaticola* CBS 118814 (ex-type) (23.6−51.1 ×

3.4−4.3 μm vs. 50−80 × 3−5 μm) (Simmons 2007). In conclusion, the phylogenetic and morphological evidence supports this fungus as being a new species within the *Alternaria alternata* species complex.

Alternaria xinyangensis **Lin Huang, Jiao He & D.W. Li, sp. nov.**
Index Fungorum: IF901042
Fig. 9

Holotype. CHINA, Henan Province, Xinyang City, Zhenlei Mountain, 32°04'51"N, 114°07'23"E, isolated from leaf spots of *Cunninghamia lanceolata*, May 2017, Wen-Li Cui, (holotype: CFCC 59352). Holotype specimen is a living specimen being maintained via lyophilisation at the China Forestry Culture Collection Center (CFCC). Ex-type (ZLS1) is maintained at the Forest Pathology Laboratory, Nanjing Forestry University.

Etymology. Epithet is after Xinyang City where the type specimen was collected.

Host/distribution. From *C. lanceolata* in Zhenlei Mountain, Xinyang City, Henan Province, China.

Description. Mycelium superficial on the PCA, composed of septate, branched, smooth, thin-walled, white to light brown hyphae. Conidiophores macronematous, mononematous, produced laterally or terminally on the hyphae, cylindrical, erect or ascending, simple or branched, geniculate, pale brown to dark brown, smooth, 1−7 septate, (9.4−)15.3−54.9(−80.4) × (2.9−)3.7−4.8(−5.2) μm, (mean ± SD = 35.1 ± 19.8 × 4.2 ± 0.6 μm, n = 40). Conidiogenous cells apical or subapical, cylindrical, brown, smooth, (3.9−)5.3−9.6(−12.9) × (2.4−)3.3−4.9(−5.5) μm, (mean ± SD = 7.5 ± 2.2 × 4.1 ± 0.8 μm, n = 39), mono- or polytretic, with conspicuous scars after conidia have seceded. Each conidiogenous locus bears a primary chain of 2−7 conidia; each primary chain usually has 1−3 branching chains of 1−3 conidia. Newly-developed conidia subhyaline or pale greyish, ellipsoidal or subacute, thin-walled, 1−3 septate, with few or no protuberance. Mature conidia brown to dark chocolate−brown, spheroidal or ellipsoid to long-ellipsoid, with 1−6 transverse septa and 1−5 longitudinal or oblique septa, (13.8−)19.9−31.8(−37.6) × (6.9−)8.6−12.9(−17.5) μm, (mean ± SD = 25.9 ± 6.0 × 10.7 ± 2.1 μm, n = 37) in size. Secondary conidia commonly produced by means of a short apical or lateral secondary conidiophore, but rarely by conidia through an inconspicuous apical conidiogenous locus. In addition, false beaks (secondary conidiophores), unbranched, short, blunted, pale brown, (3.0−)5.3−16.0(−24.4) × (2.4−)2.8−4.1(−5.1) μm, (mean ± SD = 10.6 ± 5.4 × 3.4 ± 0.7 μm, n = 31). Conidial beakless mostly with a conical cell at the apex. Chlamydospores not observed.

Culture characteristics. Colonies on PCA incubated at 25 °C in the dark growing at 7.2 mm/d; aerial hyphae cottony, olive green, with white margins; reverse centre black to greyish; sporulation abundant; diffusible pigment absent.

Additional materials examined. CHINA, Henan Province, Xinyang City, Zhenlei Mountain, 32°04'51"N, 114°07'23"E, isolated from leaf spots of *Cunninghamia lanceolata*, May 2017, Wen-Li Cui, ZLS1-1, ZLS1-2, ZLS1-3, ZLS1-4; CHINA, Henan Province, Xinyang City, Xinyang University, 32°08'20"N, 114°02'06"E, isolated from leaf spots of *C. lanceolata*, May 2017, Wen-Li Cui, XYXY06, XYXY8-2, XYXY15, XYXY15-1, XYXY15-2, XYXY15-3, XYXY15-4, XYXY16.
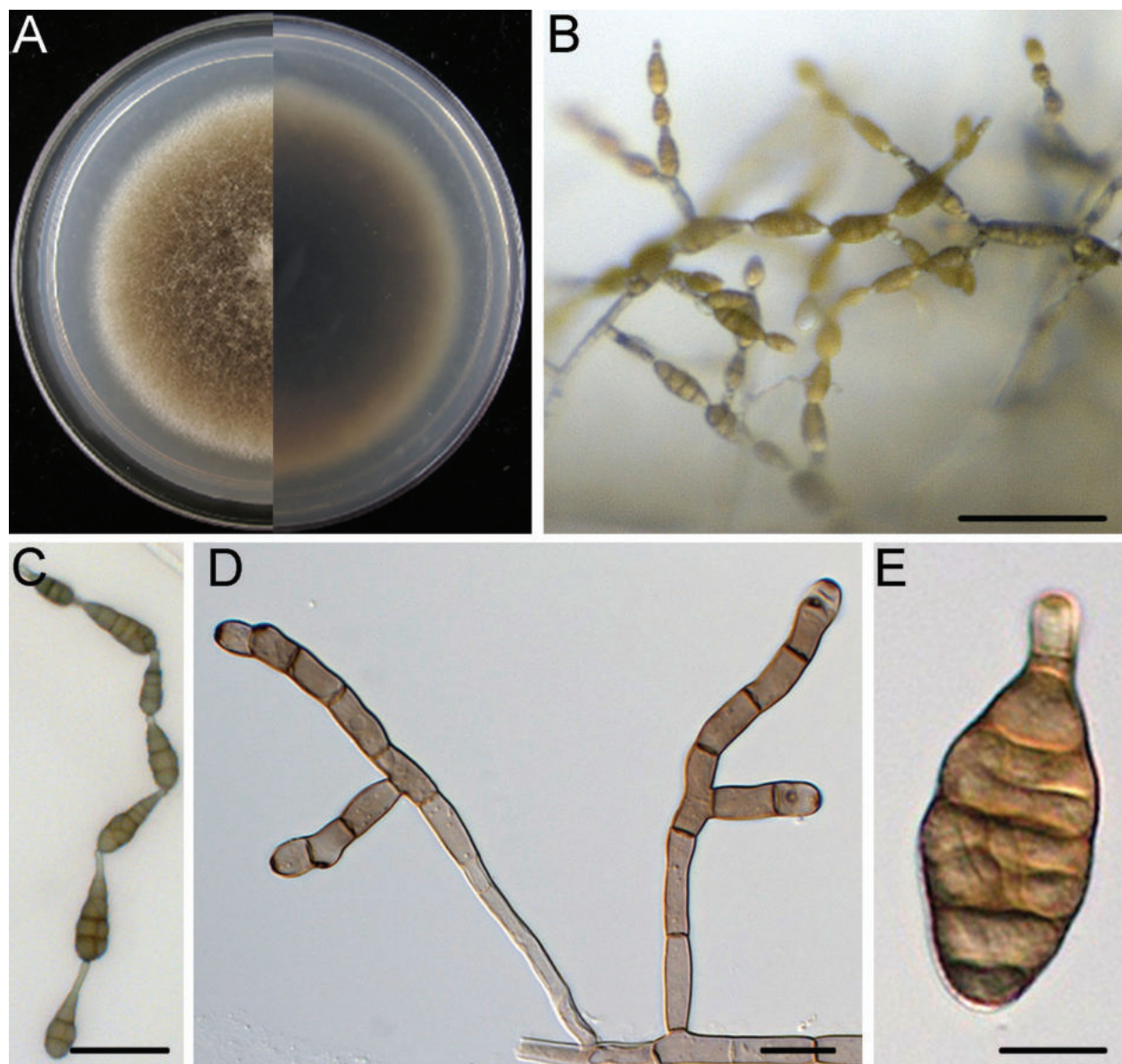
Figure 9. *Alternaria xinyangensis* (ZLS1) **A** colony on PCA after 6 days at 25 °C in the dark **B, C** sporulation patterns **D** conidiophores and conidiogenouse cells **E** conidium. Scale bars: 50 μm (**B, C**);10 μm (**D, E**).

Notes. The isolates of *A. xinyangensis* were phylogenetically close to *A. dongshanqiaoensis* (in this study, DSQ2-2), *A. citri* (ex-epitype, CBS 107.27), *A. cinerariae* (ex-epitype, CBS 612.72) and *A. kikuchiana* (ex-type, CBS 107.53) (Fig. 1). Between *A. xinyangensis* isolates and *A. dongshanqiaoensis* DSQ2-2, there were 1/453 differences in Alt a1, 1/510 in ITS, 8/664 in OPA10-2, 1/401 in endoPG, 1/757 in RPB2, 1/996 in SSU and 3/293 in TEF1. Between *A. xinyangensis* isolates and *A. citri* (ex-epitype, CBS 107.27), there were 1/453 differences in Alt a1, 3/510 in ITS, 8/664 in OPA10-2, 1/401 in endoPG, 1/996 in SSU and 3/293 in TEF1. Between *A. xinyangensis* isolates and *A. cinerariae* (ex-epitype, CBS 612.72), there were 1/453 differences in Alt a1, 3/510 in ITS, 8/664 in OPA10-2, 1/401 in endoPG, 1/996 in SSU and 3/293 in TEF1. Between *A. xinyangensis* isolates and *A. kikuchiana* (ex-type, CBS 107.53), there were 3/453 differences in Alt a1, 3/510 in ITS, 2/401 in endoPG, 1/757 in RPB2, 1/996 in

SSU and 3/293 in TEF1. The PHI analysis showed that there was no significant recombination between *A. xinyangensis* isolates and their related species (Φ_w = 0.1647) (Fig. 2A). Distinguishing characteristics of this new species and other similar species of *Alternaria* spp. are shown in Table 2. Morphologically, conidial number in chains of the *A. xinyangensis* isolates were less than those of *A. dongshanqiaoensis* DSQ2-2 (2−7 conidia vs. 5−9 conidia). Conidia of the *A. xinyangensis* isolates were smaller than those of *A. citri* CBS 107.27 (ex-epitype) (19.9−31.8 × 8.6−12.9 μm vs. 25−40 × 15−25 μm) (Pierce 1902). Secondary conidiophores of the *A. xinyangensis* isolates were significantly shorter than those of *A. cinerariae* CBS 612.72 (ex-epitype) (5.3−16.0 × 2.8−4.1 μm vs. 80−159 × 5−9 μm) (Nishikawa and Nakashima 2020). Conidia in chains of the *A. xinyangensis* isolates were less than those of *A. kikuchiana* CBS 107.53 (ex-type) (2−7 conidia vs. 6−9 conidia) (Nishikawa and Nakashima 2019). In conclusion, the phylogenetic and morphological evidence supports this fungus as being a new species within the *Alternaria alternata* species complex.

Pathogenicity assays

Pathogenicity was tested on detached Chinese fir leaves *in vitro* following Koch's postulates for *A. xinyangensis* (ZLS1), *A. kunyuensis* (XXG21), *A. cunninghamiicola* (DSQ3-2), *A. dongshanqiaoensis* (DSQ2-2), *A. longqiaoensis* (HN43-14), *A. shandongensis* (SDHG12) and *A. hunanensis* (HN43-10-2). At five days' post-inoculation, all the tested isolates caused leaf necrosis, with dark brown lesions. The control group remained symptom-less (Fig. 10A). After statistical analysis, these strains showed different levels of virulence. The virulence of
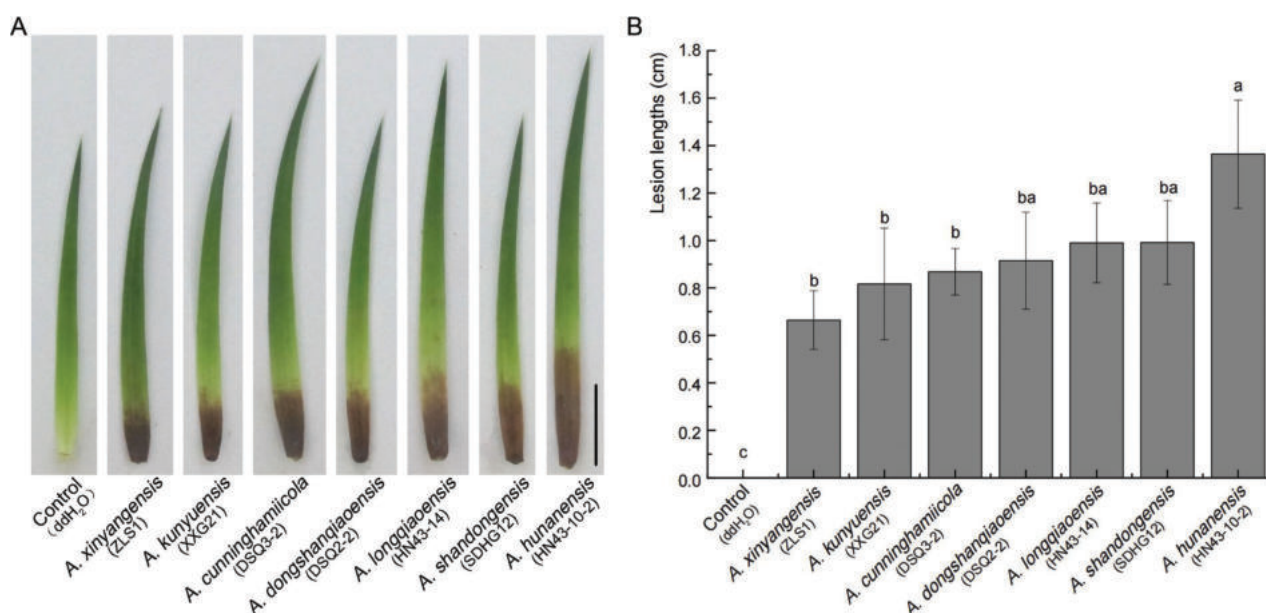

Figure 10. Symptoms on detached Chinese fir leaves **A** inoculated with isolates: *A. xinyangensis* (ZLS1), *A. kunyuensis* (XXG21), *A. cunninghamiicola* (DSQ3-2), *A. dongshanqiaoensis* (DSQ2-2), *A. longqiaoensis* (HN43-14), *A. shandongensis* (SDHG12) and *A. hunanensis* (HN43-10-2) **B** lesion length on detached Chinese fir leaves inoculated with *A. xinyangensis* (ZLS1), *A. kunyuensis* (XXG21), *A. cunninghamiicola* (DSQ3-2), *A. dongshanqiaoensis* (DSQ2-2), *A. longqiaoensis* (HN43-14), *A. shandongensis* (SDHG12) and *A. hunanensis* (HN43-10-2). Error bars represent standard error and different letters indicate significant difference, based on LSD's range test at $P < 0.05$ (n = 12). Scale bar: 10 mm (**A**).

A. hunanensis (HN43-10-2) was the strongest in all the *Alternaria* species studied, and its pathogenicity was significantly higher than those of *A. xinyangensis* (ZLS1), *A. kunyuensis* (XXG21) and *A. cunninghamiicola* (DSQ3-2) (P < 0.05), respectively, while there was no significant difference in pathogenicity amongst *A. xinyangensis* (ZLS1), *A. dongshanqiaoensis* (DSQ2-2), *A. shandongensis* (SDHG12), *A. kunyuensis* (XXG21), *A. longqiaoensis* (HN43-14) and *A. cunninghamiicola* (DSQ3-2) (P ≥ 0.05) (Fig. 10B).

The inoculated fungal isolates were re-isolated from the diseased spots on the inoculated leaves, but no fungus was isolated from the control leaves. Therefore, Koch's postulates were satisfied and these isolates ZLS1, XXG21, DSQ3-2, DSQ2-2, HN43-14, SDHG12 and HN43-10-2 were determined to be the pathogens of leaf blight on *C. lanceolata*.

Discussion

This study represents the first reports of leaf blight disease of Chinese fir in China caused by *Alternaria* spp. Phylogenetic analyses of the combined polylocus data set and morphological study showed that the 48 isolates obtained in this study grouped within Section *Alternaria*. It is surprising that the diversity of *Alternaria* species was so abundant in Chinese fir. It includes seven new species: *Alternaria cunninghamiicola* sp. nov., *A. dongshanqiaoensis* sp. nov., *A. hunanensis* sp. nov., *A. kunyuensis* sp. nov., *A. longqiaoensis* sp. nov., *A. shandongensis* sp. nov. and *A. xinyangensis* sp. nov. The detached leaves of Chinese fir were selected for pathogenicity tests that confirmed the potential virulence. To our knowledge, it is the first comprehensive study on *Alternaria* species causing leaf blight disease on Chinese fir including diversity and pathogenicity of the pathogens.

Morphology was not the main means of identification, as *Alternaria* isolates could differ morphologically due to the different cultivating conditions and the overlap in the spore sizes of some species (Rahimloo and Ghosta 2015). Armitage et al. (2015) reported that the morphological characteristics used to delineate species in *Alternaria* sect. *Alternata* are phenotypically similar and may vary amongst many morpho-species. These characteristics may be deceptive in the identification of these small-spored *Alternaria* species and would require stringent identification via phylogenetic studies (Kgatle et al. 2018). In this study, the single-locus phylogenies showed unclear resolution because of the limited number of informative sites per locus. For example, the SSU distinguishes *A. longqiaoensis* effectively with other species, but there is little resolution to distinguish between other species. The TEF1 gene could be informative for *A. xinyangensis*, *A. shandongensis*, and *A. kunyuensis* but not for *A. cunninghamiicola*, *A. dongshanqiaoensis*, *A. longqiaoensis* and *A. hunanensis*. In addition, it is also noted that the ITS region is a good phylogenetic marker, which could be informative for these isolates in this study, while LSU gene for distinguishing these isolates has a little effect. Perhaps these loci evolve at various rates and have different effective ways of evolution at several phylogenetic scales. For instance, Lawrence et al. (2013) reported that TEF1 and RPB2 are slow-evolving genes used to resolve early divergences in *Alternaria*, while Alt a1 is fast-evolving and can be used to infer evolutionary relationships at lower phylogenetic scales (Aung et al. 2020). Combined analyses of all nine loci are, thus, the major approach to identify *Alternaria* species.

A previous multi-locus phylogenetic study Woudenberg et al. (2013) established the taxonomic conclusions of morpho-species known under *A. alternata* based on the multi-locus phylogenetic analysis. Subsequently, Woudenberg et al. (2015) used the same analysis to determine the discrete lineages of *Alternaria* spp. in section *Alternaria*, which showed a 97−98% genomic similarity, concluding that species, such as *A. angustiovoide*, *A. citri*, *A. lini*, *A. mali* (CBS 106.24), *A. malvae* and *A. tenuissima* (CBS 918.96) did not make discrete groupings, but all are synonymous with *A. alternata* sensu stricto. Although Woudenberg et al. (2015) assigned 35 morpho-species as synonyms of *Alternaria alternata*, their affinities are still unclear due to inconsistencies, lack of morphological details and a comparison of single nucleotide polymorphisms. However, further studies, based on combined multi-locus phylogeny, showed that recent *A. alternata* species may not constitute a monophyletic group in DNA sequence-based phylogenies (Li et al. 2023). Morphological characters and phylogenetic analyses of the nine loci showed all 48 *Alternaria* isolates clustered in the Sect. *Alternata* in the phylogenetic tree and divide into seven distinct clusters in the current study. We compared these strains, based on morphology and phylogeny. Interestingly, our phylogenetic analyses show that the morpho-species of *A. alternata* can be separated into different clades and our novel taxa from Chinese fir are both morphologically and phylogenetically distinct from the *A. alternata* complex and other species in *Alternaria* sect. *Alternaria*. Herein, based on these most recent classifications, these isolates from Chinese fir in this study are, thus, identified as the *A. alternata* complex including *A. cunninghamiicola*, *A. dongshanqiaoensis*, *A. hunanensis*, *A. kunyuensis*, *A. longqiaoensis*, *A. shandongensis* and *A. xinyangensis*.

The results of pathogenicity tests indicate that the seven new *Alternaria* species were pathogenic to Chinese fir. *Alternaria hunanensis* exhibited the strongest virulence in the *Alternaria* species from the present study, and *A. xinyangensis*, *A. kunyuensis* and *A. cunninghamiicola* with weaker virulence especially in shoots of Chinese fir. Nevertheless, compared with our previous study, *Alternaria* species showing weaker virulence than those of *Colletotrichum* spp. (He et al. 2022) and *Fusarium* spp. (unpublished) and the results may explain why most of *Alternaria* species are facultative parasites and their pathogenicities are not too strong. *Alternaria* spp. may prefer to be saprobes or secondary pathogens growing in senescent, near-dead or dead plant tissues. The diseases caused by these pathogens often attack senescent and diseased leaves before crop maturity or when the growth of the hosts is poor. In addition, according to previous studies, some *Alternaria* taxa carry out facultative parasitism life cycles mainly depending on the following three aspects: damaging the cell walls of their hosts by mechanical penetration and the degrading enzymes, producing mycotoxins that target the cytoplasmic membrane, mitochondria, chloroplast and influencing the activity of enzymes related metabolisms, and mediating pathogenicity through signal transduction (Thomma 2003; Kang et al. 2013). At present, there are few studies on the pathogenic mechanism of *Alternaria* species, without revealing the specific process of host infection. Therefore, the thorough study of its pathogenic mechanism is the basis and key to solving the damage from *Alternaria*.

Until now, over 360 species of *Alternaria* are reported as plant pathogens and saprobes, resulting in the decline of forest quality and fruit decay during

storage and resulting in huge economic losses (Wijayawardene et al. 2020; Li et al. 2023). For example, *A. citri* caused orange brown spot disease (Peever et al. 2004); *A. yali-inficiens* caused black spots of Japanese pear (Roberts 2005); *A. alternata*, *A. longipes* (Ellis & Everh.) E.W. Mason and *A. yali-inficiens* caused tobacco brown spots (Wang et al. 2018); *A. malicola* caused fruit spot on apple in China (Dang et al. 2018); *A. yunnanensis* Z.Y. Cai, X.Y. Liu, Y.X. Liu & Y.P. Shi caused foliage spots of rubber tree in China (Cai et al. 2019); *A. koreana* O. Hassan, B.B.N.D. Romain, J.S. Kim & T. Chang caused leaf spots of ovate-leaf *Atractylodes* in South Korea (Romain et al. 2022) and *A. capsicicola* Nasehi, Kadir & Abed-Asht. [nom. inval., Art. F.5.1 (Shenzhen)] caused leaf spots of pepper in Malaysia (Nasehi et al. 2014). Surprisingly, *A. alternata* had been considered as a saprobic fungus and to be nonpathogenic on Chinese cabbage (*Brassica rapa* L. pekinensis group) (Liu and Ke 1992; Zhang et al. 1998). However, *A. alternata* had been confirmed to be pathogenic on Chinese cabbage (Shi et al. 2021). In addition, many recent studies reported various diseases caused by *Alternaria* species. For example, Xiang et al. (2023) reported the black spots caused by *A. alternata* on persimmon fruit in China. Yan et al. (2023) identified *A. tenuissima* causing leaf spots on *Lonicera caerulea* L. in Heilongjiang Province, China. Zhou et al. (2023) characterised *A. alstroemeriae* E.G. Simmons & C.F. Hill, a causal agent of grey spots on tobacco in China. Dantes et al. (2022) discovered *A. cinerariae* causing leaf blight on *Farfugium japonicum* (L.) Kitam. in South Carolina, USA. To our knowledge, however, so far, there is no detailed record that *Alternaria* spp. have been identified as pathogens on Chinese fir, except *Alternaria* sp. reported by Anonymous (1976).

In summary, our study provides the first systematic and polyphasic study from morphological, molecular and pathogenicity aspects to study *Alternaria* spp. associated with Chinese fir and reports seven novel species, *A. cunninghamiicola*, *A. dongshanqiaoensis*, *A. hunanensis*, *A. kunyuensis*, *A. longqiaoensis*, *A. shandongensis* and *A. xinyangensis* causing leaf blight on Chinese fir. However, more studies are necessary on these new taxa in order to elucidate their host range, specificity, mechanism of infection, and global distribution, as well as their potential impact on the Chinese fir industry.

Additional information

Conflict of interest

The authors have declared that no competing interests exist.

Ethical statement

No ethical statement was reported.

Funding

Author contributions

LH designed research. WLC collected samples. JH and WLC isolated cultures and performed DNA isolation and PCR amplification. JH conducted the pathogenicity test and morphological analysis, and wrote the original draft. DWL and LH reviewed and edited the draft. All authors read and approved the final manuscript.

Author ORCIDs

Jiao He ⓘ https://orcid.org/0000-0002-4146-2223
De-Wei Li ⓘ https://orcid.org/0000-0002-2788-7938
Wen-Li Cui ⓘ https://orcid.org/0009-0005-7515-7672
Lin Huang ⓘ https://orcid.org/0000-0001-7536-0914

Data availability

All of the data that support the findings of this study are available in the main text or Supplementary Information.

References

Andrew M, Peever TL, Pryor BM (2009) An expanded multilocus phylogeny does not resolve morphological species within the small-spored *Alternaria* species complex. Mycologia 101(1): 95–109. https://doi.org/10.3852/08-135

Anonymous (1976) Preliminary study on anthracnose and red blight of *Cunninghamia lanceolata* 杉木炭疽病和赤枯病初步研究. Hunan Forestry Science and Technology 湖南林业科技 06: 9–11.

Armitage A, Barbara D, Harrison R, Lane C, Sreenivasaprasad S, Woodhall J, Clarkson J (2015) Discrete lineages within *Alternaria alternata* species group: Identification using new highly variable loci and support from morphological characters. Fungal Biology 119(11): 994–1006. https://doi.org/10.1016/j.funbio.2015.06.012

Aung SLL, Liu HF, Pei DF, Lu BB, Oo MM, Deng JX (2020) Morphology and molecular characterization of a fungus from the *Alternaria alternata* species complex causing black spots on *Pyrus sinkiangensis* (Koerle pear). Mycobiology 48(3): 233–239. https://doi.org/10.1080/12298093.2020.1745476

Berbee ML, Pirseyedi M, Hubbard S (1999) *Cochliobolus* phylogenetics and the origin of known, highly virulent pathogens, inferred from ITS and glyceraldehyde-3-phosphate dehydrogenase gene sequences. Mycologia 91(6): 964–977. https://doi.org/10.1080/00275514.1999.12061106

Bigelow PDM (2003) Molecular characterization of *Embellisia* and *Nimbya* species and their relationship to *Alternaria*, *Ulocladium* and *Stemphylium*. Mycologia 95(6): 1141–1154. https://doi.org/10.1080/15572536.2004.11833024

Cai ZY, Liu YX, Shi YP, Dai LM, Li LL, Mu HJ, Lv ML, Liu XY (2019) *Alternaria yunnanensis* sp. nov., a new *Alternaria* species causing foliage spot of rubber tree in China. Mycobiology 47(1): 66–75. https://doi.org/10.1080/12298093.2019.1575584

Chen MM (2002) Forest Fungi Phytogeography: Forest Fungi Phytogeography of China, North America, and Siberia and International Quarantine of Tree Pathogens. Pacific Mushroom Research and Education Center, Sacramento, 469 pp.

Chen YJ, Meng Q, Zeng L, Tong HR (2018) Phylogenetic and morphological characteristics of *Alternaria alternata* causing leaf spot disease on *Camellia sinensis* in China. Australasian Plant Pathology 47(3): 335–342. https://doi.org/10.1007/s13313-018-0561-0

Chou HH, Wu WS (2002) Phylogenetic analysis of internal transcribed spacer regions of the genus *Alternaria*, and the significance of filament-beaked conidia. Mycological Research 106(2): 164–169. https://doi.org/10.1017/S0953756201005317

Crous PW, Schoch CL, Hyde KD, Wood AR, Gueidan C, de Hoog GS, Groenewald JZ (2009a) Phylogenetic lineages in the *Capnodiales*. Studies in Mycology 64: 17–47. https://doi.org/10.3114/sim.2009.64.02

Crous PW, Verkley GJM, Groenewald JZ (2009b) Fungal biodiversity. CBS laboratory manual series no. 1. CBS-KNAW Fungal Biodiversity Centre, Utrecht.

Cui WL, Bian JY, Li DW, Wang JW, Huang L (2020a) First report of leaf blight on Chinese fir (*Cunninghamia lanceolata*) caused by *Bipolaris setariae* in China. Plant Disease 104(9): 2523–2523. https://doi.org/10.1094/PDIS-12-19-2685-PDN

Cui WL, Lu XQ, Bian JY, Qi XL, Li DW, Huang L (2020b) *Curvularia spicifera* and *Curvularia muehlenbeckiae* causing leaf blight on *Cunninghamia lanceolata*. Plant Pathology 69(6): 1139–1147. https://doi.org/10.1111/ppa.13198

Damm U, Mostert L, Crous PW, Fourie PH (2008) Novel *Phaeoacremonium* species associated with necrotic wood of *Prunus* trees. Persoonia 20(1): 87–102. https://doi.org/10.3767/003158508X324227

Dang JL, Gleason ML, Li LN, Wang C, Niu CK, Zhang R, Sun GY (2018) *Alternaria malicola* sp. nov., a new pathogen causing fruit spot on apple in China. Plant Disease 102(7): 1273–1282. https://doi.org/10.1094/PDIS-07-17-1027-RE

Dantes W, Colburn C, Williamson MR, Yang X (2022) First report of *Alternaria cinerariae* causing leaf blight on *Farfugium japonicum* in South Carolina, USA. Plant Disease 107(6): e1953. https://doi.org/10.1094/PDIS-09-22-2221-PDN

Dey PK (1933) An *Alternaria* blight of the linseed plant. Indian Journal of Agricultural Sciences 3: 881–896.

El-Goorani MA, Sommer NF (1981) Effects of modified atmospheres on postharvest pathogens of fruits and vegetables. Horticultural Reviews 3: 412–461. https://doi.org/10.1002/9781118060766.ch10

Fisher PJ, Petrini O (1992) Fungal saprobes and pathogens as endophytes of rice (*Oryza sativa* L.). The New Phytologist 120(1): 137–143. https://doi.org/10.1111/j.1469-8137.1992.tb01066.x

Gannibal PB, Orina AS, Gasich EL (2022) A new section for *Alternaria helianthiinficiens* found on sunflower and new asteraceous hosts in Russia. Mycological Progress 21(2): 1–34. https://doi.org/10.1007/s11557-022-01780-6

Ghafri AA, Maharachchikumbura SSN, Hyde KD, Al-Saady NA, Al-Sadi AM (2019) A new section and a new species of *Alternaria* encountered from Oman. Phytotaxa 405(6): 279–289. https://doi.org/10.11646/phytotaxa.405.6.1

He J, Li DW, Zhu YN, Si YZ, Huang JH, Zhu LH, Ye JR, Huang L (2022) Diversity and pathogenicity of *Colletotrichum* species causing anthracnose on *Cunninghamia lanceolata*. Plant Pathology 71(8): 1757–1773. https://doi.org/10.1111/ppa.13611

Hong SG, Pryor BM (2004) Development of selective media for the isolation and enumeration of *Alternaria* species from soil and plant debris. Canadian Journal of Microbiology 50(7): 461–468. https://doi.org/10.1139/w04-036

Hong SG, Cramer RA, Lawrence CB, Pryor BM (2005) Alt a 1 allergen homologs from *Alternaria* and related taxa: Analysis of phylogenetic content and secondary structure. Fungal Genetics and Biology 42(2): 119–129. https://doi.org/10.1016/j.fgb.2004.10.009

Huang L, Li QC, Zhang Y, Li DW, Ye JR (2016) *Colletotrichum gloeosporioides* sensu stricto is a pathogen of leaf anthracnose on evergreen spindle tree (*Euonymus japonicus*). Plant Disease 100(4): 672–678. https://doi.org/10.1094/PDIS-07-15-0740-RE

Huang L, Zhu YN, Yang JY, Li DW, Li Y, Bian LM, Ye JR (2018) Shoot blight on Chinese fir (*Cunninghamia lanceolata*) is caused by *Bipolaris oryzae*. Plant Disease 102(3): 500–506. https://doi.org/10.1094/PDIS-07-17-1032-RE

Huson DH (1998) SplitsTree: Analyzing and visualizing evolutionary data. Bioinformatics 14(1): 68–73. https://doi.org/10.1093/bioinformatics/14.1.68

Huson DH, Bryant D (2006) Application of phylogenetic networks in evolutionary studies. Molecular Biology and Evolution 23(2): 254–267. https://doi.org/10.1093/molbev/msj030

Hyde KD, Norphanphoun C, Chen J, Dissanayake AJ, Doilom M, Hongsanan S, Jayawardena RS, Jeewon R, Perera RH, Thongbai B, Wanasinghe DN, Wisitrassameewong K, Tibpromma S, Stadler M (2018) Thailand's amazing diversity: Up to 96% of fungi in northern Thailand may be novel. Fungal Diversity 93(1): 215–239. https://doi.org/10.1007/s13225-018-0415-7

Inderbitzin P, Shoemaker RA, O'Neill NR, Turgeon BG, Berbee ML (2006) Systematics and mating systems of two fungal pathogens of opium poppy: The heterothallic *Crivellia papaveracea* with a *Brachycladium penicillatum* asexual state and a homothallic species with a *Brachycladium papaveris* asexual state. Canadian Journal of Botany 84(8): 1304–1326. https://doi.org/10.1139/b06-067

Jayawardena RS, Hyde KD, Jeewon R, Ghobad-Nejhad M, Wanasinghe DN, Liu N, Phillips AJL, Oliveira-Filho JRC, da Silva GA, Gibertoni TB, Abeywikrama P, Carris LM, Chethana KWT, Dissanayake AJ, Hongsanan S, Jayasiri SC, McTaggart AR, Perera RH, Phutthacharoen K, Savchenko KG, Shivas RG, Thongklang N, Dong W, Wei D, Wijayawardena NN, Kang J-C (2019a) One stop shop II: taxonomic update with molecular phylogeny for important phytopathogenic genera: 26–50 (2019). Fungal Diversity 94: 41–129. https://doi.org/10.1007/s13225-019-00418-5

Jayawardena RS, Hyde KD, McKenzie EHC, Jeewon R, Phillips AJL, Perera RH, de Silva NI, Maharachchikumburua SSN, Samarakoon MC, Ekanayake AH, Tennakoon DS, Dissanayake AJ, Norphanphoun C, Lin C, Manawasinghe IS, Tian Q, Brahmanage R, Chomnunti P, Hongsanan S, Jayasiri SC, Halleen F, Bhunjun CS, Karunarathna A, Wang Y (2019b) One stop shop III: taxonomic update with molecular phylogeny for important phytopathogenic genera: 51–75 (2019). Fungal Diversity 98: 77–160. https://doi.org/10.1007/s13225-019-00433-6

Kalyaanamoorthy S, Minh BQ, Wong TKF, von Haeseler A, Jermiin LS (2017) ModelFinder: Fast model selection for accurate phylogenetic estimates. Nature Methods 14(6): 587–589. https://doi.org/10.1038/nmeth.4285

Kang ZT, Jiang LM, Luo YY, Liu CJ, Li XR (2013) Research progress on the pathogenic mechanism of plant pathogenic *Alternaria* fungi 植物病原链格孢属真菌的致病机制研究进展. Life Science 生命科学 25: 908–914. https://doi.org/10.13376/j.cbls/2013.09.009

Katoh K, Standley D (2013) MAFFT multiple sequence alignment software version 7: Improvements in performance and usability. Molecular Biology and Evolution 30(4): 772–780. https://doi.org/10.1093/molbev/mst010

Kgatle MG, Truter M, Ramusi TM, Flett B, Aveling TAS (2018) *Alternaria alternata*, the causal agent of leaf blight of sunflower in South Africa. European Journal of Plant Pathology 151(3): 677–688. https://doi.org/10.1007/s10658-017-1402-7

Kobayashi T, Zhao JZ (1987) Two fungi associated with needle blight of *Cunninghamia lanceolata*. Nippon Kingakkai Kaiho 28: 289–294.

Kumar S, Glen S, Michael L, Christina K, Koichiro T (2018) MEGA X: Molecular evolutionary genetics analysis across computing platforms. Molecular Biology and Evolution 35(6): 1547–1549. https://doi.org/10.1093/molbev/msy096

Lan X, Dong LJ, Huang KY, Chen DX, Li DW, Mo LY (2015) Main species and prevention research on diseases and pests of *Cunninghamia lanceolata*. Guangxi Forestry Science 44: 162–167. https://doi.org/10.19692/j.cnki.gfs.2015.02.014

Lawrence DP, Park MS, Pryor BM (2012) *Nimbya* and *Embellisia* revisited, with nov. comb for *Alternaria celosiae* and *A. perpunctulata*. Mycological Progress 11(3): 799–815. https://doi.org/10.1007/s11557-011-0793-7

Lawrence DP, Gannibal PB, Peever TL, Pryor BM (2013) The sections of *Alternaria*: Formalizing species-group concepts. Mycologia 105(3): 530–546. https://doi.org/10.3852/12-249

Lawrence DP, Rotondo F, Gannibal PB (2015) Biodiversity and taxonomy of the pleomorphic genus *Alternaria*. Mycological Progress 15(1): 1–22. https://doi.org/10.1007/s11557-015-1144-x

Li MF, He J, Ding L, Kang J, Zhang Q, Zheng Q (2007) Single spore strains without producing fruit body isolated from *Cordyceps militeris* and their RAPD analysis. Southwest China Journal of Agricultural Sciences 20: 547–550. https://doi.org/10.16213/j.cnki.scjas.2007.03.050

Li YM, Wang YJ, Jiang GY (2020) Application of origin software in data extraction and analysis in physical chemistry experiments: taking the combustion heat measurement of naphthalene as an example. Education Teaching Forum 50: 375–377.

Li J, Jiang HB, Jeewon R, Hongsanan S, Bhat DJ, Tang SM, Mortimer PE, Xu JC, Camporesi E, Bulgakov TS, Zhao GJ, Suwannarach N, Phookamsak R (2023) *Alternaria*: Update on species limits, evolution, multi-locus phylogeny, and classification. Studies in Fungi 8(1): 1–61. https://doi.org/10.48130/SIF-2023-0001

Liu HR, Ke GL (1992) The component and the perennial change of population of black spot pathogen in Cruciferae vegetable crops 十字花科蔬菜黑斑病原种群组成及季节变化. Acta Agriculturae Boreali-occidentalis Sinica 西北农业学报 1: 6–10.

Liu YJ, Whelen S, Hall BD (1999) Phylogenetic relationships among ascomycetes: Evidence from an RNA polymerse II subunit. Molecular Biology and Evolution 16(12): 1799–1808. https://doi.org/10.1093/oxfordjournals.molbev.a026092

Liu F, Mbenoun M, Barnes I, Roux J, Wingfield MJ, Li G, Li J, Chen S (2015a) New *Ceratocystis* species from *Eucalyptus* and *Cunninghamia* in South China. Antonie van Leeuwenhoek 107(6): 1451–1473. https://doi.org/10.1007/s10482-015-0441-3

Liu JK, Hyde KD, Jones EBG, Ariyawansa HA, Bhat DJ, Boonmee S, Maharachchikumbura SSN, McKenzie EHC, Phookamsak R, Phukhamsakda C, Shenoy BD, Abdel-Wahab MA, Buyck B, Chen J, Chethana KWT, Singtripop C, Dai DQ, Dai YC, Daranagama DA, Dissanayake AJ, Doilom M, D'souza MJ, Fan XL, Goonasekara ID, Hirayama K, Hongsanan S, Jayasiri SC, Jayawardena RS, Karunarathna SC, Li WJ, Mapook A, Norphanphoun C, Pang KL, Perera RH, Peršoh D, Pinruan U, Senanayake IC, Somrithipol S, Suetrong S, Tanaka K, Thambugala KM, Tian Q, Tibpromma S, Udayanga D, Wijayawardene NN, Wanasinghe D, Wisitrassameewong K, Zeng XY, Abdel-Aziz FA, Adamčík S, Bahkali AH, Boonyuen N, Bulgakov T, Callac P, Chomnunti P, Greiner K, Hashimoto A, Hofstetter V, Kang JC, Lewis D, Li XH, Liu XZ, Liu ZY, Matsumura M, Mortimer PE, Rambold G, Randrianjohany E, Sato G, Sri-Indrasutdhi V, Tian CM, Verbeken A, von Brackel W, Wang Y, Wen TC, Xu JC, Yan JY, Zhao RL, Camporesi E (2015b) Fungal diversity notes 1–110: Taxonomic and phylogenetic contributions to fungal species. Fungal Diversity 72(1): 1–197. https://doi.org/10.1007/s13225-015-0324-y

Mitakakis TZ, Clift A, McGee PA (2001) The effect of local cropping activities and weather on the airborne concentration of allergenic *Alternaria* spores in rural Australia. Grana 40(4–5): 230–239. https://doi.org/10.1080/001731301317223268

MycoBank (2023) MycoBank. https://www.mycobank.org

Nasehi A, Kadir JB, Abed Ashtiani F, Nasr-Esfahani M, Wong MY, Rambe SK, Ghadirian H, Mahmodi F, Golkhandan E (2014) *Alternaria capsicicola* sp. nov., a new species causing leaf spot of pepper (*Capsicum annuum*) in Malaysia. Mycological Progress 13: 1041–1048. https://doi.org/10.1007/s11557-014-0991-1

Nees VE (1816) Das System der Pilze und Schwämme. Wurzburg, Germany, 329 pp.

Nguyen LT, Schmidt HA, von Haeseler A, Minh BQ (2015) IQ-TREE: A fast and effective stochastic algorithm for estimating maximum-likelihood phylogenies. Molecular Biology and Evolution 32(1): 268–274. https://doi.org/10.1093/molbev/msu300

Nishikawa J, Nakashima C (2019) Morphological and molecular characterization of the strawberry black leaf spot pathogen referred to as the strawberry pathotype of *Alternaria alternata*. Mycoscience 60(1): 1–9. https://doi.org/10.1016/j.myc.2018.05.003

Nishikawa J, Nakashima C (2020) Japanese species of *Alternaria* and their species boundaries based on host range. Fungal Systematics and Evolution 5(1): 197–281. https://doi.org/10.3114/fuse.2020.05.13

Peever TL, Su G, Carpenter-Boggs L, Timmer LW (2004) Molecular systematics of citrus-associated *Alternaria* species. Mycologia 96(1): 119–134. https://doi.org/10.1080/15572536.2005.11833002

Pierce NB (1902) Black rot of oranges. Botanical Gazette (Chicago, Ill.) 33(3): 234–235. https://doi.org/10.1086/328217

Polizzotto R, Andersen B, Martini M, Grisan S, Assante G, Musetti R (2012) A polyphasic approach for the characterization of endophytic *Alternaria* strains isolated from grapevines. Journal of Microbiological Methods 88(1): 162–171. https://doi.org/10.1016/j.mimet.2011.11.009

Preuss CGT (1852) Uebersicht untersuchter Pilze, besonders aus der Umgegend von Hoyerswerda. Linnaea 25: 723–742.

Pryor BM, Gilbertson RL (2000) Molecular phylogenetic relationships amongst *Alternaria* species and related fungi based upon analysis of nuclear ITS and mt SSU rDNA sequences. Mycological Research 104(11): 1312–1321. https://doi.org/10.1017/S0953756200003002

Quaedvlieg W, Binder M, Groenewald JZ, Summerell BA, Carnegie AJ, Burgess TI, Crous PW (2014) Introducing the consolidated species concept to resolve species in the Teratosphaeriaceae. Persoonia 33(1): 1–40. https://doi.org/10.3767/003158514X681981

Rahimloo T, Ghosta Y (2015) The occurrence of *Alternaria* species on cabbage in Iran. Zemdirbyste 102(3): 343–350. https://doi.org/10.13080/z-a.2015.102.044

Rambaut A (2014) FigTree v 1.4.2. Institute of evolutionary biology, University of Edinburgh. http://tree.bio.ed.ac.uk/software/figtree/

Reddy MVB, Angers P, Castaigne F, Arul J (2000) Chitosan effects on blackmold rot and pathogenic factors produced by *Alternaria alternata* in postharvest tomatoes. Journal of the American Society for Horticultural Science 125(6): 742–747. https://doi.org/10.21273/JASHS.125.6.742

Roberts RG (2005) *Alternaria yaliinficiens* sp. nov. on Ya Li pear fruit: From interception to identification. Plant Disease 89(2): 134–145. https://doi.org/10.1094/PD-89-0134

Romain BBND, Hassan O, Kim JS, Chang T (2022) *Alternaria koreana* sp. nov., a new pathogen isolated from leaf spot of ovate-leaf Atractylodes in South Korea. Molecular Biology Reports 49(1): 413–420. https://doi.org/10.1007/s11033-021-06887-9

Ronquist F, Teslenko M, van der Mark P, Ayres DL, Darling A, Hohna S, Larget B, Liu L, Suchard MA, Huelsenbeck JP (2012) MrBayes 3.2: Efficient Bayesian phylogenetic

inference and model choice across a large model space. Systematic Biology 61(3): 539–542. https://doi.org/10.1093/sysbio/sys029

Rosa LH, Vaz ABM, Caligiorne RB, Campolina S, Rosa CA (2009) Endophytic fungi associated with the Antarctic grass *Deschampsia antarctica* Desv. (Poaceae). Polar Biology 32(2): 161–167. https://doi.org/10.1007/s00300-008-0515-z

Runa F, Park MS, Pryor BM (2009) *Ulocladium* systematics revisited: Phylogeny and taxonomic status. Mycological Progress 8(1): 35–47. https://doi.org/10.1007/s11557-008-0576-y

Schulz B, Wanke U, Draeger S, Aust HJ (1993) Endophytes from herbaceous plants and shrubs: Effectiveness of surface sterilization methods. Mycological Research 97(12): 1447–1450. https://doi.org/10.1016/S0953-7562(09)80215-3

Seifert KA, Morgan-Jones G, Gams W, Kendrick B (2011) The genera of Hyphomycetes. CBS-KNAW Fungal Biodiversity Centre Utrecht, Utrecht, The Netherlands.

Shi X, Zeng K, Wang X, Liang Z, Wu X (2021) Characterization of *Alternaria* species causing leaf spot on Chinese cabbage in Shanxi province of China. Journal of Plant Pathology 103(1): 283–293. https://doi.org/10.1007/s42161-020-00740-x

Simmons EG (1992) *Alternaria* taxonomy: current status, viewpoint, challenge. In: Chelkowski J, Visconti A (Eds) *Alternaria* biology, plant diseases and metabolites. Elsevier, Amsterdam, 35 pp.

Simmons EG (1993) *Alternaria* themes and variations (63–72). Mycotaxon 48: 91–107.

Simmons EG (1995) *Alternaria* themes and variations (112–144). Mycotaxon 55: 55–163.

Simmons EG (1999) *Alternaria* themes and variations (226–235): Classification of citrus pathogens. Mycotaxon 70: 263–323. https://doi.org/10.1046/j.1439-0507.1999.00531.x

Simmons EG (2007) *Alternaria*: An Identification Manual. CBS Biodiversity Series, 775 pp.

Simmons EG, Roberts RG (1993) *Alternaria* themes and variations (73). Mycotaxon 48: 109–140.

Sung GH, Sung JM, Hywel Jones NL, Spatafora JW (2007) A multi-gene phylogeny of Clavicipitaceae (Ascomycota, Fungi): Identification of localized incongruence using a combinational bootstrap approach. Molecular Phylogenetics and Evolution 44(3): 1204–1223. https://doi.org/10.1016/j.ympev.2007.03.011

Thomma BP (2003) *Alternaria* spp.: From general saprophyte to specific parasite. Molecular Plant Pathology 4(4): 225–236. https://doi.org/10.1046/j.1364-3703.2003.00173.x

Tian LY, Lian T, Ke SK, Qin CS, Xu JJ, Zhao DY, Qiu HL, Yang H, Jin XF, Li NL (2019) Fungal diseases of Chinese fir in northern Guangdong. 粤北地区杉木真菌性病害种类. Forestry and Environmental Sciences 35: 90–96.

Wallroth CFW (1833) Flora Cryptogamica Germaniae Sectio 2. Germany, J.L, Schrag, Nurnberg.

Wanasinghe DN, Phukhamsakda C, Hyde KD, Jeewon R, Lee HB, Gareth Jones EB, Tibpromma S, Tennakoon DS, Dissanayake AJ, Jayasiri SC, Gafforov Y, Camporesi E, Bulgakov TS, Ekanayake AH, Perera RH, Samarakoon MC, Goonasekara ID, Mapook A, Li W-J, Senanayake IC, Li J, Norphanphoun C, Doilom M, Bahkali AH, Xu J, Mortimer PE, Tibell L, Tibell S, Karunarathna SC (2018) Fungal diversity notes 709–839: Taxonomic and phylogenetic contributions to fungal taxa with an emphasis on fungi on Rosaceae. Fungal Diversity 89(1): 1–236. https://doi.org/10.1007/s13225-018-0395-7

Wang J, Cen B, Jiang Z, Peng S, Tong Z, Li G (1995) Identification of the pathogen which causes Chinese fir shoot blight. Journal of South China Agricultural University 4: 47–49.

Wang P, Ou Y, Zhang Q, Sun W, Zhu H, Qi N, Chen Y (2018) Research advance in tobacco brown spot 烟草赤星病研究进展. Anhui Agricultural Science 安徽农业科学 46: 33–36. https://doi.org/10.13989/j.cnki.0517-6611.2018.21.008

Wangeline AL, Reeves FB (2007) Two new *Alternaria* species from selenium-rich habitats in the Rocky Mountain Front Range. Mycotaxon 99: 83–89.

White TJ, Bruns S, Lee S, Taylor J, Innis MA, Gelfand DH, Sninsky J (1990) Amplification and direct sequencing of fungal ribosomal RNA genes for phylogenetics. In: Innis MA, Gelfand DH, Sninsky JJ, White TJ (Eds) PCR Protocols: A Guide to Methods and Applications, 315–322. https://doi.org/10.1016/B978-0-12-372180-8.50042-1

Wijayawardene NN, Hyde KD, Al-Ani LKT, Tedersoo L, Haelewaters D, Rajeshkumar KC, Zhao R-L, Aptroot A, Leontyev DV, Saxena RK, Tokarev YS, Dai D-Q, Letcher PM, Stephenson SL, Ertz D, Lumbsch HT, Kukwa M, Issi IV, Madrid H, Phillips AJL, Selbmann L, Pfliegler WP, Horváth E, Bensch K, Kirk PM, Kolaříková K, Raja HA, Radek R, Papp V, Dima VS, Ma J, Malosso E, Takamatsu S, Rambold G, Gannibal PB, Triebel D, Gautam AK, Avasthi S, Suetrong S, Timdal E, Fryar SC, Delgado G, Réblová M, Doilom M, Dolatabadi S, Pawłowska J, Humber RA, Kodsueb R, Sánchez-Castro I, Goto BT, Silva DKA (2020) Outline of Fungi and fungus-like taxa. Mycosphere: Journal of Fungal Biology 11(1): 1060–1456. https://doi.org/10.5943/mycosphere/11/1/8

Wiltshire SP (1933) The foundation species of *Alternaria* and *Macrosporium*. Transactions of the British Mycological Society 18(2): 135–160. https://doi.org/10.1016/S0007-1536(33)80003-9

Wiltshire SP (1945) Danish species of *Alternaria* and *Stemphylium* taxonomy, parasitism, economical significance. The Quarterly Review of Biology 160: 313–314. https://doi.org/10.1038/160313b0

Woudenberg JH, Groenewald JZ, Binder M, Crous PW (2013) *Alternaria* redefined. Studies in Mycology 75: 171–212. https://doi.org/10.3114/sim0015

Woudenberg JH, van der Merwe NA, Jurjević Ž, Groenewald JZ, Crous PW (2015) Diversity and movement of indoor *Alternaria alternata* across the mainland USA. Fungal Genetics and Biology. Fungal Genetics and Biology 81: 62–72. https://doi.org/10.1016/j.fgb.2015.05.003

Xiang M, Wang Y, Wang D, Fu Y, Zeng J, Ouyang D, Chen J, Chen M (2023) First report of black spot disease caused by *Alternaria alternata* on persimmon fruit in China. Plant Disease 107(8): e2525. https://doi.org/10.1094/PDIS-02-23-0234-PDN

Xu YM, Liu YJ (2017) First report of *Nigrospora sphaerica* causing leaf blight on *Cunninghamia lanceolata* in China. Plant Disease 101(2): 389. https://doi.org/10.1094/PDIS-09-16-1229-PDN

Yan H (2020) Potential analysis of launching forest management carbon sequestration projects by the managementof Chinese Fir forest. 杉木林分经营碳汇项目发展的潜力分析. Journal of Wuyi University 武夷学院学报 39: 14–17. https://doi.org/10.14155/j.cnki.35-1293/g4.2020.09.004

Yan H, Mi Y, Man Z, Zang H, Guo L, Huo J, Li Y, Chen Z, Zhang B, Sang M, Li C, Cheng Y (2023) First report of leaf spot disease caused by *Alternaria tenuissima* on *Lonicera caerulea* L. in Heilongjiang Province, China. Plant Disease 107(10): e3298. https://doi.org/10.1094/PDIS-04-23-0794-PDN

Zhang TY (2003) *Alternaria*. Flora Fungorum Sinicorum.

Zhang TY, Zhang JZ, Chen WQ, Ma XL, Gao MX (1999) Taxonomic studies of *Alternaria* from China. VII. New taxa on Fagaceae, Magnoliaceae, Meliaceae, and Moraceae. Mycotaxon 72: 433–442. https://doi.org/10.13346/j.mycosystema.1999.02.002

Zhang S, Cui C, Xu L (1998) Study on the population composition and pathogenic types of black spot in Chinese cabbage in Heilongjiang province 黑龙江省大白菜黑斑病菌种群组成与致病型分化的研究. Southeast University Press 东南大学出版社, Nanjing, Jiangsu, China 中国江苏南京, 556–559.

Zhang D, Gao FL, Jakovli I, Zou H, Wang GT (2020) PhyloSuite: An integrated and scalable desktop platform for streamlined molecular sequence data management and evolutionary phylogenetics studies. Molecular Ecology Resources 20(1): 348–355. https://doi.org/10.1111/1755-0998.13096

Zheng W, Chen J, Hao Z, Shi J (2016) Comparative analysis of the chloroplast genomic information of *Cunninghamia lanceolata* (Lamb.) Hook with sibling species from the genera *Cryptomeria* D. Don, *Taiwania* Hayata, and *Calocedrus* Kurz. International Journal of Molecular Sciences 17(7): e1084. https://doi.org/10.3390/ijms17071084

Zhou H, Hou CL (2019) Three new species of *Diaporthe* from China based on morphological characters and DNA sequence data analyses. Phytotaxa 422(2): 157–174. https://doi.org/10.11646/phytotaxa.422.2.3

Zhou ZC, Tang X, Hu S, Zhu W, Wu X, Sang WJ, Peng L, Ding H (2023) First report of grey spot on tobacco caused by *Alternaria alstroemeriae* in China. Plant Disease 107(8): e2546. https://doi.org/10.1094/PDIS-11-22-2705-PDN

Supplementary material 1

Supplementary information

Authors: Jiao He, De-Wei Li, Wen-Li Cui, Lin Huang

Data type: docx

Explanation note: **table S1.** Fungal cultures isolated from Chinese fir in this study. **table S2.** Primers used for PCR amplification and DNA sequences.

Link: https://doi.org/10.3897/mycokeys.101.115370.suppl1

Morphological and phylogenetic analyses reveal three new species of *Fusarium* (Hypocreales, Nectriaceae) associated with leaf blight on *Cunninghamia lanceolata* in China

Jiao He[1], De-Wei Li[2], Wen-Li Cui[1], Li-Hua Zhu[1], Lin Huang[1]

1 Co-Innovation Center for Sustainable Forestry in Southern China, Nanjing Forestry University, Nanjing, Jiangsu 210037, China
2 The Connecticut Agricultural Experiment Station Valley Laboratory, Windsor, CT 06095, USA
Corresponding author: Lin Huang (lhuang@njfu.edu.cn)

Abstract

Chinese fir (*Cunninghamia lanceolata*) is a special fast-growing commercial tree species in China with high economic value. In recent years, leaf blight disease on *C. lanceolata* has been observed frequently. The diversity of *Fusarium* species associated with leaf blight on *C. lanceolata* in China (Fujian, Guangxi, Guizhou, and Hunan provinces) was evaluated using morphological study and molecular multi-locus analyses based on RNA polymerase second largest subunit (*RPB2*), translation elongation factor 1-alpha (*TEF-1α*), and RNA polymerase largest subunit (*RPB1*) genes/region as well as the pairwise homoplasy index tests. A total of five *Fusarium* species belonging to four *Fusarium* species complexes were recognized in this study. Two known species including *Fusarium concentricum* and *F. fujikuroi* belonged to the *F. fujikuroi* species complex, and three new *Fusarium* species were described, i.e., *F. fujianense* belonged to the *F. lateritium* species complex, *F. guizhouense* belonged to the *F. sambucinum* species complex, and *F. hunanense* belonged to the *F. solani* species complex. To prove Koch's postulates, pathogenicity tests on *C. lanceolata* revealed a wide variation in pathogenicity and aggressiveness among the species, of which *F. hunanense* HN33-8-2 caused the most severe symptoms and *F. fujianense* LC14 led to the least severe symptoms. To our knowledge, this study also represented the first report of *F. concentricum*, *F. fujianense*, *F. fujikuroi*, *F. guizhouense*, and *F. hunanense* causing leaf blight on *C. lanceolata* in China.

Key words: *Cunninghamia lanceolata*, *Fusarium*, leaf blight, new species, pathogenicity

Introduction

The genus *Fusarium* (Nectriaceae) is one of the most renowned genera that contains many phytopathogenic fungi. The members of this genus can directly incite diseases in plants, humans, and domesticated animals (Rabodonirina et al. 1994; Boonpasart et al. 2002; Vismer et al. 2002). *Fusarium* was included in the top 10 globally most important genera of plant pathogenic fungi based on scientific and economic importance (Dean et al. 2012), in particular because of the members of the *F. sambucinum* species complex (FSAMSC) and *F. oxysporum* species complex (FOSC) (O'Donnell et al. 2015; Gräfenhan et al. 2016)

that comprises some of the most destructive agricultural pathogens. *Fusarium graminearum* and 21 related species comprising the *F. sambucinum* species complex lineage 1 (FSAMSC-1) are the most important *Fusarium* head blight (FHB) pathogens of cereal crops world-wide (Goswami and Kistler 2005; Kelly et al. 2016). Further impactful fusaria include the members of the *F. fujikuroi* species complex (FFSC), *F. verticillioides* (teleomorphic synonym, *Gibberella moniliformis*), *F. fujikuroi* (teleomorphic synonym, *G. fujikuroi*), and *F. proliferatum* (teleomorphic synonym, *G. intermedia*), which are well known for their abilities to cause devastating diseases, such as rice bakanae, maize ear rot and soybean root rot, leading to considerable reductions in crop yields and economic income (O'Donnell et al. 2015; Qiu et al. 2020). The members of the *F. solani* species complex (FSSC) cause plant diseases, mostly root and crown rots and vascular wilts on a wide range of plants, including soybeans, potato, cucurbits, peas, sweet potato, Chinese rose, and various legumes (Coleman 2016; Summerell 2019; He et al. 2021).

There has been confusion in *Fusarium* taxonomy for a long time because of the nine-species system of Snyder and Hansen (1940), the misleading overlaps caused by convergent evolution and character loss, the phenomenon of cultural degeneration, and firm opinions of the taxonomists and plant pathologists who have been working on them. First described by Link (1809) and typified by *Fusarium roseum* (presently *F. sambucinum* nom. cons.) (Gams et al. 1997), the generic and species concepts in *Fusarium* have endured significant changes since the cornerstone of phenotypically-based taxonomic treatments that grouped species into sections, morphological varieties or forms and later formae speciales based on pathogenicity and host ranges (Wollenweber and Reinking 1935; Snyder and Hansen 1940; Toussoun and Nelson 1968; Gerlach and Nirenberg 1982; Nelson et al. 1983; Burgess et al. 1988). Later, the species were redistributed into species complexes after the introduction of modern molecular tools (O'Donnell et al. 2000; Geiser et al. 2013; O'Donnell et al. 2013; Aoki et al. 2014). O'Donnell et al. (2022) indicates that *Fusarium* is assessed to have >400 phylospecies and *ca*. 1/3 of the phylospecies have not been formally described; clearly, morphology alone is insufficient to differentiate most of these species. To solve the species delimitation and identification dilemma, a polyphasic approach has gradually been applied and several online databases (*Fusarium*-ID, *Fusarium* MLST and FUSARIOID-ID) have been established based on different taxonomic opinions (O'Donnell et al. 2012; Crous et al. 2021; Torres-Cruz et al. 2022). Despite these significant contributions, debates surrounding the generic delimitation of *Fusarium* and whether the genus *Neocosmospora* (also known as *F. solani* species complex, FSSC) belongs to *Fusarium* remain (Crous et al. 2021; Geiser et al. 2021; Wang et al. 2022). There has been a consensus for over a century that the FSSC is part of *Fusarium*, which was affirmed by molecular phylogenetic analyses and codified in a proposal to recognize *Fusarium* as a monophyletic group that includes the FSSC (Geiser et al. 2013). A disagreement on the generic concept of *Fusarium* has become more contentious in the last decade. Geiser et al. (2013) advocated "recognizing the genus *Fusarium* as the sole name for a group that includes virtually all *Fusarium* species of importance in plant pathology, mycotoxicology, medicine, and basic research", and the retained genus *Fusarium* includes *F. solani* species complex (FSSC). This treatment was subsequently challenged by Lombard

et al. (2015) who split the genus *Fusarium* into seven genera and segregated the FSSC as *Neocospmospora*. Later, Sandoval-Denis and Crous (2018) and Sandoval-Denis et al. (2019) justified the treatment of Lombard et al. (2015) based on the phylogenetic analyses using four loci and dispute that the Geiser et al. (2013) concept of *Fusarium* is polyphyletic. O'Donnell et al. (2020) rebutted the polyphyletic conclusions of Sandoval-Denis and Crous (2018) and Sandoval-Denis et al. (2019). Geiser et al. (2021) examined the conclusion of Sandoval-Denis and Crous (2018) and Sandoval-Denis et al. (2019), developed a phylogeny according to sequences of 19 orthologous protein-coding genes and show that *Fusarium* including the FSSC is monophyletic. Thus, 40 species described as *Neocosmospora* are recently recombined in *Fusarium* (Aoki et al. 2020, 2021a, b). Crous et al. (2021) insist that fusarium-like are polyphyletic in Nectriaceae and dispute that a narrower generic concept with a combination of features is necessary for the majority of fusarioid species based on the phylogenetic analyses using sequence data of eight loci. They segregate the Wollenweber concept of *Fusarium* into 20 genera with synapomorphic characteristics (Crous et al. 2021). O'Donnell et al. (2022) opined that *Fusarium* remains the best scientific, nomenclatural and practical taxonomic option available. However, the disagreement is far from settled.

The narrow generic concept of *Fusarium* is leading to a large number of name changes and confusions among plant pathologists, medical mycologists, quarantine officials, regulatory agencies, biologists, and other professionals. Rebuilding the correct systematic position of a large number of fungal names cannot be achieved without repeated studies (de Hoog et al. 2023). The purpose of choosing *Fusarium*, not *Neocosmospora* or other generic names is to maintain the stability of the name *Fusarium* in plant pathology and minimize confusion. We hope more independent studies in the future will resolve the phylogenetic disputes on *Fusarium s. l*.

Morphology is a fundamental component of the generic and species concepts of fungi and must not be overlooked. Key morphological features for generic circumscription include characteristics of sexual morphs such as perithecial morphology, the presence and nature of a basal stroma, ascus characters, and ascospore shape, septation, color as well as surface ornamentation (Rossman et al. 1999), but sexual stage rarely develop. Therefore, diagnostic characters are the dimensions and characteristics of aerial conidiophores and conidiogenous cells (mono- vs. poly-phialides), presence/absence and characteristics of sporodochia, the types of conidia produced, e.g., aerial microconidia, and aerial and sporodochial macroconidia. Finally, the presence or absence of chlamydospores may be important (Leslie and Summerell 2006). However, the morphology of fungal structures will vary dramatically depending on the selection of media and growth conditions, which may compromise the identification process, and some *Fusarium* strains are similar in colony morphology and biology, which also makes it difficult to directly differentiate strains (Crous et al. 2021).

Current *Fusarium* taxonomy is dominated by molecular phylogenetic studies. Many protein-coding genes have been explored for identification and taxonomic purposes in *Fusarium*. The 28S large subunit (LSU) nrDNA, internal transcribed spacer region and intervening 5.8S nrRNA gene (ITS), large subunit of the ATP citrate lyase (*acl1*), RNA polymerase II largest subunit (*rpb1*), RNA polymerase II second largest subunit (*rpb2*), α-actin (*act*), β-tubulin (*tub2*), calmodulin

(*cmdA*), histone H3 (*his3*), and translation elongation factor 1-alpha (*tef1*) loci are currently used (Lombard et al. 2015; Sandoval-Denis et al. 2018; Crous et al. 2021). However, *TEF-1α* and *RPB2* sequences appear to be the most useful in taxonomic studies of fungi of the *Fusarium* genus. Both offer high discriminatory power and are well represented in public databases (O'Donnell 2000). *TEF-1α* is commonly the first-choice identification marker as it has very good resolution power for most species, while *RPB2* allows for enhanced discrimination between closely related species (Crous et al. 2021). Additional genetic markers, often employed in association with the previously mentioned genes in multigene phylogenetic analyses, include *TUB2*, *HIS3*, *CAM*, and *RPB1*. These markers have variable resolution or applicability depending on the genus or species complex (Crous et al. 2021). One of the latest studies has used 19 loci to provide a much better phylogeny of *Fusarium* (Geiser et al. 2021). At present, Genealogical Concordance Phylogenetic Species Recognition (GCPSR) (Taylor et al. 2000) based multilocus data analyses have resolved *Fusarium* into >400 phylogenetically distinct species distributed among 23 monophyletic species complexes and several single-species lineages (O'Donnell et al. 2015; Summerell 2019; O'Donnell et al. 2020; Geiser et al. 2021).

Chinese fir (*Cunninghamia lanceolata* (Lamb.) Hook.) is an evergreen coniferous tree species. Because of its fast growth, straight trunk, and high economic value, it is widely cultivated in the Yangtze River Basin and the southern Qinling Mountains in China. It is the main afforestation tree species in southern China. Average timber volume is estimated at 500−800 m³/ha, and in China, *C. lanceolata* contributes 40% of the total commercial timber production (Zheng et al. 2016). However, *C. lanceolata* is often damaged by many diseases and insect pests (Lan et al. 2015). Some common insect pests include *Semanotus sinoauster*, *Callidium villosulum*, and *Lobesia cunninghamiacola* (Lan et al. 2015). *Bartalinia cunninghamiicola*, *Berkeleyomyces basicola* (≡ *Thielaviopsis basicola*), *Bipolaris oryzae*, *Bi. setariae*, *Ceratocystis acaciivora*, *Chalaropsis* sp., *Colletotrichum cangyuanense*, *C. fructicola*, *C. gloeosporioides*, *C. kahawae*, *C. karstii*, *C. siamense*, *Curvularia spicifera*, *Cur. muehlenbeckiae*, *Ceratocystis collisensis*, *Diaporthe anhuiensis*, *Dia. citrichinensis*, *Dia. unshiuensis*, *Dia. hongkongensis*, *Discosia pini*, *Lophodermium uncinatum*, *Nigrospora sphaerica*, *Rhizoctonia solani*, *Fusarium oxysporum* f. *pini*, and *Fusarium* sp. have been reported as pathogens on *C. lanceolata* (Anonymous 1979; Kobayashi and Zhao 1987; Wang et al. 1995; Chen 2002; Lan et al. 2015; Liu et al. 2015; Xu and Liu 2017; Huang et al. 2018; Tian et al. 2019; Zhou and Hou 2019; Cui et al. 2020a, b; He et al. 2022; Li et al. 2022; Dai et al. 2023; Liao et al. 2023).

An investigation of fungal diseases on leaves of *C. lanceolata* covering its main cultivation regions of *C. lanceolata* in China was conducted from 2016 to 2020 (unpublished data) and samples of leaf blight were collected. The foliar symptoms ranged from leaf spots, anthracnose to leaf blight. The leaf blight disease mainly caused pale brown to brownish necrotic needles on *C. lanceolata*. Our preliminary study showed that a number of fungi were responsible for the foliar diseases of *C. lanceolata* in the field, including *Alternaria* spp., *Bipolaris* spp., *Colletotrichum* spp., *Curvularia* spp., *Fusarium* spp., and *Pestalotiopsis* spp. The main aim of the present study is to determine the *Fusarium* spp. associated with *C. lanceolata*.

Materials and methods

Isolation of the potential fungal pathogen

A total of 20 isolates of *Fusarium* spp. were isolated from leaf blight disease samples of *C. lanceolata*, which were collected in four provinces (Fujian, Guangxi, Guizhou, and Hunan) in China (Suppl. material 1: table S1). Small sections (2 × 3 mm) were cut from the margins of infected tissues and surface sterilized in 75% alcohol for 30 s, then in 1% sodium hypochlorite (NaOCl) for 90 s, followed by three rinses with sterile water (Huang et al. 2016), then blotted dry with sterilized filter paper, placed on 2% potato dextrose agar (PDA) Petri plates with 100 mg/L ampicillin, and then cultured for 3 days at 25 °C in the dark. Fungal isolates were purified with the monosporic isolation method described by Li et al. (2007) using the spores produced with liquid cultures. Single-spore isolates were maintained on PDA plates. The obtained isolates were stored in the Forest Pathology Laboratory at Nanjing Forestry University. Holotype specimens of new species from this study were deposited at the China Forestry Culture Collection Center (**CFCC**), Chinese Academy of Forestry, Beijing, China.

DNA extraction, PCR amplification and sequencing

Genomic DNA of 20 isolates was extracted using a modified CTAB method (Damm et al. 2008). The fungal plugs of each isolate were grown on the PDA plates for 5 days and then collected in a 2 mL tube. Then, 500 µL of chloroform and 500 µL of hexadecyltrimethyl ammonium bromide (CTAB) extraction buffer (0.2 M Tris, 1.4 M NaCl, 20 mM EDTA, 0.2 g/L CTAB) were added into the tubes, which were placed in a shaker at 25 °C at 200 rpm for 2-h. The mixture was centrifuged at 15,800 × g for 5 min. Then, 300 µL of the supernatant was transferred into a new tube, and 600 µL of 100% ethanol was added. The suspension was centrifuged at 15,800 × g for 5 min. At that point, 600 µL of 70% ethanol was added into the precipitate. The suspension was centrifuged at 15,800 × g for 5 min, and the supernatant was discarded. The DNA pellet was dried and re-suspended in 30 µL ddH$_2$O.

The polymerase chain reaction (PCR) amplification was carried out on the extracted DNA. *TEF-1α*, *RPB2*, and *RPB1* were amplified with the primer sets of EF1/EF2 (O'Donnell et al. 1998), 5f2/7cr (Liu et al. 1999), and Fa/G2R (O'Donnell et al. 2010), respectively. The primer sequences were listed in Suppl. material 1: table S2.

PCR was performed in a 30 µl reaction volume containing 2 µL of genomic DNA (*ca*. 200 ng/µL), 15 µL of 2× Taq Plus Master Mix (Dye Plus) (Vazyme P212-01), 1 µL of 10 µM forward primer, 1 µL of 10 µM reverse primer, and 11 µL of ddH$_2$O. The parameters for PCR protocol were 94 °C for 4 min, followed by 34 cycles of 30 s at 94 °C, annealing at a suitable temperature for the 30 s for different loci: 55 °C for *TEF-1α*, *RPB2*, and *RPB1*, 72 °C for 60 s, and a final elongation step at 72 °C for 10 min. All DNA sequencing was performed at Shanghai Sangon Biotechnology Company (Nanjing, China). The sequences derived in this study were deposited in GenBank. GenBank accession numbers of all isolates used for phylogenetic analyses were listed in Table 1.

Table 1. Cultures, specimens and DNA accession numbers included in this study.

Species name	Culture/specimen[1]	Host	Country/area	GenBank/ENA accession number[2]		
				TEF−1α	RPB2	RPB1
Fusarium fujikuroi species complex						
F. acutatum	CBS 402.97[T] (Ex-type)	Unknown	India	KR071754	KT154005	MT010947
F. agapanthi	NRRL 54463[HT] (Ex-holotype)	African lily	Australia and Italy	KU900630	KU900625	KU900620
	NRRL 54464[HT]	African lily	Australia and Italy	–	KU900627	KU900622
F. ananatum	CBS 118516[T]	Unknown	Unknown	–	KU604269	MT010937
F. awaxy	LGMF 1930[HT]	stalk, *Zea mays*	Brazil	MG839004	MK766941	–
F. bactridioides	CBS 100057[T]	*Pinus leiophylla*	Arizona, USA	KC514053	–	MT010939
F. begoniae	CBS 452.97[T]	Begonia elatior hybrid	Germany	KC514054	MT010964	–
F. brevicatenulatum	CBS 404.97[T]	*Striga asiatica*	Madagascar	MT011005	MT010979	MT010948
	NRRL 25447[T]	Unknown	Unknown	MN193859	MN193887	
F. concentricum	MUCL 55980	*Musa* sp.	China	LT574935	LT575016	–
	MUCL 55983	*Musa* sp.	China	LT574938	LT575019	–
	CBS 450.97[T]	*Musa sapientum* fruit	Costa Rica	MT010992	MT010981	MT010942
	SJ1-10 *	Chinese fir	China	ON734385	ON734365	OR683264
	SJ1-10-1 *	Chinese fir	China	ON734386	ON734366	OR683265
	SJ1-10-2 *	Chinese fir	China	ON734387	ON734367	OR683266
	SJ1-10-3 *	Chinese fir	China	ON734388	ON734368	OR683267
F. circinatum	NRRL 25331[T] = CBS 405.97	Monterrey pine tree	USA	AF160295	JX171623	–
F. fujikuroi	HJYB-4	*Zanthoxylum armatum*	China	MT902140	MT902141	–
	MUCL 55986	*Musa* sp.	China	LT574941	LT575022	–
	CBS 221.76[T]	*Oryza sativa* culm	Taiwan	KR071741	KU604255	–
	HN43-17-1 *	Chinese fir	China	ON734397	ON734377	OR683276
	HN43-17-1-1 *	Chinese fir	China	ON734398	ON734378	OR683277
	HN43-17-1-2 *	Chinese fir	China	ON734399	ON734379	OR683278
	HN43-17-1-3 *	Chinese fir	China	ON734400	ON734380	OR683279
F. lactis	NRRL 25200[NT] = CBS 411.97 (Ex-neotype)	*Ficus carica*	USA	AF160272	–	MT010954
F. mangiferae	NRRL 25226[T] = BBA 69662	*Mangifera indica*	India	AF160281	JX171622	–
F. nygamai	NRRL 13448[T] = CBS 749.97	Necrotic sorghum root	Australia	AF160273	EF470114	MT010955
F. pseudocircinatum	NRRL 22946[T] = CBS 126.73	*Solanum* sp.	Ghana	AF160271	–	MT010952
F. pseudonygamai	NRRL 13592[T] = CBS 417.97	*Pennisetum typhoides*	Nigeria	AF160263	–	MT010951
F. ramigenum	NRRL 25208[T] = CBS 418.97	*Ficus carica*	USA	AF160267	KF466412	MT010959
F. sacchari	NRRL 13999 = CBS 223.76	*Saccharum officinarum*	India	AF160278	JX171580	–
F. subglutinans	NRRL 22016[T] = CBS 747.97	Corn	USA	AF160289	JX171599	–
F. thapsinum	NRRL 22045 = CBS 733.97	*Sorghum bicolor*	South Africa	AF160270	JX171600	–
F. udum	NRRL 22949 = CBS 178.32	unknown	Germany	AF160275	–	–
F. xyrophilum	NRRL 62721	*Xyris* spp.	Guyana	–	MN193905	MW402721
	NRRL 62710	*Xyris* spp.	Guyana	–	MN193903	MW402720
F. zealandicum (Outgroup)	CBS 111.93[T]	*Hoheria populnea* bark	New Zealand	HQ728148	HM626684	–
F. lateritium species complex						
F. cassiae	MFLUCC 18-0573[HT]	*Cassia fistula*	Thailand	MT212205	MT212197	–
F. citri-sinensis	YZU 191316[T]	*Citrus sinensis* fruit	China	MW855826	MW855854	–
	YZU 181391	*Citrus sinensis* fruit	China	MW855825	OM913582	–
F. fujianense	LC14 *	Chinese fir	China	ON734389	ON734369	OR683268
	LC14-1 *	Chinese fir	China	ON734390	ON734370	OR683269
F. fujianense	LC14-2 *	Chinese fir	China	ON734391	ON734371	OR683270
	LC14-3 *	Chinese fir	China	ON734392	ON734372	OR683271
F. lateritium	NRRL 52786	unknown	Germany	JF740854	JF741180	JF741009
F. lateritium	NRRL 25122[LT] (Ex-lectotype)	unknown	Germany	JF740747	JF741075	JF740959

Species name	Culture/specimen[1]	Host	Country/area	GenBank/ENA accession number[2]		
				TEF−1α	RPB2	RPB1
F. magnoliae-champaca	MFLUCC 18-0580[HT]	*Magnolia champaca*	Thailand	–	MT212198	–
F. massalimae	URM 8239[T]	*Handroanthus chrysotrichus*	Brazil	MN939763	MN939767	–
	FCCUFG 05[HT]	*Handroanthus chrysotrichus*	Brazil	MN939764	MN939768	–
F. sarcochroum	CPC 28118	*Citrus limon*	Castellò, Spain	LT746213	LT746326	LT746298
	CPC 28075[NT]	*Citrus reticulata*	Alginet, Spain	LT746211	LT746324	LT746296
F. stilboides	CBS 746.79[T]	*Citrus* sp.	New Zealand	MW928843	MW928832	–
F. sublunatum (Outgroup)	CBS 189.34[T]	*Musa sapientum* and *Theobroma cacao*	USA	–	KM232380	–
F. sambucinum species complex						
F. acaciae-mearnsii	NRRL 26754[T]	*Acacia mearnsii*	South Africa	AF212448	KM361658	KM361640
F. aethiopicum	NRRL 46718	wheat seed	Ethiopia	FJ240296	KM361670	KM361652
	NRRL 46726	wheat seed	Ethiopia	MW233126	MW233470	MW233298
	NRRL 6227	*Triticum aestivum*	New South Wales, Australia	HM744692	JX171560	JX171446
	FRC R09335	*Triticum aestivum*	New South Wales, Australia	GQ915501	GQ915485	
F. concentricum (Outgroup)	CBS 450.97[T]	*Musa sapientum* fruit	Costa Rica	–	MT010981	MT010942
F. cortaderiae	NRRL 29297	*Cortaderia* sp.	New Zealand	MW233098	MW233442	MW233270
F. culmorum	NRRL 25475[T]	Barley	Denmark	MW233082	MW233425	MW233253
F. guizhouense	GZ7-20-1 *	Chinese fir	China	ON734381	ON734361	OR683260
	GZ7-20-1-1 *	Chinese fir	China	ON734382	ON734362	OR683261
	GZ7-20-1-2 *	Chinese fir	China	ON734383	ON734363	OR683262
	GZ7-20-1-3 *	Chinese fir	China	ON734384	ON734364	OR683263
F. graminearum	NRRL 31084	unknown	unknown	MW233103	JX171644	JX171531
F. langsethiae	NRRL 53439	oat kernel	Norway	HM744691	HQ154479	–
F. longipes	NRRL 20695	soil	USA	GQ915509	GQ915493	–
F. louisianense	NRRL 54197	*Triticum aestivum*	USA	KM889633	MW233478	MW233306
F. mesoamericanum	NRRL 25797	*Musa* sp.	Honduras	AF212441	MW233426	MW233254
F. poae	LC6917	*Oryza sativa*	China	MW620088	MW474613	MW024655
	LC13783	*Hordeum vulgare*	China	MW620087	MW474612	MW024654
	NRRL 26941[T]	Barley	USA	–	KU171706	KU171686
F. pseudograminearum	NRRL 28062[HT]	Unknown	Unknown	MW233090	JX171637	JX171524
F. sambucinum	MAFF 150447	Squash	Japan	LC637559	LC637561	–
	CBS 146.95[HT]	*Solanum tuberosum*	United Kingdom	KM231941	KM232381	–
F. sibiricum	NRRL 53432	Oat	Russia	HM744686	HQ154474	–
	NRRL 53430	Oat	Russia	HM744684	MW233474	MW233302
F. sporotrichioides	CBS 131779	*Avena sativa*	Canada	JX119003	JX162545	–
F. transvaalense	LLC3337	Soil	Australia	OP487291	OP486855	OP486422
	NRRL 31008	Soil	Australia	MW233102	MW233446	MW233274
F. venenatum	CBS 458.93[T]	Winter wheat	Australia	KM231942	KM232382	–
	NRRL 25413	Unknown	United Kingdom	MW233080	MW233423	MW233251
F. solani species complex						
F. ambrosium	NRRL 22346	*Euwallacea fornicatus*	India	FJ240350	EU329503	KC691587
	NRRL 20438	*Euwallacea fornicatus*	India	AF178332	JX171584	JX171470
F. bataticola	CBS 144397	*Ipomoea batatas*	USA	AF178343	EU329509	MW218099
	CBS 144398[T]	*Ipomoea batatas*	USA	AF178344	FJ240381	MW218100
F. borneense	CBS 145462	Bark or recently dead tree	Indonesia	AF178352	EU329515	MW834213
F. breviconum	CBS 203.31	Twig	Philippines	LR583599	LR583820	MW218103
F. cicatricum (Outgroup)	CBS 125552	Dead twig	Slovenia	HM626644	HQ728153	–
F. cryptoseptatum	CBS 145463[T]	Bark	French Guiana	AF178351	EU329510	MW834215
F. cucurbiticola	CBS 410.62	*Cucurbita viciifolia*	Netherlands	DQ247640	LR583824	MW834216
	CBS 616.66[T]	*Cucurbita viciifolia*	Netherlands	DQ247592	LR583825	MW834217

Species name	Culture/specimen[1]	Host	Country/area	GenBank/ENA accession number[2]		
				TEF−1α	RPB2	RPB1
F. euwallaceae	CBS 135854[T]	*Euwallacea* sp. on *Persea americana*	Israel	JQ038007	JQ038028	JQ038021
	NRRL 62626	*Euwallacea* sp. on *Persea americana*	USA	KC691532	KU171702	KU171682
F. haematococcum	CBS 119600[ET]	Dying tree	Sri Lanka	DQ247510	LT960561	–
F. helgardnirenbergiae	CBS 145469[T]	Bark	French Guiana	AF178339	EU329505	–
F. hunanense	HN33-8-2 *	Chinese fir	China	ON734393	ON734373	OR683272
	HN33-8-2-1 *	Chinese fir	China	ON734394	ON734374	OR683273
	HN33-8-2-2 *	Chinese fir	China	ON734395	ON734375	OR683274
	HN33-8-2-3 *	Chinese fir	China	ON734396	ON734376	OR683275
F. illudens	NRRL 22090	*Beilschmiedia tawa*	New Zealand	AF178326	JX171601	JX171488
F. kuroshium	CBS 142642[T]	*Euwallacea* sp. on *Platanus racemosa*	USA	KX262216	LR583837	MW834227
F. kurunegalense	CBS 119599[T]	Recently cut tree	Sri Lanka	DQ247511	LR583838	MW834228
F. lichenicola	CBS 279.34[T]	Human	Somalia	LR583615	LR583840	–
F. mahasenii	CBS 119594[T]	Dead branch on live tree	Sri Lanka	DQ247513	LT960563	MW834231
F. neocosmosporiellum	CBS 446.93[T]	Soil	Japan	LR583670	LR583898	MW834257
F. oligoseptatum	CBS 143241[T]	*Euwallacea validus* on *Ailanthus altissima*	USA	KC691538	LR583854	–
	NRRL 62578	*Euwallacea validus* on *Ailanthus altissima*	USA	KC691537	KC691626	KC691595
F. phaseoli	NRRL 31041[T]	*Glycine max*	USA	AY220193	JX171643	JX171530
F. piperis	CBS 145470[T]	*Piper nigrum*	Brazil	AF178360	EU329513	MW834241
F. plagianthi	NRRL 22632	*Hoheria glabrata*	New Zealand	AF178354	JX171614	JX171501
F. protoensiforme	CBS 145471[T]	Dicot tree	Venezuela	AF178334	EU329498	MW834244
F. pseudensiforme	CBS 130.78	*Cocos nucifera*	Indonesia	DQ247635	LR583868	MW834245
	CBS 125729[T]	Dead tree	Sri Lanka	KC691555	KC691645	KC691615
F. rectiphorum	CBS 125727[T]	Dead tree	Sri Lanka	DQ247509	LR583871	MW834249
F. samuelsii	CBS 114067[T]	Bark	Guyana	LR583644	LR583874	MW834252
F. staphyleae (Outgroup)	NRRL 22316	*Staphylea trifolia*	USA	AF178361	EU329502	JX171496
Fusarium sp.	YZU 171871	*Citrus sinensis*	China	MK370098	MK370099	–
	YZU 171870	*Citrus sinensis*	China	MH423886	MH423885	–
F. venezuelense	CBS 145473[T]	Bark	Venezuela	AF178341	EU329507	–
F. xiangyunensis	ZF-2018	Soil	China	MH992629	–	–
F. yamamotoi	CBS 144395	*Xanthoxylum piperitum* branch	Japan	AF178328	EU329496	MW218112
	CBS 144396[ET]	*Xanthoxylum piperitum* trunk	Japan	AF178336	FJ240380	MW218113

[1] BBA: Biologische Bundesanstalt für Land- und Forstwirtschaft, Institut für Mikrobiologie, Berlin, Germany; CBS: Westerdijk Fungal Biodiversity Institute (WI), Utrecht, The Netherlands; CPC: Collection of P.W. Crous, held at WI; HMAS: Herbarium Mycologicum Academiae Sinicae, Chinese Academy of Sciences, Beijing, China; NRRL: Agricultural Research Service Culture Collection, National Center for Agricultural Utilization Research, USDA, Peoria, IL, USA; URM: the University Recife Mycology culture collection at the Universidade Federal de Pernambuco, Recife, Brazil; FCCUFG: Fungal Culture Collection of the Universidade Federal de Goiás; FRC: Fusarium Research Center, University Park, PA, USA; MUCL: Mycotheque de lUniversite Catholique de Louvain, Louvain-la-Neuve, Belgium; [ET]: Ex-epitype, [LT]: Ex-lectotype, [NT]: Ex-neotype, [HT]: Ex-holotype, [T]: Ex-type, *: Sequences generated in this study.
[2] TEF-1α: translation elongation factor 1-alpha; RPB2: RNA polymerase second largest subunit; RPB1: RNA polymerase largest subunit.

Phylogenetic analyses

The sequences generated in this study were compared against nucleotide sequences in GenBank using BLAST to determine closely related taxa. Alignments of different loci, including the sequences obtained from this study and sequences downloaded from the GenBank, were initially performed with the MAFFT v.7 online server (https://mafft.cbrc.jp/alignment/server/) (Katoh and

Standley 2013) and then manually adjusted in MEGA v. 10 (Kumar et al. 2018). The post-alignment sequences of multiple loci were concatenated in Phylo-Suite software (Zhang et al. 2020). Maximum Likelihood (ML) and Bayesian Inference (BI) analyses were conducted with PhyloSuite software using IQ-TREE ver. 1.6.8 (Nguyen et al. 2015) and MrBayes v. 3.2.6 (Ronquist et al. 2012), respectively. ModelFinder was used to carry out statistical selection of best-fit models of nucleotide substitution using the corrected Akaike information criterion (AIC) (Kalyaanamoorthy et al. 2017) (Suppl. material 1: table S3). For ML analyses the default parameters were used and bootstrap support (BS) was carried out using the rapid bootstrapping algorithm with the automatic halt option. Bayesian analyses included two parallel runs of 2,000,000 generations, with the stop rule option and a sampling frequency set to each 1,000 generations. The 50% majority rule consensus trees and posterior probability (PP) values were calculated after discarding the first 25% of the samples as burn-in. Phylogenetic trees were visualized in FigTree v. 1.4.2 (http://tree.bio.ed.ac.uk/software/figtree/) (Rambaut 2014).

Phylogenetically related but ambiguous species were analyzed using the genealogical concordance phylogenetic species recognition (GCPSR) model by performing a pairwise homoplasy index (PHI) test as described by Quaedvlieg et al. (2014). The PHI test was performed in SplitsTree4 (Huson 1998; Huson and Bryant 2006) in order to determine the recombination level within phylogenetically closely related species using a concatenated multi-locus dataset (*TEF-1α*, *RPB2* and *RPB1*). If the pairwise homoplasy index results were below a 0.05 threshold ($\Phi_w < 0.05$), it indicates significant recombination present in the dataset. The relationship among the closely related species was visualized by constructing splits graphs.

Morphological study

One representative isolate was randomly selected from each *Fusarium* species for morphological research according to the method of Leslie and Summerell (2006). The isolates were transferred from the actively growing edge of a 4-day old colony by cutting mycelial blocks (6 mm in diameter), plated on to fresh potato dextrose agar (PDA) (Crous et al. 2021), oatmeal agar (OMA) (Crous et al. 2021), corn meal agar (CMA) (Thompson et al. 2013), and synthetic nutrient-poor agar (SNA) (Crous et al. 2021) plates and incubated at 25 °C in the dark. Alternatively, the isolates were also plated on to carnation leaf agar (CLA) (Crous et al. 2021) to induce sporulation when this failed on other media. The growth rate was recorded by measuring the diameter of the colonies until day 5, and the mean growth rate was calculated per day. The colony characters including colony color, texture, and pigment production were also recorded. The morphology and size of ascomata and conidiomata were studied and recorded using a Zeiss stereo microscope (SteRo Discovery v20). The shape, color and size of conidiophores, conidia were observed using a ZEISS Axio Imager A2m microscope (ZEISS, Germany) with differential interference contrast (DIC) optics. At least 30 measurements per structure were performed using Carl Zeiss Axio Vision software to determine their sizes, unless no or fewer individual structures were produced.

Pathogenicity tests

The fungal isolates HN43-17-1, SJ1-10, LC14, GZ7-20-1, and HN33-8-2 were randomly selected from the *Fusarium* species for Koch's postulates test. A conidial suspension of 10^6 conidia/ml of each isolate was used for inoculation.

For *in vitro* inoculation, healthy young leaves of *C. lanceolata* were collected from 1-year-old *C. lanceolata* plants on the campus of Nanjing Forestry University, Jiangsu, China. Detached leaves were surface-sterilized with 75% ethanol, washed three times with sterile water, and air-dried on sterile filter paper. A 10 µl aliquot of conidial suspension was transferred to a sterile plastic tube (6 mm diameter, 20 mm deep), in which a leaf was placed so that the base of the leaf was immersed in the conidial suspension. The control was treated with the same amount of double-distilled water. Leaves in the tubes were then put in plastic trays (40 × 25 cm), covered with a piece of plastic wrap to maintain relative humidity at 99%, and incubated at 25 °C in the dark for 5 days. Each treatment had eight replicates, and the experiment was conducted three times. Symptom development on the detached leaves was evaluated by determining the means of lesion lengths at 5 days post inoculation (dpi). The data were analyzed by analysis of variance (ANOVA) using SPSS v. 18 software. LSD's range test was used to determine significant differences among or between different treatments (Chung et al. 2020). Origin v. 8.0 software was used to draw histograms (Li et al. 2020).

For *in vivo* inoculation, shoots from *C. lanceolata* tissue culture seedlings provided by Fujian Yangkou Forest Farm, Fujian, China were used. Fifty-four bottles of seedlings (cultured with 0.6% water agar medium, one seedling per bottle) were prepared. A 10 µl aliquot of conidial suspension was applied onto each of the leader shoots. The same volume of distilled water was used as a control. After inoculation, the seedlings were incubated at 28 °C with a 12-h/12-h light/dark photoperiod for 10 days. The experiment was conducted three times, and each treatment had three replicates. Pathogens were re-isolated from the resulting lesions and identified as afore-described.

Results

Phylogenetic analyses

A total of 20 *Fusarium* isolates were isolated from the diseased *C. lanceolata* samples showing the symptom of leaf blight and used for phylogenetic analyses. Three-locus phylogenetic analysis used 37 isolates of 22 related taxa from the *F. fujikuroi* species complex. *Fusarium zealandicum* CBS 111.93 (ex-type) was used as the out-group. A total of 2219 characters (*RPB1*: 1-901, *RPB2*: 902-1692, *TEF-1α*: 1693-2219) were included in the phylogenetic analyses. The Bayesian Inference (BI) and Maximum-likelihood (ML) phylogenetic analyses of the isolates of *F. fujikuroi* species complex produced topologically similar trees. The BI posterior probabilities (PP) were plotted on the ML tree (Fig. 1). In the combined analyses, four isolates (SJ1-10, SJ1-10-1, SJ1-10-2, and SJ1-10-3) were placed in the same clade with *F. concentricum* with high support (ML-BS/BI-PP = 100/1). Four isolates (HN43-17-1, HN43-17-1-1, HN43-17-1-2, and HN43-17-1-3) clustered in *F. fujikuroi* clade with high supports (ML-BS/BI-PP = 100/1).
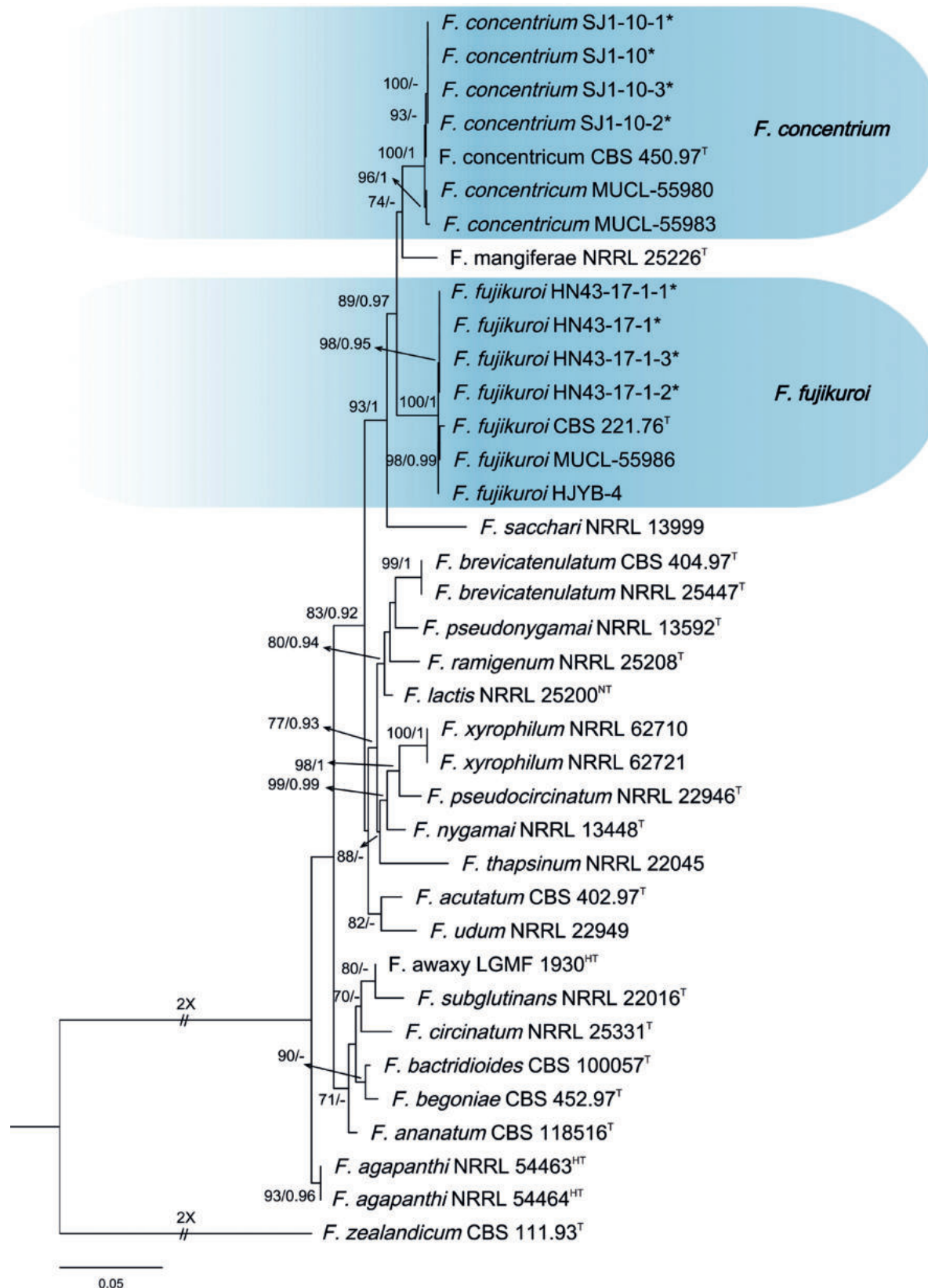
Figure 1. Phylogenetic relationships of 37 isolates of the *Fusarium fujikuroi* species complex with related taxa derived from concatenated sequences of the *TEF-1α*, *RPB2*, and *RPB1* genes/region using Bayesian inference (BI) and maximum likelihood (ML) methods. Bootstrap support values from ML ≥ 70% and BI posterior values ≥ 0.9 are shown at nodes (ML/BI). *Fusarium zealandicum* CBS 111.93[T] was the outgroup. * indicates strains of this study. [T] indicates ex-types or ex-epitypes. [LT]: Ex-lectotype, [NT]: Ex-neotype, [HT]: Ex-holotype.

The three-locus phylogenetic analysis used 16 isolates of 8 related taxa from the *F. lateritium* species complex. *Fusarium sublunatum* CBS 189.34 (ex-type) was used as the out-group. A total of 2063 characters (*RPB1*: 1-615, *RPB2*: 616-1391, *TEF-1α*: 1392-2063) were included in the phylogenetic analyses. The Bayesian Inference (BI) and Maximum-likelihood (ML) phylogenetic analyses of the isolates of *F. lateritium* species complex produced topologically similar trees. The BI posterior probabilities (PP) were plotted on the ML tree (Fig. 2). Phylogenetic analyses showed that the four isolates (LC14, LC14-1, LC14-2, and LC14-3) clustered in a distinct clade with high supports (ML-BS/BI-PP = 97/0.99), which was distinct from all other known species and closely related to *F. citri-sinensis* (ex-type, YZU 191316), *F. cassiae* (ex-holotype, MFLUCC 18-0573), *F. stilboides* (ex-type, CBS 746.79) (Fig. 2). When applying the GCPSR concept to these isolates, the concatenated sequence dataset of three-loci (*TEF-1α*, *RPB2*, and *RPB1*) was subjected to the PHI test showed that no significant recombination was detected among these isolates/taxa (Φ_w = 0.2461) (Fig. 3A), which was a solid support for the proposition that these isolates belonged to four distinct taxa.

The three-locus phylogenetic analysis used 41 isolates of 29 related taxa from the *F. solani* species complex. *Fusarium staphyleae* NRRL 22316 and
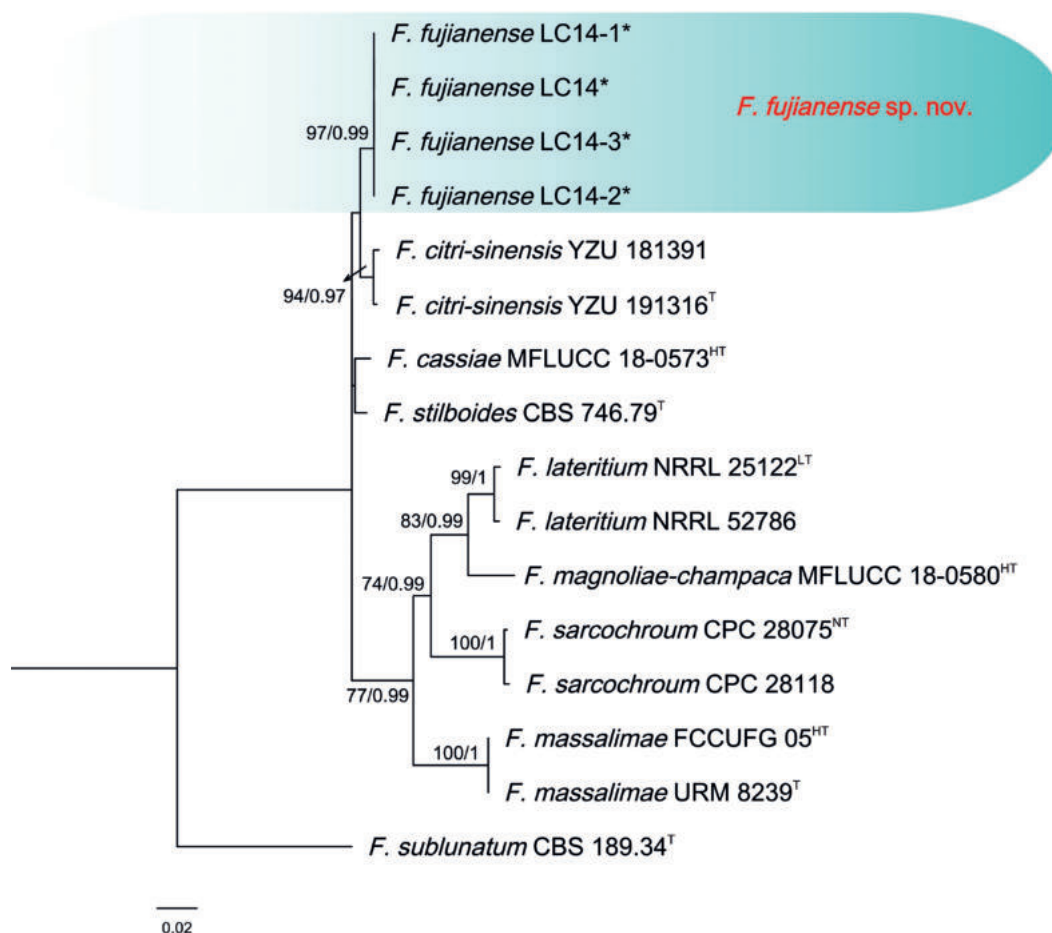

Figure 2. Phylogenetic relationships of 16 isolates of the *Fusarium lateritium* species complex with related taxa with concatenated sequences of the *TEF-1α*, *RPB2*, and *RPB1* loci using Bayesian inference (BI) and maximum likelihood (ML) methods. Bootstrap support values from ML ≥ 70% and BI posterior values ≥ 0.9 are shown at nodes (ML/BI). *Fusarium sublunatum* CBS 189.34[T] was the outgroup. * indicates strains of this study. [T] indicates the ex-type strains. [LT]: Ex-lectotype, [NT]: Ex-neotype, [HT]: Ex-holotype.
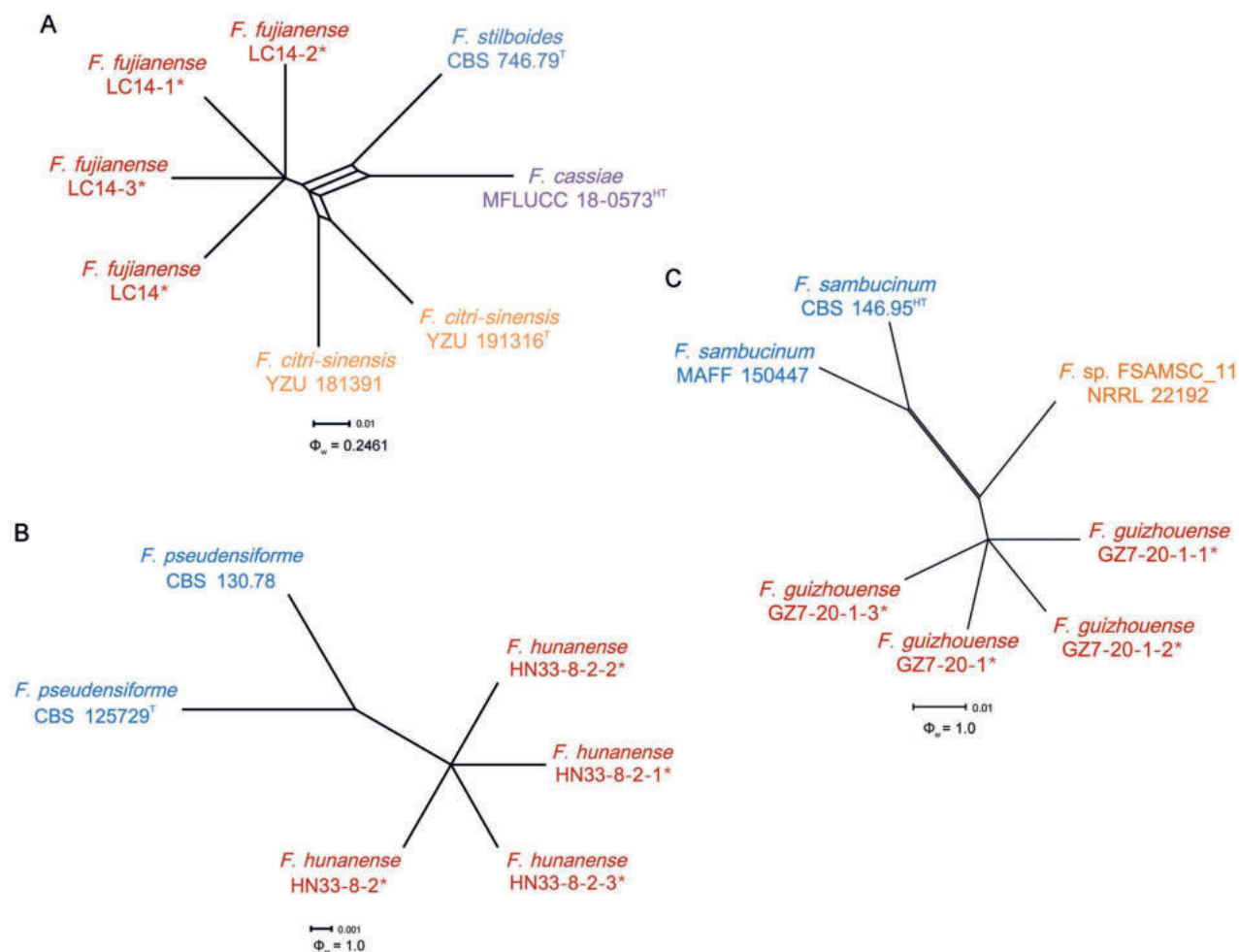
Figure 3. Splitgraphs showing the results of the pairwise homoplasy index (PHI) test of three newly described taxa and closely related species using both LogDet transformation and splits decomposition **A** the PHI of *Fusarium fujianense* sp. nov. with their phylogenetically related isolates or species **B** the PHI of *F. hunanense* sp. nov. with their phylogenetically related isolates or species **C** the PHI of *F. guizhouense* sp. nov. with their phylogenetically related isolates or species. PHI test value (Φ_w) < 0.05 indicate significant recombination within a dataset. * indicates isolates of this study. ^T indicates ex-types. ^{HT} indicates ex-holotypes.

F. cicatricum CBS 125552 were used as the out-group. A total of 2023 characters (*RPB1*: 1-640, *RPB2*: 641-1440, *TEF-1α*: 1441-2023) were included in the phylogenetic analyses. The Bayesian Inference (BI) and Maximum-likelihood (ML) phylogenetic analyses of the isolates of *F. solani* species complex produced topologically similar trees. The BI posterior probabilities (PP) were plotted on the ML tree (Fig. 4). Phylogenetic analyses showed that the four isolates (HN33-8-2, HN33-8-2-1, HN33-8-2-2, and HN33-8-2-3) clustered in a distinct clade with high supports (ML-BS/BI-PP = 100/1). These isolates were distinct from all other known species and closely related to *F. pseudensiforme* (ex-type, CBS 125729) (Fig. 4). When applying the GCPSR concept to this species, the concatenated sequence dataset of three-loci (*TEF-1α*, *RPB2*, and *RPB1*) was subjected to the PHI test showed that no significant recombination was detected among these isolates/taxa (Φw = 1.0) (Fig. 3B), which was a good support for the proposition that these isolates belonged to two distinct taxa.

The three-locus phylogenetic analysis used 30 isolates of 18 related taxa from the *F. sambucinum* species complex. *Fusarium concentricum* CBS 450.97
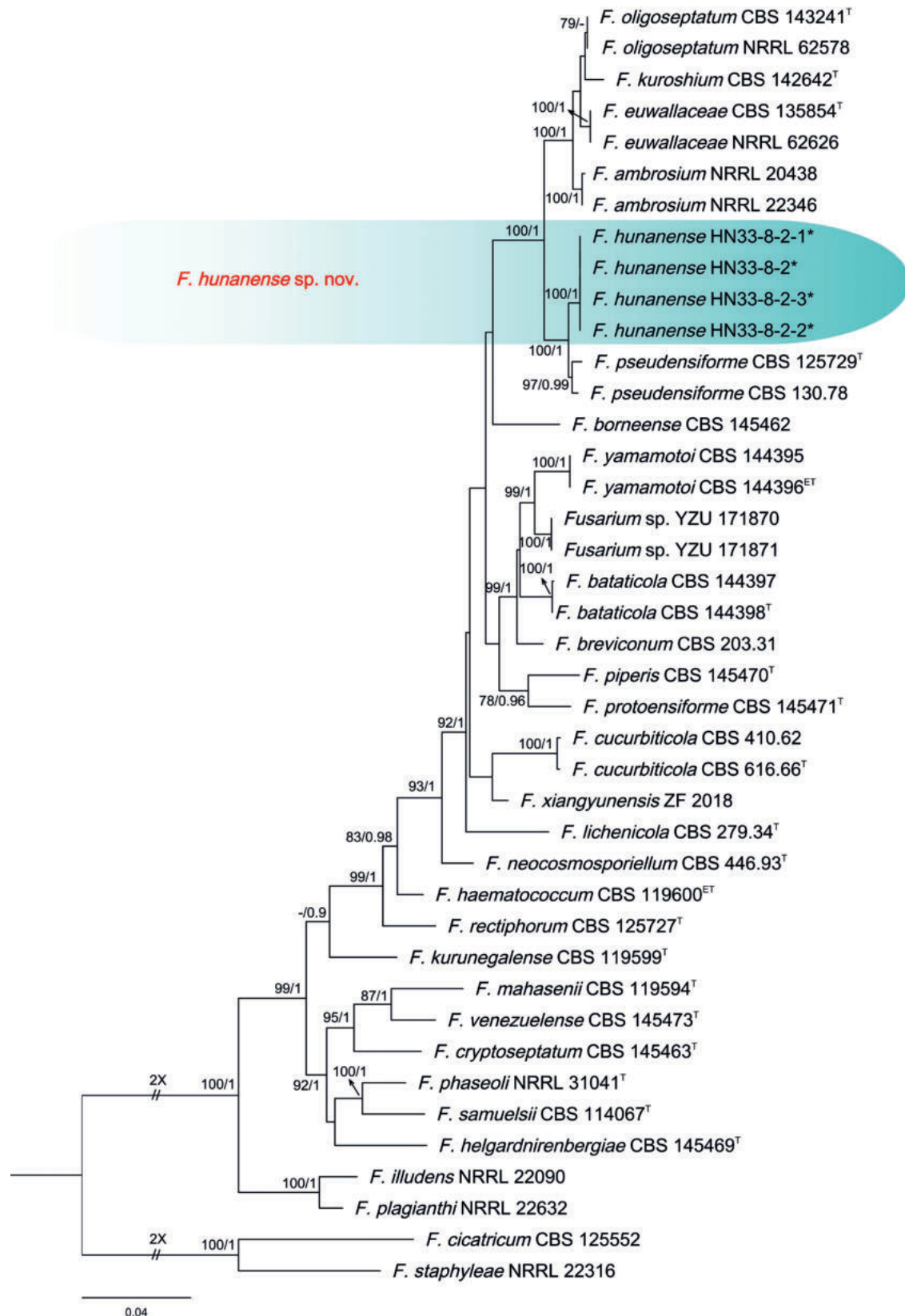
Figure 4. Phylogenetic relationships of 41 isolates of the *Fusarium solani* species complex with related taxa with concatenated sequences of the *TEF-1α*, *RPB2*, and *RPB1* loci using Bayesian inference (BI) and maximum likelihood (ML) methods. Bootstrap support values from ML ≥ 70% and BI posterior values ≥ 0.9 are shown at nodes (ML/BI). *Fusarium staphyleae* NRRL 22316 and *F. cicatricum* CBS 125552 were the outgroup. * indicates strains of this study. [T] indicates the ex-type strains. [ET] indicates ex-epitypes.

(ex-type) was used as the out-group. A total of 2115 characters (*RPB1*: 1-641, *RPB2*: 642-1538, *TEF-1α*: 1539-2115) were included in the phylogenetic analyses. The Bayesian Inference (BI) and Maximum-likelihood (ML) phylogenetic analyses of the isolates of *F. sambucinum* species complex produced topologically similar trees. The BI posterior probabilities (PP) were plotted on the ML tree (Fig. 5). Phylogenetic analyses showed that the four isolates (GZ7-20-1, GZ7-20-1-1, GZ7-20-1-2, and GZ7-20-1-3) clustered in a distinct clade with high supports (ML-BS/BI-PP = 100/1), which was distinct from all other known species and identified as closely related to *F. venenatum* (ex-type, CBS 458.93), *F. poae* (ex-type, NRRL 26941), and *F. sambucinum* (ex-holotype, CBS 146.95) (Fig. 5). When applying the GCPSR concept to these isolates, the concatenated sequence dataset of three-loci (*TEF-1α*, *RPB2*, and *RPB1*) was subjected to the PHI test and showed that no significant recombination was detected among these isolates/taxa (Φ_w = 0.7313) (Fig. 3C). The split tree decomposition network of these multiple combinations was clearly detected within four separate groups.

Taxonomy

The results of the molecular analyses and observations of morphological characteristics in culture indicated that the 20 isolates from *C. lanceolata* belonged to five *Fusarium* species, among which two were known taxa (*F. concentricum* and *F. fujikuroi*) and three were new to science (*F. fujianense*, *F. guizhouense*, and *F. hunanense*). This study selected the representative strains of each *Fusarium* species SJ1-10 (*F. concentricum*), LC14 (*F. fujianense*), HN43-17-1 (*F. fujikuroi*), GZ7-20-1 (*F. guizhouense*), and HN33-8-2 (*F. hunanense*) for detailed morphological characterization.

Fusarium concentricum Nirenberg & O'Donnell, Mycologia 90 (3): 442 (1998)
MycoBank No: 444884
Suppl. material 1: fig. S1

Description. Sexual state not observed. Asexual state: sporulation abundant from sporodochia, rarely from conidiophores formed directly on the substrate mycelium. Conidiophores in the aerial mycelium branched, bearing terminal or intercalary monophialides, often reduced to single phialides. Phialides subulate to subcylindrical, smooth, thin-walled, (2.3−)4.9−15.5(−18.3) × (1.1−)1.4−2.8(−3.5) μm, (mean ± SD = 10.2 ± 5.3 × 2.1 ± 0.7 μm, n = 9), without periclinal thickening. Microconidia in the aerial mycelium hyaline, ellipsoidal to falcate, smooth, thin-walled, 0−1-septate, (3.8−)5.9−9.1(−11.3) × (1.9−)2.5−3.4(−4.3) μm (mean ± SD = 7.5 ± 1.6 × 3.0 ± 0.5 μm, n = 60), forming small false heads on the tips of monophialides. Sporodochia pale orange colored, formed abundantly on carnation leaves. Conidiophores in sporodochia (27.7−)40.6−49.8(−51.7) μm, (mean ± SD = 45.2 ± 4.6 μm, n = 35), verticillately branched and densely packed, bearing apical whorls of 2−3 monophialides or rarely single lateral monophialides; sporodochial phialides subulate to subcylindrical, (9.5−)11.4−16.5(−20.4) × (2.2−)2.7−4.0(−4.7) μm, (mean ± SD = 13.9 ± 2.5 × 3.4 ± 0.6 μm, n = 45), smooth, thin-walled. Sporodochial macroconidia falcate, curved dorsiventrally with almost parallel sides tapering slightly towards both ends, with
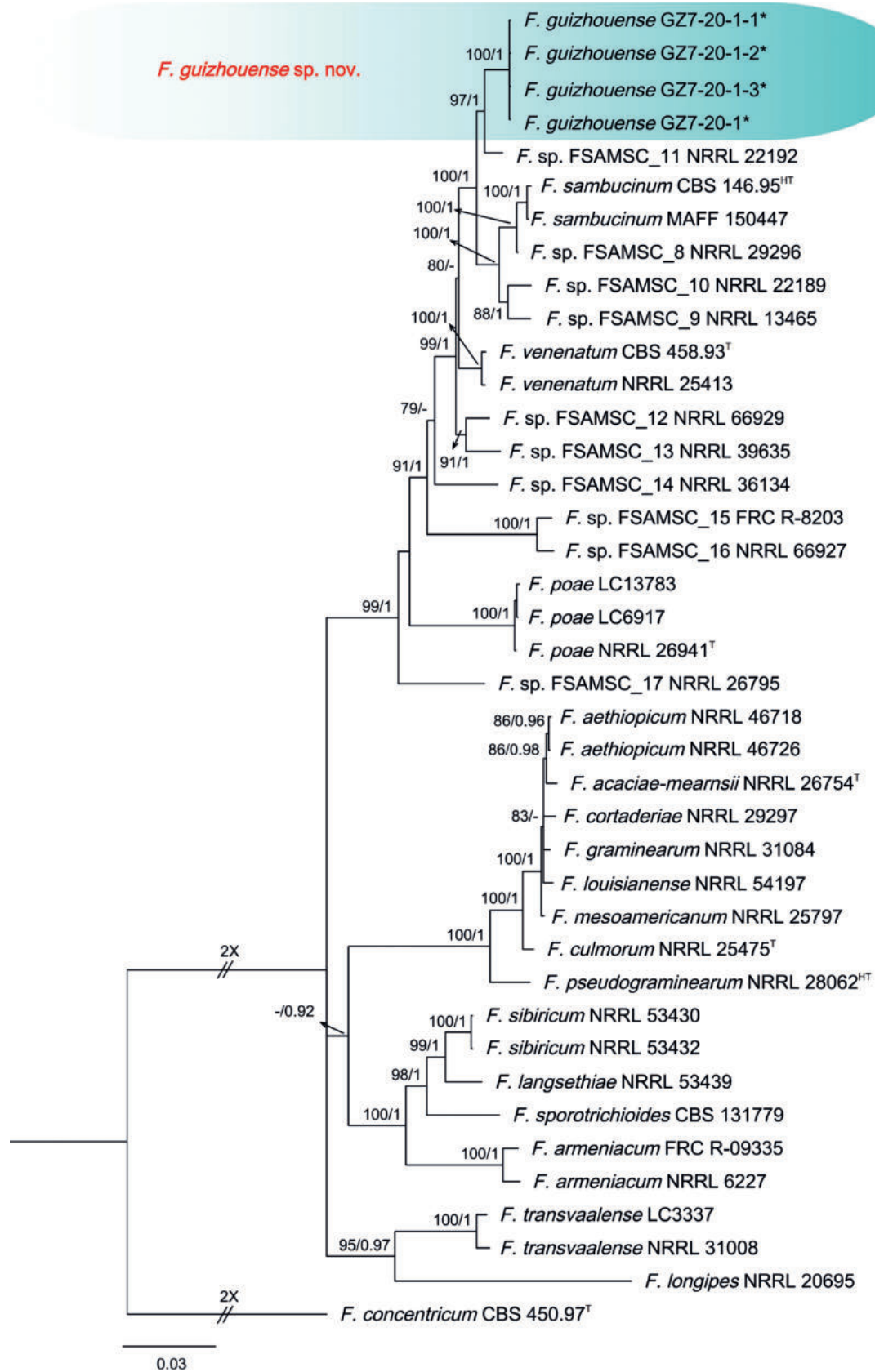
Figure 5. Phylogenetic relationships of 30 isolates of the *Fusarium sambucinum* species complex with related taxa with concatenated sequences of the *TEF-1α, RPB2*, and *RPB1* loci using Bayesian inference (BI) and maximum likelihood (ML) methods. Bootstrap support values from ML ≥ 70% and BI posterior values ≥ 0.9 are shown at nodes (ML/BI). *F. concentricum* CBS 450.97[T] was the outgroup. * indicates strains of this study. [T] indicates the ex-type strains. [HT] indicates ex-holotypes.

a blunt to papillate, curved apical cell and a foot cell, 3-septate, (23.2−)30.2−40.5(−43.7) × (3.4−)3.9−4.9(−5.5) μm, (mean ± SD = 35.3 ± 5.2 × 4.4 ± 0.5 μm, n = 60), 4-septate, (35.5−)38.0−48.8(−49.4) × (3.4−)3.4−4.3(−4.4) μm, (mean ± SD = 43.4 ± 5.4 × 3.9 ± 0.4 μm, n = 10), 5-septate, (49.5−)49.7−57.2(−59.1) × (3.5−)3.6−4.2(−4.2) μm, (mean ± SD = 53.4 ± 3.6 × 3.9 ± 0.3 μm, n = 10), hyaline, thin- and smooth-walled. Chlamydospores absent.

Culture characteristics. Colonies on PDA growing in the dark with an average growth rate of 9.3 mm/d at 25 °C. Colony surface white to pale purple, flat or slightly raised at the center; colony margins irregular, filiform. Reverse light yellow. Odor absent. Colonies on SNA incubated at 25 °C in the dark were regular, round, aerial mycelium absent or scant, growing at 13.1 mm/d. Colonies on OMA incubated at 25 °C in the dark were regular, round, aerial mycelium abundant, loose to densely floccose, growing at 13.2 mm/d. Reverse light purple. Colonies on CMA incubated at 25 °C in the dark were regular, round, colony surface and reverse pale gray at the center, aerial mycelium absent or scarce, growing at 11.9 mm/d.

Materials examined. CHINA, Guangxi Zhuang Autonomous Region, Liuzhou City, Sanjiang Dong Autonomous County, Guyi Town, 25°25'48"N, 109°28'47"E, isolated from leaf spots of *Cunninghamia lanceolata*, May 2017, Wen-Li Cui, isolates: SJ1-10, SJ1-10-1, SJ1-10-2, SJ1-10-3.

Notes. The isolate SJ1-10 in this study was in the same clade with *F. concentricum* CBS 450.97 (ex-type). Morphologically, 0-septate microconidia (3.8−11.3 × 1.9−4.3 μm) of the isolate SJ1-10 were similar with the 0-septate microconidia (7.0−12.2 ×2.3−3.9 μm) of the ex-type (CBS 450.97) of *F. concentricum* (Nirenberg and O'Donnell 1998). Five-septate macroconidia (49.5−59.1 × 3.5−4.2 μm) of the isolate SJ1-10 were similar with the 5-septate macroconidia (49.0−64.8 × 3.6−4.0 μm) of the ex-type (CBS 450.97) of *F. concentricum* (Nirenberg and O'Donnell 1998).

Fusarium fujikuroi **Nirenberg, Mitteilungen der Biologischen Bundesanstalt für Land- und Forstwirtschaft 169: 32 (1976)**
MycoBank No: 314213
Suppl. material 1: fig. S2

Description. Sexual state not observed. Asexual state: Sporulation abundant from sporodochia, rarely from conidiophores formed directly on the substrate mycelium. Conidiophores in the aerial mycelium branched, bearing terminal or intercalary phialides. Phialides subulate to subcylindrical, smooth, thin-walled, (11.5−)14.7−22.9(−30.0) μm × (1.8−)2.0−3.6(−4.0) μm, (mean ± SD = 18.8 ± 4.1 μm × 2.8 ± 0.8 μm, n = 37), without periclinal thickening; microconidia hyaline, short clavate to cylindrical, slender to relatively straight, smooth, thin-walled, 0-septate, (5.4−)6.7−11.3(−15.5) × (2.0−)2.5−3.5(−4.4) μm, (mean ± SD = 9.0 ± 2.3 × 3.0 ± 0.5 μm, n = 81), forming small false heads on the tips of phialides. Chlamydospores formed occasionally, mostly in pairs or chains, terminal or intercalary, globose to subglobose, smooth-walled, (6.0−)6.2−8.0(−8.3) × (4.4−)4.4−5.2(−5.6) μm, (mean ± SD = 7.1 ± 0.9 × 4.8 ± 0.4 μm, n = 6). Sporodochia and macroconidia not observed.

Culture characteristics. Colonies on PDA growing in the dark with an average growth rate of 13.9 mm/d at 25 °C. Colony surface white to purple, flat or slight-

ly raised at the center; colony round, regular, margins filiform, aerial mycelium abundant. Reverse purple with white periphery. Odor absent. Colonies on SNA incubated at 25 °C in the dark were regular, round, growing at 8.1 mm/d. Colony surface pure white, aerial mycelium absent or scant. Reverse pure white, without diffusible pigments. Colonies on OMA incubated at 25 °C in the dark were regular, round, aerial mycelium abundant, loose to densely floccose, growing at 12.5 mm/d. Colony white to dark purple and with white to dark violet pigmentation. Colonies on CMA incubated at 25 °C in the dark were regular, round, colony surface and reverse white, aerial mycelium absent or scant, growing at 11.3 mm/d.

Materials examined. CHINA, Hunan province, Yiyang City, Heshan District, Henglongqiao Town, 28°27'24"N, 112°29'7"E, isolated from leaf spots of *Cunninghamia lanceolata*, May 2017, Wen-Li Cui, isolates: HN43-17-1, HN43-17-1-1, HN43-17-1-2, HN43-17-1-3.

Notes. The isolate HN43-17-1 in this study was in the same clade with *F. fujikuroi* CBS 221.76 (ex-type). Morphologically, 0-septate microconidia, (5.4–15.5 × 2–4.4 μm) of the isolate HN43-17-1 were more variable than the 0-septate microconidia (12.2–12.9 × 3.4–3.7 μm) of the ex-type (CBS 221.76) of *F. fujikuroi* (Ibrahim et al. 2016).

Fusarium fujianense Lin Huang, Jiao He & D.W. Li, sp. nov.

Index Fungorum Number: IF900473

Fig. 6

Etymology. Epithet is after Fujian province where the type specimen was collected.

Holotype. CHINA, Fujian Province, Nanping City, Shunchang County, Yangkou Forest Farm, 26°48'36"N, 117°52'48"E, isolated from leaf spots of *Cunninghamia lanceolata*, May 2017, Wen-Li Cui, (holotype: CFCC 57576). Holotype specimen is a living specimen being maintained via lyophilization at the China Forestry Culture Collection Center (CFCC). Ex-type (LC14) is maintained at the Forest Pathology Laboratory, Nanjing Forestry University.

Host/distribution. From *C. lanceolata* in Yangkou Forest Farm, Shunchang County, Nanping City, Fujian Province, China.

Description. Sexual state not observed. Asexual state: Sporulation abundant from sporodochia, rarely from conidiophores formed directly on the substrate mycelium. Conidiophores in the aerial mycelium unbranched, bearing terminal or intercalary monophialides, often reduced to single phialides. Phialides subulate to subcylindrical, smooth, thin-walled, (9.2–)10.3–16.3(–18.0) μm × (2.5–)2.6–3.4(–3.6) μm, (mean ± SD = 13.3 ± 3.0 μm × 3.0 ± 0.4 μm, n = 11), without periclinal thickening; microconidia subcylindrical to clavate, hyaline, smooth- and thin-walled, 0-septate, (5.6–)6.0–8.2(–8.3) μm × (1.9–)2.1–2.5(–2.7) μm, (mean ± SD = 7.1 ± 1.1 μm × 2.3 ± 0.2 μm, n=11), forming small false heads on the tips of monophialides. Sporodochia pale orange colored, formed abundantly on PDA after 40 days. Conidiophores in sporodochia (9.7–)18.8–31.5(–37.9) μm, (mean ± SD = 25.1 ± 6.4 μm, n = 37), irregularly branched and densely packed, bearing apical whorls of monophialides or 2–3 ployphialides; sporodochial phialides subulate to subcylindrical, (5.6–)10.0–16.1(–18.8) × (1.4–)2.5–3.9(–4.8) μm, (mean ± SD = 12.7 ± 3.4 × 3.2 ± 0.7 μm, n = 39), smooth, thin-walled. Sporodochial mesoconidia falcate, curved dorsiventrally with almost parallel sides ta-
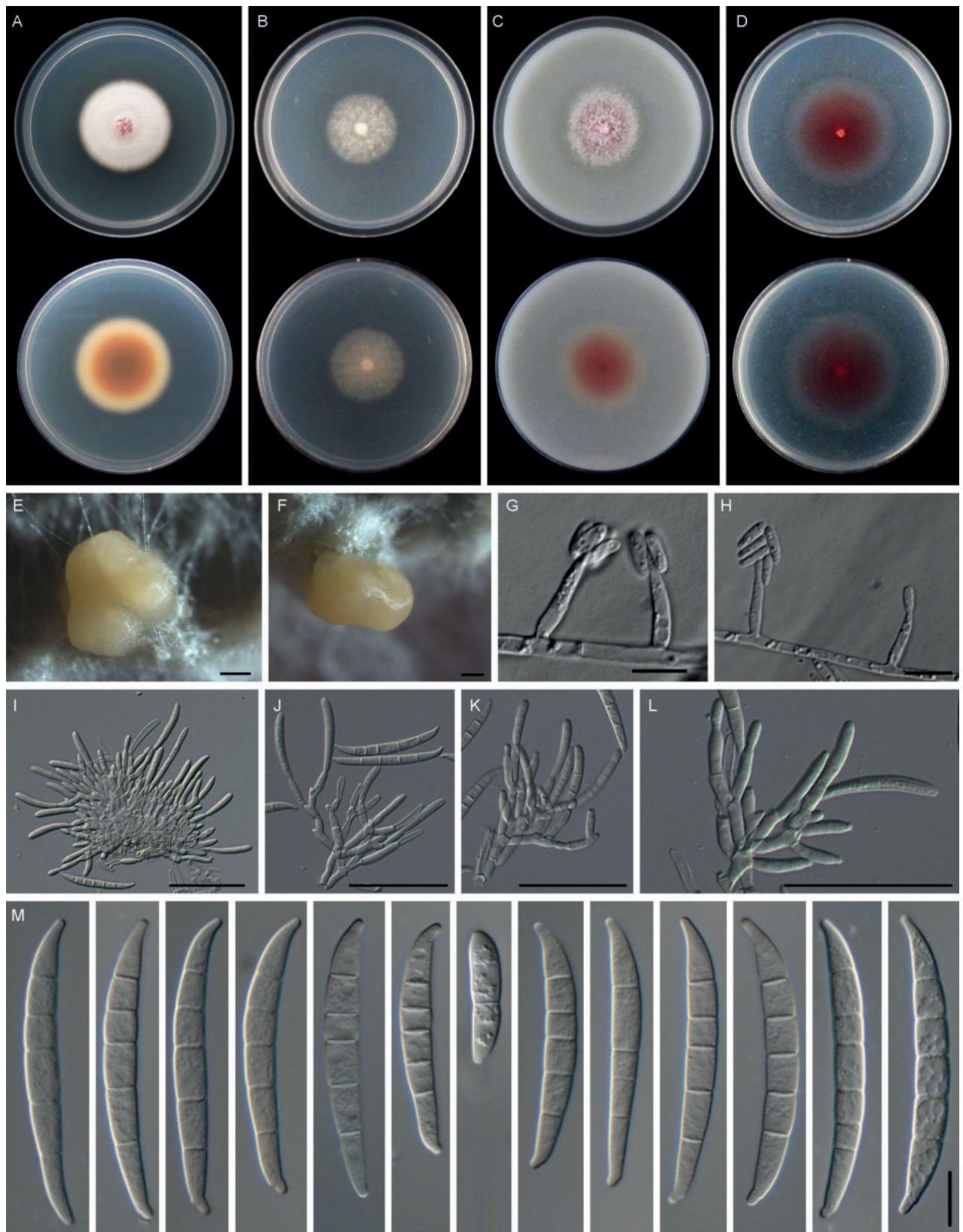
Figure 6. *Fusarium fujianense* (LC14) **A–D** colonies on PDA, SNA, OMA, and CMA, respectively, after 5 days at 24 °C in the dark **E, F** sporodochia formed on PDA **G, H** aerial conidiophores, phialides, and microconidia **I–L** sporodochial conidiophores, phialides, and macroconidia **M** mesoconidium (1-septate) and macroconidia (4–6-septate). Scale bars: 200 μm (**E, F**); 10 μm (**G–M**).

pering slightly towards both ends, with a blunt to papillate, curved apical cell and a foot-like basal cell, 1-septate, (21.8−)22.0−23.6(−23.8) × (4.7−)4.9−5.3(−5.3) μm, (mean ± SD = 22.8 ± 0.8 × 5.1 ± 0.2 μm, n = 6), macroconidia 4−6-septate, (40.2−)45.9−59.1(−63.4) × (4.5−)4.8−5.8(−6.9) μm, (mean ± SD = 52.5 ± 6.6 × 5.3 ± 0.5 μm, n = 18), hyaline, smooth, thin-walled. Chlamydospores absent.

Culture characteristics. Colonies on PDA growing in the dark with an average growth rate of 6.2 mm/d at 25 °C. Colony surface white to red, flat or slightly raised at the center; colony margins regular, round. Reverse red with white periphery. Odor absent. Colonies on SNA incubated at 25 °C in the dark were regular, round, growing at 5.4 mm/d. Colony surface pure white, aerial mycelium abundant. Reverse pure white, without diffusible pigments. Colonies on OMA incubated at 25 °C in the dark were regular, round, aerial mycelium abundant, loose to densely floccose, growing at 6.0 mm/d. Reverse red with white periphery. Colonies on CMA incubated at 25 °C in the dark were regular, round, colony surface and reverse red with white periphery, aerial mycelium absent or scant, growing at 7.1 mm/d.

Additional materials examined. Chına, Fujian Province, Nanping City, Shunchang County, Yangkou Forest Farm, 26°48'36"N, 117°52'48"E, isolated from leaf spots of *Cunninghamia lanceolata*, May 2017, Wen-Li Cui, isolates: LC14-1, LC14-2, LC14-3.

Notes. The isolates of *F. fujianense* were phylogenetically closely related to *F. citri-sinensis* (ex-type, YZU 191316), *F. cassiae* (ex-holotype, MFLUCC 18-0573), and *F. stilboides* (ex-type, CBS 746.79) (Fig. 2). Between *F. fujianense* isolates and ex-type of *F. citri-sinensis* YZU 191316, there were 13/672 differences in *TEF-1α*, and 8/776 in *RPB2*. Between *F. fujianense* isolates and ex-holotype of *F. cassiae* MFLUCC 18-0573, there were 25/672 differences in *TEF-1α*, and 7/776 in *RPB2*. Between *F. fujianense* isolates and ex-type of *F. stilboides* CBS 746.79, there were 16/672 differences in *TEF-1α*, and 2/776 in *RPB2*. The *RPB1* sequences of *F. stilboides* CBS 746.79, *F. cassiae* MFLUCC 18-0573, and *F. citri-sinensis* YZU 191316 were missing. The PHI analysis showed that there was no significant recombination between *F. fujianense* isolates and its related species (Φw = 0.2461) (Fig. 3A). Morphologically, *F. fujianense* differed from *F. citri-sinensis* in colony characteristics on PDA. The former developed dense mycelia and abundant red pigmentation, while the latter was characterized by sparse and loose aerial mycelia and pale pink pigment (Zhao et al. 2022). *F. fujianense* can be differentiated from *F. cassiae* in having abundant red pigmentation produced in PDA vs. without diffusible pigments in *F. cassiae* (Perera et al. 2020). *F. fujianense* can be distinguished from *F. stilboides* by having different 0-septate conidia (5.6−8.3 × 1.9−2.7 μm vs. 7−14 × 2−2.5 μm) (Booth and Waterston 1964). Thus, *F. fujianense* is recognized as a novel species in *F. lateritium* species complex.

Fusarium guizhouense Lin Huang, Jiao He & D.W. Li, sp. nov.
Index Fungorum Number: IF900474
Fig. 7

Etymology. Epithet is after Guizhou Province where the type specimen was collected.

Holotype. Chına, Guizhou Province, Qiandongnan Miao and Dong Autonomous Prefecture, Cengong County, Kelou Town, 27°22'58"N, 108°22'9"E, isolated

from leaf spots of *Cunninghamia lanceolata*, May 2017, Wen-Li Cui, (holotype: CFCC 57575). Holotype specimen is a living specimen maintained via lyophilization at the China Forestry Culture Collection Center (CFCC). Ex-type (GZ7-20-1) is maintained at the Forest Pathology Laboratory, Nanjing Forestry University.

Host/distribution. From *C. lanceolata* in Kelou Town, Cengong County, Qiandongnan Miao and Dong Autonomous Prefecture, Guizhou Province, China.

Description. Sexual state not observed. Asexual state: Sporulation abundant from sporodochia, rarely from conidiophores formed directly on the substrate mycelium. Conidiophores in the aerial mycelium absent. Sporodochia bright orange colored, formed abundantly on carnation leaves. Conidiophores in sporodochia (13.8−)18.8−25.8(−29.8) μm, (mean ± SD = 22.3 ± 3.5 μm, n = 39), irregularly branched and densely packed, bearing apical whorls of 1−4 phialides; sporodochial phialides subulate to subcylindrical, (8.2−)10.6−14.7(−16.9) × (2.7−)3.1−4.0(−4.8) μm, (mean ± SD = 12.6 ± 2.0 × 3.6 ± 0.5 μm, n = 40), smooth, thin-walled. Sporodochial macroconidia colorless, straight or slightly curved, wider at the middle or apical part, tapering towards the base, with a blunt and often curved apical cell and a foot-like to slightly notched basal cell, 4−5-septate. Four-septate conidia: (30.8−)33.3−40.9(−40.6) × (4.5−)5.3−6.4(−6.9) μm, (mean ± SD = 37.1 ± 3.8 × 5.9 ± 0.5 μm, n = 52), five-septate conidia: (33.4−)38.0−45.4(−51.3) × (5.0−)5.7−6.9(−7.5) μm, (mean ± SD = 41.7 ± 3.7 × 6.3 ± 0.6 μm, n = 60), smooth, thin-walled. Chlamydospores absent.

Culture characteristics. Colonies on PDA growing in the dark with an average growth rate of 16.7 mm/d at 25 °C. Colony color white at first, becoming buff, felty to cottony. Aerial mycelium abundant, loose to densely floccose; margins irregular and fimbriate. Reverse pale buff with white periphery. Odor absent. Colonies on SNA incubated at 25 °C in the dark were irregular, growing at 9.7 mm/d. Colony surface pure white, aerial mycelium scant, forming irregular rings at the periphery of the colony; margins lobate or serrate. Reverse pure white, without diffusible pigments. Colonies on OMA incubated at 25 °C in the dark were irregular, aerial mycelium abundant, loose to densely floccose, growing at 13.1 mm/d. Colony in reverse was white with litter gray pigmentation. Colonies on CMA incubated at 25 °C in the dark were round, colony surface and reverse white, flat, radially striated, membranous to dusty, aerial mycelium scant or absent; colony margins irregular, lobate or serrate, growing at 9.6 mm/d.

Additional materials examined. CHINA, Guizhou province, Qiandongnan Miao and Dong Autonomous Prefecture, Cengong County, Kelou Town, 27°22'58"N, 108°22'9"E, isolated from leaf spots of *Cunninghamia lanceolata*, May 2017, Wen-Li Cui, isolates: GZ7-20-1-1, GZ7-20-1-2, GZ7-20-1-3.

Notes. The isolates of *F. guizhouense* were phylogenetically close to *F. sambucinum* (ex-holotype, CBS 146.95), *F. poae* (ex-type, NRRL 26941), and *F. venenatum* (ex-type, CBS 458.93) (Fig. 5). Between *F. guizhouense* isolates and ex-holotype of *F. sambucinum* CBS 146.95, there were 34/577 differences in *TEF-1α*, 8/897 in *RPB2*. The *RPB1* sequence of *F. sambucinum* CBS 146.95 was missing. Between *F. guizhouense* isolates and ex-type of *F. poae* NRRL 26941, there were 24/897 differences in *RPB2*, 26/641 in *RPB1*. The *TEF-1α* sequence of *F. poae* NRRL 26941 was missing. Between *F. guizhouense* isolates and ex-type of *F. venenatum* CBS 458.93, there were 20/577 differences in *TEF-1α*, 8/897 in *RPB2*. The *RPB1* sequence of *F. venenatum* CBS 458.93 was missing. The PHI analysis showed that there was no significant recombination between *F. guizhouense* isolates and
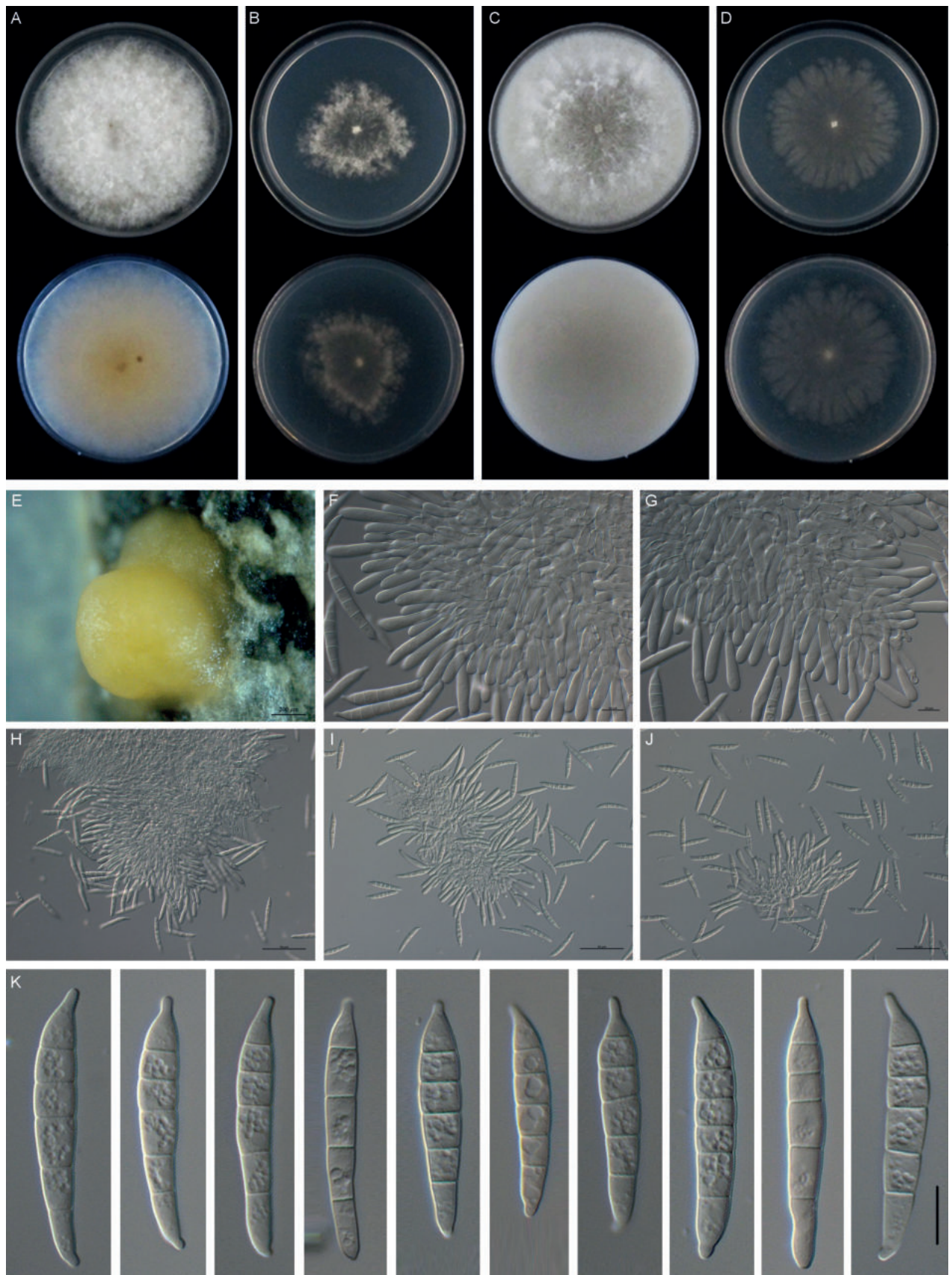
Figure 7. *Fusarium guizhouense* (GZ7-20-1) **A–D** colonies on PDA, SNA, OMA, and CMA, respectively, after 5 days at 24 °C in the dark **E** sporodochia formed on the surface of carnation leaves **F–J** sporodochial conidiophores, phialides, and macroconidia **K** macroconidia (4–6-septate). Scale bars: 200 μm (**E**); 10 μm (**F, G, K**); 50 μm (**H–J**).

its related species (Φ_w = 0.7313) (Fig. 3C). Morphologically, Sporodochial phialides of the *F. guizhouense* isolates (10.6−14.7 × 3.1−4.0 µm) were smaller than those of *F. sambucinum* NRRL 22203 (ex-lectotype) (14.0−18.0 × 3.8−4.5 µm) (Nirenberg 1995). *Fusarium* sp. FSAMSC_11 (NRRL 22192) is closely related to *F. guizhouense*, but it has no morphological data available (Laraba et al. 2021). Further study on this isolate (NRRL 22192) is necessary to determine its taxonomic placement. In conclusion, the phylogenetic and morphological evidence support this fungus being a new species within the *F. sambucinum* species complex.

Fusarium hunanense Lin Huang, Jiao He & D.W. Li, sp. nov.
Index Fungorum Number: IF900475
Fig. 8

Etymology. Epithet is named after Hunan Province where the type specimen was collected.

Holotype. CHINA, Hunan Province, Yiyang City, Heshan District, Henglongqiao Town, 28°27'24"N, 112°29'7"E, isolated from leaf spots of *Cunninghamia lanceolata*, May 2017, Wen-Li Cui, (holotype: CFCC 57574). Holotype specimen is a living specimen maintained via lyophilization at the China Forestry Culture Collection Center (CFCC). Ex-type (HN33-8-2) is maintained at the Forest Pathology Laboratory, Nanjing Forestry University.

Host/distribution. From *C. lanceolata* in Henglongqiao Town, Heshan District, Yiyang City, Hunan Province, China.

Description. Sexual state not observed. Asexual state: sporulation abundant from erect conidiophores formed on the agar surface or aggregated in sporodochia. Conidiophores in the aerial mycelium, mostly unbranched, rarely basally dichotomously branched, forming monophialides on the apices; phialides slender, subulate to subcylindrical, monophialidic, smooth, thin-walled, (29.6−)31.6−54.6(−74.1) × (2.0−)2.2−2.8(−3.0) µm, (mean ± SD = 43.1± 11.5 × 2.5 ± 0.3 µm, n = 17), with slight periclinal thickening at the tip and a short flared apical collarette. Sporodochia cream colored, produced on the surface of carnation leaves and PDA medium. Conidiophores in sporodochia (26.0−)29.3−39.1(−46.8) µm, (mean ± SD = 34.1 ± 5.1 µm, n = 39), irregularly branched, short stipitate, occasionally in whorls bearing terminal 2−4 monophialides; sporodochial phialides subulate to subcylindrical, smooth, thin-walled, (11.4−)15.5−22.1(−28.6) × (3.3−)4.0−5.2(−6.0) µm, (mean ± SD = 18.8 ± 3.3 × 4.6 ± 0.6 µm, n = 51), with periclinal thickening and a small, flared collarette. Sporodochial macroconidia cylindrical to falcate, gently curved, typically with a blunt and almost rounded apical cell and a barely notched foot cell, 3−6-septate, hyaline, smooth, thin-walled. Three-septate conidia: (22.1−)22.6−39.4(−54.7) × (5.0−)5.5−6.7(−7.4) µm, (mean ± SD = 31.0 ± 8.4 × 6.1 ± 0.6 µm, n = 11); four-septate conidia: (50.3−)54.4−68.2(−69.6) × (6.9−)6.9−7.7(−8.0) µm, (mean ± SD = 61.3 ± 6.9 × 7.3 ± 0.4 µm, n = 10); five-septate conidia: (51.8−)60.6−73.0(−78.2) × (6.4−)6.1−7.1(−8.5) µm, (mean ± SD = 66.8 ± 6.2 × 6.6 ± 0.5 µm, n = 31); six-septate conidia: (69.8−)70.7−77.7(−79.6) × (7.1−)7.5−8.3(−8.3) µm, (mean ± SD = 74.2 ± 3.5 µm × 7.9 ± 0.4 µm, n = 10). Chlamydospores developed in large numbers in hyphae and also in mature macroconidia. The chlamydospores were 0−1-septate, globose to ellipsoidal, constricted at the septum, intercalary or terminal

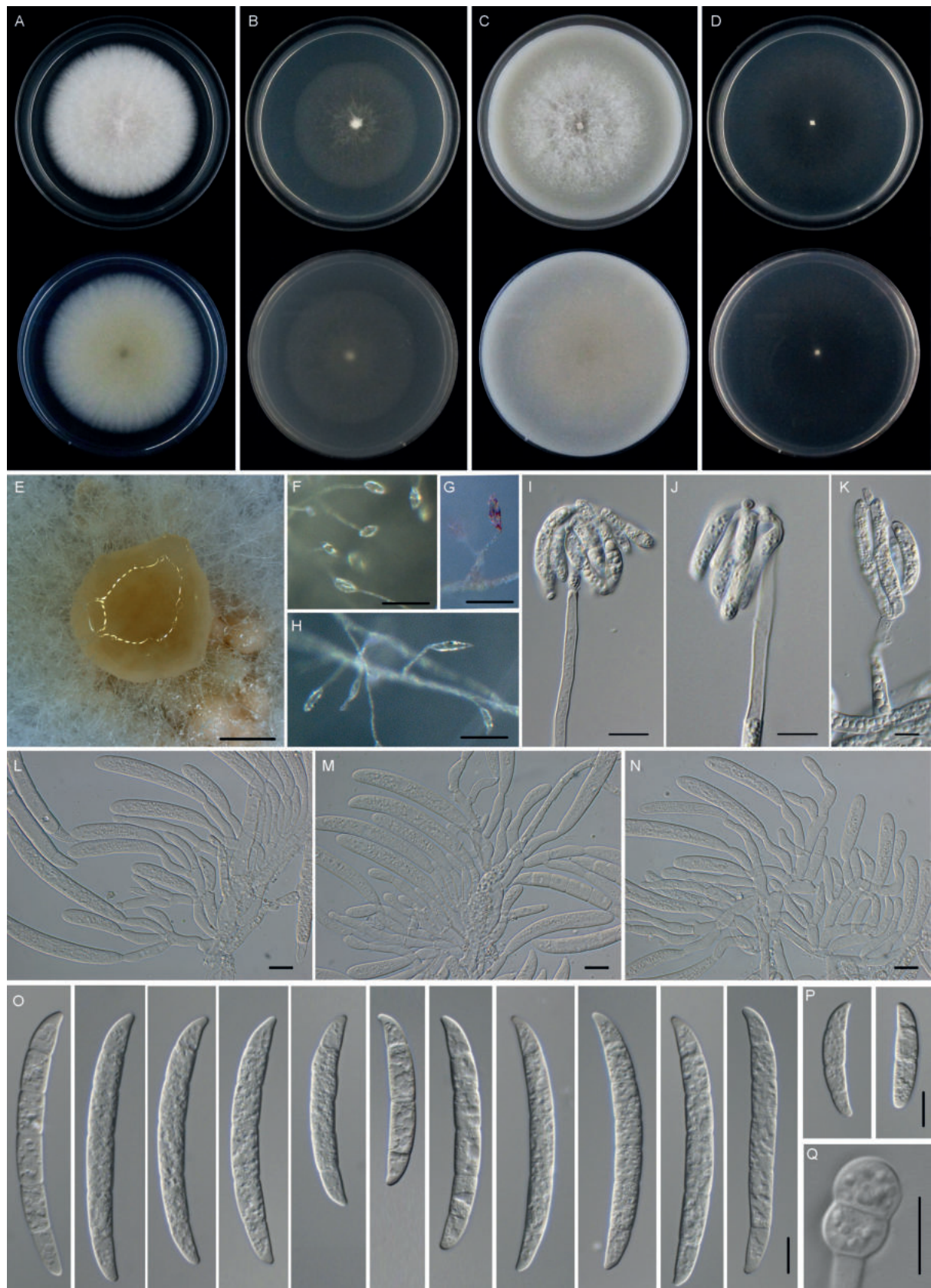**Figure 8.** *Fusarium hunanense* (HN33-8-2) **A–D** colonies on PDA, SNA, OMA, and CMA, respectively, after 5 days at 24 °C in the dark **E** sporodochia formed on PDA **F–K** aerial conidiophores, phialides, and conidia **L–N** sporodochial conidiophores, phialides, and conidia **O, P** macroconidia (3–6-septate) **Q** chlamydospore. Scale bars: 1,000 µm (**E**); 50 µm (**F–H**); 10 µm (**I–Q**).

in chains or solitary with mostly a pale color and smooth, (11.7−)11.7−12.9(−13.5) × (7.7−)7.7−8.5(−8.6) μm, (mean ± SD = 12.3 ± 0.6 × 8.1 ± 0.4 μm, n = 6).

Culture characteristics. Colonies on PDA growing in the dark with an average growth rate of 9.2 mm/d at 25 °C. Colony color white, flat, margins regular and fimbriate. Aerial mycelia abundant. Odor absent. Reverse white to pale luteous. Colonies on SNA incubated at 25 °C in the dark growing at 7.2 mm/d. Colony surface pure white, aerial mycelium scant. Reverse pure white, without diffusible pigments. Colonies on OMA incubated at 25 °C in the dark growing at 10.1 mm/d, color white, flat, velvety to felty with abundant floccose aerial mycelium. Reverse white without diffusible pigments. Colonies on CMA incubated at 25 °C in the dark were round, colony surface and reverse white, flat, aerial mycelium absent, hyphae hyaline, growing at 9.1 mm/d.

Additional materials examined. Chᴉɴᴀ, Hunan province, Yiyang City, Heshan District, Henglongqiao Town, 28°27'24"N, 112°29'7"E, isolated from leaf spots of *Cunninghamia lanceolata*, May 2017, Wen-Li Cui, isolates: HN33-8-2-1, HN33-8-2-2, HN33-8-2-3.

Notes. The isolates of *F. hunanense* were phylogenetically close to *F. pseudensiforme* (ex-type, CBS 125729) (Fig. 4). Between *F. hunanense* isolates and ex-type of *F. pseudensiforme* CBS 125729, there were 8/583 differences in *TEF-1α*, 3/800 in *RPB2*, and 9/640 in *RPB1*. The PHI analysis showed that there was no significant recombination among *F. hunanense* isolates and its related species (Φ_w = 1.0) (Fig. 3B). Morphologically, 5-septate sporodochial macroconidia of the *F. hunanense* isolates (60.6−73.0 × 6.1−7.1 μm) were longer than those of *F. pseudensiforme* CBS 125729 (ex-type) (50−63 × 5.2−7.2 μm) (Nalim et al. 2011). In conclusion, the phylogenetic and morphological evidence supported this fungus being a new species within the *F. solani* species complex.

Pathogenicity assays. Pathogenicity was tested on detached *C. lanceolata* leaves *in vitro* following Koch's postulates for *F. hunanense* (HN33-8-2), *F. concentricum* (SJ1-10), *F. guizhouense* (GZ7-20-1), *F. fujikuroi* (HN43-17-1), and *F. fujianense* (LC14). At five days post-inoculation, all the tested isolates caused leaf necrosis, with dark brown lesions. The control remained unchanged (Fig. 9A). Equivalently, shoots of tissue-culture seedlings of *C. lanceolata* were inoculated by *F. hunanense* (HN33-8-2), *F. concentricum* (SJ1-10), *F. guizhouense* (GZ7-20-1), *F. fujikuroi* (HN43-17-1), and *F. fujianense* (LC14) *in vivo*. After ten days post-inoculation, all isolates caused necrotic lesions on shoots of *C. lanceolata*. The control remained healthy (Fig. 9B). Statistically, these isolates showed different levels of virulence. *Fusarium hunanense* (HN33-8-2) was significantly more virulent than those of *F. concentricum* (SJ1-10), *F. guizhouense* (GZ7-20-1), *F. fujikuroi* (HN43-17-1), and *F. fujianense* (LC14), while *F. fujianense* (LC14) was the least virulent (Fig. 9C).

The fungal isolates used for inoculation were re-isolated from the diseased spots on the inoculated leaves and shoots, but no fungus was isolated from the leaves and shoots of the control. Koch's postulates were satisfied, and these isolates HN33-8-2, SJ1-10, GZ7-20-1, HN43-17-1, and LC14 were determined to be the pathogens of leaf blight on *C. lanceolata*.

Discussion

In this study, the pathogens causing leaf blight of *C. lanceolata* in China, focusing especially on Fujian, Guangxi, Guizhou, and Hunan provinces, were determined
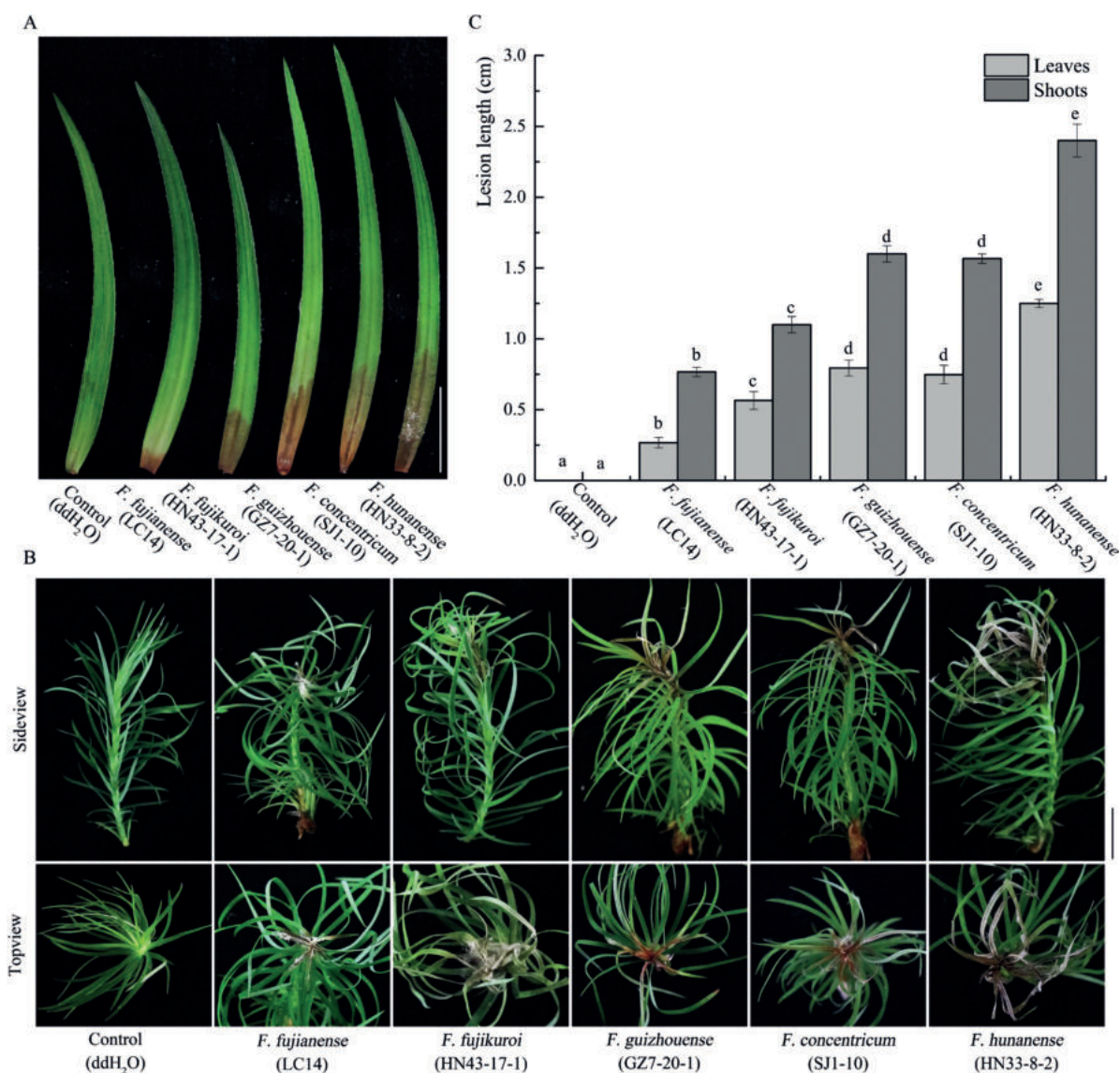
Figure 9. Symptoms on detached *Cunninghamia lanceolata* leaves (**A**) and shoots of tissue-culture seedlings of *C. lanceolata* (**B**) inoculated with isolates: *Fusarium fujianense* (LC14), *F. fujikuroi* (HN43-17-1), *F. guizhouense* (GZ7-20-1), *F. concentricum* (SJ1-10), and *F. hunanense* (HN33-8-2). Scale bar: 10 mm. C, Lesion length on detached *C. lanceolata* leaves inoculated with *F. fujianense* (LC14), *F. fujikuroi* (HN43-17-1), *F. guizhouense* (GZ7-20-1), *F. concentricum* (SJ1-10), and *F. hunanense* (HN33-8-2). Error bars represent standard deviation, and different letters indicate significant difference based on LSD's range test at *P* < 0.05 (n = 8).

by the inoculation tests using the shoots of tissue-culture seedlings of *C. lanceolata*. Phylogenetic and morphological analyses were used to evaluate the diversity of *Fusarium* species from the symptomatic *C. lanceolata* leaves. Three of the species newly described here (*F. fujianense*, *F. hunanense*, and *F. guizhouense*) and two known species (*F. fujikuroi* and *F. concentricum*) were associated with leaf blight of *C. lanceolata*. To date, *F. oxysporum* f. *pini* has been reported from *C. lanceolata* in Taiwan, China (Anonymous 1979). *Fusarium oxysporum* and *Fusarium* sp. have been reported to cause *C. lanceolata* seedlings damping off in mainland China (Chen 2002; Tian et al. 2019). However, none of the five species of *Fusarium* were previously reported to be pathogens of this disease. The taxonomic and phylogenetic analyses are the basis of research for various fields of

Fusarium biology. Because often *Fusarium* isolates show morphological variation during their growth in culture, their identification faces certain difficulties and challenges. Microscopically, the most typical feature of the genus *Fusarium s.l.* is its identifiable spindle- or canoe-shaped macroconidia (hyaline, multicellular, in clusters, macroconidia with or without foot cells at the base). If microconidia are present, the shape, number of cells, and mode of conidiogenesis (chains or false heads) are important in identification (Leslie and Summerell 2006).

Phylogenetic analyses based on DNA sequence diversity plays a crucial role, and many molecular markers, such as ITS, *TUB2*, *HIS3*, and *CAL* etc. have been used. However, *RPB2* and *TEF-1α* sequences appear to be the most useful in taxonomic studies of fungi, especially for the members of the genus *Fusarium* (O'Donnell 2000; O'Donnell et al. 2013; Crous et al. 2021). In the previous results of this study, it was found that, compared to *TEF-1α* and *RPB2* gene sequences, the ITS possesses relatively little phylogenetic signal, and the *TUB2* sequence is too short, thus the two loci have been eliminated. In the present study, the phylogeny inferred from concatenate multi-locus sequences (*TEF-1α*, *RPB2*, and *RPB1*) as suggested from previous studies (Sandoval-Denis et al. 2018) grouped isolates from *C. lanceolata* into five species belonging to four *Fusarium* species complexes with high supports. It should be noted here that, *TEF-1α*, *RPB2* and *RPB1* genes used to distinguish these species have rich information, but relatively few *RPB1* sequences are available in the databases, so there were some limitations using *RPB1*.

At present, the taxonomic studies on *Fusarium* are very divisive, especially segregating the *Fusarium solani* species complex as *Neocosmospora* (Lombard et al. 2015; de Hoog et al. 2023). The disagreement has become wider in recent years. Both sides have their support. In addition to the previous publications, the studies published in 2023 reflect such a dilemma. Chen et al. (2023) recognized nine genera of fusarioid and considered these nine genera are well-supported in their present phylogenomic study and different from *Fusarium*, while Zeng and Zhuang (2023) recognized 14 genera. At the same time, some mycologists, plant pathologists, and medical mycologists supported the broad concept of *Fusarium* and preferred the species complexes of *Fusarium*. *Fusarium bilaiae* Gagkaeva & al., a new cryptic species from sunflower, has been described in the *Fusarium fujikuroi* species complex using the tef, tub, and rpb2 sequences (Gagkaeva et al. 2023). In a Brazilian study on *Fusarium* from melons, Silva et al. (2023) favored *Fusarium solani* species complex (FSSC) and reported that among the 31 isolates, 29 isolates were *Fusarium falciforme* (Carrión) Summerb. & Schroers, (=*Neocosmospora falciformis* (Carrión) L. Lombard & Crous) and two isolates were *F. suttonianum* (Sand.-Den. & Crous) O'Donnell, Geiser & T. Aoki (≡*Neocosmospora suttoniana* Sand.-Den. & Crous) using sequences of *EF-1α* and *RPB2*. The position paper by de Hoog et al. (2023) to the medical community showed how complicated the disagreement has become at present. de Hoog et al. (2023) indicated that the phylogenetic relationship between *Fusarium* and *Neocosmospora* may justify their segregation, and it seems necessary to maintain the fusarium-like genera proposed by Crous et al. (2021). However, de Hoog et al. (2023) also opined that the segregation of *Neocosmospora* was not obligatory for the medical fields to be adopted immediately and recommended waiting until taxonomists settle their disagreement (de Hoog et al. 2023). Thus, de Hoog et al. (2023) recommended using the names under *Fusarium* species complexes, not the names under the segregated genera. This is the opinion with which we agree.

Species delineation needs polyphasic support. In addition to phylogenetic analyses and morphological studies, genealogical concordance analysis enables to determine sexual recombination and provides an operational criterion to verify the species borderline (de Hoog et al. 2023). This method was used in our present studies and no significant genetic recombination was in the new species that we described.

Pathogenicity tests showed that all five species were able to infect host plants. However, these species displayed differences in virulence on *C. lanceolata*. It is well known that *F. fujikuroi* is the causal agent of the rice disease bakanae in the major rice-growing regions in the world (Leslie and Summerell 2006). Besides rice, *F. fujikuroi* has been reported as saprobe or endophyte of vanilla (Pinaria et al. 2010) and isolated from human skin (O'Donnell et al. 2010). However, the predominant presence of *F. fujikuroi* from leaves of *C. lanceolata* has not been reported. This result could also be explained by the crop planting history of the sample site. We speculated that the fields have been previously planted with rice, which are highly susceptible to *F. fujikuroi* among other *Fusarium* species. *Fusarium concentricum* was described as a new species by Nirenberg and O'Donnell (1998), which was predominantly isolated from *Musa × paradisiaca* (banana) in Central America and *Nilaparvata lugens* (Asian brown leaf hopper) in South Korea. *Nilaparvata lugens* is a serious pest on rice in Asia (Wu et al. 2018). It is possible that this insect serves as a vector for this pathogen's dispersal. Very little is known about the pathogenicity and biology of *F. concentricum* (Leslie and Summerell 2006). However, *F. fujikuroi* and *F. concentricum* are reported to cause leaf blight on *C. lanceolata* for the first time.

The present study introduces new insights into the biodiversity of *Fusarium* species associated with *C. lanceolata* in China. A remarkable diversity of *Fusarium* species spanning several species complexes was found from four provinces, China. Furthermore, three new species of *Fusarium* were described, with demonstrated pathogenicity to *C. lanceolata*. However, considering the limited geographic areas studied, it is likely that additional *Fusarium* species would also be isolated if more areas were studied. Meanwhile, this also shows that despite the widespread distribution of *C. lanceolata* in China, and previous knowledge about its associated microbes, the fungal species-richness in *C. lanceolata* remains underestimated. Therefore, more studies are necessary on these new taxa in order to elucidate their host range, specificity, and global distribution, as well as their potential impact on the *C. lanceolata* industry.

Additional information

Conflict of interest

The authors have declared that no competing interests exist.

Ethical statement

No ethical statement was reported.

Funding

Author contributions

LHZ and LH designed research; JH and WLC performed experiments; JH, DWL and LHZ analyzed data; JH wrote the original draft; and DWL and LH reviewed and edited the manuscript. All authors have read and approved the final manuscript.

Author ORCIDs

Jiao He ⓘ https://orcid.org/0000-0002-4146-2223
De-Wei Li ⓘ https://orcid.org/0000-0002-2788-7938
Wen-Li Cui ⓘ https://orcid.org/0009-0005-7515-7672
Li-Hua Zhu ⓘ https://orcid.org/0000-0003-2740-4980
Lin Huang ⓘ https://orcid.org/0000-0001-7536-0914

Data availability

All of the data that support the findings of this study are available in the main text or Supplementary Information.

References

Anonymous (1979) List of Plant Diseases in Taiwan. Pl. Protect. Soc., Republ. of China, 404 pp.

Aoki T, O'Donnell K, Geiser DM (2014) Systematics of key phytopathogenic *Fusarium* species: Current status and future challenges. Journal of General Plant Pathology 80(3): 189–201. https://doi.org/10.1007/s10327-014-0509-3

Aoki T, Geiser DM, Kasson MT, O'Donnell K (2020) Nomenclatural novelties. Index Fungorum: Published Numbers 440(3): 1–5.

Aoki T, Geiser DM, O'Donnell K (2021a) Nomenclatural novelties. Index Fungorum: Published Numbers 496: 1–2.

Aoki T, Geiser DM, O'Donnell K (2021b) Nomenclatural novelties. Index Fungorum: Published Numbers 486: 1.

Boonpasart S, Kasetsuwan N, Puangsricharern V, Pariyakanok L, Jittpoonkusol T (2002) Infectious keratitis at King Chulalongkorn Memorial Hospital: a 12-year retrospective study of 391 cases. Journal of the Medical Association of Thailand = Chotmaihet thangphaet 85 Suppl 1: S217–230.

Booth C, Waterston J (1964) *Fusarium stilboides*. [Descriptions of Fungi and Bacteria]. CABI International, Sheet, 30 pp.

Burgess LW, Liddell CM, Summerell BA (1988) Laboratory manual for fusarium research: incorporating a key and descriptions of common species found in Australasia (2nd ed.). University of Sydney S, Australia.

Chen MM (2002) Forest Fungi Phytogeography: Forest Fungi Phytogeography of China, North America, and Siberia and International Quarantine of Tree Pathogens. Pacific Mushroom Research and Education Center, Sacramento, California, 469 pp.

Chen YP, Su PW, Hyde K, Maharachchikumbura S (2023) Phylogenomics and diversification of Sordariomycetes. Mycosphere 14(1): 414–451. https://doi.org/10.5943/mycosphere/14/1/5

Chung PC, Wu HY, Wang YW, Ariyawansa HA, Hu HP, Hung TH, Tzean SS, Chung CL (2020) Diversity and pathogenicity of *Colletotrichum* species causing strawberry anthracnose in Taiwan and description of a new species, *Colletotrichum miaoliense* sp. nov. Scientific Reports 10(1): e14664. https://doi.org/10.1038/s41598-020-70878-2

Coleman JJ (2016) The *Fusarium solani* species complex: Ubiquitous pathogens of agricultural importance. Molecular Plant Pathology 17(2): 146–158. https://doi.org/10.1111/mpp.12289

Crous PW, Lombard L, Sandoval-Denis M, Seifert KA, Schroers HJ, Chaverri P, Gené J, Guarro J, Hirooka Y, Bensch K, Kema GHJ, Lamprecht SC, Cai L, Rossman AY, Stadler M, Summerbell RC, Taylor JW, Ploch S, Visagie CM, Yilmaz N, Frisvad JC, Abdel-Azeem AM, Abdollahzadeh J, Abdolrasouli A, Akulov A, Alberts JF, Araújo JPM, Ariyawansa HA, Bakhshi M, Bendiksby M, Ben Hadj Amor A, Bezerra JDP, Boekhout T, Câmara MPS, Carbia M, Cardinali G, Castañeda-Ruiz RF, Celis A, Chaturvedi V, Collemare J, Croll D, Damm U, Decock CA, de Vries RP, Ezekiel CN, Fan XL, Fernández NB, Gaya E, González CD, Gramaje D, Groenewald JZ, Grube M, Guevara-Suarez M, Gupta VK, Guarnaccia V, Haddaji A, Hagen F, Haelewaters D, Hansen K, Hashimoto A, Hernández-Restrepo M, Houbraken J, Hubka V, Hyde KD, Iturriaga T, Jeewon R, Johnston PR, Jurjević Ž, Karalti I, Korsten L, Kuramae EE, Kušan I, Labuda R, Lawrence DP, Lee HB, Lechat C, Li HY, Litovka YA, Maharachchikumbura SSN, Marin-Felix Y, Matio Kemkuignou B, Matočec N, McTaggart AR, Mlčoch P, Mugnai L, Nakashima C, Nilsson RH, Noumeur SR, Pavlov IN, Peralta MP, Phillips AJL, Pitt JI, Polizzi G, Quaedvlieg W, Rajeshkumar KC, Restrepo S, Rhaiem A, Robert J, Robert V, Rodrigues AM, Salgado-Salazar C, Samson RA, Santos ACS, Shivas RG, Souza-Motta CM, Sun GY, Swart WJ, Szoke S, Tan YP, Taylor JE, Taylor PWJ, Tiago PV, Váczy KZ, van de Wiele N, van der Merwe NA, Verkley GJM, Vieira WAS, Vizzini A, Weir BS, Wijayawardene NN, Xia JW, Yáñez-Morales MJ, Yurkov A, Zamora JC, Zare R, Zhang CL, Thines M (2021) Fusarium: More than a node or a foot-shaped basal cell. Studies in Mycology 98(4): e100116. https://doi.org/10.1016/j.simyco.2021.100116

Cui WL, Bian JY, Li DW, Wang JW, Huang L (2020a) First report of leaf blight on Chinese fir (*Cunninghamia lanceolata*) caused by *Bipolaris setariae* in China. Plant Disease 104(9): 2523–2523. https://doi.org/10.1094/PDIS-12-19-2685-PDN

Cui WL, Lu XQ, Bian JY, Qi XL, Li DW, Huang L (2020b) *Curvularia spicifera* and *Curvularia muehlenbeckiae* causing leaf blight on *Cunninghamia lanceolata*. Plant Pathology 69(6): 1139–1147. https://doi.org/10.1111/ppa.13198

Dai XK, Zhang ML, Liu T, Chen XY, Zhu TH (2023) Brown leaf spot of *Cunninghamia lanceolata* caused by *Colletotrichum kahawae* in Sichuan province, China. Plant Disease 107(8): e2548. https://doi.org/10.1094/PDIS-12-22-2794-PDN

Damm U, Mostert L, Crous PW, Fourie PH (2008) Novel *Phaeoacremonium* species associated with necrotic wood of *Prunus* trees. Persoonia 20(1): 87–102. https://doi.org/10.3767/003158508X324227

de Hoog S, Walsh TJ, Ahmed SA, Alastruey-Izquierdo A, Alexander BD, Arendrup MC, Babady E, Bai FY, Balada-Llasat J-M, Borman A, Chowdhary A, Clark A, Colgrove R, Cornely O, Dingle T, Dufresne P, Fuller J, Gangneux J-P, Gibas C, Zhang S (2023) A conceptual framework for nomenclatural stability and validity of medically important fungi: A proposed global consensus guideline for fungal name changes supported by ABP, ASM, CLSI, ECMM, ESCMID-EFISG, EUCAST-AFST, FDLC, IDSA, ISHAM, MMSA, and MSGERC. Journal of Clinical Microbiology 61(11): e00873–e00823. https://doi.org/10.1128/jcm.00873-23

Dean R, Van Kan JAL, Pretorius ZA, Hammond-Kosack K, Di Pietro A, Spanu PD, Rudd JJ, Dickman M, Kahmann R, Ellis J, Foster GD (2012) The Top 10 fungal pathogens in molecular plant pathology. Molecular Plant Pathology 13(4): 414–430. https://doi.org/10.1111/j.1364-3703.2011.00783.x

Gagkaeva T, Orina A, Gomzhina M, Gavrilova O (2023) *Fusarium bilaiae*, a new cryptic species in the *Fusarium fujikuroi* complex associated with sunflower. Mycologia 115(6): 1–15. https://doi.org/10.1080/00275514.2023.2259277

Gams W, Nirenberg HI, Seifert KA, Brayford D, Thrane U (1997) Proposal to conserve the name *Fusarium sambucinum* (Hyphomycetes). Taxon 46(1): 111–113. https://doi.org/10.2307/1224298

Geiser DM, Aoki T, Bacon CW, Baker SE, Bhattacharyya MK, Brandt ME, Brown DW, Burgess LW, Chulze S, Coleman JJ, Correll JC, Covert SF, Crous PW, Cuomo CA, De Hoog GS, Di Pietro A, Elmer WH, Epstein L, Frandsen RJ, Freeman S, Gagkaeva T, Glenn AE, Gordon TR, Gregory NF, Hammond-Kosack KE, Hanson LE, Jímenez-Gasco Mdel M, Kang S, Kistler HC, Kuldau GA, Leslie JF, Logrieco A, Lu G, Lysøe E, Ma LJ, McCormick SP, Migheli Q, Moretti A, Munaut F, O'Donnell K, Pfenning L, Ploetz RC, Proctor RH, Rehner SA, Robert VA, Rooney AP, Bin Salleh B, Scandiani MM, Scauflaire J, Short DP, Steenkamp E, Suga H, Summerell BA, Sutton DA, Thrane U, Trail F, Van Diepeningen A, Vanetten HD, Viljoen A, Waalwijk C, Ward TJ, Wingfield MJ, Xu JR, Yang XB, Yli-Mattila T, Zhang N (2013) One fungus, one name: Defining the genus *Fusarium* in a scientifically robust way that preserves longstanding use. Phytopathology 103(5): 400–408. https://doi.org/10.1094/PHYTO-07-12-0150-LE

Geiser DM, Al-Hatmi AMS, Aoki T, Arie T, Balmas V, Barnes I, Bergstrom GC, Bhattacharyya MK, Blomquist CL, Bowden RL, Brankovics B, Brown DW, Burgess LW, Bushley K, Busman M, Cano-Lira JF, Carrillo JD, Chang HX, Chen CY, Chen W, Chilvers M, Chulze S, Coleman JJ, Cuomo CA, de Beer ZW, de Hoog GS, Del Castillo-Múnera J, Del Ponte EM, Diéguez-Uribeondo J, Di Pietro A, Edel-Hermann V, Elmer WH, Epstein L, Eskalen A, Esposto MC, Everts KL, Fernández-Pavía SP, da Silva GF, Foroud NA, Fourie G, Frandsen RJN, Freeman S, Freitag M, Frenkel O, Fuller KK, Gagkaeva T, Gardiner DM, Glenn AE, Gold SE, Gordon TR, Gregory NF, Gryzenhout M, Guarro J, Gugino BK, Gutierrez S, Hammond-Kosack KE, Harris LJ, Homa M, Hong CF, Hornok L, Huang JW, Ilkit M, Jacobs A, Jacobs K, Jiang C, Jiménez-Gasco MDM, Kang S, Kasson MT, Kazan K, Kennell JC, Kim HS, Kistler HC, Kuldau GA, Kulik T, Kurzai O, Laraba I, Laurence MH, Lee T, Lee YW, Lee YH, Leslie JF, Liew ECY, Lofton LW, Logrieco AF, López-Berges MS, Luque AG, Lysøe E, Ma LJ, Marra RE, Martin FN, May SR, McCormick SP, McGee C, Meis JF, Migheli Q, Mohamed Nor NMI, Monod M, Moretti A, Mostert D, Mulè G, Munaut F, Munkvold GP, Nicholson P, Nucci M, O'Donnell K, Pasquali M, Pfenning LH, Prigitano A, Proctor RH, Ranque S, Rehner SA, Rep M, Rodríguez-Alvarado G, Rose LJ, Roth MG, Ruiz-Roldán C, Saleh AA, Salleh B, Sang H, Scandiani MM, Scauflaire J, Schmale DG III, Short DPG, Šišić A, Smith JA, Smyth CW, Son H, Spahr E, Stajich JE, Steenkamp E, Steinberg C, Subramaniam R, Suga H, Summerell BA, Susca A, Swett CL, Toomajian C, Torres-Cruz TJ, Tortorano AM, Urban M, Vaillancourt LJ, Vallad GE, van der Lee TAJ, Vanderpool D, van Diepeningen AD, Vaughan MM, Venter E, Vermeulen M, Verweij PE, Viljoen A, Waalwijk C, Wallace EC, Walther G, Wang J, Ward TJ, Wickes BL, Wiederhold NP, Wingfield MJ, Wood AKM, Xu JR, Yang XB, Yli-Mattila T, Yun SH, Zakaria L, Zhang H, Zhang N, Zhang SX, Zhang X (2021) Phylogenomic analysis of a 55.1-kb 19-gene dataset resolves a monophyletic *Fusarium* that includes the *Fusarium solani* species complex. Phytopathology 111(7): 1064–1079. https://doi.org/10.1094/PHYTO-08-20-0330-LE

Gerlach W, Nirenberg HI (1982) The genus *Fusarium*: A pictorial atlas. Mitteilungen aus der Biologischen Bundesanstalt fuer Land und Forstwirtschaft. Berlin Dahlem 209: 1–406. https://doi.org/10.2307/3792677

Goswami RS, Kistler HC (2005) Pathogenicity and in planta mycotoxin accumulation among members of the *Fusarium graminearum* species complex on wheat and rice. Phytopathology 95(12): 1397–1404. https://doi.org/10.1094/PHYTO-95-1397

Gräfenhan T, Johnston PR, Vaughan MM, McCormick SP, Proctor RH, Busman M, Ward TJ, O'Donnell K (2016) *Fusarium praegraminearum* sp. nov., a novel nivalenol

Jiao He et al.: *Fusarium* species associated with Chinese fir

mycotoxin-producing pathogen from New Zealand can induce head blight on wheat. Mycologia 108(6): 1229–1239.

He J, Li DW, Zhang Y, Ju YW, Huang L (2021) *Fusarium rosicola* sp. nov. causing vascular wilt on *Rosa chinensis*. Plant Pathology 70(9): 2062–2073. https://doi.org/10.1111/ppa.13452

He J, Li DW, Zhu YN, Si YZ, Huang JH, Zhu LH, Ye JR, Huang L (2022) Diversity and pathogenicity of *Colletotrichum* species causing anthracnose on *Cunninghamia lanceolata*. Plant Pathology 71(8): 1757–1773. https://doi.org/10.1111/ppa.13611

Huang L, Li QC, Zhang Y, Li DW, Ye JR (2016) *Colletotrichum gloeosporioides* sensu stricto is a pathogen of leaf anthracnose on evergreen spindle tree (*Euonymus japonicus*). Plant Disease 100(4): 672–678. https://doi.org/10.1094/PDIS-07-15-0740-RE

Huang L, Zhu YN, Yang JY, Li DW, Li Y, Bian LM, Ye JR (2018) Shoot blight on Chinese fir (*Cunninghamia lanceolata*) is caused by *Bipolaris oryzae*. Plant Disease 102(3): 500–506. https://doi.org/10.1094/PDIS-07-17-1032-RE

Huson DH (1998) SplitsTree: Analyzing and visualizing evolutionary data. Bioinformatics 14(1): 68–73. https://doi.org/10.1093/bioinformatics/14.1.68

Huson DH, Bryant D (2006) Application of phylogenetic networks in evolutionary studies. Molecular Biology and Evolution 23(2): 254–267. https://doi.org/10.1093/molbev/msj030

Ibrahim NF, Mohd MH, Mohamed Nor NMI, Zakaria L (2016) *Fusarium fujikuroi* causing fusariosis of pineapple in peninsular Malaysia. Australasian Plant Disease Notes, Australasian Plant Pathology Society 11(1): 1–21. https://doi.org/10.1007/s13314-016-0206-5

Kalyaanamoorthy S, Minh BQ, Wong TKF, von Haeseler A, Jermiin LS (2017) ModelFinder: Fast model selection for accurate phylogenetic estimates. Nature Methods 14(6): 587–589. https://doi.org/10.1038/nmeth.4285

Katoh K, Standley D (2013) MAFFT multiple sequence alignment software version improvements in performance and usability. Molecular Biology and Evolution 30(4): 772–780. https://doi.org/10.1093/molbev/mst010

Kelly A, Proctor RH, Belzile F, Chulze SN, Clear RM, Cowger C, Elmer W, Lee T, Obanor F, Waalwijk C, Ward TJ (2016) The geographic distribution and complex evolutionary history of the NX-2 trichothecene chemotype from *Fusarium graminearum*. Fungal Genetics and Biology 95: 39–48. https://doi.org/10.1016/j.fgb.2016.08.003

Kobayashi T, Zhao JZ (1987) Two fungi associated with needle blight of *Cunninghamia lanceolata*. Nippon Kingakkai Kaiho 28(3): 289–294.

Kumar S, Glen S, Michael L, Christina K, Koichiro T (2018) MEGA X: Molecular evolutionary genetics analysis across computing platforms. Molecular Biology and Evolution 35(6): 1547–1549. https://doi.org/10.1093/molbev/msy096

Lan X, Dong LJ, Huang KY, Chen DX, Li DW, Mo LY (2015) Main species and prevention research on diseases and pests of *Cunninghamia lanceolata*. Guangxi Forestry Science 44: 162–167. https://doi.org/10.19692/j.cnki.gfs.2015.02.014

Laraba I, McCormick SP, Vaughan MM, Geiser DM, O'Donnell K (2021) Phylogenetic diversity, trichothecene potential, and pathogenicity within *Fusarium sambucinum* species complex. PLOS ONE 16(1): e0245037. https://doi.org/10.1371/journal.pone.0245037

Leslie JF, Summerell BA (2006) The *Fusarium* Laboratory Manual. Blackwell Publishing Professional, USA. https://doi.org/10.1002/9780470278376

Li MF, He J, Ding L, Kang J, Zhang Q, Zheng Q (2007) Single spore strains without producing fruit body isolated from *Cordyceps militeris* and their RAPD analysis. Xi Nan Nong Ye Xue Bao 20: 547–550. https://doi.org/10.16213/j.cnki.scjas.2007.03.050

Li YM, Wang YJ, Jiang GY (2020) Application of origin software in data extraction and analysis in physical chemistry experiments: taking the combustion heat measurement of naphthalene as an example. Education Teaching Forum 50: 375–377.

Li X, He SQ, Gao Y, Xing SJ, Ren H, Yang H, Gao YT, Wang JY, Li NP, Duan JF, Yang J, Huang Q (2022) *Ceratocystis* and related genera causing wilt of *Cunninghamia lanceolata* Yunnan, China. Forest Pathology 52(1): e12744. https://doi.org/10.1111/efp.12744

Liao YCZ, Sun JW, Li DW, Nong ML, Zhu LH (2023) First report of top blight of *Cunninghamia lanceolata* caused by *Diaporthe unshiuensis* and *Diaporthe hongkongensis* in China. Plant Disease 107(3): e962. https://doi.org/10.1094/PDIS-06-22-1467-PDN

Link JHF (1809) Observationes in ordines plantarum naturales. Dissertatio Ima. Gesellschaft Naturforschender Freunde zu Berlin. Magazin 3(1): 3–42.

Liu YJ, Whelen S, Hall BD (1999) Phylogenetic relationships among ascomycetes: Evidence from an RNA polymerse II subunit. Molecular Biology and Evolution 16(12): 1799–1808. https://doi.org/10.1093/oxfordjournals.molbev.a026092

Liu F, Mbenoun M, Barnes I, Roux J, Wingfield MJ, Li G, Li J, Chen S (2015) New *Ceratocystis* species from *Eucalyptus* and *Cunninghamia* in South China. Antonie van Leeuwenhoek 107(6): 1451–1473. https://doi.org/10.1007/s10482-015-0441-3

Lombard L, van der Merwe NA, Groenewald JZ, Crous PW (2015) Generic concepts in Nectriaceae. Studies in Mycology 80(1): 189–245. https://doi.org/10.1016/j.simyco.2014.12.002

Nalim FA, Samuels GJ, Wijesundera RL, Geiser DM (2011) New species from the *Fusarium solani* species complex derived from perithecia and soil in the old world tropics. Mycologia 103(6): 1302–1330. https://doi.org/10.3852/10-307

Nelson PE, Toussoun TA, Marasas WFO (1983) *Fusarium* species: an illustrated manual for identification. Universtity Park, Penn., 193 pp.

Nguyen LT, Schmidt HA, von Haeseler A, Minh BQ (2015) IQ-TREE: A fast and effective stochastic algorithm for estimating maximum-likelihood phylogenies. Molecular Biology and Evolution 32(1): 268–274. https://doi.org/10.1093/molbev/msu300

Nirenberg HI (1995) Morphological differentiation of *Fusarium sambucinum* Fuckel sensu stricto, *F. torulosum* (Berk. & Curt.) Nirenberg comb. nov. and *F. venenatum* Nirenberg sp. nov. Mycopathologia 129(3): 131–141. https://doi.org/10.1007/BF01103337

Nirenberg HI, O'Donnell K (1998) New *Fusarium* species and combinations within the *Gibberella fujikuroi* species complex. Mycologia 90(3): 434–458. https://doi.org/10.1080/00275514.1998.12026929

O'Donnell K (2000) Molecular phylogeny of the *Nectria haematococca-Fusarium solani* species complex. Mycologia 92(5): 919–938. https://doi.org/10.1080/00275514.2000.12061237

O'Donnell K, Kistler HC, Cigelnik E, Ploetz RC (1998) Multiple evolutionary origins of the fungus causing Panama disease of banana: Concordant evidence from nuclear and mitochondrial gene genealogies. Proceedings of the National Academy of Sciences of the United States of America 95(5): 2044–2049. https://doi.org/10.1073/pnas.95.5.2044

O'Donnell K, Nirenberg HI, Aoki T, Cigelnik E (2000) A multigene phylogeny of the *Gibberella fujikuroi* species complex: Detection of additional phylogenetically distinct species. Mycoscience 41(1): 61–78. https://doi.org/10.1007/BF02464387

O'Donnell K, Sutton DA, Rinaldi MG, Sarver BA, Balajee SA, Schroers HJ, Summerbell RC, Robert VA, Crous PW, Zhang N, Aoki T, Jung K, Park J, Lee YH, Kang S, Park B, Geiser DM (2010) Internet-accessible DNA sequence database for identifying fusaria from human and animal infections. Journal of Clinical Microbiology 48(10): 3708–3718. https://doi.org/10.1128/JCM.00989-10

O'Donnell K, Humber RA, Geiser DM, Kang S, Park B, Robert VARG, Crous PW, Johnston PR, Aoki T, Rooney AP, Rehner SA (2012) Phylogenetic diversity of insecticolous fusaria inferred from multilocus DNA sequence data and their molecular identification via FUSARIUM-ID and Fusarium MLST. Mycologia 104(2): 427–445. https://doi.org/10.3852/11-179

O'Donnell K, Rooney AP, Proctor RH, Brown DW, McCormick SP, Ward TJ, Frandsen RJ, Lysøe E, Rehner SA, Aoki T, Robert VA, Crous PW, Groenewald JZ, Kang S, Geiser DM (2013) Phylogenetic analyses of RPB1 and RPB2 support a middle cretaceous origin for a clade comprising all agriculturally and medically important fusaria. Fungal Genetics and Biology 52: 20–31. https://doi.org/10.1016/j.fgb.2012.12.004

O'Donnell K, Ward TJ, Robert VARG, Crous PW, Geiser DM, Kang S (2015) DNA sequence-based identification of *Fusarium*: Current status and future directions. Phytoparasitica 43(5): 583–595. https://doi.org/10.1007/s12600-015-0484-z

O'Donnell K, Al-Hatmi AMS, Aoki T, Brankovics B, Cano-Lira JF, Coleman JJ, de Hoog GS, Di Pietro A, Frandsen RJN, Geiser DM, Gibas CFC, Guarro J, Kim HS, Kistler HC, Laraba I, Leslie JF, López-Berges MS, Lysøe E, Meis JF, Monod M, Proctor RH, Rep M, Ruiz-Roldán C, Šišić A, Stajich JE, Steenkamp ET, Summerell BA, van der Lee TAJ, van Diepeningen AD, Verweij PE, Waalwijk C, Ward TJ, Wickes BL, Wiederhold NP, Wingfield MJ, Zhang N, Zhang SX (2020) No to *Neocosmospora*: Phylogenomic and practical reasons for continued inclusion of the *Fusarium solani* species complex in the genus *Fusarium*. MSphere 5(5): e00810–e00820. https://doi.org/10.1128/mSphere.00810-20

O'Donnell K, Whitaker BK, Laraba I, Proctor RH, Brown DW, Broders K, Kim H-S, McCormick SP, Busman M, Aoki T, Torres-Cruz TJ, Geiser DM (2022) DNA sequence-based identification of *Fusarium*: A work in progress. Plant Disease 106(6): 1597–1609. https://doi.org/10.1094/PDIS-09-21-2035-SR

Perera R, Hyde K, Maharachchikumbura S, Jones E, McKenzie E, Stadler M, Lee H, Samarakoon MC, Ekanayaka A, Erio C, Liu JK (2020) Fungi on wild seeds and fruits. Mycosphere 11(1): 2108–2480. https://doi.org/10.5943/mycosphere/11/1/14

Pinaria AG, Liew ECY, Burgess LW (2010) *Fusarium* species associated with vanilla stem rot in Indonesia. Australasian Plant Pathology 39(2): 176–183. https://doi.org/10.1071/AP09079

Qiu J, Lu Y, He D, Lee YW, Ji F, Xu J, Shi J (2020) *Fusarium fujikuroi* species complex associated with rice, maize, and soybean from Jiangsu province, China: Phylogenetic, pathogenic, and toxigenic analysis. Plant Disease 104(8): 2193–2201. https://doi.org/10.1094/PDIS-09-19-1909-RE

Quaedvlieg W, Binder M, Groenewald JZ, Summerell BA, Carnegie AJ, Burgess TI, Crous PW (2014) Introducing the consolidated species concept to resolve species in the Teratosphaeriaceae. Persoonia 33(1): 1–40. https://doi.org/10.3767/003158514X681981

Rabodonirina M, Piens MA, Monier MF, Guého E, Fière D, Mojon M (1994) *Fusarium* infections in immunocompromised patients: Case reports and literature review. European Journal of Clinical Microbiology & Infectious Diseases 13(2): 152–161. https://doi.org/10.1007/BF01982190

Rambaut A (2014) FigTree v 1.4.2. Institute of evolutionary biology, University of Edinburgh. http://tree.bio.ed.ac.uk/software/figtree/

Ronquist F, Teslenko M, van der Mark P, Ayres DL, Darling A, Hohna S, Larget B, Liu L, Suchard MA, Huelsenbeck JP (2012) MrBayes 3.2: Efficient Bayesian phylogenetic inference and model choice across a large model space. Systematic Biology 61(3): 539–542. https://doi.org/10.1093/sysbio/sys029

Rossman AY, Samuels GJ, Rogerson CT, Lowen R (1999) Genera of Bionectriaceae, Hypocreaceae and Nectriaceae (Hypocreales, Ascomycetes). Studies in Mycology 42(42): 1–248.

Sandoval-Denis M, Crous PW (2018) Removing chaos from confusion: Assigning names to common human and animal pathogens in *Neocosmospora*. Persoonia 41(1): 109–129. https://doi.org/10.3767/persoonia.2018.41.06

Sandoval-Denis M, Guarnaccia V, Polizzi G, Crous PW (2018) Symptomatic citrus trees reveal a new pathogenic lineage in *Fusarium* and two new *Neocosmospora* species. Persoonia 40(1): 1–25. https://doi.org/10.3767/persoonia.2018.40.01

Sandoval-Denis M, Lombard L, Crous PW (2019) Back to the roots: A reappraisal of *Neocosmospora*. Persoonia 43(1): 90–185. https://doi.org/10.3767/persoonia.2019.43.04

Silva S, Costa M, Cardoso A, Nascimento L, Barroso K, Nunes G, Pfenning L, Ambrósio M (2023) *Fusarium falciforme* and *Fusarium suttonianum* cause root rot of melon in Brazil. Plant Pathology 72(4): 721–730. https://doi.org/10.1111/ppa.13701

Snyder WC, Hansen HN (1940) The species concept in *Fusarium*. American Journal of Botany 27(2): 64–67. https://doi.org/10.1002/j.1537-2197.1940.tb14217.x

Summerell BA (2019) Resolving *Fusarium*: Current status of the genus. Annual Review of Phytopathology 57(1): 323–339. https://doi.org/10.1146/annurev-phyto-082718-100204

Taylor JW, Jacobson DJ, Kroken S, Kasuga T, Geiser DM, Hibbett DS, Fisher MC (2000) Phylogenetic species recognition and species concepts in fungi. Fungal Genetics and Biology 31(1): 21–32. https://doi.org/10.1006/fgbi.2000.1228

Thompson RS, Aveling TAS, Blanco Prieto R (2013) A new semi-selective medium for *Fusarium graminearum*, *F. proliferatum*, *F. subglutinans* and *F. verticillioides* in maize seed. South African Journal of Botany 84: 94–101. https://doi.org/10.1006/fgbi.2000.1228

Tian LY, Lian T, Ke SK, Qin CS, Xu JJ, Zhao DY, Qiu HL, Yang H, Jin XF, Li NL (2019) Fungal diseases of Chinese fir in northern Guangdong. 粤北地区杉木真菌性病害种类. Forestry and Environmental Sciences 35(04): 90–96.

Torres-Cruz TJ, Whitaker BK, Proctor RH, Broders K, Laraba I, Kim H-S, Brown DW, O'Donnell K, Estrada-Rodríguez TL, Lee Y-H, Cheong K, Wallace EC, McGee CT, Kang S, Geiser DM (2022) FUSARIUM-ID v.3.0: An updated, downloadable resource for *Fusarium* species identification. Plant Disease 106(6): 1610–1616. https://doi.org/10.1094/PDIS-09-21-2105-SR

Toussoun TA, Nelson PE (1968) *Fusarium*: A Pictorial Guide to the Identification of *Fusarium* Especies According to the Taxonomic System of Snyder and Hansen. The Pa Sta. Univ. Press., University Park, London, 51 pp.

Vismer HF, Marasas WF, Rheeder JP, Joubert JJ (2002) *Fusarium dimerum* as a cause of human eye infections. Medical Mycology 40(4): 399–406. https://doi.org/10.1080/mmy.40.4.399.406

Wang J, Cen B, Jiang Z, Peng S, Tong Z, Li G (1995) Identification of the pathogen which causes Chinese fir shoot blight. 杉木枯梢病的病原鉴定. Journal of South China Agricultural University 16(4): 47–49.

Wang M, Crous PW, Sandoval-Denis M, Han S-L, Liu F, Liang J, Duan W, Cai L (2022) *Fusarium* and allied genera from China: Species diversity and distribution. Persoonia 48(1): 1–53. https://doi.org/10.3767/persoonia.2022.48.01

Wollenweber HW, Reinking OA (1935) Die Fusarien: Ihre Beschreibung, Schadwirkung und Bekämpfung.

Wu SF, Zeng B, Zheng C, Mu XC, Zhang Y, Hu J, Zhang S, Gao CF, Shen JL (2018) The evolution of insecticide resistance in the brown planthopper (*Nilaparvata lugens*

Stål) of China in the period 2012–2016. Scientific Reports 8(1): e4586. https://doi.org/10.1038/s41598-018-22906-5

Xu YM, Liu YJ (2017) First report of *Nigrospora sphaerica* causing leaf blight on *Cunninghamia lanceolata* in China. Plant Disease 101(2): e389. https://doi.org/10.1094/PDIS-09-16-1229-PDN

Zeng ZQ, Zhuang WY (2023) Three new species of *Fusicolla* (Hypocreales) from China. Journal of Fungi 9(5): e572. https://doi.org/10.3390/jof9050572

Zhang D, Gao FL, Jakovli I, Zou H, Wang GT (2020) PhyloSuite: An integrated and scalable desktop platform for streamlined molecular sequence data management and evolutionary phylogenetics studies. Molecular Ecology Resources 20(1): 348–355. https://doi.org/10.1111/1755-0998.13096

Zhao L, Wei X, Huang CX, Yi JP, Deng JX, Cui MJ (2022) *Fusarium citri-sinensis* sp. nov. (Ascomycota: Nectriaceae) isolated from fruit of *Citrus sinensis* in China. Phytotaxa 555(3): 259–266. https://doi.org/10.11646/phytotaxa.555.3.5

Zheng W, Chen J, Hao Z, Shi J (2016) Comparative analysis of the chloroplast genomic information of *Cunninghamia lanceolata* (Lamb.) Hook with sibling species from the genera *Cryptomeria* D. Don, *Taiwania* Hayata, and *Calocedrus* Kurz. International Journal of Molecular Sciences 17(7): e1084. https://doi.org/10.3390/ijms17071084

Zhou H, Hou CL (2019) Three new species of *Diaporthe* from China based on morphological characters and DNA sequence data analyses. Phytotaxa 422(2): 157–174. https://doi.org/10.11646/phytotaxa.422.2.3

Supplementary material 1

Supplementary data

Authors: Jiao He, De-Wei Li, Wen-Li Cui, Li-Hua Zhu, Lin Huang
Data type: docx
Explanation note: **table S1.** Fungal cultures isolated from Chinese fir in this study. **table S2.** Genes/region and respective primer pairs used in the study. **table S3.** Nucleotide substitution models used in the phylogenetic analyses. **fig. S1.** *Fusarium concentricum* (SJ1-10). A–D, Colonies on PDA, SNA, OMA, and CMA, respectively, after 5 days at 24°C in the dark; E–F, sporodochia formed on PDA and the surface of carnation leaves, respectively; G–H, aerial conidiophores; I–J, sporodochial conidiophores, phialides, and conidia; K–L, aerial phialides and conidia; M, microconidia (0–1-septate) and macroconidia (3–5-septate). **fig. S2.** *Fusarium fujikuroi* (HN43-17-1). A–D, Colonies on PDA, SNA, OMA, and CMA, respectively, after 5 days at 24°C in the dark; E–H, aerial conidiophores, phialides, and microconidia; H, microconidia (0-septate); I, chlamydospore.

Link: https://doi.org/10.3897/mycokeys.101.113128.suppl1

Research Article

Two new phyllospheric species of *Colacogloea* (Colacogloeaceae, Pucciniomycotina) identified in China

Yun-Feng Lu[1,2], Chun-Yue Chai[1,2], Feng-Li Hui[1,2]

1   *School of Life Science and Agricultural Engineering, Nanyang Normal University, Nanyang 473061, China*
2   *Research Center of Henan Provincial Agricultural Biomass Resource Engineering and Technology, Nanyang Normal University, Nanyang 473061, China*
Corresponding author: Feng-Li Hui (*fenglihui@yeah.net*)

Abstract

During our ongoing survey of basidiomycetous yeasts associated with plant leaves in virgin forest, five *Colacogloea* strains were isolated in the Baotianman Nature Reserve, Henan Province, central China. Phenotypes from cultures and a phylogeny based on the internal transcribed spacer (ITS) regions and the D1/D2 domains of the large sub-unit (LSU) rRNA gene were employed to characterize and identify these isolates. As a result, two new species, namely *Colacogloea celtidis* **sp. nov.** and *C. pararetinophila* **sp. nov.**, are introduced herein. In the phylogeny of combined ITS and LSU dataset, the new species *C. celtidis* **sp. nov.** formed a clade with the unpublished *Colacogloea* strain (KBP: Y-6832), and together these formed the sister group to *C. armeniacae*, while *C. pararetinophila* **sp. nov.** was retrieved as a sister to *C. retinophila*. A detailed description and illustration of both new species, as well as the differences between them and their closest relatives in the genus are provided. Results from the present study will add to our knowledge of the biodiversity of *Colacogloea* in China.

Key words: Basidiomycota, Microbotryomycetes, phyllosphere, phylogenetic analysis, taxonomy

OPEN ⊖ ACCESS

Introduction

The genus *Colacogloea* consists of relatively rare and under-sampled dimorphic basidiomycetes (Sampaio et al. 2011). It was first proposed by Oberwinkler et al. (1990) to accommodate a single species, *C. effusa* (synonyms: *C. peniophorae*) which was initially described as *Platygloea effusa* (Bourdot and Galzin 1909). The genus *Colacogloea* was later expanded by the inclusion of *C. bispora* (originally described as *Platygloea bispora*) as a new combination (comb. nov.) (Oberwinkler et al. 1999), as well as two new species, *C. papilionacea* and *C. allantospora*, proposed by Kirschner and Oberwinkler (2000) and Bandoni et al. (2002), respectively. In 2015, Wang et al. revised the genus *Colacogloea* based on a multi-gene phylogeny, and transferred eight asexual species to the genus as the new combinations, *C. cycloclastica*, *C. diffluens*, *C. eucalyptica*, *C. falcata*, *C. foliorum*, *C. philyla*, *C. retinophila*, and *C. terpenoidalis* (Wang et al. 2015a, 2015b). Since then, six new members of the genus, *C. subericola* (originally described as *Rhodotorula subericola*) from Spain (Belloch et al. 2007; Li et al.

2020), *C. demeterae* from Germany (Yurkov et al. 2016), and *C. aletridis*, *C. hydrangeae*, *C. armeniacae* and *C. rhododendri* from China (Li et al. 2020; Wang et al. 2021), were introduced based on morphological analyses and phylogenetic data. Recent incorporations into the genus are *C. bettinae*, *C. biconidiata*, *C. fennica*, *C. microspora*, and *C. universitatis-gandavensis* isolated from the hymenium of *Peniophorella pubera* and *P. praetermissa* (Schoutteten et al. 2023). The genus *Colacogloea* was included in the newly proposed family Colacogloeaceae within Microbotryomycetes (Wang et al. 2015b).

Until now, 23 species have been accepted in the genus *Colacogloea* (Wang et al. 2021; Schoutteten et al. 2023). Among them, *C. allantospora*, *C. bettinae*, *C. biconidiata*, *C. bispora*, *C. effusa*, *C. fennica*, *C. microspora*, *C. papilionacea*, *C. philyla*, and *C. universitatis-gandavensis* are known from their sexual states, which mostly developed in the fructifications of Polyporales, with transversely septate basidia, "simple" septal pores, and colacosomes (Oberwinkler et al. 1990; Sampaio et al. 2011; Schoutteten et al. 2023). The other 13 species are asexual morphs that resemble yeasts from the genus *Rhodotorula* and reproduce by polar budding (Hamamoto et al. 2011; Sampaio 2011; Wang et al. 2015b). Physiologically, the members of the genus *Colacogloea* all lack fermentative ability, possess Q-10 as a predominant ubiquinone, and assimilate various carbon sources, but not myo-inositol and methanol (Hamamoto et al. 2011; Sampaio 2011; Sampaio et al. 2011; Wang et al. 2015b).

The Baotianman Nature Reserve, located in Henan Province, Central China, measures 4,285 ha. With a forest coverage rate of 98%, it is classified as World Biosphere Reserve by the United Nations Educational, Scientific and Cultural Organization (UNESCO). The reserve encompasses a virgin forest with more than 2000 species of vascular plant. The local climate is typical of a transitional climate from northern subtropical zone to warm temperate zone, with cold dry winters, and fresh rainy summers, and an annual mean temperature of 15 °C (Hu et al. 2022). These weather patterns make Baotianman an excellent location for studying fungal diversity. During the survey, we collected several yeast strains of interest and used morphological comparison together with phylogenetic analyses to determine their classifications. As a result, we identified and characterized two new species of *Colacogloea*.

Materials and methods

Sample collection and yeast isolation

Leaf samples collected from Baotianman Nature Reserve were stored in sterile flasks and transported to the laboratory within 24 h. Yeast strains were isolated from leaf surfaces by the improved ballistospore-fall method as described in previous papers (Nakase and Takashima 1993; Hu et al. 2022). Vaseline was used to affix the semi-withered leaves onto the insides of Petri dishes filled with yeast extract-malt extract (YM) agar (0.3% yeast extract, 0.3% malt extract, 0.5% peptone, 1% glucose, and 2% agar). The dishes were then incubated at 20 °C until visible colonies had formed. Different yeast morphotypes were selected from these colonies and purified by streaking on separate YM agar plates. After purification, yeast strains were suspended in YM broth supplemented with 20% (v/v) glycerol and stored at −80 °C. Cultures of

Table 1. Yeast strains and isolation sources investigated in this study.

	Strain	Source	Location
Colacogloea celtidis	NYUN 2210184[T]	Leaf of *Celtis bungeana*	Getiaopa, Baotianman Nature Reserve, Neixiang, Henan Province, China
	NYUN 221136	Undetermined leaf	Mayigou, Baotianman Nature Reserve, Neixiang, Henan Province, China
Colacogloea pararetinophila	NYNU 2110393[T]	Undetermined leaf	Mayigou, Baotianman Nature Reserve, Neixiang, Henan Province, China
	NYNU 2110421	Undetermined leaf	Tianmanpubu, Baotianman Nature Reserve, Neixiang, Henan Province, China
	NYNU 2211185	Undetermined leaf	Tianmanpubu, Baotianman Nature Reserve, Neixiang, Henan Province, China

all obtained isolates were preserved at the Microbiology Lab, Nanyang Normal University, Henan, China. All isolates used in this study and their origins are presented in Table 1.

Morphological and physiological characterization

Morphological and physiological characteristics of yeast strains were defined according to methods established by Kurtzman et al. (2011). Colony characteristics were observed and recorded on YM agar after two weeks of incubation at 20 °C. To investigate mycelium formation, colonies were transferred to corn meal (CM) agar (2% cornmeal infusion and 2% agar) slide cultures and incubated at 20 °C for two weeks. Tests of sexual reproductive potential were conducted for individual strains and strain pairs on potato dextrose agar (PDA) (20% potato infusion, 2% glucose, and 1.5% agar), CM agar, and yeast carbon base plus 0.01% ammonium sulphate (YCBS) agar for two months and observed at weekly intervals (Sampaio et al. 2011; Li et al. 2020). The inverted-plate method (do Carmo-Sousa and Phaff 1962) was used to observe the ballistoconidium-forming activity of all yeasts after two weeks of incubation on CM agar at 20 °C. Glucose fermentation was carried out in liquid medium using Durham fermentation tubes. Carbon and nitrogen source assimilation tests were conducted in liquid medium and starved inoculum was used for the nitrogen test (Kurtzman et al. 2011). Cycloheximide resistance was performed in liquid medium, while urea hydrolysis was conducted on agar slants. Acid production and diazonium blue B (DBB) reactions were investigated using Petri dishes with solid medium. Growth at different temperatures (15, 20, 25, 30, 35, and 37 °C) was determined by the amount of cultivation on YM agar. Cell morphology was examined using a Leica DM 2500 microscope (Leica Microsystems GmbH, Wetzlar, Germany) and a Leica DFC295 digital microscope color camera under bright field, phase contrast, or differential interference contrast (DIC) environment. All novel taxonomic descriptions and proposed names were deposited in the MycoBank database (http://www.mycobank.org; 29 October 2023).

DNA extraction, PCR amplification, and sequencing

The total genomic DNA was extracted from yeast strains using the Ezup Column Yeast Genomic DNA Purification Kit according to the manufacturer's

instructions (Sangon Biotech Co., Shanghai, China). Two nuclear loci, which include the ITS regions and the D1/D2 domains of the LSU rRNA gene, were amplified using ITS1/ITS4 (White et al. 1990) and NL1/NL4 (Kurtzman and Robnett 1998) primers, respectively. The amplifications were performed in a 25 µL reaction-volume tube containing 9.5 µL of ddH_2O, 12.5 µL of 2 × Taq PCR Master Mix with blue dye (Sangon Biotech Co., Shanghai, China), 1 µL of DNA template, and 1 µL of each primer. The following parameters were used to amplify the ITS and D1/D2 regions: an initial denaturation step of 2 min at 95 °C, followed by 35 cycles of 30 s at 95 °C, 30 s at 51 °C, 40 s at 72 °C, and a final extension of 10 min at 72 °C (Wang et al. 2014). The PCR products were purified and sequenced at Sangon Biotech Co., Ltd (Shanghai, China) with the same primers. We determined the identity and accuracy of the newly-obtained sequences by comparing them to sequences in GenBank and assembled them using BioEdit 7.1.3.0 (Hall 1999). All newly generated sequences were deposited in the GenBank database (https://www.ncbi.nlm.nih.gov/genbank/), and the accession numbers are listed in Table 2.

Phylogenetic analysis

A total of 57 nucleotide sequences that belonged to 27 taxa were included in the phylogenetic analyses. Except for 10 sequences recognized in this study, the other sequences were obtained from previous studies (Li et al. 2020; Wang et al. 2021) and GenBank (Table 2). *Udeniozyma ferulica* CBS 7416[T] was used as the outgroup. The phylogenetic relationships of the new *Colacogloea* species and their relatives were determined using a combined ITS and LSU sequence dataset. Sequences of the individual loci were aligned with Clustal X 1.83 (Thompson et al. 1997) or MAFFT 7.110 (Katoh and Standley 2013) using default settings. PhyloSuite V1.2.2 (Zhang et al. 2020) was used to concatenate the aligned sequences of the different loci. The few ambiguously aligned regions of the ITS and LSU alignments were removed with Gblocks v.0.91b, by keeping the default settings but allowing all gap positions when not ambiguous and manually adjusted in Sequencher 5.4.5 (Katoh et al. 2019; Castresana 2000).

Phylogenetic analyses were carried out using maximum likelihood (ML) and Bayesian inference (BI) methods. The ML analysis was conducted with RAxML v. 8.2.3 (Stamatakis 2014) using a GTRGAMMA substitution model. ML bootstrap values (MLBS) of the nodes were evaluated using 1,000 rapid bootstrap replicates. For the BI approach, ModelFinder (Kalyaanamoorthy et al. 2017) was used to determine the appropriate substitution model that would best fit the DNA evolution for the combined dataset. MrBayes 3.2.7a (Ronquist et al. 2012) in the CIPRES Science Gateway version 3.3 was used to analyze the BI data. Best-fit evolution models were determined as GTR+I+G for the ITS and LSU partitions. Six simultaneous Markov chains were run for 50 million generations and trees were sampled every 1,000th generation. The first 25% of created sample trees were discarded as they represent the burn-in phase of analysis. The remaining trees were used to calculate the Bayesian posterior probabilities (BPP) of the clades.

The resulting trees were viewed in FigTree v. 1.4.3 (Andrew 2016) and processed with Adobe Illustrator CS5. Branches that received MLBS ≥ 50% and BPP ≥ 0.95 were considered significantly supported.

Table 2. Taxon names, strain numbers, and GenBank accession numbers used for phylogenetic analyses. Entries in bold were newly generated for this study.

Species Name	Strain No.	GenBank Accession No	
		ITS	LSU D1/D2
Colacogloea aletridis	CBS 15459[T]	NR_174802	MK050450
Colacogloea armeniacae	CGMCC 2.6134[T]	MT252007	MT252007
Colacogloea bettinae	DSM 112418[T]	OQ870173	OQ875008
Colacogloea biconidiata	DSM 112405[T]	OQ870175	OQ875010
Colacogloea celtidis	**NYUN 2210184[T]**	**OP954665**	**OP954664**
Colacogloea celtidis	**NYUN 221136**	**OR727350**	**OR727349**
Colacogloea cycloclastica	CBS 8448[T]	NR_154750	NG_058729
Colacogloea demeterae	CBS 12500[T]	—	FN428967
Colacogloea diffluens	CBS 5233[T]	NR_073289	NG_058991
Colacogloea effusa	DSM 113583[ET]	OQ870184	OQ875017
Colacogloea eucalyptica	CBS 8499[T]	NR_111685	NG_058758
Colacogloea falcata	CBS 7368[T]	NR_073297	NG_058723
Colacogloea fennica	DSM 113583[ET]	OQ870184	OQ875017
Colacogloea foliorum	CBS 5234[T]	NR_073331	NG_058992
Colacogloea hydrangeae	CBS 15463[T]	NR_174803	MK050451
Colacogloea microspora	DSM 112413[T]	OQ870193	OQ875026
Colacogloea papilionacea	RoKi 618[T]	—	EF450545
Colacogloea pararetinophila	**NYNU 2110393[T]**	**OM014194**	**OM014193**
Colacogloea pararetinophila	**NYNU 2110421**	**OR727348**	**OR727347**
Colacogloea pararetinophila	**NYNU 2211185**	**OR727352**	**OR727351**
Colacogloea philyla	CBS 6272[T]	NR_073274	NG_058993
Colacogloea retinophila	CBS 8446[T]	NR_154830	NG_058994
Colacogloea rhododendri	CBS 15652[T]	NR_174804	MK050452
Colacogloea subericola	CBS 10442[T]	NR_137680	NG_060065
Colacogloea terpenoidalis	CBS 8445[T]	NR_154749	NG_058995
Colacogloea universitatis-gandavensis	NS 20-022P[T]	—	OQ875007
Colacogloea sp.	KBP: Y-6832	ON263266	ON263266
Chrysozyma griseoflava	CBS 7284[T]	NR_073303	NG_058746
Udeniozyma ferulica	CBS 7416[T]	NR_073330	NG_058429
Yurkovia longicylindrica	CGMCC 2.5603[T]	NR_174799	MK050441

CBS, CBS-KNAW Collections, Westerdijk Fungal Biodiversity Institute, Utrecht, The Netherlands; DSM, German Collection of Microorganisms and Cell Cultures GmbH, Braunschweig, Germany; CGMCC, China General Microbiological Culture Collection Center, Beijing, China; NYNU, Microbiology Lab, Nanyang Normal University, Henan, China; T, ex-type strain; ET, ex-epitype strain. Species obtained in this study are in bold.

Results

Phylogenetic analysis

During this study, five strains of *Colacogloea* were discovered in the Baotian-man Nature Reserve. To reveal the phylogenetic position of the specimens, we

performed phylogenetic analyses with combined ITS and LSU sequence data. The dataset consisted of 1,272 characters (674 characters from ITS and 598 characters from LSU), of which 715 were constant, 536 were variable, 366 were parsimony-informative, and 164 were singleton. ML and BI analyses generated similar topologies, with the BI analysis reaching an average standard deviation of split frequencies of 0.009922. The consensus topology from the ML analysis with MLBS (≥ 50%) and BPP (≥ 0.95) labeled on branches is shown (Fig. 1). In the phylogenetic trees, five strains isolated in this study formed two strongly supported groups (100% MLBS/1 BPP), and were clearly distinct from other known species of *Colacogloea*.
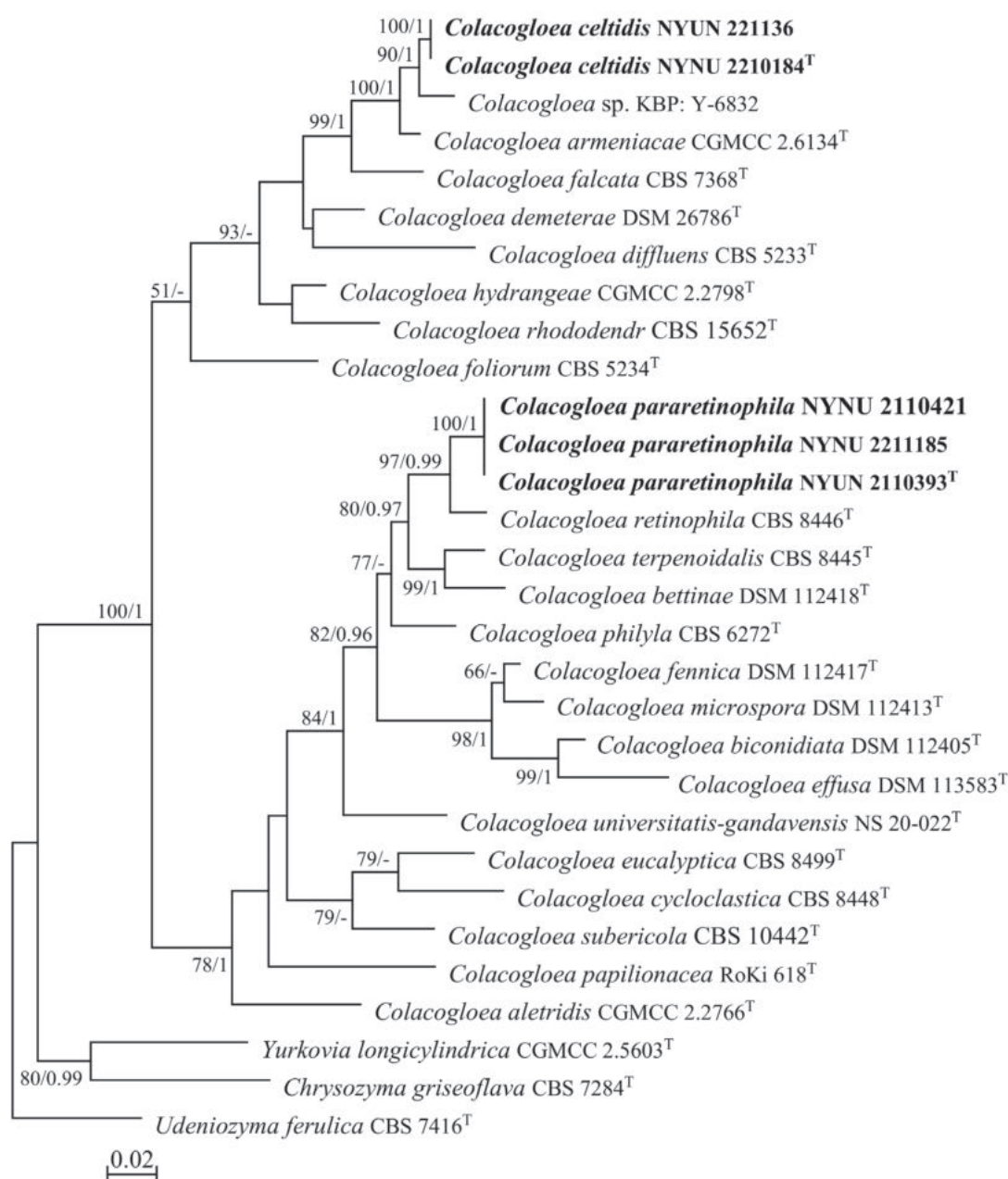

Figure 1. Maximum likelihood (ML) phylogram of *Colacogloea* species based on combined ITS and LSU sequence data. *Udeniozyma ferulica* CBS 7416[T] was used as the outgroup. Branches are labeled with MLBS ≥ 50% and BPP ≥ 0.95. New strains described in this study are shown in bold.

The two strains NYUN 2210184ᵀ and NYUN 221136 possess identical sequences in both the D1/D2 domains and ITS regions, indicating they belong to same species. The NYUN 2210184ᵀ group formed a well-supported clade and then grouped with the unpublished strain *Colacogloea* sp. KBP: Y-6832 and *C. armeniacae*, with strong support (100 MLBS/1 BPP; Fig. 1). The D1/D2 sequences of this group differed by only 3 nt substitutions (~0.5%) from *Colacogloea* sp. KBP: Y-6832; however, there were 16 nt (~2.9%) differences in the ITS regions, which indicates that the isolate KBP: Y-6832 may represent a different species. Similarly, the NYUN 2210184ᵀ group differed from the type strain of the closest known species *C. armeniacae* by 6 nt (~1%) substitutions in the D1/D2 domains and by more than 15 nt (~2.5%) mismatches in the ITS regions. According to the basidiomycetous yeast species thresholds proposed by Fell et al. (2000), Scorzetti et al. (2002), and Vu et al. (2016), strains that differ by two or more nucleotide substitutions in the D1/D2 domains or 1–2% nucleotide differences in the ITS regions may represent different taxa. Therefore, the differences in both the D1/D2 and ITS sequences were significant enough for the NYUN 2210184ᵀ group to be considered a distinct *Colacogloea* species.

Three strains NYNU 2110393ᵀ, NYNU 2110421, and 2211185 formed a well-supported clade (100% MLBS/1 BPP; Fig. 1). They shared a 100% of nucleotide identity based on their D1/D2 and ITS sequences, indicating that they are conspecific. The closest relative of the NYNU 2110393ᵀ group is *C. retinophila*, but differed from the type strain of the latter by six nt (~1%) substitutions in the D1/D2 domains and 31 nt (~5%) mismatches in the ITS regions, respectively. According to the criteria mentioned above, this data clearly supports the distinction between the NYNU 2110393ᵀ group and *C. retinophila* at the species level.

Taxonomy

Colacogloea celtidis C.Y. Chai & F.L. Hui, sp. nov.
MycoBank No: 850696
Fig. 2A

Etymology. The specific epithet "*celtidis*" refers to *Celtis*, the plant genus, from which the type strain was isolated.

Typus. China, Henan Province, Neixiang County, Baotianman Nature Reserve, Getiaopa (33°29'07"N, 111°52'51"E), in phylloplane from leaf of *Celtis bungeana*, October 2022, J.Z. Li, NYUN 2210184 (holotype GDMCC 2.332ᵀ preserved as a metabolically inactive state, culture ex-type KCTC 37265 and CICC 33577).

Description. On YM agar, after two weeks at 20 °C, the streak culture is cream, butyrous, and smooth. The margin is entire. In YM broth, after 7 d at 20 °C, cells are long cylindrical, 2.3–3.0 × 7.0–10.2 μm and single, budding is polar. After 1 mo at 20 °C, a ring and sediment are present. In Dalmau plate culture on corn meal agar, hyphae and pseudohyphae are not formed. Sexual structures are not observed for individual strains and strain pairs on PDA, CM agar and YCBS agar for two months. Ballistoconidia are not produced. Glucose fermentation is absent. Glucose, salicin, D-xylose (weak), D-arabinose, 5-keto-D-gluconate, ethanol (weak), glycerol, ribitol, D-mannitol, D-glucitol, succinate, D-gluconate, D-glucosamine (weak), 2-keto-D-gluconate, D-glucuronate, and glucono-1,5-lactone are assimilated as sole carbon sources. Inulin, sucrose, raffinose, melibiose, galactose,
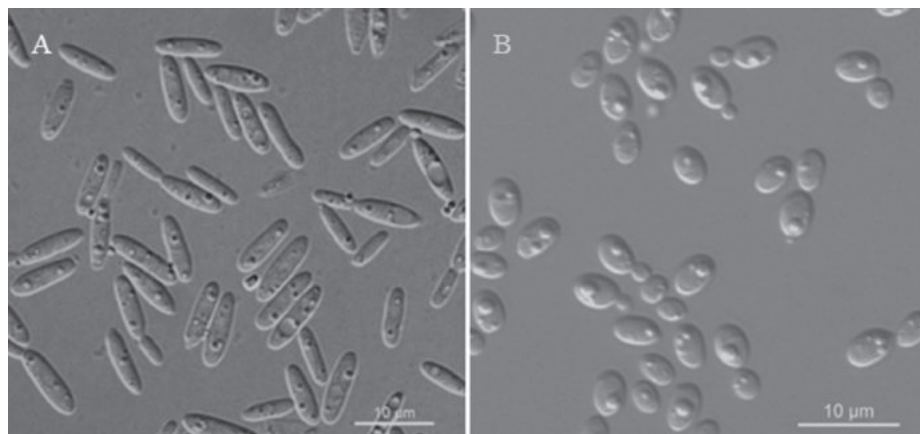
Figure 2. Vegetative cells of *Colacogloea celtidis* sp. nov. NYUN 2210184^T (**A**) and *Colacogloea pararetinophila* sp. nov. NYNU 2110393^T (**B**) following growth in YM broth for 7 days at 20 °C. Scale bars: 10 μm.

lactose, trehalose, maltose, melezitose, methyl-α-D-glucoside, cellobiose, L-sorbose, L-rhamnose, L-arabinose, D-ribose, methanol, erythritol, galactitol, myo-inositol, DL-lactate, and citrate are not assimilated. Nitrate, nitrite (delayed and weak), ethylamine (delayed and weak), and L-lysine (delayed) are assimilated as sole nitrogen sources. Cadaverine is not assimilated. Maximum growth temperature is 30 °C. Growth in vitamin-free medium is positive. Starch-like substances are not produced. Urease activity is positive. Diazonium Blue B reaction is positive.

Additional strain examined. CHINA, Henan Province, Neixiang County, Baotianman Nature Reserve, Mayigou (33°30'44"N, 111°55'47"E) in phylloplane from undetermined leaf, October 2022, J.Z. Li, NYNU 221136.

GenBank accession numbers. Holotype NYUN 2210184^T (ITS: OP954665, D1/D2: OP954664); additional strain NYUN 221136 (ITS: OR727350, D1/D2: OR727349).

Note. Phylogenetic analyses revealed that *C. celtidis* sp. nov. formed a single clade with high support (100 MLBP/1 BPP; Fig. 1). *C. eltise* sp. nov. can be physiologically differentiated from its closest known species *C. armeniacae* (Wang et al. 2021) by its ability to grow in D-xylose and D-arabinose and inability to grow in trehalose and cellobiose (Table 3).

***Colacogloea pararetinophila* C.Y. Chai & F.L. Hui, sp. nov.**
MycoBank No: 850697
Fig. 2B

Etymology. The specific epithet "*pararetinophila*" refers to its phylogenetic similarity to *C. retinophila*.

Typus. China, Henan Province, Neixiang County, Baotianman Nature Reserve, Mayigou (33°30'44"N, 111°55'47"E) in phylloplane from undetermined leaf, October 2021, W.T. Hu and R.Z. Qiao, NYNU 2110393 (holotype CICC 33533^T preserved as a metabolically inactive state, culture ex-type JCM 35724 and GDMCC 2.268).

Description. On YM agar, after two weeks at 20 °C, the streak culture is cream, butyrous, and smooth. The margin is entire. In YM broth, after 7 d at

Table 3. Physiological and biochemical characteristics that differ between the new species and closely related species.

Characteristics	*C. celtidis*	*C. armeniacae**	*C. pararetinophila*	*C. retinophila**
Carbon assimilation				
Trehalose	−	+	w	+
Cellobiose	−	+	−	−
Salicin	+	−/d/w	w	−
D-Xylose	w	−	+	s
D-Arabinose	+	−	+	s
D-Ribose	−	−/d/w	+	−
D-Glucuronate	+	+	−	+
Nitrogen assimilation				
Nitrate	+	+	+	−
Nitrite	d/w	+	+	−
L-Lysine	d	−	+	n
Growth tests				
0.1% Cycloheximide	−	n	+	−

+, positive reaction; −, negative reaction; d, delayed positive; s, slowly positive; w, weakly positive; n, data not available. All data from this study, except* which were obtained from the original description (Sampaio 2011; Wang et al. 2021).

20 °C, cells are ovoid or ellipsoidal, 2.0–2.6 × 2.8–4.2 μm and single, budding is polar. After 1 mo at 20 °C, a ring and sediment are present. In Dalmau plate culture on corn meal agar, hyphae and pseudohyphae are not formed. Sexual structures are not observed for individual strains and strain pairs on PDA, CM agar and YCBS agar for two months. Ballistoconidia are not produced. Glucose fermentation is absent. Glucose, trehalose (weak), salicin (weak), D-xylose, D-arabinose, 5-keto-D-gluconate, D-ribose, ethanol, glycerol, ribitol, D-mannitol, D-glucitol, succinate (weak), citrate (weak), D-gluconate, D-glucosamine, 2-keto-D-gluconateare, and glucono-1,5-lactone assimilated as sole carbon sources. Inulin, sucrose, raffinose, melibiose, galactose, lactose, maltose, melezitose, methyl-α-D-glucoside, cellobiose, L-sorbose, L-rhamnose, L-arabinose, methanol, erythritol, galactitol, myo-inositol, DL-lactate, and D-glucuronate are not assimilated. Nitrate, nitrite, ethylamine, and L-lysine are assimilated as sole nitrogen sources. Cadaverine is not assimilated. Maximum growth temperature is 37 °C. Growth in vitamin-free medium is positive. Starch-like substances are not produced. Urease activity is positive. Diazonium Blue B reaction is positive.

Additional strain examined. China, Henan Province, Neixiang County, Baotianman Nature Reserve, Tianmanpubu (33°30'26"N, 112°02'28"E) in phylloplane from undetermined leaf, October 2021, W.T. Hu and R.Z. Qiao, NYNU 2110421 and October 2022, J.Z. Li, NYUN 2211185.

GenBank accession numbers. Holotype NYNU 2110393[T] (ITS: OM014194, D1/D2: OM014193); additional strains NYNU 2110421 (ITS: OR727348, D1/D2: OR727347) and NYUN 2211185 (ITS: OR727352, D1/D2: OR727351).

Note. Phylogenetic analyses revealed that *C. pararetinophila* sp. nov. has a close relationship with *C. retinophila* with high support values (100 MLBP/1 BPP; Fig.1). *C. pararetinophila* sp. nov. can be physiologically differed from its closest

relative *C. retinophila* (Sampaio 2011) in the ability to assimilate salicin and D-ribose and inability to assimilate D-glucuronate. In addition, *C. pararetinophila* sp. nov. can grow in 0.1% cycloheximide while *C. retinophila* cannot (Table 3).

Discussion

Traditional methods of classification for *Colacogloea* species are based primarily on phenotypical features, such as colony morphology, cell shape, basidia formation, details of physiological and biochemical characteristics, etc. (Sampaio et al. 2011). The classification based on these phenotypical features, however, was in many cases not consistent with the results obtained from phylogenetic analyses. For example, *R. cycloclastica*, *R. philyla*, and *R. retinophila*, originally classified in the polyphyletic anamorphic genus *Rhodotorula*, are nested within the genus *Colacogloea* based on phylogenetic analyses (Sampaio et al. 2011; Wang et al. 2015a). As a result, these three species were then reassigned to the genus *Colacogloea*, according to the International Code of Nomenclature for Algae, Fungi, and Plants (McNeill et al. 2012). Therefore, a combination of phenotypical characteristics and phylogenetic analysis has been adopted as the standard method for concretely identifying *Colacogloea* species (Wang et al. 2015b).

In this study, we introduce *C. celtidis* sp. nov. and *C. pararetinophila* sp. nov. as two new species of *Colacogloea*, and describe them in asexual morphs based on molecular analyses and morphological features. Our phylogenetic analyses indicated that the genus of *Colacogloea* has two subclades (Fig. 1), which are in concordance with previous studies (Wang et al. 2015a; Li et al. 2020; Wang et al. 2021; Schoutteten et al. 2023). *C. celtidis* sp. nov., with its sister species *C. armeniacae*, form a well-separated clade in subclade I, which is comprised of anamorphic species only. *C. pararetinophila* sp. nov., with its sister species *C. retinophila*, form a monophyletic lineage in subclade II, which includes eight teleomorphic species and seven anamorphic species. In previous studies, the two sub-clades were well supported in phylogenetic trees from the four protein-coding genes and the combined seven-loci analysis (Wang et al. 2015a; Wang et al. 2021; Schoutteten et al. 2023). Multi-gene phylogenetic analyses suggest that the two sub-clades of the genus *Colacogloea* seem to represent two genera, although that was not well supported in the phylogenetic tree produced by this study (Fig. 1). Therefore, further analyses using more molecular data or genomic data are needed to clarify the possible heterogeneity of the genus.

Colacogloea species are widely distributed and are found in different habitats. Filamentous morphs of *Colacogloea* species were mainly isolated from the hymenia of corticioid fungi, especially from the genera *Peniophorella* and *Tubulicrinis* (Sampaio et al. 2011; Schoutteten et al. 2023). The yeast morphs of *Colacogloea* species can be isolated from leaves, fruits, tree bark, plant residues, soil, insects, and tunnels (Belloch et al. 2007; Hamamoto et al. 2011; Sampaio 2011; Sampaio et al. 2011; Yurkov et al. 2016; Li et al. 2020; Wang et al. 2021), but most of them are found mostly in association with plant materials, especially leaves. Moreover, the yeast morphs of *C. papilionacea* and *C. philyla*, that were isolated from insects and insect tunnels, were also collected from plants (Kirschner and Oberwinkler 2000; Sampaio 2011; Sampaio et al. 2011).

In this study, the five isolates of two new species also have an association with plant leaves, like most of the other anamorphic species in the genus. Taken together, these findings might indicate that the plant is a common habitat of *Colacogloea* species in the yeast morphs.

Acknowledgements

Additional information

Conflict of interest

The authors have declared that no competing interests exist.

Ethical statement

No ethical statement was reported.

Funding

Author contributions

Data curation: YFL, CYC. Methodology: YFL. Molecular phylogeny: YFL, CYC. Writing – original draft: YFL. Writing – review and editing: CYC, FLH. All authors read and approved the final manuscript.

Author ORCIDs

Yun-Feng Lu ⓘ https://orcid.org/0000-0003-0284-5560
Chun-Yue Chai ⓘ https://orcid.org/0000-0001-7753-6223
Feng-Li Hui ⓘ https://orcid.org/0000-0001-7928-3055

Data availability

All of the data that support the findings of this study are available in the main text or Supplementary Information.

References

Andrew R (2016) FigTree: Tree figure drawing tool Version 1.4.3. Institute of Evolutionary Biology, United Kingdom, University of Edinburgh Press.

Bandoni RJ, Krug J, Ginns J (2002) On some *Colacogloea* species from Canada. Czech Mycology 54(1−2): 31−43. https://doi.org/10.33585/cmy.54105

Belloch C, Villa-Carvajal M, Alvarez-Rodríguez ML, Coque JJ (2007) *Rhodotorula subericola* sp. nov., an anamorphic basidiomycetous yeast species isolated from bark of *Quercus suber* (cork oak). International Journal of Systematic and Evolutionary Microbiology 57(Pt 7): 1668−1671. https://doi.org/10.1099/ijs.0.64766-0

Bourdot H, Galzin L (1909) Hyménomycètes de France (I. Héterobasidiés). Bulletin Tri-mestriel de la Societe Mycologique de France 25: 15–36.

Castresana J (2000) Selection of conserved blocks from multiple alignments for their use in phylogenetic analysis. Molecular Biology and Evolution 17(4): 540–552. https://doi.org/10.1093/oxfordjournals.molbev.a026334

do Carmo-Sousa L, Phaff HJ (1962) An improved method for the detection of spore discharge in the Sporobolomycetaceae. Journal of Bacteriology 83(2): 434–435. https://doi.org/10.1128/jb.83.2.434-435.1962

Fell JW, Boekhout T, Fonseca A, Scorzetti G, Statzell-Tallman A (2000) Biodiversity and systematics of basidiomycetous yeasts as determined by large-subunit rDNA D1/D2 domain sequence analysis. International Journal of Systematic and Evolutionary Microbiology 50(Pt 3): 1351–1371. https://doi.org/10.1099/00207713-50-3-1351

Hall TA (1999) Bioedit: A user-friendly biological sequence alignment editor and analysis program for Windows 95/98/NT. Nucleic Acids Symposium Series 41: 95–98.

Hamamoto M, Boekhout T, Nakase T (2011) *Sporobolomyces* Kluyver & van Niel (1924). In: Kurtzman CP, Fell JW, Boekhout T (Eds) The Yeasts – a Taxonomic Study, 5th edn., vol. 3. Amsterdam, Elsevier, 1929–1990. https://doi.org/10.1016/B978-0-444-52149-1.00156-7

Hu WT, Chu SB, Li Y, Hui FL (2022) *Hyphopichia xiaguanensis* f.a., sp. nov., an ascomycet-ous yeast species isolated from plant leaves. International Journal of Systematic and Evolutionary Microbiology 72(Pt 5): 5398. https://doi.org/10.1099/ijsem.0.005398

Kalyaanamoorthy S, Minh BQ, Wong TKF, Von Haeseler A, Jermiin LS (2017) Modelfind-er: Fast model selection for accurate phylogenetic estimates. Nature Methods 14(6): 587–589. https://doi.org/10.1038/nmeth.4285

Katoh K, Standley DM (2013) MAFFT multiple sequence alignment software version 7: Improvements in performance and usability. Molecular Biology and Evolution 30(4): 772–780. https://doi.org/10.1093/molbev/mst010

Katoh K, Rozewicki J, Yamada KD (2019) MAFFT online service: Multiple sequence alignment, interactive sequence choice and visualization. Briefings in Bioinformatics 20(4): 1160–1166. https://doi.org/10.1093/bib/bbx108

Kirschner R, Oberwinkler F (2000) A new species of *Colacogloea* with zygoconidia. Sydowia 52: 195–203.

Kurtzman CP, Robnett CJ (1998) Identification and phylogeny of ascomycetous yeasts from analysis of nuclear large subunit (26S) ribosomal DNA partial sequences. Antonie van Leeuwenhoek International Journal of General and Molecular Microbiology 73(4): 331–371. https://doi.org/10.1023/A:1001761008817

Kurtzman CP, Fell JW, Boekhout T (2011) Methods for isolation, phenotypic character-ization and maintenance of yeasts. In: Kurtzman CP, Fell JW, Boekhout T (Eds) The Yeasts – a Taxonomic Study, 5th edn, vol. 1. Amsterdam, Elsevier, 87–110. https://doi.org/10.1016/B978-0-444-52149-1.00007-0

Li AH, Yuan FX, Groenewald M, Bensch K, Yurkov AM, Li K, Han PJ, Guo LD, Aime MC, Sampaio JP, Jindamorakot S, Turchetti B, Inacio J, Fungsin B, Wang QM, Bai FY (2020) Diversity and phylogeny of basidiomycetous yeasts from plant leaves and soil: Proposal of two new orders, three new families, eight new genera and one hundred and seven new species. Studies in Mycology 96: 17–140. https://doi.org/10.1016/j.simyco.2020.01.002

McNeill J, Barrie FR, Buck WR, Demoulin V, Greuter W, Hawksworth DL, Herendeen PS, Knapp S, Marhold K, Prado J, Prud'homme van Reine WF, Smith GF, Wiersma JH, Turland NJ (2012) International Code of Nomenclature for algae, fungi, and plants

(Melbourne Code). Regnum Vegetabile 154. A.R.G. Gantner Verlag KG, 140 pp. [Königstein: Koeltz Scientific Books]

Nakase T, Takashima M (1993) A simple procedure for the high frequency isolation of new taxa of ballistosporous yeasts living on the surfaces of plants. RIKEN Review 3: 33–34.

Oberwinkler F, Bauer R, Bandoni RJ (1990) *Colacogloea*: A new genus in the auricularioid Heterobasidiomycetes. Canadian Journal of Botany 68(12): 2531–2536. https://doi. org/10.1139/b90-318

Oberwinkler F, Bauer R, Tschen J (1999) The mycoparasitism of *Platygloea bispora*. Kew Bulletin 54(3): 763–769. https://doi.org/10.2307/4110873

Ronquist F, Teslenko M, van der Mark P, Ayres DL, Darling A, Höhna S, Larget B, Liu L, Suchard MA, Huelsenbeck JP (2012) MrBayes3.2: Efficient Bayesian phylogenetic inference and model choice, across a large model space. Systems Biology 61(3): 539–542. https://doi.org/10.1093/sysbio/sys029

Sampaio JP (2011) *Rhodotorula* Harrison (1928). In: Kurtzman CP, Fell JW, Boekhout T (Eds) The Yeasts – a Taxonomic Study, 5th edn, vol. 3. Amsterdam, Elsevier, 1873–1927. https://doi.org/10.1016/B978-044481312-1/50110-6

Sampaio JP, Kirschner R, Oberwinkler F (2011) *Colacogloea* Oberwinkler & Bandoni (1990). In: Kurtzman CP, Fell JW, Boekhout T (Eds) The Yeasts – a Taxonomic Study, 5th edn, vol. 3. Amsterdam, Elsevier, 1403–1408. https://doi.org/10.1016/B978-0-444-52149-1.00107-5

Schoutteten N, Yurkov A, Leroux O, Haelewaters D, Van Der Straeten D, Miettinen O, Boekhout T, Begerow D, Verbeken A (2023) Diversity of colacosome-interacting my-coparasites expands the understanding of the evolution and ecology of Microbotryo-mycetes. Studies in Mycology 106: 41–94. https://doi.org/10.3114/sim.2022.106.02

Scorzetti G, Fell JW, Fonseca A, Statzell-Tallman A (2002) Systematics of basidiomyce-tous yeasts: A comparison of large subunit D1/D2 and internal transcribed spacer rDNA regions. FEMS Yeast Research 2(4): 495–517. https://doi.org/10.1016/S1567-1356(02)00128-9

Stamatakis A (2014) RAxML Version 8: A tool for phylogenetic analyses and post analyses of large phylogenies. Bioinformatics (Oxford, England) 30(9): 1312–1313. https://doi.org/10.1093/bioinformatics/btu033

Thompson JD, Gibson TJ, Plewniak F, Jeanmougin F, Higgins DG (1997) The CLUSTAL_X windows interface: Flexible strategies for multiple sequence alignment aided by quality analysis tools. Nucleic Acids Research 25(24): 4876–4882. https://doi. org/10.1093/nar/25.24.4876

Vu D, Groenewald M, Szöke S, Cardinali G, Eberhardt U, Stielow B, de Vries M, Verkleij GJ, Crous PW, Boekhout T, Robert V (2016) DNA barcoding analysis of more than 9 000 yeast isolates contributes to quantitative thresholds for yeast species and genera delimita-tion. Studies in Mycology 85(1): 91–105. https://doi.org/10.1016/j.simyco.2016.11.007

Wang QM, Theelen B, Groenewald M, Bai FY, Boekhout T (2014) Moniliellomycetes and Malasseziomycetes, two new classes in Ustilaginomycotina. Persoonia 33(1): 41–47. https://doi.org/10.3767/003158514X682313

Wang QM, Groenewald M, Takashima M, Theelen B, Han PJ, Liu XZ, Boekhout T, Bai FY (2015a) Phylogeny of yeasts and related filamentous fungi within Pucciniomycotina determined from multigene sequence analyses. Studies in Mycology 81(1): 27–54. https://doi.org/10.1016/j.simyco.2015.08.002

Wang QM, Yurkov AM, Göker M, Lumbsch HT, Leavitt SD, Groenewald M, Theelen B, Liu XZ, Boekhout T, Bai FY (2015b) Phylogenetic classification of yeasts and relat-

ed taxa within Pucciniomycotina. Studies in Mycology 81(1): 149–189. https://doi.org/10.1016/j.simyco.2015.12.002

Wang GS, Sun Y, Wangmu, Wang Q-M (2021) *Colacogloea armeniacae* sp. nov., a novel pucciniomycetous yeast species isolated from apricots. Mycoscience 62(1): 42–46. https://doi.org/10.47371/mycosci.2020.08.005

White TJ, Bruns T, Lee S, Taylor J (1990) Amplification and direct sequencing of fungal ribosomal RNA genes for phylogenetics. In: Innis MA, Gelfand DH, Sninsky JJ, White TJ (Eds) PCR Protocols: A Guide to Methods and Applications. Academic Press, 315–322. https://doi.org/10.1016/B978-0-12-372180-8.50042-1

Yurkov AM, Wehde T, Federici J, Schäfer AM, Ebinghaus M, Lotze-Engelhard S, Mittelbach M, Prior R, Richter C, Röhl O, Begerow D (2016) Yeast diversity and species recovery rates from beech forest soils. Mycological Progress 15(8): 845–859. https://doi.org/10.1007/s11557-016-1206-8

Zhang D, Gao F, Jakovlić I, Zou H, Zhang J, Li WX, Wang GT (2020) PhyloSuite: An integrated and scalable desktop platform for streamlined molecular sequence data management and evolutionary phylogenetics studies. Molecular Ecology Resources 20(1): 348–355. https://doi.org/10.1111/1755-0998.13096

Supplementary material 1

Molecular data

Authors: Yun-Feng Lu, Chun-Yue Chai, Feng-Li Hui

Data type: fasta

Explanation note: A dataset of ITS and LSU for Fig. 1.

Link: https://doi.org/10.3897/mycokeys.101.114872.suppl1

MycoKeys

Morphological characteristics and phylogenetic evidence reveal two new species and the first report of *Comoclathris* (Pleosporaceae, Pleosporales) on dicotyledonous plants from China

Rong Xu[1,2], Wenxin Su[2], Yang Wang[3], Shangqing Tian[2], Yu Li[1], Chayanard Phukhamsakda[2,4]

1 *School of Food Science and Engineering, Yangzhou University, Yangzhou 225127, China*
2 *Internationally Cooperative Research Center of China for New Germplasm Breeding of Edible Mushroom, Jilin Agricultural University, Changchun 130118, China*
3 *College of Plant Protection, Shenyang Agricultural University, Shenyang, 110866, China*
4 *Center of Excellence Win Fungal Research, Mae Fah Luang University, Chiang Rai 57100, Thailand*
Corresponding authors: Chayanard Phukhamsakda (*chayanard.phu@mfu.ac.th*); Yu Li (*yuli966@126.com*)

Abstract

Two novel *Comoclathris* species were identified from dicotyledonous plants (*Clematis* sp. and *Xanthoceras sorbifolium*) in China. The results were supported by morphological characters and Maximum Likelihood (ML) and Bayesian Inference (BI) analyses. Multi-gene phylogenetic analyses of the ITS, LSU, SSU and *rpb*2 sequences revealed two new species *Comoclathris clematidis* and *C. xanthoceratis*, which are phylogenetically distinct. The new species are phylogenetically closely related to *C. arrhenatheri*. However, they are distinguishable from *C. arrhenatheri* by having comparatively larger asci and ascospores. This study improves our knowledge of *Comoclathris* as no species has been previously described from China. This suggests such taxa may be rare and it is likely that new taxa will be discovered from hosts and environments that have not yet been extensively investigated.

Key words: Ascomycota, *Clematis*, new species, saprobes, taxonomy, *Xanthoceras sorbifolium*

Introduction

Clements (1909) introduced the genus *Comoclathris* with *C. lanata* Clem as the type species. The species was originally assigned to the Diademaceae, based on having ascomata with flat circular lid-like opening (Shoemaker and Babcock 1992). Previously, *Comoclathris* was considered a synonym of *Platyspora* (Ariyawansa et al. 2014) and *Comoclathris* has been associated with an asexual morph resembling *Alternaria*-like (Simmons 1967); thus, the genus was temporarily referred to Pleosporaceae, based to these morphological characteristics (Zhang et al. 2012; Woudenberg et al. 2013). Two strains of *Comoclathris compressa* (CBS 157.53 and CBS 156.53) were treated as representative sequences which formed a well-supported clade within the family Pleosporaceae (Ariyawansa et al. 2014). Subsequently, *Comoclathris* was placed into Pleosporaceae, based on phylogenetic evidence coupled with

morphological characteristics (Ariyawansa et al. 2015; Thambugala et al. 2017; Wijayawardene et al. 2017; Wanasinghe et al. 2018).

Comoclathris can be distinguished from *Pleospora*, *Pleoseptum* and *Clathrospora* by its applanate and dark reddish-brown muriform ascospores with a single longitudinal septum and ascomata with circular lid-like opening (versus two or more rows of longitudinal septa of *Clathrospora* species) (Shoemaker and Babcock 1992; Zhang et al. 2012; Ariyawansa et al. 2014, 2015). Thirty-eight epithets have been recorded as *Comoclathris* in Species Fungorum (2023); however, most lack molecular data, including the type species *C. lanata*. *Comoclathris* has been found from America, Antarctica, Argentina, Austria, Bulgaria, Canada, Central Asia, Finland, Greece, India, Iran, Iraq, Italy, Netherlands, Norway, Pakistan, Portugal, Romania, Russia, Spain, Sweden, Switzerland, Syria, Tunisia, Turkey, Ukraine and Yugoslavia (Ahmad 1978; Shoemaker and Babcock 1992; Chlebicki 2002; Checa 2004; Pande 2008; Woudenberg et al. 2013; Eriksson 2014; Thambugala et al. 2017; Hongsanan et al. 2020). Most *Comoclathris* species are saprobes, with recent reports from Italy (Hyde et al. 2016; Wanasinghe et al. 2018; Brahmanage et al. 2020).

The aim of this study was to explore the diversity of *Comoclathris* species from dicotyledonous plants in China. Two new *Comoclathris* species (*C. clematidis* and *C. xanthoceratis*) from Jilin and Yunnan Provinces, China are described. The morphology was compared to other *Comoclathris* species. Maximum Likelihood and Bayesian Inference phylogenetic analyses were performed to confirm the taxonomic position of the isolates using ITS, LSU, SSU and *rpb*2 datasets. The results improve our understanding of the occurrence and distribution of *Comoclathris* species from China, thus expanding the knowledge of fungal biodiversity. This is also the first report of *Comoclathris* on dicotyledonous plants in China.

Materials and methods

Sample collection, morphological study and isolation

Dried wood samples were collected from Jilin (Temperate zone, 43°10'N, 124°20'E) and Yunnan Provinces (Subtropical region, 25°23'N, 102°42'E) in China. The samples were transferred to the laboratory in plastic bags with labels indicating the details of the collection. The characteristics of specimens were observed using a Zeiss Stemi 2000C stereomicroscope, equipped with a Leica DFC450C digital camera (Leica, Germany). Morphological characteristics of ascomata (n = 5), peridium (n = 10), hamathecium (n = 20), asci (n = 20), ascospores (n = 40) and other microscopic characteristics associated with ascomata were documented using a Zeiss AX10 microscope, equipped with an Axiocam 506 digital camera (ZEISS, Germany). The ZEN 3.4 application (blue edition) was used for microscopic measurements (ZEISS, Germany). The photos were edited using Adobe Photoshop CC2020 (Adobe Systems, USA).

Single spore isolation was used to obtain pure cultures (Senanayake et al. 2020) and germinated spores were cultured at 25 °C on potato dextrose agar (PDA). Type specimens were deposited in the Herbarium of Mycology, Jilin Agricultural University (HMJAU), Changchun, China and isotypes were deposited in Mae Fah Luang University (MFLU) Herbarium, Chiang Rai, Thailand. Ex-type

cultures were deposited in the International Cooperation Research Center of China for New Germplasm Breeding of Edible Mushrooms Culture Collection (CCMJ). The new taxa were registered in MycoBank (Crous et al. 2004).

DNA extraction, PCR amplification and sequencing

Pure mycelia were harvested after two weeks of incubation at 25 °C on PDA. The internal transcribed spacer regions (ITS), large subunit (LSU), small subunit (SSU) and RNA polymerase II second-largest subunit (*rpb*2) were amplified by polymerase chain reaction (PCR) using ITS5/ITS4, NS1/NS4 (White et al. 1990), LR0R/LR5 (Vilgalys and Hester 1990) and fRPB2-5F/fRPB2-7cR (Liu et al. 1999) primers, respectively. The amplification reactions and conditions for ITS, LSU and SSU were performed using the conditions described by Xu et al. (2022). The amplification conditions for *rpb*2 annealing conditions were different: 94 °C for 5 min, then 35 cycles of denaturation at 94 °C for 30 s, annealing at 56 °C for 45 s, elongation at 72 °C for 90 s and a final extension at 72 °C for 10 min. The amplification reactions were performed using 20 µl PCR mixtures containing 9 µl ddH$_2$O, 10 µl of 2× EsTaq MasterMix (Dye), 0.4 µl (200 ng/µl) of DNA template and 0.3 µl of 2 µmol/µl of forward and reverse primers. The PCR products were verified on 1% agarose electrophoresis gels stained with 0.5 ml of 10,000X standard DNA dye (Biotium, United States). Purification and sequencing of amplified PCR fragments were performed by Sangon Biotech Co, Shanghai, China.

Sequencing and sequence alignment

Sequences obtained from this study were searched in the GenBank database (http://blast.ncbi.nlm.nih.gov/) using BLAST. The newly-obtained sequences and data from recent publications (Brahmanage et al. 2020; Crous et al. 2021) were used in the analysis (Table 1). *Neocamarosporium betae* (CBS 523.66) and *N. calvescens* (CBS 246.79) were used as the outgroup in the phylogenetic analyses. The sequences were edited using BioEdit v. 7.1.3.0 and aligned with MAFFT v. 7 (Hall 1999; Katoh and Standley 2013). The alignments were trimmed using trimAl v. 1.2 under the gappyout option (Capella-Gutierrez et al. 2009). The datasets were combined using SequenceMatrix v. 1.7.8 (Vaidya et al. 2011). The newly-generated sequence data were deposited in GenBank (Benson et al. 2013).

Phylogenetic analysis

The phylogenetic analyses were performed using Maximum Likelihood (ML) and Bayesian Inference (BI) methods. RAxML-HPC2 on XSEDE, implemented in the CIPRES web portal (http://www.phylo.org/portal2/), was used for ML analysis, with a rapid bootstrapping algorithm of 1000 replicates (Stamatakis 2014). The suitability of the DNA model was analysed using jModelTest v. 2.1.10 on the CIPRES online portal for posterior probability. The best fit evolutionary models for individual and combined datasets were calculated under the Akaike Information Criterion (AIC) (Nylander 2004) and are as follows: GTR+I+G model for the ITS alignment, K80+I model for the LSU and SSU alignments, GTR+G model for the *rpb*2 alignment and SYM+I+G model for the combined datasets. Bayesian Inference analyses were carried out by using MrBayes v.

Table 1. Taxa used in the phylogenetic analyses and their corresponding GenBank accession numbers. The ex-type strains are indicated in bold and the newly-generated sequences are shown in cells with light grey shading.

Taxa	Strain	Host/Substrate	Country	GenBank accession numbers				References
				ITS	LSU	SSU	*rpb*2	
Comoclathris ambigua	CBS 366.52	–	USA	KY940748	AY787937	–	KT216533	(Woudenberg et al. 2017)
C. antarctica	**WA0000074564**	**Soil**	**Antarctica**	**MW040594**	**MW040597**	**–**	**–**	(Crous et al. 2021)
C. arrhenatheri	MFLUCC 15-0465	*Arrhenatherum elatius*	Italy	KX965737	KY000647	KX986348	KX938346	(Thambugala et al. 2017)
C. arrhenatheri	MFLUCC 15-0476	*Dactylis glomerata*	Italy	KY026595	KY000648	KX986349		
C. clematidis	**CCMJ 13076**	***Clematis* sp.**	**China**	**OQ534243**	**OQ534239**	**OQ676454**	**OQ547800**	This study
C. clematidis	CCMJ 13077	*Clematis* sp.	China	OQ534244	OQ534240	OQ676455	OQ547801	
C. compressa	CBS 156.53	*Castilleja miniata*	USA	–	KC584372	KC584630	KC584497	(Woudenberg et al. 2013)
C. compressa	CBS 157.53	–	USA	–	MH868679	KC584631	KC584498	
C. europaeae	**MFLU 20-0391**	**–**	**Italy**	**MT370396**	**MT370421**	**MT370367**	**MT729650**	(Brahmanage et al. 2020)
C. flammulae	**MFLU 20-0397**	***Clematis flammula***	**Italy**	**MT370397**	**MT370422**	**MT370368**	**MT729651**	
C. flammulae	MFLU 20-0399	*Colutea arborescens*	Italy	MT370395	MT370420	MT370366	–	
C. galatellae	**MFLUCC 18-0773**	***Galatella villosa***	**Ukraine**	**MN632549**	**MN632550**	**MN632551**	**–**	(Hongsanan et al. 2020)
C. incompta	CBS 467.76	*Olea europaea*	Greece	–	GU238087	GU238220	KC584504	(Aveskamp et al. 2010)
C. incompta	CH-16	*Olea europaea*	Tunisia	KU973716	KU973729	–	–	(Moral et al. 2017)
C. italica	**MFLUCC 15-0073**	***Thalictrum* sp.**	**Italy**	**KX500109**	–	–	–	(Tibpromma et al. 2015,)
C. lini	**MFLUCC 14-0968**	***Linum* sp.**	**Italy**	**KR049218**	**KR049219**	**KT210389**	–	(Nwanasinghe et al. 2015)
C. lini	MFLUCC 14-0561	*Ononis spinosa*	Italy	KT591614	KT591615	KT591616	–	
C. lonicerae	**MFLU 20-0385**	***Lonicera* sp.**	**Italy**	**MT370394**	**MT370419**	**MT370365**	**MT729649**	(Brahmanage et al. 2020)
C. lonicerae	MFLU 18-1236	*Colutea arborescens*	Italy	OL744429	OL744433	OL744435	OL771441	
C. permunda	MFLUCC 14-0974	*Phleum* sp.	Italy	KY659561	KY659564	KY659568	–	(Vu et al. 2019)
C. pimpinellae	**MFLUCC 14-1159**	***Pimpinella tragium***	**Russia**	**KU987665**	**KU987666**	**KU987667**	**–**	(Li et al. 2016)
C. rosae	**MFLU 15-0203**	***Rosa canina***	**Italy**	**MG828876**	**MG828992**	**MG829103**	**MG829249**	(Wanasinghe et al. 2018)
C. rosae	MFLU 16-0234	*Rosa canina*	Italy	MG828877	MG828993	MG829104	MG829250	
C. rosarum	**MFLUCC 14-0962**	***Rosa canina***	**Italy**	**MG828878**	**MG828994**	**MG829105**	**MG829251**	
C. rosigena	**MFLU 16-0229**	***Rosa canina***	**Italy**	**MG828879**	**MG828995**	**MG829106**	**MG829252**	
C. sedi	**MFLUCC 13-0763**	***Rosa* sp.**	**Italy**	**KP334717**	**KP334707**	**KP334727**	–	(Ariyawansa,et al. 2014)
C. sedi	MFLUCC 13-0817	*Sedum* sp.	Italy	KP334715	KP334705	KP334725	–	
C. spartii	**MFLUCC 13-0214**	***Spartium junceum***	**Italy**	**KM577159**	**KM577160**	**KM577161**	–	(Cours et al. 2014)
C. typhicola	CBS 602.72	–	Netherlands	MH860592	MH872288	–	–	(Vu et al. 2019)
C. xanthoceratis	**CCMJ 13078**	*Xanthoceras sorbifolium*	**China**	**OQ534245**	**OQ534241**	**OQ676456**	**OQ547802**	This study
C. xanthoceratis	CCMJ 13079	*Xanthoceras sorbifolium*	China	OQ534246	OQ534242	OQ676457	OQ547803	
Neocamarosporium betae	CBS 523.66	*Beta vulgaris*	Netherlands	FJ426981	MH870520	EU754080	KT389670	(Aveskamp et al. 2009)
N. calvescens	CBS 246.79	*Atriplex calotheca*	Germany	MH861203	EU754131	EU754032	KC584500	(Vu et al. 2019)

3.2.6 on the CIPRES web platform (Ronquist and Huelsenbeck 2003). Tree samples were taken every 1000th generation while Markov chains were run for 15,000,000 generations. Phylogenetic trees were illustrated in FigTree v. 1.4.4 (Rambaut 2018) and altered in Adobe Illustrator CS v. 6. RAxML bootstrap support values greater than or equal to 98% and Bayesian posterior probabilities equal to 1.00 were considered as strong statistical support. The data used in this study were deposited in the Zenodo repository (accession number doi: 10.5281/zenodo.7675986).

Results

Phylogenetic analyses

The combined multi-loci (ITS, LSU, SSU and *rpb*2) sequence dataset consisted of 32 taxa and 3,280 characters including gaps (ITS: 1–559 bp, LSU: 560–1,441 bp, SSU: 1,442–2,415 bp and *rpb*2: 2,416–3,280 bp). The best-scoring RAxML tree had a final log-likelihood value of -10805.548630. There were 691 distinct alignment patterns with 26.80% undetermined characters or gaps in the matrix. Estimated base frequencies were as follows: A = 0.254018, C = 0.226589, G = 0.268862, T = 0.250530; substitution rates AC = 2.459854, AG = 4.593060, AT = 1.418628, CG = 1.005203, CT = 7.378387 and GT = 1.000000. The proportion of invariable sites (I) was estimated to be 0.690973 and the gamma distribution shape parameter (α) was estimated to be 0.927322. A total of 4,592 trees were sampled in the BI analysis after the 20% burn-in with a stop value of 0.009967. The ML and BI trees were similar in topology (Fig. 1). Phylogenetic results demonstrated that *Comoclathris clematidis* and *C. xanthoceratis* formed a distinct lineage and clustered with *C. arrhenatheri* with strong statistical support (98% ML and 1.00 BPP). *Comoclathris clematidis* (CCMJ13076 and CCMJ 13077) and *C. xanthoceratis* (CCMJ 13078 and CCMJ 13079) formed a closely-related clade with high statistical support (100% ML and 1.00 BPP).

Taxonomy

***Comoclathris clematidis* R. Xu, Phukhams. & Y. Li, sp. nov.**
MycoBank No: 847614
Fig. 2

Etymology. Refers to the host genus, *Clematis*.

Description. *Saprobic* on dried branches of *Clematis* species. **Sexual morph: *Ascomata*** 150–230 × 120–150 μm ($\bar{x}$ = 176 × 138 μm, n = 5), solitary, scattered or aggregated in small groups, immersed to erumpent, subglobose, elongated, black, without a distinct ostiole. ***Peridium*** 10–20 μm wide at the base, 15–20 μm wide at the sides, comprising thick-walled cells of ***textura angularis***, dark brown to black. ***Hamathecium*** comprising numerous, 1–3.5 μm wide ($\bar{x}$ = 2.0 μm, n = 20), filamentous, septate, rarely branched pseudoparaphyses, hyaline, embedded in a gelatinous matrix, extending above the asci. ***Asci*** 114–174 × 27–43 μm ($\bar{x}$ = 140 × 34 μm, n = 20), 8-spored, bitunicate, fissitunicate, cylindrical-clavate, short pedicellate, apically rounded, with an ocular chamber. ***Ascospores*** 22–39 × 8–21 μm ($\bar{x}$ = 30 × 14 μm, n = 40), 1–2-seriate, partially overlapping, broadly fusiform, initially 3-septate and yellowish, becoming brown, verrucose or echinulate wall, muriform, with 3 transversely septa and a vertical septum in second and third cells, constricted at the septa, with obtuse ends, smooth-walled, surrounded by a thick mucilaginous sheath. **Asexual morph**: Undetermined.

Culture characteristics. Colonies on PDA reaching 40 mm diam. after three weeks at 25 °C. Cultures from above, circular, flat to umbonate, covered with flocculent aerial mycelium, velvety on the surface, greenish-olivaceous, dense, entire edge; reverse black in the middle, green olivaceous radiating outwardly, white mycelium at the edge.
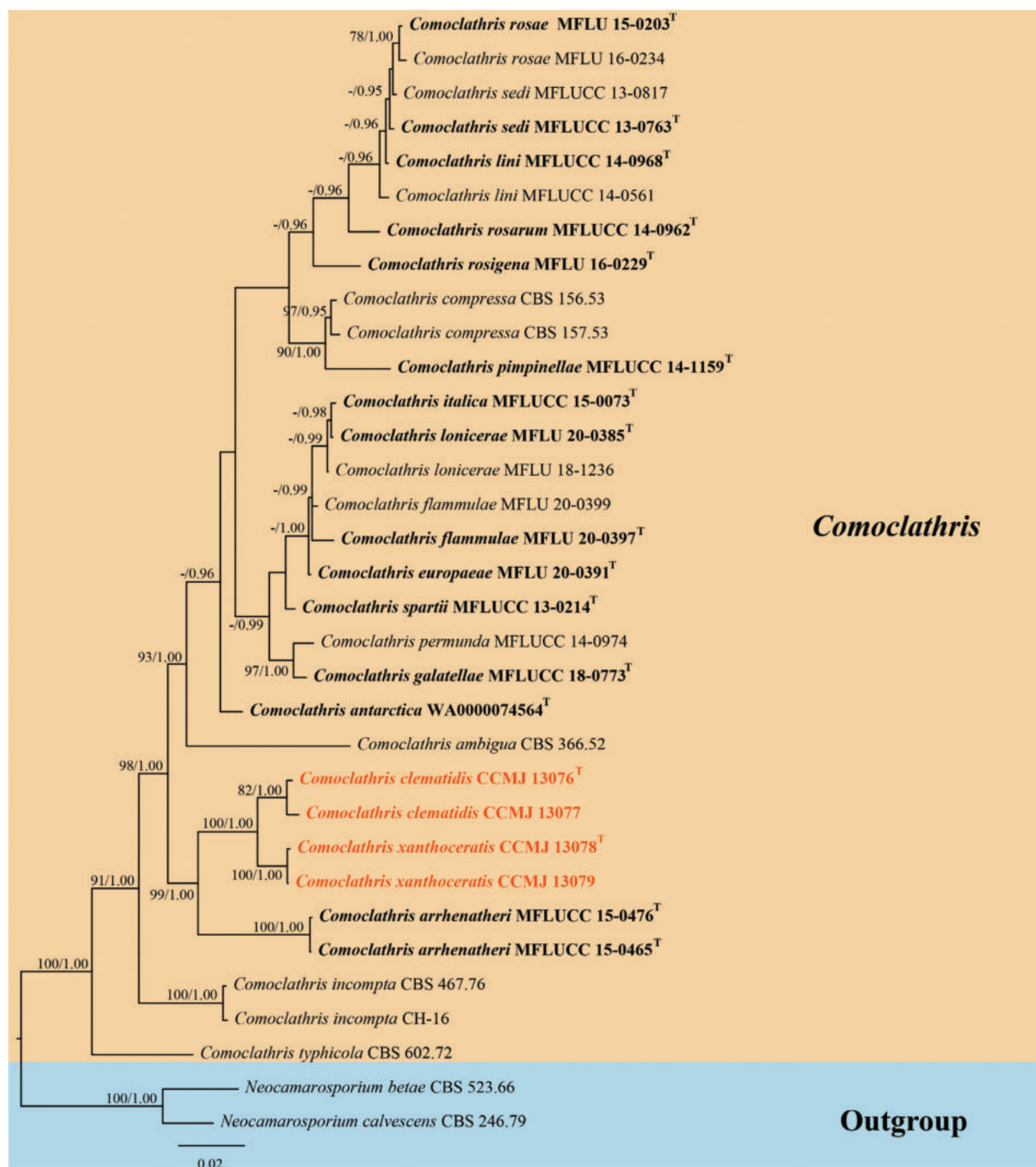
Figure 1. The Bayesian 50% majority-rule consensus phylogram, based on a concatenated ITS, LSU, SSU and *rpb*2 dataset of *Comoclathris*. The tree is rooted with *Neocamarosporium betae* (CBS 523.66) and *N. calvescens* (CBS 246.79). RAxML bootstrap support values ≥ 70% (ML, left) and Bayesian posterior probabilities ≥ 0.90 (BPP, right) are shown near the nodes. The new isolates are indicated in orange. The type strains are in bold and labelled with T.

Material examined. CHINA. Yunnan Province, Kunming, on the dead aerial branch of *Clematis* sp. (Ranunculaceae), 24 April 2021, S. Tibpromma, S42, HMJAU 64844 (**holotype**); ex-type, CCMJ 13076; MFLU 23-0384 (isotype), ex-isotype, CCMJ 13077.

Notes. In the phylogenetic analyses, *Comoclathris clematidis* (CCMJ 13076 and CCMJ 13077) clustered with *C. xanthoceratis* (CCMJ 13078 and CCMJ

13079) with 82% ML and 100 BPP within *Comoclathris* (Fig. 1). *Comoclathris clematidis* was found on dried stems of *Clematis* species in the subtropical zone of Yunnan Province, China. The majority of *Comoclathris* species are found in temperate regions, but only *C. incompta* (CH-16) has been identified in subtropical regions (Moral et al. 2017). *Comoclathris clematidis* differs from *C. flammulae* which was also found on *Clematis* by its larger asci (114−174 × 27−43 μm vs. 50−55 × 13−17 μm) and larger ascospores (22−39 × 8−21 μm vs. 16−22 × 10−16 μm). In addition, *C. clematidis* contains fewer transverse septa in ascospores (3 transverse septa vs. 6 transverse septa) (Brahmanage et al. 2020). The new species *Comoclathris clematidis* is distinguishable from *Comoclathris sedi* which was also isolated from *Clematis* by having larger asci (114−174 × 27−43 μm vs. 80−110 × 16−18 μm), larger ascospores (22−39 × 8−21 μm vs. 19−20 × 8−10 μm) and fewer ascospore septa (3 transverse septa vs. 4−5 transverse septa) (Ariyawansa et al. 2015). The ascomata of *C. clematidis* are immersed to superficial and appear as black spots or convex surfaces, while the ascomata of *C. xanthoceratis* are immersed to semi-immersed and covered with dark brown setae. *Comoclathris clematidis* has cylindrical-clavate asci and verrucose or echinulate ascospore walls, while *C. xanthoceratis* has clavate asci and smooth-walled ascospores. Both *C. clematidis* and *C. xanthoceratis* have ascospores with 3 transverse septa and 2 vertical septa. In addition, the two species show different culture characteristics and only *C. xanthoceratis* produce ascocarps in the culture. The ITS and *rpb*2 base pair differences between the two species are 0.95% (5/526, no gaps) and 4.69% (34/725, no gaps), respectively.

In the BLASTn search, the *rpb*2 sequence was 89.53% similar to *Comoclathris arrhenatheri* (MFLUCC 15-0465) with 100% query cover, translating to 89.53% similarity. The LSU sequence was 98.76% similar to *C. permunda* (CBS: 127967) with 99% query cover, translating to 97.77% similarity, while the SSU sequence was 98.58% similar to *C. lini* (MFLUCC 14-0968) with 100% query cover, translating to 98.58% similarity. The ITS region was 97.93% similar to *Comoclathris* sp. (14APR) with 93% query cover, translating to 91.07% similarity. Therefore, *Comoclathris clematidis* was introduced as a novel species.

***Comoclathris xanthoceratis* R. Xu, Phukhams. & Y. Li, sp. nov.**
MycoBank No: 847615
Fig. 3

Etymology. Refers to the host genus, *Xanthoceras*.

Description. *Saprobic* on dried stems of *Xanthoceras sorbifolium*. **Sexual morph: *Ascomata*** solitary, scattered or aggregated in small groups, 147−221 × 114−130 μm ($\bar{x}$ = 187−124 μm, n = 5), immersed to semi-immersed, sub-globose, black, elongated, covered with dark brown setae, without a distinct ostiole. ***Peridium*** 13−20 μm wide at the base, 20−32 μm wide at the sides, comprising thick-walled cells of ***textura angularis***, dark brown to black; inner layer composed of thin-walled cells of ***textura angularis***, hyaline. ***Hamathecium*** comprising 1.5−4.0 μm wide, septate, filiform, embedded in a gelatinous matrix, rarely branched pseudoparaphyses, extending above the asci. ***Asci*** 8-spored, bitunicate, fissitunicate, 99−165 × 36−48 μm ($\bar{x}$ = 127 × 42 μm, n = 20), clavate,
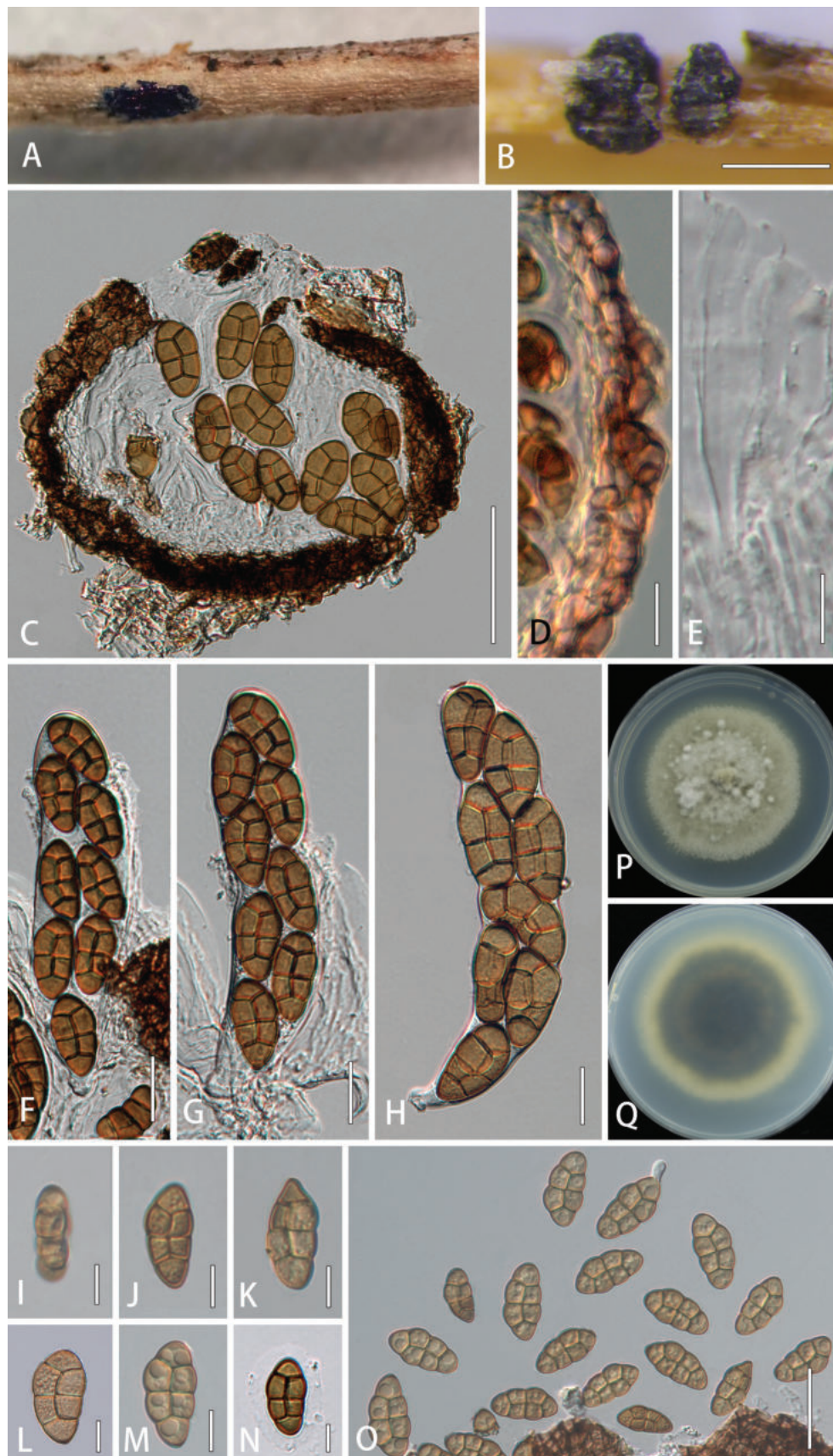
Figure 2. *Comoclathris clematidis* (HMJAU 64844, holotype) **A, B** appearance of ascomata on host substrate **C** vertical section of ascoma **D** peridium **E** pseudoparaphyses **F−H** asci **I−O** ascospores **P, Q** culture characteristics on PDA after three weeks at 25 °C. Scale bars: 200 µm (**B**); 50 µm (**C**); 20 µm (**E−H, O**); 10 µm (**D, I−N**).
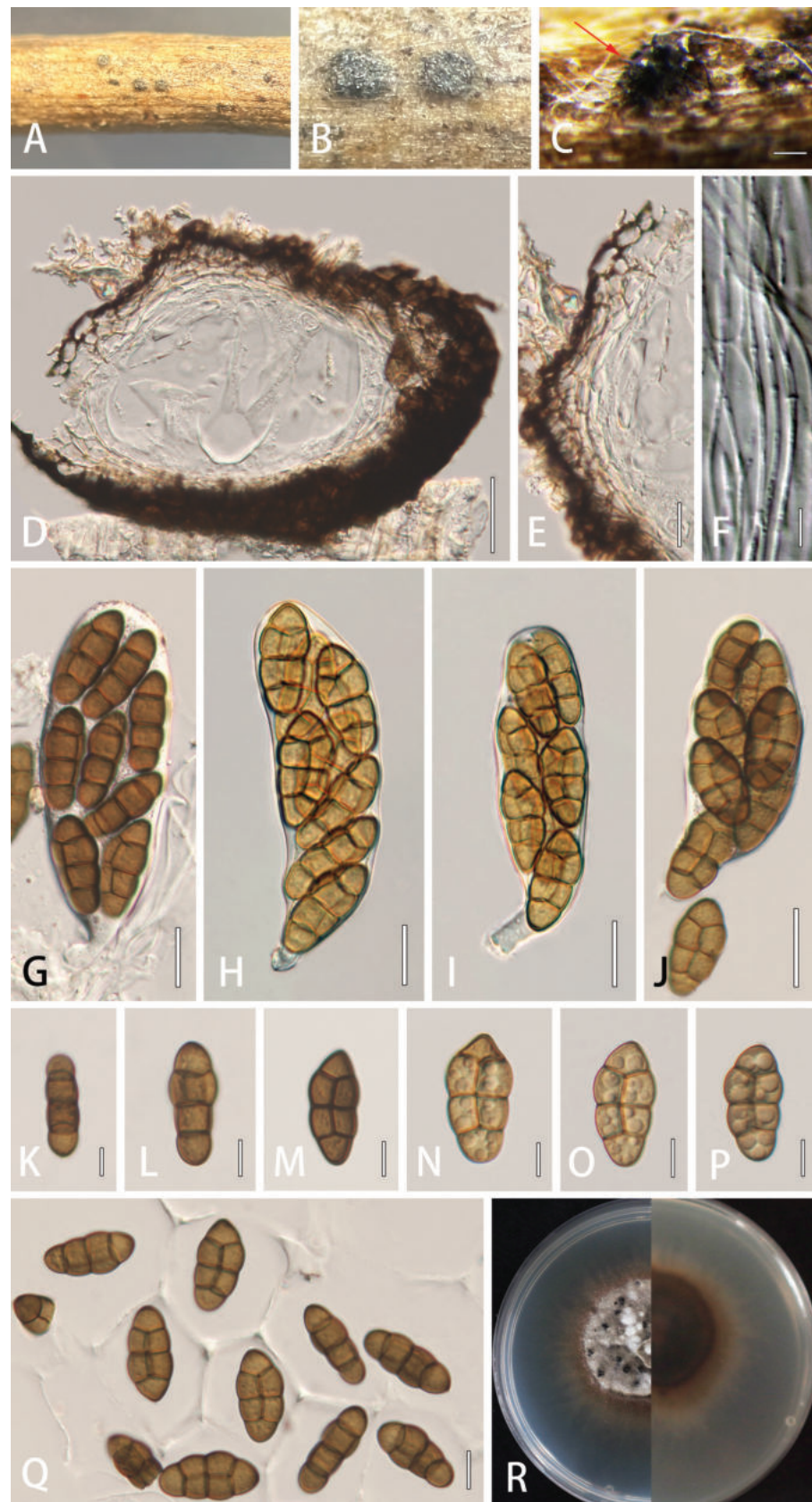
Figure 3. *Comoclathris xanthoceratis* (HMJAU 64846, holotype) **A–C** appearance of ascomata on host substrate **D** vertical section of ascoma **E** peridium **F** pseudoparaphyses **G–J** asci (**H, I**) asci production from the sterile condition) **K–Q** ascospores **R** culture characteristics on PDA after three weeks at 25 °C (black dots indicate the sexual reproduction in culture condition). Scale bars: 200 μm (**C**); 50 μm (**D**); 20 μm (**G–J**); 10 μm (**E, K–Q**); 5 μm (**F**).

short pedicellate, apically rounded, with an ocular chamber. **Ascospores** 23−42 × 9−19 μm ($\overline{x}$ = 37 × 16 μm, n = 40), 1−2-seriate, muriform, broadly fusiform, with 3 transverse septa and a vertical septum in second and third cells, brown to dark brown, with obtuse ends, smooth-walled, surrounded by a thick muci-laginous sheath. **Asexual morph**: Undetermined.

Culture characteristics. Colonies on PDA reaching 30 mm diam. after three weeks at 25 °C. Cultures from above, dense, round, umbonate, wrinkled and folded, papillate with white aerial mycelium, radial edge, orange at the margin; reverse reddish, white mycelium present at the margin.

Material examined. CHINA. Jilin Province, Changchun, on dead stem of *Xanthoceras sorbifolium* Bunge (Sapindaceae), 2 July 2022, Rong Xu, XR71, HM-JAU 64846 (**holotype**); ex-type, CCMJ 13078; MFLU 23-0385 (isotype), ex-iso-type, CCMJ 13079.

Notes. *Comoclathris xanthoceratis* (CCMJ 13078 and CCMJ 13079) is closely related to *C. clematidis* (CCMJ 13076 and CCMJ 13077) (100% ML and 1.00 BPP). The two species are phylogenetically closely related to *C. arrhenatheri* (MFLUCC 15-0465). However, there are distinct differences in morphology (Thambugala et al. 2017). The asci of *C. arrhenatheri* are smaller than *C. clematidis* and *C. xanthoceratis* (*C. arrhenatheri* vs. *C. clematidis* vs. *C. xanthoceratis*: 70−95 × 18.5−25 vs. 114−174 × 27−43 vs. 99−165 × 36−48 μm, respectively). *Comoclathris arrhenatheri* have ascospores with 4 transverse septa and 2−3 vertical septa, while *C. clematidis* and *C. xanthoceratis* only have 3 transverse septa and 2 vertical septa. Additionally, the ascospores of *C. arrhenatheri* are short-er than *C. clematidis* and *C. xanthoceratis* (*C. arrhenatheri* vs. *C. clematidis* vs. *C. xanthoceratis*: 16.5−22 × 7.7−10.2 vs. 22−39 × 8−21 vs. 23−42 × 9−19 μm).

A pairwise comparison of the ITS region between *C. xanthoceratis* and *C. arrhenatheri* demonstrated 8.95% (46/514, no gaps) base-pairs difference, while there were 74 base-pair difference in the *rpb*2 gene (10.2%, no gaps). Hence, *C. xanthoceratis* is introduced as a new species, based on morphological and nucleotide differences. This is also the first report of *Comoclathris* species found on *Xanthoceras sorbifolium*.

Discussion

In this study, we described two new *Comoclathris* species from China, based on morphological and multi-locus phylogenic analyses. The identifying morpho-logical features of *Comoclathris* include operculate perithecia and muriform, asymmetrical, strongly divided ascospores (Shoemaker and Babcock 1992; Wanasinghe et al. 2018). Phylogenetic analyses, based on four combined loci (ITS, LSU, SSU and *rpb*2), as well as morphological characters, are important for the identification of *Comoclathris* species (Table 2). The phylogeny presented here is similar to previous studies (Thambugala et al. 2017; Wijayawardene et al. 2017; Wanasinghe et al. 2018; Brahmanage et al. 2020; Hongsanan et al. 2020), demonstrating a robust backbone tree in this study.

In the phylogenetic analyses, many species appear to be conspecific and their phylogenetic placement remains to be resolved. It implied that the concept of sub-division, based on molecular phylogeny alone, has been inaccurate. For example, Wanasinghe et al. (2015) introduced *C. lini* as a new species, although *C. lini* grouped in a well-supported clade with *C. sedi* (100% ML and 1.00 BPP). *Comoclathris lini* is

Table 2. Synopsis of *Comoclathris* species with the newly-introduced species in bold.

Taxa	Sexual Morph			Asexual morph		Reference
	Ascomata	Asci	Ascospores	Conidiomata	Conidia	
Comoclathris antarctica	339 (± 103) × 299 (± 97) μm, separate or in groups, dark brown to almost black, strongly enclosed in aerial hyphae, ovoid to spherical, without distinct ostiole, neck very short, operculum semi-spherical, flattened; perithecial hyphae dark; wall of 2–3 cell layers.	72–84 × 18–26 μm, mostly 8-spored, immature asci shorter (~ 60 μm), cylindrical to clavate, bitunicate with a rounded apex.	31 × 13.5 μm, lanceolate to ovoid, clavate, yellow to pale brown, elongated, asymmetrical with a blunt apex, muriform, with 6–8 transvers septa, apical cell not divided.	Undetermined		(Crous et al. 2021)
C. arrhenatheri	100–150 × 80–120 μm, solitary, scattered or aggregated in small groups, immersed to erumpent, black, elongate, subglobose, covered with pale to dark brown setae, without a distinct ostiole.	65–95 × 18.5–25 μm, 8-spored, cylindrical-clavate, short pedicellate, apically rounded, with an ocular chamber.	16.5–22 × 7.7–10.2 μm, 1–2 seriate, partially overlapping initially yellowish, 1-septate, becoming yellow to pale brown and muriform, with 4 transverse septa and 2–3 vertical septa.	Undetermined		(Thambugala et al. 2017)
C. clematidis	**150–230 × 120–150 μm solitary, scattered or aggregated in small groups, immersed to erumpent, subglobose, elongated, black, without a distinct ostiole.**	**114–174 × 27–43 μm, 8-spored, cylindrical-clavate, short pedicellate, apically rounded, with an ocular chamber.**	**22–39 × 8–21 μm, 1–2 seriate, partially overlapping, broadly fusiform, initially 3 septate and yellowish, becoming brown, muriform, with 3 transversely septa and a vertical septum, with a thick mucilaginous sheath.**	**Undetermined**		**This study**
C. compressa	200–520 × 150–320 μm, scattered, immersed, sub-epidermal, later superficial, depressed globose, with smooth, straight to bent, tapered, brown hairs.	80–120 × 20–30 μm, numerous, saccate, with tetraserlate to biseriate spores.	24–29 × 10–14 μm, fusoid, straight, transversely 3-septate, with 1 longitudinal septum in central cells, dark reddish-brown, with guttules, smooth, with a uniform sheath 2–3 μm wide.	Undetermined		(Shoemaker et al. 1992)
C. europaeae	240–250 × 145–165 μm, solitary, scattered, semi-immersed to slightly erumpent, dark brown to black, globose to subglobose, without a distinct ostiole.	60–70 × 15–18 μm, 8-spored, cylindrical-clavate, pedicellate, apex rounded, with an indistinct ocular chamber.	20–22 × 11–13 μm, uni-to biseriate, partially overlapping, muriform, brown, transversely septate or muriform, with 7 transverse septa.	Undetermined		(Brahmanage et al. 2020)
C. flammulae	105–130 × 80–90 μm, solitary or aggregated, immersed, globose to subglobose, dark brown to black, without a distinct ostiole.	50–55 × 13–17 μm, 8-spored, cylindrical-clavate, short pedicellate, rounded at the apex, with an indistinct ocular chamber.	16–22 × 10–16 μm, overlapping uni-to biseriate, yellowish-brown when immature, becoming dark brown at maturity, clavate, with acute ends, muriform, with 6 transverse septa, 1–2 longitudinal septa.	Undetermined		(Brahmanage et al. 2020)
C. galatellae	200–550 × 230–340 μm, immersed, erumpent to superficial, broadly to narrowly oblong and flattened, ostiolate.	50–90 × 14–17 μm, 8-spored, cylindrical to clavate, with furcate pedicel and minute ocular chamber.	20–30 × 6–8 μm, uni-seriate or partially overlapping, mostly ellipsoidal, brown or pale brown, muriform, 2–4 transverse septa, 1–2 longitudinal septa, without sheath.	None	2–4 × 1–2 μm, oval to ellipsoid, hyaline, aseptate, guttulate.	(Hongsanan et al. 2020)
C. italica	180–240 × 200–250 μm, semi-immersed to erumpent, solitary, scattered, broadly oblong to flattened, dark brown to black, coriaceous, cupulate when dry.	100–120 × 30–35 μm, 8-spored, clavate, short pedicellate, thick-walled at the apex, with a minute ocular chamber.	30–35 × 10–15 μm, overlapping 1–3 seriate, initially 1 septate and hyaline, becoming brown at maturity, muriform, mostly ellipsoidal, 6–8 transversely septate, with 1–2 vertical septa.	Undetermined		(Thambugala et al. 2017)
C. lini	260–290 × 300–350 μm, superficial, solitary, scattered, broadly oblong and flattened, dark brown to black, coriaceous, cupulate when dry, ostiolate.	110–130 × 15–25 μm, 8-spored, cylindrical to cylindrical-clavate, pedicellate, thick walled at the apex, with a minute ocular chamber.	20–25 × 10–12 μm, overlapping, initially hyaline, becoming brown at maturity, mostly ellipsoidal, with upper part widest, muriform, with 4–6 transverse septa and 4–6 vertical septa.	Undetermined		(Wanasinghe et al. 2015)

Taxa	Sexual Morph			Asexual morph		Reference
	Ascomata	Asci	Ascospores	Conidiomata	Conidia	
C. lonicerae	370–485 × 255–360 μm, solitary or aggregated, scattered, semi-immersed to erumpent, globose to subglobose, dark brown to black, without a distinct ostiole.	180–192 × 60–74 μm, 8-spored, broadly cylindrical to cylindrical clavate, short pedicellate, rounded at the apex, with an indistinct, shallow ocular chamber.	55–70 × 20–30 μm, overlapping uni or biseriate, yellowish-brown, transversely septate or muriform, with 3–5 transverse septa, 1–2 longitudinal septa, with rounded ends.		Undetermined	(Brahmanage et al. 2020)
C. permunda	150–200 × 150–200 μm, semi-immersed to erumpent, solitary, scattered, broadly oblong to flattened, dark brown to black, coriaceous, cupulate when dry, with brown to reddishbrown, setae.	90–110 × 19–22 μm, 8-spored, cylindrical-clavate, with a 20–30 μm long pedicel, thick-walled at the apex, with a minute ocular chamber.	22–28 × 9–12 μm, overlapping 1–2-seriate, muriform, mostly ellipsoidal, 2–4 transversely septate, with 1–2 vertical septa, initially hyaline, becoming golden brown at maturity, surrounded by a thick, hyaline, mucilaginous sheath.		Undetermined	(Thambugala et al. 2017)
C. pimpinellae	155–135 × 88–95 μm, solitary or aggregated, semi-immersed or rarely somewhat superficial, globose to subglobose, dark brown to black.	58–75 × 14–16 μm, 8-spored, cylindrical-clavate, short-pedicellate, rounded at the apex, with indistinct, shallow, ocular chamber.	14–16 × 5–8 μm, overlapping biseriate, yellow to light brown, transversely septate or muriform, with 3 transverse septa, central segments with 2 longitudinal septa, end segments with 2 angular septa, surrounded by a thick, hyaline, a mucilaginous sheath.		Undetermined	(Li et al. 2016)
C. rosae	120–150 × 175–200 μm diam, immersed to erumpent, globose or subglobose, dark brown to black, coriaceous.	70–110 × 15–30 μm, 8-spored, cylindrical-clavate to clavate, pedicellate, thick-walled at the apex, with minute ocular chamber.	20–30 × 8–15 μm, overlapping 1–2 seriate, mostly ellipsoidal, muriform, 4–7 transversely septate, with 1–2 vertical septa, conically rounded at both ends.		Undetermined	(Wanasinghe et al. 2018)
C. rosarum	200–300 × 300–400 μm diam, immersed to erumpent, globose or subglobose, dark brown to black, coriaceous.	150–200 × 35–50 μm, 8-spored, clavate, pedicellate, thick-walled at the apex, with minute ocular chamber.	40–60 × 20–25 μm, overlapping 1–2 seriate, mostly ellipsoidal, muriform, 6–7 transversely septate, with 2–4 vertical septa, deeply constricted at the middle septum.		Undetermined	(Wanasinghe et al. 2018)
C. rosigena	180–220 × 300–400 μm, immersed to erumpent, globose or subglobose, dark brown to black, coriaceous.	150–180 × 45–60 μm, 8-spored, cylindrical-clavate to clavate, pedicellate, thick-walled at the apex, with minute ocular chamber.	40–60 × 16–24 μm, overlapping biseriate, mostly ellipsoidal, muriform, 5–7 transversely septate, with 1 vertical septum, slightly constricted at the middle septum.		Undetermined	(Wanasinghe et al. 2018)
C. sedi	200–250 × 290–350 μm, scattered or aggregated on the host stem, subglobose or nearly globose, superficial, coriaceous, brown to blackish-brown with a blunt ostiole.	80–110 × 16–18 μm, 8-spored, cylindrical to cylindrical-clavate, with a short knob-like pedicel and indistinct shallow ocular chamber.	19–20 × 8–10 μm, 1–2 overlapping seriate, fusiform, muriform, with 4–5 transverse septa and 1–2 longitudinal septa, not constricted at the septa.		Undetermined	(Ariyawansa et al. 2015)
C. spartii	Up to 200 μm diam., solitary, scattered or aggregated in small groups, immersed in host tissue, dark brown to black, globose to subglobose, without a distinct ostiole.	100–180 × 23–28 μm, 8-spored cylindrical-clavate, stipitate, apex rounded, with a small apical chamber.	25–34 × 9–14.5 μm, uni- to biseriate in asci, muriform, yellow to pale brown, broadly fusiform, with obtuse ends, constricted at the primary septum, surrounded by a mucilaginous sheath.		Undetermined	(Crous et al. 2014)
C. typhicola	350–400 μm diam. Ostiole 100–125 μm diam.	100–125 × 25–30 μm, numerous, clavate, hyaline.	45–50 × 10–12.5 μm, muriform, oval to cylindrical, straight, rounded at one end, slightly tapered at the other, hyaline when immature, light yellow to yellow.		Undetermined	(Adamska et al. 2012)
C. xanthoceratis	**147–221 × 114–130 μm, solitary, scattered or aggregated in small groups,, immersed to semi-immersed, subglobose, black, elongated, covered with dark brown setae, without a distinct ostiole.**	**99–165 × 36–48 μm, 8-spored, bitunicate, fissitunicate, clavate, short pedicellate, apically rounded, with an ocular chamber.**	**23–42 × 9–19 μm, 1–2 seriate, muriform, broadly fusiform, with 3 transverse septa and a vertical septum in second and third cells, brown to dark brown, with obtuse ends, smooth-walled, with a thick mucilaginous sheath.**		**Undetermined**	**This study**

different from *C. sedi* in having comparatively larger asci and different ascospore septa (4–6 transverse septa, 4–6 longitudinal septa vs. 4–5 transverse septa, 1–2 longitudinal septa). In our study, the base pair differences amongst ITS, LSU and *rpb*2 of *Comoclathris clematidis* and *C. xanthoceratis* were 0.95% (5/526, no gaps), 0.12% (1/803, no gaps) and 4.69% (34/725, no gaps), respectively. There were no differences in the SSU sequences between the two species. The *rpb*2 can be used as an effective barcode to distinguish *Comoclathris* species including *C. clematidis* and *C. xanthoceratis* as it is phylogenetically informative and reflects interspecific relationships (Woudenberg et al. 2013; Ariyawansa et al. 2015; Thambugala et al. 2017; Wanasinghe et al. 2018; Brahmanage et al. 2020). Thus, we recommend using morphological characters coupled with molecular phylogeny to delineate *Comoclathris*, especially including *rpb*2 marker as a protein-coding locus.

The host specificity of *Comoclathris* remains unclear. A single *Comoclathris* species can be found colonising more than one host, while various *Comoclathris* species have also been associated with the same host (Ariyawansa et al. 2015; Thambugala et al. 2017; Wanasinghe et al. 2018; Brahmanage et al. 2020). For example, *C. flammulae* and *C. lonicerae* were found on *Colutea arborescens* (Brahmanage et al. 2020), while *C. rosae*, *C. rosarum* and *C. rosigena* were found on *Rosa canina* (Wanasinghe et al. 2018). Some *Comoclathris* species have been associated with different hosts. *Comoclathris arrhenatheri* was collected from *Arrhenatherum elatius* and *Dactylis glomerata* (Thambugala et al. 2017, Italy), while *C. flammulae* was collected from *Clematis flammula* and *Colutea arborescens* in Italy (Brahmanage et al. 2020).

Comoclathris members are mostly distributed in the temperate areas (i.e. Greece, Italy, Netherlands, Russia, Ukraine and USA), while only *C. incompta* (CH-16) and *C. antarctica* (WA0000074564) have been reported in the subtropical and Arctic zones, respectively (Moral et al. 2017; Crous et al. 2021). In this study, *C. clematidis* (CCMJ 13076 and CCMJ 13077) was collected from *Clematis* species (Ranunculaceae) in Kunming City, which is located in the subtropical region. *Comoclathris xanthoceratis* (CCMJ 13078 and CCMJ 13079) was isolated from *Xanthoceras sorbifolium* (Sapindaceae) in Changchun, Jilin Province (temperate zone), which is consistent with many previous studies (Woudenberg et al. 2013; Ariyawansa et al. 2015; Hyde et al. 2016; Li et al. 2016; Thambugala et al. 2017; Wijayawardene et al. 2017; Wanasinghe et al. 2018; Brahmanage et al. 2020; Hongsanan et al. 2020). This study also extends the knowledge of the host range and geographic distribution of *Comoclathris* species.

Acknowledgements

Additional information

Conflict of interest

The authors have declared that no competing interests exist.

Ethical statement

No ethical statement was reported.

Funding

Author contributions

Data curation, Rong Xu and Wengxin Su; Formal analysis, Shangqing Tian; Funding acquisition, Chayanard Phukhamsakda and Yu Li; Investigation, Rong Xu and Wengxin Su; Project administration, Chayanard Phukhamsakda and Yu Li; Software, Yang Wang; Supervision, Chayanard Phukhamsakda; Writing – original draft, Rong Xu; Writing – review and editing: Chayanard Phukhamsakda and Yu Li. All authors have read and agreed to the published version of the manuscript.

Author ORCIDs

Rong Xu https://orcid.org/0000-0002-7744-6321
Wenxin Su https://orcid.org/0000-0002-5470-5853
Yang Wang https://orcid.org/0000-0002-5899-3987
Shangqing Tian https://orcid.org/0000-0003-4758-3023
Yu Li https://orcid.org/0000-0003-4966-701X
Chayanard Phukhamsakda https://orcid.org/0000-0002-1033-937X

Data availability

All of the data that support the findings of this study are available in the main text or supplementary information.

References

Adamska I (2012) Interesting instances of Ascomycota on *Acorus*, *Phragmites* and *Typha*. Phytopathologia 64: 19–27.

Ahmad S (1978) Ascomycetes of Pakistan Part II. Biological Society of Pakistan Monograph 8: 1–144.

Ariyawansa HA, Phookamsak R, Tibpromma S, Kang JC, Hyde KD (2014) A molecular and morphological reassessment of Diademaceae. The Scientific World Journal 675348: 1–11. https://doi.org/10.1155/2014/675348

Ariyawansa HA, Thambugala KM, Manamgoda DS, Jayawardena RS, Camporesi E, Boonmee S, Wanasinghe DN, Phookamsak R, Hongsanan S, Singtripop C, Chukeatirot E, Kang JC, Jones EBG, Hyde KD (2015) Towards a natural classification and backbone tree for Pleosporaceae. Fungal Diversity 71(1): 85–139. https://doi.org/10.1007/s13225-015-0323-z

Aveskamp MM, Verkley GJ, de Gruyter J, Murace MA, Perelló A, Woudenberg JH, Groenewald JZ, Crous PW (2009) DNA phylogeny reveals polyphyly of *Phoma* section *Peyronellaea* and multiple taxonomic novelties. Mycologia 101(3): 363–382. https://doi.org/10.3852/08-199

Aveskamp MM, Gruyter JD, Woudenberg JHC, Verkley GJM, Crous PW (2010) Highlights of the Didymellaceae: A polyphasic approach to characterise *Phoma* and related pleosporalean genera. Studies in Mycology 65(65): 1–60. https://doi.org/10.3114/sim.2010.65.01

Benson DA, Cavanaugh M, Clark K, Karsch-Mizrachi I, Lipman DJ, Ostell J, Sayers EW (2013) GenBank. Nucleic Acids Research 41(D1): D36–D42. https://doi.org/10.1093/nar/gks1195

Brahmanage RS, Dayarathne MC, Wanasinghe DN, Thambugala KM, Jeewon R, Chethana KWT, Samarakoon MC, Tennakoon DS, De Silva NI, Camporesi E, Raza M, Yan JY, Hyde KD (2020) Taxonomic novelties of saprobic Pleosporales from selected dicotyledons and grasses. Mycosphere 11(1): 2481–2541. https://doi.org/10.5943/mycosphere/11/1/15

Capella-Gutierrez S, Silla-Martínez JM, Gabaldón T (2009) TrimAl: A tool for automated alignment trimming in large-scale phylogenetic analyses. Bioinformatics 25(15): 1972–1973. https://doi.org/10.1093/bioinformatics/btp348

Checa J (2004) Dothideales dictiospóricos-dictyosporic dothideales. Flora Mycologica Iberica 6: 1–162.

Chlebicki A (2002) Biogeographic relationships between fungi and selected glacial relict plants. Monographiae Botanicae 90: 1–230. https://doi.org/10.5586/mb.2002.001

Clements FE (1909) The genera of fungi. The HW Wilson Company, 244 pp. https://doi.org/10.5962/bhl.title.54501

Crous PW, Gams W, Stalpers JA, Robert V, Stegehuis G (2004) MycoBank: An online initiative to launch mycology into the 21st century. Studies in Mycology 50: 19–22. https://edepot.wur.nl/31039

Crous PW, Wingfield MJ, Schumacher RK, Summerell BA, Giraldo A, Gene J, Guarro J, Wanasinghe DN, Hyde KD, Camporesi E, Jones EB (2014) Fungal Planet description sheets: 281–319. Persoonia 33(1): 212–289. https://doi.org/10.3767/003158514X685680

Crous PW, Cowan DA, Maggs-Kölling G, Yilmaz N, Thangavel R, Wingfield MJ, Noordeloos ME, Dima B, Brandrud TE, Jansen GM, Morozova OV, Vila J, Shivas RG, Tan YP, Bishop-Hurley S, Lacey E, Marney TS, Larsson E, Le Floch G, Lombard L, Nodet P, Hubka V, Alvarado P, Berraf-Tebbal A, Reyes JD, Delgado G, Eichmeier A, Jordal JB, Kachalkin AV, Kubátová A, Maciá-Vicente JG, Malysheva EF, Papp V, Rajeshkumar KC, Sharma A, Spetik M, Szabóová D, Tomashevskaya MA, Abad JA, Abad ZG, Alexandrova AV, Anand G, Arenas F, Ashtekar N, Balashov S, Bañares Á, Baroncelli R, Bera I, Biketova A, Blomquist CL, Boekhout T, Boertmann D, Bulyonkova TM, Burgess TL, Carnegie AJ, Cobo-Diaz JF, Corriol G, Cunnington JH, Da Cruz MO, Damm U, Davoodian N, Santiago ALCM, Dearnaley J, de Freitas LWS, Dhileepan K, Dimitrov R, Di Piazza S, Fatima S, Fuljer F, Galera H, Ghosh A, Giraldo A, Glushakova AM, Gorczak M, Gouliamova DE, Gramaje D, Groenewald M, Gunsch CK, Gutiérrez A, Holdom D, Houbraken J, Ismailov AB, Istel Ł, Iturriaga T, Jeppson M, Jurjević Ž, Kalinina LB, Kapitonov VI, Kautmanová I, Khalid AN, Kiran M, Kiss L, Kovács Á, Kurose D, Kušan I, Lad S, Læssøe T, Lee HB, Luangsa-Ard JJ, Lynch M, Mahamedi AE, Malysheva VF, Mateos A, Matočec N, Mešić A, Miller AN, Mongkolsamrit S, Moreno G, Morte A, Mostowfizadeh-Ghalamfarsa R, Naseer A, Navarro-Ródenas A, Nguyen TTT, Noisripoom W, Ntandu JE, Nuytinck J, Ostrý V, Pankratov TA, Pawłowska J, Pecenka J, Pham THG, Polhorský A, Pošta A, Raudabaugh DB, Reschke K, Rodríguez A, Romero M, Rooney-Latham S, Roux J, Sandoval-Denis M, Th. Smith M, Steinrucken TV, Svetasheva TY, Tkalčec Z, van der Linde EJ, v.d. Vegte M, Vauras J, Verbeken A, Visagie CM, Vitelli JS, Volobuev SV, Weill A, Wrzosek M, Zmitrovich IV, Zvyagina EA, Groenewald JZ (2021) Fungal Planet description sheets: 1182–1283. Persoonia 46: 313–528. https://doi.org/10.3767/persoonia.2021.46.11

Eriksson OE (2014) Checklist of the non-lichenized ascomycetes of Sweden. Symbolae Botanicae Upsalienses 36(2): 1–499.

Hall TA (1999) BioEdit: A user-friendly biological sequence alignment editor and analysis program for windows 95/98/NT. Nucleic Acids Symposium Series 41: 95–98.

Hongsanan S, Hyde KD, Phookamsak R, Wanasinghe DN, McKenzie EHC, Sarma VV, Boonmee S, Lücking R, Bhat DJ, Liu NG, Tennakoon DS, Pem D, Karunarathna A, Jiang SH, Jones EBG, Phillips AJL, Manawasinghe IS, Tibpromma S, Jayasiri SC, Sandamali

DS, Jayawardena RS, Wijayawardene NN, Ekanayaka AH, Jeewon R, Lu YZ, Dissanayake AJ, Zeng XY, Luo ZL, Tian Q, Phukhamsakda C, Thambugala KM, Dai DQ, Chethana KWT, Samarakoon MC, Ertz D, Bao DF, Doilom M, Liu JK, Pérez-Ortega S, Suija A, Senwanna C, Wijesinghe SN, Konta S, Niranjan M, Zhang SN, Ariyawansa HA, Jiang HB, Zhang JF, Norphanphoun C, de Silva NI, Thiyagaraja V, Zhang H, Bezerra JDP, Miranda-González R, Aptroot A, Kashiwadani H, Harishchandra D, Sérusiaux E, Aluthmuhandiram JVS, Abeywickrama PD, Devadatha B, Wu HX, Moon KH, Gueidan C, Schumm F, Bundhun D, Mapook A, Monkai J, Chomnunti P, Suetrong S, Chaiwan N, Dayarathne MC, Yang J, Rathnayaka AR, Bhunjun CS, Xu JC, Zheng JS, Liu G, Feng Y, Xie N (2020) Refined families of Dothideomycetes: Dothideomycetidae and Pleosporomycetidae. Mycosphere 11(1): 1553–2107. https://doi.org/10.5943/mycosphere/11/1/13

Hyde KD, Hongsanan S, Jeewon R, Bhat DJ, McKenzie EHC, Jones EBG, Phookamsak R, Ariyawansa HA, Boonmee S, Zhao Q, Abdel-Aziz FA, Abdel-Wahab MA, Banmai S, Chomnunti P, Cui BK, Daranagama DA, Das K, Dayarathne MC, de Silva NI, Dissanayake AJ, Doilom M, Ehanayaka AH, Gibertoni TB, Neto A, Huang SK, Jayasiri SC, Jayawardena RS, Konta S, Lee HB, Li WJ, Lin CG, Liu JK, Lu YZ, Luo ZL, Manawasinghe IS, Manimohan P, Mapook A, Niskanen T, Norphanphoun C, Papizadeh M, Perera RH, Phukhamsakda C, Richter C, de Santiago ALCM, Drechsler-Santos ER, Senanayake IC, Tanaka K, Tennakoon TMDS, Thambugala KM, Tian Q, Tibpromma S, Thongbai B, Vizzini A, Wanasinghe DN, Wijayawardene NN, Wu HX, Yang J, Zeng XY, Zhang H, Zhang JF, Bulgakov TS, Camporesi E, Bahkali AH, Amoozegar MA, Araujo-Neta LS, Ammirati JF, Baghela A, Bhatt RP, Bojantchev D, Buyck B, de Silva GA, de Lima CLF, de Oliveira RJV, de Souza CAF, Dai YC, Dima B, Duong TT, Ercole E, Mafalda-Freire F, Ghosh A, Hashimoto A, Kamolhan S, Kang JC, Karunarathna SC, Kirk PM, Kytovuori I, Lantieri A, Liimatainen K, Liu ZY, Liu XZ, Lucking R, Medardi G, Mortimer PE, Nguyen TTT, Promputtha I, Raj KNA, Reck MA, Lumyong S, Shahzadeh-Fazeli SA, Stadler M, Soudi MR, Su HY, Takahashi T, Tangthirasunun N, Uniyal P, Wang Y, Wen TC, Xu JC, Zhang ZK, Zhao YC, Zhou JL, Zhu L (2016) Fungal diversity notes 367–490: Taxonomic and phylogenetic contributions to fungal taxa. Fungal Diversity 80: 1–270. https://doi.org/10.1007/s13225-016-0373-x

Katoh K, Standley K (2013) MAFFT Multiple Sequence Alignment Software Version 7: Improvements in performance and usability. Molecular Biology and Evolution 30(4): 772–780. https://doi.org/10.1093/molbev/mst010

Li GJ, Hyde KD, Zhao RN, Hongsanan S, Abdel-Aziz FA, AbdelWahab MA, Alvarado P, Alves-Silva G, Ammirati JF, Ariyawansa HA, Baghela A, Bahkali AH, Beug M, Bhat DJ, Bojantchev D, Boonpratuang T, Bulgakov TS, Camporesi E, Boro MC, Ceska O, Chakraborty D, Chen JJ, Chethana KWT, Chomnunti P, Consiglio G, Cui BK, Dai DQ, Dai YC, Daranagama DA, Das K, Dayarathne MC, Crop ED, De Oliveira RJV, de Souza CAF, de Souza JI, Dentinger BTM, Dissanayake AJ, Doilom M, Drechsler-Santos ER (2016) Fungal divers notes 253–366: Taxonomic and phylogenetic contributions to fungal taxa. Fungal Diversity 78(1): 1–237. https://doi.org/10.1007/s13225-016-0366-9

Liu YJ, Whelen S, Hall BD (1999) Phylogenetic relationships among ascomycetes: evidence from an RNA polymerase II subunit. Molecular Biology and Evolution 16: 1799–1808. https://doi.org/10.1093/oxfordjournals.molbev.a026092

Moral J, Agusti-Brisach C, Perez-Rodriguez M, Xavier C, Rhouma A, Trapero A (2017) Identification of fungal species associated with branch dieback of olive and resistance of table cultivars to *Neofusicoccum mediterraneum* and *Botryosphaeria dothidea*. Plant Disease 101(2): 306–316. https://doi.org/10.1094/PDIS-06-16-0806-RE

Nylander JAA (2004) MrModeltest v2 Program distributed by the author. Evolutionary Biology Centre, Uppsala University.

Pande A (2008) Ascomycetes of Peninsular India. Scientific Publishers, Jodhpur, 584 pp.

Rambaut A (2018) FigTree v.1.4.4. University of Edinburgh, Edinburgh.

Ronquist F, Huelsenbeck JP (2003) MrBayes 3: Bayesian phylogenetic inference under mixed models. Bioinformatics 19(12): 1572–1574. https://doi.org/10.1093/bioinformatics/btg180

Senanayake IC, Rathnayaka AR, Marasinghe DS, Calabon MS, Gentekaki E, Lee HB, Hurdeal VG, Pem D, Dissanayake LS, Wijesinghe SN, Bundhun D, Nguyen TT, Goonasekara ID, Abeywickrama PD, Bhunjun CS, Jayawardena RS, Wanasinghe DN, Jeewon R, Bhat DJ, Xiang MM (2020) Morphological approaches in studying fungi: Collection, examination, isolation, sporulation and preservation. Mycosphere 11(1): 2678–2754. https://doi.org/10.5943/mycosphere/11/1/20

Shoemaker RA, Babcock CE (1992) Applanodictyosporous Pleosporales: *Clathrospora*, *Comoclathris*, *Graphyllium*, *Macrospora*, and *Platysporoides*. Canadian Journal of Botany 70(8): 1617–1658. https://doi.org/10.1139/b92-204

Simmons EG (1967) Typification of *Alternaria*, *Stemphylium*, and *Ulocladium*. Mycologia 59(1): 67–92. https://doi.org/10.1080/00275514.1967.12018396

Species Fungorum (2023) Species Fungorum. http://www.speciesfungorum.org/Names/Names.asp [Accessed 26 September 2023]

Stamatakis A (2014) RAxML Version 8: A tool for phylogenetic analysis and post-analysis of large phylogenies. Bioinformatics 30(9): 1312–1313. https://doi.org/10.1093/bioinformatics/btu033

Thambugala KM, Wanasinghe DN, Phillips AJL, Camporesi E, Bulgakov TS, Phukhamsakda C, Ariyawansa HA, Goonasekara ID, Phookamsak R, Dissanayake A, Tennakoon DS, Tibpromma S, Chen YY, Liu ZY, Hyde KD (2017) Mycosphere notes 1 – 50: Grass (Poaceae) inhabiting Dothideomycetes. Mycosphere 8(4): 697–796. https://doi.org/10.5943/mycosphere/8/4/13

Tibpromma S, Promputtha I, Phookamsak R, Boonmee S, Hydem KD (2015) Phylogeny and morphology of *Premilcurensis* gen. nov. (Pleosporales) from stems of *Senecio* in Italy. Phytotaxa 236(1): 40. https://doi.org/10.11646/phytotaxa.236.1.3

Vaidya G, Lohman DJ, Meier R (2011) SequenceMatrix: Concatenation software for the fast assembly of multi-gene datasets with character set and codon information. Cladistics 27(2): 171–180. https://doi.org/10.1111/j.1096-0031.2010.00329.x

Vilgalys R, Hester M (1990) Rapid genetic identification and mapping of enzymatically amplified ribosomal DNA from several *Cryptococcus* species. Journal of Bacteriology 172(8): 4238–4246. https://doi.org/10.1128/jb.172.8.4238-4246.1990

Vu D, Groenewald M, Vries MD, Gehrmann T, Stielow B, Eberhardt U, Al-Hatmi A, Groenewald JZ, Cardinali G, Houbraken J (2019) Large-scale generation and analysis of filamentous fungal DNA barcodes boosts coverage for kingdom fungi and reveals thresholds for fungal species and higher taxon delimitation. Studies in Mycology 92: 135–154. https://doi.org/10.1016/j.simyco.2018.05.001

Wanasinghe D, Ebgareth J, Camporesi E, Hyde KD (2015) A new species of the genus *Comoclathris* (Pleosporaceae). Journal of Fungal Research 13(4): 260–268. https://doi.org/10.13341/j.jfr.2014.2057

Wanasinghe DN, Phukhamsakda C, Hyde KD, Jeewon R, Lee HB, Jones EBG, Tibpromma S, Tennakoon DS, Dissanayake AJ, Jayasiri SC, Gafforov Y, Camporesi E, Bulgakov TS, Ekanayake AH, Perera RH, Samarakoon MC, Goonasekara ID, Mapook A, Li WJ, Senanayake IC, Li JF, Norphanphoun C, Doilom M, Bahkali AH, Xu JC, Mortimer PE, Tibell L, Tibell S, Karunarathna SC (2018) Fungal diversity notes 709–839: Taxonomic and phylogenetic contributions to fungal taxa with

an emphasis on fungi on Rosaceae. Fungal Diversity 89(1): 1–236. https://doi.org/10.1007/s13225-018-0395-7

White TJ, Bruns TD, Lee SB, Taylor JW (1990) Amplification and direct sequencing of fungal ribosomal RNA genes for phylogenetics. PCR protocols: a guide to methods and applications 18(1): 315–322. https://doi.org/10.1016/B978-0-12-372180-8.50042-1

Wijayawardene NN, Hyde KD, Rajeshkumar KC, Hawksworth DL, Madrid H, Kirk PM, Braun U, Singh RV, Crous PW, Kukwa M, Lu¨cking R, Kurtzman CP, Yurkov A, Haelewaters D, Aptroot A, Lumbsch HT, Timdal E, Ertz D, Etayo J, Phillips AJL, Groenewald JZ, Papizadeh M, Selbmann L, Dayarathne MC, Weerakoon G, Jones EBG, Suetrong S, Tian Q, Castan˜eda-Ruiz RF, Bahkali AH, Pang KL, Tanaka K, Dai DQ, Sakayaroj J, Hujslova´ M, Lombard L, Shenoy BD, Suija A, Maharachchikumbura SSN, Thambugala KM, Wanasinghe DN, Sharma BO, Gaikwad S, Pandit G, Zucconi L, Onofri S, Egidi E, Raja HA, Kodsueb R, Ca'ceres MES, Pe'rez-Ortega S, Fiuza PO, Monteiro JS, Vasilyeva LN, Shivas RG, Prieto M, Wedin M, Olariaga I, Lateef AA, Agrawal Y, Fazeli SAS, Amoozegar MA, Zhao GZ, Pfliegler WP, Sharma G, Oset M, Abdel-Wahab MA, Takamatsu S, Bensch K, de Silva NI, De Kese A, Karunarathna A, Boonmee S, Pfister DH, Lu Y-Z, Luo Z-L, Boonyuen N, Daranagama DA, Senanayake IC, Jayasiri SC, Samarakoon MC, Zeng X-Y, Doilom M, Quijada L, Rampadarath S, Heredia G, Dissanayake AJ, Jayawardana RS, Perera RH, Tang LZ, Phukhamsakda C, Herna'ndez-Restrepo M, Ma X, Tibpromma S, Gusmao LFP, Weerahewa D, Karunarathna SC (2017) Notes for genera: Ascomycota. Fungal Diversity 86(1): 1–594. https://doi.org/10.1007/s13225-017-0386-0

Woudenberg JHC, Groenewald JZ, Binder M, Crous PW (2013) *Alternaria* redefined. Studies in Mycology 75(1): 171–212. https://doi.org/10.3114/sim0015

Woudenberg JHC, Hanse B, Van Leeuwen GCM, Groenewald JZ, Crous PW (2017) *Stemphylium* revisited. Studies in Mycology 87: 77–103. https://doi.org/10.1016/j.simyco.2017.06.001

Xu R, Su WX, Tian SQ, Bhunjun CS, Tibpromma S, Hyde KD, Li Y, Phukhamsakda C (2022) Synopsis of Leptosphaeriaceae and introduction of three new taxa and one new record from China. Journal of Fungi (Basel, Switzerland) 8(5): 416. https://doi.org/10.3390/jof8050416

Zhang Y, Crous PW, Schoch CL, Hyde KD (2012) Pleosporales. Fungal Diversity 53(1): 1–221. https://doi.org/10.1007/s13225-011-0117-x

Supplementary material 1

Phylogram generated from maximum likelihood analysis based on combined ITS, LSU, SSU, and rpb2 sequnence data

Authors: Rong Xu, Wenxin Su, Yang Wang, Shangqing Tian, Yu Li, Chayanard Phukhamsakda

Data type: pdf

Link: https://doi.org/10.3897/mycokeys.101.113040.suppl1

Species diversity and major host/substrate associations of the genus *Akanthomyces* (Hypocreales, Cordycipitaceae)

Yao Wang[1,2*], Zhi-Qin Wang[1,2*], Run Luo[1,2], Sisommay Souvanhnachit[1,2], Chinnapan Thanarut[3], Van-Minh Dao[4], Hong Yu[1,2]

1 Yunnan Herbal Laboratory, College of Ecology and Environmental Sciences, Yunnan University, Kunming, Yunnan, China
2 The International Joint Research Center for Sustainable Utilization of Cordyceps Bioresources in China and Southeast Asia, Yunnan University, Kunming, Yunnan, China
3 Faculty of Agricultural Production, Maejo University, Chiang Mai, Thailand
4 Institute of Regional Research and Development, Ministry of Science and Technology, Hanoi, Vietnam
Corresponding author: Hong Yu (hongyu@ynu.edu.cn; herbfish@163.com)

Abstract

Akanthomyces, a group of fungi with rich morphological and ecological diversity in Cordycipitaceae (Ascomycota, Hypocreales), has a wide distribution amongst diverse habitats. By surveying arthropod-pathogenic fungi in China and Southeast Asia over the last six years, nine *Akanthomyces* spp. were found and identified. Five of these were shown to represent four known species and an undetermined species of *Akanthomyces*. Four of these were new species and they were named *A. kunmingensis* and *A. subaraneicola* from China, *A. laosensis* from Laos and *A. pseudonoctuidarum* from Thailand. The new species were described and illustrated according to the morphological characteristics and molecular data. *Akanthomyces araneogenus*, which was isolated from spiders from different regions in China, Thailand and Vietnam, was described as a newly-recorded species from Thailand and Vietnam. The phylogenetic positions of the nine species were evaluated, based on phylogenetic inferences according to five loci, namely, ITS, nr*LSU*, *TEF*, *RPB1* and *RPB2*. In this study, we reviewed the research progress achieved for *Akanthomyces* regarding its taxonomy, species diversity, geographic distribution and major host/substrate associations. The morphological characteristics of 35 species in *Akanthomyces*, including four novel species and 31 known taxa, were also compared.

Key words: Arthropod-pathogenic fungi, Cordycipitaceae, morphology, new species, phylogenetic analyses

Introduction

Akanthomyces Lebert is one of the oldest genera in the family Cordycipitaceae (Ascomycota, Hypocreales). This genus was established by Lebert in 1858 on the basis of the type species, *A. aculeatus* Lebert, which was found on a moth in France (Lebert 1858). Morphologically, *Akanthomyces* species have been characterised asexually by white, cream or flesh-coloured cylindrical, attenuated synnematal growth covered by a hymenium-like layer of phialides producing

one-celled catenulate conidia (Mains 1950; Samson and Evans 1974; Hsieh et al. 1997). These phialides are ellipsoidal, cylindrical or narrowly cylindrical and gradually or abruptly taper to a more or less distinct neck (Hsieh et al. 1997). Owing to extensive overlap in their morphological characteristics, *Akanthomyces* was once considered as a synonym of *Lecanicillium* W. Gams & Zare, an anamorph within Cordycipitaceae with verticillium-like morphology (Gams and Zare 2001); however, many species originally described in *Lecanicillium* do not form a single monophyletic clade and are distributed throughout Cordycipitaceae (Wang et al. 2020). Kepler et al. (2017) phylogenetically established the genetic boundaries in Cordycipitaceae and they proposed that *Lecanicillium* should be rejected and, instead, could be considered as a synonym of *Akanthomyces* (Kepler et al. 2017). Kepler et al. (2017) also showed that the type species of *Lecanicillium*, *L. lecanii* (Zimm.) Zare & W. Gams (as *Cordyceps confragosa* (Mains) G.H. Sung, J.M. Sung, Hywel-Jones & Spatafora), as well as several other *Lecanicillium* species, namely, *L. attenuatum* Zare & W. Gams, *L. muscarium* (Petch) Zare & W. Gams and *L. sabanense* Chir.-Salom., S. Restrepo & T.I. Sanjuan, fall within *Akanthomyces*. The teleomorph of *Akanthomyces* was originally described as *Torrubiella* Boud. and it was characterised by producing superficial perithecia on a loose mat of hyphae (subiculum) or a highly reduced non-stipitate stroma (Boudier 1885). According to the most complete taxonomic treatment of Cordycipitaceae to date, this connection was verified by DNA sequencing; since *Akanthomyces* was described earlier than *Torrubiella*, the taxonomic revision recommended *Akanthomyces* as the name of this genus (Kepler et al. 2017).

Over the past two decades, our efforts have been applied to the investigation of Cordycipitoid fungi, especially those located in China and Southeast Asia. To date, our study team has collected over 18,000 specimens and 7,500 strains of *Cordyceps* Fr. *sensu lato*, representing more than 450 species in total (Wang et al. 2020). These specimens and strains sufficiently revealed that Cordycipitaceae is the most complex group in Hypocreales with its varied morphological characteristics and wide-ranging hosts. Some of the genera with sexual and asexual morphs, such as *Akanthomyces* and *Hevansia* Luangsa-ard, Hywel-Jones & Spatafora, share numerous similar morphological characteristics. The genus *Hevansia* was erected to accommodate asexual morphs on spiders that were previously described under *Akanthomyces*. The type species *Hevansia novoguineensis* (Samson & B.L. Brady) Luangsa-ard, Hywel-Jones & Spatafora, which was previously described as *Akanthomyces novoguineensis* Samson & B.L. Brady, differs from *Akanthomyces* by the immersed perithecia of the teleomorph in a disc sitting at the top of a well-formed stipe (Aini et al. 2020); however, *H. novoguineensis* must now be an akanthomyces-like teleomorph (Kepler et al. 2017; Aini et al. 2020). Some *Akanthomyces*, *Samsoniella* Mongkols., Noisrip., Thanakitp., Spatafora & Luangsa-ard and *Cordyceps* species produce similar isaria-like asexual conidiogenous structures, such as flask-shaped phialides produced in whorls and conidia with divergent chains (Wang et al. 2020; Wang et al. 2022). Due to the extensive overlap in morphological characteristics and the lack of distinctive phenotypic variation, species in many genera, *Akanthomyces* in particular, are not easily classified and identified. Thus, more known species and new species in the genus *Akanthomyces*

need to be introduced and supported by more detailed morphological and phylogenetic evidence in combination with a larger taxon sampling.

In surveys of arthropod-pathogenic fungi from different regions in Yunnan and Hunan Province, China; Chiang Mai Province, Thailand; Nghe An Province, Vietnam; and Oudomxay Province, Laos, over the last six years, approximately nine *Akanthomyces* spp. were collected and identified. In this study, we aimed to: 1) reveal the hidden species diversity of the genus *Akanthomyces* according to phylogenetic analyses and morphological observation and 2) systematically review the geographical distribution and major host/substrate associations of *Akanthomyces* species by surveying the literature to the greatest extent possible and combining the results with those generated in our study.

Materials and methods

Soil and specimen collection

All of the soil samples were collected from Yunnan Province in China. Fungal specimens were obtained from six locations between 2017 and 2022, namely, two different locations in Yunnan Province, China, one location in Hunan Province, China, one location in Chiang Mai Province, Thailand, one location in Nghe An Province, Vietnam and one location in Oudomxay Province, Laos. Soil samples and specimens were noted and photographed in the field and then they were carefully put in plastic containers at a low temperature. After that, they were brought to the laboratory and stored at 4 °C prior to examination and isolation.

Fungal isolation and culture

The *Akanthomyces* strains were isolated from the soil samples, based on the methods described by Wang et al. (2015) and Wang et al. (2023b). Briefly, 2 g of soil were added to a flask containing 20 ml sterilised water and glass beads. The soil suspension was shaken for about 10 min and then diluted 100 times. Subsequently, 200 µl of the diluted soil suspension was spread on Petri dishes with solidified onion garlic agar (OGA: 20 g of grated garlic and 20 g of onion were boiled in 1 litre of distilled water for 1 h; the boiled biomass was then filtered-off and 2% agar was added). Czapek yeast extract agar (CYA, Advanced Technology and Industrial Co., Ltd., China) and potato dextrose agar (PDA, Difco, USA) were used and all media had 50 mg/l rose Bengal and 100 mg/l kanamycin added. Conidia developing on invertebrate cadavers were transplanted on to plates of PDA and cultured at 25 °C. Colonies of the isolated filamentous fungi appearing in the culture were transferred on to fresh PDA media. Each purified fungal strain was transferred to PDA slants and cultured at 25 °C until its hyphae spread across the entire slope. The emerging fungal spores were washed with sterile physiological saline to form a suspension containing 1×10^3 cells/ml. To obtain monospore cultures, a sample of the spore suspension was placed on PDA on a Petri dish utilising a sterile micropipette and then the dish was incubated at 25 °C. Voucher specimens and the corresponding isolated strains were deposited in the Yunnan Herbal Herbarium (**YHH**) and the Yunnan Fungal Culture Collection (**YFCC**), respectively, of Yunnan University, Kunming, China.

Morphological observations

The specimens were examined with an Olympus SZ61 stereomicroscope (Olympus Corporation, Tokyo, Japan). Fungal structures of the specimens, such as synnemata, phialides and conidia, were mounted on glass slides with a drop of lactophenol cotton blue solution. Cultures on PDA slants were transferred to PDA plates and then they were incubated at 25 °C for 14 d. For morphological evaluation, microscope slides were prepared by placing mycelia from the cultures on PDA medium blocks (5 mm diameter) and then overlaid with a coverslip. Micro-morphological observations and measurements were performed with a light microscope (CX40, Olympus Corporation, Tokyo, Japan) and a scanning electron microscope (Quanta 200 FEG, FEI Company, Hillsboro, USA). The individual length and width measurements were recorded for 30–100 replicates and included the absolute minima and maxima.

DNA extraction, PCR and sequencing

The specimens and axenic living cultures were prepared for DNA extraction. Genomic DNA was extracted utilising a Genomic DNA Purification kit (Qiagen GmbH, Hilden, Germany), based on the manufacturer's instructions. The primer pair ITS5/ITS4 was used to amplify a fraction of the internal transcribed spacer regions of the rDNA (ITS rDNA) (White et al. 1990). Primer pair LR5/LR0R (Vilgalys and Hester 1990; Rehner and Samuels 1994) was used to amplify a fraction of the nuclear ribosomal large subunit (nr*LSU*) and EF1-983F/EF1-2218R primers (Rehner and Buckley 2005) were used to amplify translation elongation factor 1α (*TEF*). For amplification of the largest and second largest subunits of RNA polymerase II (*RPB1* and *RPB2*), PCR primer pairs RPB1-5′F/RPB1-5′R and RPB2-5′F/RPB2-5′R (Bischoff et al. 2006; Sung et al. 2007) were employed. All of the PCR reactions were performed in a final volume of 50 μl and contained 25 μl of 2 × *Taq* PCR Master Mix (Tiangen Biotech Co., Ltd., Beijing, China), 0.5 μl of each primer (10 μM), 1 μl of genomic DNA and 23 μl of RNase-free water. Target gene amplification and sequencing were performed, based on the methods detailed in our prior study (Wang et al. 2020).

Phylogenetic analyses

The phylogenetic analyses were based on five genes, namely, ITS, nr*LSU*, *TEF*, *RPB1* and *RPB2*, sequences. The sequences were retrieved from GenBank (http://www.ncbi.nlm.nih.gov/, accessed on 1 March 2023) and combined with those generated in our study. Taxon information and GenBank accession numbers are listed in Table 1. Sequences were aligned with MAFFT v.7 (http://mafft.cbrc.jp/alignment/server/, accessed on 1 March 2023). The aligned sequences were then manually corrected when necessary. After alignment, the sequences of the genes were concatenated. Conflicts amongst the five genes were resolved with PAUP* 4.0b10 (Swofford et al. 2002). The results showed that the phylogenetic signals for the five loci were congruent (P = 0.02). The data partitions were defined for the combined dataset with PartitionFinder v.1.1.1 (Lanfear et al. 2012). Phylogenetic analyses were conducted utilising Bayesian Inference (BI) and Maximum Likelihood (ML) methods, respectively. The model selected for BI

Table 1. Specimen information and GenBank accession numbers for sequences used in this study.

Species	Voucher information	Host/Substrate	GenBank accession numbers					Reference
			ITS	nr*LSU*	*TEF*	*RPB1*	*RPB2*	
Akanthomyces aculeatus	HUA 186145	–	–	MF416520	MF416465	–	–	Kepler et al. (2017)
Akanthomyces aculeatus	TS772	Lepidoptera; Sphingidae	KC519371	KC519370	KC519366	–	–	Sanjuan et al. (2014)
Akanthomyces araneicola	GY29011[T]	Araneae; spider	MK942431	–	MK955950	MK955944	MK955947	Chen et al. (2019)
Akanthomyces araneogenus	GZUIF DX2[T]	Araneae; spider	MH978179	–	MH978187	MH978182	MH978185	Chen et al. (2018)
Akanthomyces araneogenus	**YFCC 1811934**	**Araneae; spider**	**OQ509518**	**OQ509505**	**OQ506281**	**OQ511530**	**OQ511544**	**This study**
	YFCC 2206935	**Araneae; spider**	**OQ509519**	**OQ509506**	**OQ506282**	**OQ511531**	**OQ511545**	**This study**
Akanthomyces araneosus	KY11341[T]	Araneae; spider	ON502826	ON502832	ON525443	–	ON525442	Chen et al. (2022)
Akanthomyces attenuatus	CBS 170.76[T]	Lepidoptera; *Carpocapsa pomonella*	MH860970	OP752153	OP762607	OP762611	OP762615	Manfrino et al. (2022)
Akanthomyces bashanensis	CQ05621[T]	Araneae; spider	OQ300412	OQ300420	OQ325024	–	OQ349684	Chen et al. (2023)
Akanthomyces beibeiensis	CQ05921[T]	Araneae; spider	OQ300415	OQ300424	OQ325028	–	OQ349688	Chen et al. (2023)
Akanthomyces coccidioperitheciatus	NHJ 6709	Araneae; spider	JN049865	EU369042	EU369025	EU369067	EU369086	Kepler et al. (2012)
Akanthomyces dipterigenus	CBS 126.27	Hemiptera; *Icerya purchasi*	AJ292385	KM283797	KM283820	KR064300	KM283862	Kepler et al. (2017)
Akanthomyces dipterigenus	**YFCC 2107933**	**Soil**	**OQ509520**	**OQ509507**	**OQ506283**	**OQ511532**	**OQ511546**	**This study**
Akanthomyces kanyawimiae	TBRC 7242	Araneae; spider	MF140751	MF140718	MF140838	MF140784	MF140808	Mongkolsamrit et al. (2018)
	TBRC 7243	Unidentified	MF140750	MF140717	MF140837	MF140783	MF140807	Mongkolsamrit et al. (2018)
Akanthomyces kunmingensis	**YFCC 1708939**	**Araneae; spider**	**OQ509521**	**OQ509508**	**OQ506284**	**OQ511533**	**OQ511547**	**This study**
	YFCC 1808940[T]	**Araneae; spider**	**OQ509522**	**OQ509509**	**OQ506285**	**OQ511534**	**OQ511548**	**This study**
Akanthomyces laosensis	**YFCC 1910941[T]**	**Lepidoptera; Noctuidae**	**OQ509523**	**OQ509510**	**OQ506286**	**OQ511535**	**OQ511549**	**This study**
	YFCC 1910942	**Lepidoptera; Noctuidae**	**OQ509524**	**OQ509511**	**OQ506287**	**OQ511536**	**OQ511550**	**This study**
Akanthomyces lecanii	CBS 101247	Hemiptera; *Coccus viridis*	JN049836	AF339555	DQ522359	DQ522407	DQ522466	Kepler et al. (2012)
Akanthomyces lepidopterorum	GZAC SD05151[T]	Lepidoptera (pupa)	MT705973	–	–	–	MT727044	Chen et al. (2020b)
Akanthomyces muscarius	CBS 455.70B	–	–	MH871560	–	–	–	Kepler et al. (2017)
Akanthomyces neoaraneogenus	GZU1031Lea[T]	Araneae; spider	KX845703	–	KX845697	KX845699	KX845701	Chen et al. (2017)
Akanthomyces neocoleopterorum	GY11241[T]	Coleoptera	MN093296	–	MN097813	MN097816	MN097812	Chen et al. (2020a)
	GY11242	Coleoptera	MN093298	–	MN097815	MN097817	MN097814	Chen et al. (2020a)
Akanthomyces noctuidarum	BCC 36265[T]	Lepidoptera; Noctuidae	MT356072	MT356084	MT477978	MT477994	MT477987	Aini et al. (2020)
	BCC 47498	Lepidoptera; Noctuidae	MT356074	MT356086	MT477980	MT477996	MT477988	Aini et al. (2020)
	BCC 28571	Lepidoptera; Noctuidae	MT356075	MT356087	MT477981	MT478009	MT478006	Aini et al. (2020)
Akanthomyces pissodis	CBS 118231[T]	Coleoptera; *Pissodes strobi*	–	KM283799	KM283822	KM283842	KM283864	Chen et al. (2020b)
Akanthomyces pseudonoctuidarum	**YFCC 1808943[T]**	**Lepidoptera; Noctuidae**	**OQ509525**	**OQ509512**	**OQ506288**	**OQ511537**	**OQ511551**	**This study**
	YFCC 1808944	**Lepidoptera; Noctuidae**	**OQ509526**	**OQ509513**	**OQ506289**	**OQ511538**	**OQ511552**	**This study**
Akanthomyces pyralidarum	BCC 28816[T]	Lepidoptera; Pyralidae	MT356080	MT356091	MT477982	MT478000	MT478007	Aini et al. (2020)
	BCC 32191	Lepidoptera; Pyralidae	MT356081	MT356092	MT477983	MT478001	MT477989	Aini et al. (2020)

Species	Voucher information	Host/Substrate	GenBank accession numbers					Reference
			ITS	nr*LSU*	*TEF*	*RPB1*	*RPB2*	
Akanthomyces sabanensis	ANDES-F 1023	Hemiptera; *Pulvinaria caballeroramosae*	KC633237	–	KC633267	KC875222	–	Kepler et al. (2017)
	ANDES-F 1024	Hemiptera; *Pulvinaria caballeroramosae*	KC633232	KC875225	KC633266	–	KC633249	Kepler et al. (2017)
***Akanthomyces* sp.**	**YFCC 945**	**Soil**	**OQ509531**	**–**	**OQ506294**	**OQ511543**	**OQ511557**	**This study**
Akanthomyces subaraneicola	**YFCC 2107937ᵀ**	**Araneae; spider**	**OQ509527**	**OQ509514**	**OQ506290**	**OQ511539**	**OQ511553**	**This study**
	YFCC 2107938	**Araneae; spider**	**OQ509528**	**OQ509515**	**OQ506291**	**OQ511540**	**OQ511554**	**This study**
Akanthomyces sulphureus	TBRC 7248ᵀ	Araneae; spider	MF140758	MF140722	MF140843	MF140787	MF140812	Mongkolsamrit et al. (2018)
	TBRC 7249	Araneae; spider	MF140757	MF140721	MF140842	MF140786	MF140734	Mongkolsamrit et al. (2018)
Akanthomyces sulphureus	**YFCC 1710936**	**Araneae; spider**	**OQ509529**	**OQ509516**	**OQ506292**	**OQ511541**	**OQ511555**	**This study**
Akanthomyces thailandicus	TBRC 7245ᵀ	Araneae; spider	MF140754	–	MF140839	–	MF140809	Mongkolsamrit et al. (2018)
Akanthomyces tiankengensis	KY11571ᵀ	Araneae; spider	ON502848	ON502825	ON525447	–	ON525446	Chen et al. (2022)
	KY11572	Araneae; spider	ON502821	ON502827	ON525449	–	ON525448	Chen et al. (2022)
Akanthomyces tortricidarum	BCC 72638ᵀ	Lepidoptera; Tortricidae	MT356076	MT356088	MT478004	MT477997	MT477992	Aini et al. (2020)
	BCC 41868	Lepidoptera; Tortricidae	MT356077	MT356089	MT477985	MT477998	MT478008	Aini et al. (2020)
Akanthomyces tuberculatus	HUA 186131	Lepidoptera (adult moth)	–	MF416521	MF416466	–	–	Kepler et al. (2017)
Akanthomyces uredinophilus	KACC 44066	Rust	–	KM283784	KM283808	KM283830	KM283850	Park et al. (2016)
	KACC 44082ᵀ	Rust	–	KM283782	KM283806	KM283828	KM283848	Park et al. (2016)
	KUN 101466	Insect	MG948305	MG948307	MG948315	MG948311	MG948313	Park et al. (2016)
	KUN 101469	Insect	MG948306	MG948308	MG948316	MG948312	MG948314	Park et al. (2016)
Akanthomyces waltergamsii	TBRC 7251	Araneae; spider	MF140747	MF140713	MF140833	MF140781	MF140805	Mongkolsamrit et al. (2018)
	TBRC 7252ᵀ	Araneae; spider	MF140748	MF140714	MF140834	MF140782	MF140806	Mongkolsamrit et al. (2018)
Akanthomyces waltergamsii	**YFCC 883**	**Araneae; spider**	**OQ509530**	**OQ509517**	**OQ506293**	**OQ511542**	**OQ511556**	**This study**
Akanthomyces zaquensis	HMAS 246915ᵀ	Fungi; *Ophiocordyceps sinensis*	MT789699	MT789697	MT797812	MT797810	–	Wang et al. (2023a)
	HMAS 246917	Fungi; *Ophiocordyceps sinensis*	MT789698	MT789696	MT797811	MT797809	–	Wang et al. (2023a)
Samsoniella aurantia	TBRC 7271ᵀ	Lepidoptera	MF140764	MF140728	MF140846	MF140791	MF140818	Mongkolsamrit et al. (2018)
Samsoniella inthanonensis	TBRC 7915ᵀ	Lepidoptera (pupa)	MF140761	MF140725	MF140849	MF140790	MF140815	Mongkolsamrit et al. (2018)

Boldface: data generated in this study. Ex-type materials are marked with "T".

analysis was from jModelTest version 2.1.4 (Darriba et al. 2012). The following models were implemented in the analysis: GTR + I + G for partitions of ITS, nr*L-SU* and *TEF* and GTR + I for partitions of *RPB1* and *RPB2*. The BI analysis was executed on MrBayes v.3.2.7a for five million generations (Ronquist et al. 2012). GTR + FO + G was selected as the optimal model for ML analysis and 1000 rapid bootstrap replicates were performed on the dataset. ML phylogenetic analyses were conducted in RAxML 7.0.3 (Stamatakis et al. 2008). Additional ML analyses were performed using IQ-TREE v. 2.1.3 with ultrafast bootstrapping for the estimation of branch support (Minh et al. 2020). Further, ML analysis (IQ-TREE) was applied to single-locus genealogies for ITS, nr*LSU, TEF, RPB1* and *RPB2*.

Identification of host arthropods

The host arthropods of *Akanthomyces* spp. were identified on the basis of morphological characteristics and they were further identified utilising molecular analyses according to the mitochondrial cytochrome oxidase I gene (*cox1*) and mitochondrial cytochrome b gene (*cytb*). Genomic DNA was extracted from the head and leg areas of the cadavers of the hosts by utilising the CTAB method (Liu et al. 2001). The *cox1* and *cytb* loci were amplified with the primer pair Hep-cox1F/Hep-cox1R and Hep-cytbF/Hep-cytbR, respectively (Simon et al. 1994). Sequences were analysed with MEGA v.6.06 software (Tamura et al. 2013) and processed by Standard Nucleotide BLAST (GenBank, NCBI nucleotide database) to assess similarity with reported arthropod sequences.

Results

Sequencing and phylogenetic analyses

The five DNA loci (ITS, nr*LSU*, *TEF*, *RPB1*, *RPB2*) were readily amplified and sequenced and there was a fairly high success rate in this study. Preliminary phylogenetic analyses, based on the combined five-gene sequences from 116 fungal taxa Cordycipitaceae and *Trichoderma* Pers., confirmed the presence and positions of *Akanthomyces* and related genera within Cordycipitaceae. The concatenated five-gene dataset consisted of 4,453 bp (ITS = 639 bp, nr*LSU* = 921 bp, *TEF* = 1,044 bp, *RPB1* = 758 bp and *RPB2* = 1,091 bp). Ten well-supported clades were recognized, which accommodate species of the genera *Akanthomyces*, *Ascopolyporus* Möller, *Beauveria* Vuill., *Blackwellomyces* Spatafora & Luangsa-ard, *Cordyceps*, *Gibellula* Cavara, *Hevansia*, *Samsoniella*, *Simplicillium* W. Gams & Zare and *Trichoderma* (Suppl. material 1: fig. S1). The phylogenetic analyses also revealed the species diversity of the genus *Akanthomyces*. This suggested that the group should be genetically composed of at least 30 species (Suppl. material 1: fig. S1). The further phylogenetic analyses, based on combined partial ITS+nr*LSU*+*TEF*+*RPB1*+*RPB2* sequences consisting of 56 fungal taxa (Table 1), resolved the majority of the *Akanthomyces* lineages into separate terminal branches (Fig. 1). The dataset consisted of 4,401 bp of sequence data (ITS = 619 bp, nr*LSU* = 896 bp, *TEF* = 1,022 bp, *RPB1* = 731 bp and *RPB2* = 1,133 bp). *Samsoniella aurantia* Mongkols., Noisrip., Thanakitp., Spatafora & Luangsa-ard (strain TBRC 7271) and *S. inthanonensis* Mongkols., Noisrip., Thanakitp., Spatafora & Luangsa-ard (strain TBRC 7915) within Cordycipitaceae were used as the outgroup sequences for this dataset. This revealed a similar tree and cluster topology, as shown in Suppl. material 1: fig. S1. Amongst the hosts of *Akanthomyces*, Araneae (spider) and Lepidoptera (adult moth) are the two major orders. Most of the spider pathogens form a monophyletic clade, separated from the pathogens of moths, themselves forming also an apparent monophyletic clade (Fig. 1). The phylogenetic analyses also suggested the existence of distinct species in the spider pathogens and adult moth entomopathogens clade that we proposed as new species: *A. kunmingensis* and *A. subaraneicola*, which were found in the spider pathogens clade; and *A. laosensis* and *A. pseudonoctuidarum*, which were found in the adult moth entomopathogens clade (Fig. 1).
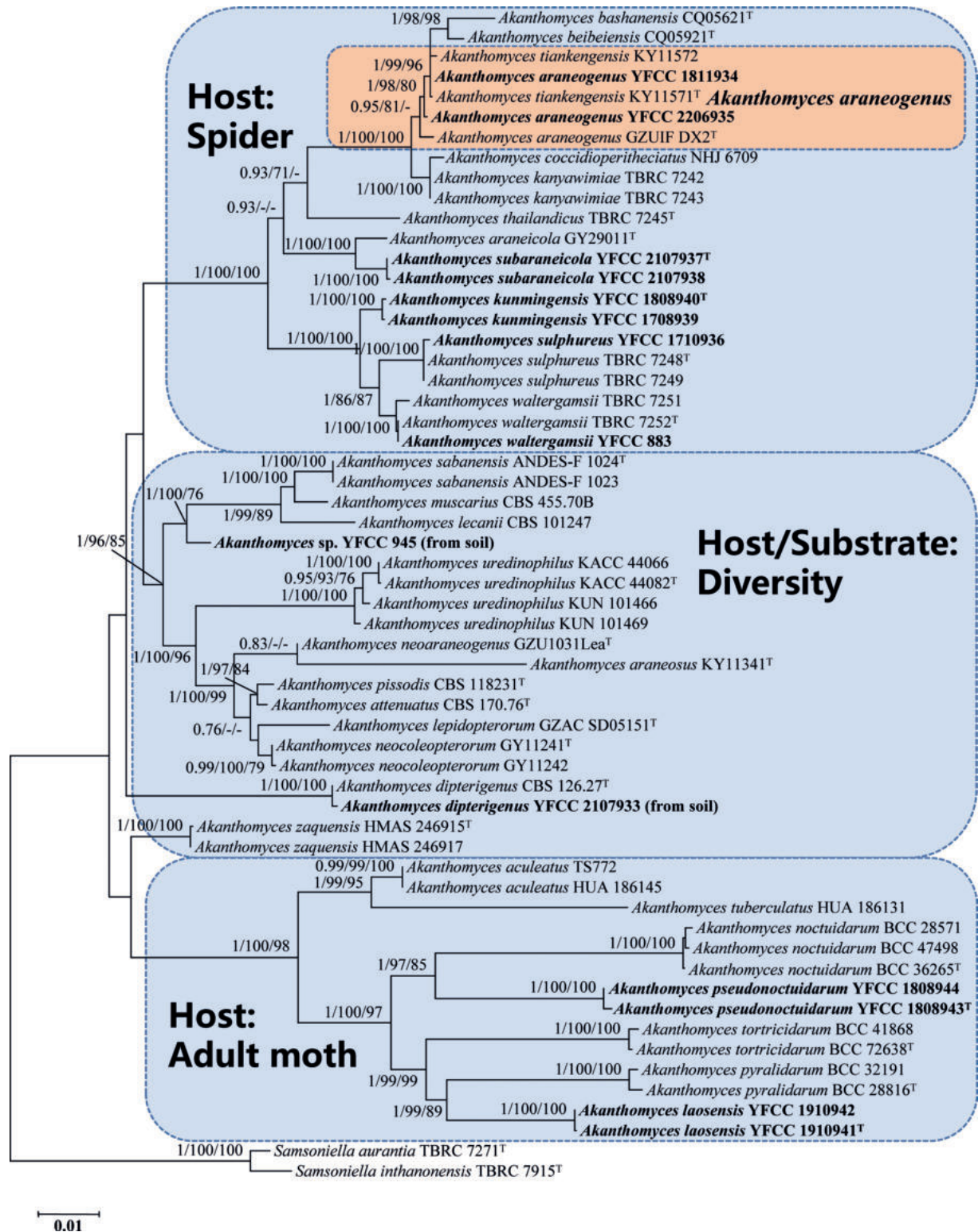
Figure 1. Phylogenetic tree of *Akanthomyces* species, based on combined partial ITS + nr*LSU* + *TEF* + *RPB1* + *RPB2* sequences. Numbers at the branches indicate support values (BI-PP/IQ-TREE-BS/ RAxML-BS) above 0.7/70%/70%. Ex-type materials are marked with "T". Isolates in bold type are those analysed in this study.

Despite differing topologies between individual loci (ITS, nr*LSU*, *TEF*, *RPB1* and *RPB2*), the newly-proposed species usually stood out as distinct clades to other known species. Some novel species always recovered the sister relation-

ship to a particular known species for all loci. For example, the newly-discovered species *A. kunmingensis* had a close genetic relationship with *A. waltergamsii*. They were regarded as different species with strong support from ITS, nr*LSU*, *TEF*, *RPB1* and *RPB2* (Suppl. material 1: figs S2–S6). The new species *A. subaraneicola* was sisters to *A. araneicola* and this relationship received significant bootstrap support from ITS, *TEF*, *RPB1* and *RPB2* (Suppl. material 1: figs S2, S4–S6). Meanwhile, *A. laosensis* was inferred to form a sister clade to either *A. pyralidarum* (ITS, *RPB1* and *RPB2*) or *A. tortricidarum* (nr*LSU* and *TEF*). Similarly, despite the differing position of *A. pseudonoctuidarum* between different markers, it always formed a clade that could be distinguished from its closely-related species, *A. noctuidarum* and *A. tortricidarum*.

Morphological features

The morphological characteristics of the five species, as well as photomicrographs of morphological structures, are shown in Figs 2–6. The detailed fungal morphological descriptions are supplied in the Taxonomy section.

Taxonomy

Akanthomyces kunmingensis Hong Yu bis, Y. Wang & Z.Q. Wang, sp. nov.
MycoBank No: 848307
Fig. 2

Etymology. Named after the location, Kunming City, where the species was collected.

Type. CHINA. Yunnan Province, Kunming City, Wild Duck Lake Forest Park (25.2181°N, 102.8503°E, 2100 m above sea level), on a spider on a dead stem, 14 August 2018, collected by Yao Wang (holotype: YHH 16988; ex-type living culture: YFCC 1808940).

Description. *Sexual morph*: Undetermined. *Asexual morph*: Synnemata arising from spider body, cream to light yellow, erect, irregularly branched, producing a mass of conidia at the upper apex, powdery and floccose. Colonies on PDA reaching 15–20 mm in diameter after 14 days at 25 °C, circular, white and fluffy mycelium, middle bulge, reverse pale yellow to light brown. Hyphae smooth-walled, branched, septate, hyaline, 0.5–2.8 µm wide. Conidiophores smooth-walled, cylindrical, solitary, sometimes verticillate, 4.3–9.5 × 1.2–2.0 µm (n = 30). Phialides consisting of a cylindrical, somewhat inflated base, verticillate on conidiophores, usually in whorls of 4–5 or solitary on hyphae, 6.2–29.4 × 1.1–2.5 µm (n = 30). Conidia smooth and hyaline, ellipsoidal to long oval, one-celled, 1.9–3.5 × 1.1–1.8 µm (n = 50), often in chains. Size and shape of phialides and conidia similar in culture and on natural substratum.

Host. Spider (Araneae).

Habit. On spiders on dead stems.

Distribution. Kunming City, Yunnan Province, China.

Other material examined. CHINA. Yunnan Province, Kunming City, Songming County, Dashao Village (25.3924°N, 102.5589°E, 2700 m above sea level), on a spider on a dead stem, 12 August 2017, Yao Wang (YHH 2301006; living culture: YFCC 1708939).
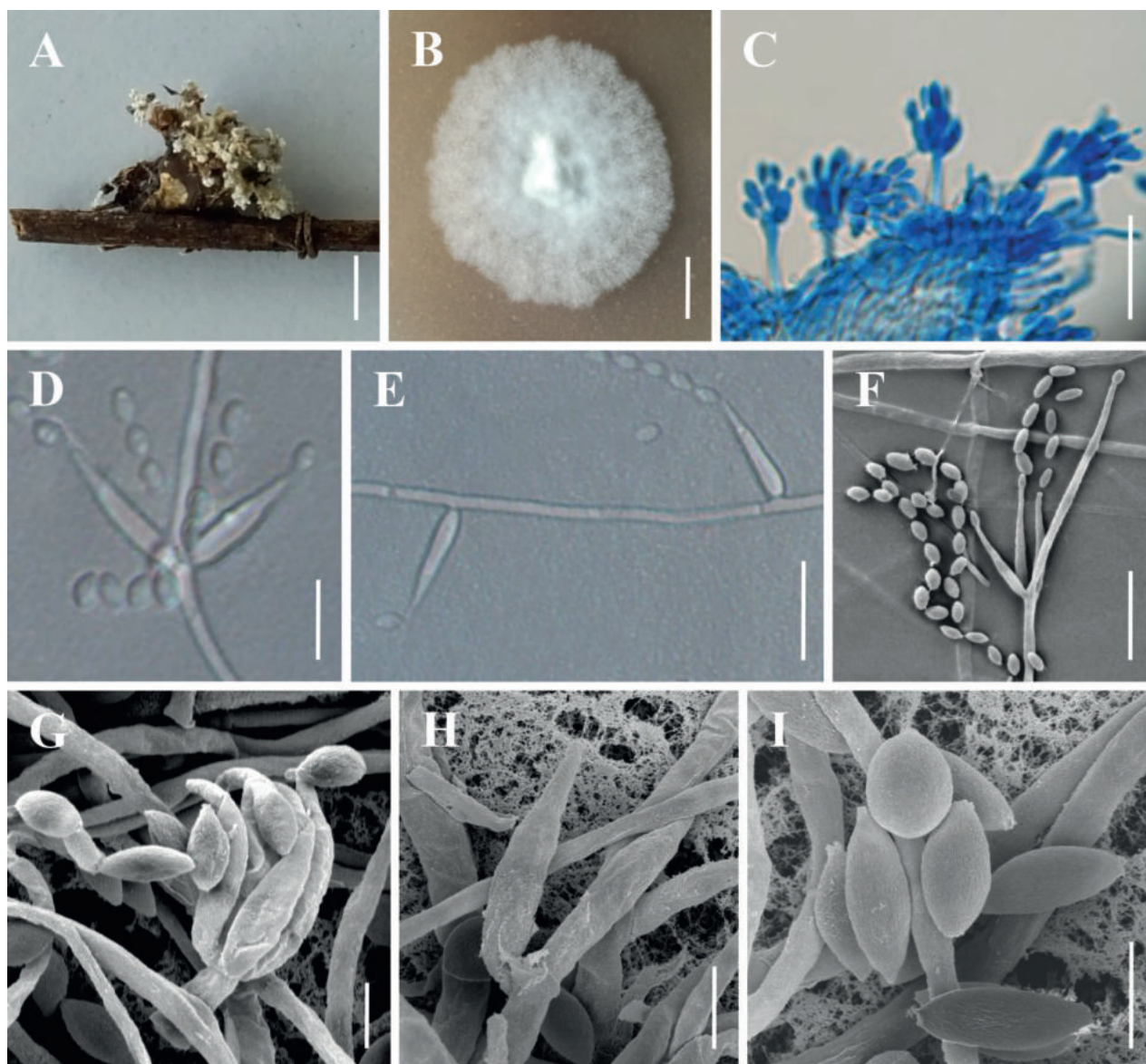
Figure 2. Morphology of *Akanthomyces kunmingensis* **A** the type specimen (YHH 16988) **B** culture character on PDA medium **C** conidiogenous structures on the host **D−H** conidiophores, conidiogenous cells and conidia **I** conidia. Scale bars: 3 mm (**A**); 10 mm (**B**); 10 μm (**C, E, F**); 5 μm (**D**); 2 μm (**G−I**).

Commentary. In regard to phylogenetic relationships, *Akanthomyces kunmingensis* forms a distinct lineage in the genus *Akanthomyces* with high credible support (1/100%/100%) and it is closely related to *A. sulphureus* and *A. waltergamsii* (Fig. 1). Morphologically, *A. kunmingensis* is so similar to *A. waltergamsii* that it was once referred to as *A. waltergamsii* by Wang et al. (2020); however, a morphological observation revealed a significant difference of conidia shapes between *A. kunmingensis* and *A. waltergamsii*. *Akanthomyces kunmingensis* usually produces a variety of shapes of conidia (viz. spherical, ellipsoidal to long oval or fusiform), while *A. waltergamsii* produces only ellipsoidal and fusiform conidia. Moreover, *A. kunmingensis* can be distinguished from *A. sulphureus* and *A. waltergamsii* by its longer phialides (6.2−29.4 μm) and smaller conidia (1.9−3.5 × 1.1−1.8 μm) (Table 3).

Akanthomyces laosensis Hong Yu bis & Y. Wang, sp. nov.
MycoBank No: 848308
Fig. 3

Etymology. Named after the location, Laos, where the species was collected.

Type. Laos. Oudomxay Province, Muang Xay County, Nagang Village (20.7143°N, 102.0957°E, 698 m above sea level), on the adult of Noctuidae on the underside of a dicotyledonous leaf, 5 October 2019, collected by Yao Wang (holotype: YHH 2301008; ex-holotype living culture: YFCC 1910941).

Description. *Sexual morph*: Undetermined. *Asexual morph*: Specimens examined in this study can be found on the underside of dicotyledonous leaves.
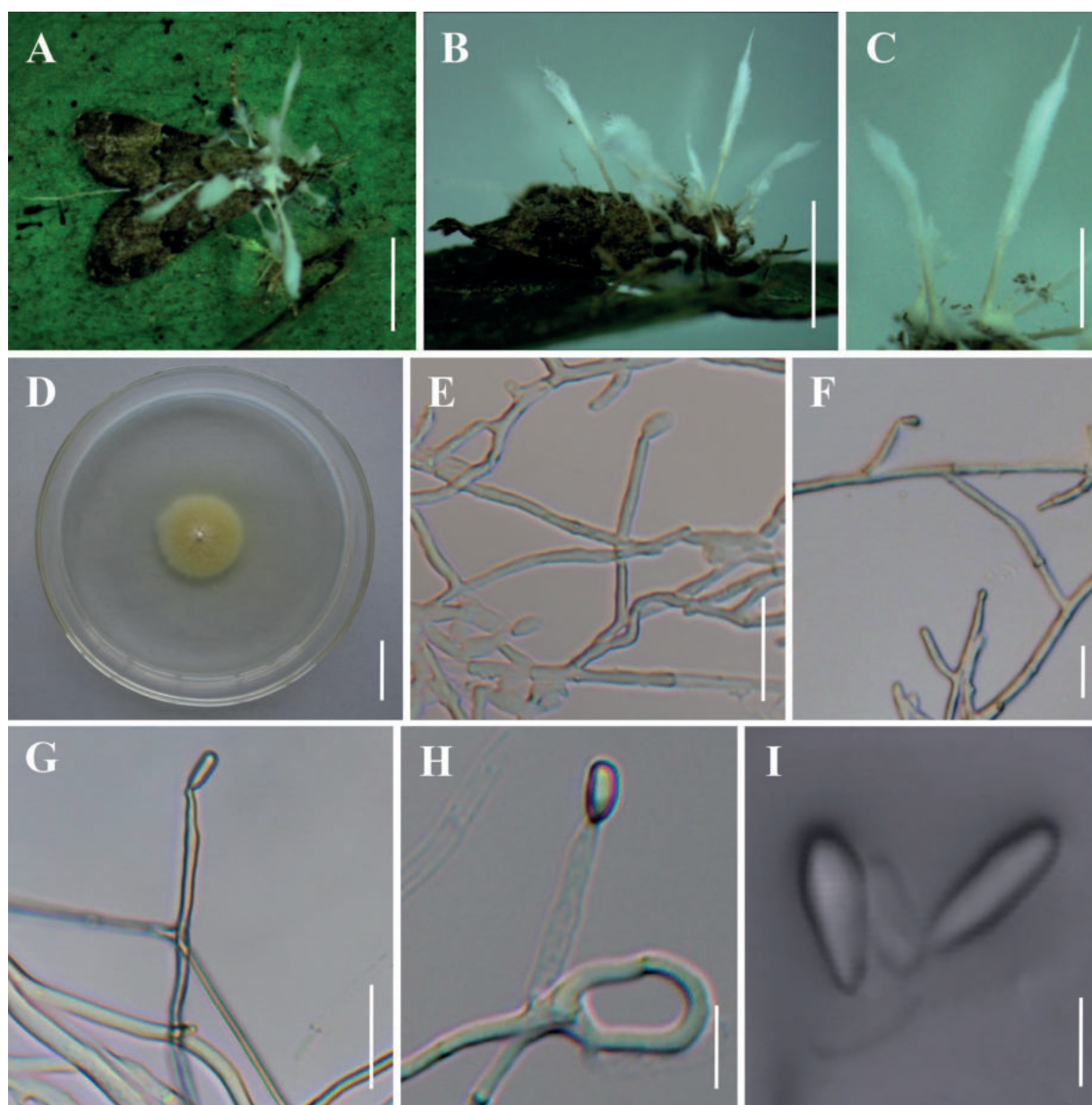

Figure 3. Morphology of *Akanthomyces laosensis* **A, B** fungus on adult moth **C** long synnemata **D** culture character on PDA medium **E–H** conidiophores, conidiogenous cells and conidia **I** conidia from long synnemata. Scale bars: 10 mm (**A, B**); 5 mm (**C**); 20 mm (**D**); 20 μm (**E–G**); 10 μm (**H**); 5 μm (**I**).

Synnemata arose at the head and in the middle of the host body, white, up to 15.6 mm long and 0.6–1.3 mm wide, rarely branched, feathery to clavate with acute or blunt ends. Colonies on PDA moderately fast-growing at 25 °C, reaching 23–26 mm in diameter in 14 days, circular, flat, white in the middle with a light yellow edge, reverse light yellow. Hyphae smooth-walled, branched, septate, hyaline, 0.8–3.5 μm wide. Conidiogenous cells monophialidic, produced along the synnemata or solitary on hyphae in culture. Phialides smooth-walled, hyaline, cylindrical, 11.5–30.0 × 2.0–4.2 μm (n = 30). Conidia smooth and hyaline, cylindrical or long oval, one-celled, 4.1–9.8 × 2.3–4.2 μm (n = 30). Size and shape of phialides and conidia similar in culture and on natural substratum.

Host. Adult moth (Noctuidae, Lepidoptera).

Habit. On the adults of Noctuidae sp. on the underside of leaves of plants.

Distribution. Muang Xay County, Oudomxay Province, Laos.

Other material examined. Laos. Oudomxay Province, Muang Xay County, Nam Kit Park (20.6651°N, 102.0007°E, 695 m above sea level), on an adult moth on the underside of a leaf, 1 October 2019, Yao Wang (YHH 2301000; living culture: YFCC 1910942).

Commentary. Phylogenetically, *Akanthomyces laosensis* forms a distinct lineage and is closely related to *A. pyralidarum* with strong statistical support (1/99%/89%) (Fig. 1). Morphologically, *A. laosensis* is distinctly different from *A. pyralidarum* because of its longer synnemata (up to 15.6 mm). Furthermore, *A. laosensis* was determined to occur on an adult of Noctuidae sp., while *A. pyralidarum* was located on an adult of Pyralidae sp. In fact, the species is easily distinguished from other known species in the genus of *Akanthomyces* by its longer phialides (11.5–30.0 μm) and larger conidia (4.1–9.8 × 2.3–4.2 μm) (Table 3).

Akanthomyces pseudonoctuidarum Hong Yu bis & Y. Wang, sp. nov.

MycoBank No: 848309

Fig. 4

Etymology. Referring to macromorphological resemblance of *A. noctuidarum*, but *A. pseudonoctuidarum* is phylogenetically distinct.

Type. Thailand. Chiang Mai Province, Chiang Mai City, Sansai District, Maejo Farm (18.9177°N, 99.0520°E, 317 m above sea level), on the adult of Noctuidae on the underside of a dicotyledonous leaf, 22 August 2018, collected by Hong Yu (holotype: YHH 2301010; ex-type living culture: YFCC 1808943).

Description. *Sexual morph*: Undetermined. ***Asexual morph*:** Synnemata arising from moth body, cream to light yellow, erect, simple, cylindrical to clavate, 800–2000 × 120–350 μm. Conidia and reproductive structures on natural substratum not observed. Colonies on PDA moderately fast-growing at 25 °C, reaching a diameter of 25–28 mm within 14 days, circular, flat to raised, white and fluffy mycelium, reverse cream to pale yellow. Hypha smooth-walled, hyaline, septate, 1.0–2.9 μm wide. Conidiophores smooth-walled, cylindrical, solitary, 6.5–13.8 × 1.8–3.6 μm (n = 30). Conidiogenous cells monophialidic or polyphialidic. Phialides verticillate, usually in whorls of 2–3 or solitary on hyphae, cylindrical with papillate end, hyaline, 6.8–26.0 × 2.1–3.6 μm (n = 30).
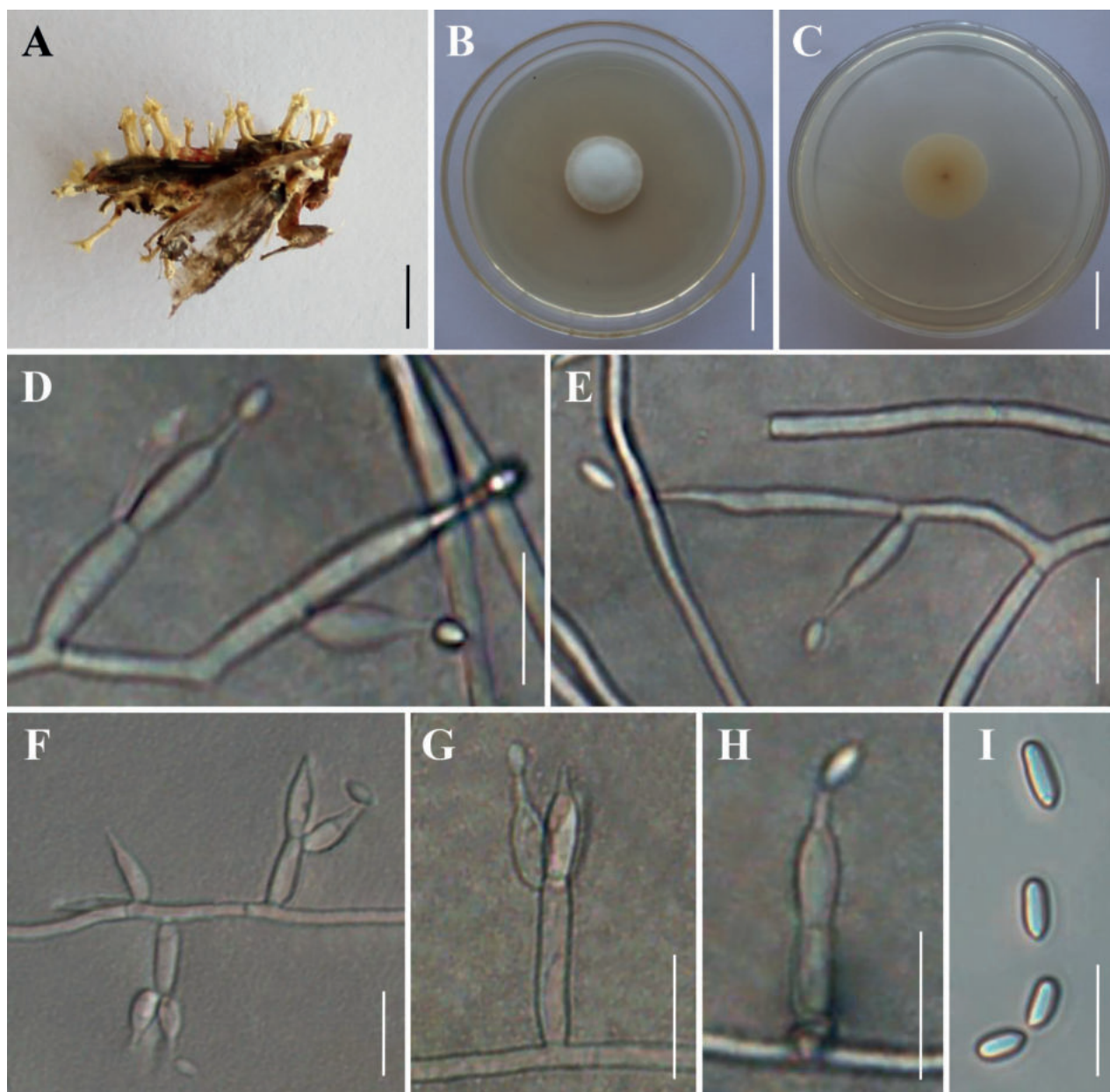
Figure 4. Morphology of *Akanthomyces pseudonoctuidarum* **A** adult moth infected by *A. pseudonoctuidarum* **B, C** culture character on PDA medium **D–H** conidiophores, conidiogenous cells and conidia **I** conidia. Scale bars: 2 mm (**A**); 20 mm (**B, C**); 10 μm (**D–I**).

Conidia smooth and hyaline, ellipsoidal to long oval, one-celled, 2.6−6.4 × 1.5−2.2 μm (n = 30).

Host. Adult moth (Noctuidae, Lepidoptera).

Habit. On the adults of Noctuidae sp. on the underside of leaves of plants.

Distribution. Chiang Mai City, Chiang Mai Province, Thailand.

Other material examined. Thailand, Chiang Mai Province, Chiang Mai City, Mae Rim District, Queen Sirikit Botanic Garden (18.8990°N, 98.8605°E, 536 m above sea level), on an adult of Noctuidae, 26 August 2018, collected by Yao Wang (YHH 2301011; living culture: YFCC 1808944).

Commentary. *Akanthomyces pseudonoctuidarum* is similar to its phylogenetically closely-related species *A. noctuidarum* in macromorphology. They have the same hosts (the adults of Noctuidae sp.) and *Isaria*-like asexual

conidiogenous structures, producing cream or light yellow synnemata. However, *A. pseudonoctuidarum* is easily recognised by its larger synnemata (800–2000 × 120–350 µm), longer phialides (6.8–26.0 µm) and larger conidia (2.6–6.4 × 1.5–2.2 µm) (Table 3). It was easily distinguished phylogenetically from *A. noctuidarum* (Fig. 1; 1/97%/85%). Both the morphological study and phylogenetic analyses of combined ITS, nr*LSU*, *TEF*, *RPB1* and *RPB2* sequence data supported that this fungus is a distinct species in the genus *Akanthomyces*.

Akanthomyces subaraneicola Hong Yu bis, Y. Wang & Z.Q. Wang, sp. nov.

MycoBank No: 848310

Fig. 5

Etymology. "Subaraneicola" refers to morphologically resembling *A. araneicola*, but phylogenetically distinct.

Type. CHINA. Hunan Province, Huaihua City, Zhongpo National Forest Park (27.5724°N, 109.9664°E, 615 m above sea level), on a spider emerging from leaf litter on the forest floor, 10 July 2021, collected by Yao Wang (holotype: YHH 2301004; ex-type living culture: YFCC 2107937).

Description. *Sexual morph*: Undetermined. *Asexual morph*: Mycosed hosts covered by white to pale yellow mycelia, producing numerous powdery conidia, synnemata not observed. Colonies on PDA reaching 24–28 mm in diameter within 14 days at 25 °C, circular, white and fluffy mycelium in the centre, cottony with a raised mycelial density at the outer ring, reverse white to pale yellow. Hyphae smooth-walled, branched, septate, hyaline, 1.6–3.2 µm wide. Conidiophores smooth-walled, cylindrical, solitary, sometimes verticillate, 6.5–12.3 × 1.6–3.5 µm (n = 30). Conidiogenous cells monophialidic or polyphialidic. Phialides consisting of a cylindrical, somewhat inflated base, verticillate on conidiophores, usually in whorls of 2–5, or solitary on hyphae, 12.1–38.2 × 1.3–3.2 µm (n = 30). Conidia smooth and hyaline, ellipsoidal to long oval, one-celled, 3.0–5.4 × 1.8–3.4 µm (n = 50), often in chains. Size and shape of phialides and conidia similar in culture and on natural substratum.

Host. Spider (Araneae).

Habit. On spiders on dead stems or emerging from leaf litter on the forest floor.

Distribution. Hunan and Yunnan Province, China.

Other material examined. CHINA, Yunnan Province, Kunming City, Wild Duck Lake Forest Park (25.1244°N, 102.8716°E, 1900 m above sea level), on a spider on a dead stem, 28 July 2021, Yao Wang (YHH 2301005; living culture: YFCC 2107938).

Commentary. Morphologically, *Akanthomyces subaraneicola* resembles the phylogenetic sister species *A. araneicola*. They were found to be parasitic on spiders (Araneae) and they are easily recognised by having white to pale yellow mycelia covering the hosts with a mass of conidia; however, our morphological observation revealed a significant difference in the shape and size of conidia between *A. subaraneicola* and *A. araneicola*. *Akanthomyces subaraneicola* usually produces large ellipsoidal to long oval conidia (3.0–5.4 × 1.8–3.4 µm), while *A. araneicola* produces small fusiform conidia (2.5–5.0 × 1.3–1.9 µm) (Table 3). In addition, molecular phylogenetic analyses indicated that they are distinct species (Fig. 1; 1/100%/100%).
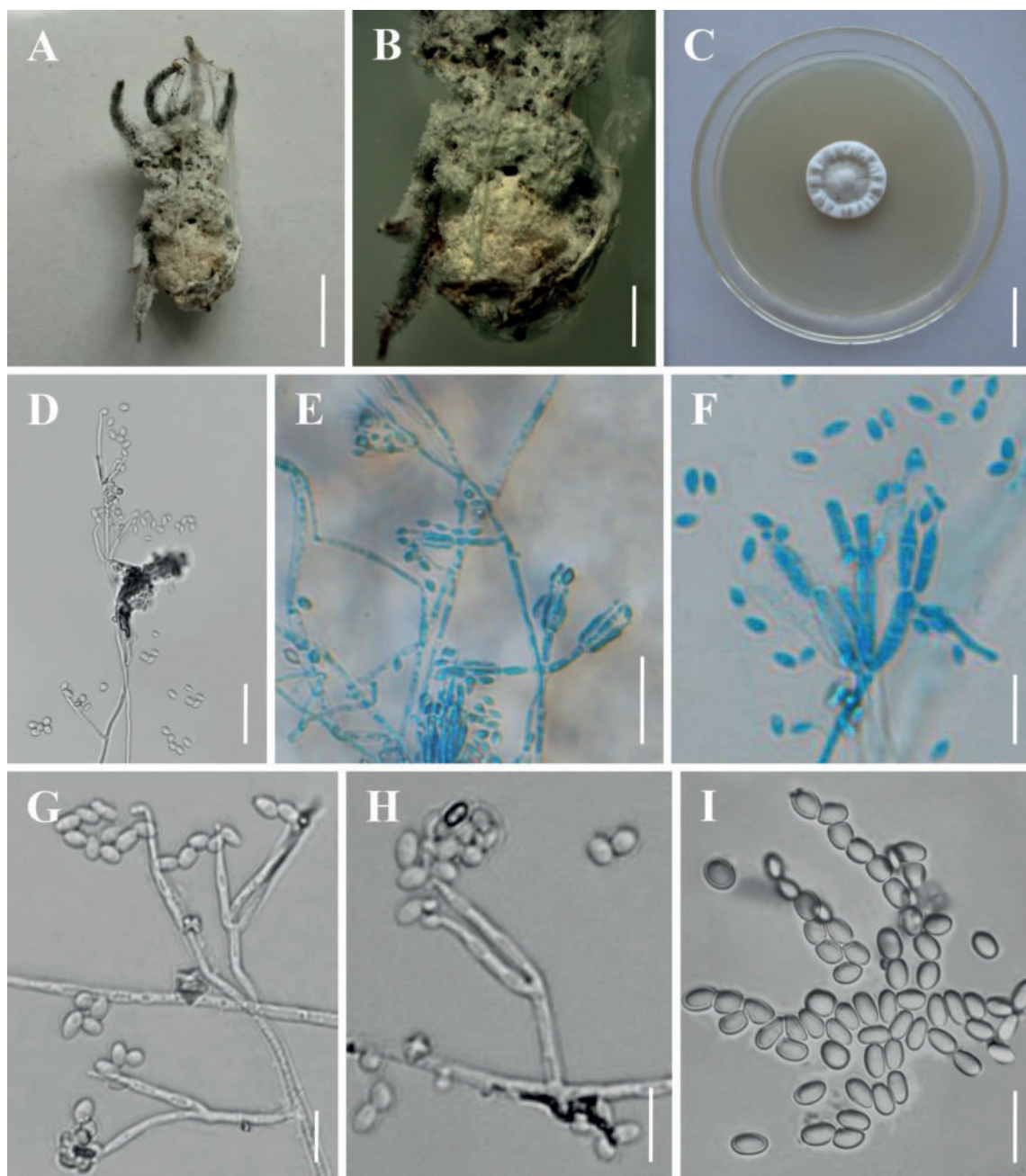
Figure 5. Morphology of *Akanthomyces subaraneicola* **A, B** fungus on spider **C** culture character on PDA medium **D–H** conidiophores, conidiogenous cells and conidia **I** conidia. Scale bars: 10 mm (**A**); 5 mm (**B**); 20 mm (**C**); 30 μm (**D**); 20 μm (**E**); 10 μm (**F–I**).

Akanthomyces araneogenus Z.Q. Liang, W.H. Chen & Y.F. Han, Phytotaxa 379(1): 69 (2018)

MycoBank No: 816114

Fig. 6

Akanthomyces tiankengensis W.H. Chen, Y.F. Han, J.D. Liang & Z.Q. Liang, Microbiology Spectrum 10(5): e01975-22, 6 (2022). Synonym.

Description. *Sexual morph*: Undetermined. *Asexual morph*: Mycosed hosts covered with white to pale yellow mycelia, occasionally several synnemata aris-

ing from all of the parts of the host. Colonies on PDA moderately fast-growing at 25 °C, reaching a diameter of 25–36 mm in 14 days at 25 °C, circular, middle bulge, white to yellowish, reverse yellowish. Hyphae smooth-walled, branched, septate, hyaline, 0.5–2.9 μm wide. Conidiophores smooth-walled, cylindrical, solitary, 10.6–22.4 × 1.3–2.6 μm (n = 30). Phialides consisting of a cylindrical, somewhat inflated base, verticillate on conidiophores, usually in whorls of 2–3 or solitary on hyphae, 8.1–17.8 × 1.1–3.6 μm (n = 30). Conidia smooth and hyaline, one-celled, globose, 1.6–2.4 μm in diameter or ellipsoidal to fusiform, 2.2–4.1 × 1.1–2.3 μm (n = 50), often in chains. Size and shape of phialides and conidia similar in culture and on natural substratum.

Host. Spider (Araneae).

Habit. On the spiders on dead stems or emerging from leaf litter.

Distribution. Guizhou and Yunnan Province, China; Chiang Mai Province, Thailand; Nghe An Province, Vietnam.
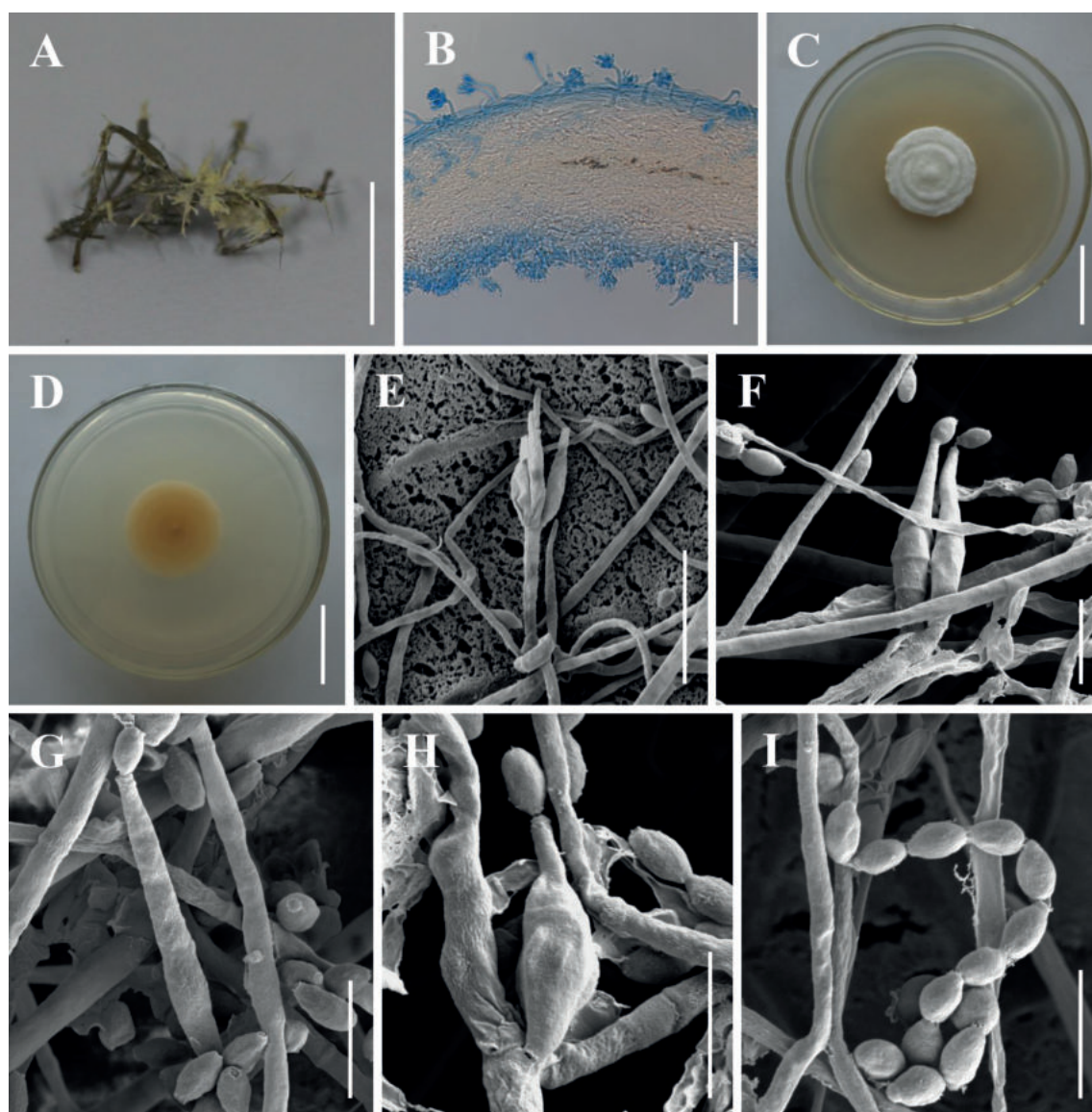

Figure 6. Morphology of *Akanthomyces araneogenus* **A** fungus on spider **B** conidiogenous structures on the host **C,D** culture character on PDA medium **E–H** conidiophores, conidiogenous cells and conidia **I** conidia. Scale bars: 5 mm (**A**); 30 μm (**B**); 30 mm (**C, D**); 10 μm (**E**); 5 μm (**F–I**).

Material examined. Thailand, Chiang Mai Province, Chiang Mai City, Queen Sirikit Botanic Garden (18.8990°N, 98.8604°E, 547 m above sea level), on a spider on a dead stem, 20 November 2018, Yao Wang (YHH 2301001; living culture: YFCC 1811934). VIETNAM, Nghe An Province, Pu Mat National Park (18.9292°N, 104.5889°E, 621 m above sea level), on spiders emerging from leaf litter on the forest floor, 28 April 2017, Yao Wang (YHH 2301007, YHH 2301012; living culture: YFCC 1704946, YFCC 1704947). China, Yunnan Province, Dai Autonomous Prefecture of Xishuangbanna, Mengla County (21.1817°N, 101.7252°E, 875 m above sea level), on a spider on a dead stem, 12 June 2022, Zhi-Qin Wang (YHH 2301002; living culture: YFCC 2206935).

Commentary. In our phylogenetic analyses, *Akanthomyces araneogenus* ex-type strain (GZUIF DX2) and *A. tiankengensis* ex-type isolate (KY11571) and our two samples isolated from the spiders formed a well-supported clade (Fig. 1). From a phylogenetic point of view, *A. tiankengensis* could not be distinguished from *A. araneogenus*, being inside the clade of the latter. Previous morphological observations revealed several differences in the characteristics between *A. araneogenus* and *A. tiankengensis* (Chen et al. 2018; Chen et al. 2022); however, our samples from different regions showed diversity of morphology in this study. The colony colour and the shape and size of the phialides and conidia of *A. araneogenus* and *A. tiankengensis*, amongst other morphological features, have been noted in our samples. There is reason to believe that distinguishing the two species is difficult because of the extensive overlap in morphological characteristics. Thus, we propose that *A. tiankengensis* is a synonym of *A. araneogenus*.

Discussion

In this study, *Akanthomyces* comprised at least 36 species with a cosmopolitan distribution (Table 2). A collection of 31 isolates of unknown identity were shown to represent four known species, four new species and an undetermined species of *Akanthomyces*. The phylogenetic positions of the four known species were evaluated, based on phylogenetic inferences according to five loci, namely, ITS, nr*LSU*, *TEF*, *RPB1* and *RPB2*, including *A. araneogenus* from China, Thailand and Vietnam, *A. dipterigenus* and *A. waltergamsii* from China and *A. sulphureus* from Vietnam (see Table 2 and Fig. 1). The four new species, given the names *A. kunmingensis* and *A. subaraneicola* from China, *A. laosensis* from Laos and *A. pseudonoctuidarum* from Thailand, were recognised according to morphological characteristics and molecular data. The isolate YFCC 945 from China represented an unknown species in the genus *Akanthomyces*. Unfortunately, the isolate did not produce conidia or reproductive structures when grown on PDA and other media and they were, thus, tentatively treated as an undetermined species of *Akanthomyces*, pending further investigation.

The highest species diversity of *Akanthomyces* occurred in subtropical and tropical regions, especially in China and Southeast Asia (see Table 2). Based on our update, there are at least 17 *Akanthomyces* species in China and Yunnan Province has the most. There is also high species diversity of *Akanthomyces* in Southeast Asia, where more than 11 species have been recorded (Table 2). Thailand, Vietnam and Laos are located in tropical regions with extremely rich biodiversity in Southeast Asia. The forests exhibit a significant variety of plant and animal life attributed to the tropical monsoon climate, characterised by high temperatures

and rainfall (Lao et al. 2021). These have created a favourable environment for the development of arthropod-pathogenic fungi, including *Akanthomyces* spp.

Akanthomyces species inhabit diverse hosts/substrates that range from eight orders of Arthropoda, namely, Acari, Araneae, Coleoptera, Hemiptera, Hymenoptera, Lepidoptera, Orthoptera and Thysanoptera, to plants, other fungi, peat, water and rusts (see Table 2). Amongst the hosts of *Akanthomyces*, Araneae and Lepidoptera are the two major orders. Our study also found that the majority of *Akanthomyces* species are spider pathogens or adult moth entomopathogens, with the exception of a few other entomopathogens and generalists that have a remarkably broad host/substrate range (Table 2 and Fig. 1). In this study, we identified an extension of the host/substrate range to also include soil, as shown in Fig. 1. The family Cordycipitaceae has been shown to evolve from an ancestor which is ecologically versatile and most probably inhabit the soil/environment and diversified into groups of entomopathogens and mycoparasites (Sung et al. 2007; Kepler et al. 2017; Wang et al. 2020; Zhou et al. 2022). *Akanthomyces* have been principally shown to be arthropod-pathogenic fungi in this study. The fact that *Akanthomyces* can be found in soil might suggest some kind of convergence/reversion.

Due to the difficulty of isolation and the limitation of cultivation conditions, studies on the development and application of *Akanthomyces* species are still currently limited. As generalists that have a remarkably broad host/substrate range, *A. gracilis* and *A. muscarius* have a high potential for interspecific transmission and biological control of pest insects (Samson and Evans 1974; Zare and Gams 2001; Kuchár et al. 2019; Nicoletti and Becchimanzi 2020). *Akanthomyces lecanii* is an effective mycoparasite of several rust fungi, green mould and fungi causing root rot diseases (*Pythium ultimum*), as well as of several powdery mildew pathogens and it is receiving increasing attention as a versatile biocontrol agent of a number of plant pathogens (Benhamou and Brodeur 2001). The members of the genus *Akanthomyces* contain species ranging from specialists with very narrow host ranges to generalists that attack a wide range of arthropods and they might be used as an ideal model system for research on fungal arthropod pathology and fungal-pathogen speciation and host adaptation (Hu et al. 2014). Coleopterans, lepidopterans and spiders are the major host groups of arthropod-pathogenic fungi within Hypocreales (Shrestha et al. 2019). The findings indicate that the majority of the hosts of *Akanthomyces* are distributed in lepidopterans and spiders, with a few in coleopterans (see Table 2). These arthropod-pathogenic fungi with special nutritional preferences are more likely to produce numerous distinctive bioactive compounds. It is hoped that this study will generate continued interest amongst mycologists, arachnologists and related experts and researchers to use such fungal resources through in vitro growth and extraction of useful bio-active secondary metabolites (extrolites).

Fungal species diversity and their host/substrate associations are important aspects of fungal ecology. A strong taxonomic basis that is dependent on advances in nucleic acid sequence technology is one of the main fundamental needs in fungal ecology (Zhang et al. 2021) and is even crucial to studies on species diversity and their host–substrate associations. However, it is regrettable that a growing number of researchers have relied heavily on molecular biology techniques to the complete exclusion of fungal isolation and characterisation utilising classical methods (Walker et al. 2019; Zhang et al. 2021). Although fungal research has entered the molecular era, phenotypic and culture-based

Table 2. Species diversity, host/substrate and geographic distribution of *Akanthomyces* species.

Species	Host/Substrate	Know distribution	References
Akanthomyces aculeatus	Adult moth (Noctuidae; Sphingidae)	USA (Connecticut; Washington; Ontario); Brazil (Salvador); Amazon countries	Mains (1950); Sanjuan et al. (2014)
Akanthomyces angustispora	Coleopterous larva	USA (Nashville)	Mains (1950)
Akanthomyces aranearum	Spider (Araneae)	USA (North Carolina; Maine); Ceylon; Netherlands; Ghana (Begoro); China	Mains (1950); Samson and Evans (1974); Hsieh et al. (1997); Zare and Gams (2001)
Akanthomyces araneicola	Spider (Araneae)	China (Guizhou)	Chen et al. (2019)
Akanthomyces araneogenus	**Spider (Araneae)**	China (Guizhou; **Yunnan**); **Thailand (Chiang Mai); Vietnam (Nghe An)**	Chen et al. (2018); **This study**
Akanthomyces araneosus	Spider (Araneae)	China (Guizhou)	Chen et al. (2022)
Akanthomyces attenuatus	*Cydia pomonella* (Lepidoptera, Tortricidae); leaf litter of *Acer saccharum*; *Symplocarpus foetidus* (plants); *Astrocaryum sciophilum* (plants)	Poland; USA; Canada; French	Zare and Gams (2001); Ellsworth et al. (2013); Barthélemy et al. (2019)
Akanthomyces clavata	*Hapithus agitator* (Orthoptera, Gryllidae)	USA (Florida)	Mains (1950)
Akanthomyces coccidioperitheciatus	Spider (Araneae)	Japan	Kepler et al. (2017); Johnson et al. (2009)
Akanthomyces dipterigenus	Hemiptera: *Icerya purchasi* (Coccidae); *Myzus persicae* (Aphididae); *Macrosiphoniella sanborni* (Aphididae); *Citrus aphid* (Aphididae); **soil**	UK; Sri Lanka; Peru; **China (Yunnan)**	Kepler et al. (2017); Zare and Gams (2001); **This study**
Akanthomyces fragilis	Orthopterous larva	Trinidad; Guiana; Brazil	Mains (1950); Petch (1937)
Akanthomyces gracilis	Hymenoptera, Formicidae (*Paltothyreus tarsatus*; *Platythyrea conradti*; *Polyrhachis militaris*; *Polyrhachis monista*; *Polyrhachis decemdentata*; *Camponotus brutus*; *Oecophylla longinoda*; *Crematogaster bequarti*; *Crematogaster clariventris*; *Macromischoides inermis*; *Macromischoides aculeatus*; *Dorylus* sp.); Coleoptera (beetle larvae, beetle imago); Lepidoptera larva, Hemiptera (Pyrrhocoridae; Cercopidae)	Ghana (Begoro); China (Guizhou)	Samson and Evans (1974); Liang et al. (2013)
Akanthomyces johnsonii	Leaf and stem (*Arctium* sp., *Begonia* sp., *Coffea* sp., *Dianthus* sp., *Ipomoea* sp., *Kalanchoe* sp., *Lycopersicon* sp., *Peperomia* sp., and *Sargassum* sp.); often associated with species of *Botryosporium*	Ghana; Indonesia; Australia (Great Barrier Reef); UK; USA; Canada	Vincent et al. (1988)
Akanthomyces kanyawimiae	Spider (Araneae)	Thailand (Phetchabun; Chanthaburi)	Mongkolsamrit et al. (2018)
Akanthomyces kunmingensis	**Spider (Araneae)**	**China (Yunnan)**	**This study**
Akanthomyces laosensis	**Adult moth (Lepidoptera, Noctuidae)**	**Laos (Oudomxay)**	**This study**
Akanthomyces lecanii	Hemiptera, Coccidae: *Pulvinaria floccifera*; *Coccus viridis*; scale insect. *Tetranychus urticae* (Acari: Tetranychidae); *Pistacia vera* (plants); *Ammophila arenaria* (plants); *Dactylis glomerata* (plants); *Deschampsia flexuosa* (plants); *Elymus farctus* (plants); *Laretia acaulis* (plants); *Pinus sylvestris* (plants); *Shorea thumbuggaia* (plants); *Taxus baccata* (plants)	W. Indies; Dominican Republic; Peru; Jamaica; USA; Sri Lanka; Indonesia; Turkey; China; Iran; Spain; Finland; Chile; Italy; Poland; India	Kepler et al. (2017); Zare and Gams (2001); Dash et al. (2018); Dolatabad et al. (2017); Nicoletti and Becchimanzi (2020)
Akanthomyces lepidopterorum	Pupa of Lepidoptera	China (Guizhou)	Chen et al. (2020b)
Akanthomyces muscarius	*Trialeurodes vaporariorum* (Hemiptera, Aleyrodidae); *Brachycaudus helichrysi* (Hemiptera, Aphididae); *Cecidophyopsis ribis* (Acari, Eriophyidae); *Cossus cossus* (Lepidoptera, Cossidae); *Zyginidia pullula* (Hemiptera, Cicadellidae); *Thrips tabaci* (Thysanoptera, Thripidae); peat; contaminated pesticide solution; *Pteridium aquilinum* (Pteridophyta); leaves of *Nypa fruticans* (Plants); *Hemileia vastatrix* (Fungi); water from domestic supply; laboratory glyphosate solution; *Acer campestre* (plants); *Laurus nobilis* (plants); *Myrtus communis* (plants); *Nypa fruticans* (plants); *Quercus robur* (plants); *Prunus cerasus* (plants); cabbage plants	UK; Italy; New Caledonia; Thailand; New Zealand	Kepler et al. (2017); Zare and Gams (2001); Nicoletti and Becchimanzi (2020); Vinit et al. (2018); Aghdam and Fotouhifar 2017; Kuchár et al. (2019)
Akanthomyces neoaraneogenus	Spider (Araneae)	China (Guizhou)	Chen et al. (2017); Mains (1949)

Species	Host/Substrate	Know distribution	References
Akanthomyces neocoleopterorum	Ladybug (Coleoptera)	China (Guizhou)	Chen et al. (2020a)
Akanthomyces noctuidarum	Adult moth (Lepidoptera, Noctuidae)	Thailand (Narathiwat; Nakhon Ratchasima; Kamphaeng Phet)	Aini et al. (2020)
Akanthomyces pissodis	Adult of *Pissodes strobi* (Coleoptera, Curculionidae)	Canada	Cope and Leal (2005)
Akanthomyces pseudonoctuidarum	**Adult moth (Lepidoptera, Noctuidae)**	**Thailand (Chiang Mai)**	**This study**
Akanthomyces pyralidarum	Adult moth (Lepidoptera, Pyralidae)	Thailand (Kanchanaburi; Chiang Mai; Phetchabun)	Aini et al. (2020)
Akanthomyces ryukyuenis	Spider (Araneae)	Japan	Kobayasi and Shimizu (1982)
Akanthomyces sabanensis	*Pulvinaria caballeroramosae* (Hemiptera, Coccidae)	Colombia	Chirivi-Salomón et al. (2015)
Akanthomyces subaraneicola	**Spider (Araneae)**	**China (Hunan; Yunnan)**	**This study**
Akanthomyces sulphureus	**Spider (Araneae)**	Thailand (Nakhon Ratchasima; Surat Thani); **Vietnam (Nghe An)**	Mongkolsamrit et al. (2018); **This study**
Akanthomyces thailandicus	Spider (Araneae)	Thailand (Chiang Mai)	Mongkolsamrit et al. (2018)
Akanthomyces tiankengensis	Spider (Araneae)	China (Guizhou)	Chen et al. (2022)
Akanthomyces tortricidarum	Adult moth (Lepidoptera, Tortricidae)	Thailand (Nakhon Ratchasima; Kamphaeng Phet)	Aini et al. (2020)
Akanthomyces tuberculatus (= A. pistillariaeformis)	Adult moth (Lepidoptera); Hymenoptera, Formicidae; Hemiptera, Pyrrhocoridae	China (Zhejiang; Yunnan); Begoro; Trinidad	Mains (1950); Samson and Evans (1974); Liang et al. (2007)
Akanthomyces uredinophilus	Rust; decayed insect	Korea (Gangwon; North Chungcheong); China (Yunnan)	Park et al. (2016); Wei et al. (2018)
Akanthomyces waltergamsii	**Spider (Araneae)**	Thailand (Saraburi; Naknon Ratchasima); **China (Yunnan)**	Mongkolsamrit et al. (2018); **This study**
Akanthomyces zaquensis	The stroma and the sclerotium of *Ophiocordyceps sinensis* (Fungi)	China (Qinghai)	Wang et al. (2023a)

Table 3. Morphological comparison of *Akanthomyces* species.

Species	Perithecia (μm)	Asci (μm)	Part-spores (μm)	Synnemata (mm)	Conidiophores (μm)	Phialides (μm)	Conidia (μm)	References
Akanthomyces aculeata				Arising from various parts of the insect, terete, narrowing upwards, 1–8 × 0.1–0.5, yellowish		Subcylindrical or narrowly ellipsoidal, 6–16 × 2.5–4, narrowing above to an acute apex, terminated by a short sterigma up to 4 long	Broadly ellipsoidal or obovoid often acute at the lower end, 3–6 × 2–3	Mains (1950)
Akanthomyces aranearum				Arising from all parts of the host, cylindrical to clavate, 0.8–10 × 0.1–0.2, simple or occasionally slightly branched, brown		Obovoid or ellipsoidal 6–12 × 4–8, rounded above and abruptly narrowing into a short sterigma, asperulate	Narrowly obclavate often acute at the lower end, narrowing upwards, rounded or obtuse at the upper end, 8–14 × 1.5–3	Mains (1950)
Akanthomyces araneicola				Synnemata not observed	Mononematous, with single phialide or whorls of two to six phialides or *Penicillium*-like from hyphae directly	Cylindrical, somewhat inflated base, 8.1–16.9 × 1.3–1.9, tapering to a thin neck	Mostly fusiform, 2.5–5.0 × 1.3–1.9	Chen et al. (2019)
Akanthomyces araneogenus				Occasionally several white synnemata arise from all parts of the host	Mononematous or synnematous, 21.6–48 × 1.2–2.2, *Penicillium*-like from hyphae directly	Cylindrical, somewhat inflated base, 4.3–17.3 × 0.9–3.1, tapering to a thin neck	Globose, 1.3–2.4 in diam, or ellipsoidal, 2.1–3.3 × 1.1–1.6	Chen et al. (2018)
Akanthomyces araneosus				Synnemata not observed	Erect conidiophores usually arose from the aerial hyphae	Solitary or in groups of two, 16.9–18.1 × 1.3–1.9 with a cylindrical basal portion and tapered into a short, distinct neck	Fusiform, 3.1–5.0 × 1.0–1.8	Chen et al. (2022)
Akanthomyces angustispora				Arising from the body and head of the host, simple or branched, 8–13 × 0.2–0.6, flesh coloured		Oblong or narrowly ellipsoidal, 6–14 × 3–4, narrowing above into an acute apex terminated by a short sterigma	Narrowly clavate, 4.5–6 × 1.2–1.4	Mains (1950)
Akanthomyces attenuatus						9–15.5 × 1–2	Cylindrical with attenuate base, occasionally 2-celled, 4.5–6.5 × 1.5–2.0	Zare and Gams (2001); Kepler et al. (2017)
Akanthomyces clavata				Numerous, arising from various parts of the host, light brown, clavate, 0.5–2.0 × 0.06–0.25		Subcylindrical, 17.1–21.4 × 2.8–4.3, narrowing above to acute apices, terminated by short sterigmata	Ellipsoidal to oblong, 4.5–8.5 × 2.1–2.5	Mains (1950)
Akanthomyces dipterigenus						20–40 × 1.2–2.7, tapering towards the apex	Ellipsoidal to oblong-oval, 5.0–10.5 × 1.5–2.5	Zare and Gams (2001); Kepler et al. (2017)
Akanthomyces fragilis				Numerous arising from all parts of the host, clavate, 0.7–1.5 × 0.03–0.09		Subcylindrical to narrowly clavate, 7–10 × 2.5–3, verrucose in the upper portions	Subcylindrical, somewhat narrowed and rounded at the ends, 6.5–9 × 1.5	Mains (1950)
Akanthomyces gracilis				Arising from the natural body openings and intersegmental and appendage joints, usually white to yellow-brown, cylindrical, 0.7–3 × 0.1–0.5		Cylindrical basal part tapering to a slender neck, 7–10 × 1.5–2.5	Ellipsoidal to fusiform, 2.5–3 × 1–1.6	Samson and Evans (1974)

Species	Perithecia (µm)	Asci (µm)	Part-spores (µm)	Synnemata (mm)	Conidiophores (µm)	Phialides (µm)	Conidia (µm)	References
Akanthomyces johnsonii				Gregarious, white, 0.4–4 tall, with a stipe 0.025–0.1 wide, subulate to cylindrical	Unbranched or with metulae arising at right angles to the stipe hyphae, 4–6 × 2–3	10–20 long, ellipsoidal to cylindrical body 2.5–4 wide, tapering into a narrow neck 3–5 × 1–1.5	Broadly fusoid with more or less truncate poles with minute frills, 3–4 × (l–)1.5–2	Vincent et al. (1988)
Akanthomyces kanyawimiae				Up to 1.5 long, up to 0.4 wide, covered by dense white to cream mycelia	Erect, verticillate with phialides in whorls of two to five	(8–)9–12(–15) × 2–3, with cylindrical basal portion, tapering into a long neck, (2–)3–5.5(–7) × 1–1.5	Cylindrical to ellipsoidal, (2–)2.5–3.5(–5) × (1.5–)2(–3)	Mongkolsamrit et al. (2018)
Akanthomyces kunmingensis				**Cream to light yellow, erect, irregularly branched**	**Cylindrical, solitary, sometimes verticillate, with phialides in whorls of four to five 4.3–9.5 × 1.2–2.0**	**Cylindrical, somewhat inflated base, 6.2–29.4 × 1.1–2.5**	**Ellipsoidal to long oval, 1.9–3.5 × 1.1–1.8**	**This study**
Akanthomyces laosensis				**Arising at the head and in the middle of the host body, white, up to 15.6 long, 0.6–1.3 wide, feathery in clavate with acute or blunt end**	**Monophialidic, produced along the synnemata or solitary on hyphae in culture**	**Cylindrical, 11.5–30.0 × 2.0–4.2**	**Cylindrical or long oval, 4.1–9.8 × 2.3–4.2**	**This study**
Akanthomyces lecanii	Ovoid, 350–650 × 200–375	200–350 × 3.5–4				Relatively short, 11–20 (–30) × 1.3–1.8, aculeate and strongly tapering	Typically short-ellipsoidal, 2.5–3.5 (–4.2) × 1–1.5	Kepler et al. (2017); Zare and Gams (2001); Shrestha et al. (2019)
Akanthomyces lepidopterorum				Synnemata not observed	Mononematous, with single phialide or two phialides	Cylindrical, somewhat inflated base, 12.7–25.8 × 1.4–1.7, tapering to a thin neck	Mostly cylindrical, 3.5–5.6 × 1.4–2.1, forming mostly globose heads	Chen et al. (2020b)
Akanthomyces muscarius						(15–)20–35 × 1.0–1.7	Ellipsoidal to subcylindrical, (2–)2.5–5.5(–6) × 1–1.5(–1.8)	Kepler et al. (2017); Zare and Gams (2001)
Akanthomyces neoaraneogenus				Synnemata not observed	Moderately branched, with (1–)2–6 (–8) phialides	30–64 × 1.1–3.2	Forming mostly globose heads, cylindrical, 3.2–8.6 × 1.3–1.6	Chen et al. (2017); Mains (1949)
Akanthomyces neocoleopterorum				Synnemata not observed	Mononematous, with single phialide or whorls of two to five phialides, or *Verticillium*-like from hyphae directly	Cylindrical, somewhat inflated base, 19.9–29.6 × 1.6–2.0, tapering to a thin neck	Mostly cylindrical, 3.3–6.6 × 1.5–1.8	Chen et al. (2020a)
Akanthomyces noctuidarum	Ovoid, (530–)623–993(–1000) × (290–)308–413(–425)	(170–)196–423(–550) × (2–)2.7–3.8(–4)	(6–)7–10.7(–13) × 1	Arising from moth body and wing veins, white to cream, erect, cylindrical to clavate, (650–)668–1191(–1500) × (50–)53.4–102(–120) µm	Monophialidic or polyphialidic	Cylindrical with papillate end, hyaline, (5–)6.8–9(–10) × (1.8–)2–2.4(–3)	Cylindrical with round end, (3–)3.5–4.5(–6) × 1	Aini et al. (2020)
Akanthomyces pissodis				Synnemata not observed			Cylindrical to ovoid or oval, 4–9.2 × 1.6–2.4	Cope and Leal (2005)
Akanthomyces pseudonoctuidarum				**Arising from moth body, cream to light yellow, erect, cylindrical to clavate, 0.8–2 × 0.12–0.35**	**Cylindrical, solitary, 6.5–13.8 × 1.8–3.6**	**Cylindrical with papillate end, 6.8–26.0 × 2.1–3.6**	**Ellipsoidal to long oval, 2.6–6.4 × 1.5–2.2**	**This study**

Species	Perithecia (µm)	Asci (µm)	Part-spores (µm)	Synnemata (mm)	Conidiophores (µm)	Phialides (µm)	Conidia (µm)	References
Akanthomyces pyralidarum	Ovoid to obpyriform, (290–)342–580(–650) × (150–)186–291(–340)	(170–)222–329(–360) × (2–)2.5–.3(–4)	(5–)5.9–9.4(–12) × 1	Synnemata not observed	Not observed	Not observed	Not observed	Aini et al. (2020)
Akanthomyces ryukyuensis	Pyriformia, 570–630 × 170–250	5 wide, cap 3 wide	1 × 1–4					Kobayasi and Shimizu (1982)
Akanthomyces sabanensis				Synnemata not observed	Generally arising from submerged hyphae, moderately branched	Solitary or in whorls of 2–4, 13–19 long, from 1.0–2.0 gradually tapering to 0.5–1.0	Ellipsoidal to ovoid, usually straight, 3.5–4.5 × 1.5–2.0	Chirivi-Salomón et al. (2015); Kepler et al. (2017)
Akanthomyces sulphureus	Narrowly ovoid, (650–)676(–680) × (240–)324.5(–330)	Up to 500 long, 2–3 wide	(300–)336(–450) × 1–1.5	Synnemata not observed	Erect, verticillate with phialides in whorls of two to three	(10–)16(–20) × 2–2.5, with a cylindrical basal portion, tapering into a thin neck, 1 × 0.5	Cylindrical to ellipsoidal, (4–)4.5–5.5(–6) × 2–3	Mongkolsamrit et al. (2018)
Akanthomyces subaraneicola				**Synnemata not observed**	**Cylindrical, solitary or verticillate with phialides in whorls of two to five, 6.5–12.3 × 1.6–3.5**	**Cylindrical, somewhat inflated base, 12.1–38.2 × 1.3–3.2**	**Ellipsoidal to long oval, 3.0–5.4 × 1.8–3.4**	**This study**
Akanthomyces thailandicus	Narrowly ovoid, (700–)752–838(–850) × (300–)305–375(–400)	Up to 550 long, 5–7 wide	4–6 × 1–1.5	Synnemata not observed	Erect, forming verticillate branches with solitary phialides	(12–)13.5–21(–30) × 1–2, awl-shaped, *lecanicillium*-like	Cylindrical to ellipsoidal (3–)4–6(–7) × 1.5–2	Mongkolsamrit et al. (2018)
Akanthomyces tiankengensis				Synnemata not observed	Erect, usually aring from the aerial hyphae	Solitary or in groups of two, 13.9–17.1 × 1.1 – 1.6 with a cylindrical basal portion and tapering into a short, distinct neck	Fusiform, 2.3–3.0 × 1.5–2.3	Chen et al. (2022)
Akanthomyces tortricidarum				Long synnemata aring at the head and in the middle of the host body, up to 5 long, 0.12–0.15 wide, cylindrical to clavate, short synnemata aring on moth body, wings and legs, (197–)200–267(–300) × (15–)17.7–31.6(40–)µm, white to cream	Monophialidic or polyphialidic	Long synnemata: (5–)6–8(–10) × (1.8–)2–2.7(–3), short synnemata: (5–)6.2–8.3(–10) × (1.8–)2–2.5(–3), cylindrical to ellipsoidal with papillate end	Fusoid, long synnemata: (1–)2.5–3(–3.2) × (0.8–)1–1.4(–2), short synnemata: (1–)1.8–2.7(–3) × 1–2	Aini et al. (2020)
Akanthomyces tuberculatus (= A. pistillariaeformis)	Narrowly ovoid or conoid, 420–900 × 180–370	300–600 × 4–5	2–6 × 0.5–1	Arising from all parts of the moths, clavate, 0.4–1.0 long, the stipe 0.025–0.05 thick		Subcylindrical, 6–10 × 2–3, narrowing above into an acute apex terminated by a short sterigma 2–3 long	Fusoid to subcylindrical narrowing at the ends, 2.5–5 × 1–1.5	Mains (1950)
Akanthomyces uredinophilus				Synnemata not observed		Produced singly or in whorls of up to 3–4(–5) on prostrate hyphae, 20–60 × 1–2.5(–3)	Cylindrical, oblong, or ellipsoid, 3–9 × 1.8–3	Park et al. (2016)
Akanthomyces waltergamsii				Arising on legs of spider, erect, up to 1.5 long, 0.1–0.12 wide	Usually forming verticillate branches with phialides in whorls of two to five	(10–)16(–22) × (1–)1.5(–2), with cylindrical to ellipsoidal basal portion, tapering into a thin neck, 1–3 × 1	Ellipsoidal or fusiform, (2–)3.5(–4) × 2–3	Mongkolsamrit et al. (2018)
Akanthomyces zaquensis				Synnemata not observed		8.0–40.0 long, rarely over 100, 0.6–1.2 at the base, tapering to about 0.4 at the tips	Long-ellipsoidal to almost cylindrical, (1.5–)3.0–6.0(–7.0) × 0.5–1.2(–1.5)	Wang et al. (2023a)

studies are still an invaluable tool for fungal biology and ecology exploration (Walker et al. 2019). In addition to molecular data, morphological and ecological characteristics have a pivotal role in taxonomy and phylogenetic identification of fungi. In our work, we surveyed the literature to the greatest extent possible, combined that with the results of those obtained by morphological methods (optical microscope and electron microscope) in our study, to list and compare the morphological characteristics of 35 *Akanthomyces* species (Table 3). The morphological comparison revealed obvious differences in the size of ascospores and asci, morphology of the synnemata, conidiogenous structures and conidial shape and size, although the morphological features generally overlapped. Our statistics showed that at least 20 *Akanthomyces* species are specialists with narrow host ranges and they are either spider pathogens or adult moth entomopathogens (Table 2). They cause mortality of spiders and adult moths by nature. The cadavers are usually found attached to the underside of leaves or on tree trunks, barks, decaying logs, branches, grass, leaf litter and forest floors (Shrestha et al. 2019). These ecological characteristics are phylogenetically informative for distinguishing species of *Akanthomyces* and they contribute to the timely discovery of new *Akanthomyces* species in nature.

Additional information

Conflict of interest

The authors have declared that no competing interests exist.

Ethical statement

No ethical statement was reported.

Funding

Author contributions

All authors have contributed equally.

Author ORCIDs

Yao Wang https://orcid.org/0000-0002-1262-6700
Hong Yu https://orcid.org/0000-0002-2149-5714

Data availability

All of the data that support the findings of this study are available in the main text or Supplementary Information.

References

Aghdam SA, Fotouhifar KB (2017) Introduction of some endophytic fungi of sour cherry trees (*Prunus cerasus*) in Iran. Rostaniha 18: 77–94.
Aini AN, Mongkolsamrit S, Wijanarka W, Thanakitpipattana D, Luangsaard JJ, Budiharjo A (2020) Diversity of *Akanthomyces* on moths (Lepidoptera) in Thailand. MycoKeys 71: 1–22. https://doi.org/10.3897/mycokeys.71.55126

Barthélemy M, Elie N, Pellissier L, Wolfender JL, Stien D, Touboul D, Eparvier V (2019) Structural identification of antibacterial lipids from Amazonian palm tree endophytes through the molecular network approach. International Journal of Molecular Sciences 20(8): 2006–2018. https://doi.org/10.3390/ijms20082006

Benhamou N, Brodeur J (2001) Pre-inoculation of Ri T-DNA transformed cucumber roots with the mycoparasite, *Verticillium lecanii*, induces host defense reactions against *Pythium ultimum* infection. Physiological and Molecular Plant Pathology 58(3): 133–146. https://doi.org/10.1006/pmpp.2001.0322

Bischoff JF, Rehner SA, Humber RA (2006) *Metarhizium frigidum* sp. nov.: A cryptic species of *M. anisopliae* and a member of the *M. flavoviride* complex. Mycologia 98(5): 737–745. https://doi.org/10.1080/15572536.2006.11832645

Boudier E (1885) Note sur un nouveau genre et quelques nouvelles especes des Pyrenomycetes. Revue Mycologique Toulouse 7: 224–227.

Chen WH, Han YF, Liang ZQ, Jin DC (2017) *Lecanicillium araneogenum* sp. nov., a new araneogenous fungus. Phytotaxa 305(1): 29–34. https://doi.org/10.11646/phytotaxa.305.1.4

Chen WH, Liu C, Han YF, Liang JD, Liang ZQ (2018) *Akanthomyces araneogenum*, a new *Isaria*-like araneogenous species. Phytotaxa 379(1): 66–72. https://doi.org/10.11646/phytotaxa.379.1.6

Chen WH, Liu C, Han YF, Liang JD, Tian WY, Liang ZQ (2019) *Akanthomyces araneicola*, a new araneogenous species from Southwest China. Phytotaxa 409(4): 227–232. https://doi.org/10.11646/phytotaxa.409.4.5

Chen WH, Han YF, Liang JD, Liang ZQ (2020a) *Akanthomyces neocoleopterorum*, a new verticillium-like species. Phytotaxa 432: 119–124. https://doi.org/10.11646/phytotaxa.432.2.2

Chen WH, Han YF, Liang JD, Liang ZQ (2020b) *Akanthomyces lepidopterorum*, a new lecanicillium-like species. Phytotaxa 459: 117–123. https://doi.org/10.11646/phytotaxa.459.2.3

Chen WH, Liang JD, Ren XX, Zhao JH, Han YF, Liang ZQ (2022) Species diversity of *Cordyceps*-like fungi in the Tiankeng karst region of China. Microbiology Spectrum 10(5): e01975–e22. https://doi.org/10.1128/spectrum.01975-22

Chen WH, Liang JD, Ren XX, Zhao JH, Han YF (2023) Study on species diversity of *Akanthomyces* (Cordycipitaceae, Hypocreales) in the Jinyun Mountains, Chongqing, China. MycoKeys 98: 299–315. https://doi.org/10.3897/mycokeys.98.106415

Chiriví-Salomón JS, Danies G, Restrepo S, Sanjuan T (2015) *Lecanicillium sabanense* sp. nov. (Cordycipitaceae) a new fungal entomopathogen of coccids. Phytotaxa 234(1): 63–74. https://doi.org/10.11646/phytotaxa.234.1.4

Cope HH, Leal I (2005) A new species of *Lecanicillium* isolated from the white pine weevil, *Pissodes strobi*. Mycotaxon 94: 331–340.

Darriba D, Taboada GL, Doallo R, Posada D (2012) jModelTest 2: More models, new heuristics and parallel computing. Nature Methods 9(8): e772. https://doi.org/10.1038/nmeth.2109

Dash CK, Bamisile BS, Ravindran K, Qasim M, Lin Y, Islam SU, Hussain M, Wang L (2018) Endophytic entomopathogenic fungi enhance the growth of *Phaseolus vulgaris* L. (Fabaceae) and negatively affect the development and reproduction of *Tetranychus urticae* Koch (Acari: Tetranychidae). Microbial Pathogenesis 125: 385–392. https://doi.org/10.1016/j.micpath.2018.09.044

Dolatabad HK, Javan-Nikkhah M, Shier WT (2017) Evaluation of antifungal, phosphate solubilisation, and siderophore and chitinase release activities of endophytic fungi

from *Pistacia vera*. Mycological Progress 16(8): 777–790. https://doi.org/10.1007/s11557-017-1315-z

Ellsworth KT, Clark TN, Gray CA, Johnson JA (2013) Isolation and bioassay screening of medicinal plant endophytes from eastern Canada. Canadian Journal of Microbiology 59(11): 761–765. https://doi.org/10.1139/cjm-2013-0639

Gams W, Zare R (2001) A revision of *Verticillium* sect. Prostrata. III. Generic classification. Nova Hedwigia 72(3–4): 329–337. https://doi.org/10.1127/nova.hedwigia/72/2001/329

Hsieh LS, Tzean SS, Wu WJ (1997) The genus *Akanthomyces* on spiders from Taiwan. Mycologia 89(2): 319–324. https://doi.org/10.1080/00275514.1997.12026788

Hu X, Xiao G, Zheng P, Shang Y, Su Y, Zhang X, Liu X, Zhan S, St Leger RJ, Wang C (2014) Trajectory and genomic determinants of fungal-pathogen speciation and host adaptation. Proceedings of the National Academy of Sciences of the United States of America 111: 16796–16801. https://doi.org/10.1073/pnas.1412662111

Johnson D, Sung GH, Hywel-Jones NL, Luangsa-Ard JJ, Bischoff JF, Kepler RM, Spatafora JW (2009) Systematics and evolution of the genus *Torrubiella* (Hypocreales, Ascomycota). Mycological Research 113(3): 279–289. https://doi.org/10.1016/j.mycres.2008.09.008

Kepler RM, Sung GH, Ban S, Nakagiri A, Chen MJ, Huang B, Li Z, Spatafora JW (2012) New teleomorph combinations in the entomopathogenic genus *Metacordyceps*. Mycologia 104(1): 182–197. https://doi.org/10.3852/11-070

Kepler RM, Luangsa-ard JJ, Hywel-Jones NL, Quandt CA, Sung GH, Rehner SA, Aime MC, Henkel TW, Sanjuan T, Zare R, Chen MJ, Li ZZ, Rossman AY, Spatafora JW, Shrestha B (2017) A phylogenetically-based nomenclature for Cordycipitaceae (Hypocreales). IMA Fungus 8(2): 335–353. https://doi.org/10.5598/imafungus.2017.08.02.08

Kobayasi Y, Shimizu D (1982) *Cordyceps* species from Japan 5. Bulletin of the National Science Museum Series B 8: 111–123.

Kuchár M, Glare TR, Hampton JG, Dickie IA, Christey MC (2019) Virulence of the plant-associated endophytic fungus *Lecanicillium muscarium* to diamondback moth larvae. New Zealand Plant Protection 72: 253–259. https://doi.org/10.30843/nzpp.2019.72.257

Lanfear R, Calcott B, Ho SYW, Guindon S (2012) Partitionfinder: Combined selection of partitioning schemes and substitution models for phylogenetic analyses. Molecular Biology and Evolution 29(6): 1695–1701. https://doi.org/10.1093/molbev/mss020

Lao TD, Le TAH, Truong NB (2021) Morphological and genetic characteristics of the novel entomopathogenic fungus *Ophiocordyceps langbianensis* (Ophiocordycipitaceae, Hypocreales) from Lang Biang Biosphere Reserve, Vietnam. Scientific Reports 11(1): e1412. https://doi.org/10.1038/s41598-020-78265-7

Lebert H (1858) Ueber einige neue oder unvollkommen gekannte Krankheiten der Insekten, welche durch Entwicklung niederer Pflanzen im lebenden Körper enstehen. Zeitschrift für Wissenschaftliche Zoologie 9: 439–453.

Liang ZQ, Liu AY, Liu ZY (2007) *Cordyceps*. Flora Fungorum sinicorum (Vol. 32). Science Press, Beijing.

Liang ZQ, Chen WH, Han YF, Zou X (2013) A combined identification of morphological traits and DELTA system to *Akanthomyces gracilis* from China. Journal of Fungal Research 11: 242–245.

Liu ZY, Liang ZQ, Whalley AJS, Yao YJ, Liu AY (2001) *Cordyceps brittlebankisoides*, a new pathogen of grubs and its anamorph, *Metarhizium anisopliae* var. *majus*. Journal of Invertebrate Pathology 78(3): 178–182. https://doi.org/10.1006/jipa.2001.5039

Mains EB (1949) New species of *Torrubiella*, *Hirsutella* and *Gibellula*. Mycologia 41(3): 303–310. https://doi.org/10.1080/00275514.1949.12017774

Mains EB (1950) Entomogenous species of *Akanthomyces*, *Hymenostilbe* and *Insecticola* in North America. Mycologia 42(4): 566–589. https://doi.org/10.1080/00275514.1950.12017861

Manfrino R, Gutierrez A, Diez del Valle F, Schuster C, Ben Gharsa H, López Lastra C, Leclerque A (2022) First description of *Akanthomyces uredinophilus* comb. nov. from Hemipteran insects in America. Diversity 14(12): e1118. https://doi.org/10.3390/d14121118

Minh BQ, Schmidt HA, Chernomor O, Schrempf D, Woodhams MD, Von Haeseler A, Lanfear R (2020) IQ-TREE 2: New models and efficient methods for phylogenetic inference in the genomic era. Molecular Biology and Evolution 37(5): 1530–1534. https://doi.org/10.1093/molbev/msaa015

Mongkolsamrit S, Noisripoom W, Thanakitpipattana D, Wutikhun T, Spatafora JW, Luangsa-Ard J (2018) Disentangling cryptic species with *Isaria*-like morphs in Cordycipitaceae. Mycologia 110(1): 230–257. https://doi.org/10.1080/00275514.2018.1446651

Nicoletti R, Becchimanzi A (2020) Endophytism of *Lecanicillium* and *Akanthomyces*. Agriculture 10(6): 1–16. https://doi.org/10.3390/agriculture10060205

Park MJ, Hong SB, Shin HD (2016) *Lecanicillium uredinophilum* sp. nov. associated with rust fungi from Korea. Mycotaxon 130(4): 997–1005. https://doi.org/10.5248/130.997

Petch T (1937) Notes on entomogenous fungi. Transactions of the British Mycological Society 21(1–2): 34–67. https://doi.org/10.1016/S0007-1536(37)80005-4

Rehner SA, Buckley E (2005) A *Beauveria* phylogeny inferred from nuclear ITS and EF1-a sequences: Evidence for cryptic diversification and links to *Cordyceps teleomorphs*. Mycologia 97(1): 84–98. https://doi.org/10.3852/mycologia.97.1.84

Rehner SA, Samuels GJ (1994) Taxonomy and phylogeny of *Gliocladium* analysed from nuclear large subunit ribosomal DNA sequences. Mycological Research 98(6): 625–634. https://doi.org/10.1016/S0953-7562(09)80409-7

Ronquist F, Teslenko M, van der Mark P, Ayres DL, Darling A, Höhna S, Larget B, Liu L, Suchard MA, Huelsenbeck JP (2012) MrBayes 3.2: Efficient Bayesian phylogenetic inference and model choice across a large model space. Systematic Biology 61(3): 539–542. https://doi.org/10.1093/sysbio/sys029

Samson RA, Evans HC (1974) Notes on entomogenous fungi from Ghana II. The genus *Akanthomyces*. Acta Botanica Neerlandica 23(1): 28–35. https://doi.org/10.1111/j.1438-8677.1974.tb00913.x

Sanjuan T, Tabima J, Restrepo S, Læssøe T, Spatafora JW, Franco-Molano AE (2014) Entomopathogens of Amazonian stick insects and locusts are members of the *Beauveria* species complex (*Cordyceps* sensu stricto). Mycologia 106(2): 260–275. https://doi.org/10.3852/13-020

Shrestha B, Kubátová A, Tanaka E, Oh J, Yoon DH, Sung JM, Sung GH (2019) Spider-pathogenic fungi within Hypocreales (Ascomycota): Their current nomenclature, diversity, and distribution. Mycological Progress 18(8): 983–1003. https://doi.org/10.1007/s11557-019-01512-3

Simon C, Frati F, Beckenbach A, Crespi B, Liu H, Flook P (1994) Evolution, weighting, and phylogenetic utility of mitochondrial gene sequences and a compilation of conserved polymerase chain reaction primers. Annals of the Entomological Society of America 87(6): 651–701. https://doi.org/10.1093/aesa/87.6.651

Stamatakis A, Hoover P, Rougemont J (2008) A rapid bootstrap algorithm for the RAxML web servers. Systematic Biology 57(5): 758–771. https://doi.org/10.1080/10635150802429642

Sung GH, Hywel-Jones NL, Sung JM, Luangsa-ard JJ, Shrestha B, Spatafora JW (2007) Phylogenetic classification of *Cordyceps* and the clavicipitaceous fungi. Studies in Mycology 57: 5–59. https://doi.org/10.3114/sim.2007.57.01

Swofford DL (2002) PAUP*. Phylogenetic analysis using parsimony (*and other methods), version 4.0b10. Sinauer Associates, Sunderland.

Tamura K, Stecher G, Peterson D, Filipski A, Kumar S (2013) MEGA6: Molecular evolutionary genetics analysis version 6.0. Molecular Biology and Evolution 30(12): 2725–2729. https://doi.org/10.1093/molbev/mst197

Vilgalys R, Hester M (1990) Rapid genetic identification and mapping of enzymatically amplified ribosomal DNA from several *Cyptococcus* species. Journal of Bacteriology 172(8): 4238–4246. https://doi.org/10.1128/jb.172.8.4238-4246.1990

Vincent MA, Seifert KA, Samson RA (1988) *Akanthomyces johnsonii*, a saprophytic synnematous hyphomycete. Mycologia 80(5): 685–688. https://doi.org/10.1080/00275514.1988.12025601

Vinit K, Doilom M, Wanasinghe DN, Bhat DJ, Brahmanage RS, Jeewon R, Xiao Y, Hyde KD (2018) Phylogenetic placement of *Akanthomyces muscarius*, a new endophyte record from *Nypa fruticans* in Thailand. Current Research in Environmental & Applied Mycology 8(3): 404–417. https://doi.org/10.5943/cream/8/3/10

Walker LM, Cedeño-Sanchez M, Carbonero F, Herre EA, Turner BL, Wright SJ, Stephenson SL (2019) The response of litter-associated Myxomycetes to long-term nutrient addition in a lowland tropical forest. The Journal of Eukaryotic Microbiology 66(5): 757–770. https://doi.org/10.1111/jeu.12724

Wang Y, Wang YR, Han YF, Liang ZQ (2015) A new thermotolerant species of *Taifanglania*. Junwu Xuebao 34: 345–349. https://doi.org/10.13346/j.mycosystema.140136

Wang YB, Wang Y, Fan Q, Duan DE, Zhang GD, Dai RQ, Dai YD, Zeng WB, Chen ZH, Li DD, Tang DX, Xu ZH, Sun T, Nguyen TT, Tran NL, Dao VM, Zhang CM, Huang LD, Liu YJ, Zhang XM, Yang DR, Sanjuan T, Liu XZ, Yang ZL, Yu H (2020) Multigene phylogeny of the family Cordycipitaceae (Hypocreales): New taxa and the new systematic position of the Chinese cordycipitoid fungus *Paecilomyces hepiali*. Fungal Diversity 103(1): 1–46. https://doi.org/10.1007/s13225-020-00457-3

Wang ZQ, Wang Y, Dong QY, Fan Q, Dao VM, Yu H (2022) Morphological and phylogenetic characterization reveals five new species of *Samsoniella* (Cordycipitaceae, Hypocreales). Journal of Fungi 8(7): e747. https://doi.org/10.3390/jof8070747

Wang YH, Wang WJ, Wang K, Dong CH, Hao JR, Kirk PM, Yao YJ (2023a) *Akanthomyces zaquensis* (Cordycipitaceae, Hypocreales), a new species isolated from both the stroma and the sclerotium of *Ophiocordyceps sinensis* in Qinghai, China. Phytotaxa 579(3): 198–208. https://doi.org/10.11646/phytotaxa.579.3.5

Wang Y, Tang DX, Luo R, Wang YB, Thanarut C, Dao VM, Yu H (2023b) Phylogeny and systematics of the genus *Clonostachys*. Frontiers in Microbiology 14: e1117753. https://doi.org/10.3389/fmicb.2023.1117753

Wei DP, Wanasinghe DN, Chaiwat TA, Hyde KD (2018) *Lecanicillium uredinophilum* known from rusts, also occurs on animal hosts with chitinous bodies. Asian Journal of Mycology 1(1): 63–73. https://doi.org/10.5943/ajom/1/1/5

White TJ, Bruns T, Lee S, Taylor JW (1990) Amplification and direct sequencing of fungal ribosomal RNA genes for phylogenetics. PCR protocols, 315–322. https://doi.org/10.1016/B978-0-12-372180-8.50042-1

Zare R, Gams W (2001) A revision of *Verticillium* section *Prostrata*. IV. The genera *Lecanicillium* and *Simplicillium* gen. nov. Nova Hedwigia 73(1–2): 1–50. https://doi.org/10.1127/nova.hedwigia/73/2001/1

Zhang ZY, Shao QY, Li X, Chen WH, Liang JD, Han YF, Huang JZ, Liang ZQ (2021) Culturable fungi from urban soils in China I: Description of 10 new taxa. Microbiology Spectrum 9(2): e00867–e21. https://doi.org/10.1128/Spectrum.00867-21

Zhou YM, Zhi JR, Qu JJ, Zou X (2022) Estimated divergence times of *Lecanicillium* in the family Cordycipitaceae provide insights into the attribution of *Lecanicillium*. Frontiers in Microbiology 13: e859886. https://doi.org/10.3389/fmicb.2022.859886

Supplementary material 1

Supplementary information

Authors: Yao Wang, Zhi-Qin Wang, Run Luo, Sisommay Souvanhnachit, Chinnapan Thanarut, Van-Minh Dao, Hong Yu

Data type: docx

Explanation note: **fig. S1.** Phylogenetic relationships among the genus *Akanthomyces* and its allies in Cordycipitaceae based on Bayesian inference (BI) and maximum likelihood (ML) analyses of a five-locus (ITS, nr*LSU*, *TEF*, *RPB1*, and *RPB2*) dataset. **fig. S2.** Phylogenetic tree of *Akanthomyces* based on Maximum Likelihood (IQ-TREE) analysis from the ITS sequences. Statistical support values (≥70%) are shown at the nodes for ML boostrap support. **fig. S3.** Phylogenetic tree of *Akanthomyces* based on Maximum Likelihood (IQ-TREE) analysis from the nr*LSU* sequences. **fig. S4.** Phylogenetic tree of *Akanthomyces* based on Maximum Likelihood (IQ-TREE) analysis from the *TEF* sequences. **fig. S5.** Phylogenetic tree of *Akanthomyces* based on Maximum Likelihood (IQ-TREE) analysis from the *RPB1* sequences. **fig. S6.** Phylogenetic tree of *Akanthomyces* based on Maximum Likelihood (IQ-TREE) analysis from the *RPB2* sequences.

Link: https://doi.org/10.3897/mycokeys.101.109751.suppl1

MycoKeys

Three new species of *Cortinarius* section *Delibuti* (Cortinariaceae, Agaricales) from China

Pan Long[1], Song-Yan Zhou[2], Sai-Nan Li[1], Fei-Fei Liu[2], Zuo-Hong Chen[1]

1 *College of Life Science, Hunan Normal University, Changsha 410081, China*
2 *Key Laboratory for Plant Diversity and Biogeography of East Asia, Kunming Institute of Botany, Chinese Academy of Sciences, Kunming 650201, China*
Corresponding author: Zuo-Hong Chen (chenzuohong@263.net)

Abstract

Three new species of *Cortinarius* section *Delibuti*, namely *C. fibrillososalor*, *C. pseudosalor*, and *C. subtropicus* are described as new to science based on morphological and phylogenetic evidences. *Cortinarius pseudosalor* is extremely morphologically similar to *C. salor*, but it differs from the latter by smaller coarsely verrucose basidiospores. *Cortinarius fibrillososalor* can be easily differentiated by its fibrillose pileus. The pileus of *C. subtropicus* becomes brown without lilac tint at maturity comparing with other members of section *Delibuti*. A combined dataset of ITS and LSU sequences was used for phylogenetic analysis. The phylogenetic reconstruction of section *Delibuti* revealed that these three new species clustered and formed independent lineages with full support respectively. A key to the three new species and related species of section *Delibuti* is provided in this work.

Key words: Morphology, new taxa, phylogeny, taxonomy

Introduction

The genus *Cortinarius* (Pers.) Gray (Cortinariaceae, Agaricales), which is known for its high species diversity, comprises more than 3000 taxa and exhibits a global distribution (Garnica et al. 2005; Willis 2018). However, the taxonomy of this genus faces an extremely complex challenge due to the overlapping morphological variation within species (Seidl 2000; Dima et al. 2021). Different classification systems of *Cortinarius* have been proposed by many taxonomists based on the comparison of the morphological characteristics, geographical distribution, ecological traits, chemical features, DNA barcode markers, or diverse combinations of the above through introducing the infrageneric concepts such as subgenus, section, or clade (Moser 1969; Moser and Horak 1975; Singer 1986; Bidaud et al. 1994; Brandrud 1998; Peintner et al. 2002; Garnica et al. 2003; Peintner et al. 2004; Garnica et al. 2005; Stefani et al. 2014; Garnica et al. 2016; Niskanen et al. 2016; Soop et al. 2019). Recently, according to the data of shallow whole genome sequencing and a five-locus analysis of 245 species, the genus *Cortinarius* was elevated to the Cortinariaceae rank, encompassing 10 genera, namely *Aureonarius* Niskanen & Liimat., *Austrocortinarius* Niskanen & Liimat., *Calonarius* Niskanen & Liimat., *Cortinarius*, *Cystinarius* Niskanen & Liimat., *Hygronarius* Niskanen & Liimat., *Mystinarius*

Niskanen & Liimat., *Phlegmacium* (Fr.) Wünsche, *Thaxterogaster* Singer and *Volvanarius* Niskanen & Liimat. (Liimatainen et al. 2022).

Cortinarius sect. *Delibuti* (Fr.) Sacc., typified by *C. delibutus* Fr., is widely distributed (Høiland and Holst-Jensen 2000; Peintner et al. 2004). Section *Delibuti* species possess a viscid to glutinous pileus and glutinous cylindrical to clavate stipe, a duplex pileipellis with a gelatinous layer, subglobose and moderately warty basidiospores, basidiome in shades of bluish, yellow, brown, or green, lilac-blue lamellae while brown in the mature stage and a ring zone usually on the upper part of the stipe (Peintner et al. 2004; Garnica et al. 2005; Soop et al. 2019). As a comparatively old lineage, sect. *Delibuti* used to be placed in the myxacioid group or subgenus *Myxacium* (Fr.) Trog (Singer 1986; Brandrud et al. 1990, 1992; Seidl 2000; Garnica et al. 2005). In other views, sect. *Delibuti* was also placed in phlegmacioid group or subg. *Phlegmacium*, including subsections *Delibuti* and *Anomali* (Antonio and Aguirre 2004; Peintner et al. 2004). Based on four- locus (nrITS, nrL-SU, *rpb1*, and *rpb2*) phylogenetic analysis, sect. *Delibuti* was placed within larger entity-Anomaloid sections, including sections *Anomali*, *Bolares*, *Delibuti*, *Spilomei* and *Subtorti* (Soop et al. 2019). More recently, sect. *Delibuti* was placed in *Cortinarius* subgen. *Camphorati* Liimat., Niskanen & Ammirati, encompassing sections *Anomali*, *Bolares*, *Lilacinocinerei* and *Subtorti* by Liimatainen et al. (2022).

The research on *Cortinarius* has mainly been conducted in Europe and North America, while it is still lacking in East Asia (Peintner et al. 2002; Garnica et al. 2003; Peintner et al. 2004; Garnica et al. 2005; Liimatainen et al. 2014; Stefani et al. 2014; Garnica et al. 2016; Niskanen et al. 2016; Soop et al. 2019, Liimatainen et al. 2022). To date, fewer than 30 species were originally reported from China, and only two new species in sect. *Delibuti* were originally found in China (Yang 1998; Wei and Yao 2013; Xie et al. 2019, 2020, 2021a, 2021b, 2022; Luo and Bau 2021, Zhang et al. 2023; Zhou et al. 2023). With the combination of morphological observations and phylogenetic analysis, we describe three species belonging to sect. *Delibuti* as new to science in this study.

Materials and methods

Specimens

The specimens were collected from central and southwestern China during 2012–2022. The vouchers are all deposited in the Mycological Herbarium of Hunan Normal University (MHHNU) and Cryptogamic Herbarium of Kunming Institute of Botany, Chinese Academy of Sciences (KUN-HKAS). Detailed information is listed in Table 1.

Morphological observation

The descriptions of macromorphological characters were based on field records and photographs. Color codes were used following Kornerup and Wanscher (1978). The size of basidiomes, as determined by pileus width, was described as small (< 5.0 cm), medium-sized (5.0–9.0 cm) or large (> 9.0 cm). Microscopic features were observed from dried specimens that were mounted with 5% aqueous KOH and stained with 1% Congo red solution under a light microscope (Motic Ltd., China). Melzer's reagent was used as an indicator of the

Table 1. List of sequences of *Cortinarius* used for phylogenetic analyses. The sequences newly generated in this study are in bold, and all type specimens are highlighted with an asterisk.

Species	Voucher	Locality	GenBank Accession No.		Reference
			ITS	**LSU**	
Cortinarius anomalus	TUB011883	Europe, Germany	AY669645	AY669645	Garnica et al. (2005)
C. anomalus *	CFP1154 (S)	Europe, Ångermanland	KX302224	–	Dima et al. (2016)
C. barlowensis *	JFA13140	North America	FJ717554	–	Harrower et al. (2011)
C. bolaris	T40	Europe, Norway	KC842426	KC842496	Stensrud et al. (2014)
C. bolaris *	CFP1008	Europe	KX302233	–	Dima et al. (2016)
C. bolaris	TUB0118524	Europe, Germany	AY669596	AY669596	Garnica et al. (2005)
C. calaisopus *	PDD 94050	New Zealand, Dunedin	NR157880	MH108373	Genbank
C. calaisopus	PDD103678/CO2106	New Zealand	KF727395	KF727338	Soop et al. (2019)
C. camphoratus	SMI193	North America, Canada	FJ039626	–	Harrower et al. (2011)
C. delibutus	F17048	North America, Canada	FJ717515	FJ717515	Harrower et al. (2011)
C. delibutus	SAT01-301-12	North America, USA	FJ717513	–	Harrower et al. (2011)
C. dysodes	PDD70499/CO1038 HT	New Zealand	GU233340	GU233394	Soop et al. (2019)
C. ferrusinus *	JB8106 13	Europe	KY657254	–	Genbank
**C. fibrillososalor* **	**MHHNU 32494**	**East Asia, China, Hunan**	**OR647481**	**OR647506**	**This study**
C. fibrillososalor	**MHHNU 33520**	**East Asia, China: Hunan**	**OR647485**	**OR647507**	**This study**
C. fibrillososalor	**MHHNU 33509**	**East Asia, China, Hunan**	**OR647483**	–	**This study**
C. fibrillososalor	**MHHNU 8657**	**East Asia, China, Hunan**	**OR647355**	**OR647497**	**This study**
C. fibrillososalor	**MHHNU 32070**	**East Asia, China, Hunan**	**OR660685**	**OR647503**	**This study**
C. illibatus	HMJAU48760	East Asia, China, Heilongjiang	MW911735	–	Xie et al. (2021a)
C. illibatus	OS574	Europe	KC842441	KC842511	Stensrud et al. (2014)
C. pseudocamphoratus *	HMJAU48694	East Asia, China, Xizang	NR_176776	–	Xie et al. (2022)
C. putorius	TN07411 HT	North America, USA	KR011124	–	Ariyawansa et al. (2015)
C. rotundisporus	PDD96298/ JAC12057	New Zealand	MH101550	MH108389	Soop et al. (2019)
C. rotundisporus	PERTH 05255074	Australia	AY669612	AY669612	Garnica et al. (2005)
C. salor	TUB011838	Europe, Germany	AY669592	AY669592	Garnica et al. (2005)
C. spilomeus *	S: CFP1137	Europe	KX302267	–	Dima et al. (2016)
C. spilomeus	TUB011523	Europe	AY669654	AY669654	Garnica et al. (2005)
C. pseudosalor	**MHHNU 8349**	**East Asia, China, Hunan**	**OR647352**	–	**This study**
**C. pseudosalor * **	**MHHNU 32082**	**East Asia, China, Hubiei**	**OR660686**	**OR647504**	**This study**
C. pseudosalor	**MHHNU 32148**	**East Asia, China, Hubiei**	**OR660688**	**OR647505**	**This study**
C. subsalor	HMJAU48758	East Asia, China, Zhejiang	MW911733	–	Xie et al. (2021a)
C. subsalor *	HMJAU48759	East Asia, China, Zhejiang	MW911734	–	Xie et al. (2021a)
C. subtortus	F16111	North America	FJ157044	FJ157044	Harrower et al. (2011)
C. subtortus	TUB011382	Europe	AY174857	AY174857	Garnica et al. (2003)
C. subtropicus	**MHHNU 31954**	**East Asia, China, Hunan**	**OR647356**	**OR647498**	**This study**
C. subtropicus	**KUN-HKAS 75760**	**East Asia, China, Guangxi**	**OR647491**	**OR647509**	**This study**
C. subtropicus	**MHHNU 31964**	**East Asia, China, Hunan**	**OR660684**	**OR647501**	**This study**
C. subtropicus	**MHHNU 31981**	**East Asia, China, Hunan**	**OR660687**	**OR647502**	**This study**
**C. subtropicus* **	**MHHNU 33533**	**East Asia, China, Hunan**	**OR647488**	**OR647508**	**This study**
C. tasmacamphoratus	HO A20606A0	Australia, Tasmania	AY669633	AY669633	Garnica et al. (2005)
C. tessiae	PDD107517/CO1450	New Zealand	MG019356	MG019356	Soop et al. (2019)
C. tessiae	PDD72611	New Zealand	HM060317	HM060316	Genbank
C. tetonensis *	JFA10350	North America	MZ580436	–	Dima et al. (2016)
C. tibeticisalor *	HMJAU48764	East Asia, China, Xizang	MW911730	–	Xie et al. (2021a)
C. tibeticisalor	HMJAU48762	East Asia, China: Xizang	MW911731	–	Xie et al. (2021a)
C. tibeticisalor	HMJAU48763	East Asia, China, Xizang	MW911732	–	Xie et al. (2021a)
C. viridipileatus	OTA61977	New Zealand	MK546592	MK546595	Nilsen et al. (2021)
C. viridipileatus	OTA64087	New Zealand	MK546593	MK546596	Nilsen et al. (2021)

amyloidity of basidiospores. In the description of basidiospores, the abbreviation [n/m/p] represents that the measurements were made on n basidiospores from m basidiomes of p collections. At least twenty matured basidiospores and basidia from each of the basidiomes were measured. The range (a)b−c(d) stands for the dimensions of basidiospores in which b−c contains a minimum of 90% of the measured values, while a and d indicate the extreme values. In addition, a Q value shows the ratio of length to width of basidiospores, and a Qm value shows the average Q ± standard deviation. A JSM-6380LV scanning electron microscope (JEOL Ltd., Tokyo, Japan) was used for the observation of ornamentations of basidiospores.

DNA extraction, PCR amplification and sequencing

Total genomic DNA was extracted by a Fungal DNA Mini Kit (Omega, USA). ITS 4 and ITS 5 (White et al. 1990), LROR and LR5/LR7 (Vilgalys and Hester 1990), were used for amplification of internal transcribed spacer (ITS), nuclear ribosomal large subunit (nrLSU), respectively. Each PCR mixture contained 1× PCR buffer, 1.5 mM MgCl2, 0.2 mM dNTPs, 0.4 µM of each primer, 1.25 U of Taq polymerase, and 1−2 µl DNA template in a total volume of 25 µl. PCRs were performed with an Eppendorf Mastercycler thermal cycler (Eppendorf Inc., Germany) as follows: initial denaturation at 94 °C for 4 min (ITS; nrLSU; *tef1-α*); followed by 30−35 cycles of 94 °C for 30 s (ITS; nrLSU), 54 °C for 30 s (ITS) or 55 °C for 1 min (nrLSU), and 72 °C for 30 s (ITS), 1 min (nrLSU); and a final extension at 72 °C for 7−10 min. Amplified PCR products were detected by gel electrophoresis on 2% agarose gels and then sent to Tsingke Biological Technology (China) for sequencing.

Phylogenetic analyses

The sequences newly generated in this study and downloaded from GenBank were used for phylogenetic analysis (Table 1). Alignment was performed by MAFFT v7.149b (Katoh and Standley 2013) and adjusted manually by MEGA5 (Tamura et al. 2011). SequenceMatrix 1.7.8 (Vaidya et al. 2011) was applied to generate multigene matrixes. GTR+I+G was selected as the best-fit model for combined matrix based on the Akaike Information Criterion (AIC) by MrModeltest 2.3 (Nylander 2004). Maximum likelihood (ML) analysis was performed using the W-IQ-TREE web service (http://iqtree.cibiv.univie.ac.at/) with 1000 ultrafast bootstrap replicates (Trifinopoulos et al. 2016). Bayesian inference (BI) was performed in MrBayes v3.2 (Ronquist et al. 2012). Four Metropolis-coupled Monte Carlo Markov chains were run for 5000000 generations, sampling every 1000th generation. Subsequently, the sampled trees were summarized after omitting the first 25% of trees as burn-in.

Results

Phylogenetic analyses

In the concatenated dataset (ITS+LSU), a total of 78 sequences (48 ITS, 30 LSU) from 48 samples were used for phylogenetic analyses among sect. *Delibuti*, sect. *Subtorti*, sect. *Camphorati*, sect. *Bolares*, sect. *Spilomei*, and sect. *Anomali*,
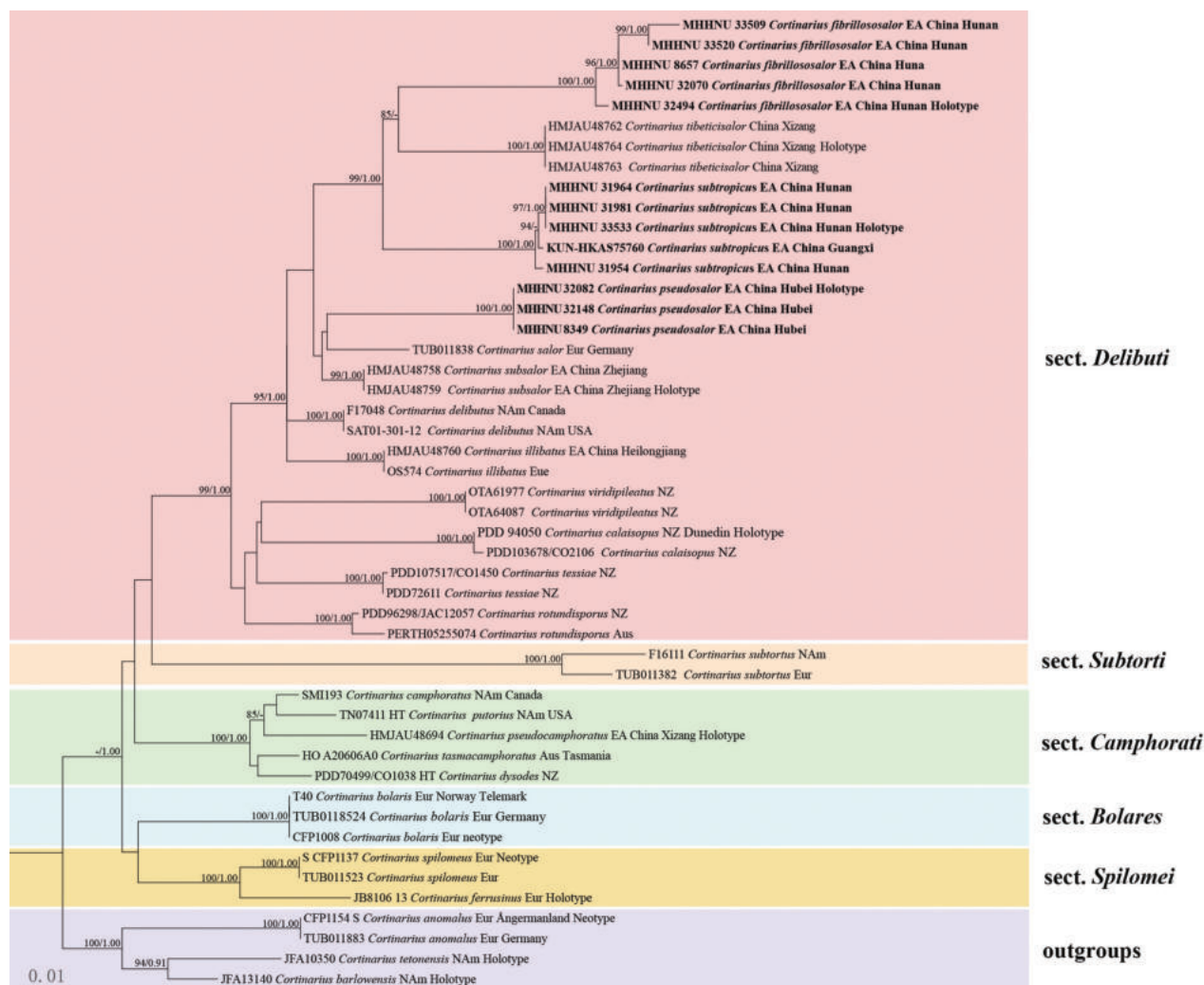
Figure 1. Phylogenetic tree of *Cortinarius* sect. *Delibuti* inferred from a combined matrix of ITS and LSU through maximum likelihood and Bayesian inference. Bayesian posterior probabilities (PP) > 0.90 and bootstrap values (BP) >85% are reported at the nodes (PP/BP); "−" indicates that the support value was less than the respective threshold. The three newly described species are highlighted in bold. Aus: Australia; EA: East Asia; Eur: Europe; NAm: North America; NZ: New Zealand.

of which 24 sequences (13 ITS, 11 LSU) were newly yielded in this study (Table 1). The estimates of tree topology inferred from ML and Bayesian analyses were extremely similar. The ML phylogenetic tree is shown with both bootstrap values (BP) and posterior probabilities (PP) annotated near the nodes (Fig. 1).

The phylogenetic relationship of sections within the genus *Cortinarius* in the present study was unclear and weakly supported. In the multi-locus tree, the monophyly of sect. *Delibuti* was supported with well-supported values (BP = 99%, PP = 1.00), including 12 species. Section *Camphorati* was also monophyletic with fully supported values (BP = 100%, PP = 1.00), emcompassing 5 species. In sect. *Delibuti*, *C. delibutus*, *C. illibatus*, *C. salor*, *C. subsalor*, *C. tibeticisalor*, and three novel species, namely *C. fibrillososalor*, *C. pseudosalor*, and *C. subtropicus*, formed a monophyletic lineage (BP = 95%, PP = 1.00). *Cortinarius fibrillososalor*, *C. subtropicus*, and *C. tibeticisalor* formed a clade only be found in East Asia (BP = 99%, PP = 1.00), while *C. tibeticisalor* has a special olive-green tint, was only distributed in Tibetan Plateau (Xie et al. 2021a). However, *C. pseudosalor*, *C. salor* and *C. subsalor* clustered with low support

values, leaving the position not determined. In addition, 13 specimens from *C. pseudosalor*, *C. fibrillososalor* and *C. subtropicus* collected in this study were fully supported (BP = 100%, PP = 1.00), and the phylogenetic relationships of *C. fibrillososalor*, *C. tibeticisalor* and *C. subtropicus* were clarified (BP = 100%, PP = 1.00).

Taxonomy

Cortinarius fibrillososalor P. Long & Z.H. Chen, sp. nov.
MycoBank No: 850393
Figs 2, 3

Etymology. *Fibrillososalor* (Latin) refers to the species morphologically similar to *Cortinarius salor*, but with fibrils on the pileus.

Figure 2. Basidiomes of *Cortinarius fibrillososalor* (**a, b** MHHNU 32494 **c, d** MHHNU 8657).
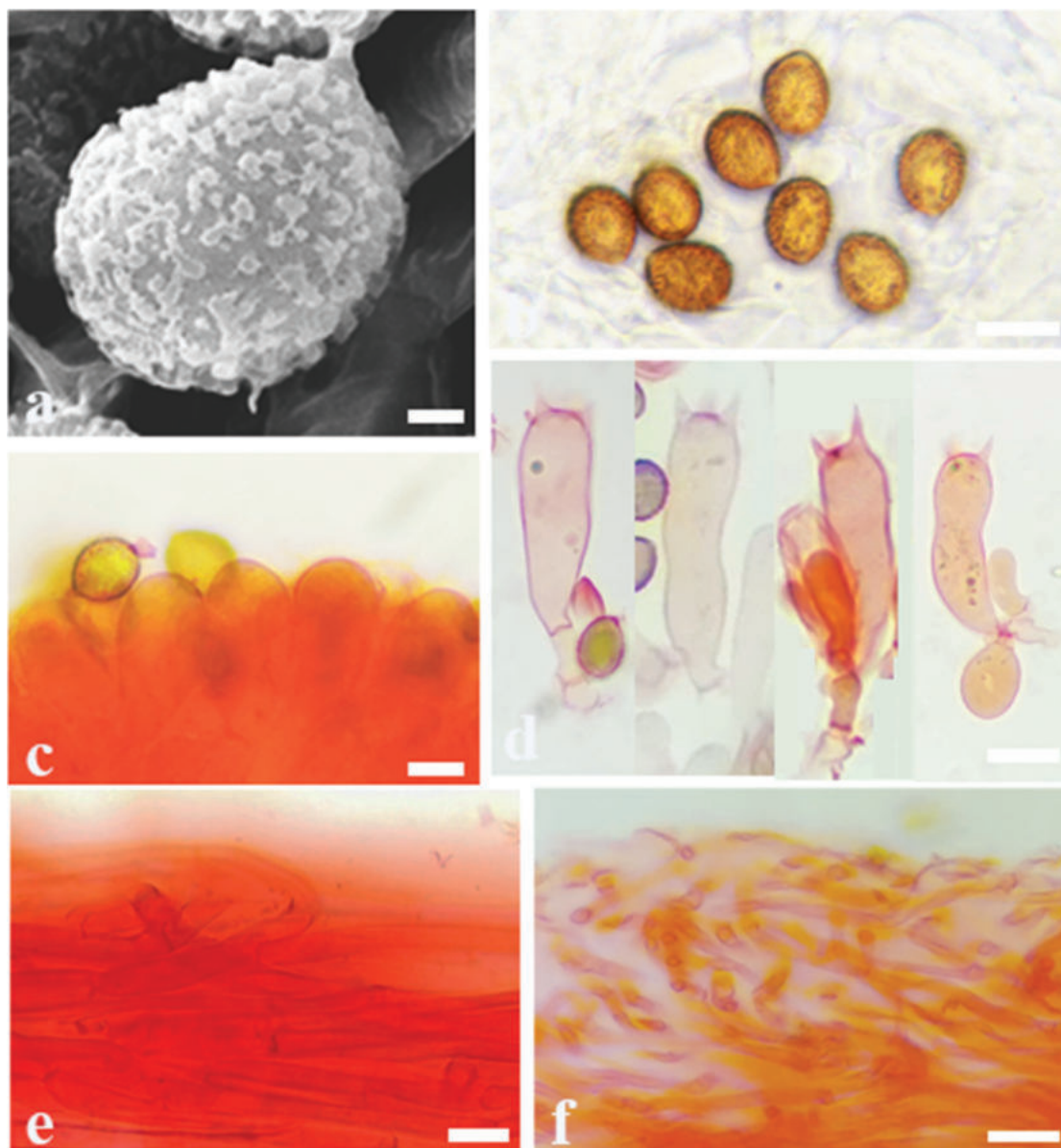
Figure 3. Microscopic features of *Cortinarius fibrillososalor* (MHHNU 32494) **a** scanning electron micrograph of basidiospore **b** basidiospores **c** lamellae edge **d** basidia with probasidium **e** stipitipellis **f** pileipellis; Scale bars: 1 μm (**a**); 10 μm (**b–e**); 20 μm (**f**).

Holotype. CHINA, Hunan Province: Sangzhi County, Badagongshan National Nature Reserve, at 29.782541°N, 110.084472°E, alt. 1424 m, 8 September 2020, Z.H. Chen, P. Long and S.N. Li, (MHHNU 32494).

Diagnosis. Differs from the other species of sect. *Delibuti* from its fibrillose pileus.

Description. Basidiomes small to medium-sized, telamonia-like, development type stipiocarpic. Pileus 2.9–5.2 cm, at first broadly convex, then lower convex to plane, broadly umbonate at the centre, margin incurved or decurved to upturned; at first violaceous (17B6–17B8), tinged brown (5B4–5C6) at the centre then becoming whitish mauve (16A1–16A2), finely fibrillose, with brown (5A5–5C7) universal veil remains at margin; surface silky when dry or glutinous when wet. Context thin, creamy white, soft, beige (3A1–A2) when bruised.

Lamellae adnate to adnexed, lilac (17A2–17B2) to brownish (6C5–6D7), moderately distant, sometimes margin wavy. Stipe cylindrical to clavate, bend, gradually slender to the apex, 3.4–5.9 cm long, 0.4–0.8 cm wide, violaceous (17A4–17B5) when young then fading to whitish mauve (16A2–16A3) tint, leaving an ochraceous (5B6–5D8) ringon the upper stem, hollow. Odour indistinct.

Basidiospores [100/5/5] (6.5–) 7.0–8.8 (–9.2) × (5.0–) 5.9–7.2 (–8.1) μm, av. 8.1 × 6.5 μm, Q = 1.14 (1.16) – 1.31 (1.45), Qm = 1.24 ± 0.02, broadly globose to long ellipsoid, rarely subglobose, yellowish brown, moderately verrucose, without amyloid and dextrinoid reaction. Basidia (27–) 28–35 × (8–) 9–11 μm, 4-spored, sterigmata up to 2.4–3.7 μm, clavate to subcylindrical, colourless or with amber yellow oily inclusions or granules. Pileipellis duplex, hyphae 4–8 μm wide, epicutis strongly gelatinous, 68–128 μm thick, composed of colourless or amber yellow, irregularly arranged and strongly interwoven hyphae, hypocuits 25–38 μm thick, composed of colourless or amber yellow, nearly parallel cylindrical hyphae. Lamellar edges fertile. Cystidia absent. Lamellar trama regular, 40–80 μm thick, composed of parallel arranged hyphae, hyphae 3–6 μm wide. Stipitipellis gelatinous, stipe hyphae 3–6 μm wide, thin-walled, cylindrical, interwoven. Clamp connections present in all tissues.

Habitat, ecology and distribution. Solitary to gregarious on soil in evergreen broad-leaved forest, known from Hunan, China; July to September.

Additional specimens examined. China, Hunan Province: Sangzhi County, Badagongshan National Nature Reserve, at 29.769154°N, 110.086577°E, alt. 1405 m, 31 July 2020, Z.H. Chen, P. Long and S.N. Li, (MHHNU 32070). China, Hunan Province: Sangzhi County, Badagongshan National Nature Reserve, at 29.769154°N, 110.477086°E, alt.1482 m, 28 July 2022, Z.H. Chen, J. Wen and Z.J. Jiang (MHHNU 33509, MHHNU 33520). China, Hunan Province: Sangzhi County, Badagongshan National Nature Reserve, at 29.404913°N, 109.491158°E, alt. 1500 m, 10 September 2015, P. Zhang, (MHHNU 8657).

Notes. *Cortinarius fibrillososalor* can be differentiated from other species of section *Deliduti* for its fibrillose pileus, usually under evergreen broad-leaved forest at 1405–1500m. In addition, basidiospores broadly globose to long ellipsoid, rarely subglobose while other members in this section usually subglobose to broadly ellipsoid.

Cortinarius pseudosalor P. Long & Z.H. Chen, sp. nov.
MycoBank No: 850392
Figs 4, 5

Etymology. *Pseudosalor* (Latin) refers to the species morphologically similar to *Cortinarius salor*.

Holotype. China, Hubei Province: Hefeng County, Mulinzi National Nature Reserve, at 30.058935°N, 110.209541°E, alt.1413 m, 1 August 2020, Z.H. Chen, P. Long and S.N. Li, (MHHNU 32082).

Diagnosis. This species differs from other species in sect. *Deliduti* for its high morphological similarity with *C. salor*, but having smaller coarsely verrucose basidiospores.

Description. Basidiomes small to medium-sized, development type stipiocarpic. Pileus 2.8–6.5 cm, at first broadly convex, then lower convex to plane, mar-

Figure 4. Basidiomes of *Cortinarius pseudosalor* (**a, b** MHHNU 32082 **c, d** MHHNU 8349).

gin incurved when young, decurved to upturned at maturity; bluish violaceous (18A3–18C5) when young, tinge of white at the centre when chapped, later fading to ochraceous grey (5B6–5C7) when old with brown (5B8–5C8) universal veil remains at margin; dry, viscid. Context dirty white, soft. Lamellae adnexed, pale yellow (1A2) with lilac tint (16A1–16A2) then brownish (5B6–5D7), moderately distant, sometimes margin wavy. Stipe clavate, gradually slender to the apex, 4–8.4 cm long, 0.4–1.0 cm wide, violaceous (16A2–16A4) when young then fading to upper dirty white, whitish mauve (16A2) at base, leaving an ochraceous ring (5B8–5C8) on the upper stem, hollow in centre. Odour indistinct.

Basidiospores [60/3/3] (7.3–) 7.4–8.4 × (5.7–) 6.0–7.4 (–7.5) μm, av. 7.9 × 6.7 μm, Q = (1.11) 1.12– (1.26) 1.27, Qm = 1.18 ± 0.11, subglobose to broadly ellipsoid, yellowish brown, coarsely verrucose, without amyloid and dextrinoid reaction. Basidia (29–) 30–38 × (8–) 9–12 μm, 4-spored, sterigmata up to 3.7–5.0 μm, clavate to subcylindrical, colourless or with amber yellow granules. Pileipellis duplex obviously, hyphae 2–6 μm wide, epicutis gelatinous, 50–75 μm
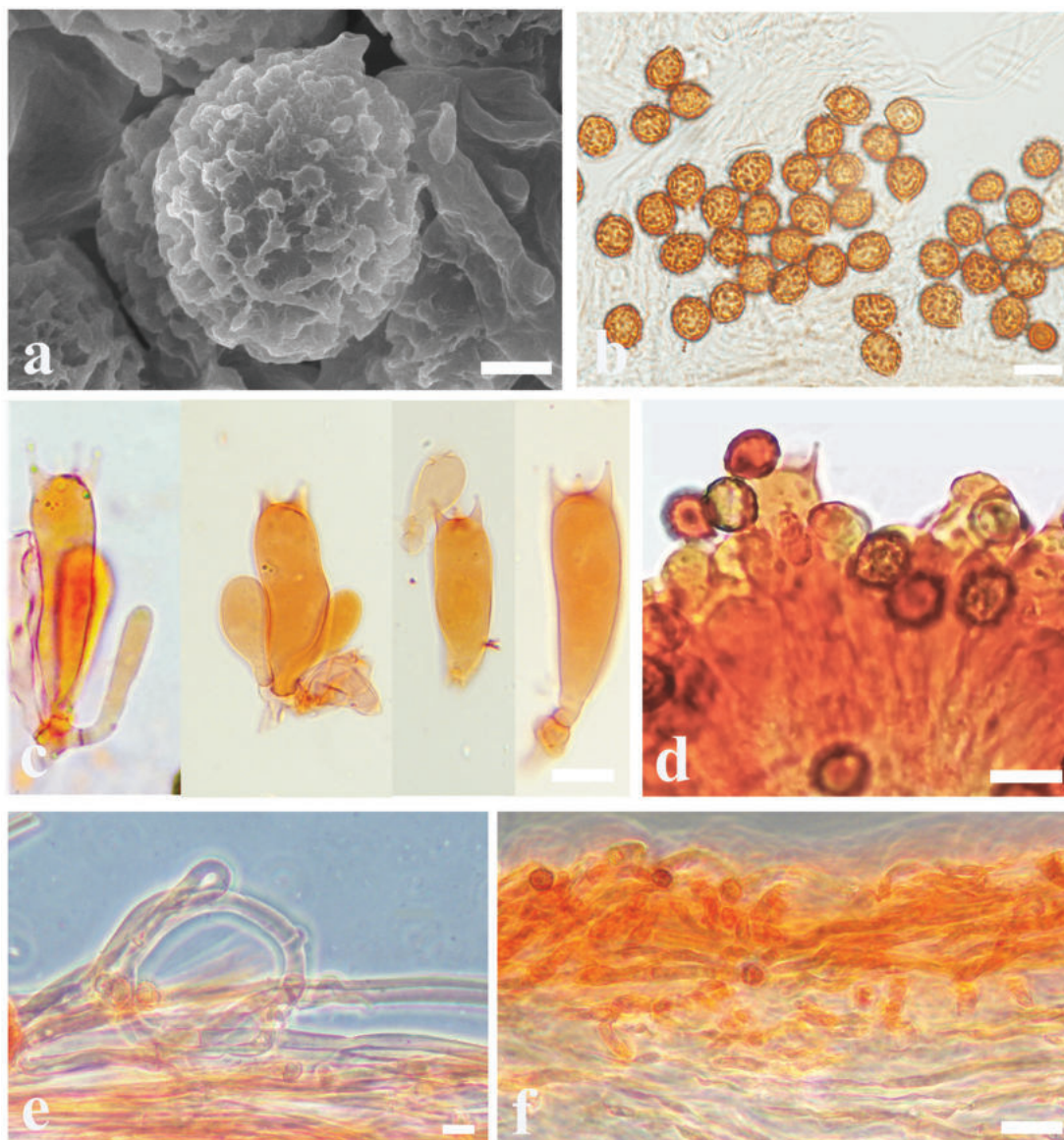
Figure 5. Microscopic features of *Cortinarius pseudosalor* (MHHNU 32082) **a** scanning electron micrograph of basidiospore **b** basidiospores **c** basidia with probasidium **d** lamellae edge **e** stipitipellis **f** pileipellis. Scale bars: 1 μm (**a**); 10 μm (**b–e**); 20 μm (**f**).

thick, composed of colourless or amber yellow, moderately interwoven hyphae, hypocuits 50–75 μm thick, composed of colourless or amber yellow, hyphae nearly parallel cylindrical. Lamellar edges fertile. Cystidia absent. Lamellar trama regular, 45–55 μm thick, composed of hyphae and inflated cells, hyphae 2–5 μm wide, inflated cells 14–24 × 5–9 μm. Stipitipellis gelatinous, stipe hyphae 2–7 μm wide, thin-walled, cylindrical, weakly interwoven. Clamp connections present in all tissues.

Habitat, ecology and distribution. Solitary to gregarious on soil in coniferous and broad-leaved mixed forest or evergreen broad-leaved forest, known from Hunan and Hubei, China; August.

Additional specimens examined. China, Hunan Province: Yongshun County, Xiaoxi National Nature Reserve, at 28.4215–28.5355°N, 110.650–110.2135°E,

alt. 1000–1300 m, 30 August 2014, P. Zhang, (MHHNU 8349); Hubei Province: Hefeng County, Xiaping Town, at 30.046382°N, 110.136712°E, alt. 1223 m, 2 August 2020, Z.H. Chen, P. Long and S.N. Li, (MHHNU 32148).

Notes. *Cortinarius pseudosalor* is easily misidentified as *C. salor* for their high morphological similarity, except the former has smaller coarsely verrucose basidiospores. Besides, *C. pseudosalor* distributed in Central China under coniferous and broad-leaved mixed forest or evergreen broad-leaved forest at alt. 1000–1413 m.

Cortinarius subtropicus P. Long & Z.H. Chen, sp. nov.

MycoBank No: 850394

Figs 6, 7

Etymology. *Subtropicus* (Latin) refers to subtropical distribution range of the species.

Holotype. CHINA, Hunan Province: Sangzhi County, Badagongshan National Nature Reserve, at 29.050057°N, 110.477119°E, alt. 1642 m, 29 July 2022, Z.H. Chen, J. Wen and Z.J. Jiang, (MHHNU 33533).

Diagnosis. Differs from the other species of sect. *Deliburi* species in having an epicutis pileipellis that can be easily separated from the context of the pileus.

Description. Basidiomes small, development type stipiocarpic. Pileus 2.1–4.6 cm, at first broadly convex, then lower convex to plane, broadly umbonate at the centre, margin incurved; at first violaceous (15A4–15B7), tinged brown (6A5–6C7) at the centre then becoming orange brown (5B2–5B6), brown (5A4–5B6) universal veil remains at margin; surface smooth when dry or glutinous when wet, pileipellis is easy to separate. Context thin, creamy white, soft, beige (3A1–A2) when bruised. Lamellae adnate, bluish violet (18A2–18B2) with pale greyish (18B1) to brownish (5A4–5B7), rust brown (5C7) when dry, moderately distant. Stipe cylindrical to weakly clavate, bend, gradually slender to the apex, 6.4–7.2 cm long, 0.5–1.0 cm wide, lilac (15A2–15B2) when young, dirty white at maturity, leaving an ochraceous (5D7) to orange (5B6) ring on the upper stem, hollow in centre, crumbly. Odour indistinct.

Basidiospores [120/6/6] (6.6–) 7.0–9.1 (–10.3) × (5.9–)6.1–7.9 (– 10.3) μm, av. 7.8 × 6.4 μm, Q = 1.10–1.38 (1.41), Qm = 1.24 ± 0.01, subglobose to ellipsoid, yellowish brown, moderately verrucose, without amyloid and dextrinoid reaction. Basidia 32–48 × 9–12 μm, 4-spored, sterigmata 2.8–4.9 μm, clavate to subcylindrical, colourless or with amber yellow oily inclusions. Pileipellis duplex, hyphae 4–8 μm wide, epicutis gelatinous, 30–40 μm thick, composed of colourless or amber yellow, irregularly arranged and moderately interwoven hyphae, hypocuits 130–200 μm thick, composed of colourless or amber yellow, nearly parallel cylindrical hyphae. Lamellar edges fertile. Cystidia absent. Lamellar trama regular, 40–80 μm thick, composed of parallel arranged hyphae, hyphae 3–6 μm wide. Stipitipellis gelatinous, stipe hyphae 3–6 μm wide, thin-walled, cylindrical, subparallel arranged. Clamp connections present in all tissues of the basidiome.

Habitat, ecology and distribution. Solitary to gregarious on soil in under evergreen broad-leaved forest, on the ground, known from Hunan, China; July.

Figure 6. Basidiomes of *Cortinarius subtropicus* (**a, b** MHHNU 33533 **c, d** MHHNU 31964).

Additional specimens examined. CHINA, Hunan Province: Sangzhi County, Badagongshan National Nature Reserve, at 29.683144°N, 109.754104°E, alt. 1645 m, 27 July 2020, Z.H. Chen, P. Long and S.N. Li, (MHHNU 31954). CHINA, Hunan Province: Sangzhi County, Badagongshan National Nature Reserve, at 29.6767°N, 109.750696°E, alt. 1625 m, 28 July 2020, Z.H. Chen, P. Long and S.N. Li, (MHHNU 31964). CHINA, Hunan Province: Sangzhi County, Badagongshan National Nature Reserve, at 29.676642°N, 109.750674°E, alt. 1625 m, 28 July 2020, Z.H. Chen, P. Long and S.N. Li, (MHHNU 31981). CHINA, Guangxi Province: Xingan County, Maoershan National Nature Reserve, alt. 1900 m, 24 July 2012, X.B. Liu, (KUN-HKAS 75760).

Notes. *Cortinarius subtropicus* has an epicutis pileipellis that can be easily separated from the context of the pileus. Besides, pileus become brown without lilac or dark olive tint at maturity comparing with other members of section *Delibuti*.
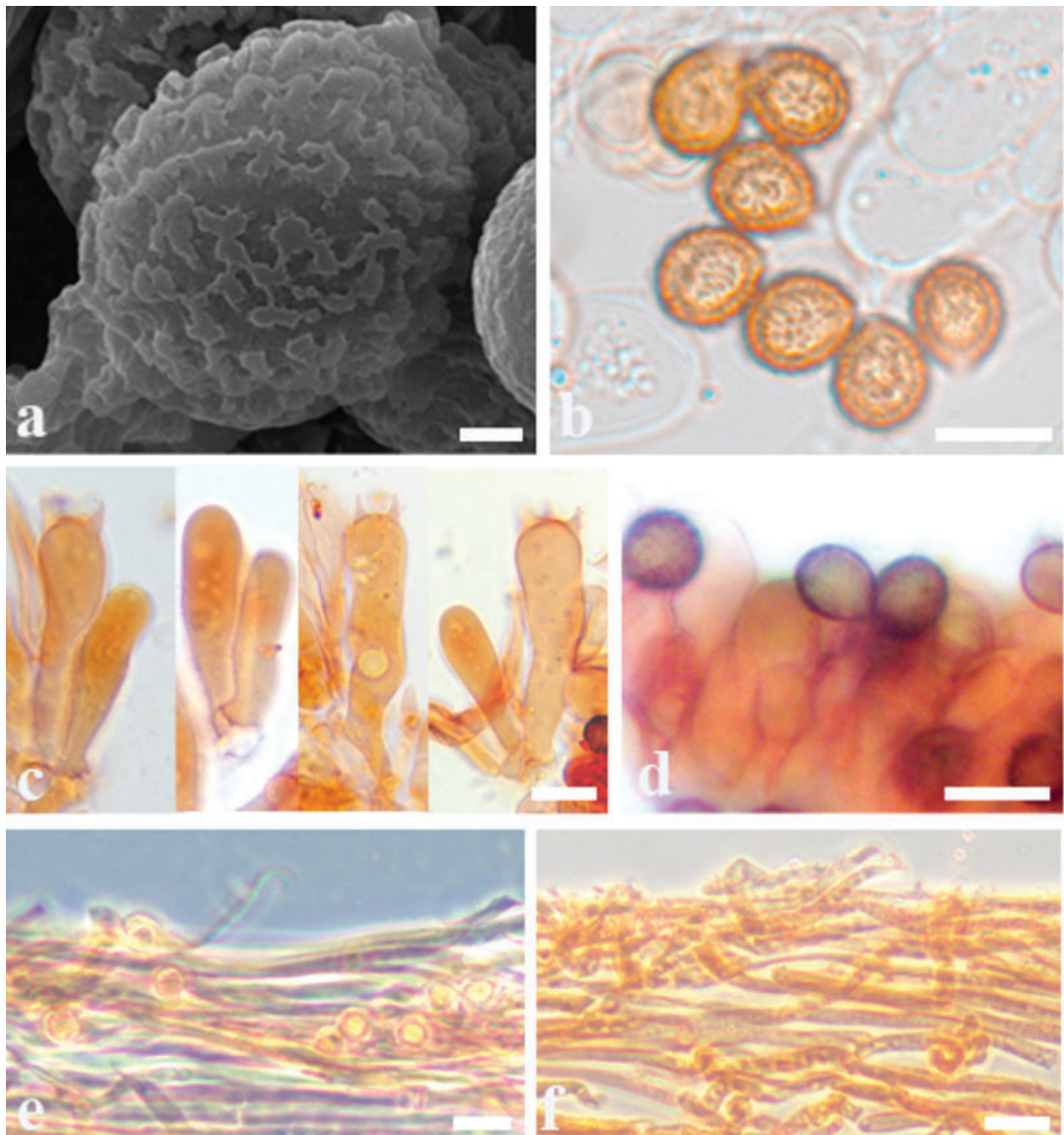
Figure 7. Microscopic features of *Cortinarius subtropicus* (MHHNU 33533) **a** scanning electron micrograph of basidiospores **b** basidiospores **c** basidia with probasidium **d** lamellae edge **e** stipitipellis **f** pileipellis. Scale bars: 1 µm (**a**); 10 µm (**b−e**); 20 µm (**f**).

A key to species of *Cortinarius* sect. *Delibuti*

1   Only distributed in the Northern Hemisphere **2**

−   Only distributed in the Southern Hemisphere or distributed both in Northern and Southern Hemisphere **12**

2   Pileus usually ochraceous yellow without bluish hue...................................**3**

−   Pileus usually bluish violet, sometimes yellow brown **4**

3   Lamellae usually bluish violet at first, veil yellow to pale brown ....
....***C. delibutus***

−   Lamellae pale ochraceous with tinge of pinkish violet, veil not yellowish.....
....***C. illibatus***

4   Distributed in Europe ± North America **5**

−   Distributed in China, East Asia..**8**

5   Growing under coniferous trees and broadleaved trees; pileus bluish violet ... **6**
–   Only growing under coniferous trees (*Abies* and *Picea*); pileus usually orange .... ***C. largodelibutus***
6   Basidiomes small to medium-sized, pileus deep bluish violet to ochraceous; Veil violet to ochraceous **7**
–   Basidiomes small, pileus yellow to olive-ochre at the centre, greyish blue to violet at margin then fading quickly; veil yellow ....***C. betulinus***
7   Pileus usually olive brown; growing under coniferous trees (*Picea*) and broadleaved trees (*Betula*) ....***C. transiens***
–   Pileus usually deep bluish violet; growing under broadleaved trees (*Quercus*, *Fagus*, *Corylus*) ....***C. salor***
8   Pileus usually dark olivaceous to brown at maturity; distributed in Tibetan Plateau of China ....***C. tibeticisalor***
–   Pileus usually ochraceous yellow at maturity; distributed in Central China ± Eastern China...**9**
9   Pileus with fibrils, basidiospores broadly globose to long ellipsoid, rarely subglobose ....***C. fibrillososalor***
–   Pileus without fibrils, basidiospores subglobose to broadly ellipsoid **10**
10   Basidiospores average length >8 µm...***C. subsalor***
–   Basidiospores average length <8 µm..**11**
11   Pileipellis is easy to separate; epicutis of pileipellis less than 40 µm thick, distributed from 1625 m to 1900 m ....***C. subtropicus***
–   Epicutis of pileipellis more than 50 µm thick, distributed from 1000 m to 1413 m ....***C. pseudosalor***
12   Growing under trees of *Nothofagus* **13**
–   Growing under trees of Myrtaceae..**15**
13   Pileus glutinous, greyish yellow to greyish orange, stipe violet, then becoming white to pale brownish, basidiospores ellipsoid, distributed in Northern and Southern Hemisphere ....***C. illitus***
–   Pileus viscid, with a green hue; basidiospores subglobose, distributed in Southern Hemisphere **14**
14   Pileus blue–green to aerugineous; stipe blue green; distributed in Australasia ....***C. tessiae***
–   Pileus dark green; stipe white with a purple hue; distributed in New Zealand...***C. viridipileatus***
15   Basidiomes distinctly viscid to glutinous, stipe viscid, mainly greyish blue-green...***C. rotundisporus***
–   Basidiomes weakly viscid, stipe often dry, mainly yellow-green to olive....... .... ***C. calaisopus***

Discussion

In this study, three species of *Cortinarius* sect. *Delibuti*, namely *C. fibrillososalor*, *C. pseudosalor*, and *C. subtropicus*, were described as new to science based on phylogenetic analyses and morphological characteristics. The phylogenetic relationships of *C. fibrillososalor* and *C. subtropicus* in *C.* sect. *Delibuti* were resolved with close phylogenetic relationship with *C. tibeticisalor*. However, the phylogenetic position of *C. pseudosalor* is still unclear as no supported sister relationship was revealed in the phylogenetic analysis.

Cortinarius fibrillososalor, *C. pseudosalor*, *C. salor*, *C. subsalor*, *C. subtropicus* and *C. tibeticisalor* have morphological homogeneity of the basidiomes. The macromorphological characters of *C. pseudosalor*, and *C. salor* are similar to basidiomes, coloured bluish violet, while *C. subsalor* is coloured purple to purplish red in pileus centre. Besides, *C. pseudosalor* has smaller coarsely verrucose basidiospores comparing *C. salor* and *C. subsalor* (Kibby and Tortelli 2021; Xie et al. 2021a). Meanwhile, *C. salor* is characterized by its lilaceous lamellae all the time and the narrow distribution in European woodlands, while *C. pseudosalor* and *C. subsalor* occurs in Asia (Xie et al. 2021a). *Cortinarius fibrillososalor* with violaceous to whitish mauve tint differ from other species in this section in the appearance of fibrils on the pileus and its broadly globose to long ellipsoid basidiospores (Kibby and Tortelli 2021; Xie et al. 2021a). *Cortinarius subtropicus* was found in the subtropical monsoon climate region of the Hunan and Guangxi provinces distributed from 1625 m to 1900 m. *Cortinarius tibeticisalor was* only distributed in Tibetan Plateau and was usually olivaceous to brown at maturity, while olivaceous species in sect. *Delibuti* mainly occurred in the South Pacific (Soop et al. 2019; Xie et al. 2021a).

Phylogenetic analysis was first applied to the taxonomic study of *Cortinarius* with ITS (Liu et al. 1997). Later, phylogenetic relationships were inferred mainly based on ITS, LSU sequences, and *rpb1*, *rpb2* were also confirmed to help elucidate the relationships of species in *Cortinarius* (Frøslev et al. 2005; Soop et al. 2019; Xie et al. 2022). Species delimitation could be justified by the combination of ITS and LSU sequences (Nilsen et al. 2021; Zhou et al. 2023), a two-locus dataset (ITS and LSU) was used for the research of three new species and their similar species in the present study. However, it needs more sequence data and DNA markers for recognising higher taxonomic rank such as subgenus or genus. In section rank, a two-locus dataset (ITS, LSU) and four-locus dataset (ITS, LSU, *rpb1* and *rpb2*) were first employed for phylogenetic analyses, and the latter provided a higher BP value and clearer tree structure, although with limited *rpb1* and *rpb2* (Soop et al. 2019). Besides, the first phylogenomic study based on shallow whole genome sequencing was conducted for Cortinariaceae revision (Liimatainen et al. 2022).

Acknowledgements

Additional information

Conflict of interest

The authors have declared that no competing interests exist.

Ethical statement

No ethical statement was reported.

Data availability

All of the data that support the findings of this study are available in the main text or Supplementary Information. The sequence data generated in this study are deposited in NCBI GenBank.

References

Antonio J, Aguirre C (2004) Fungi Non Delineati Vol. 29. Edizioni Candusso, Italy, 3.

Ariyawansa HA, Hyde KD, Jayasiri SC, Buyck B, Chethana KWT, Dai DQ, Dai YC, Daranagama DA, Jayawardena RS, Lücking R, Ghobad-Nejhad M, Niskanen T, Thambugala KM, Voigt K, Zhao RL, Li GJ, Doilom M, Boonmee S, Yang ZL, Cai Q, Cui YY, Bahkali AH, Chen J, Cui BK, Chen JJ, Dayarathne MC, Dissanayake AJ, Ekanayaka AH, Hashimoto A, Hongsanan S, Jones EBJ, Larsson E, Li WJ, Li QR, Liu JK, Luo ZL, Maharachchikumbura SSN, Mapook A, McKenzie EHC, Norphanphoun C, Konta S, Pang KL, Perera RH, Phookamsak R, Phukhamsakda C, Pinruan U, Randrianjohany E, Singtripop C, Tanaka K, Tian CM, Tibpromma S, Abdel-Wahab MA, Wanasinghe DN, Wijayawardene NN, Zhang JF, Zhang H, Abdel-Aziz FA, Wedin M, Westberg M, Ammirati JF, Bulgakov TS, Lima DX, Callaghan TM, Callac P, Chang CH, Coca LF, Dal-Forno M, Dollhofer V, Fliegerová K, Greiner K, Griffith GW, Ho HM, Hofstetter V, Jeewon R, Kang JC, Wen TC, Kirk PM, Kytövuori I, Lawrey JD, Xing J, Li H, Liu ZY, Liu XZ, Liimatainen K, Lumbsch HT, Matsumura M, Moncada B, Nuankaew S, Parnmen S, Santiago ALCMA, Sommai S, Song Y, Souza CAF, Souza-Motta CM, Su HY, Suetrong S, Wang Y, Wei SF, Wen TC, Yuan HS, Zhou LW, Réblová M, Fournier J, Camporesi E, Luangsa-ard JJ, Tasanathai K, Khonsanit A, Thanakitpipattana D, Somrithipol S, Diederich P, Millanes AM, Common RS, Stadler M, Yan JY, Li XH, Lee HW, Nguyen TTT, Lee HB, Battistin E, Marsico O, Vizzini A, Vila J, Ercole E, Eberhardt U, Simonini G, Wen HA, Chen XH, Miettinen O, Spirin V (2015) Fungal diversity notes 111–252-taxonomic and phylogenetic contributions to fungal taxa. Fungal Diversity 75(1): 27. https://doi.org/10.1007/s13225-015-0346-5

Bidaud A, Moënne-Loccoz P, Reumaux P (1994) Atlas des Cortinaires, Clé générale des sous-genres, sections, sous-sections et séries. Èditions Fèdération mycologique Dauphiné-Savoie, France, 121–198, 222–263.

Brandrud TE (1998) *Cortinarius* subgenus *Phlegmacium* section *Phlegmacioides* (= *Variecolores*) in Europe. Edinburgh Journal of Botany 55(1): 65–156. https://doi.org/10.1017/S0960428600004364

Brandrud TE, Lindstrom H, Marklund H, Melot J, Muskos S (1990) *Cortinarius* Flora Photographica I (English version). *Cortinarius* HB, Matfors, 60 pp.

Brandrud TE, Lindstrom H, Marklund H, Melot J, Muskos S (1992) *Cortinarius* Flora Photographica II (English version). *Cortinarius* HB, Matfors, 60 pp.

Dima B, Lindström H, Liimatainen K, Olson Å, Soop K, Kytövuori I, Dahlberg A, Niskanen T (2016) Typification of Friesian names in *Cortinarius* sections *Anomali*, *Spilomei*, and *Bolares*, and description of two new species from northern Europe. Mycological Progress 15(9): 903–919. https://doi.org/10.1007/s11557-016-1217-5

Dima B, Liimatainen K, Niskanen T, Bojantchev D, Harrower E, Papp V, Nagy LG, Kovács GM, Ammirati JF (2021) Type studies and fourteen new North American species of *Cortinarius* section *Anomali* reveal high continental species diversity. Mycological Progress 20(11): 1399–1439. https://doi.org/10.1007/s11557-021-01738-0

Frøslev TG, Matheny PB, Hibbett D (2005) Lower level relationships in the mushroom genus *Cortinarius* (Basidiomycota, Agaricales): A comparison of RBP1, RPB2 and ITS phylogenies. Molecular Phylogenetics and Evolution 37(2): 602–618. https://doi.org/10.1016/j.ympev.2005.06.016

Garnica S, Weiss M, Oberwinkler F (2003) Morphological and molecular phylogenetic studies in South American *Cortinarius* species. Mycological Research 107(10): 1143–1156. https://doi.org/10.1017/S0953756203008414

Garnica S, Weiß M, Oertel B, Oberwinkler F (2005) A framework for a phylogenetic classification in the genus *Cortinarius* (Basidiomycota, Agaricales) derived from morphological and molecular data. Canadian Journal of Botany 83(11): 1457–1477. https://doi.org/10.1139/b05-107

Garnica S, Schön ME, Abarenkov K, Riess K, Liimatainen K, Niskanen T, Dima B, Soop B, Frøslev TG, Jeppesen TS, Peintner U, Kuhnert-Finkernagel R, Brandrud TE, Saar G, Oerter B, Ammirati JF (2016) Determining threshold values for barcoding fungi: Lessons from *Cortinarius* (Basidiomycota), a highly diverse and widespread ectomycorrhizal genus. FEMS Microbiology Ecology 92(4): fiw045. https://doi.org/10.1093/femsec/fiw045

Harrower E, Ammirati JF, Cappuccino AA, Ceska O, Kranabetter JM, Kroeger P, Lim S, Taylor T, Berbee ML (2011) *Cortinarius* species diversity in British Columbia and molecular phylogenetic comparison with European specimen sequences. Botany 89(11): 799–810. https://doi.org/10.1139/b11-065

Høiland K, Holst-Jensen A (2000) *Cortinarius* phylogeny and possible taxonomic implications of ITS rDNA sequences. Mycologia 92(4): 694–710. https://doi.org/10.1080/00275514.2000.12061210

Katoh K, Standley DM (2013) MAFFT multiple sequence alignment software version 7: Improvements in performance and usability. Molecular Biology and Evolution 30(4): 772–780. https://doi.org/10.1093/molbev/mst010

Kibby G, Tortelli M (2021) The genus *Cortinarius* in Britain. privately published, Great Britain, 20–22.

Kornerup A, Wanscher JH (1978) Methuen handbook of colour, 3rd edn. Methuen, London, 252 pp.

Liimatainen K, Niskanen T, Dima B, Kytövuori I, Ammirati JF, Frøslev TG (2014) The largest type study of Agaricales species to date: Bringing identification and nomenclature of *Phlegmacium* (*Cortinarius*) into the DNA era. Persoonia 33(1): 98–140. https://doi.org/10.3767/003158514X684681

Liimatainen K, Kim JT, Pokorny L, Kirk PM, Dentinger B, Niskanen T (2022) Taming the beast: A revised classification of Cortinariaceae based on genomic data. Fungal Diversity 112(1): 89–170. https://doi.org/10.1007/s13225-022-00499-9

Liu Y, Rogers SO, Ammirati JF (1997) Phylogenetic relationships in *Dermocybe* and related *Cortinarius* taxa based on nuclear ribosomal DNA internal transcribed spacers. Canadian Journal of Botany 75(4): 519–532. https://doi.org/10.1139/b97-058

Luo Y, Bau T (2021) *Cortinarius jiaoheensis* (Cortinariaceae), a new species of *Cortinarius* subgenus *Telamonia* section *Flexipedes*, from northeast China. Phytotaxa 494(1): 113–121. https://doi.org/10.11646/phytotaxa.494.1.7

Moser M (1969) Uber einige kritische oder neue Cortinarien aus der untergattung Myxacium Fr. aus Smaland und Halland. Friesia 9: 142–150.

Moser M, Horak E (1975) Cortinarius Fr. und nahe verwandte Gattungen in Sudamerika. Beihefte zur Nova Hedwigia 52: 1–628.

Nilsen AR, Macrae OC, Andrew KM, Wang XY, Tana MCT, Soop K, Brown CM, Summerfield TC, Orlovich DA (2021) Studies of New Zealand *Cortinarius*: Resolution of taxonomic conflicts in section *Subcastanelli* (Agaricales), new species and key to rozitoid species. New Zealand Journal of Botany 59(4): 457–475. https://doi.org/10.1080/0028825X.2021.1879877

Niskanen T, Liimatainen K, Kytövuori I, Lindström H, Dentinger B, Ammirati JF (2016) *Cortinarius* subgenus *Callistei* in North America and Europe-type studies, diversity, and distribution of species. Mycologia 108(5): 1018–1027. https://doi.org/10.3852/16-033

Nylander JAA (2004) MrModeltest v2. Program distributed by the author. Evolutionary Biology Centre, Uppsala University.

Peintner U, Horak E, Moser MM, Vilgalys R (2002) Phylogeny of *Rozites*, *Cuphocybe* and *Rapacea* inferred from ITS and LSU rDNA sequences. Mycologia 94(4): 620–629. https://doi.org/10.1080/15572536.2003.11833190

Peintner U, Moncalvo JM, Vilgalys R (2004) Toward a better understanding of the infrageneric relationships in *Cortinarius* (Agaricales, Basidiomycota). Mycologia 96(5): 1042–1058. https://doi.org/10.1080/15572536.2005.11832904

Ronquist F, Teslenko M, van der Mark P, Ayres DL, Darling A, Höhn S, Larget B, Liu L, Suchard MA, Huelsenbeck JP (2012) MrBayes 3.2: Efficient Bayesian phylogenetic inference and model choice across a large model space. Systematic Biology 61(3): 539–542. https://doi.org/10.1093/sysbio/sys029

Seidl MT (2000) Phylogenetic relationships within *Cortinarius* subgenus *Myxacium*, sections *Defibulati* and *Myxacium*. Mycologia 92(6): 1091–1102. https://doi.org/10.1080/00275514.2000.12061257

Singer R (1986) The Agaricales in modern taxonomy 4th ed. Koenigstein, Koeltz Scientific Books, 981 pp.

Soop K, Dima B, Cooper JA, Park D, Oertel B (2019) A phylogenetic approach to a global supraspecific taxonomy of *Cortinarius* (Agaricales) with an emphasis on the southern mycota. Persoonia 42(1): 261–290. https://doi.org/10.3767/persoonia.2019.42.10

Stefani F, Jones RH, May TW (2014) Concordance of seven gene genealogies compared to phenotypic data reveals multiple cryptic species in Australian dermocyboid *Cortinarius* (Agaricales). Molecular Phylogenetics and Evolution 71: 249–260. https://doi.org/10.1016/j.ympev.2013.10.019

Stensrud Ø, Orr RJS, Reier-Røberg K, Schumacher T, Høiland K (2014) Phylogenetic relationships in *Cortinarius* with focus on North European species. Karstenia 54(2): 57–71. https://doi.org/10.29203/ka.2014.464

Tamura K, Peterson D, Peterson N, Stecher G, Nei M, Kumar S (2011) MEGA5: Molecular Evolutionary Genetic Analysis using Maximum Likelihood, Evolutionary Distance, and Maximum Parsimony Methods. Molecular Biology and Evolution 28(10): 2731–2739. https://doi.org/10.1093/molbev/msr121

Trifinopoulos J, Nguyen LT, von Haeseler A, Minh BQ (2016) W-IQTREE: A fast online phylogenetic tool for maximum likelihood analysis. Nucleic Acids Research 44(W1): 1–4. https://doi.org/10.1093/nar/gkw256

Vaidya G, Lohman DJ, Meier R (2011) Sequence matrix: Concatenation software for the fast assembly of multi-gene datasets with character set and codon information. Cladistics 27(2): 171–180. https://doi.org/10.1111/j.1096-0031.2010.00329.x

Vilgalys R, Hester M (1990) Rapid genetic identification and mapping of enzymatically amplified ribosomal DNA from several Cryptococcus species. Journal of Bacteriology 172(8): 4238–4246. https://doi.org/10.1128/jb.172.8.4238-4246.1990

Wei TZ, Yao YJ (2013) *Cortinarius korfii*, a new species from China. Junwu Xuebao 32(3): 557–562. https://doi.org/10.13346/j.mycosystema.2013.03.017

White TJ, Bruns T, Lee S, Taylor J (1990) Amplification and direct sequencing of fungal ribosomal RNA genes for phylogenetics. Academic Press, San Diego, 315–322. https://doi.org/10.1016/B978-0-12-372180-8.50042-1

Willis KJ (2018) State of the World's Fungi. Royal Botanic Gardens, Kew, London, 18–23.

Xie ML, Li D, Wei SL, Ji RQ, Li Y (2019) *Cortinarius subcaesiobrunneus* sp. nov., (Cortinariaceae, Agaricales) a new species from northwest China. Phytotaxa 392(3): 217–224. https://doi.org/10.11646/phytotaxa.392.3.4

Xie ML, Wei TZ, Fu YP, Li D, Qi L, Xing PJ, Cheng GH, Ji RQ, Li Y (2020) Three new species of *Cortinarius* subgenus *Telamonia* (Cortinariaceae, Agaricales) from China. MycoKeys 69: 91–109. https://doi.org/10.3897/mycokeys.69.49437

Xie ML, Chen JL, Phukhamsakda C, Dima B, Fu YP, Ji RQ, Wang K, Wei TZ, Li Y (2021a) *Cortinarius subsalor* and *C. tibeticisalor* spp. nov., two new species from the section *Deliburi* from China. PeerJ 9: e11982. https://doi.org/10.7717/peerj.11982

Xie ML, Wei TZ, Dima B, Fu YP, Ji RQ, Li Y (2021b) *Cortinarius khinganensis* (Agaricales), a new species of section *Illumini* from Northeast China. Phytotaxa 500(1): 1–10. https://doi.org/10.11646/phytotaxa.500.1.1

Xie ML, Phukhamsakda C, Wei TZ, Li JP, Wang K, Wang Y, Ji RQ, Li Y (2022) Morphological and phylogenetic evidence reveal five new *Telamonioid* species of *Cortinarius* (Agaricales) from East Asia. Journal of Fungi (Basel, Switzerland) 8(3): 257. https://doi.org/10.3390/jof8030257

Yang ZL (1998) Revision of the genera *Rozites* and *Descolea* from China. Fungal Science 13(3 & 4): 61–74. https://doi.org/10.7099/FS.199812.0061

Zhang QY, Jin C, Zhou HM, Ma ZY, Zhang YZ, Liang JQ, Si J, Li HJ (2023) Enlargement of the knowledge of *Cortinarius* section *Anomali* (Agaricales, Basidiomycota): Introducing three new species from China. Frontiers in Cellular and Infection Microbiology 13: 1–15. https://doi.org/10.3389/fcimb.2023.1215579

Zhou SY, Long P, Yang ZL (2023) Three new species and a new record of *Cortinarius* section *Camphorati* from southwestern China. Mycologia 115(6): 904–917. https://doi.org/10.1080/00275514.2023.2251365

Supplementary material 1

Multiple sequence alignment

Authors: Pan Long, Song-Yan Zhou, Sai-Nan Li, Fei-Fei Liu, Zuo-Hong Chen
Data type: fas
Link: https://doi.org/10.3897/mycokeys.101.114705.suppl1

Multigene phylogeny and morphology reveal three new species of *Cytospora* isolated from diseased plant branches in Fengtai District, Beijing, China

Aoli Jia[1,2], Baoyue Chen[3], Hongyan Lu[3], Yu Xing[3], Bin Li[3], Xinlei Fan[1,2]

1   *State Key Laboratory of Efficient Production of Forest Resources, Beijing Forestry University, Beijing 100083, China*
2   *Key Laboratory for Silviculture and Conservation of the Ministry of Education, Beijing Forestry University, Beijing 100083, China*
3   *Forestry Workstation, Fengtai District Bureau of Forestry and Parks of Beijing Municipality, Beijing 100055, China*
Corresponding author: Xinlei Fan (*xinleifan@bjfu.edu.cn*)

Abstract

Members of *Cytospora* include saprobes, endophytes and important plant pathogens, which are widely distributed on various wood hosts and have a wide global distribution. In this study, the species definitions were conducted, based on multigene phylogeny (ITS, *act*, *rpb2*, *tef1-α* and *tub2* genes) and comparisons of morphological characters. A total of 22 representative isolates obtained from 21 specimens in Fengtai District of Beijing City were identified as seven species of *Cytospora*, including four known species (*C. albodisca*, *C. ailanthicola*, *C. euonymina*, *C. haidianensis*) and three novel species (*C. fengtaiensis*, *C. pinea*, *C. sorbariae*). The results provide an understanding of the taxonomy of *Cytospora* species associated with canker and dieback diseases in Fengtai District, Beijing, China.

Key words: Canker disease, Diaporthales, pathogens, taxonomy

Introduction

The genus *Cytospora* was established by Ehrenberg (1818) and classified in Cytosporaceae, Diaporthales, Sordariomycetes (Wijayawardene et al. 2018; Fan et al. 2020). It includes numerous important pathogens associated with canker and dieback diseases of woody plants, with a worldwide distribution and broad host range (Sinclair et al. 1987; Adams et al. 2005, 2006; Lawrence et al. 2018; Fan et al. 2020; Lin et al. 2023a, b). Dieback and stem canker caused by *Cytospora* lead to the growth weakness or death of host plants, thereby causing significant economic and ecological losses (Sinclair et al. 1987; Adams et al. 2005). Currently, 695 species epithets of *Cytospora* have been listed in Index Fungorum (www.indexfungorum.org; accessed on 24 November 2023).

The taxonomy and correspondence between sexual and asexual morphs of *Cytospora* is quite confusing. Previous *Cytospora* species and their related sexual morphs viz. *Leucostoma*, *Valsa*, *Valsella* and *Valseutypella* were listed by old fungal literature for their identification (Fries 1823; Saccardo 1884; Kobayashi 1970; Barr 1978; Sutton 1980; Gvritishvili 1982; Spielman 1983, 1985). Adams

et al. (2005) revised the genus *Cytospora* from *Eucalyptus* with 28 species and accepted all sexual genera combined under *Valsa*, either as subgenera or species without additional infrageneric rank, regarding the sexual genera (*Leucocytospora*, *Leucostoma*, *Valsella* and *Valseutypella*) as synonyms of *Valsa*. Based on the one fungus = one name initiative (Wingfield et al. 2012), Fan et al. (2015a, b) and Rossman et al. (2015) recommended to use *Cytospora*, the oldest name having priority over *Valsa*.

Cytospora canker symptoms initially appear on trunks and branches as slightly sunken bark with brown discolouration of the xylem, which may result in trunk and branch cracking (Adams et al. 2005). The asexual morph of *Cytospora* is characterised by the pycnidial stromata submerged in cortex with single or multiple locule(s), with or without conceptacle, filamentous conidiophores producing hyaline, allantoid, eguttulate and smooth conidia. The sexual morph is characterised by the ascomata submerged in the substrate with an erumpent pseudostroma, with or without necks. Asci are unitunicate, clavate to cylindrical with four or eight ascospores which are biseriate or multi-seriate, elongate-allantoid, thin-walled, hyaline and aseptate (Spielman 1983, 1985; Adams et al. 2005).

Currently, use of polyphasic approaches, such as morphological and phylogenetic analyses to define species of *Cytospora* has been proposed (Norphanphoun et al. 2017; Fan et al. 2020). In morphology, presence or absence of conceptacle, quantity and arrangement of locule(s), shape and size of conidiophores and conidial size are significantly taxonomic. In phylogeny, the current studies use the internal transcribed spacer (ITS), the partial actin (*act*), the RNA polymerase II subunit (*rpb2*), the translation elongation factor *1-α* (*tef1-α*) and the beta-tubulin (*tub2*) genes to perform phylogenetic analysis.

Beijing is the capital city of China, located in the northern part of the North China Plain with more than 1,000 species of tree hosts (Liu et al. 2022). As more plant species were recorded in this city, the exploration of fungal diversity gradually increased as most fungi are often linked to particular host plants as pathogens or endophytes. With the modern taxonomic approaches applying, more than 30 *Cytospora* species have been reported in the last five years in Beijing (Fan et al. 2020; Pan et al. 2021; Lin et al. 2023a, b). Fengtai is one of the districts in Beijing with high forest cover and rich tree species which is located in the south-western suburbs of Beijing. However, there are few studies associated with fungal diversity in Fengtai District. A research to explore more hidden species of *Cytospora* in this region is considered imperative. Therefore, a survey on the diversity of *Cytospora* on diseased branches was conducted in Fengtai District from 2022 to 2023. The objectives of this study were to summarise the systematic study of *Cytospora* species in Fengtai District and to clarify the systematics and taxonomy of *Cytospora* species with detailed descriptions and illustrations and compare it to known species in the genus.

Materials and methods

Sample collection and isolation

Twenty-one fresh specimens with typical conidiomata and/or ascomata were collected from diseased branches or twigs of wood hosts which are distributed

in Beigong National Forest Park, Century Forest Park, Garden Expo Park, Lotus Pond Park and Qianling Mountain in Fengtai District, Beijing City. Sampled trees expressed general symptoms and signs of canker diseases including elongate, slightly sunken and discoloured areas in the bark, several prominent dark conidiomata and/or ascomata immersed in bark, erumpent through the surface of bark when mature (Fig. 1). A total of 22 isolates were obtained by removing a mucoid spore mass from conidiomata and/or ascomata, spreading the suspension on the surface of 1.8% potato dextrose agar (PDA) (potato, 200 g; glucose, 20 g; agar, 20 g; distilled water, to complete 1000 ml) media in a Petri dish and incubating at 25 °C for up to 24 h. Hyphal tips were removed to a new PDA plate twice to obtain a pure culture. Specimens were deposited in the Museum of Beijing Forestry University (BJFC) and at the working Collection of X.L. Fan (CF), housed at the BJFU. Axenic cultures are maintained in the China Forestry Culture Collection Centre (CFCC).

Morphological analyses

The identification of species was based on morphological characteristics of the ascomata or conidiomata formed on infected host materials. Macro-morphological features (structure and size of conidiomata and ascomata, ectostromatic disc and ostioles) were photographed using a Leica stereomicroscope (M205 FA) (Leica Microsystems, Wetzlar, Germany). Micromorphological features (conidiophores, conidiogenous cells, asci and conidia/ascospores) were photographed using a Nikon Eclipse 80i microscope (Nikon Corporation, Tokyo, Japan), equipped with a Nikon digital sight DS-Ri2 high resolution colour camera with differential interference contrast. Over 30 conidiomata were sectioned and 50 conidia were selected randomly to measure their lengths and widths. Colony diameters were measured and the colony colours described after 3 days and 14 days according to the colour charts of Rayner (1970).

DNA extraction, PCR amplification and sequencing

Mycelium used for DNA extraction was grown on PDA for three days and obtained from the cellophane surface by scraping. The genomic DNA was extracted using the modified CTAB method (Doyle and Doyle 1990). PCR amplifications and sequencing of five genes (ITS, *act*, *rpb2*, *tef1-α* and *tub2*) were performed. The primers and PCR conditions are listed in Table 1. PCR products were electrophoresed in 1% agarose gel and the DNA was sequenced by the Sino Geno Max Biotechnology Company Limited (Beijing, China). DNA sequences generated by the forward and reverse primers combination were used to obtain consensus sequences using Seqman v. 7.1.0 (DNASTAR Inc., Madison, WI, USA).

Phylogenetic analyses

The phylogenetic analyses were performed, based on the individual datasets of each gene region and combined five genes (ITS, *act*, *rpb2*, *tef1-α* and *tub2*) to compare *Cytospora* species from the current study with other sequences ob-
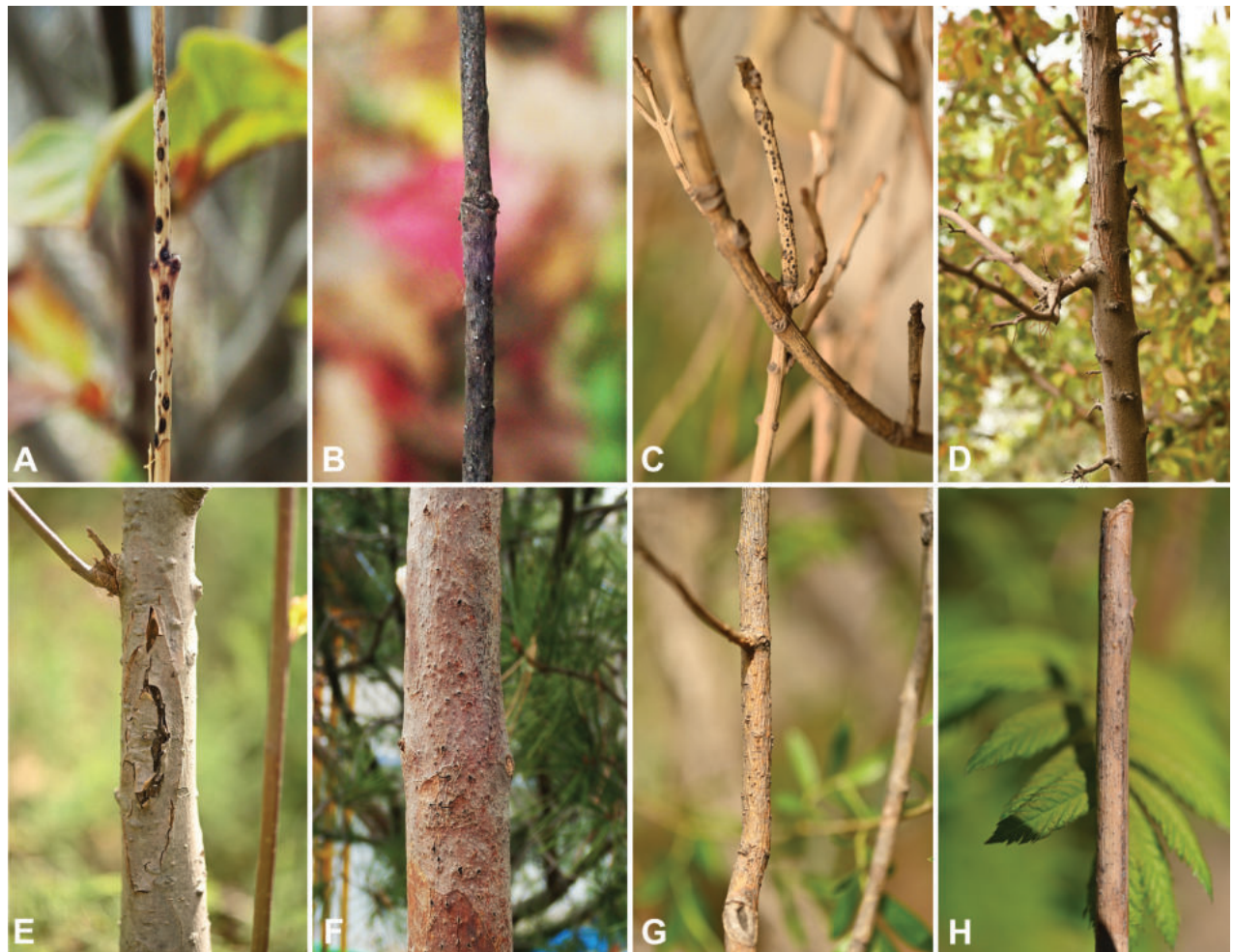
Figure 1. Disease symptoms associated with *Cytospora* species collected from Fengtai District, Beijing, China **A** *Acer palmatum* 'Atropurpureum' **B** *Acer pictum* subsp. *Mono.* **C** *Euonymus japonicus* **D** *Malus* 'American' **E** *Malus × micromalus* **F** *Pinus bungeanae* **G** *Salix babylonica* **H** *Sorbaria sorbifolia*.

tained from GenBank. The sequence datasets used in this study were based on Lin et al. (2023b). Sequence alignments of the individual gene were performed in MAFFT v. 6 (Katoh and Standley 2013) and adjusted by MEGA v. 6.0 (Tamura et al. 2013). Ambiguous regions were excluded from alignments. Phylogenetic analyses were conducted using the programme PhyML v. 3.0 (Guindon et al. 2010) for Maximum Likelihood (ML) analysis and MrBayes v. 3.1.2 (Ronquist and Huelsenbeck 2003) for Bayesian Inference (BI) analysis. For ML analysis, the substitution model (GTR+G+I model) for each dataset was selected following recent studies (Fan et al. 2020; Pan et al. 2020, 2021). Confidence levels for the nodes were determined using 1,000 replicates of bootstrapping methods (Hillis and Bull 1993). For BI analysis, the best-fit evolutionary models for each partitioned locus were estimated in MrModelTest v. 2.3 (Posada and Crandall 1998) with a Markov Chain Monte Carlo algorithm. Phylograms were plotted in FigTree v. 1.4.3 (http://tree.bio.ed.ac.uk/software/figtree) and edited in Adobe Illustrator CS6 v.16.0.0 (https://www.adobe.com/cn/products/illustrator.html). Sequence data were submitted to GenBank (https://www.ncbi.nlm.nih.gov) (Table 2). The multigene sequence alignments and the trees obtained were deposited in TreeBASE (https://treebase.org; study ID S30958).

Table 1. Genes used in this study with PCR primers, primer DNA sequence, optimal annealing temperature and corresponding references.

Locus	PCR primers	PCR: thermal cycles: (Annealing temp. in bold)	References of primers used
ITS	ITS1	(95 °C: 30 s, 51 °C: 30 s, 72 °C: 1min) × 35 cycles	White et al. (1990)
	ITS4		
act	ACT-512F	(95 °C: 45 s, 55 °C: 45 s, 72 °C: 1min) × 35 cycles	Carbone and Kohn (1999)
	ACT-783R		
rpb2	RPB2-5F	(95 °C: 30 s, 52 °C: 1 min, 72 °C:1 min) × 35 cycles	Liu et al. (1999)
	RPB2-7cR		
tef1-α	728F	(95 °C: 15 s, 55 °C: 20 s, 72 °C: 1min) × 35 cycles	Rehner et al. (2005)
	1567R		
tub2	T1	(95 °C: 30 s, 55 °C: 30 s, 72 °C: 1min) × 35 cycles	Glass and Donaldson (1995)
	Bt2b		

Table 2. Strains of *Cytospora* used in the molecular analyses in this study.

Species	Strain	Host	Origin	GenBank accession numbers				
				ITS	*act*	*rpb2*	*tef1-α*	*tub2*
Cytospora ailanthicola	CFCC 89970	*Ailanthus altissima*	Ningxia, China	MH933618	MH933526	MH933592	MH933494	MH933565
Cytospora ailanthicola	**CFCC 59446**	**Salix matsudana**	**Beijing, China**	**OR826163**	**OR831996**	**OR832018**	**OR832040**	**OR832062**
Cytospora albodisca	CFCC 53161	*Platycladus orientalis*	Beijing, China	MW418406	MW422899	MW422909	MW422921	MW422933
Cytospora albodisca	CFCC 54373	*Platycladus orientalis*	Beijing, China	MW418407	MW422900	MW422910	MW422922	MW422934
Cytospora albodisca	**CFCC 59467**	**Malus × micromalus**	**Beijing, China**	**OR826179**	**OR832012**	**OR832034**	**OR832056**	**OR832076**
Cytospora albodisca	**CFCC 59537**	**Euonymus japonicus**	**Beijing, China**	**OR826180**	**OR832013**	**OR832035**	**OR832057**	**OR832077**
Cytospora alba	CFCC 55462^T	*Salix matsudana*	Gansu, China	MZ702593	OK303457	OK303516	OK303577	OK303644
Cytospora alba	CFCC 55463^T	*Salix matsudana*	Gansu, China	MZ702594	OK303458	OK303517	OK303578	OK303645
Cytospora ampulliformis	MFLUCC 16-0583^T	*Sorbus intermedia*	Russia	KY417726	KY417692	KY417794	NA	NA
Cytospora ampulliformis	MFLUCC 16-0629	*Acer platanoides*	Russia	KY417727	KY417693	KY417795	NA	NA
Cytospora amydgali	CBS 144233^T	*Prunus dulcis*	California, USA	MG971853	MG972002	NA	MG971659	MG971718
Cytospora atrocirrhata	CFCC 89615	*Juglans regia*	Qinghai, China	KR045618	KF498673	KU710946	KP310858	KR045659
Cytospora atrocirrhata	CFCC 89616	*Juglans regia*	Qinghai, China	KR045619	KF498674	KU710947	KP310859	KR045660
Cytospora atrocirrhata	CXY 1401	*Populus* sp.	Inner Mongolia, China	JX534242	NA	NA	NA	KM034904
Cytospora atrocirrhata	CXY 1402	*Populus* sp.	Inner Mongolia, China	JX534243	NA	NA	NA	KM034903
Cytospora avicennae	IRAN 4199C^T	*Malus domestica*	Nahavand, Iran	MW295650	MZ014511	MW824358	MW394145	NA
Cytospora avicennae	IRAN 4625C	*Malus domestica*	Arak, Iran	OM368648	NA	NA	OM372510	NA
Cytospora azerbaijanica	IRAN 4201C^T	*Malus domestica*	Urmia, Iran	MW295526	MZ014513	MW824360	MW394147	NA
Cytospora azerbaijanica	IRAN 4627C	*Malus domestica*	Miandoab, Iran	OM368650	NA	NA	OM372512	NA
Cytospora beilinensis	CFCC 50493^T	*Pinus armandii*	Beijing, China	MH933619	MH933527	NA	MH933495	MH933561
Cytospora beilinensis	CFCC 50494	*Pinus armandii*	Beijing, China	MH933620	MH933528	NA	MH933496	MH933562
Cytospora berberidis	CFCC 89927^T	*Berberis dasystachya*	Qinghai, China	KR045620	KU710990	KU710948	KU710913	KR045661
Cytospora berberidis	CFCC 89933	*Berberis dasystachya*	Qinghai, China	KR045621	KU710991	KU710949	KU710914	KR045662
Cytospora bungeanae	CFCC 50495^T	*Pinus bungeanae*	Shanxi, China	MH933621	MH933529	MH933593	MH933497	MH933563
Cytospora bungeanae	CFCC 50496	*Pinus bungeanae*	Shanxi, China	MH933622	MH933530	MH933594	MH933498	MH933564
Cytospora calamicola	MFLUCC 15-0397	*Calamus*	Thailand	NR_185736	NA	NA	ON734013	NA
Cytospora californica	CBS 144234^T	*Juglans regia*	California, USA	MG971935	MG972083	NA	MG971645	NA
Cytospora carbonacea	CFCC 89947	*Ulmus pumila*	Qinghai, China	KR045622	KP310842	KU710950	KP310855	KP310825
Cytospora carpobroti	CMW 48981^T	*Carpobrotus edulis*	South Africa	MH382812	NA	NA	MH411212	MH411207
Cytospora celtidicola	CFCC 50497^T	*Celtis sinensis*	Anhui, China	MH933623	MH933531	MH933595	MH933499	MH933566
Cytospora celtidicola	CFCC 50498	*Celtis sinensis*	Anhui, China	MH933624	MH933532	MH933596	MH933500	MH933567

Species	Strain	Host	Origin	GenBank accession numbers				
				ITS	*act*	*rpb2*	*tef1-α*	*tub2*
Cytospora centrivillosa	MFLUCC 16-1206[T]	*Sorbus domestica*	Italy	MF190122	NA	MF377600	NA	NA
Cytospora centrivillosa	MFLUCC 17-1660	*Sorbus domestica*	Italy	MF190123	NA	MF377601	NA	NA
Cytospora ceratosperma	CFCC 89624	*Juglans regia*	Gansu, China	KR045645	NA	KU710976	KP310860	KR045686
Cytospora ceratosperma	CFCC 89625	*Juglans regia*	Gansu, China	KR045646	NA	KU710977	KP31086	KR045687
Cytospora ceratospermopsis	CFCC 89626[T]	*Juglans regia*	Shaanxi, China	KR045647	KU711011	KU710978	KU710934	KR045688
Cytospora ceratospermopsis	CFCC 89627	*Juglans regia*	Shaanxi, China	KR045648	KU711012	KU710979	KU710935	KR045689
Cytospora chrysosperma	CFCC 89629	*Salix psammophila*	Shaanxi, China	KF765673	NA	KF765705	NA	NA
Cytospora chrysosperma	CFCC 89981	*Populus alba* subsp. *pyramidalis*	Gansu, China	MH933625	MH933533	MH933597	MH933501	MH933568
Cytospora chrysosperma	CFCC 89982	*Ulmus pumila*	Tibet, China	KP281261	KP310835	NA	KP310848	KP310818
Cytospora cinnamomea	CFCC 53178[T]	*Prunus armeniaca*	Xinjiang, China	MK673054	MK673024	NA	NA	MK672970
Cytospora coryli	CFCC 53162[T]	*Corylus mandshurica*	Beijing, China	MN854450	NA	MN850751	MN850758	MN861120
Cytospora corylina	CFCC 54684[T]	*Corylus heterophylla*	Beijing, China	MW839861	MW815951	MW815937	MW815886	MW883969
Cytospora corylina	CFCC 54685	*Corylus heterophylla*	Beijing, China	MW839862	MW815952	MW815938	MW815887	MW883970
Cytospora corylina	CFCC 54686	*Corylus heterophylla*	Beijing, China	MW839863	MW815953	MW815939	MW815888	MW883971
Cytospora corylina	CFCC 54687	*Corylus heterophylla*	Beijing, China	MW839864	MW815954	MW815940	MW815889	MW883972
Cytospora cotini	MFLUCC 14-1050[T]	*Cotinus coggygria*	Russia	KX430142	NA	KX430144	NA	NA
Cytospora cotoneastricola	CF 20197027	*Cotoneaster* sp.	Tibet, China	MK673072	MK673042	MK673012	MK672958	MK672988
Cytospora cotoneastricola	CF 20197028	*Cotoneaster* sp.	Tibet, China	MK673073	MK673043	MK673013	MK672959	MK672989
Cytospora cotoneastricola	CF 20197030	*Cotoneaster* sp.	Tibet, China	MK673074	MK673044	MK673014	MK672960	MK672990
Cytospora cotoneastricola	CF 20197031[T]	*Cotoneaster* sp.	Tibet, China	MK673075	MK673045	MK673015	MK672961	MK672991
Cytospora curvata	MFLUCC 15-0865[T]	*Salix alba*	Russia	KY417728	KY417694	KY417796	NA	NA
Cytospora curvispora	CFCC 54000[T]	*Corylus heterophylla*	Beijing, China	MW839851	MW815931	MW815945	MW815880	MW883963
Cytospora curvispora	CFCC 54001	*Corylus heterophylla*	Beijing, China	MW839853	MW815932	MW815946	MW815881	MW883964
Cytospora curvispora	CFCC 54676	*Corylus heterophylla*	Beijing, China	MW839854	MW815933	MW815947	MW815882	MW883965
Cytospora curvispora	CFCC 54677	*Corylus heterophylla*	Beijing, China	MW839855	MW815934	MW815948	MW815883	MW883966
Cytospora curvispora	CFCC 54678	*Corylus heterophylla*	Beijing, China	MW839856	MW815935	MW815949	MW815884	MW883967
Cytospora curvispora	CFCC 54679	*Corylus heterophylla*	Beijing, China	MW839857	MW815936	MW815950	MW815885	MW883968
Cytospora davidiana	CXY 1350[T]	*Populus davidiana*	Inner Mongolia, China	KM034870	NA	NA	NA	NA
Cytospora diopuiensis	MFLUCC 18-1419[T]	Undefined wood	Chiang Mai, Thailand	MK912137	MN685819	NA	NA	NA
Cytospora diopuiensis	CFCC55884	*Kerria japonica* f. *pleniflora*	Beijing, China	OK316819	NA	OK358569	OK358471	OK358473
Cytospora diopuiensis	CFCC55885	*Kerria japonica* f. *pleniflora*	Beijing, China	OK316820	NA	OK358570	OK358472	OK358474
Cytospora diopuiensis	CFCC 56961	*Koelreuteria paniculata*	Beijing, China	ON376918	ON390905	ON390908	ON390914	ON390923
Cytospora diopuiensis	CFCC 56970	*Koelreuteria paniculata*	Beijing, China	ON376917	ON390904	ON390907	ON390913	ON390922
Cytospora diopuiensis	CFCC 56971	*Koelreuteria paniculata*	Beijing, China	ON376919	ON390906	NA	ON390915	NA
Cytospora discotoma	CFCC 53137[T]	*Platycladus orientalis*	Beijing, China	MW418404	MW422897	MW422907	MW422919	MW422931
Cytospora discotoma	CFCC 54368	*Platycladus orientalis*	Beijing, China	MW418405	MW422898	MW422908	MW422920	MW422932
Cytospora donetzica	MFLUCC 15-0864	*Crataegus monogyna*	Russia	KY417729	KY417695	KY417797	NA	NA
Cytospora donetzica	MFLUCC 16-0574[T]	*Crataegus monogyna*	Russia	KY417731	KY417697	KY417799	NA	NA
Cytospora donglingensis	CFCC 53159[T]	*Platycladus orientalis*	Beijing, China	MW418412	MW422903	MW422915	MW422927	MW422939
Cytospora donglingensis	CFCC 53160	*Platycladus orientalis*	Beijing, China	MW418414	MW422905	MW422917	MW422929	MW422941
Cytospora donglingensis	CFCC 54371	*Platycladus orientalis*	Beijing, China	MW418413	MW422904	MW422916	MW422928	MW422940
Cytospora donglingensis	CFCC 54372	*Platycladus orientalis*	Beijing, China	MW418415	MW422906	MW422918	MW422930	MW422942
Cytospora elaeagni	CFCC 89632	*Elaeagnus angustifolia*	Ningxia, China	KR045626	KU710995	KU710955	KU710918	KR045667

Species	Strain	Host	Origin	GenBank accession numbers				
				ITS	*act*	*rpb2*	*tef1-α*	*tub2*
Cytospora elaeagni	CFCC 89633	*Elaeagnus angustifolia*	Ningxia, China	KF765677	KU710996	KU710956	KU710919	KR045668
Cytospora elaeagnicola	CFCC 52882ᵀ	*Elaeagnus angustifolia*	Xinjiang, China	MK732341	MK732344	MK732347	NA	NA
Cytospora elaeagnicola	CFCC 52883	*Elaeagnus angustifolia*	Xinjiang, China	MK732342	MK732345	MK732348	NA	NA
Cytospora elaeagnicola	CFCC 52884	*Elaeagnus angustifolia*	Xinjiang, China	MK732343	MK732346	MK732349	NA	NA
Cytospora ershadii	IRAN 4197C	*Malus domestica*	Nahavand, Iran	MW295510	NA	NA	MW394143	NA
Cytospora ershadii	IRAN 4198Cᵀ	*Malus domestica*	Arak, Iran	MW295523	MZ014510	MW824357	MW394144	NA
Cytospora erumpens	CFCC 50022	*Prunus padus*	Shanxi, China	MH933627	MH933534	NA	MH933502	MH933569
Cytospora erumpens	MFLUCC 16-0580ᵀ	*Salix × fragilis*	Russia	KY417733	KY417699	KY417801	NA	NA
Cytospora erumpens	CFCC 53163	*Prunus padus*	Xinjiang, China	MK673059	MK673029	MK673000	MK672948	MK672975
Cytospora eucalypti	CBS 144241	*Eucalyptus globulus*	California, USA	MG971907	MG972056	NA	MG971617	MG971772
Cytospora euonymicola	CFCC 50499ᵀ	*Euonymus kiautschovicus*	Shaanxi, China	MH933628	MH933535	MH933598	MH933503	MH933570
Cytospora euonymicola	CFCC 50500	*Euonymus kiautschovicus*	Shaanxi, China	MH933629	MH933536	MH933599	MH933504	MH933571
Cytospora euonymina	CFCC 89993ᵀ	*Euonymus kiautschovicus*	Shanxi, China	MH933630	MH933537	MH933600	MH933505	MH933590
Cytospora euonymina	CFCC 89999	*Euonymus kiautschovicus*	Shanxi, China	MH933631	MH933538	MH933601	MH933506	MH933591
Cytospora euonymina	**CFCC 59444**	**Salix babylonica**	**Beijing, China**	**OR826164**	**OR831997**	**OR832019**	**OR832041**	**NA**
Cytospora euonymina	**CFCC 59479**	**Salix babylonica**	**Beijing, China**	**OR826165**	**OR831998**	**OR832020**	**OR832042**	**NA**
Cytospora fengtaiensis	**CFCC 59442**	**Acer palmatum 'Atropurpureum'**	**Beijing, China**	**OR826166**	**OR831999**	**OR832021**	**OR832043**	**OR832063**
Cytospora fengtaiensis	**CFCC 59449ᵀ**	**Acer palmatum 'Atropurpureum'**	**Beijing, China**	**OR826167**	**OR832000**	**OR832022**	**OR832044**	**OR832064**
Cytospora fengtaiensis	**CFCC 59525**	**Acer palmatum 'Atropurpureum'**	**Beijing, China**	**OR826168**	**OR832001**	**OR832023**	**OR832045**	**OR832065**
Cytospora fengtaiensis	**CFCC 59526**	**Acer palmatum 'Atropurpureum'**	**Beijing, China**	**OR826169**	**OR832002**	**OR832024**	**OR832046**	**OR832066**
Cytospora fengtaiensis	**CFCC 59527**	**Acer palmatum 'Atropurpureum'**	**Beijing, China**	**OR826170**	**OR832003**	**OR832025**	**OR832047**	**OR832067**
Cytospora fraxinigena	BBH 42442	*Fraxinus ornus*	NA	MF190133	NA	NA	NA	NA
Cytospora fraxinigena	MFLUCC 14-0868ᵀ	*Fraxinus ornus*	Italy	MF190133	NA	NA	NA	NA
Cytospora fugax	CXY 1371	*Populus simonii*	Jilin, China	KM034852	NA	NA	NA	KM034891
Cytospora fugax	CXY 1381	*Populus ussuriensis*	Heilongjiang, China	KM034853	NA	NA	NA	KM034890
Cytospora galegicola	MFLUCC 18-1199ᵀ	*Galega officinalis*	Forlì-Cesena, Italy	MK912128	MN685810	MN685820	NA	NA
Cytospora gigalocus	CFCC 89620ᵀ	*Juglans regia*	Qinghai, China	KR045628	KU710997	KU710957	KU710920	KR045669
Cytospora gigalocus	CFCC 89621	*Juglans regia*	Qinghai, China	KR045629	KU710998	KU710958	KU710921	KR045670
Cytospora gigaspora	CFCC 50014	*Juniperus procumbens*	Shanxi, China	KR045630	KU710999.	KU710959	KU710922	KR045671
Cytospora gigaspora	CFCC 89634ᵀ	*Salix psammophila*	Shaanxi, China	KF765671	KU711000	KU710960	KU710923	KR045672
Cytospora globosa	MFLU 16-2054ᵀ	*Abies alba*	Italy	MT177935	NA	MT432212	MT454016	NA
Cytospora granati	CBS 144237ᵀ	*Punica granatum*	California, USA	MG971799	MG971949	NA	MG971514	MG971664
Cytospora haidianensis	CFCC 54056	*Euonymus alatus*	Beijing, China	MT360041	MT363978	MT363987	MT363997	MT364007
Cytospora haidianensis	CFCC 54057ᵀ	*Euonymus alatus*	Beijing, China	MT360042	MT363979	MT363988	MT363998	MT364008
Cytospora haidianensis	CFCC 54184	*Euonymus alatus*	Beijing, China	MT360043	MT363980	MT363989	MT363999	MT364009
Cytospora haidianensis	**CFCC 59450**	**Euonymus japonicus**	**Beijing, China**	**OR826171**	**OR832004**	**OR832026**	**OR832048**	**OR832068**
Cytospora haidianensis	**CFCC 59475**	**Malus 'American'**	**Beijing, China**	**OR826172**	**OR832005**	**OR832027**	**OR832049**	**OR832069**
Cytospora haidianensis	**CFCC 59471**	**Acer pictum subsp. mono**	**Beijing, China**	**OR826173**	**OR832006**	**OR832028**	**OR832050**	**OR832070**

Species	Strain	Host	Origin	GenBank accession numbers				
				ITS	*act*	*rpb2*	*tef1-α*	*tub2*
Cytospora haidianensis	**CFCC 59536**	**Acer pictum subsp. mono**	**Beijing, China**	**OR826174**	**OR832007**	**OR832029**	**OR832051**	**OR832071**
Cytospora hippophaës	CFCC 89639	*Hippophaë rhamnoides*	Gansu, China	KR045632	KU711001	KU710961	KU710924	KR045673
Cytospora hippophaës	CFCC 89640	*Hippophaë rhamnoides*	Gansu, China	KF765682	KF765730	KU710962	KP310865	KR045674
Cytospora huairouensis	CFCC 56940	*Prunus armeniaca*	Beijing, China	ON188758	OR662079	OR662096	OR662113	OR662060
Cytospora huairouensis	CFCC 56973	*Prunus armeniaca*	Beijing, China	ON188759	OR662080	OR662097	OR662114	OR662061
Cytospora huairouensis	CFCC 57286	*Prunus armeniaca*	Beijing, China	ON188760	OR662081	OR662098	OR662115	OR662062
Cytospora iranica	IRAN 4200C[T]	*Malus domestica*	Arak, Iran	MW295652	MZ014512	MW824359	MW394146	NA
Cytospora iranica	IRAN 4628C	*Malus domestica*	Nahavand, Iran	OM368651	NA	NA	OM372513	NA
Cytospora japonica	CFCC 89956	*Prunus cerasifera*	Ningxia, China	KR045624	KU710993	KU710953	KU710916	KR045665
Cytospora japonica	CFCC 89960	*Prunus cerasifera*	Ningxia, China	KR045625	KU710994	KU710954	KU710917	KR045666
Cytospora joaquinensis	CBS 144235	*Populus deltoides*	California, USA	MG971895	MG972044	NA	MG971605	MG971761
Cytospora junipericola	BBH 42444	*Juniperus communis*	Italy	MF190126	NA	NA	MF377579	NA
Cytospora junipericola	MFLU 17-0882[T]	*Juniperus communis*	Italy	MF190125	NA	NA	MF377580	NA
Cytospora juniperina	CFCC 50501[T]	*Juniperus przewalskii*	Sichuan, China	MH933632	MH933539	MH933602	MH933507	NA
Cytospora juniperina	CFCC 50502	*Juniperus przewalskii*	Sichuan, China	MH933633	MH933540	MH933603	MH933508	MH933572
Cytospora juniperina	CFCC 50503	*Juniperus przewalskii*	Sichuan, China	MH933634	MH933541	MH933604	MH933509	NA
Cytospora kantschavelii	CXY 1383	*Populus maximowiczii*	Jilin, China	KM034867	NA	NA	NA	NA
Cytospora kantschavelii	CXY 1386	*Populus maximowiczii*	Chongqing, China	KM034867	NA	NA	NA	NA
Cytospora kuanchengensis	CFCC 52464[T]	*Castanea mollissima*	Hebei, China	MK432616	MK442940	MK578076	NA	NA
Cytospora kuanchengensis	CFCC 52465	*Castanea mollissima*	Hebei, China	MK432617	MK442941	MK578077	NA	NA
Cytospora longispora	CBS 144236[T]	*Prunus domestica*	California, USA	MG971905	MG972054	NA	MG971615	MG971764
Cytospora longistiolata	MFLUCC 16-0628	*Salix × fragilis*	Russia	KY417734	KY417700	KY417802	NA	NA
Cytospora leucosperma	CFCC 89622	*Pyrus bretschneideri*	Gansu, China	KR045616	KU710988	KU710944	KU710911	KR045657
Cytospora leucosperma	CFCC 89894	*Pyrus bretschneideri*	Qinghai, China	KR045617	KU710989	KU710945	KU710912	KR045658
Cytospora leucostoma	CFCC 50023	*Cornus alba*	Shanxi, China	KR045635	KU711003	KU710964	KU710926	KR045676
Cytospora leucostoma	CFCC 50024	*Prunus pseudocerasus*	Qinghai, China	MH933640	MH933547	MH933605	NA	MH933576
Cytospora leucostoma	CFCC 53140	*Prunus sibirica*	Beijing, China	MN854445	MN850760	MN850746	MN850753	MN861115
Cytospora leucostoma	CFCC 53141	*Prunus sibirica*	Beijing, China	MN854446	MN850761	MN850747	MN850754	MN861116
Cytospora leucostoma	CFCC 53156	*Juglans mandshurica*	Beijing, China	MN854447	MN850762	MN850748	MN850755	MN861117
Cytospora leucostoma	CFCC 53167	*Prunus armeniaca*	Xinjiang, China	MK673056	MK673026	MK672998	MK672946	MK672972
Cytospora leucostoma	CFCC 53169	*Prunus persica*	Beijing, China	MK673080	MK673050	MK673020	MK672966	MK672996
Cytospora leucostoma	CFCC 53170	*Prunus persica*	Beijing, China	MK673081	MK673051	MK673021	MK672967	MK672997
Cytospora leucostoma	CFCC 54680	*Corylus heterophylla*	Beijing, China	MW839857	MW815941	MW815955	MW815890	MW883973
Cytospora leucostoma	CFCC 54681	*Corylus heterophylla*	Beijing, China	MW839857	MW815942	MW815956	MW815891	MW883974
Cytospora leucostoma	CFCC 54682	*Corylus heterophylla*	Beijing, China	MW839857	MW815943	MW815957	MW815892	MW883975
Cytospora leucostoma	CFCC 54683	*Corylus heterophylla*	Beijing, China	MW839857	MW815944	MW815958	MW815893	MW883976
Cytospora lumnitzericola	MFLUCC 17-0508[T]	*Lumnitzera racernosa*	Tailand	MG975778	MH253457	MH253453	NA	NA
Cytospora macropycnidia	CBS 149338	*Vitis vinifera*	USA	OP038094	OP003977	OP095265	OP106954	OP079909
Cytospora mali	CFCC 50028	*Malus pumila*	Gansu, China	MH933641	MH933548	MH933606	MH933513	MH933577
Cytospora mali	CFCC 50029	*Malus pumila*	Ningxia, China	MH933642	MH933549	MH933607	MH933514	MH933578
Cytospora mali	CFCC 50030	*Malus pumila*	Shaanxi, China	MH933643	MH933550	MH933608	MH933524	MH933579
Cytospora mali	CFCC 50031	*Crataegus* sp.	Shanxi, China	KR045636	KU711004	KU710965	KU710927	KR045677

Species	Strain	Host	Origin	GenBank accession numbers				
				ITS	*act*	*rpb2*	*tef1-α*	*tub2*
Cytospora mali	CFCC 50044	*Malus baccata*	Qinghai, China	KR045637	KU711005	KU710966	KU710928	KR045678
Cytospora mali-spectabilis	CFCC 53181ᵀ	*Malus spectabilis* 'Royalty'	Xinjiang, China	MK673066	MK673036	MK673006	MK672953	MK672982
Cytospora melnikii	CFCC 89984	*Rhus typhina*	Xinjiang, China	MH933678	MH933551	MH933609	MH933515	MH933580
Cytospora melnikii	MFLUCC 15-0851	*Malus domestica*	Russia	KY417735	KY417701	KY417803	NA	NA
Cytospora melnikii	MFLUCC 16-0635	*Populus nigra* var. *italica*	Russia	KY417736	KY417702	KY417804	NA	NA
Cytospora myrtagena	CFCC 52454	*Castanea mollissima*	Shaanxi, China	MK432614	MK442938	MK578074	NA	NA
Cytospora myrtagena	CFCC 52455	*Castanea mollissima*	Shaanxi, China	MK432615	MK442939	MK578075	NA	NA
Cytospora nivea	MFLUCC 15-0860	*Salix acutifolia*	Russia	KY417737	KY417703	KY417805	NA	NA
Cytospora nivea	CFCC 89641	*Elaeagnus angustifolia*	Ningxia, China	KF765683	KU711006	KU710967	KU710929	KR045679
Cytospora nivea	CFCC 89643	*Salix psammophila*	Shaanxi, China	KF765685	NA	KU710968	KP310863	KP310829
Cytospora notastroma	NE_TFR5	*Populus tremuloides*	USA	JX438632	NA	NA	JX438543	NA
Cytospora notastroma	NE_TFR8	*Populus tremuloides*	USA	JX438633	NA	NA	JX438542	NA
Cytospora ochracea	CFCC 53164ᵀ	*Cotoneaster* sp.	Xinjiang, China	MK673060	MK673030	MK673001	MK672949	MK672976
Cytospora oleicola	CBS 144248ᵀ	*Olea europaea*	California, USA	MG971944	MG972098	NA	MG971660	MG971752
Cytospora olivacea	CFCC 53174	*Prunus cerasifera*	Xinjiang, China	MK673058	MK673028	MK672999	NA	MK672974
Cytospora olivacea	CFCC 53175	*Prunus dulcis*	Xinjiang, China	MK673062	MK673032	MK673003	NA	MK672978
Cytospora olivacea	CFCC 53176ᵀ	*Sorbus tianschanica*	Xinjiang, China	MK673068	MK673038	MK673008	MK672955	MK672984
Cytospora olivacea	CFCC 53177	*Prunus virginiana*	Xinjiang, China	MK673071	MK673041	MK673011	NA	MK672987
C. olivarum	UCD634-Oe CBS 145585	*Olea europaea*	Ventura Co., CA, U.S.A.	MK514094	MK509025	NA	MK509030	MK509035
C. olivarum	UCD644-Oe	*Olea europaea*	Ventura Co., CA, U.S.A.	MK514095	MK509026	NA	MK509031	MK509036
Cytospora palm	CXY 1276	*Cotinus coggygria*	Beijing, China	JN402990	NA	NA	KJ781296	NA
Cytospora palm	CXY 1280ᵀ	*Cotinus coggygria*	Beijing, China	JN411939	NA	NA	KJ781297	NA
Cytospora paracinnamomea	CFCC 55453ᵀ	*Salix matsudana*	Gansu, China	MZ702594	OK303456	OK303515	OK303576	OK303643
Cytospora paracinnamomea	CFCC 55455ᵀ	*Salix matsudana*	Gansu, China	MZ702598	OK303460	OK303519	OK303580	OK303647
Cytospora parakantschavelii	MFLUCC 15-0857ᵀ	*Populus × sibirica*	Russia	KY417738	KY417704	KY417806	NA	NA
Cytospora parakantschavelii	MFLUCC 16-0575	*Pyruspyraster*	Russia	KY417739	KY417705	KY417807	NA	NA
Cytospora parapistaciae	CBS 144506ᵀ	*Pistacia vera*	California, USA	MG971804	MG971954	NA	MG971519	MG971669
Cytospora parasitica	MFLUCC 15-0507ᵀ	*Malus domestica*	Russia	KY417740	KY417706	KY417808	NA	NA
Cytospora parasitica	XJAU 2542-1	*Malus* sp.	Xinjiang, China	MH798884	NA	NA	MH813452	NA
Cytospora parasitica	CFCC 53171	*Malus pumila*	Xinjiang, China	MK673061	MK673031	MK673002	MK672950	MK672977
Cytospora parasitica	CFCC 53172	*Malus pumila*	Xinjiang, China	MK673069	MK673039	MK673009	MK672956	MK672985
Cytospora parasitica	CFCC 53173	*Berberis* sp.	Xinjiang, China	MK673070	MK673040	MK673010	MK672957	MK672986
Cytospora paratranslucens	MFLUCC 15-0506ᵀ	*Populus alba* var. *bolleana*	Russia	KY417741	KY417707	KY417809	NA	NA
Cytospora paratranslucens	MFLUCC 16-0627	*Populus alba*	Russia	KY417742	KY417708	KY417810	NA	NA
Cytospora paraplurivora	FDS-439	*Prunus armeniaca*	Canada	OL640182	OL631586	NA	OL631589	NA
Cytospora paraplurivora	FDS-564	*Prunus persica* var. *nucipersica*	Canada	OL640183	OL631587	NA	OL631590	NA
Cytospora paraplurivora	FDS-623	*Prunus persica* var. *persica*	Canada	OL640181	OL631588	NA	OL631591	NA
Cytospora phialidica	MFLUCC 17-2498	*Alnus glutinosa*	Italy	MT177932	NA	MT432209	MT454014	NA
Cytospora piceae	CFCC 52841ᵀ	*Picea crassifolia*	Xinjiang, China	MH820398	MH820406	MH820395	MH820402	MH820387
Cytospora piceae	CFCC 52842	*Picea crassifolia*	Xinjiang, China	MH820399	MH820407	MH820396	MH820403	MH820388
Cytospora pinea	**CFCC 59521ᵀ**	**Pinus bungeanae**	**Beijing, China**	**OR826181**	**OR832014**	**OR832036**	**OR832058**	**OR832078**
Cytospora pinea	**CFCC 59522**	**Pinus bungeanae**	**Beijing, China**	**OR826182**	**OR832015**	**OR832037**	**OR832059**	**OR832079**
Cytospora pinea	**CFCC 59523**	**Pinus bungeanae**	**Beijing, China**	**OR826183**	**OR832016**	**OR832038**	**OR832060**	**OR832080**
Cytospora pinea	**CFCC 59524**	**Pinus bungeanae**	**Beijing, China**	**OR826184**	**OR832017**	**OR832039**	**OR832061**	**OR832081**

Species	Strain	Host	Origin	GenBank accession numbers				
				ITS	*act*	*rpb2*	*tef1-α*	*tub2*
Cytospora pingbianensis	MFLUCC 18-1204ᵀ	Undefined wood	Yunnan, China	MK912135	MN685817	MN685826	NA	NA
Cytospora pistaciae	CBS 144238ᵀ	*Pistacia vera*	California, USA	MG971802	MG971952	NA	MG971517	MG971667
Cytospora platanicola	MFLU 17-0327	*Platanus hybrida*	Italy	MH253451	MH253449	MH253450	NA	NA
Cytospora platyclada	CFCC 50504ᵀ	*Platycladus orientalis*	Yunnan, China	MH933645	MH933552	MH933610	MH933516	MH933581
Cytospora platyclada	CFCC 50505	*Platycladus orientalis*	Yunnan, China	MH933646	MH933553	MH933611	MH933517	MH933582
Cytospora platyclada	CFCC 50506	*Platycladus orientalis*	Yunnan, China	MH933647	MH933554	MH933612	MH933518	MH933583
Cytospora platycladicola	CFCC 50038ᵀ	*Platycladus orientalis*	Gansu, China	KT222840	MH933555	MH933613	MH933519	MH933584
Cytospora platycladicola	CFCC 50039	*Platycladus orientalis*	Gansu, China	KR045642	KU711008	KU710973	KU710931	KR045683
Cytospora plurivora	CBS 144239ᵀ	*Olea europaea*	California, USA	MG971861	MG972010	NA	MG971572	MG971726
Cytospora populicola	CBS 144240	*Populus deltoides*	California, USA	MG971891	MG972040	NA	MG971601	MG971757
Cytospora populina	CFCC 89644ᵀ	*Salix psammophila*	Shaanxi, China	KF765686	KU711007	KU710969	KU710930	KR045681
Cytospora populinopsis	CFCC 50032ᵀ	*Sorbus aucuparia*	Ningxia, China	MH933648	MH933556	MH933614	MH933520	MH933585
Cytospora populinopsis	CFCC 50033	*Sorbus aucuparia*	Ningxia, China	MH933649	MH933557	MH933615	MH933521	MH933586
Cytospora predappioensis	MFLUCC 17-2458ᵀ	*Platanus hybrida*	Italy	MG873484	NA	NA	NA	NA
Cytospora prunicola	MFLU 17-0995ᵀ	*Prunus* sp.	Italy	MG742350	MG742353	MG742352	NA	NA
Cytospora pruni-mume	CFCC 53179	*Prunus armeniaca*	Xinjiang, China	MK673057	MK673027	NA	MK672947	MK672973
Cytospora pruni-mume	CFCC 53180ᵀ	*Prunus mume*	Xinjiang, China	MK673067	MK673037	MK673007	MK672954	MK672983
Cytospora prunina	CFCC 58997	*Prunus armeniaca*	Beijing, China	OR578808	NA	NA	NA	OR662077
Cytospora prunina	CFCC 58998	*Prunus armeniaca*	Beijing, China	OR578809	NA	NA	NA	OR662078
Cytospora pruinopsis	CFCC 50034ᵀ	*Ulmus pumila*	Shaanxi, China	KP281259	KP310836	KU710970	KP310849	KP310819
Cytospora pruinopsis	CFCC 50035	*Ulmus pumila*	Jilin, China	KP281260	KP310837	KU710971	KP310850	KP310820
Cytospora pruinopsis	CFCC 53153	*Ulmus pumila*	Beijing, China	MN854451	MN850763	MN850752	MN850759	MN861121
Cytospora pruinosa	CFCC 50036	*Syringa oblata*	Qinghai, China	KP310800	KP310832	NA	KP310845	KP310815
Cytospora pruinosa	CFCC 50037	*Syringa oblata*	Qinghai, China	MH933650	MH933558	NA	MH933522	MH933589
Cytospora pubescentis	MFLUCC 18-1201ᵀ	*Quercus pubescens*	Forlì-Cesena, Italy	MK912130	MN685812	MN685821	NA	NA
Cytospora punicae	CBS 144244	*Punica granatum*	California, USA	MG971943	MG972091	NA	MG971654	MG971798
Cytospora quercicola	MFLU 17-0881	*Quercus* sp.	Italy	MF190128	NA	NA	NA	NA
Cytospora quercicola	MFLUCC 14-0867ᵀ	*Quercus* sp.	Italy	MF190129	NA	NA	NA	NA
Cytospora ribis	CFCC 50026	*Ulmus pumila*	Qinghai, China	KP281267	KP310843	KU710972	KP310856	KP310826
Cytospora ribis	CFCC 50027	*Ulmus pumila*	Qinghai, China	KP281268	KP310844	NA	KP310857	KP310827
Cytospora rosae	MFLU 17-0885	*Rosa canina*	Italy	MF190131	NA	NA	NA	NA
Cytospora rosicola	CF 20197024ᵀ	*Rosa* sp.	Tibet, China	MK673079	MK673049	MK673019	MK672965	MK672995
Cytospora rosigena	MFLUCC 18-0921ᵀ	*Rosa* sp.	Russia	MN879872	NA	NA	NA	NA
Cytospora rostrata	CFCC 89909	*Salix cupularis*	Gansu, China	KR045643	KU711009	KU710974	KU710932	KR045684
Cytospora rostrata	CFCC 89910	*Salix cupularis*	Gansu, China	KR045644	KU711010	KU710975	KU710933	NA
Cytospora rusanovii	MFLUCC 15-0853	*Populus × sibirica*	Russia	KY417743	KY417709	KY417811	NA	NA
Cytospora rusanovii	MFLUCC 15-0854ᵀ	*Salix babylonica*	Russia	KY417744	KY417710	KY417812	NA	NA
Cytospora salicacearum	MFLUCC 15-0509	*Salix alba*	Russia	KY417746	KY417712	KY417814	NA	NA
Cytospora salicacearum	MFLUCC 15-0861	*Salix × fragilis*	Russia	KY417745	KY417711	KY417813	NA	NA
Cytospora salicacearum	MFLUCC 16-0587	*Prunus cerasus*	Russia	KY417742	KY417708	KY417810	NA	NA
Cytospora salicacearum	MFLUCC 16-0576	*Populus nigra* var. *italica*	Russia	KY417741	KY417707	KY417809	NA	NA
Cytospora salicicola	MFLUCC 14-1052ᵀ	*Salix alba*	Russia	KU982636	KU982637	NA	NA	NA
Cytospora salicicola	MFLUCC 15-0866	*Salix* sp.	Thailand	KY417749	KY417715	KY417817	NA	NA
Cytospora salicina	MFLUCC 15-0862	*Salix alba*	Russia	KY417750	KY417716	KY417818	NA	NA
Cytospora salicina	MFLUCC 16-0637	*Salix ×fragilis*	Russia	KY417751	KY417717	KY417819	NA	NA
Cytospora schulzeri	CFCC 50042	*Malus pumila*	Gansu, China	KR045650	KU711014	KU710981	KU710937	KR045691

Species	Strain	Host	Origin	GenBank accession numbers				
				ITS	*act*	*rpb2*	*tef1-α*	*tub2*
Cytospora sibiraeae	CFCC 50045^T	*Sibiraea angustata*	Gansu, China	KR045651	KU711015	KU710982	KU710938	KR045692
Cytospora sibiraeae	CFCC 50046	*Sibiraea angustata*	Gansu, China	KR045652	KU711015	KU710983	KU710939	KR045693
Cytospora sophorae	CFCC 50047	*Styphnolobium japonicum*	Shanxi, China	KR045653	KU711017	KU710984	KU710940	KR045694
Cytospora sophorae	CFCC 50048	*Magnolia grandiflora*	Shanxi, China	MH820401	MH820409	MH820397	MH820405	MH820390
Cytospora sophorae	CFCC 89598	*Styphnolobium japonicum*	Gansu, China	KR045654	KU711018	KU710985	KU710941	KR045695
Cytospora sophoricola	CFCC 89596	*Styphnolobium japonicum var. pendula*	Gansu, China	KR045656	KU711020	KU710987	KU710943	KR045697
Cytospora sophoricola	CFCC 89595^T	*Styphnolobium japonicum var. pendula*	Gansu, China	KR045655	KU711019	KU710986	KU710942	KR045696
Cytospora sophoriopsis	CFCC 55469	*Salix matsudana*	Gansu, China	MZ702583	OK303445	OK303504	OK303565	OK303632
Cytospora sophoriopsis	CFCC 89600	*Styphnolobium japonicum*	Gansu, China	KR045623	KU710992	KU710951	KU710915	KP310817
Cytospora sorbariae	**CFCC 59443**	**Sorbaria sorbifolia**	**Beijing, China**	**OR826175**	**OR832008**	**OR832030**	**OR832052**	**OR832072**
Cytospora sorbariae	**CFCC 59445^T**	**Sorbaria sorbifolia**	**Beijing, China**	**OR826176**	**OR832009**	**OR832031**	**OR832053**	**OR832073**
Cytospora sorbariae	**CFCC 59529**	**Sorbaria sorbifolia**	**Beijing, China**	**OR826177**	**OR832010**	**OR832032**	**OR832054**	**OR832074**
Cytospora sorbariae	**CFCC 59530**	**Sorbaria sorbifolia**	**Beijing, China**	**OR826178**	**OR832011**	**OR832033**	**OR832055**	**OR832075**
Cytospora sorbi	MFLUCC 16-0631^T	*Sorbus aucuparia*	Russia	KY417752	KY417718	KY417820	NA	NA
Cytospora sorbicola	MFLUCC 16-0584^T	*Acer pseudoplatanus*	Russia	KY417755	KY417721	KY417823	NA	NA
Cytospora sorbicola	MFLUCC 16-0633	*Cotoneaster melanocarpus*	Russia	KY417758	KY417724	KY417826	NA	NA
Cytospora sorbina	CF 20197660^T	*Sorbus tianschanica*	Xinjiang, China	MK673052	MK673022	NA	MK672943	MK672968
Cytospora spiraeae	CFCC 50049^T	*Spiraeasalicifolia*	Gansu, China	MG707859	MG708196	MG708199	NA	NA
Cytospora spiraeae	CFCC 50050	*Spiraeasalicifolia*	Gansu, China	MG707860	MG708197	MG708200	NA	NA
Cytospora spiraeicola	CFCC 53138^T	*Spiraeasalicifolia*	Beijing, China	MN854448	NA	MN850749	MN850756	MN861118
Cytospora spiraeicola	CFCC 53139	*Tilia nobilis*	Beijing, China	MN854449	NA	MN850750	MN850757	MN861119
Cytospora tamaricicola	CFCC 50507	*Rosa multifolora*	Yunnan, China	MH933651	MH933559	MH933616	MH933525	MH933587
Cytospora tamaricicola	CFCC 50508^T	*Tamarix chinensis*	Yunnan, China	MH933652	MH933560	MH933617	MH933523	MH933588
Cytospora tanaitica	MFLUCC 14-1057^T	*Betula pubescens*	Russia	KT459411	KT459413	NA	NA	NA
Cytospora thailandica	MFLUCC 17-0262^T	*Xylocarpus moluccensis*	Thailand	MG975776	MH253459	MH253455	NA	NA
Cytospora thailandica	MFLUCC 17-0263^T	*Xylocarpus moluccensis*	Thailand	MG975777	MH253460	MH253456	NA	NA
Cytospora tibetensis	CF 20197026	*Cotoneaster* sp.	Tibet, China	MK673076	MK673046	MK673016	MK672962	MK672992
Cytospora tibetensis	CF 20197029	*Cotoneaster* sp.	Tibet, China	MK673077	MK673047	MK673017	MK672963	MK672993
Cytospora tibetensis	CF 20197032^T	*Cotoneaster* sp.	Tibet, China	MK673078	MK673048	MK673018	MK672964	MK672994
Cytospora tibouchinae	CPC 26333^T	*Tibouchina semidecandra*	France	KX228284	NA	NA	NA	NA
Cytospora translucens	CXY 1351	*Populus davidiana*	Inner Mongolia, China	KM034874	NA	NA	NA	KM034895
Cytospora translucens	CXY 1359	*Populus × Beijingensis*	Beijing, China	KM034871	NA	NA	NA	KM034894
Cytospora ulmi	MFLUCC 15-0863^T	*Ulmus minor*	Russia	KY417759	NA	NA	NA	NA
Cytospora verrucosa	CFCC 53157^T	*Platycladus orientalis*	Beijing, China	MW418408	NA	MW422911	MW422923	MW422935
Cytospora verrucosa	CFCC 53158	*Platycladus orientalis*	Beijing, China	MW418410	MW422901	MW422913	MW422925	MW422937
Cytospora verrucosa	CFCC 54369	*Platycladus orientalis*	Beijing, China	MW418409	NA	MW422912	MW422924	MW422936
Cytospora verrucosa	CFCC 54370	*Platycladus orientalis*	Beijing, China	MW418411	MW422902	MW422914	MW422926	MW422938
Cytospora vinacea	CBS 141585^T	*Vitis interspecific hybrid 'Vidal'*	USA	KX256256	NA	NA	KX256277	KX256235
Cytospora viridistroma	CBS 202.36^T	*Cercis canadensis*	USA	MN172408	NA	NA	MN271853	NA

Species	Strain	Host	Origin	GenBank accession numbers				
				ITS	*act*	*rpb2*	*tef1-α*	*tub2*
Cytospora viticola	Cyt2	*Vitis interspecific* hybrid 'Frontenac'	USA	KX256238	NA	NA	KX256259	KX256217
Cytospora viticola	CBS 141586[T]	*Vitis vinifera* 'CabernetFranc'	USA	KX256239	NA	NA	KX256260	KX256218
Cytospora xinjiangensis	CFCC 53182	*Rosa* sp.	Xinjiang, China	MK673064	MK673034	MK673004	MK672951	MK672980
Cytospora xinjiangensis	CFCC 53183[T]	*Rosa* sp.	Xinjiang, China	MK673065	MK673035	MK673005	MK672952	MK672981
Cytospora xinglongensis	CFCC 52458[T]	*Castanea mollissima*	Hebei, China	MK432622	MK442946	MK578082	NA	NA
Cytospora xinglongensis	CFCC 52459	*Castanea mollissima*	Hebei, China	MK432623	MK442947	MK578083	NA	NA
Cytospora xylocarpi	MFLUCC 17-0251[T]	*Xylocarpus granatum*	Thailand	MG975775	MH253458	MH253454	NA	NA
Cytospora yakimana	CBS 149297	*Vitis vinifera*	USA	OM976602	ON012555	ON045093	ON012569	ON086750
Cytospora yakimana	CBS 149298	*Vitis vinifera*	USA	OM976603	ON012556	ON045094	ON012570	ON086751
Cytospora zhaitangensis	CFCC 56227[T]	*Euonymus japonicus*	Beijing, China	OQ344750	OQ398760	OQ398789	OQ410623	OQ398733
Cytospora zhaitangensis	CFCC 57537	*Euonymus japonicus*	Beijing, China	OQ344751	OQ398761	OQ398790	OQ410624	OQ398734
Diaporthe vaccinii	CBS 160.32	*Vaccinium macrocarpon*	USA	KC343228	JQ807297	NA	KC343954	KC344196

[1]Acronyms: ATCC: American Type Culture Collection, Virginia, USA; BBH: BIOTEC Bangkok Herbarium, National Science and Technology Development Agency, Thailand; CBS: Westerdijk Fungal Biodiversity Institute (CBS-KNAW Fungal Biodiversity Centre), Utrecht, The Netherlands; CFCC: China Forestry Culture Collection Centre, Beijing, China; CMW: Culture Collection of Michael Wingfield, University of Pretoria, South Africa; CPC: Culture Collection of Pedro Crous, The Netherlands; IMI: Culture Collection of the International Mycological Institute, CABI Bioscience, Egham, Surrey, UK; MFLU: Mae Fah Luang University herbarium, Thailand; MFLUCC: Mae Fah Luang University Culture Collection, Thailand; MUCC: Murdoch University Culture Collection, Perth, Australia; NE: Gerard Adams Collections, University of Nebraska, Lincoln NE, USA; PPRI: Culture Collection of the Plant Protection Research Institute, Agriculture Research Center, Pretoria, South Africa; XJAU: Xinjiang Agricultural University, Xinjiang, China; NA: not applicable. All the new isolates used in this study are in bold and the type materials are marked with T.

Results

Phylogenetic analyses

Each gene region and the combined matrix of five gene sequences of *Cytospora* were both considered. The concatenated alignment comprised sequences from 296 strains and *Diaporthe vaccinii* CBS 160.32 was selected as the outgroup. *Cytospora* ingroup strains with a total of 3166 characters including gaps (615 characters for ITS, 344 for *act*, 731 for *rpb2*, 811 for *tef1-α* and 665 for *tub2*). ML bootstraps (ML BS ≥ 60%) and Bayesian posterior probabilities (BPP ≥ 0.90) have been shown above the branches (Fig. 2). For ML analysis, the substitution model (GTR+G+I model) for each dataset was selected following recent studies (Fan et al. 2020; Pan et al. 2020, 2021). Confidence levels for the nodes were determined using 1,000 replicates of bootstrapping methods (Hillis and Bull 1993). The matrix had 1992 distinct alignment patterns. Estimated base frequencies are as follows: A = 0.244402, C = 0.286560, G = 0.238889, T = 0.230150; substitution rates: AC = 1.282426, AG = 3.546575, AT = 1.431177, CG = 0.946427, CT = 6.172877, GT = 1.000000; gamma distribution shape parameter: α = 0.364165. For BI analysis, the best-fit model of nucleotide evolution was deduced on the AIC (ITS and *act*: GTR+I+G; *rpb2* and *tef1-α*: TrN+I+G; and *tub2*: HKY+I+G).

The topologies resulting from ML and BI analyses of the concatenated dataset were similar. In the present study, 22 isolates formed seven clades representing seven species, of which four clades were grouped with the strains of four known species (*C. ailanthicola*, *C. albodisca*, *C. euonymina*, *C. haidianensis*). Isolates in other three clades were separated from all other species and were also highly supported (ML/BI = 100/1) (Fig. 2), representing three new species (*C. fengtaiensis*, *C. pinea*, *C. sorbariae*), which have been described below.
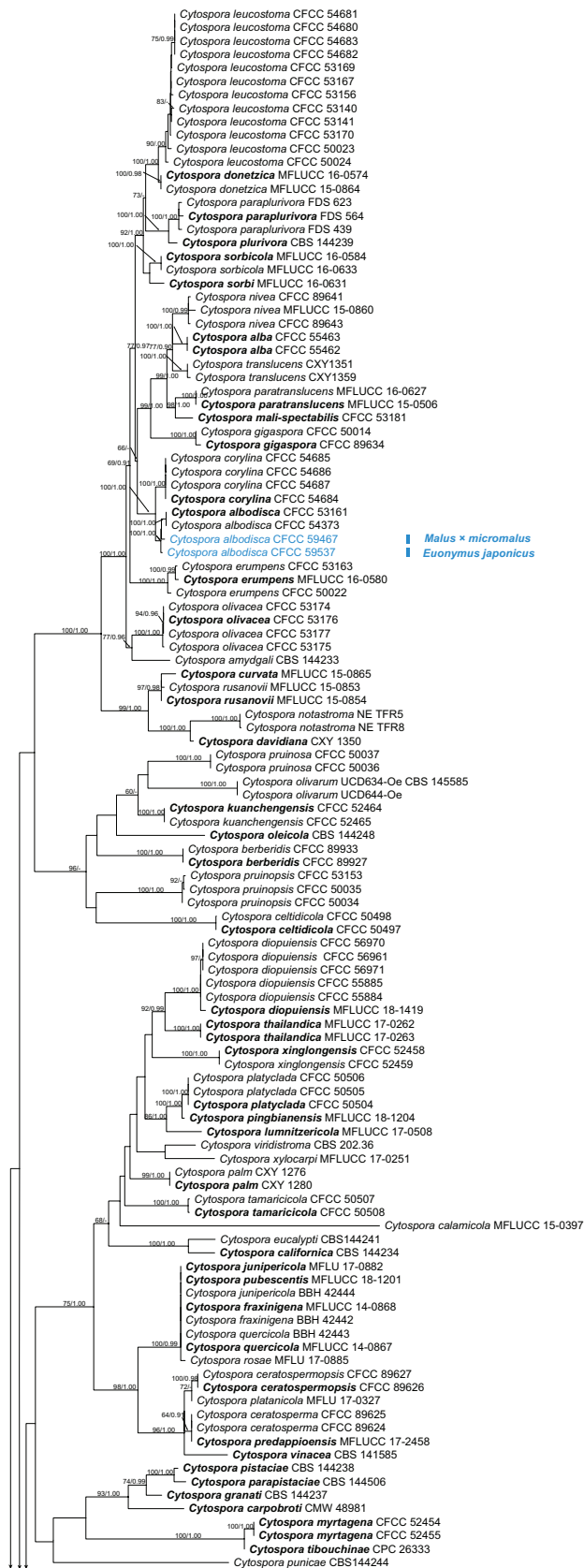
Figure 2. Phylogram of *Cytospora* based on Maximum Likelihood (ML) analysis of the dataset of combined ITS, *act*, *rpb2*, *tef1-a* and *tub2* genes. Numbers above the branches indicate ML bootstrap values (ML-BS ≥ 60%) and Bayesian Posterior Probabilities (BPP ≥ 0.9). Ex-type isolates are in bold. Isolates in this study marked with its hosts and highlighted in two different colours where the novel species are shown in dark blue and the known species are shown in light blue.
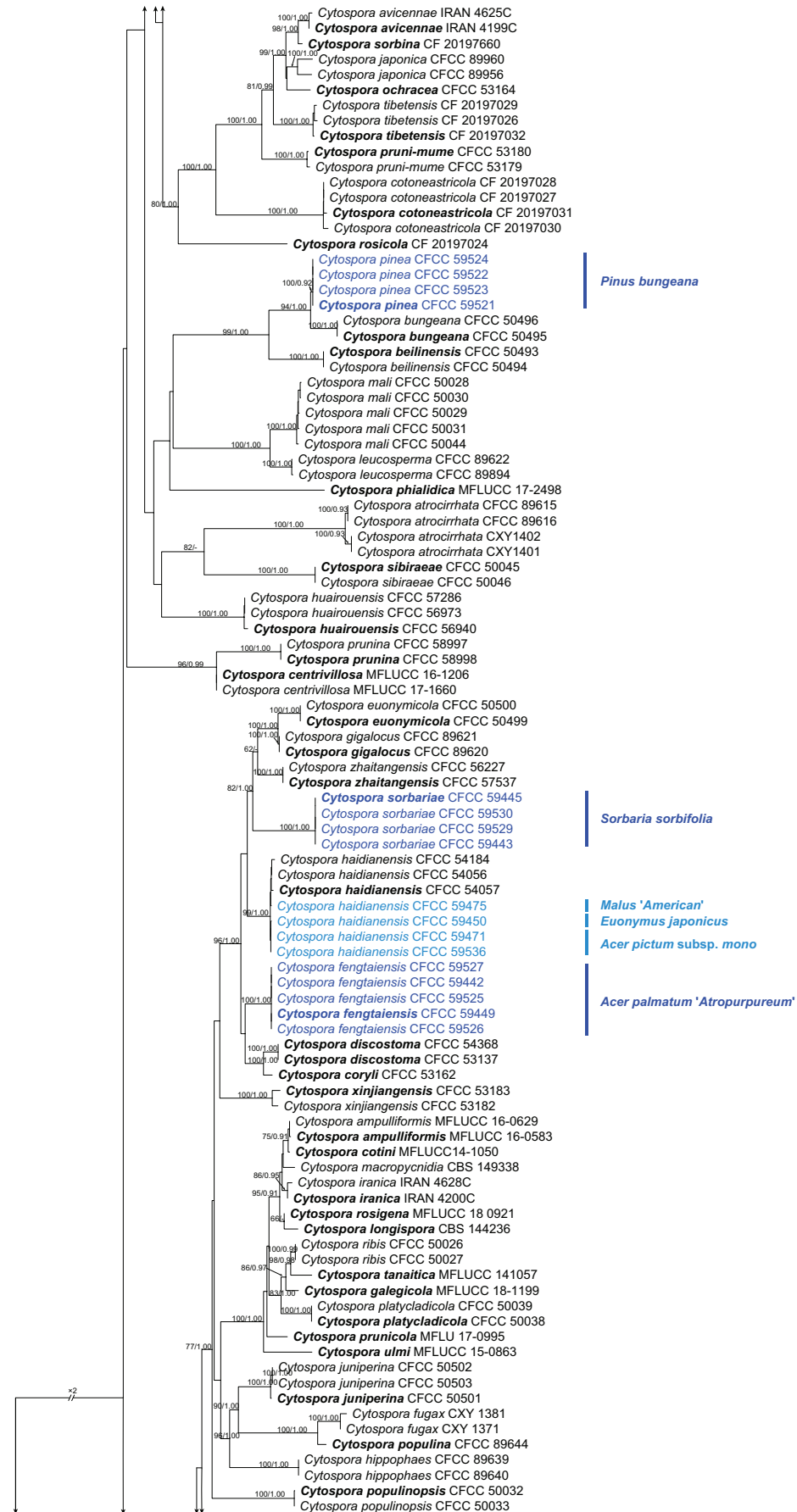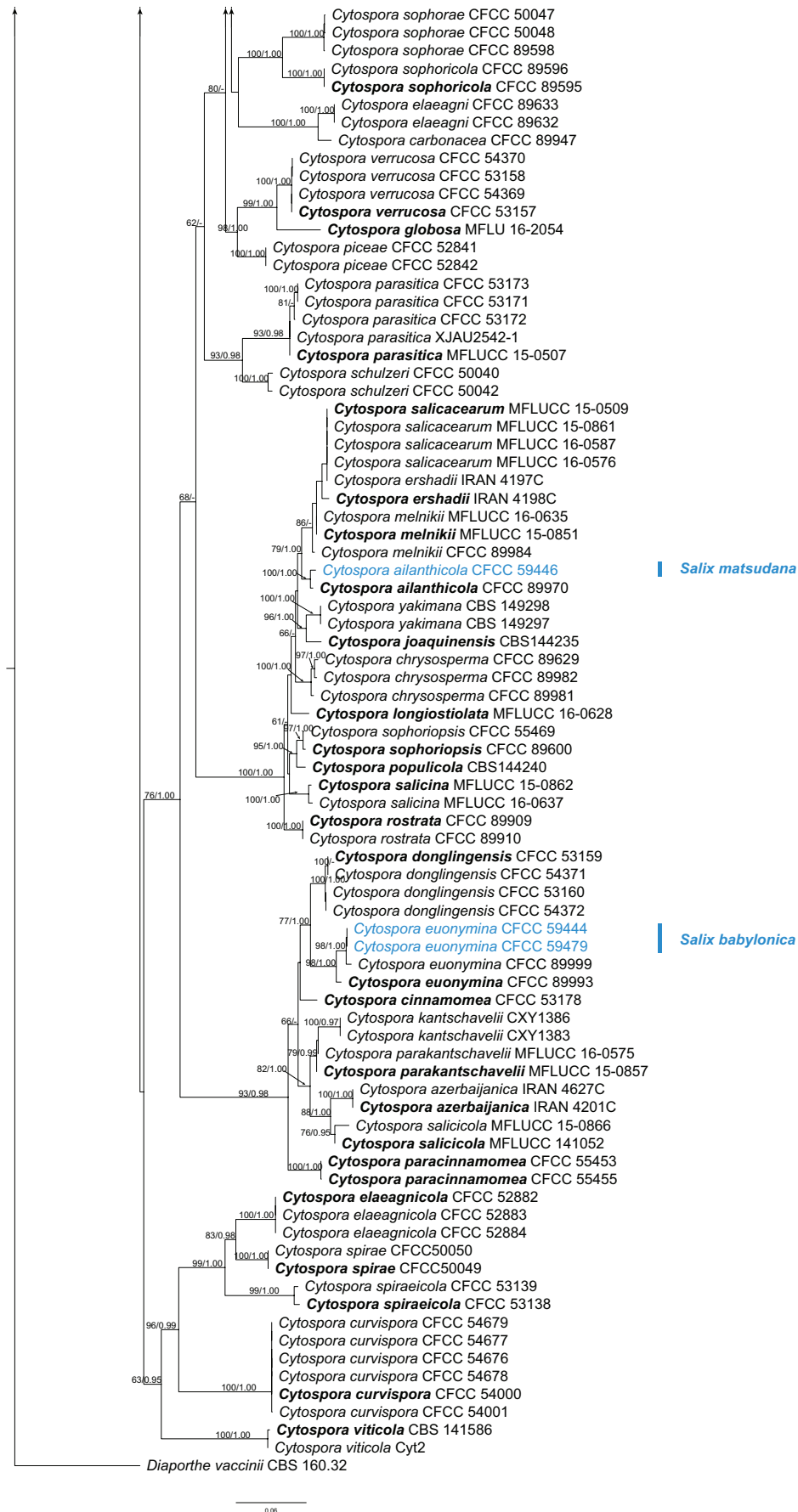
Figure 2. Continued.

Figure 2. Continued.

Taxonomy

Cytospora ailanthicola X.L. Fan & C.M. Tian, Persoonia 45: 13 (2020)
Fig. 3

Description. *Sexual morph*: not observed. *Asexual morph*: *Conidiomata pycnidial*, immersed in the bark, scattered, producing black area on bark, circular to ovoid, with multiple locules, occasionally slightly erumpent through the surface. *Conceptacle* absent. *Ectostromatic disc* inconspicuous, grey to black, circular to ovoid, producing one ostiole per disc when mature. *Ostiole* in the centre of the disc, black, 50−110 μm in diam. *Locules* numerous, subdivided frequently by invaginations with common walls, circular to ovoid, 300−500 μm in diam. *Conidiophores* hyaline, unbranched, approximately cylindrical, 6.5−9 × 1−1.5 (av. = 8 ± 1.5 × 1.3 ± 0.2, n = 50) μm. *Conidiogenous cells* enteroblastic, phialidic. *Conidia* hyaline, elongate-allantoid, smooth, aseptate, 2.8−3 × 0.8−1.2 (av. = 3 ± 0.3 × 1 ± 0.2, n = 50) μm.

Culture characteristics. Cultures on PDA are initially white, growing fast up to 5 cm after 3 d and entirely covering the 6 cm Petri dish after 7 d, with fluffy and whitish aerial mycelium, producing black pycnidia with cream to yellowish conidial drops exuding from the ostioles after 30 d. *Pycnidia* aggregated on surface.

Materials examined. CHINA, Beijing City, Fengtai Distinct, Qianling Mountain scenic area, 39°51'12.28"N, 116°5'17.74"E, from branches of *Salix matsudana*, 12 Apr 2023, A.L. Jia & X.L. Fan (BJFC CF20230400, living culture CFCC 59446).

Notes. *Cytospora ailanthicola* was first observed on branches of *Ailanthus altissima* in China by Fan et al. (2020). Lin et al. (2022) confirmed this species was a pathogen with strong virulence caused by poplar canker disease. In this study, CFCC 59446 was isolated from symptomatic branches of *Salix matsudana* in Beijing, which clustered in a well-supported clade with *C. ailanthicola* ex-holotype CFCC 89970 (ML/BI = 100/1). Therefore, CFCC 59446 is identified as *C. ailanthicola*.
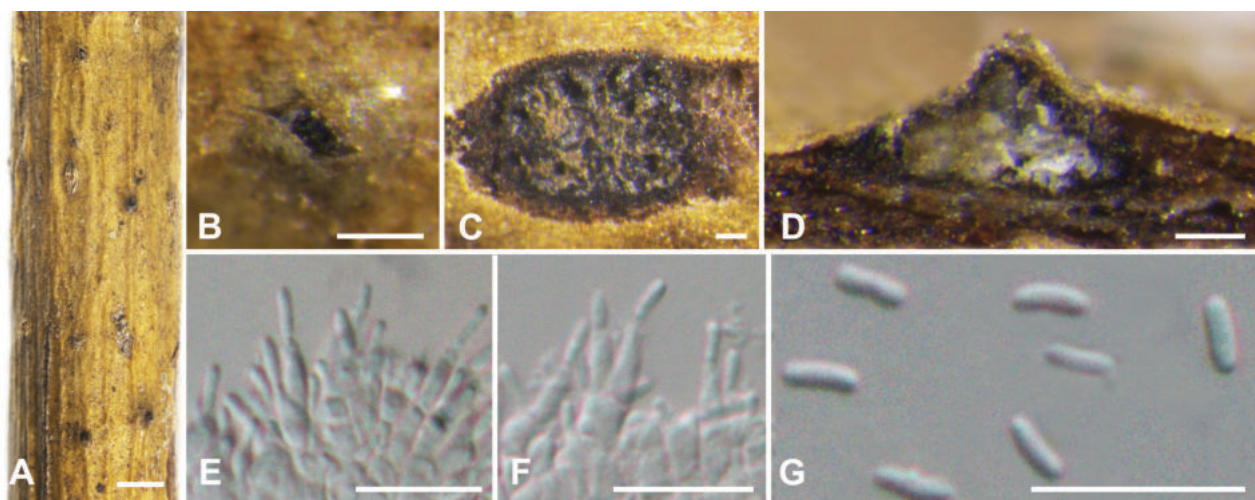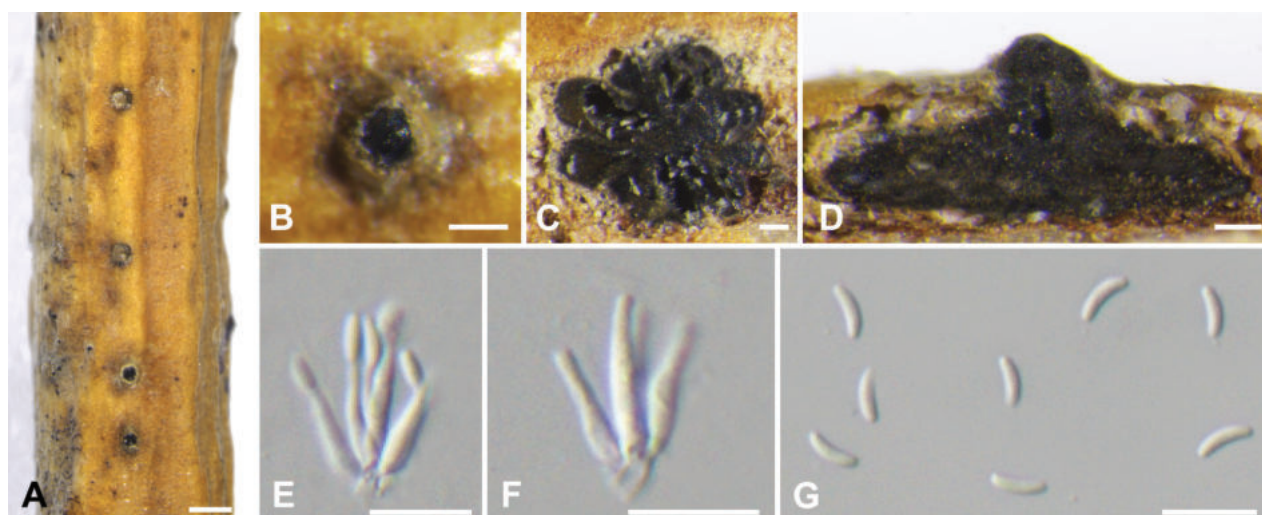

Figure 3. *Cytospora ailanthicola* from *Salix matsudana* (BJFC CF20230400) **A, B** habit of conidiomata on branch **C** transverse section through conidiomata **D** longitudinal section through conidiomata **E, F** conidiophores and conidiogenous cells **G** conidia. Scale bars: 1 mm (**A**); 200 μm (**B**); 100 μm (**C, D**); 10 μm (**E−G**)

Cytospora albodisca M. Pan & X.L. Fan, Front. Plant Sci. 12 (636460): 3 (2021).
Fig. 4

Description. *Sexual morph*: not observed. *Asexual morph*: *Conidiomata pycnidial*, semi-immersed in the bark, scattered, producing black area on bark, circular to ovoid, with multiple locules, occasionally slightly erumpent through the surface. *Conceptacle* absent. *Ectostromatic disc* conspicuous, black, discoid, circular to ovoid, 680–1200 μm in diam., producing one ostiole per disc when mature. *Ostiole* grey to black, in the centre of the disc, 140–300 μm in diam. *Locules* numerous, subdivided frequently by invaginations with common walls, circular to ovoid, 500–1200 μm in diam. *Conidiophores* hyaline, unbranched, approximately cylindrical, 7–11× 0.8–2 (av. = 9 ± 2.2 × 1.3 ± 0.3, n = 50) μm. *Conidiogenous cells* enteroblastic, phialidic. *Conidia* hyaline, elongate-allantoid, smooth, aseptate, 5–7 × 1–2 (av. = 6 ± 0.5 × 1.5 ± 0.3, n = 50) μm.
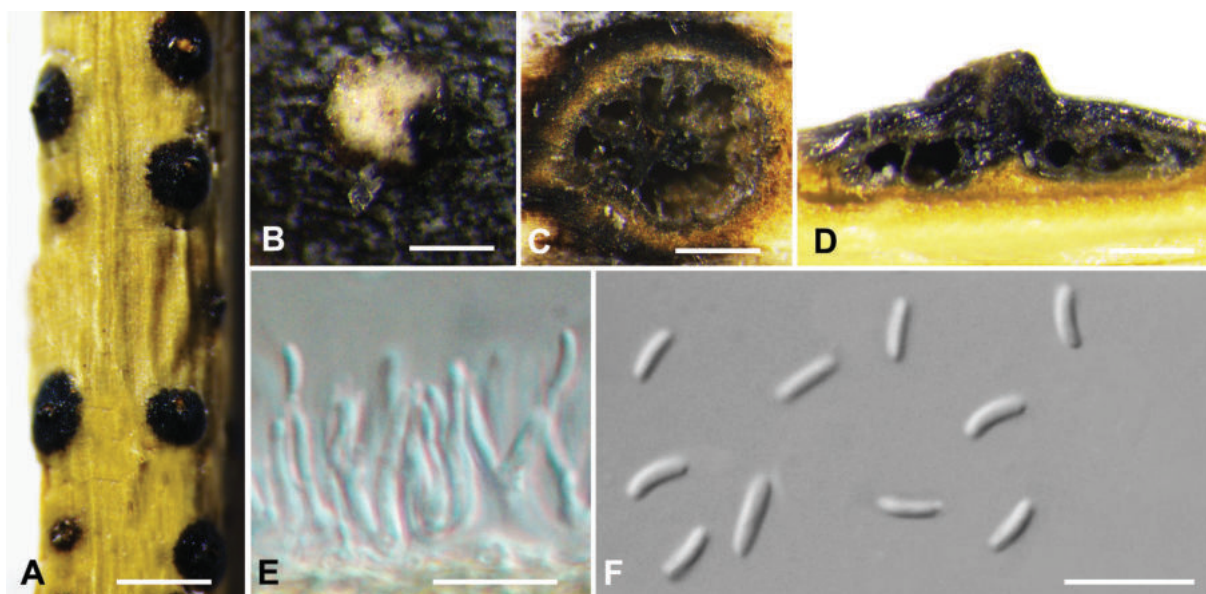
Culture characteristics. Cultures on PDA are initially white, growing fast up to 5 cm in diam. after 3 d and entirely covering the 6 cm Petri dish after 5 d, becoming dark herbage green to dull green after 7–10 d. Colonies are sparse in the centre and compact to the margin. After 30 d, *pycnidia* distributed irregularly on surface.

Materials examined. China, Beijing City, Fengtai Distinct, Qianling Mountain scenic area, 39°51'12.28"N, 116°5'17.74"E, from branches of *Malus × micromalus*, 12 Apr 2023, A.L. Jia & X.L. Fan (BJFC CF20230401, living culture CFCC 59467); Qianling Mountain scenic area, 39°51'12.28"N, 116°5'17.74"E, from branches of *Euonymus japonicus*, 12 Apr 2023, A.L. Jia & X.L. Fan (BJFC CF20230402, living culture CFCC 59537).

Notes. *Cytospora albodisca* was described by Pan et al. (2021) associated with canker disease of *Platycladus orientalis* in China. It can be identified by having ascostroma surrounded by a black conceptacle, producing allantoid, aseptate ascospores (8 × 14 × 2–3.5 μm). In this study, the asexual morph of *Cytospora al-*
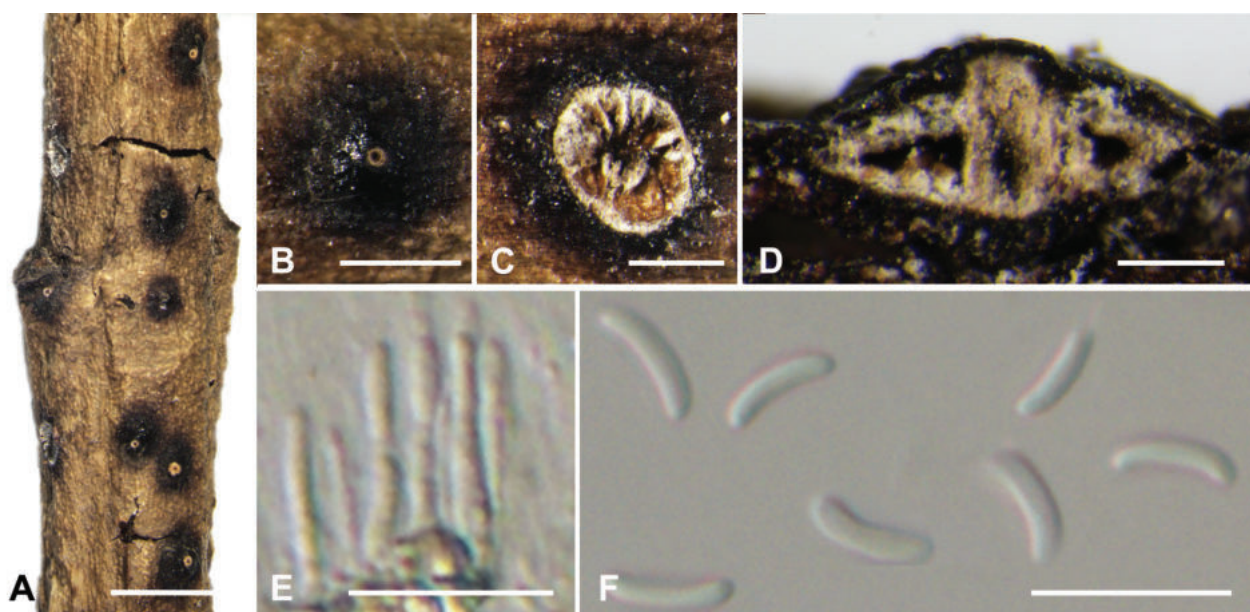
Figure 4. *Cytospora albodisca* from *Euonymus japonicus* (BJFC CF20230402) **A, B** habit of conidiomata on branch **C** transverse section through conidiomata **D** longitudinal section through conidiomata **E** conidiophores and conidiogenous cells **F** conidia. Scale bars: 2 mm (**A**); 1 mm (**B**); 500 μm (**C**); 200 μm (**D**); 10 μm (**E**, F).

bodisca is characterised by the pycnidial stromata submerged in the cortex with multiple locules, filamentous conidiophores producing hyaline, allantoid, eguttulate and smooth conidia. Phylogenetically, the isolates (CFCC 59459 and 59537) clustered together with *C. albodisca* with high statistical support (ML/BI = 100/1) (Fig. 2). Therefore, the isolate in this study was confirmed to be *C. albodisca*.

Cytospora euonymina X.L. Fan & C.M. Tian, Persoonia 45: 21 (2020)
Fig. 5

Description. *Sexual morph*: not observed. ***Asexual morph*: *Conidiomata pycnidial*,** immersed in the bark, scattered, producing black area on bark, erumpent through the surface, with multiple locules. ***Conceptacle*** absent. ***Ectostromatic disc*** honey to dark mouse grey, conspicuous, circular to ovoid, 200−500µm in diam, with one ostiole per disc. ***Ostiole*** in the centre of the disc, black, conspicuous, 80−200 µm diam. ***Locules*** numerous, subdivided frequently by invaginations with common walls, 400−750 µm in diam. ***Conidiophores*** borne along the locules, hyaline, unbranched or occasionally branched at the base or in the middle, thin-walled, 8−12 × 1.5−2 (av. = 10 ± 2.1 × 1.8 ± 0.3, n = 50) µm, embedded in a gelatinous layer. ***Conidiogenous cells*** enteroblastic, phialidic. ***Conidia*** hyaline, elongate-allantoid, smooth, aseptate, 5−7 × 1−2 (av. = 6 ± 0.5 × 1.5 ± 0.3, n = 50) µm.

Culture characteristics. Cultures on PDA are initially white, irregular, lacking aerial mycelium, fast growing up to 5 cm diam. after 3 d. Colonies pale white to light salmon after 30 d, pycnidia distributed sparsely over the medium surface.

Materials examined. CHINA, Beijing City, Fengtai Distinct, Qianling Mountain scenic area, 39°51'12.28"N, 116°5'17.74"E, from branches of *Salix babylonica*, 12 Apr 2023, A.L. Jia & X.L. Fan (BJFC CF20230403, living culture CFCC 59444; BJFC CF20230404, living culture CFCC 59479).

Notes. *Cytospora euonymina* was isolated from *Euonymus kiautschovicus* in Shanxi Province, China (Fan et al. 2020). It is characterised by having pycnidia covered by the darkened cuticle. Lin et al. (2023b) reported this species from
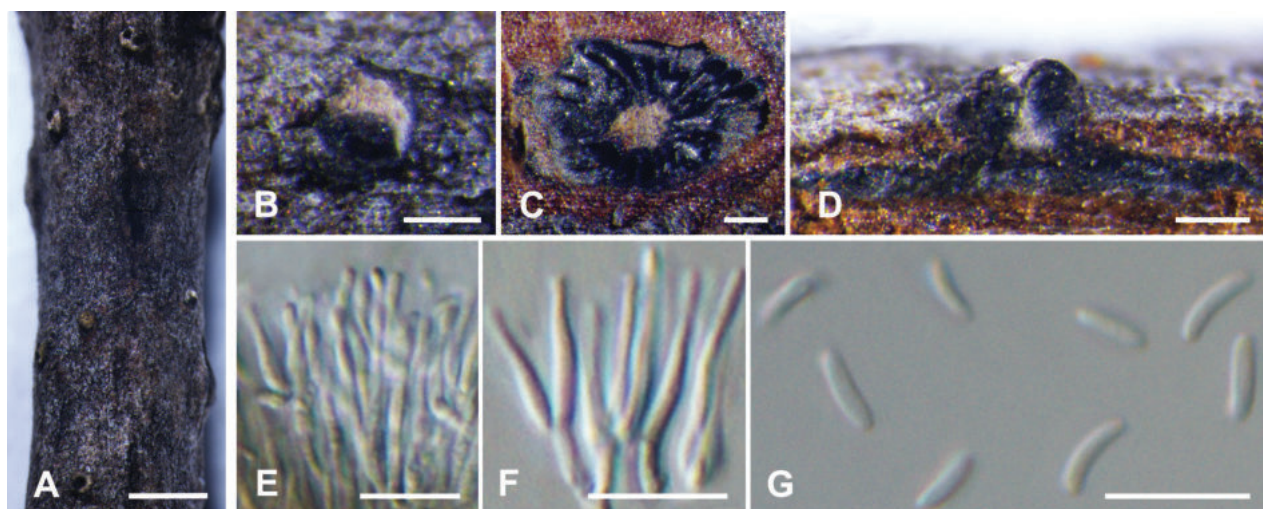

Figure 5. *Cytospora euonymina* from *Salix babylonica* (BJFC CF20230403) **A, B** habit of conidiomata on branch **C** transverse section through conidiomata **D** longitudinal section through conidiomata **E, F** conidiophores and conidiogenous cells **G** conidia. Scale bars: 500 µm (**A**); 200 µm (**B**); 100 µm (**C, D**); 10 µm (**E−G**).

leaves of *Euonymus japonicus.* In this study, two isolates grouped together with *C. euonymina* in ML and BI trees (ML/BI = 98/1). Therefore, they were identified as *C. euonymina*. Additionally, CFCC 59444 and 59479 extends its host range which were isolated from branches of *Salix babylonica* in the current study.

Cytospora fengtaiensis A.L. Jia & X.L. Fan, sp. nov.
MycoBank No: 850894
Fig. 6

Etymology. Named after the place where it was first collected, Fengtai District, Beijing City.

Typification. CHINA. Beijing City, Fengtai District, Qianling Mountain scenic area, 39°51'12.28"N, 116°5'17.74"E, from branches of *Acer palmatum* 'Atropurpureum', 7 Apr 2023, A.L. Jia & X.L. Fan (holotype BJFC CF20230405, ex-holotype living culture CFCC 59449); 39°51'12.51"N, 116°5'17.32"E, from branches of *Acer palmatum* 'Atropurpureum', 7 Apr 2023, A.L. Jia & X.L. Fan (paratype BJFC CF20230406, ex-paratype living culture CFCC 59442.

Description. *Sexual morph*: not observed. ***Asexual morph*: *Conidiomata pycnidial*,** immersed in the bark, scattered, producing black area on bark, circular to ovoid, with multiple locules, occasionally slightly erumpent through the surface. ***Conceptacle*** absent. ***Ectostromatic disc*** conspicuous, grey to black, discoid, circular to ovoid, 180−250 μm in diam., producing one ostiole per disc when mature. ***Ostiole*** grey to black, nearly at the same level as the disc surface, 70−105 μm in diam. Locules numerous, subdivided frequently by invaginations with common walls, circular to ovoid, 560−800 μm in diam. ***Conidiophores*** hyaline, unbranched, approximately cylindrical, 11−17 × 1.5−2 (av. = 14.7 ± 2.7 × 1.6 ± 0.3, n = 50) μm. ***Conidiogenous cells*** enteroblastic, phialidic. ***Conidia*** hyaline, elongate-allantoid, smooth, aseptate, 5−6 × 1−2 (av. = 5.5 ± 0.5 × 1.6 ± 0.2, n = 50) μm.

Figure 6. *Cytospora fengtaiensis* from *Acer palmatum* 'Atropurpureum' (BJFC CF20230405) **A, B** habit of conidiomata on branch **C** transverse section through conidiomata **D** longitudinal section through conidiomata **E** conidiophores and conidiogenous cells **F** conidia. Scale bars: 1 mm (**A**); 200 μm (**B−D**); 10 μm (**E, F**).

Culture characteristics. Cultures on PDA are initially white to pale vinaceous, growing slowly up to 3 cm after 3 d and entirely covering the 6 cm Petri dish after 7 d, becoming fawn after 14 d. Colonies are flat with a uniform texture, Colony margin irregular. After 30 d, *pycnidia* aggregated on surface.

Additional materials examined. CHINA. Beijing City, Fengtai District, Qianling Mountain scenic area, 39°51'11.45"N, 116°5'15.36"E, from branches of *Acer palmatum 'Atropurpureum'*, 7 Apr 2023, A.L. Jia & X.L. Fan (BJFC CF20230407, living culture CFCC 59525; BJFC CF20230408, living cultures CFCC 59526 and 59527).

Notes. *Cytospora fengtaiensis* is associated with canker disease of *Acer palmatum 'Atropurpureum'* in the current study. It can be identified by its conidiomata producing larger black areas on bark. Phylogenetically, five isolates in this study formed a distinct lineage in the phylogenetic trees of each individual gene (ITS, *act*, *rpb2*, *tef1-α* and *tub2*) and the combined gene dataset (Fig. 2).

Cytospora haidianensis X. Zhou & X.L. Fan, Forests 11: 524 (2020)
Fig. 7

Description. *Sexual morph*: not observed. *Asexual morph*: *Conidiomata pycnidial*, immersed in the bark, scattered, producing black area on bark, circular to ovoid, with multiple locules, occasionally slightly erumpent through the surface. *Conceptacle* absent. *Ectostromatic disc* isabelline to dark brick, conspicuous, circular to ovoid, 130−350 µm in diam, with one ostiole per disc. *Ostiole* in the centre of the disc, black, conspicuous, 90−180 µm in diam. *Locules* numerous, subdivided frequently by invaginations with common walls, circular to ovoid, 500−1200 µm in diam. *Conidiophores* hyaline, branched at the base or unbranched, approximately cylindrical, 12−19 × 1−1.5 (av. = 15.5 ± 4.3 × 1.1 ± 0.4, n = 50) µm. *Conidiogenous cells* enteroblastic, phialidic, subcylindrical to cylindrical. *Conidia* hyaline, elongate-allantoid, smooth, aseptate, thin-walled, 4.8−6 × 1.5−2 (av. = 5.3 ± 0.7 × 1.7 ± 0.3, n = 50) µm.

Cultural characteristics. Colonies on PDA are initially white after 3 d, becoming light brown after 14 d. The colonies are thin with a uniform texture, lacking aerial mycelium. *Pycnidia* were randomly observed on the surface of the colony after 30 d.

Materials examined. CHINA, Beijing City, Fengtai Distinct, Beigong National Forest Park, 39°52'20.46"N, 116°7'47.60"E, from branches of *Euonymus japonicus*, 12 Apr 2023, A.L. Jia & X.L. Fan (BJFC CF20230409, living culture CFCC 59450); Beigong National Forest Park, 39°52'20.46"N, 116°7'47.60"E, from branches of *Malus 'American'*, 12 Apr 2023, A.L. Jia & X.L. Fan (BJFC CF20230410, living culture CFCC 59475); Century Forest Park, 39°49'43"N, 116°14'27"E, from branches of *Acer pictum* subsp. *mono*, 18 May 2023, A.L. Jia & Y.X. Li (BJFC CF20230411, living culture CFCC 59471; BJFC CF20230412, living culture CFCC 59536).

Notes. *Cytospora haidianensis* was first introduced by Zhou et al. (2020) and which was isolated from *Euonymus alatus* in Beijing, China. This species has numerous locules with a central column of ostiolar tissue (Zhou et al. 2020). In this study, four isolates grouped together with *C. haidianensis* in ML and BI trees (ML/BI = 100/1). Therefore, they are identified as *Cytospora haidianensis*. The current study extends its host range to *Buxus megistophylla*, *Malus 'American'* and *Acer pictum* subsp. *mono*.
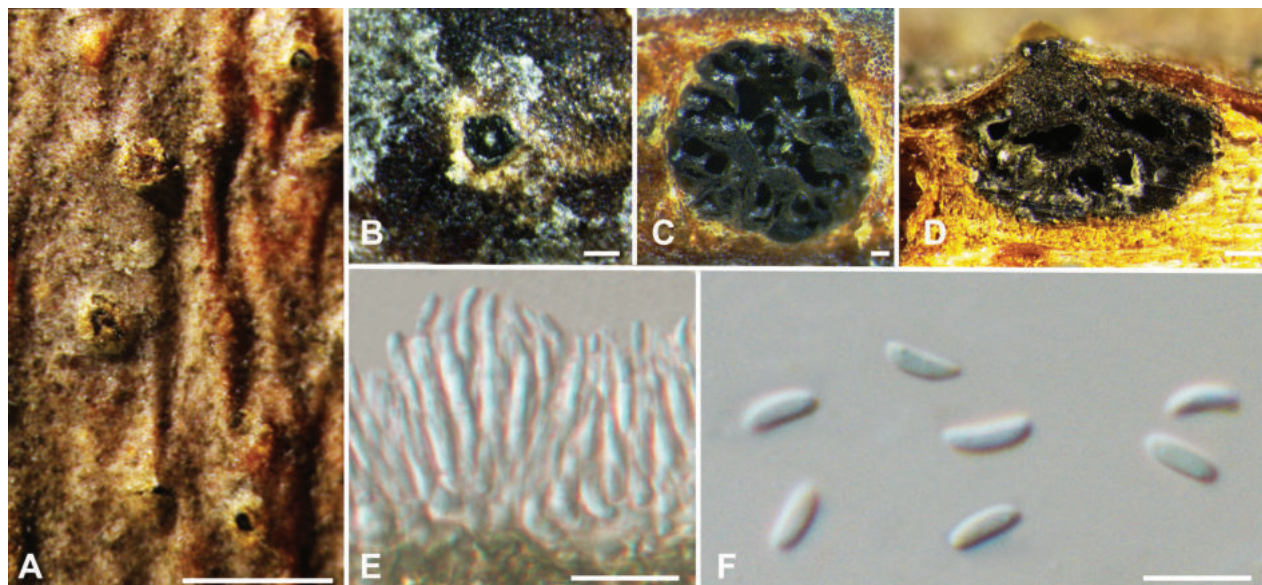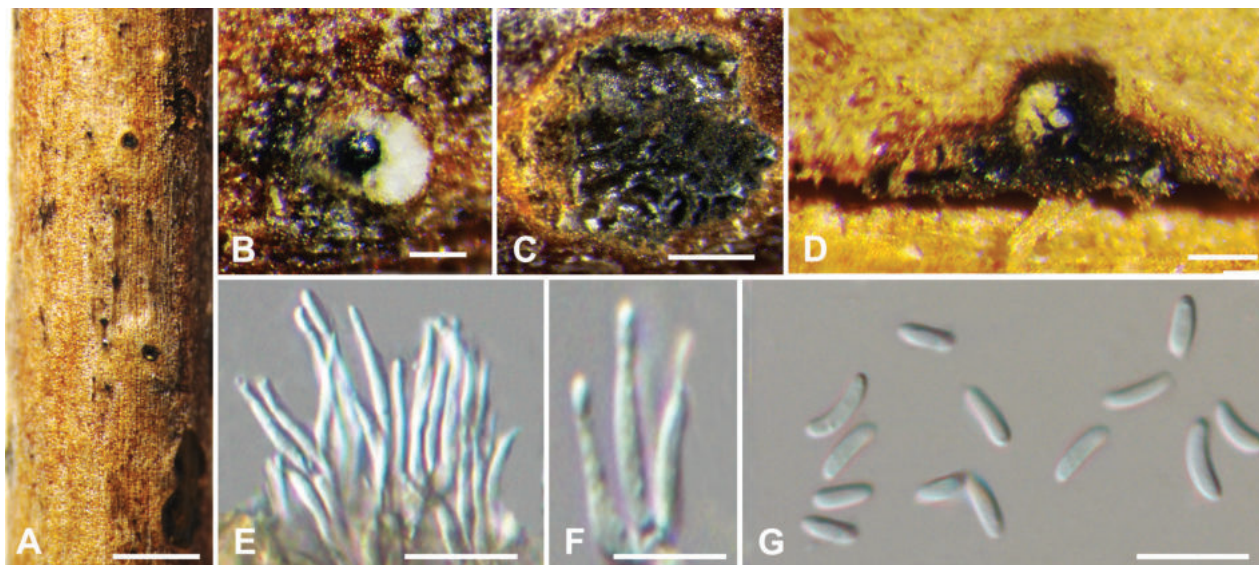
Figure 7. *Cytospora haidianensis* from *Salix babylonica* (BJFC CF20230411) **A, B** habit of conidiomata on branch **C** transverse section through conidiomata **D** longitudinal section through conidiomata **E, F** conidiophores and conidiogenous cells **G** conidia. Scale bars: 1 mm (**A**); 200 μm (**B–D**); 10 μm (**E–G**).

Cytospora pinea A.L. Jia & X.L. Fan, sp. nov.

MycoBank No: 850895

Fig. 8

Etymology. Named after the host genus on which it was collected, *Pinus*.

Typification. China, Beijing City, Fengtai Distinct, Lotus Pond Park, 39°53'27.64"N, 116°18'49.21"E, from branches of *Pinus bungeanae*, 9 Feb 2023, X.L. Fan (holotype BJFC CF20230413, ex-holotype living culture CFCC 59521; 39°53'27.21"N, 116°18'49.56"E, from branches of *Pinus bungeanae*, 9 Feb 2023, X.L. Fan (paratype BJFC CF20230415, ex-paratype living culture CFCC 59523).

Description. *Sexual morph*: not observed. *Asexual morph*: *Conidiomata pycnidial*, immersed in bark, scattered, nearly flat, slightly erumpent through the bark surface in a large area, with multiple locules. *Conceptacle* absent. *Ectostromatic disc* light brown to black, inconspicuous, circular to ovoid, with one *ostiole* per disc. *Ostiole* black, conspicuous, 150–200 μm diam. *Locules* numerous, irregular, subdivided frequently by invaginations with common walls, 980–1130 μm diam. *Conidiophores* borne along the locules, hyaline, branched at the base, in the middle or unbranched, thin-walled, 15–22 × 1.5–2.5 μm (av. = 18 ± 2.3 × 2 ± 0.3 μm, n = 30), embedded in a gelatinous layer. *Conidiogenous cells* enteroblastic, phialidic, sub-cylindrical, 3–7.5(–8) × 1–2 μm (av. = 4.5 ± 1.4 × 1.6 ± 0.3 μm, n = 50), tapering towards apices; arranged in rosettes. *Conidia* hyaline, allantoid, eguttulate, smooth, aseptate, thin-walled, 3.5–5 × 1–2 μm (av. = 4.3 ± 0.5 × 1.4 ± 0.2 μm, n = 50).

Culture characteristics. Cultures on PDA are initially white, growing slowly up to 2 cm in diam. after 3 d and becoming yellowish after 7–10 d. Colonies thin with a uniform texture, lacking aerial mycelium, entirely covering the 6 cm Petri dish after 14 d, with a regular edge. After 30 d, *pycnidia* irregularly distributed on culture surface.

Additional materials examined. China, Beijing City, Fengtai Distinct, Lotus Pond Park, 39°53'26.87"N, 116°18'43.46"E, from branches of *Pinus bungeanae*, 9 Feb 2023, X.L. Fan (BJFC CF20230414, living culture CFCC 59522; BJFC CF20230416, living culture CFCC 59524).

Figure 8. *Cytospora pinea* from *Pinus bungeanae* (BJFC CF20230413) **A, B** habit of conidiomata on branch **C** transverse section through conidiomata **D** longitudinal section through conidiomata **E** conidiophores and conidiogenous cells **F** conidia. Scale bars: 2 mm (**A**); 200 μm (**B, D**); 100 μm (**C**); 10 μm (**E, F**).

Notes. *Cytospora pinea* is associated with canker disease of *Pinus bungeanae* in China. *Cytospora pinea* is close to *C. bungeanaee* in the phylogenetic diagram (Fig. 2) and was isolated from the same host species *Pinus bungeanae* (Fan et al. 2020). It can be distinguished from *C. bungeanaee* by smaller conidiophores (3–7.5(–8) × 1–2 vs. 15–27(–30) × 1.5–2 μm in *C. bungeanaee*) and smaller locules (980–1130 vs. (1150–)1220–1480(–1600) μm in *C. bungeanaee*). Furthermore, *Cytospora pinea* has a black conspicuous ostiole per disc, whereas the ostiole of *C. bungeanaee* is inconspicuous. Phylogenetically, there are differences of 76/344 in the *act* region and 7/811 in the *tef1-α* gene with gaps.

Cytospora sorbariae **A.L. Jia & X.L. Fan, sp. nov.**
MycoBank No: 850896
Fig. 9

Etymology. Named after the host genus on which it was collected, *Sorbaria.*

Typification. China. Beijing City, Fengtai District, Beijing Garden Expo, 39°52'35.65"N, 116°11'4.02"E, from branches of *Sorbaria sorbifolia*, 7 Apr 2023, A.L. Jia & X.L. Fan (holotype BJFC CF20230417, ex-holotype living culture CFCC 59445); 39°52'35.43"N, 116°11'4.62"E, from branches of *Sorbaria sorbifolia*, 7 Apr.2023, A.L. Jia & X.L. Fan (paratype BJFC CF20230419, ex-paratype living culture CFCC 59529).

Description. Sexual morph: not observed. **Asexual morph: Conidiomata pycnidial** immersed in the bark, scattered, erumpent through the surface of bark in a large area, with multiple locules. **Conceptacle** absent. **Ectostromatic disc** brown to black, circular to ovoid, erumpent through the surface of bark in a large area, conspicuous when mature, 160–300 μm in diam., with one or two ostioles per disc. **Ostioles** grey to black, at the same or slightly above the level of the

Figure 9. *Cytospora sorbariae* from *Sorbaria sorbifolia* (BJFC CF20230417) **A, B** habit of conidiomata on branch **C** transverse section through conidiomata **D** longitudinal section through conidiomata **E, F** conidiophores and conidiogenous cells **G** conidia. Scale bars: 1 mm (**A**); 100 μm (**B–D**); 10 μm (**E–G**).

disc surface, 50–85 μm in diam. Locules numerous, subdivided frequently by invaginations with common walls, circular to ovoid, 550–750 μm in diam. ***Conidiophores*** hyaline, unbranched, approximately cylindrical, 14–18 × 1–1.5 μm. ***Conidiogenous cells*** enteroblastic, phialidic. ***Conidia*** hyaline, elongate-allantoid, smooth, aseptate, 5.5–7.5 × 1.5–2.5 (av. = 6.5 ± 0.7 × 2 ± 0.3, n = 50) μm.

Culture characteristics. Cultures on PDA are initially white, growing fast up to cover the 5.5 cm Petri dish after 3 d, becoming vinaceous buff after 7–10 d. Colonies are flat with a uniform texture, lacking aerial mycelium. Colony margin regular. After 30 d, *pycnidia* distributed irregularly on surface.

Additional materials examined. CHINA. Beijing City, Fengtai District, Beijing Garden Expo, 39°52'35.10"N, 116°11'4.31"E, from branches of *Sorbaria sorbifolia*, 7 Apr 2023, A.L. Jia & X.L. Fan (BJFC CF20230418, living culture 59443; BJFC CF20230420, living culture 59530).

Notes. *Cytospora sorbariae* is associated with canker disease of *Sorbaria sorbifolia* in the current study. It can be identified by having conidiomata with a column lenticular tissue in the centre and its distinct disc of stromata on branches. Additionally, the four strains are phylogenetically separated from all other available strains included in this study. The clear multi-gene phylogram placed it in a distinct clade with high support (ML/BI = 100/1, Fig. 2).

Discussion

The present study identified seven *Cytospora* species (*C. ailanthicola, C. albodisca, C. euonymina, C. fengtaiensis* sp. nov., *C. haidianensis, C. pinea* sp. nov. and *C. sorbariae* sp. nov.) from symptomatic branches and twigs associated with canker and dieback disease. This study represents an investigation of *Cytospora* species associated with canker disease in Fengtai District, Beijing and included a comprehensive analysis of DNA sequence data to compare the novelties with known *Cytospora* species.

In recent years, the study of *Cytospora* species on a particular host has received much attention from experts. For example, Jiang et al. (2020) identified six *Cytospora* species on Chinese chestnut (*Castanea mollissima*) which proved that *Cytospora* canker is a common disease on chestnut trees. Lin et al. (2023a) revealed the presence of *Cytospora* species from *Populus* in China and confirmed *Cytospora ailanthicola*, *C. chrysosperma*, *C. paratranslucens* and *C. sophoriopsis* as pathogens by pathogenicity tests. In this study, *Cytospora* species has a high diversity on *Malus spectabilis* and *Euonymus japonicus* (*Cytospora albodisca* and *C. haidianensis*). There are many studies about *Cytospora* related to *E. japonicus*, while few studies on *Malus spectabilis* have been recorded (Lin et al. 2023b). Therefore, many varieties of *Malus spectabilis* associated with *Cytospora* species need a systematic study and their pathogenicity is required to be confirmed in the future.

Cytospora included both generalist pathogens and specialist pathogens (Lawrence et al. 2018). Most *Cytospora* species have been discovered in a wide range of hosts (Adams et al. 2005, 2006; Lawrence et al. 2018; Norphanphoun et al. 2018; Fan et al. 2020). In this study, *Cytospora sorbariae* and *C. fengtaiensis* were introduced as two new species from the single host species, so more exhaustive sampling from other regions of the world is needed in future studies for a clear elucidation of their host ranges and distribution.

In this article, seven species, associated with *Cytospora* disease, were identified in Fengtai District, Beijing. A targeted prevention and treatment strategy is needed to be drawn up. The occurrence of *Cytospora* canker and dieback diseases can be minimised by removing dead and dying branches in the dry season and maintaining susceptible trees as strong as possible. Moreover, the occurrence of *Cytospora* canker diseases is affected by the environment, distribution and transmission (Fan et al. 2015b), which may act as potential inoculum sources for other hosts in natural and artificial environments.

This study focused on *Cytospora* species in Fengtai District of Beijing, an attractive location with a high richness of fungal species (Zhu et al. 2018b, 2019). The descriptions and molecular data of *Cytospora* in this study could provide a resource for future studies in this genus and lay the foundation for the future investigation of canker disease caused by *Cytospora* species.

Additional information

Conflict of interest

The authors have declared that no competing interests exist.

Ethical statement

No ethical statement was reported.

Funding

Author contributions

Conceptualisation: XF, AJ. Formal analysis: BC, AJ. Funding acquisition: XF. Investigation: XF, AJ, HL. Methodology: AJ. Resources: YX, BL, XF. Software: AJ, XF. Supervision:

XF. Validation: AJ, HL. Visualisation: AJ. Writing - original draft: AJ. Writing - review and editing: XF.

Author ORCIDs

Aoli Jia ⓘ https://orcid.org/0009-0004-0265-5454
Xinlei Fan ⓘ https://orcid.org/0000-0002-4946-4442

Data availability

All of the data that support the findings of this study are available in the main text.

References

Adams GC, Roux J, Wingfield MJ, Common R (2005) Phylogenetic relationships and morphology of *Cytospora* species and related teleomorphs (Ascomycota, Diaporthales, Valsaceae) from *Eucalyptus*. Studies in Mycology 52: 1–144.

Adams GC, Roux J, Wingfield MJ (2006) *Cytospora* species (Ascomycota, Diaporthales, Valsaceae), introduced and native pathogens of trees in South Africa. Australasian Plant Pathology 35(5): 521–548. https://doi.org/10.1071/AP06058

Barr ME (1978) The Diaporthales in North America with emphasis on *Gnomonia* and its segregates. Mycologia Memoir 7: 1–232.

Carbone I, Kohn LM (1999) A method for designing primer sets for speciation studies in filamentous ascomycetes. Mycologia 91(3): 553–556. https://doi.org/10.1080/00275514.1999.12061051

Doyle JJ, Doyle JL (1990) Isolation of plant DNA from fresh tissue. Focus (San Francisco, Calif.) 12: 13–15.

Ehrenberg CG (1818) Sylvae Mycologicae Berolinenses. Formis Theophili Bruschcke, Berlin, Germany.

Fan XL, Hyde KD, Liu M, Liang YM, Tian CM (2015a) *Cytospora* species associated with walnut canker disease in China, with description of a new species *C. gigalocus*. Fungal Biology 119(5): 310–319. https://doi.org/10.1016/j.funbio.2014.12.011

Fan XL, Hyde KD, Yang Q, Liang YM, Ma R, Tian CM (2015b) *Cytospora* species associated with canker disease of three anti-desertification plants in northwestern China. Phytotaxa 197(4): 227–244. https://doi.org/10.11646/phytotaxa.197.4.1

Fan XL, Bezerra JDP, Tian CM, Crous PW (2020) *Cytospora* (Diaporthales) in China. Persoonia 45(1): 1–45. https://doi.org/10.3767/persoonia.2020.45.01

Fries EM (1823) Systema mycologicum. Vol. 2, Greifswald, Germany.

Glass NL, Donaldson GC (1995) Development of primer sets designed for use with the PCR to amplify conserved genes from filamentous ascomycetes. Applied and Environmental Microbiology 61(4): 1323–1330. https://doi.org/10.1128/aem.61.4.1323-1330.1995

Guindon S, Dufayard JF, Lefort V, Anisimova M, Hordijk W, Gascuel HO (2010) New algorithms and methods to estimate maximum-likelihood phylogenies: Assessing the performance of PhyML 3.0. Systematic Biology 59(3): 307–321. https://doi.org/10.1093/sysbio/syq010

Gvritishvili MN (1982) The fungal genus *Cytospora* in the USSR. Izdatelstv Sabchota Sakarstvelo, Tbilisi, Russia.

Hillis DM, Bull JJ (1993) An empirical test of bootstrapping as a method for assess in confidence in phylogenetic analysis. Systematic Biology 42(2): 182–192. https://doi.org/10.1093/sysbio/42.2.182

Jiang N, Yang Q, Fan XL, Tian CM (2020) Identification of six *Cytospora* species on Chinese chestnut in China. MycoKeys 62: 1–25. https://doi.org/10.3897/mycokeys.62.47425

Katoh K, Standley DM (2013) MAFFT multiple sequence alignment software version 7: Improvements in performance and usability. Molecular Biology and Evolution 30(4): 772–780. https://doi.org/10.1093/molbev/mst010

Kobayashi T (1970) Taxonomic studies of Japanese Diaporthaceae with special reference to their life-histories. Tokyo, Japan, 242 pp.

Lawrence DP, Holland LA, Nouri MT, Travadon R, Trouillas FP (2018) Molecular phylogeny of *Cytospora* species associated with canker diseases of fruit and nut crops in California, with the descriptions of ten new species and one new combination. IMA Fungus 9(2): 333–369. https://doi.org/10.5598/imafungus.2018.09.02.07

Lin L, Pan M, Tian CM, Fan XL (2022) Fungal richness of *Cytospora* species associated with willow canker disease in China. Journal of Fungi (Basel, Switzerland) 8(4): 377. https://doi.org/10.3390/jof8040377

Lin L, Pan M, Bezerra JDP, Tian CM, Fan XL (2023a) Re-evaluation of the fungal diversity and pathogenicity of *Cytospora* species from *Populus* in China. Plant Disease 107(1): 83–96. https://doi.org/10.1094/PDIS-02-22-0260-RE

Lin L, Pan M, Gao H, Tian CM, Fan XL (2023b) The potential fungal pathogens of *Euonymus japonicus* in Beijing, China. Journal of Fungi (Basel, Switzerland) 9(2): 271. https://doi.org/10.3390/jof9020271

Liu YJ, Whelen S, Hall BD (1999) Phylogenetic relationships among ascomycetes: Evidence from an RNA polymerse II subunit. Molecular Biology and Evolution 16(12): 1799–1808. https://doi.org/10.1093/oxfordjournals.molbev.a026092

Liu H, Cui YM, Wang L, Zhang DK, Liu XH, Zhang GM (2022) Evaluation on plant diversity in urbanization area of Beijing City. Journal of Beijing Forestry University 44: 48–55.

Norphanphoun C, Doilom M, Daranagama DA, Phookamsak R, Wen TC, Bulgakov TS, Hyde KD (2017) Revisiting the genus *Cytospora* and allied species. Mycosphere 8(1): 51–97. https://doi.org/10.5943/mycosphere/8/1/7

Norphanphoun C, Raspé O, Jeewon R, Wen T-C, Hyde KD (2018) Morphological and phylogenetic characterization of novel *Cytospora* species associated with mangroves. MycoKeys 38: 93–120. https://doi.org/10.3897/mycokeys.38.28011

Pan M, Zhu HY, Bonthond G, Tian CM, Fan XL (2020) High diversity of *Cytospora* associated with canker and dieback of Rosaceae in China, with 10 new species Described. Frontiers in Plant Science 11: 690. https://doi.org/10.3389/fpls.2020.00690

Pan M, Zhu HY, Tian CM, Huang MR, Fan XL (2021) Assessment of *Cytospora* isolates from conifer cankers in China, with the descriptions of four new *Cytospora* species. Frontiers in Plant Science 12: 636460. https://doi.org/10.3389/fpls.2021.636460

Posada D, Crandall KA (1998) Modeltest: Testing the model of DNA substitution. Bioinformatics (Oxford, England) 14(9): 817–818. https://doi.org/10.1093/bioinformatics/14.9.817

Rayner RW (1970) A Mycological Colour Chart. Commonwealth Mycological Institute, Kew, UK, 33 pp.

Rehner SA, Buckley E (2005) A *Beauveria* phylogeny inferred from nuclear ITS and EF*1-α* sequences: Evidence for cryptic diversification and links to *Cordyceps* teleomorphs. Mycologia 97(1): 84–98. https://doi.org/10.3852/mycologia.97.1.84

Ronquist F, Huelsenbeck JP (2003) MrBayes 3: Bayesian phylogenetic inference under mixed models. Bioinformatics (Oxford, England) 19(12): 1572–1574. https://doi.org/10.1093/bioinformatics/btg180

Rossman AY, Adams GC, Cannon PF, Castlebury LA, Crous PW, Gryzenhout M, Jaklitsch WM, Mejia LC, Stoykov D, Udayanga D, Voglmayr H, Walker M (2015) Recommendations of generic names in Diaporthales competing for protection or use. IMA Fungus 6(1): 145–154. https://doi.org/10.5598/imafungus.2015.06.01.09

Saccardo PA (1884) Sylloge Fungorum III. Typis Seminarii, Italy.

Sinclair WA, Lyon HH, Johnson WT (1987) Diseases of Trees and Shrubs. Coinstock Publishing Associates. Cornell University Press, USA, 680 pp.

Spielman LJ (1983) Taxonomy and biology of *Valsa* species on hardwoods in North America, with special reference to species on maples. Cornell University, New York, USA.

Spielman LJ (1985) A monograph of *Valsa* on hardwoods in North America. Canadian Journal of Botany 63(8): 1355–1378. https://doi.org/10.1139/b85-190

Sutton BC (1980) The Coelomycetes: Fungi Imperfecti with pycnidia, acervuli and stromata. Commonwealth Mycological Institute, Kew, UK, 696 pp.

Tamura K, Stecher G, Peterson D, Filipski A, Kumar S (2013) MEGA6: Molecular evolutionary genetics analysis version 6.0. Molecular Biology and Evolution 30(12): 2725–2729. https://doi.org/10.1093/molbev/mst197

White TJ, Bruns T, Lee S, Taylor J (1990) Amplifcation and direct sequencing of fungal ribosomal RNA genes for phylogenetics. PCR Protocols: a guide to methods and applications 18: 315–322. https://doi.org/10.1016/B978-0-12-372180-8.50042-1

Wijayawardene NN, Hyde KD, Lumbsch HT, Liu JK, Maharachchikumbura SSN, Ekanayaka AH, Tian Q, Phookamsak R (2018) Outline of Ascomycota: 2017. Fungal Diversity 88(1): 167–263. https://doi.org/10.1007/s13225-018-0394-8

Wingfield MJ, Beer ZWD, Slippers B, Wingfield BD, Groenewald JZ, Lombard L, Crous PW (2012) One fungus, one name promotes progressive plant pathology. Molecular Plant Pathology 13: 604–613. https://doi.org/10.1111/j.1364-3703.2011.00768.x

Zhou X, Pan M, Li HY, Tian CM, Fan XL (2020) Dieback of *Euonymus alatus* (Celastraceae) caused by *Cytospora haidianensis* sp. nov. in China. Forests 11(5): 524. https://doi.org/10.3390/f11050524

Zhu HY, Tian CM, Fan XL (2018b) Studies of botryosphaerialean fungi associated with canker and dieback of tree hosts in Dongling Mountain of China. Phytotaxa 348(2): 63–76. https://doi.org/10.11646/phytotaxa.348.2.1

Zhu HY, Pan M, Bonthond G, Tian CM, Fan XL (2019) Diaporthalean fungi associated with canker and dieback of trees from Mount Dongling in Beijing, China. MycoKeys 59: 67–94. https://doi.org/10.3897/mycokeys.59.38055

MycoKeys

Taxonomic novelties and global biogeography of *Montagnula* (Ascomycota, Didymosphaeriaceae)

Dhanushka N. Wanasinghe[1] , Thilina S. Nimalrathna[2,3,4,5] , Li Qin Xian[1] , Turki Kh. Faraj[6] , Jianchu Xu[1,7] , Peter E. Mortimer[1]

1 Honghe Center for Mountain Futures, Kunming Institute of Botany, Chinese Academy of Sciences, Honghe County 654400, Yunnan, China

2 CAS Key Laboratory of Tropical Forest Ecology, Xishuangbanna Tropical Botanical Garden, Chinese Academy of Sciences, Menglun, Mengla, Yunnan, China

3 Southeast Asia Biodiversity Research Institute, Chinese Academy of Sciences & Center for Integrative Conservation, Xishuangbanna Tropical Botanical Garden, Chinese Academy of Sciences, Mengla, Yunnan 666303, China

4 Yunnan International Joint Laboratory of Southeast Asia Biodiversity Conservation & Yunnan Key Laboratory for Conservation of Tropical Rainforests and Asian Elephants, Menglun, Mengla, Yunnan 666303, China

5 International College, University of Chinese Academy of Sciences, Beijing, China

6 Department of Soil Science, College of Food and Agriculture Sciences, King Saud University, P.O. Box 145111, Riyadh 11362, Saudi Arabia

7 CIFOR-ICRAF China Country Program, Kunming, Yunnan, China

Corresponding authors: Jianchu Xu (jxu@mail.kib.ac.cn); Peter E. Mortimer (peter@mail.kib.ac.cn)

OPEN ACCESS

Abstract

Whilst conducting surveys of lignicolous microfungi in Yunnan Province, we collected a large number of taxa that resemble *Montagnula* (Didymosphaeriaceae, Pleosporales). Our phylogenetic study on *Montagnula* involved analysing sequence data from ribosomal RNA genes (nc18S, nc28S, ITS) and protein-coding genes (*rpb*2, *tef*1-α). We present a biphasic approach (morphological and molecular phylogenetic evidence) that supports the recognition of four new species in *Montagnula viz*., *M. lijiangensis*, *M. menglaensis*, *M. shangrilana* and *M. thevetiae*. The global diversity of *Montagnula* is also inferred from metabarcoding data and published records based on field observations. Metabarcoding data from GlobalFungi and field observations provided insights into the global diversity and distribution patterns of *Montagnula*. Studies conducted in Asia, Australia, Europe, and North America revealed a concentration of *Montagnula* species, suggesting regional variations in ecological preferences and distribution. *Montagnula* species were found on various substrates, with sediments yielding a high number of sequences. Poaceae emerged as a significant contributor, indicating a potential association between *Montagnula* species and grasses. Culture-based investigations from previously published data revealed *Montagnula* species associations with 105 plant genera (in 45 plant families), across 55 countries, highlighting their wide ecological range and adaptability. This study enhances our understanding of the taxonomy, distribution, and ecological preferences of *Montagnula* species. It emphasizes their role in the decomposition of organic matter in grasslands and savannah systems and suggests further investigation into their functional roles in ecosystem processes. The global distribution patterns and ecological interactions of *Montagnula* species underscore the need for continued research and conservation efforts.

Key words: Global distribution, microfungi, molecular phylogeny, taxonomy, Yunnan

Introduction

Fungi are the second largest group of eukaryotes, performing vital ecological functions such as decomposition, mutualism, and pathogenesis to plants and animals (Tedersoo et al. 2014). Ascomycota, which forms the largest phylum of Fungi, and includes the genus *Montagnula*, is an incredibly diverse group, with an estimated global species richness of ~154,500 species (Bánki et al. 2023). Despite their ecological and economic importance, many Ascomycota species remain undescribed, and their distribution and diversity have yet to be properly determined (Maharachchikumbura et al. 2021a, b; Wijayawardene et al. 2022). This is somewhat due to the fact that many Ascomycota species are microscopic and inconspicuous, making them difficult to find and subsequently study, or sometimes these smaller species can be overlooked with studies focussing on more charismatic species of macrofungi (Wanasinghe et al. 2022a). The investigation of taxonomic and phylogenetic systematics in Ascomycota is bridging crucial knowledge gaps and enhancing our understanding of this particular group of fungi. *Montagnula* (typified with *M. infernalis*), is an example of a relatively understudied genus within Ascomycota, and many species remain undescribed. Understanding the taxonomic, phylogenetic and host relationships between *Montagnula* species will help us better understand how they have diversified and adapted to different habitats in various ecological zones. These data are useful to make predictions about the ecology and biology of the genus and to guide future research into their interactions with other organisms and their roles in ecosystem processes. Understanding the taxonomy and phylogeny of *Montagnula* is also important for conservation purposes. With ongoing habitat destruction and climate change, it is more important than ever to understand the current diversity and distribution of fungi around the world (Wanasinghe et al. 2022a).

Therefore, our research group at the Center for Mountain Futures (CMF), has been conducting investigations into the microfungal diversity and biogeography in Yunnan Province, Southwest China. Specifically, we are focusing on various substrates such as leaf and woody litter, aiming to clarify the taxonomy of fungi on these substrates, using morphology in conjunction with multigene phylogeny. As a result, we have successfully isolated numerous anamorphic and teleomorphic Ascomycota species in Yunnan, and we have published our findings based on different themes, including their relationship with hosts, substrates, and localities (Thiyagaraja et al. 2019, 2020, 2021; Abeywickrama et al. 2020; Wanasinghe et al. 2020, 2021, 2022b, 2023; Yasanthika et al. 2020; Bundhun et al. 2021; Dissanayake et al. 2021; Gao et al. 2021; Monkai et al. 2021; Mortimer et al. 2021; Ren et al. 2021a, b, 2022a, b; Aluthmuhandiram et al. 2022; Maharachchikumbura et al. 2022; Wanasinghe and Mortimer 2022). The objectives of this study are (1) to identify the lignicolous *Montagnula* species collected from Yunnan using both morphological and phylogenetic approaches, and (2) to utilize metabarcoding data and published records based on field observations to infer the global diversity and biogeography of *Montagnula*. The analyses conducted in this study revealed four new species and four existing species of *Montagnula*, in Yunnan. The discovery of several previously undescribed Ascomycota species in the genus *Montagnula* in Yunnan Province is a significant advancement in our understanding of the diversity and distribu-

tion of this group of fungi. Furthermore, the utilization of metabarcoding data and published records based on field observations to infer the global diversity of *Montagnula* demonstrates the potential of these approaches in elucidating the biogeography of fungi on a large scale. By studying and documenting the diversity of *Montagnula* species, we can enhance our appreciation for the importance of conserving these fungi and their habitats, and take appropriate measures to mitigate the threats they face.

Materials and methods

Sample collecting

Fresh fungal materials were collected from dead woody twigs from Honghe, Kunming, Mengla, Shangri-La and Yulong Counties, all within Yunnan Province, China, during the dry season (January, March, April) and wet season (August, September). To preserve their integrity, the specimens were transported to the laboratory in Zip lock plastic bags during the dry season and in paper bags during the wet season.

Morphological observations

The morphology of external and internal macro-/micro-structures were observed as described in Wanasinghe et al. (2017, 2018a, 2020). Hand sections of the ascomata were mounted in distilled water and the following characteristics were evaluated and measured: ascomata diameter, height, color and shape; width of peridium; and height and diameter of ostioles. Length and width (at the widest point) of asci and ascospores. Images were captured with a Canon EOS 600D digital camera fitted to a Nikon ECLIPSE Ni compound microscope. Macroscopic images of colonies were documented using an iPhone XS Max (Apple Inc., Cupertino, CA, USA) with daylight. Measurements were made with the Tarosoft (R) Image Frame Work program, and images used for figures were processed with Adobe Photoshop CS5 Extended version 10.0 software (Adobe Systems, San José, CA, USA).

Isolation

Single spore isolation was conducted by following the methods described in Wanasinghe et al. (2018b). Germinated spores were individually transferred to potato dextrose agar (PDA: 39 g/L distilled water, Difco potato dextrose) plates and grown at 20 °C in the daylight.

Deposition of specimens, cultures and registering names

The living cultures were deposited at the Kunming Institute of Botany Culture Collection (KUNCC), Kunming, China. Dry herbarium materials were deposited in the herbarium of Cryptogams Kunming Institute of Botany, Academia Sinica (KUN-HKAS). MycoBank numbers have been obtained as outlined in MycoBank (http://www.MycoBank.org accessed on 21 September 2023) for the novel taxa.

DNA extraction, PCR amplifications and sequencing

Genomic DNA was extracted from the axenic mycelium as described by Phookamsak et al. (2017). Mycelia for DNA extraction from each isolate were grown on PDA for 3–4 weeks at 20 °C and total genomic DNA was extracted from approximately 150 ± 50 mg axenic mycelium scraped from the edges of the growing culture. Mycelium was ground to a fine powder with liquid nitrogen and DNA extracted using the Biospin Fungus Genomic DNA Extraction Kit-BSC14S1 (BioFlux, P.R. China) following the instructions of the manufacturer. When fungi failed to grow in culture, DNA extraction was carried out directly from fruiting bodies, adhering to the protocol outlined by Wanasinghe et al. (2018b). DNA to be used as templates for Polymerase Chain Reaction (PCR) were stored at 4 °C for use in regular work and duplicated at -20 °C for long-term storage.

We used primers ITS5/ITS4 (White et al. 1990), LR0R/LR5 (Vilgalys and Hester 1990; Rehner and Samuels 1994), NS1/NS4 (White et al. 1990), EF1-983F/EF1-2218R (Liu et al. 1999; Rehner and Buckley 2005), and fRPB2-5f/fRPB2-7cR (Sung et al. 2007) to amplify sequence data for a total of five markers: the internal transcribed spacers (ITS), partial 28S large subunit rDNA (LSU), partial 18S small subunit rDNA (SSU), translation elongation factor 1-α (*tef*1-α), and RNA polymerase II second largest subunit (*rpb*2). PCR amplifications were performed following the methods described in Wanasinghe et al. (2021). We sequenced complementary strands with the same primers used for PCR amplifications and sequencing was done from a commercial sequencing provider (BGI, Ltd Shenzhen, P.R. China). The nucleotide sequence data obtained were deposited in GenBank (Table 2).

Sequencing assembly and alignments

Sequences generated from different primers of the five genes were analysed with other sequences retrieved from GenBank (Table 2). Sequences with high similarity indices were determined from a BLAST search to find the closest matches with taxa in Didymosphaeriaceae, using recently published data (Du et al. 2021; Ren et al. 2022a; Sun et al. 2023). The multiple alignments of all consensus sequences, as well as the reference sequences were automatically generated with MAFFT v. 7 (Katoh et al. 2019), and manually corrected where necessary using BioEdit v. 7.0.5.2 (Hall 1999).

Phylogenetic inference

The single-locus datasets were examined for topological incongruence among loci for members of the analyses. The alignments were concatenated into a multi-locus alignment that was analyzed with maximum likelihood (ML) and Bayesian (BI) phylogenetic methods in the CIPRES Science Gateway (Miller et al. 2010). ML tree was obtained using RAxML-HPC2 on XSEDE v. 8.2.10 (Stamatakis 2014) with applying GTR+G+I model. Support values were obtained with 1,000 bp replicates (Felsenstein 1985). ML bootstrap values equal or greater than 75% are given above each node. The best-fit model was selected with respect to Bayesian Information Criterion (BIC) scores using the IQ-TREE web application at http://iqtree.cibiv.univie.ac.at (Trifinopoulos et al. 2016). For model selection, we restricted the pool of available models to JC, F81, HKY, SYM and GTR (Ronquist et al. 2011). BI

were performed with two parallel runs of 2 M generations, using four chains in each, and retaining one tree every 100 generations. The dataset was partitioned by gene region, and a GTR + G + I model was applied to each partition, ending the run automatically when standard deviation of split frequencies dropped below 0.01 with a burn-in fraction of 0.25. A fifty percent majority rule consensus tree was obtained after discarding the first 25% of trees, and posterior probabilities were used as a measure of nodal support. The posterior probability in BI (BYPP) greater than 0.95 are given above each node. Phylograms were visualized with FigTree v1.4.0 program (Rambaut 2012) and reorganized in Microsoft power point (2019).

The biogeographical distribution of *Montagnula*

In our initial approach, we obtained detailed geographical distribution information for the *Montagnula* genus. This data was extracted from the GlobalFungi database (https://globalfungi.com, accessed on 04 December 2023), as outlined by Větrovský et al. (2020). The database provided information on the countries and precise geographical coordinates of recorded *Montagnula* occurrences. To visualize these occurrences, we employed a range of packages in R version 4.2.1 (R Core Team 2022), including 'sf' (Pebesma and Bivand 2023), 'raster' (Hijmans 2023), 'rgdal' (Bivand et al. 2022), and 'ggplot2' (Wickham 2011). In our map, each marker signifies an individual occurrence of *Montagnula*. These occurrences are visually distinguished by a color scheme, with each color denoting the specific biome from which the samples were collected, as illustrated in Fig. 2a. Additionally, we have developed two donut charts, showcased in Fig. 2b, c, which effectively illustrate the distribution of *Montagnula* sequences. These charts present the sequence abundance as a percentage of the total, segmented across various biomes and continents, providing a clear visual breakdown of their distribution. Furthermore, we have gathered Environmental DNA (eDNA) data from diverse sources in metabarcoding studies focusing on fungi, as found in the GlobalFungi database (Fig. 3). This dataset included specifics about eDNA sources, locations of the studies, and the sequence abundance of *Montagnula* sequences. It is important to note that the sequence abundance in metabarcoding studies might not always accurately represent the actual abundance of species in a habitat. Nonetheless, these data can provide valuable insights into the potential rarity or prevalence of the group in the eDNA source. We analyzed the sequence abundance in diverse eDNA samples from different continents. Before visualization, the abundance values were normalized via a logarithmic transformation to ensure a standardized and comparable presentation of *Montagnula* sequence abundance. Post-transformation abundance data were visualized using the 'ggplot2' package, aiding in highlighting the focus areas of metabarcoding and identifying the environmental sample types from which *Montagnula* sequences were derived across various continents (Figs 2, 3).

The host relations of *Montagnula*

To illustrate the host specificity of *Montagnula* species, we utilized detailed information regarding host species from the literature (Table 1). This enabled us to create informative bar plots displaying the host preferences of *Montagnula* species (Fig. 4). This information was visualized using the 'ggplot2' package in R.

Table 1. Accepted species in *Montagnula* including their host and geographic location.

Species	Host species	Host family	Country	Reference
Montagnula acaciae	*Acacia auriculiformis*	Fabaceae	Thailand	Tennakoon et al. (2022)[#]
Montagnula aloes	*Aloe* sp.	Asphodelaceae	South Africa	Crous et al. (2012)[#]
Montagnula appendiculata	*Zea mays*	Poaceae	China	Aptroot (2004)[#]
Montagnula aquatica	Submerged wood	NA	Thailand	Sun et al. (2023)[#]
	Dead woody litter	NA	China	This study[#]
Montagnula aquilariae	*Aquilaria sinensis*	Thymelaeaceae	China	Hyde et al. (2023)[#]
	Dead woody litter	NA	China	This study[#]
Montagnula baatanensis	*Agave* sp.	Asparagaceae	USA	Crivelli (1983)
Montagnula bellevaliae	*Bellevalia romana*	Asparagaceae	Italy	Hongsanan et al. (2015)[#]
Montagnula camporesii	*Dipsacus* sp.	Caprifoliaceae	Italy	Hyde et al. (2020)[#]
Montagnula camarae	*Cytisus scoparius*	Fabaceae	Portugal	Checa (2004)
Montagnula chiangraiensis	*Chromolaena odorata*	Asteraceae	Thailand	Mapook et al. (2020)[#]
Montagnula chromolaenae	*Chromolaena odorata*	Asteraceae	Thailand	Mapook et al. (2020)[#]
Montagnula chromolaenicola	*Chromolaena odorata*	Asteraceae	Thailand	Mapook et al. (2020)[#]
	Lagerstroemia sp.	Lythraceae	China	This study[#]
Montagnula cirsii	*Cirsium* sp.	Asteraceae	Italy	Hyde et al. (2016)[#]
Montagnula cylindrospora	Human skin[##]	NA	USA	Crous et al. (2020)[#]
Montagnula dasylirionis	*Dasylirion* sp.	Asparagaceae	USA	Ramaley and Barr (1995)
Montagnula donacina	*Acacia reficiens*	Fabaceae	Namibia	Aptroot (1995)
	Acacia sp.	Fabaceae	India	Aptroot (1995)
	Adhatoda vasica	Acanthaceae	India	Aptroot (1995)
	Ailanthus altissima	Simaroubaceae	India	Aptroot (1995)
	Althaea rosea	Malvaceae	China	Aptroot (1995)
	Annona squamosa	Annonaceae	India	Aptroot (1995)
	Arundo donax	Poaceae	Portugal	Aptroot (1995)
	Bambusoideae	Poaceae	Brazil	Aptroot (1995)
	Bambusoideae	Poaceae	Papua New Guinea	Aptroot (1995)
	Cajanus cajan	Fabaceae	India	Aptroot (1995)
	Calamus australis	Arecaceae	Australia	Hyde et al. (1999)
	Careya arborea	Lecythidaceae	India	Aptroot (1995)
	Citrus aurantiifolia	Rutaceae	India	Aptroot (1995)
	Clerodendrum infortunatum	Lamiaceae	India	Aptroot (1995)
	Clerodendrum multiflorum	Lamiaceae	India	Aptroot (1995)
	Coffea arabica	Rubiaceae	Paraguay	Aptroot (1995)
	Coffea robusta	Rubiaceae	Central African Republic	Aptroot (1995)
	Craterellus odoratus[##]	Cantharellaceae	China	Zhao et al. (2018)[#]
	Duranta repens	Verbenaceae	India	Aptroot (1995)
	Ficus glomerata	Moraceae	India	Aptroot (1995)
	Funtumia africana	Apocynaceae	Sierra Leone	Aptroot (1995)
	Hibiscus sp.	Malvaceae	India	Aptroot (1995)
	Ipomoea carnea	Convolvulaceae	India	Aptroot (1995)
	Mallotus philippinensis	Euphorbiaceae	India	Aptroot (1995)
	Morus alba	Moraceae	India	Aptroot (1995)
	Litchi litchi	Sapindaceae	Myanmar	Thaung (2008)

Species	Host species	Host family	Country	Reference
Montagnula donacina	*Nerium odorum*	Apocynaceae	India	Aptroot (1995)
	Paeonia suffruticosa	Paeoniaceae	China	Li et al. (2023)#
	Phyllostachys bambusoides	Poaceae	Japan	Wang et al. (2004)
	Pistacia sp.	Anacardiaceae	India	Aptroot (1995)
	Platanus sp.	Platanaceae	USA	Wang et al. (2004)
	Premna cumingiana	Lamiaceae	Philippines	Aptroot (1995)
	Pseudosasa japonica	Poaceae	France	Aptroot (1995)
	Saccharum officinarum	Poaceae	Brazil	Aptroot (1995)
	Unknown stem	NA	India	Aptroot (1995)
	Tectona grandis	Lamiaceae	India	Aptroot (1995)
	Terminalia tomentosa	Combretaceae	India	Aptroot (1995)
	Trachycarpus fortunei	Arecaceae	China	Hyde et al. (1999)
	Unknown bark	NA	India	Aptroot (1995)
	Unknown branches	NA	Sierra Leone	Aptroot (1995)
	Unknown plant	NA	Colombia	Aptroot (1995)
	Dead wood	NA	China	Sun et al. (2023)#
	Dead wood	NA	Thailand	Ren et al. (2022a)#
	Dead wood	NA	China	This study#
	Vitis vinifera	Vitaceae	Australia	Pitt et al. (2014)#
	Wikstroemia sp.	Thymelaeaceae	USA	Aptroot (1995)
	Zea mays	Poaceae	Georgia	Aptroot (1995)
Montagnula dura	*Aconitum septentrionale*	Ranunculaceae	Sweden	Eriksson (1992)
	Lonicera etrusca	Caprifoliaceae	Spain	Checa (2004)
Montagnula gilletiana	*Fraxinus ornus*	Oleaceae	Bulgaria	Fakirova (2004)
	Retama sphaerocarpa	Fabaceae	Spain	Checa (2004)
	Ulex europaeus	Fabaceae	Spain	Checa (2004)
Montagnula graminicola	Poaceae	Poaceae	Italy	Liu et al. (2015)#
Montagnula guiyangensis	*Helwingia himalaica*	Helwingiaceae	China	Sun et al. (2023)#
Montagnula hirtula	*Cerastium latifolium*	Caryophyllaceae	Austria	Leuchtmann (1984)
	Cerastium sp.	Caryophyllaceae	Italy	Leuchtmann (1984)
	Epilobium parviflorum	Onagraceae	Switzerland	Leuchtmann (1984)
	Rubus idaeus	Rosaceae	Finland	Leuchtmann (1984)
	Rubus sp.	Rosaceae	Sweden	Eriksson (1992)
Montagnula infernalis	*Agave americana*	Asparagaceae	Portugal	Checa (2004)
	Agave americana	Asparagaceae	Spain	Checa (2004)
	Fourcroya sp.	Asparagaceae	Portugal	Ariyawansa et al. (2014)
	Furcraea gigantea	Asparagaceae	Portugal	Checa (2004)
	Furcraea gigantea	Asparagaceae	Spain	Checa (2004)
	Furcraea longaeva	Asparagaceae	Portugal	Checa (2004)
	Furcraea longaeva	Asparagaceae	Spain	Checa (2004)
Montagnula infernalis	*Furcraea macrophylla*	Asparagaceae	Bahamas	Barr (1990)
Montagnula jonesii	*Fagus sylvatica*	Fagaceae	Italy	Tennakoon et al. (2016)#
	Ficus benjamina	Moraceae	Thailand	Tennakoon et al. (2022)#
Montagnula krabiensis	*Pandanus* sp.	Pandanaceae	Thailand	Tibpromma et al. (2018)#
Montagnula lijiangensis	*Quercus* sp.	Fagaceae	China	This study#
Montagnula longipes	*Agave americana*	Asparagaceae	Algeria	Aptroot (1995)
Montagnula melanorhabdos	*Agave* sp.	Asparagaceae	Turkey	Aptroot (2006)

Species	Host species	Host family	Country	Reference
Montagnula menglaensis	*Indocalamus tessellatus*	Poaceae	China	This study#
Montagnula mohavensis	*Yucca mohavensis*	Asparagaceae	USA	Ramaley and Barr (1995)
Montagnula obtusa	*Ilex* sp.	Aquifoliaceae	USA	French (1989)
	Juglans sp.	Juglandaceae	USA	French (1989)
	Pinus pinaster	Pinaceae	Portugal	Checa (2004)
	Sorbus aucuparia	Rosaceae	Sweden	Eriksson (1992)
Montagnula opaca	*Phalaris*	Poaceae	Switzerland	Crivelli (1983)
Montagnula opulenta	*Ammophila arenaria*	Poaceae	France	Aptroot (1995)
	Ammophila arenaria	Poaceae	Germany	Aptroot (1995)
	Ammophila arenaria	Poaceae	Sweden	Aptroot (1995)
	Festuca brachyphylla	Poaceae	Canada	Aptroot (1995)
	Opuntia ficus-indica	Cactaceae	Canary Islands	Aptroot (1995)
	Opuntia ficus-indica	Cactaceae	France	Aptroot (1995)
	Opuntia ficus-indica	Cactaceae	Italy	Aptroot (1995)
	Opuntia ficus-indica	Cactaceae	Malta	Aptroot (1995)
	Opuntia ficus-indica	Cactaceae	Tunisia	Aptroot (1995)
	Opuntia sp.	Cactaceae	Cyprus	Aptroot (1995)
	Opuntia sp.	Cactaceae	Israel	Aptroot (1995)
	Opuntia sp.	Cactaceae	Italy	Aptroot (1995)
	Opuntia sp.	Cactaceae	Tunisia	Aptroot (1995)
	Opuntia tuna	Cactaceae	USA	Aptroot (1995)
	Poa abbreviata	Poaceae	Canada	Aptroot (1995)
	Puccinellia angustata	Poaceae	Greenland	Aptroot (1995)
	Stipa himalaica	Poaceae	India	Aptroot (1995)
Montagnula opuntiae	*Opuntia lindheimeri*	Cactaceae	USA	Huhndorf (1992)
Montagnula palmacea	*Chamaerops humilis*	Arecaceae	France	Aptroot (1995)
	Cocos capitata	Arecaceae	Spain	Aptroot (1995)
	Daviesia nudiflora	Fabaceae	Australia	Aptroot (1995)
	Phoenix dactylifera	Arecaceae	Egypt	Aptroot (1995)
	Phoenix dactylifera	Arecaceae	Greece	Aptroot (1995)
	Phoenix dactylifera	Arecaceae	Iraq	Aptroot (1995)
	Phoenix dactylifera	Arecaceae	Italy	Aptroot (1995)
	Phoenix dactylifera	Arecaceae	Pakistan	Aptroot (1995)
	Phoenix dactylifera	Arecaceae	Saudi Arabia	Aptroot (1995)
	Phoenix dactylifera	Arecaceae	Tunisia	Aptroot (1995)
	Phoenix sylvestris	Arecaceae	Pakistan	Aptroot (1995)
	Pitcairnia chrysantha	Bromeliaceae	Chile	Aptroot (1995)
	Unknown leaves	NA	USA	Aptroot (1995)
	Unknown petiole	NA	USA	Aptroot (1995)
Montagnula perforans	*Calamagrostis arenaria*	Poaceae	France	Aptroot (2006)
Montagnula phragmospora	*Agave americana*	Asparagaceae	Portugal	Checa (2004)
	Agave americana	Asparagaceae	Spain	Checa (2004)
	Agave hookeri	Asparagaceae	Portugal	Checa (2004)
	Agave hookeri	Asparagaceae	Spain	Checa (2004)
	Agave sp.	Asparagaceae	France	Barr (1990)
	Agave sp.	Asparagaceae	Portugal	Checa (2004)
	Agave sp.	Asparagaceae	Spain	Checa (2004)

Species	Host species	Host family	Country	Reference
Montagnula phragmospora	*Yucca brevifolia*	Asparagaceae	California	Barr (1990)
	Yucca sp.	Asparagaceae	Portugal	Checa (2004)
	Yucca sp.	Asparagaceae	Spain	Checa (2004)
Montagnula puerensis	Dead wood	NA	China	Du et al. (2021)#
Montagnula rhodophaea	*Arundo donax*	Poaceae	Italy	Leuchtmann (1984)
	Phragmites communis	Poaceae	Switzerland	Leuchtmann (1984)
Montagnula saikhuensis	*Citrus* sp.	Rutaceae	Thailand	Wanasinghe et al. (2016)#
Montagnula scabiosae	*Scabiosa* sp.	Caprifoliaceae	Italy	Hongsanan et al. (2015)#
Montagnula shangrilana	*Rhododendron* sp.	Ericaceae	China	This study#
Montagnula sp.	*Carex fuliginosa*	Cyperaceae	Austria	Scheuer (1988)
Montagnula spartii	*Aeluropus littoralis*	Poaceae	Russia	Aptroot (1995)
	Ammophila arenaria	Poaceae	Belgium	Aptroot (1995)
	Ammophila arenaria	Poaceae	Denmark	Aptroot (1995)
	Ammophila arenaria	Poaceae	Sweden	Aptroot (1995)
	Ammophila arenaria	Poaceae	United Kingdom	Aptroot (1995)
	Calamagrostis epigeios	Poaceae	Russia	Aptroot (1995)
	Calycotome spinosa	Fabaceae	France	Aptroot (1995)
	Calycotome spinosa	Fabaceae	Spain	Aptroot (1995)
	Calycotome villosa	Fabaceae	Italy	Aptroot (1995)
	Carex rostrata	Cyperaceae	Sweden	Aptroot (1995)
	Chamaerops humilis	Arecaceae	Spain	Aptroot (1995)
	Leymus arenarius	Poaceae	Russia	Aptroot (1995)
	Ephedra ciliata	Ephedraceae	Unknown country in Asia	Aptroot (1995)
	Ephedra sp.	Ephedraceae	Iran	Aptroot (1995)
	Festuca arenaria	Poaceae	France	Aptroot (1995)
	Festuca sulcata	Poaceae	Iran	Aptroot (1995)
	Genista aspalathoides	Fabaceae	Italy	Aptroot (1995)
	Gramineae	Gramineae	Austria	Aptroot (1995)
	Koeleria cristata	Poaceae	Germany	Aptroot (1995)
	Koeleria glauca	Poaceae	Denmark	Aptroot (1995)
	Linum austriacum	Linaceae	Germany	Aptroot (1995)
	Luzula spadicea	Juncaceae	Switzerland	Aptroot (1995)
	Lygeum spartum	Poaceae	Spain	Aptroot (1995)
	Melica ciliata	Poaceae	France	Aptroot (1995)
	Nardus stricta	Poaceae	Austria	Aptroot (1995)
	Puccinellia peisonis	Poaceae	Austria	Aptroot (1995)
	Sarothamnus scoparius	Fabaceae	Poland	Mulenko et al. (2008)
	Sarothamnus scoparius	Fabaceae	Switzerland	Aptroot (1995)
	Sesleria caerulea	Poaceae	Italy	Aptroot (1995)
Montagnula spartii	*Spartium junceum*	Fabaceae	Albania	Aptroot (1995)
	Spartium junceum	Fabaceae	France	Aptroot (1995)
	Spartium junceum	Fabaceae	Greece	Aptroot (1995)
	Spartium junceum	Fabaceae	Turkey	Aptroot (1995)
	Ulex sp.	Fabaceae	Spain	Aptroot (1995)
Montagnula spinosella	*Abelia triflora*	Caprifoliaceae	Spain	Checa (2004)
	Carex aterrima	Cyperaceae	Austria	Scheuer (1988)

Species	Host species	Host family	Country	Reference
Montagnula spinosella	*Carex misandra*	Cyperaceae	Norway	Holm and Holm (1993, 1994)
	Colpodium vahlianum	Poaceae	Norway	Holm and Holm (1993, 1994)
	Deschampsia caespitosa	Poaceae	Norway	Holm and Holm (1993, 1994)
	Juncus maritimus	Juncaceae	Spain	Holm and Holm (1993), Checa (2004)
	Luzula confusa	Juncaceae	Norway	Holm and Holm (1993, 1994)
Montagnula stromatosa	*Phoenix hanceana*	Arecaceae	China	Lu et al. (2000)
	Phoenix sp.	Arecaceae	China	Zhuang (2001)
	Trachycarpus fortunei	Arecaceae	China	Hyde et al. (1999)
	Trachycarpus fortunei	Arecaceae	United Kingdom	Hyde et al. (1999)
Montagnula subsuperficialis	*Panicum grumosum*	Poaceae	Argentina	Shoemaker (1989)
Montagnula thailandica	*Chromolaena odorata*	Asteraceae	Thailand	Mapook et al. (2020)[#]
	Hevea brasiliensis	Euphorbiaceae	Thailand	Senwanna et al. (2021)[#]
	Coffea arabica var. *catimor*	Rubiaceae	China	Lu et al. (2022)[#]
	Unidentified twig	NA	Thailand	Boonmee et al. (2021)[#]
Montagnula thevetiae	*Thevetia peruviana*	Apocynaceae	China	This study[#]
Montagnula thuemeniana	*Yucca* sp.	Asparagaceae	USA	Barr (1990)
Montagnula triseti	*Trisetum distichophyllum*	Poaceae	Switzerland	Crivelli (1983)
Montagnula vakrabeejae	Unidentified twig	NA	Andaman	Niranjan and Sarma (2018)
Montagnula verniciae	*Vernicia fordii*	Euphorbiaceae	China	Li et al. (2023)[#]
Montagnula yuccigena	*Yucca baccata*	Asparagaceae	Mexico	Ramaley and Barr (1995)

"[#]" Denotes molecular data available in GenBank. "[##]" Denotes none plant based. NA represents not applicable.

Table 2. GenBank accession numbers of sequences used for the phylogenetic analyses.

Taxon	Strain number	GenBank accession numbers					Reference
		ITS	LSU	SSU	*tef*1-α	*rpb*2	
Montagnula acaciae	MFLUCC 18-1636	ON117280	ON117298	ON117267	ON158093	NA	Tennakoon et al. (2022)
	NCYUCC 19-0087[T]	ON117281	ON117299	ON117268	ON158094	NA	Tennakoon et al. (2022)
Montagnula aloes	CPC 19671	JX069863	JX069847	NA	NA	NA	Crous et al. (2012)
	CBS 132531[T]	NR_111757	NG_042676	NA	NA	NA	Crous et al. (2012)
Montagnula appendiculata	CBS 109027[T]	DQ435529	AY772016	NA	NA	NA	Wanasinghe et al. (2016)
Montagnula aquatica	MFLU 22-0171[T]	OP605992	OP605986	OP600504	NA	NA	Sun et al. (2023)
Montagnula aquatica	**KUNCC 23-14425**	**OR583097**	**OR583116**	**OR583135**	**OR588088**	**OR588107**	**This study**
	KUNCC 23-14557	**OR583099**	**OR583118**	**OR583137**	**OR588090**	**OR588109**	**This study**
Montagnula aquilariae	KUNCC 22-10815[T]	OP452927	OP482265	OP482268	OP426318	NA	Hyde et al. (2023)
	KUNCC 22-10816	OP554219	OP482266	OP482269	OP426319	NA	Hyde et al. (2023)
	KUNCC 22-10815[T]	OP452927	OP482265	OP482268	OP426318	NA	Hyde et al. (2023)
	KUNCC 22-10816	OP554219	OP482266	OP482269	OP426319	NA	Hyde et al. (2023)
Montagnula aquilariae	**KUNCC 23-14430**	**OR583100**	**OR583119**	**OR583138**	**OR588091**	**OR588110**	**This study**
	KUNCC 23-14431	**OR583101**	**OR583120**	**OR583139**	**OR588092**	**OR588111**	**This study**
	KUNCC 23-14432	**OR583102**	**OR583121**	**OR583140**	**OR588093**	**OR588112**	**This study**
Montagnula bellevaliae	MFLUCC 14-0924[T]	KT443906	KT443902	KT443904	NA	NA	Hongsanan et al. (2015)
Montagnula camporesii	MFLUCC 16-1369[T]	MN401746	NG_070946	NG_068418	MN397908	MN397909	Hyde et al. (2020)
Montagnula chiangraiensis	MFLUCC 17-1420[T]	NR_168864	NG_068707	NG_070155	NA	NA	Mapook et al. (2020)
Montagnula chromolaenae	MFLUCC 17-1435[T]	NR_168865	NG_068708	NG_070156	NA	NA	Mapook et al. (2020)

Taxon	Strain number	GenBank accession numbers					Reference
		ITS	LSU	SSU	*tef*1-α	*rpb*2	
Montagnula chromolaenicola	MFLUCC 17-1469[T]	NR_168866	NG_070948	NG_070157	MT235773	MT235809	Mapook et al. (2020)
Montagnula chromolaenicola	**KUNCC 23-14426**	**OR583098**	**OR583117**	**OR583136**	**OR588089**	**OR588108**	**This study**
	KUNCC 23-14427	**OR583103**	**OR583122**	**OR583141**	**OR588094**	**OR588113**	**This study**
	KUNCC 23-14558	**OR583104**	**OR583123**	**OR583142**	**OR588095**	**OR588114**	**This study**
Montagnula cirsii	MFLUCC 13-0680	KX274242	KX274249	KX274255	KX284707	NA	Hyde et al. (2016)
Montagnula cylindrospora	CBS 146572[T]	LT796834	LN907351	NA	LT797074	LT796994	Crous et al. (2020)
Montagnula donacina	HFG07004	MF967419	MF183940	NA	NA	NA	Zhao et al. (2017)
	HVVV01	KJ628375	KJ628377	KJ628376	NA	NA	Pitt et al. (2014)
	HKAS 124552	OP605991	OP605987	NA	NA	NA	Sun et al. (2023)
	KUMCC 21-0653	OP058961	OP059052	OP059003	OP135938	NA	Ren et al. (2021)
	KUMCC 21-0579	OP058963	OP059054	OP059005	OP135940	NA	Ren et al. (2021)
	KUMCC 21-0631	OP058962	OP059053	OP059004	OP135939	NA	Ren et al. (2021)
	UESTCC 23.0030	OR253120	OR253279	OR253194	NA	NA	Unpublished
Montagnula donacina	**KUNCC 23-14428**	**OR583105**	**OR583124**	**OR583143**	**OR588096**	**OR588115**	**This study**
	KUNCC 23-14429	**OR583106**	**OR583125**	**OR583144**	**OR588097**	**OR588116**	**This study**
Montagnula graminicola	MFLUCC 13-0352[T]	KM658314	KM658315	KM658316	NA	NA	Liu et al. (2015)
Montagnula guiyangensis	HKAS 124556[T]	OP605989	OP600484	OP600500	NA	NA	Sun et al. (2023)
	GUCC 22−0817	OP605990	OP600485	OP600501	NA	NA	Sun et al. (2023)
Montagnula jonesii	MFLUCC 16-1448[T]	KY313619	KY273276	KY313618	KY313620	NA	Tennakoon et al. (2016)
	MFLU 18-0084	ON117282	ON117300	ON117269	ON158095	NA	Tennakoon et al. (2022)
Montagnula krabiensis	MFLUCC 16-0250[T]	NR168179	NG068826	NG068385	MH412776	NA	Tibpromma et al. (2018)
Montagnula lijiangensis	**HKAS 126540**	**OR583107**	**OR583126**	**OR583145**	**OR588098**	**OR588117**	**This study**
	HKAS 126541[T]	**OR583108**	**OR583127**	**OR583146**	**OR588099**	**OR588118**	**This study**
Montagnula menglaensis	**KUNCC 23-14422**	**OR583109**	**OR583128**	**OR583147**	**OR588100**	**OR588119**	**This study**
	KUNCC 23-14423	**OR583110**	**OR583129**	**OR583148**	**OR588101**	**OR588120**	**This study**
	KUNCC 23-14424[T]	**OR583111**	**OR583130**	**OR583149**	**OR588102**	**OR588121**	**This study**
Montagnula puerensis	KUMCC 20-0225[T]	MW567739	MW575866	MW575864	MW575859	NA	Du et al. (2021)
	KUMCC 20-0331	MW567740	MW575867	MW575865	MW575860	NA	Du et al. (2021)
Montagnula saikhuensis	MFLUCC 16-0315[T]	KU743209	KU743210	KU743211	NA	NA	Wanasinghe et al. (2016)
Montagnula scabiosae	MFLUCC 14-0954[T]	KT443907	KT443903	KT443905	NA	NA	Hongsanan et al. (2015)
Montagnula shangrilana	**KUNCC 23-14433**	**OR583112**	**OR583131**	**OR583150**	**OR588103**	**OR588122**	**This study**
	KUNCC 23-14434[T]	**OR583113**	**OR583132**	**OR583151**	**OR588104**	**OR588123**	**This study**
Montagnula thailandica	MFLUCC 17-0363	OL782142	OL782059	OL780525	OL875102	OL828754	Senwanna et al. (2021)
	MFLUCC 17-1508[T]	MT214352	NG070949	NG070158	MT235774	MT235810	Mapook et al. (2020)
	MFLUCC 21-0075	OP297807	OP297777	OP297791	OP321576	NA	Lu et al. (2022)
	ZHKUCC 22-0206	OP297808	OP297778	OP297792	OP321577	NA	Lu et al. (2022)
	ZHKUCC 22-0207	MZ538515	MZ538549	NA	MZ567092	NA	Boonmee et al. (2021)
Montagnula thevetiae	**HKAS 126963**	**OR583114**	**OR583133**	**OR583152**	**OR588105**	**OR588124**	**This study**
	HKAS 126964[T]	**OR583115**	**OR583134**	**OR583153**	**OR588106**	**OR588125**	**This study**
Neokalmusia jonahhulmei	KUMCC 21-0818[T]	ON007043	ON007039	ON007048	ON009133	ON009137	Wanasinghe and Mortimer (2022)
Neokalmusia jonahhulmei	KUMCC 21-0819	ON007044	ON007040	ON007049	ON009134	ON009138	Wanasinghe and Mortimer (2022)

Ex-type strains are indicated with superscript "T", and newly generated sequence is shown in bold. NA represents sequences that are unavailable in GenBank. CBS: Culture Collection of the Westerdijk Fungal Biodiversity Institute, Netherlands; CPC: Personal collection of P.W. Crous, Netherlands; HFG: Personal collection of Zhen-Zhu Zhao; GUCC: Guizhou University Culture Collection (GUCC), Guiyang, China; HKAS/KUNCC: Kunming Institute of Botany Culture Collection, China; HVVV: Personal collection of Wayne Pitt from *Vitis vinifera*; MFLUCC/MFLU: Mae Fah Luang University Culture Collection, Chiang Rai, Thailand; NCYUCC: National Chiayi University Culture Collection, Taiwan, China; UESTCC: University of Electronic Science and Technology Culture Collection; ZHKUCC: Zhongkai University of Agriculture and Engineering Culture Collection.
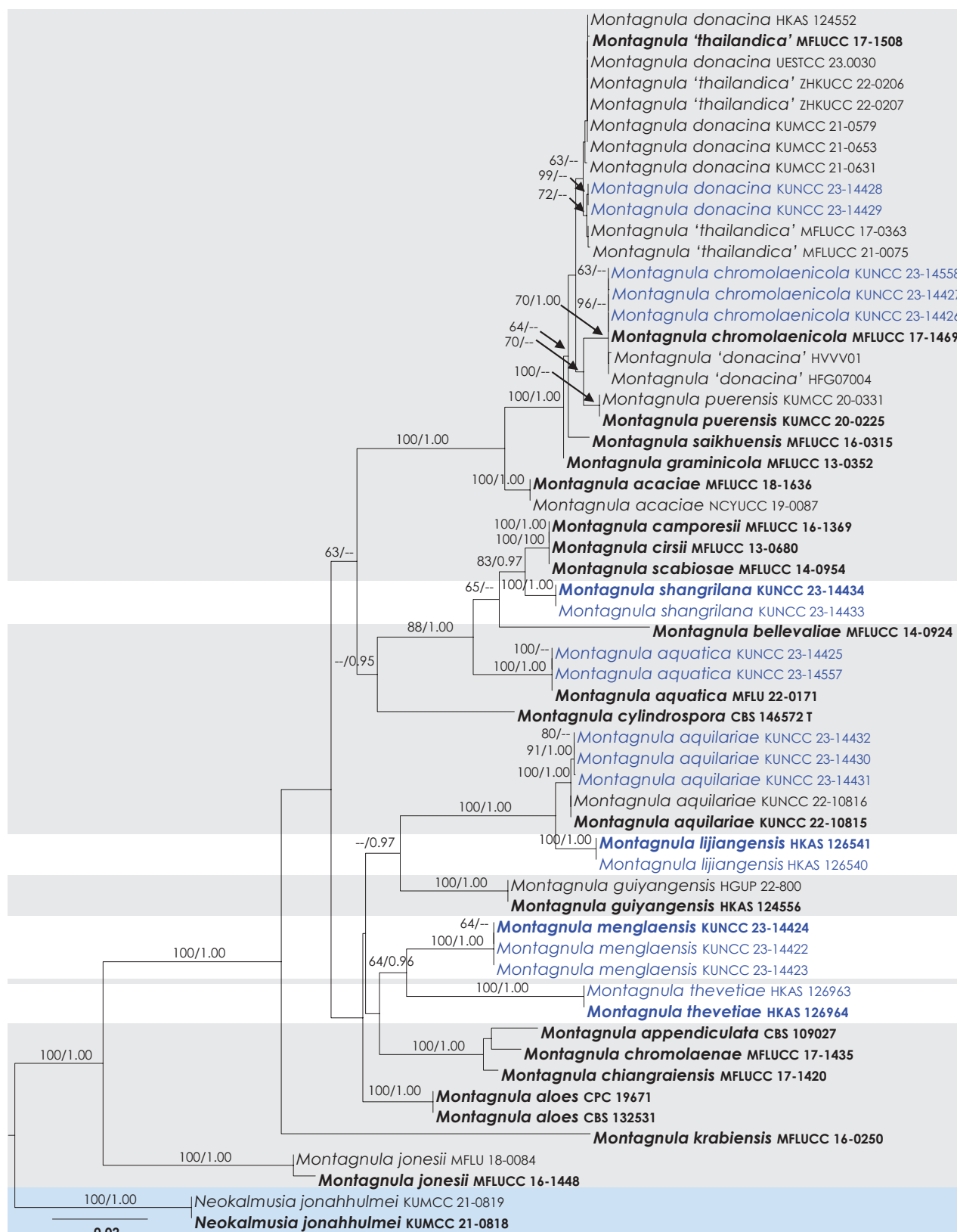
Figure 1. Phylogenetic analysis of SSU, LSU, ITS, *tef*1-α, and *rpb*2 of the *Montagnula*. Species names given in bold are ex-type, ex-epitype and ex-paratype strains. Species names highlighted in blue are generated from this study. Branch support of nodes ≥75% ML BS and ≥0.95 PP is indicated above the branches. The genus *Montagnula* is depicted within a pale gray box, with new species highlighted in white, and the outgroup indicated by a blue box.
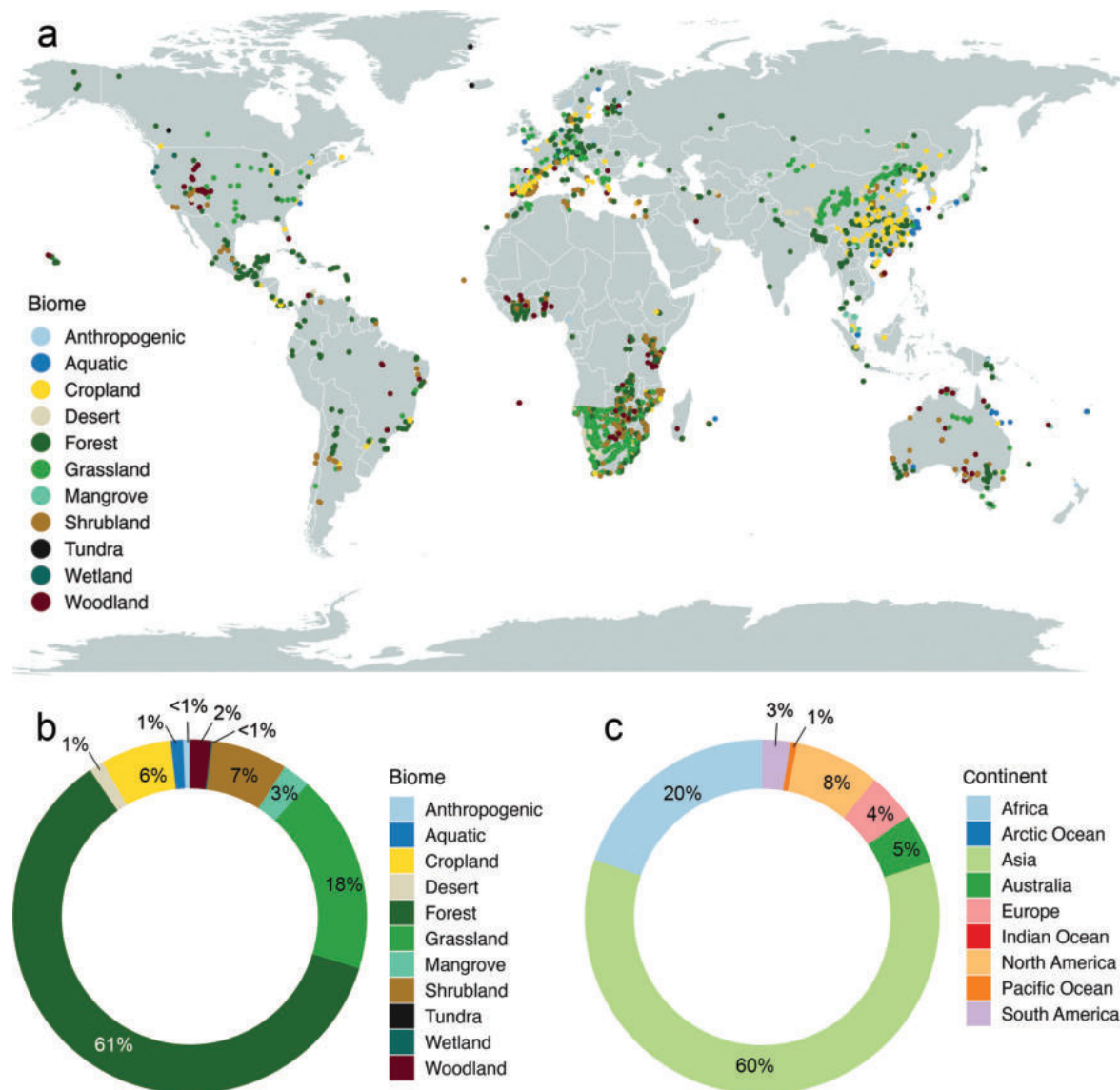
Figure 2. Geographical distribution of *Montagnula* species with known ITS sequence data. **a** the map summarizes data from the GlobalFungi database (shown by circles). Each circle symbolizes a unique sample, with each color representing the specific biome from which it has been collected **b** the distribution of *Montagnula* sequences as a percentage of total abundance across different biomes **c** the distribution of *Montagnula* sequences as a percentage of total abundance across different continents. See Suppl. material 1 for primary data.

Results

Phylogenetic analyses

In order to examine the evolutionary relationships of our new strains within *Montagnula*, phylogenetic analyses were performed based on the combined SSU, LSU, ITS, *tef*1-α, and *rpb*2 DNA sequences of 56 representatives of the genus and two strains from *Neokalmusia jonahhulmei* (KUMCC 21-0818, KUMCC 21-0819) as the outgroup taxon. The full dataset consisted of 4,268 characters including gaps (18S = 1,023 characters, 28S = 896, ITS = 508, *tef*1-α = 885, *rpb*2 = 956). The RAxML analysis of the combined dataset yielded a best-scoring tree with a final ML optimization likelihood value of -14,343.052271. The matrix had 1004 distinct
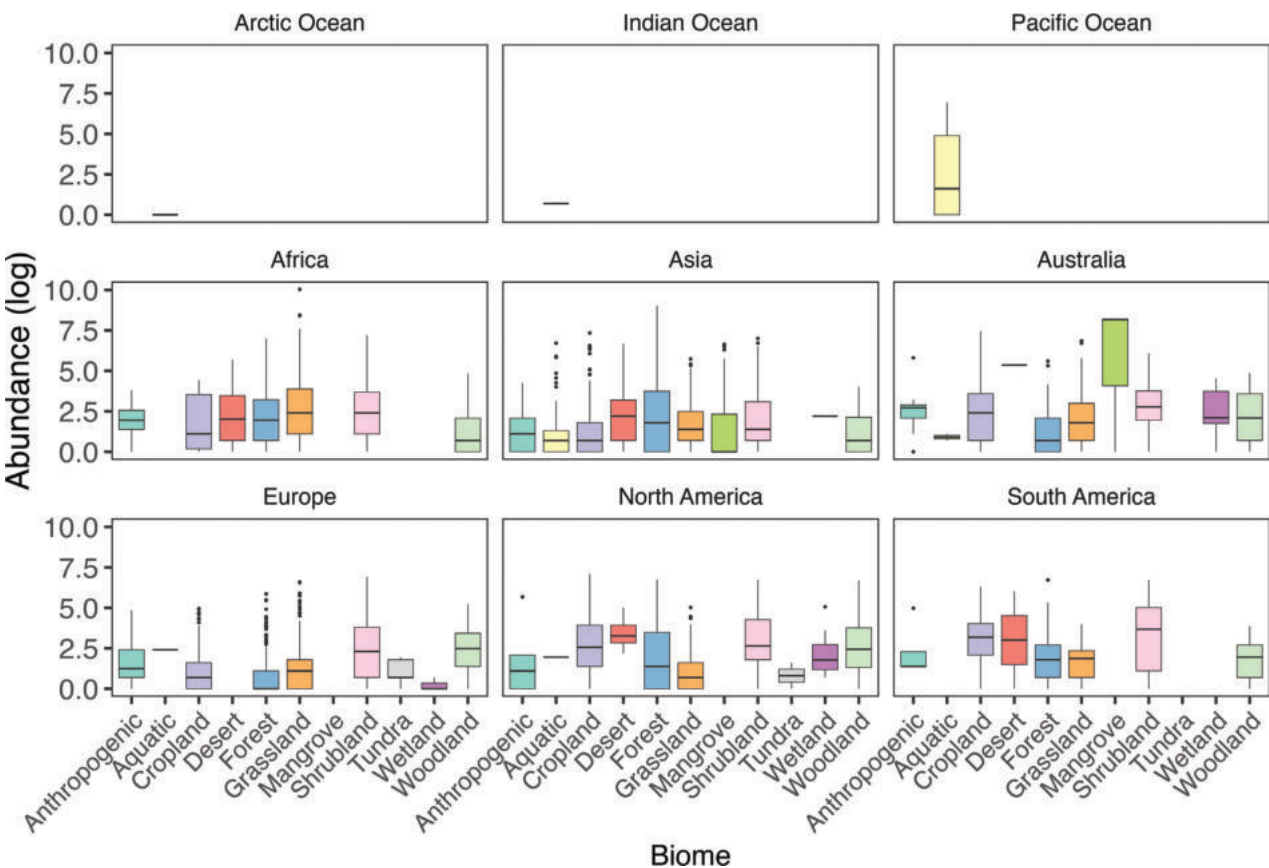
Figure 3. The distribution of *Montagnula* occurrences across oceans, continents and various substrates, as documented in the existing literature. On the x-axis, the logarithmic abundance of each record for different sources is displayed.
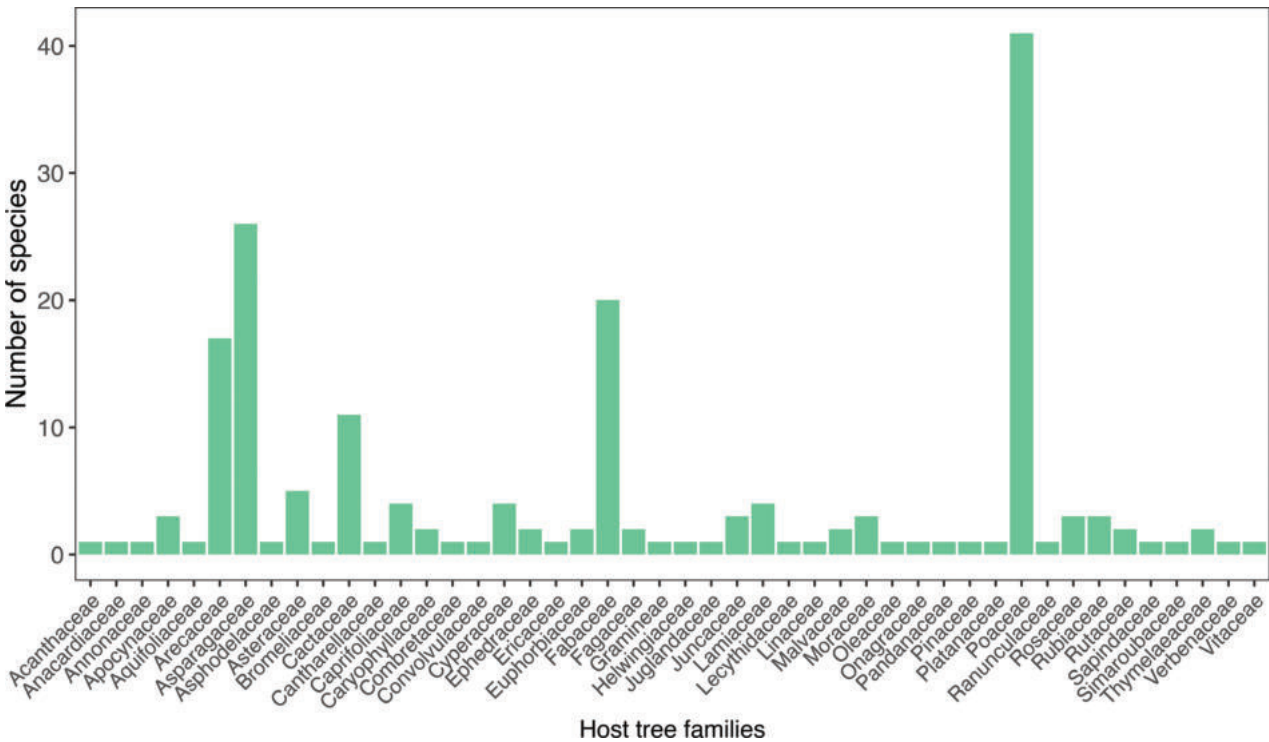
Figure 4. The species richness of recorded *Montagnula* species across different plant families (Table 1).

alignment patterns, with 23.88% undetermined characters or gaps. Parameters for the GTR + I + G model of the combined amplicons were as follows: Estimated base frequencies; A = 0.244145, C = 0.256118, G = 0.269851, T = 0.229886; substitution rates AC = 1.815063, AG = 3.954334, AT = 1.414215, CG = 1.362941, CT = 10.779403, GT = 1.000; proportion of invariable sites I = 0.559204; and gamma distribution shape parameter α = 0.542439. The Bayesian analysis ran 1,675,000 generations before the average standard deviation for split frequencies reached below 0.01 (0.009994). The analyses generated 16,751 trees, from which we sampled 12,564 trees after discarding the first 25% as burn-in. The alignment contained a total of 1,005 unique site patterns. The BI and ML trees were not in conflict; the ML tree is shown in Fig. 1. Where applicable, the phylogenetic results obtained (Fig. 1) are discussed in the descriptive notes below.

We conducted a thorough study of a compilation of data derived from multiple metabarcoding studies, which documented the occurrence of *Montagnula* species worldwide, excluding Antarctica. Among the continents, the highest number of studies were recorded in Asia, Australia, Europe, and North America (Fig. 2). These studies encompassed a diverse range of 11 distinct sources, revealing that sediments and "other" sources yielded the highest number of sequences (Fig. 3). Across different continents, the sequences obtained from various sources exhibited moderate similarity. However, in regions such as Asia, Australia, Europe, and North America, studies revealed *Montagnula* species from a diverse array of sources, in contrast to other studies, which identified species from a more limited selection of sources. Furthermore, in culture-based investigations, the primary focus was on extracting *Montagnula* species from plant substrates originating from 45 distinct plant families (Fig. 4). Among these families, Poaceae yielded the most substantial number of isolated species, followed by Asparagaceae and Fabaceae. Additionally, two records were also detected in mushrooms and human skin samples.

Taxonomy

Pleosporales Luttr. ex M.E. Barr, Prodromus to class Loculoascomycetes: 67 (1987)
Didymosphaeriaceae Munk, Dansk botanisk Arkiv 15 (2): 128 (1953)

***Montagnula* Berl., Icones Fungorum. Pyrenomycetes 2: 68 (1896)**

Notes. This study presents an updated and comprehensive phylogenetic classification of the genus *Montagnula*, incorporating SSU, LSU, ITS, *tef*1-α, and *rpb*2 DNA sequence analyses. By combining morphological and phylogenetic considerations, we have identified four new species, *M. lijiangensis*, *M. menglaensis*, *M. shangrilana* and *M. thevetiae* within the genus. Additionally, this research accounts for the existing species *viz.*, *M. aquatica*, *M. aquilariae*, *M. chromolaenicola* and *M. donacina*. The note sections of this publication provide detailed information on these taxonomic accounts, including additional discussion and supporting evidence. Each newly identified species adds to the known biodiversity within the genus, expanding our knowledge of the ecological and morphological characteristics exhibited by *Montagnula* taxa.

Montagnula aquatica **Y.R. Sun, Yong Wang bis & K.D. Hyde, Plants 12 (4, no. 738): 2 (2023)**
MycoBank No: 900129

Descriptions and illustrations. See Sun et al. (2023).

Habitat and distribution. This species is found in freshwater habitats of Chiang Rai, Thailand, terrestrial habitats of Yunnan, China, inhabiting dead wood of deciduous hosts (Sun et al. 2023, this study).

Material examined. China, Yunnan Province, Honghe Hani and Yi Autonomous Prefecture, Honghe County, Dayangjiexiang (23.389965°N, 102.225552°E, 1194 m), on dead woody litter of an unidentified plant, 13 March 2023, D.N. Wanasinghe, DWHH23-51 (HKAS 130322), new country and habitat record, living culture KUNCC 23-14425. *ibid*. 23.388966°N, 102.224786°E, 1215 m, DWHH23-51-2 (HKAS 130323), living culture KUNCC 23-14557.

Notes. Based on our phylogenetic analyses, we have determined that the newly collected strains (i.e. KUNCC 23-14425 and KUNCC 23-14557) are monophyletic with the ex-type strain of *Montagnula aquatica* (MFLU 22-0171). Further morphological investigations comparing our isolate with the type species have revealed similarities in the size range of the ascomata, asci, and ascospores, as well as the ascospore septation (Sun et al. 2023). Therefore, we document KUNCC 23-14425 and KUNCC 23-14557 as new records of *Montagnula aquatica* in China, accompanied by protein sequence data (*tef*1-α and *rpb*2) for this species. It is worth noting that the holotype of *Montagnula aquatica* was previously reported on submerged decaying wood in a freshwater habitat in Thailand, while our collection was made from a terrestrial habitat in China. This observation suggests that this fungus exhibits adaptability to a wide range of habitats, although its exploration in diverse geographic locations remains limited. The inclusion of *Montagnula aquatica* as a new record in China expands our understanding of the distribution and ecological preferences of this species in both terrestrial and aquatic habitats. Additionally, the protein sequence data obtained for this strain contributes valuable information to the existing knowledge on *Montagnula aquatica*. Further studies exploring the ecological aspects of this fungus in different geographic locations will provide deeper insights into its adaptability and potential ecological roles.

Montagnula aquilariae **T.Y. Du & Tibpromma, Mycosphere 14 (1): 705 (2023)**
MycoBank No: 846332
Fig. 5

Description. *Saprobic* on dead woody litter of an unknown deciduous host. **Teleomorph** *Ascomata* 450–600 µm high × 480–550 µm diam., immersed to semi-erumpent, gregarious or rarely clustered, globose to subglobose, ostiolate. *Ostiole* 120–220 × 70–110 µm (x̄ = 139 × 89 µm, n = 5), papillate, central, straight, dark brown to black, filled with hyaline cells, periphyses are lacking. *Peridium* 20–40 µm thick on the sides and can reach up to 60 µm near the apex, with an outer layer consisting of heavily pigmented cells that have thick walls and exhibit a *textura angularis* to *textura globulosa* texture at the apex, *textura angularis* texture at the sides and base; the innermost layer consists of narrow, hyaline compressed rows of cells that merge with pseudoparaphyses. *Hamath-*
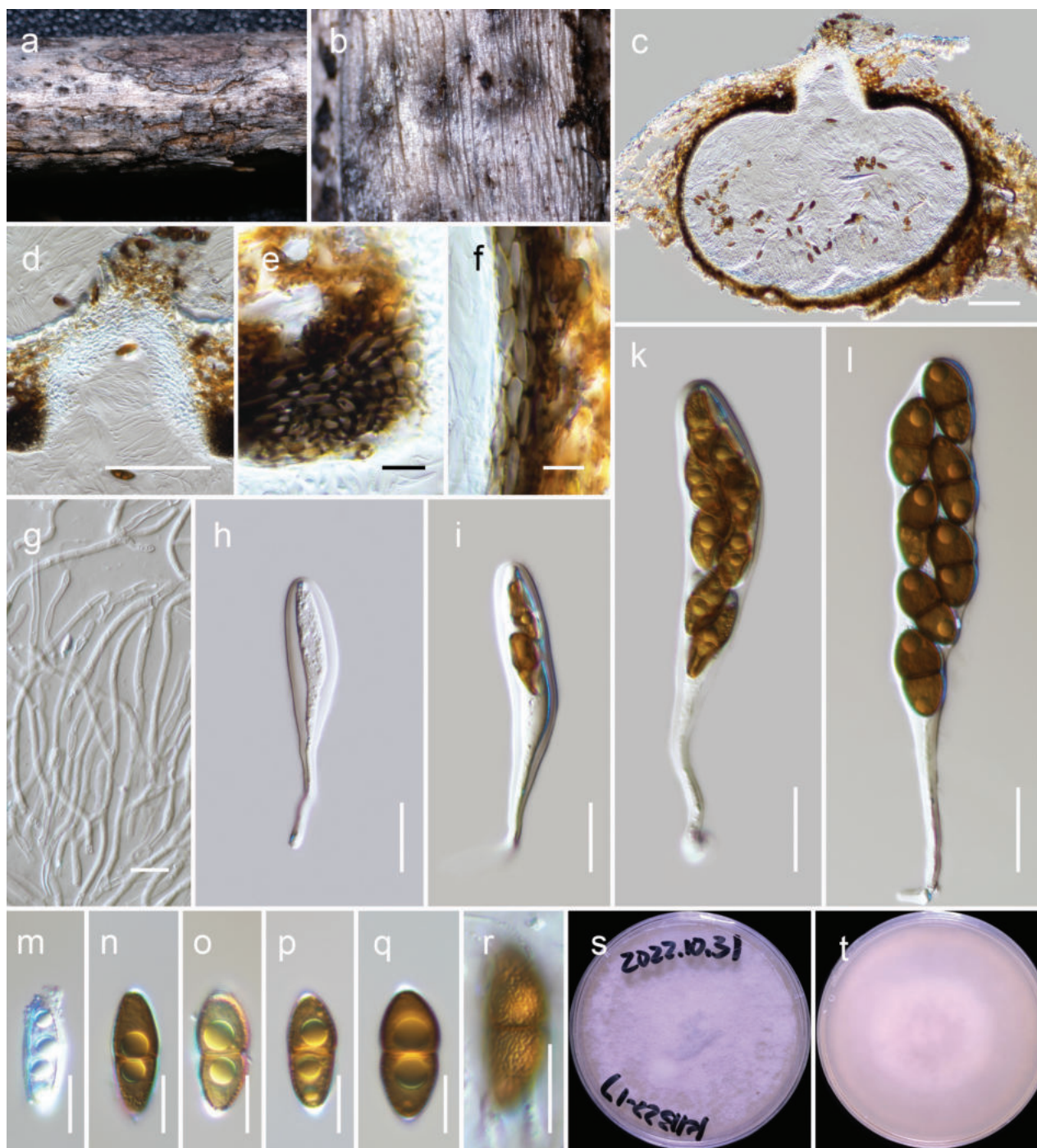
Figure 5. *Montagnula aquilariae* (HKAS 126542) **a, b** ascomata on natural wood surface **c** vertical section through an ascoma **d** ostiolar neck **e** peridium cells at the apex **f** peridium cells at the side **g** pseudoparaphyses **h–l** asci **m–r** ascospores (see verruculose feature of the ascospore in r) **s, t** culture characters on PDA (s = above, t = reverse). Scale bars: 100 μm (**c, d**); 50 μm (**e**); 10 μm (**e–g, m–r**); 20 μm (**h–l**).

ecium of 2−4 μm broad, dense, narrow, branched, cellular pseudoparaphyses. **Asci** 100−120 × 16−22 μm (x̄ = 110.8 × 18.4 μm, n = 20), bitunicate, fissituni- cate, cylindrical-clavate to clavate, pedicel 30−50 μm long, 8-spored, biseriate, with a minute ocular chamber best seen in immature ascus. **Ascospores** 20−25 × 8.5−11 μm (x̄ = 21.8 × 9.6 μm, n = 30), ellipsoidal to narrowly oblong, straight or somewhat curved, ends conically rounded, golden-brown to dark brown,

1-septate, constricted at the septum, large guttules in each cell, verruculose, with a thin mucilaginous sheath. **Anamorph** Undetermined.

Habitat and distribution. This species is found in terrestrial habitats of Yunnan, China, specifically inhabiting dead woody twigs of deciduous hosts, including *Aquilaria sinensis* (Hyde et al. 2023, this study).

Material examined. Chɪɴᴀ, Yunnan Province, Kunming City, Kunming Institute of Botany (25.141723°N, 102.750013°E, 1970 m), on dead woody litter of an unidentified plant, 24 April 2022, L. Qinxian, KIB22-17-1 (HKAS 126542), living culture KUNCC 23-14430; *ibid*. 25.141487°N, 102.748863°E, 1982 m, K2B22-17-3 (HKAS 126543), living culture KUNCC 23-14431; *ibid*. K2B22-17-4 (HKAS 126544), living culture KUNCC 23-14432.

Notes. *Montagnula aquilariae* was recently introduced by Hyde et al. (2023) based on samples obtained from *Aquilaria sinensis* in Xishuangbanna, Yunnan Province. In our new collections, three strains (KUNCC 23-14430, KUNCC 23-14431, KUNCC 23-14432) exhibited a monophyletic relationship with the previously known strains of *Montagnula aquilariae* (KUNCC 22-10815 [ex-type] and KUNCC 22-10816). Through further morphological, ecological, and nucleotide (SSU, LSU, ITS, *tef*1-α) comparisons, we have confirmed that these new strains indeed belong to *Montagnula aquilariae*. Our research also provides additional insights into the characteristics of *Montagnula aquilariae*. Specifically, we report the verruculose feature of the ascospores and present *rpb*2 sequence data for this fungus, advancing our knowledge of its morphological and genetic attributes.

***Montagnula chromolaenicola* Mapook & K.D. Hyde, Fungal Diversity 101: 35 (2020)**
MycoBank No: 557298

Descriptions and illustrations. See Mapook et al. (2020).

Habitat and distribution. This species was observed in terrestrial habitats in Mae Hong Son, Thailand, specifically on dead stems of *Chromolaena odorata* (Mapook et al. 2020). Additionally, it has also been found in terrestrial habitats in Yunnan, China, where it inhabits dead wood of deciduous hosts (this study).

Material examined. Chɪɴᴀ, Yunnan Province, Honghe County, Honghe Hani and Yi Autonomous Prefecture, Dayangjiexiang (23.389965°N, 102.225552°E, 1201 m), on a dead woody climber of an unidentified host, 13 March 2023, D.N. Wanasinghe, DWHH23-17A (HKAS 130321), living culture KUNCC 23-14426. *ibid*. 23.389295°N, 102.224780°E, 1200 m, on dead twigs of *Lagerstroemia* sp. DWHH23-33-2 (HKAS 126543), living culture KUNCC 23-14427; *ibid*. DWHH23-33-3 (HKAS 130320), living culture KUNCC 23-14558.

Notes. Through our phylogenetic analyses, we have determined that the newly isolated strains HH33 and HH17A exhibit a monophyletic relationship with the ex-type strain of *Montagnula chromolaenicola* (MFLUCC 17-1469). Upon conducting further investigations and morphological comparison of our collection with the type species, we have discovered several similarities. These include the size range of the ascomata, asci, and ascospores, as well as the ascospore septation (Mapook et al. 2020). Consequently, we hereby document our new collections (i.e. HKAS 130321, HKAS 126543 and HKAS 130320) as

new records of *Montagnula chromolaenicola* in China. In a recent study by Sun et al. (2023), *Montagnula chromolaenicola*, *M. puerensis*, *M. saikhuensis*, and *M. thailandica* were synonymized under the name *M. donacina* due to the absence of obvious branches in their phylogenetic tree and the close morphological resemblance between these species. However, it is important to note that most of these strains lack informative sequence data for *tef*1-α or *rpb*2. Our observations, on the other hand, have revealed that the inclusion of protein data in this group leads to the formation of distinct branches and independent lineages. Therefore, we propose retaining the older names for these species, except for *Montagnula thailandica*, until further research resolves this group using all available sequence data.

Montagnula donacina (Niessl) Wanas., E.B.G. Jones & K.D. Hyde, Index Fungorum 319: 1 (2017)

MycoBank No: 552762

Descriptions and illustrations. See Pitt et al. (2014).

Habitat and distribution. This species has been reported worldwide on various hosts within terrestrial habitats (see Table 2). Specifically, it has been documented in Australia (*Calamus australis*, *Vitis vinifera*), Brazil (*Bambusoideae*, *Saccharum officinarum*), Central African Republic (*Coffea robusta*), China (*Althaea rosea*, *Craterellus odoratus*, *Trachycarpus fortunei*), Colombia (unknown plant), France (*Pseudosasa japonica*), Georgia (*Zea mays*), India (*Acacia* sp., *Adhatoda vasica*, *Ailanthus altissima*, *Annona squamosa*, *Cajanus cajan*, *Careya arborea*, *Citrus aurantiifolia*, *Clerodendrum infortunatum*, *C. multiflorum*, *Duranta repens*, *Ficus glomerata*, *Hibiscus* sp., *Ipomoea carnea*, *Mallotus philippinensis*, *Morus alba*, *Nerium odorum*, *Pistacia indica*, *Tectona grandis*, *Terminalia tomentosa*), Japan (*Phyllostachys bambusoides*), Myanmar (*Nephelium litchi*), Namibia (*Acacia reficiens*), Papua New Guinea (*Bambusoideae*), Paraguay (*Coffea arabica*), Philippines (*Premna cumingiana*), Portugal (*Arundo donax*), Sierra Leone (*Funtumia africana*), Thailand (dead wood) and the USA (*Platanus* sp., *Wikstroemia* sp.).

Material examined. CHINA, Yunnan Province, Honghe (23.424892°N, 102.231417°E, 600 m), on dead woody litter of an unidentified plant, 14 August 2022, D.N. Wanasinghe, DWHH22-23-1 (HKAS 126545), living culture KUNCC 23-14428. *ibid*. DWHH22-23-2 (HKAS 126546), living culture KUNCC 23-14429.

Notes. Wanasinghe et al. (2016) regarded *Munkovalsaria* as a synonym of *Montagnula* and established *Montagnula donacina* (=*Munkovalsaria donacina*). So far, *Montagnula donacina* stands as the most extensively distributed species within the genus. Despite its global presence, there is a scarcity of molecular data available for *Montagnula donacina*. A preliminary analysis revealed only 20 sequence data entries when searching for "*Montagnula donacina*" in the NCBI database, originating from only seven strains: HFG07004, HKAS 124552, HVVV01, KUMCC 21-0579, KUMCC 21-0631, KUMCC 21-0653, and UESTCC:23.0030. Our phylogenetic analysis demonstrated a close relationship between two strains designated as *Montagnula donacina* (HVVV01 and HFG07004) and the type strain of *Montagnula chromolaenicola* (MFLUCC

17-1469). Additionally, we observed that the strains of *Montagnula thailandica* formed a monophyletic group alongside the remaining *Montagnula donacina* strains (HKAS 124552, KUMCC 21-0579, KUMCC 21-0631, KUMCC 21-0653, and UESTCC:23.0030). Furthermore, two newly generated sequences, KUNCC 23-14428 and KUNCC 23-14429, were also clustered with the strains of *Montagnula donacina*. We hereby introduce these two strains as belonging to *Montagnula donacina* and provide *rpb*2 sequence data for this species for the first time.

Montagnula lijiangensis Wanas., sp. nov.

MycoBank No: 850093

Fig. 6

Etymology. The specific epithet "lijiangensis" refers to Lijiang, Yunnan Province, where the holotype was collected.

Holotype. HKAS 126541.

Description. *Saprobic* on dead woody litter of *Quercus* sp. **Teleomorph Ascomata** 500–700 μm high × 500–600 μm diam., immersed, gregarious or rarely clustered, globose to subglobose, ostiolate. *Ostiole* 100–140 × 80–120 μm ($\overline{x}$ = 125 × 96 μm, n = 5), apapillate, central, straight, filled with hyaline cells. *Peridium* 20–30 μm thin on the sides and can reach up to 70 μm near the apex, with an outer layer consisting of heavily pigmented cells that have thick walls and exhibit a *textura angularis* texture at the apex, *textura angularis* texture at the sides and base; the innermost layer consists of narrow, hyaline compressed rows of cells. *Hamathecium* of 3–7.5 μm broad, dense, narrow, branched, cellular pseudoparaphyses that are swollen at the base. *Asci* 130–160 × 20–26 μm ($\overline{x}$ = 152.8 × 23.9 μm, n = 20), bitunicate, fissitunicate, cylindrical-clavate to clavate, pedicel 30–60 μm long, 8-spored, uni to biseriate, with a minute ocular chamber best seen in immature ascus. *Ascospores* 22–26 × 10–14 μm ($\overline{x}$ = 24.8 × 11.8 μm, n = 30), ellipsoidal to narrowly oblong, mostly straight, with conically rounded ends at the immature stage that become rounded when mature, golden-brown to dark brown, 1-septate and constricted at the septum, with large guttules in each cell, verruculose, surrounded by a thick mucilaginous sheath. **Anamorph** Undetermined.

Habitat and distribution. This species is found in terrestrial habitats of Yunnan, China, inhabiting dead woody twigs of deciduous hosts (this study).

Material examined. Сʜɪɴᴀ, Yunnan Province, Lijiang, Yulong County (26.86389°N, 99.824738°E, 2725 m), on dead woody litter of *Quercus* sp. (Fagaceae), 17 August 2021, L. Qinxian, STX09-03-1 (*holotype*, HKAS 126541, *ibid*. 26.863484°N, 99.824548°E, 2706 m, STX09-03-3 (HKAS 126540).

Notes. The analysis of two newly generated sequences revealed a monophyletic clade in our phylogenetic analysis (Fig. 1), demonstrating a close phylogenetic relationship to *Montagnula aquilariae*. This relationship is further supported by morphological features such as asci and ascospores. However, a comparison of nucleotide differences (without gaps) between these two clades (KUNCC 22-10815 and KUNCC 23-14430 vs HKAS 126541) showed 12/508 (2.3%) differences in the ITS region, 15/885 (1.7%) differences in the *tef*1-α region, and 19/956 (2%) differences in the *rpb*2 region.
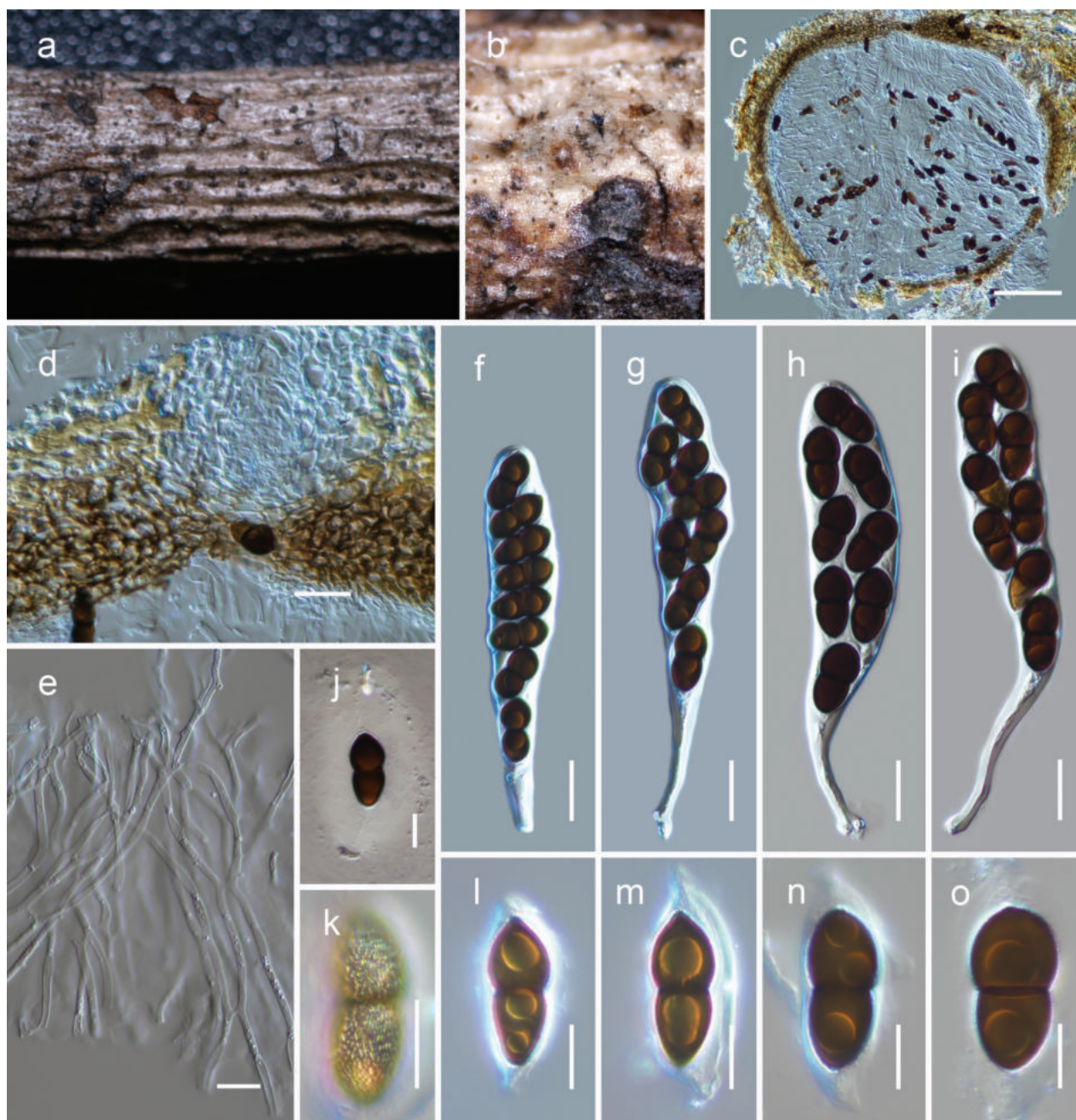
Figure 6. *Montagnula lijiangensis* (HKAS 126541, holotype) **a, b** ascomata on natural wood surface **c** vertical section through an ascoma **d** ostiolar neck and peridium cells at the apex **e** pseudoparaphyses **f–i** asci **j–o** ascospores (see verruculose feature of the ascospore in **k**). Scale bars: 100 μm (**c**); 20 μm (**d, f–i**); 10 μm (**e–o**).

***Montagnula menglaensis* Wanas., sp. nov.**
MycoBank No: 850094
Fig. 7

Etymology. The specific epithet "menglaensis" refers to Mengla County, Yunnan Province, where the holotype was collected.

Holotype. HKAS 130318.

Description. *Saprobic* on dead culms of *Indocalamus tessellatus* (Munro) Keng f. **Teleomorph *Ascomata*** 200–300 μm high × 240–320 μm diam.,
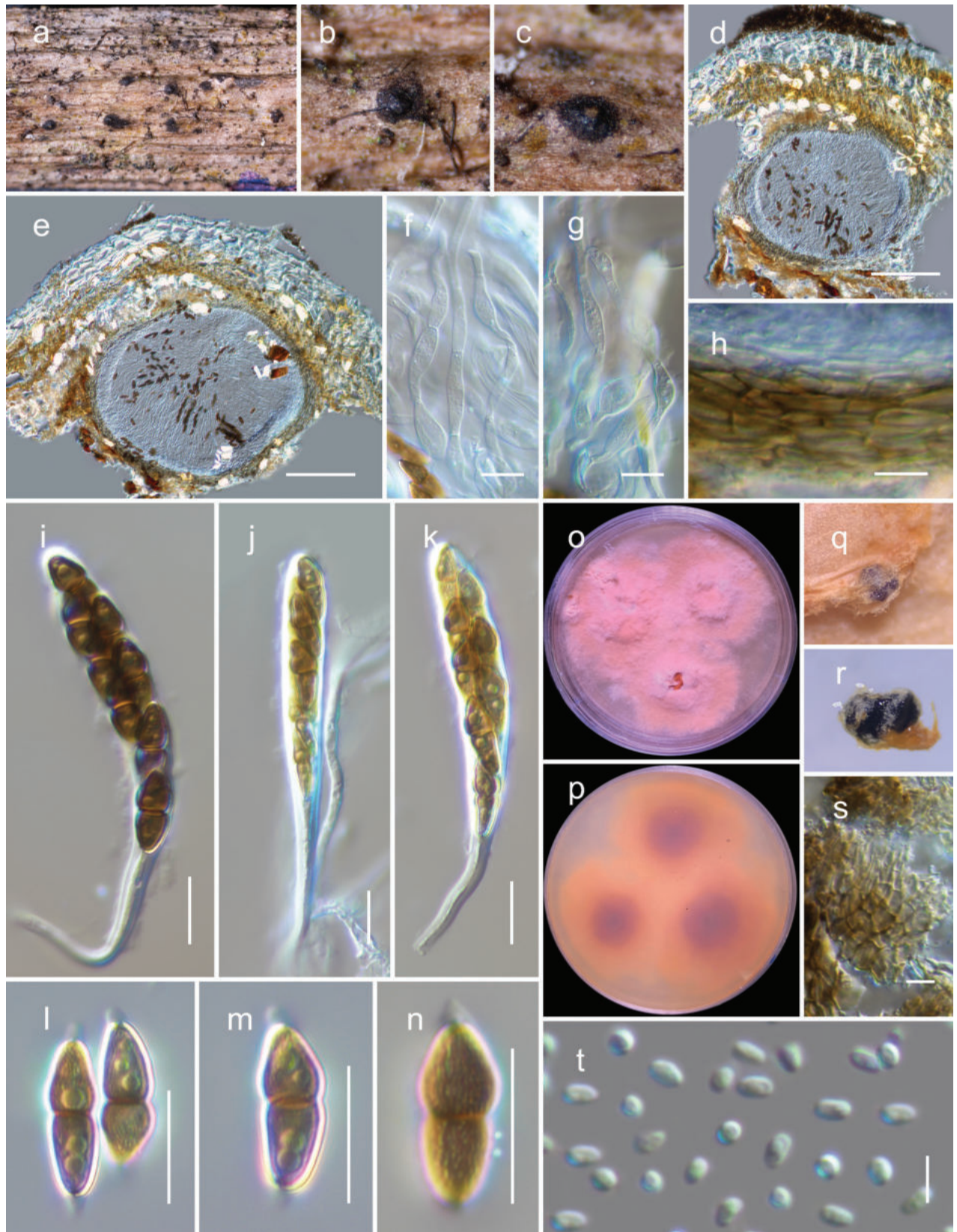
Figure 7. *Montagnula menglaensis* (HKAS 130318, holotype) **a–c** ascomata on natural wood surface **d, e** vertical section through ascomata **f, g** pseudoparaphyses **h** peridium **i–k** asci **l, m** ascospores (see verruculose feature of the ascospore in **n**) **o, p** culture characters on PDA (o = above, p = reverse) **q, r** conidiomata **s** pycnidial wall **t** conidia. Scale bars: 100 μm (**d, e**); 10 μm (**f–h, l–n, s, t**); 20 μm (**i–k**).

immersed, gregarious or rarely clustered, globose to subglobose. ***Peridium*** 10–25 µm thin with an outer layer consisting of heavily pigmented cells that have thick walls and exhibit a ***textura angularis*** texture at the sides and base; the innermost layer consists of narrow, hyaline compressed rows of cells. ***Hamathecium*** of 3–7.5 µm broad, dense, branched, cellular pseudoparaphyses that are swollen at some septa. ***Asci*** 60–80 × 9–11 µm (x̄ = 71 × 9.8 µm, n = 15), bitunicate, fissitunicate, cylindrical-clavate, pedicel 15–30 µm long, 8-spored, uni to biseriate, with a minute ocular chamber best seen in immature ascus. ***Ascospores*** 10.5–14 × 4.5–5.5 µm (x̄ = 12.6 × 5.1 µm, n = 20), ellipsoidal, mostly straight, with conically rounded ends, golden-brown to dark brown, 1-septate and constricted at the septum, upper cell wider than the lower cell, with large guttules in each cell, verruculose, and surrounded by a thin mucilaginous sheath which is thicker at both ends. **Anamorph** Coelomycetous on PDA. ***Conidiomata*** pycnidial, gregarious, immersed to superficial, globose to subglobose, dark brown to black. ***Pycnidial wall*** thin, composed of brown cells of ***textura angularis***. ***Conidiogenous cells*** did not observed. ***Conidia*** 2.3–3.3 × 1.4–2 µm (x̄ = 3 × 1.7 µm, n = 30), hyaline, aseptate, round to oblong or ellipsoidal, with small guttules.

Culture characteristics. Ascospores germinated on PDA within 24 h. Following a two-week incubation period at 25 °C, the colonies on PDA medium reached a diameter of 5 cm. These colonies exhibited an undulate margin, initially appearing creamy whitish and transitioning to orange, raised in the center. The colonies were orange at the center and a creamy orange towards the periphery when observed from the reverse side.

Habitat and distribution. This species is found in terrestrial habitats of Yunnan, China, inhabiting dead woody twigs of deciduous hosts (this study).

Material examined. CHINA, Yunnan Province, Xishuangbanna, Mengla County (21.588394°N, 101.435042°E, 776 m), on dead culms of *Indocalamus tessellatus*, 29 January 2022, L. Qinxian, ML23-7-3 (holotype, HKAS 130318), ex-type KUNCC 23-14424; *ibid*. 21.589178°N, 101.435752°E, 782 m, ML23-7-2 (HKAS 130316), living culture KUNCC 23-14422; *ibid*. ML23-7-5 HKAS 130317), living culture KUNCC 23-14423.

Notes. *Montagnula menglaensis* is described as a novel species based on its holomorph. The anamorph of *Montagnula* is rarely encountered; however, Crous et al. (2020) recently reported *Montagnula cylindrospora* based on its anamorphic features. The conidia of *Montagnula menglaensis* resemble to those of *M. cylindrospora*, although the latter fungus exhibits a more cylindrical shape.

Montagnula shangrilana Wanas., sp. nov.
MycoBank No: 850095
Fig. 8

Etymology. The specific epithet "shangrilana" refers to Shangri-La, Yunnan Province, where the holotype was collected.

Holotype. HKAS 126539.

Description. *Saprobic* on dead woody litter of *Rhododendron* sp. **Teleomorph** ***Ascomata*** 120–180 µm high × 150–210 µm diam., immersed to semi-erumpent,
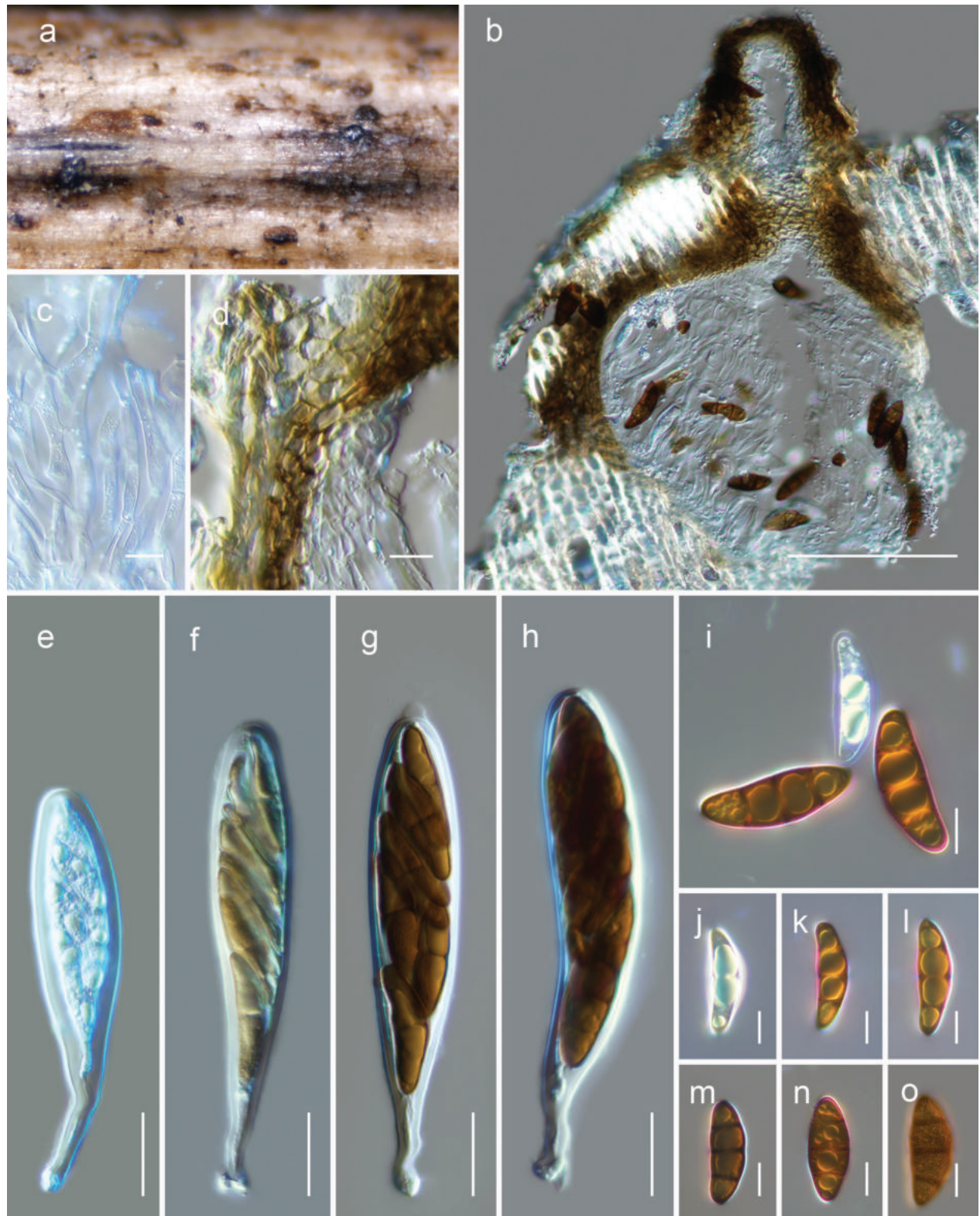
Figure 8. *Montagnula shangrilana* (HKAS 126541, holotype) **a** ascomata on natural wood surface **b** vertical section through an ascoma **c** pseudoparaphyses **d** peridium cells **e−h** asci **i−o** ascospores (see verruculose feature of the ascospore in **o**). Scale bars: 100 μm (**b**); 10 μm (**c, d, j−o**); 20 μm (**e−h**).

gregarious or rarely clustered, globose to subglobose, ostiolate. ***Ostiole*** 80−110 × 50−80 μm ($\bar{x}$ = 100 × 64 μm, n = 6), papillate, central, straight, filled with hyaline cells. ***Peridium*** 10−20 μm thin on the sides and can reach up to 40 μm near

the apex, with an outer layer consisting of heavily pigmented cells that have thick walls and exhibit a **textura angularis** arrangement at the apex, **textura angularis** texture at the sides; the innermost layer consists of hyaline compressed rows of cells. **Hamathecium** of 2–4.5 µm broad, dense, branched, cellular pseudoparaphyses. **Asci** 90–140 × 20–30 µm ($\bar{x}$ = 116.2 × 24 µm, n = 10), bitunicate, fissitunicate, cylindrical-clavate, pedicel 25–40 µm long, 8-spored, uni to biseriate, with a minute ocular chamber best seen in immature ascus. **Ascospores** 48–60 × 17–22 µm ($\bar{x}$ = 55.8 × 19.3 µm, n = 20), ellipsoidal to narrowly oblong, mostly straight, with conically rounded ends at the immature stage that become rounded when mature, golden-brown to dark brown, 3-septate, with large guttules in each cell, verruculose, surrounded by a thick mucilaginous sheath. **Anamorph** Undetermined.

Culture characteristics. Ascospores germinated on PDA within 24 h. Following a two-week incubation period at 25 °C, the colonies on PDA medium reached a diameter of 5 cm. These colonies exhibited a filiform margin, initially appearing whitish and transitioning to greenish gray, raised in the center. The colonies were grey at the center and a greenish gray towards the periphery and radiated when observed from the reverse side.

Habitat and distribution. This species is found in terrestrial habitats of Yunnan, China, inhabiting dead woody twigs of deciduous hosts, in a subalpine environment (this study).

Material examined. CHINA, Yunnan Province, Diqing Tibetan Autonomous Prefecture, Shangri-La (27.289707°N, 100.034477°E, 2744 m), on dead woody litter of *Rhododendron* sp. (Ericaceae), 22 August 2021, L. Qinxian, WTS8-2-2 (holotype, HKAS 126539), ex-type KUNCC 23-14434; *ibid*. (27.290007°N, 100.035233°E, 2833 m, WTS8-2 (HKAS 126538), living culture KUNCC 23-14433.

Notes. In the combined SSU, LSU, ITS, *tef*1-α, and *rpb*2 phylogenetic analysis, two strains of *Montagnula shangrilana* (HKAS 126538, HKAS 126539) formed a monophyletic clade closely related to *M. camporesii* (MFLUCC 16-1369), *M. cirsii* (MFLUCC 13-0680), and *M. scabiosae* (MFLUCC 14-0954). While there were slight variations in size, shape, and color, all four species shared the common characteristic of 3-transversely septate ascospores. The sequence data of *Montagnula camporesii*, *M. cirsii*, and *M. scabiosae* showed no significant differences in their base pair comparisons, suggesting that they may be conspecific. Morphologically, these three species exhibited clavate asci and ellipsoid to fusiform, brown, overlapping, 3-septate ascospores. In contrast, our newly discovered species differed from these three species by 10/508 (1.96%) differences in the ITS region, 13/885 (1.5%) differences in the *tef*1-α region, and 15/956 (1.56%) differences in the *rpb*2 region (only *M. camporesii* possesses *rpb*2).

Montagnula thevetiae Wanas., sp. nov.

MycoBank No: 850096
Fig. 9

Etymology. The specific epithet "thevetiae" refers to the host *Thevetia peruviana* from which the holotype was isolated.

    Holotype. HKAS 126964.
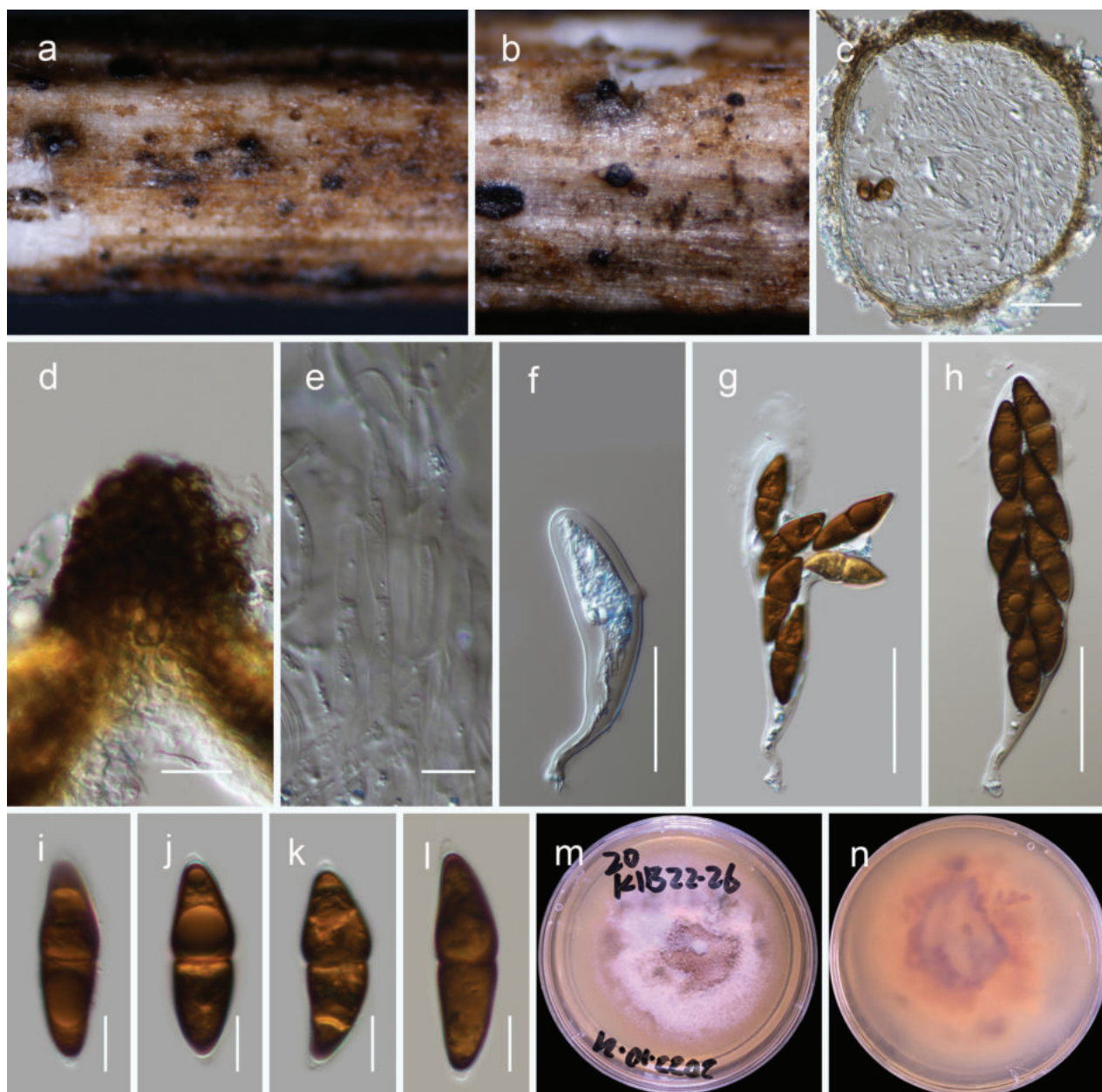
Figure 9. *Montagnula thevetiae* (HKAS 126564, holotype). **a, b** ascomata on natural wood surface **c** vertical section through an ascoma **d** closeup of ostiole **e** pseudoparaphyses **f–h** asci **j–l** ascospores **m, n** culture characteristics on PDA (m = above, n = reverse). Scale bars: 100 µm (**c**); 50 µm (**d, f–h**); 10 µm (**e, i–l**).

Description. *Saprobic* on dead twigs of *Thevetia peruviana*. **Teleomorph Ascomata** 140–160 µm high × 150–190 µm diam., immersed, gregarious or rarely clustered, globose to subglobose, ostiolate. *Ostiole* 40–65 × 50–90 µm ($\bar{x}$ = 50 × 78 µm, n = 6), papillate, central, straight, filled with hyaline to brown cells. *Peridium* 10–20 µm thin on the sides and can reach up to 30 µm near the apex, with an outer layer consisting of heavily pigmented cells that have thick walls and *textura angularis* arrangement, the inner layer consists of hyaline compressed rows of cells. *Hamathecium* of 2–3.5 µm broad, dense, branched, cellular pseudoparaphyses. *Asci* 110–160 × 25–35 µm ($\bar{x}$ = 126.4 × 30.3 µm, n = 12), bitunicate, fissitunicate, cylindrical-clavate, pedicel 25–35 µm long, 8-spored, uni to biseriate, with a minute ocular chamber best seen in immature ascus.

Ascospores 30−40 × 11.5−14 µm (x̄ = 37.3 × 12.8 µm, n = 20), ellipsoidal to narrowly oblong, straight to curved, with conically rounded ends, brown to dark brown, 1-septate, constricted at the septum, with large guttules in each cell, verruculose, surrounded by a thin mucilaginous sheath. **Anamorph** Undetermined.

Culture characteristics. Ascospores germinated on PDA within 24 h. Following a two-week incubation period at 25 °C, the colonies on PDA medium reached a diameter of 4 cm. These colonies exhibit an irregular, flattened to slightly raised morphology and display various color sectors ranging from white, creamy orange to pale brown. The reverse side of the colonies appears creamy orange, with occasional dark patches that can be observed.

Habitat and distribution. This species is found in terrestrial habitats of Yunnan, China, inhabiting dead woody twigs of *Thevetia peruviana* (this study).

Material examined. CHINA, Yunnan Province, Kunming city, Kunming Institute of Botany (25.142238°N, 102.750354°E, 1971 m), on dead twigs of *Thevetia peruviana*, 24 April 2022, L. Qinxian, K2B22-26-2 (holotype, HKAS 126964), *ibid*. (25.140859°N, 102.749045°E, 1968 m, K2B22-26 (HKAS 126963).

Notes. *Montagnula thevetiae* is isolated from the dead twigs of *Thevetia peruviana*. The newly obtained sequences of this fungus formed a monophyletic clade closely related to *Montagnula menglaensis*. Morphologically, they share similarities in having 1-septate ascospores, although *Montagnula thevetiae* exhibits a darker pigmentation. On the other hand, *Montagnula thevetiae* differs from *M. menglaensis* by 15/1023 (1.46%) differences in the SSU region, 19/895 (2.12%) differences in the LSU region, 32/508 (6.3%) differences in the ITS region, 27/885 (3%) differences in the *tef*1-α region, and 86/956 (9%) differences in the *rpb*2 region.

Discussion

Montagnula species in Yunnan Province

The study of lignicolous microfungi in Yunnan Province resulted in the collection of eight *Montagnula* species, including four novel species. This study contributes to our understanding of the diversity and distribution of *Montagnula* species and provides insight into the ecological roles played by these fungi in their respective habitats. *Montagnula aquatica* was previously documented as occurring on submerged decaying wood within a freshwater habitat in Thailand (Sun et al. 2023). However, our recent collection of this species was obtained from a terrestrial habitat in China. The holotype was collected in the Bandu District of the Chiang Rai Province, situated at an approximate elevation of 400−450 m and characterized by a tropical climate. The collection site was near to a waterfall (Sun et al. 2023). In contrast, our new collections were made in the Honghe region of Yunnan Province, which possesses an elevation of approximately 1200 m. The local environment in this region is characterized by poor, eroded soils, steep valleys, and a subtropical climate. This observation suggests that *Montagnula aquatica* may possess an adaptable nature, enabling it to thrive in a wide range of habitats across diverse geographic locations. *Montagnula aquilariae*, another species within the genus, has been identified in the terrestrial habitats of Yunnan, China. It specifically colonizes dead woody twigs of deciduous hosts, including *Aquilaria sinensis* (Hyde et al. 2023). The

holotype of this species was collected from a hilly area in Nanmo, Menghai and Xishuangbanna, situated at an elevation of ~1100 m and characterized by a tropical climate. Additional collections were made from Kunming, located within the same province but at an elevation of ~2000 m, and characterized by a warm and temperate climate. *Montagnula chromolaenicola* has been observed in terrestrial habitats in Thailand, particularly on dead stems of *Chromolaena odorata* (Mapook et al. 2020). The holotype of this species was collected from the Mae Yen mountainous area of Mae Hong Son Province, at an elevation of ~900 m. The local environment of this area exhibits a tropical savanna climate. In our study, we collected this fungus from a terrestrial habitat within the steep valleys of subtropical Honghe, Yunnan, China. In this region, *Montagnula chromolaenicola* was found to inhabit the dead woody litter of deciduous hosts. *Montagnula donacina* has been reported across various terrestrial habitats worldwide, with the majority of records originating from India (Table 1). This species primarily associates with hosts from the Poaceae family. In our study, we collected *Montagnula donacina* from the subtropical Honghe region in China, specifically on decaying woody litter at an elevation of ~600 m. *Montagnula lijiangensis* was collected from terrestrial habitats at a high elevation of ~2725 m. This species was found on dead woody litter of *Quercus* sp. within an environment characterized by a mild subtropical highland climate. *Montagnula menglaensis* was discovered in the terrestrial habitats of Mengla County, Yunnan, China. It was observed colonizing dead culms of *Indocalamus tessellatus*. The local environment of this region exhibits a tropical savanna climate, with an elevation of ~800 m. *Montagnula shangrilana* was found in the terrestrial habitats of Shangri-La, Yunnan, China, where it inhabits dead woody twigs of *Rhododendron* sp. This species has also been observed at higher elevations, reaching ~2800 m, within an environment characterized by a humid continental climate. *Montagnula thevetiae* was discovered within the terrestrial habitat of the botanical garden at the Kunming Institute of Botany in Yunnan, China. This species was found colonizing dead woody twigs of *Thevetia peruviana*. The collection site is situated at an elevation of ~2000 m and experiences a warm and temperate climate.

Taxonomic reassessment and phylogenetic analysis of *Montagnula* species

In a recent study conducted by Sun et al. (2023), *Montagnula chromolaenicola*, *M. puerensis*, *M. saikhuensis*, and *M. thailandica* were regarded as the synonyms of *M. donacina* (Wanasinghe et al. 2016). This decision was based on the absence of clear branches in their phylogenetic tree and the close morphological resemblance between these species. However, upon further examination, it was observed in this study that only *Montagnula donacina* and *M. thailandica* appear to be conspecific, based on combined gene analyses (Fig. 1). When informative sequence data such as *tef*1-α or *rpb*2 were added to the analysis for *Montagnula chromolaenicola*, *M. puerensis*, *M. saikhuensis*, and *M. thailandica*, distinct branches and independent lineages were observed (Fig. 1). This suggests that these species are separate entities. Notably, two sequences of *M. donacina* (HVVV01 and HFG07004) were found to be monophyletic with the type strain of *Montagnula chromolaenicola* (MFLUCC 17-1469), indicating that they belong

to the latter species. In the case of *Montagnula camporesii* (MFLUCC 16-1369), *M. cirsii* (MFLUCC 13-0680), and *M. scabiosae* (MFLUCC 14-0954), the type strains formed a monophyletic lineage as a single species. Nucleotide base pair comparison of LSU, SSU, and ITS between these three strains did not reveal any differences. Therefore, it is suggested that *Montagnula camporesii* and *M. cirsii* should be synonymized under *M. scabiosae*, as it is the oldest name. However, it is important to note that this taxonomic clarification was not within the scope of our study, and future studies should compare the morphology of the holomorphs to resolve any remaining taxonomic confusion. Apart from these two clades, all other species formed distinct lineages in the multi-gene phylogenetic analysis. Out of the accepted 54 species in this genus, sequence data are currently available for only 28 species, including the four new species introduced in this study. This leaves approximately 48% of the species in need of phylogenetic sorting. Hence, future studies based on taxonomy should prioritize obtaining DNA sequence data for the remaining species. They should aim to acquire informative sequence data, such as *tef*1-α and *rpb*2, for all strains, and focus on revising the taxonomy of all species within the genus *Montagnula*.

Morphological characterization of *Montagnula* species

The genus *Montagnula* exhibits rare reporting of its anamorphic features, with only one species, *M. cylindrospora*, described from its anamorph in addition to our study (Crous et al. 2020). This finding has helped confirm its phylogenetic placement within the genus. The teleomorph, rather than the anamorph, appears to be more commonly observed in the natural environment. The majority of *Montagnula* species produce immersed or semi-immersed ascomata, which are globose to subglobose in shape and possess a central papillate ostiole. However, there are a few exceptions, such as *M. camporesii*, *M. cirsii*, and *M. longipes*, which have been reported to have superficial ascomata. Upon closer examination, it becomes apparent that *Montagnula camporesii* and *M. cirsii* actually have semi-immersed ascomata, as illustrated in Hyde et al. (2016, 2020). It is worth mentioning that Aptroot (1995) did not illustrate the ascomata, and their orientation remains unclear. Additionally, only one species, *Montagnula bellevaliae*, has been reported to possess an eccentric ostiole (Hongsanan et al. 2015). The peridium cells of *Montagnula* species commonly exhibit a thick-walled arrangement with a textura angularis pattern. Notably, the cells near the apex are often thicker compared to those on the sides and base walls. A distinguishing characteristic for species within this genus is the presence of swollen cells in pseudoparaphyses. The asci, typically exhibit a cylindrical to clavate shape with a prominent pedicel. Ascospores in *Montagnula* are predominantly described as ellipsoidal to fusiform, pigmented, and septate. The majority of species (>15) have ascospores with a single septum, while some species, including *M. dasylirionis*, *M. dura*, *M. infernalis*, *M. mohavensis*, *M. phragmospora*, *M. spinosella*, and *M. yuccigena*, have been reported to possess muriform spores (Du et al. 2023). The remaining species have ascospores with either 3 or 5 septa. A distinct characteristic within the genus is the verruculose surface texture of the ascospores which is neglected by most of the studies. Only *Montagnula appendiculata*, *M. chiangraiensis*, and *M. chromolaenae* have been documented to possess polar appendages (Aptroot 2004; Mapook et al. 2020).

Ecological preferences and worldwide distribution of *Montagnula* species through culture-dependent studies

The information we gathered from our culture-based investigations revealed that *Montagnula* species were found on 105 genera in 45 distinct plant families, in 55 countries (Table 1). This highlights the wide ecological range and adaptability of *Montagnula* species across different hosts and geographic regions. Among the plant families, Poaceae emerged as the most significant contributor, yielding the highest number of isolated *Montagnula* species (Fig. 4). This finding suggests a potential association between *Montagnula* species and grasses, indicating the ecological importance of the Poaceae family in the life cycle and development of *Montagnula* species. Furthermore, *Montagnula* species were also detected in other plant families, such as Asparagaceae and Fabaceae, indicating their potential interactions with a diverse range of host plants. Among the more than 100 plant genera associated with *Montagnula* species, *Agave* (Asparagaceae), *Opuntia* (Cactaceae), *Phoenix* (Arecaceae), *Ammophila* (Poaceae), and *Yucca* (Asparagaceae) were found to have the greatest number of species, collectively representing 25% of the total count. This highlights the potential preference of *Montagnula* species for these specific plant genera within their respective families. The analysis of country-wise distribution revealed that India had the highest number of *Montagnula* entries (Table 1). The majority of these entries were attributed to *Montagnula donacina*, indicating a wide distribution of this species in India. Among the countries where *Montagnula* species were reported, China exhibited the highest diversity with nine different species, followed by Italy and the USA with seven different species each. This suggests regional variations in the diversity and distribution of *Montagnula* species. Interestingly, our study also detected *Montagnula* species in mushrooms and human skin samples, indicating their presence in alternative sources and potential interactions with other organisms. This highlights the need for further investigation into the ecological roles and potential impacts of *Montagnula* species in these non-traditional habitats. Except for Antarctica, *Montagnula donacina* has been reported from various countries across all six continents. Additionally, it has been identified in 25 different plant families. Investigating the reasons behind its wide distribution and adaptation to diverse ecological conditions would be intriguing. Future studies should focus on the morphological features, secondary metabolites, and gene data-based analyses of the species. To date, only six studies, including this one, have provided entries featuring both morphology and DNA-based sequence data evidence (Pitt et al. 2014; Zhao et al. 2018; Ren et al. 2022a; Li et al. 2023; Sun et al. 2023).

These findings elucidate the global distribution and ecological preferences of *Montagnula* species, highlighting the significance of different sources and plant families in their occurrence and potential ecological interactions. The wide range of sources from which species were identified suggests their adaptability and potential ecological roles in various ecosystems. The study also has important implications for our understanding of the ecology and biology of *Montagnula* fungi. All of the new species described in this study were found to be associated with dead wood, indicating the role that these fungi play in the decomposition of organic matter in forest ecosystems. We suggest that future studies could investigate the functional roles played by *Montagnula* fungi in ecosystem processes, such as carbon and nutrient cycling.

Global biogeography and ecological versatility of *Montagnula* based on metabarcoding data through culture-independent studies (NGS)

In addition to the taxonomic novelties, this study utilized metabarcoding data from the GlobalFungi database (Větrovský et al. 2020) to gain insights into the global diversity and distribution of *Montagnula*. Metabarcoding is a valuable tool that allows for the rapid identification of multiple species from complex environmental samples, providing confirmation of their presence in specific habitats. The analysis of multiple metabarcoding studies provided comprehensive information on the occurrence and distribution patterns of *Montagnula* species worldwide. The distribution of *Montagnula* across diverse biomes underscores their remarkable ecological adaptability and diversity. Forests, constituting 61% of their habitats, emerge as the predominant biome, indicating a strong preference or adaptation of the genus to forest ecosystems. Grasslands, accounting for 18%, also represent a significant habitat, suggesting the versatility in adapting to open and semi-open landscapes of them. Croplands (6%) and shrublands (7%) further exemplify the adaptability of *Montagnula*, thriving in both cultivated areas and natural, low-vegetation environments. Notably, woodlands and anthropogenic areas, representing 2% and 1% respectively, highlight the ability to exist in moderately wooded areas and regions significantly influenced by human activity. Additionally, their presence in aquatic environments, deserts, and wetlands, each accounting for 1% of their habitats, along with a notable 3% in mangroves, reflects the broad ecological niche of them. The marginal occurrence in tundras (0.1%) suggests a limited but notable ability to survive in extreme cold climates. The presence of *Montagnula* in such varied biomes underscores its ecological versatility and the importance of diverse habitats in understanding its biogeography.

The presence of *Montagnula* species has been documented in various regions of Africa, Arctic Ocean, Asia, Australia, Europe, Indian Ocean, North America, Pacific Ocean and South America indicating their widespread occurrence and ecological significance in these areas. In Asia, *Montagnula* species have been observed in multiple countries, including China, India, Indonesia, Iran, Japan, Malaysia, South Korea, Thailand and others (Suppl. material 1). The diverse range of habitats in these regions, such as freshwater habitats, terrestrial environments, and mountainous areas, offer suitable ecological niches for *Montagnula* colonization and growth. The detection of *Montagnula* species in different ecological contexts within Asia suggests their ability to adapt to various local conditions and substrates, contributing to their wide distribution across the continent. For example, in China, *Montagnula* species have been found in diverse habitats ranging from aquatic environments to forests and grasslands (Suppl. material 1), indicating their adaptability to different ecosystems. This adaptability may be attributed to their ability to utilize a wide range of organic materials as substrates, including decaying plant remains.

Australia also exhibits a notable presence of *Montagnula* species, indicating their occurrence in diverse habitats throughout the continent (Bissett et al. 2016; Luis et al. 2019; Turner et al. 2019; Gui et al. 2023). The unique ecosystems in Australia, including deserts, rainforests and grasslands, provide opportunities for *Montagnula* to establish themselves in different ecological niches. The metabarcoding studies were used for various biomes i.e. anthropogenic, aquatic, cropland, desert, forest, grassland, mangrove, shrubland, wetland and woodland (Fig. 3). This highlights the higher presence and distribution of *Montagnula* in different

habitats within Australia. In Europe, *Montagnula* species have been recorded in several countries, including Austria, Belgium, Czech Republic (highest), Estonia, France, Germany, Italy, Netherlands Slovenia, Sweden Switzerland and Spain (Suppl. material 1). The presence of *Montagnula* in Europe suggests their ability to adapt to different climates and ecological conditions. This broad distribution across Europe indicates the need for further investigation into the ecological preferences and potential impacts of *Montagnula* species in this region. For instance, studies in Europe have identified *Montagnula* species in different habitats, such as anthropogenic, aquatic, cropland, desert, forest, grassland, shrubland, tundra, wetland and woodland (Suppl. material 1). Africa and North America also demonstrates a diverse distribution of *Montagnula* species, with the majority of records coming from the South Africa, Namibia, Botswana, Zambia, Mozambique, Kenya, Kenya and Ivory Coast in Africa respectively. United States was having the highest number of sampling locations in North America. Comparatively, the occurrences of *Montagnula* species using metabarcoding data in China, the USA, and European countries are relatively well-documented. However, the rest of the world remains a mystery in terms of *Montagnula* distribution. For example, the majority of Asia, including India and Russia, lacks metabarcoding data for *Montagnula* species. This emphasizes the need for more extensive research and data collection to better understand the global distribution of *Montagnula* and its ecological roles.

Conclusion

Our study on *Montagnula* species has provided valuable insights into their ecological preferences and global distribution patterns. The findings indicate that these fungi exhibit a wide range of climatic distribution, suggesting their adaptability to different temperature ranges and potentially reducing their vulnerability to climate change. The ability of *Montagnula* species to utilize a diverse range of organic materials as substrates, including decaying plant remains, contributes to their widespread distribution across various habitats. Our analysis revealed a diverse range of sources from which *Montagnula* species were detected, including freshwater and terrestrial habitats, further highlighting their ecological versatility. Sediments were found to be particularly rich in *Montagnula* sequences, suggesting their potential as suitable habitats for colonization and growth. Although moderate sequence similarity was observed across different sources and continents, regional variations in ecological preferences and distribution patterns were evident. The diverse host range observed in our field collections aligns with global meta-barcoding sources, emphasizing the ability of *Montagnula* species to thrive in various ecosystems. The ecological adaptability and versatility of *Montagnula* species underscore their success in colonizing diverse habitats. Further research and investigation into their biogeography will contribute to our understanding of their global distribution, ecological roles, and potential impacts on ecosystems. This knowledge is crucial for effective conservation efforts, understanding ecosystem dynamics, and managing ecological balance in different regions.

Acknowledgments

Additional information

Author contributions

Conceptualization: DNW. Data curation: LQX, DNW. Formal analysis: TKF, DNW, TSN. Investigation: TSN, DNW. Methodology: TSN, DNW. Project administration: PEM, JX. Resources: JX. Supervision: JX, PEM. Writing – original draft: TSN, DNW. Writing – review and editing: PEM, TKF.

Author ORCIDs

Dhanushka N. Wanasinghe https://orcid.org/0000-0003-1759-3933
Thilina S. Nimalrathna https://orcid.org/0000-0002-2368-042X
Li Qin Xian https://orcid.org/0009-0006-4936-9409
Turki KH. Faraj https://orcid.org/0000-0002-6012-8474
Jianchu Xu https://orcid.org/0000-0002-2485-2254
Peter E. Mortimer https://orcid.org/0000-0003-3188-9327

Data availability

All of the data that support the findings of this study are available in the main text or Supplementary Information.

References

Abeywickrama PD, Wanasinghe DN, Karunarathna SC, Jayawardena RS, Hyde KD, Zhang W, Li X, Yan J (2020) A new host report of *Diaporthe manihotia* (Diaporthales, Ascomycota) from *Camellia* sp. in Yunnan province, China. Asian Journal of Mycology 3(1): 473–489. https://doi.org/10.5943/ajom/3/1/17

Aluthmuhandiram JVS, Wanasinghe DN, Chethana KWT, Gafforov Y, Saichana N, Hong LX, Jiye Y, Mamarakhimov O (2022) Lophiostomataceae (Dothideomycetes): Intro-

ducing *Lophiostoma khanzada-kirgizbaeva* sp. nov. and *Paucispora xishanensis* sp. nov. Phytotaxa 559(3): 247–262. https://doi.org/10.11646/phytotaxa.559.3.3

Aptroot A (1995) Redisposition of some species excluded from *Didymosphaeria* (Ascomycotina). Nova Hedwigia 60: 325–379.

Aptroot (2004) Two new ascomycetes with long gelatinous appendages collected from monocots in the tropics. Studies in Mycology 50: 307–311.

Aptroot (2006) *Mycosphaerella* and its anamorphs: 2. Conspectus of *Mycosphaerella*. CBS Biodiversity Series 5: 1–231.

Ariyawansa H, Tanaka K, Thambugala KM, Phookamsak R, Camporesi E, Hongsanan S, Monkai J, Wanasinghe DN, Tian Q, Mapook A, Chukeatirote E, Kang J-C, Xu J-C, McKenzie EHC, Jones EBG, Hyde KD (2014) A molecular phylogenetic reappraisal of the Didymosphaeriaceae (=Montagnulaceae). Fungal Diversity 68(1): 69–104. https://doi.org/10.1007/s13225-014-0305-6

Bánki O, Roskov Y, Döring M, Ower G, Vandepitte L, Hobern D, Remsen D, Schalk P, De Walt RE, Keping M (2023) Catalogue of Life Checklist (Version 2023-01-12). Catalogue of Life. https://doi.org/10.48580/dfqz

Barr ME (1990) Some dictyosporous genera and species of Pleosporales in North America. Memoirs of the New York Botanical Garden 62: 1–92.

Bissett A, Fitzgerald A, Meintjes T, Mele PM, Reith F, Dennis PG, Breed MF, Brown B, Brown MV, Brugger J, Byrne M, Caddy-Retalic S, Carmody B, Coates DJ, Correa C, Ferrari BC, Gupta VVSR, Hamonts K, Haslem A, Hugenholtz P, Karan M, Koval J, Lowe AJ, Macdonald S, McGrath L, Martin D, Morgan M, North KI, Paungfoo-Lonhienne C, Pendall E, Phillips L, Pirzl R, Powell JR, Ragan MA, Schmidt S, Seymour N, Snape I, Stephen JR, Stevens M, Tinning M, Williams K, Yeoh YK, Zammit CM, Young A (2016) Introducing BASE: The Biomes of Australian Soil Environments soil microbial diversity database. GigaScience 5(1): 1–21. https://doi.org/10.1186/s13742-016-0126-5

Bivand R, Keitt T, Rowlingson B (2022) rgdal: Bindings for the 'Geospatial' Data Abstraction Library. R package version 1.6–2. https://CRAN.R-project.org/package=rgdal

Boonmee S, Wanasinghe DN, Calabon MS, Huanraluek N, Chandrasiri SKU, Jones GEB, Rossi W, Leonardi M, Singh SK, Rana S, Singh PN, Maurya DK, Lagashetti AC, Choudhary D, Dai YC, Zhao CL, Mu YH, Yuan HS, He SH, Phookamsak R, Jiang HB, Martín MP, Dueñas M, Telleria MT, Kałucka IL, Jagodziński AM, Liimatainen K, Pereira DS, Phillips AJL, Suwannarach N, Kumla J, Khuna S, Lumyong S, Potter TB, Shivas RG, Sparks AH, Vaghefi N, Abdel-Wahab MA, Abdel-Aziz FA, Li GJ, Lin WF, Singh U, Bhatt RP, Lee HB, Nguyen TTT, Kirk PM, Dutta AK, Acharya K, Sarma VV, Niranjan M, Rajeshkumar KC, Ashtekar N, Lad S, Wijayawardene NN, Bhat DJ, Xu RJ, Wijesinghe SN, Shen HW, Luo ZL, Zhang JY, Sysouphanthong P, Thongklang N, Bao DF, Aluthmuhandiram JVS, Abdollahzadeh J, Javadi A, Dovana F, Usman M, Khalid AN, Dissanayake AJ, Telagathoti A, Probst M, Peintner U, Garrido-Benavent I, Bóna L, Merényi Z, Boros L, Zoltán B, Stielow JB, Jiang N, Tian CM, Shams E, Dehghanizadeh F, Pordel A, Javan-Nikkhah M, Denchev TT, Denchev CM, Kemler M, Begerow D, Deng CY, Harrower E, Bozorov T, Kholmuradova T, Gafforov Y, Abdurazakov A, Xu JC, Mortimer PE, Ren GC, Jeewon R, Maharachchikumbura SSN, Phukhamsakda C, Mapook A, Hyde KD (2021) Fungal diversity notes 1387–1511: Taxonomic and phylogenetic contributions on genera and species of fungal taxa. Fungal Diversity 111(1): 1–335. https://doi.org/10.1007/s13225-021-00489-3

Bundhun D, Wanasinghe DN, Maharachchikumbura SSN, Bhat DJ, Huang S-K, Lumyong S, Mortimer PE, Hyde KD (2021) *Yuxiensis granularis* gen. et sp. nov., a novel quellkörper-bearing fungal taxon added to Scortechiniaceae and inclusion of Parasympodiella-

ceae in Coronophorales based on phylogenetic evidence. Life 11(10): e1011. https://doi.org/10.3390/life11101011

Checa J (2004) Dictyosporic Dothideales. Flora Mycologica Iberica 6: 1–162.

Crivelli PG (1983) Über die heterogene Ascomycetengattung *Pleospora* Rabh.; Vorschlag für eine Aufteilung. Diss. ETH Zürich 7318: 1–213. https://doi.org/10.3929/ethz-a-000300166

Crous PW, Summerell BA, Shivas RG, Burgess TI, Decock CA, Dreyer LL, Granke LL, Guest DI, St J, Hardy GE, Hausbeck MK, Huberli D, Jung T, Koukol O, Lennox CL, Liew ECY, Lombard L, McTaggart AR, Pryke JS, Roets F, Saude C, Shuttleworth LA, Stukely MJC, Vanky K, Webster BJ, Windstam ST, Groenewald JZ (2012) Fungal planet description sheets: 107–127. Persoonia 28(1): 138–182. https://doi.org/10.3767/003158512X652633

Crous PW, Wingfield MJ, Chooi YH, Gilchrist CLM, Lacey E, Pitt JI, Roets F, Swart WJ, Cano-Lira JF, Valenzuela-Lopez N, Hubka V, Shivas RG, Stchigel AM, Holdom DG, Jurjević Ž, Kachalkin AV, Lebel T, Lock C, Martín MP, Tan YP, Tomashevskaya MA, Vitelli JS, Baseia IG, Bhatt VK, Brandrud TE, De Souza JT, Dima B, Lacey HJ, Lombard L, Johnston PR, Morte A, Papp V, Rodríguez A, Rodríguez-Andrade E, Semwal KC, Tegart L, Abad ZG, Akulov A, Alvarado P, Alves A, Andrade JP, Arenas F, Asenjo C, Ballarà J, Barrett MD, Berná LM, Berraf-Tebbal A, Bianchinotti MV, Bransgrove K, Burgess TI, Carmo FS, Chávez R, Čmoková A, Dearnaley JDW, Santiago ALCMA, Freitas-Neto JF, Denman S, Douglas B, Dovana F, Eichmeier A, Esteve-Raventós F, Farid A, Fedosova AG, Ferisin G, Ferreira RJ, Ferrer A, Figueiredo CN, Figueiredo YF, Reinoso-Fuentealba CG, Garrido-Benavent I, Cañete-Gibas CF, Gil-Durán C, Glushakova AM, Gonçalves MFM, González M, Gorczak M, Gorton C, Guard FE, Guarnizo AL, Guarro J, Gutiérrez M, Hamal P, Hien LT, Hocking AD, Houbraken J, Hunter GC, Inácio CA, Jourdan M, Kapitonov VI, Kelly L, Khanh TN, Kisło K, Kiss L, Kiyashko A, Kolařík M, Kruse J, Kubátová A, Kučera V, Kučerová I, Kušan I, Lee HB, Levicán G, Lewis A, Liem NV, Liimatainen K, Lim HJ, Lyons MN, Maciá-Vicente JG, Magaña-Dueñas V, Mahiques R, Malysheva EF, Marbach PAS, Marinho P, Matočec N, McTaggart AR, Mešić A, Morin L, Muñoz-Mohedano JM, Navarro-Ródenas A, Nicolli CP, Oliveira RL, Otsing E, Ovrebo CL, Pankratov TA, Paños A, Paz-Conde A, Pérez-Sierra A, Phosri C, Pintos Á, Pošta A, Prencipe S, Rubio E, Saitta A, Sales LS, Sanhueza L, Shuttleworth LA, Smith J, Smith ME, Spadaro D, Spetik M, Sochor M, Sochorová Z, Sousa JO, Suwannasai N, Tedersoo L, Thanh HM, Thao LD, Tkalčec Z, Vaghefi N, Venzhik AS, Verbeken A, Vizzini A, Voyron S, Wainhouse M, Whalley AJS, Wrzosek M, Zapata M, Zeil-Rolfe I, Groenewald JZ (2020) Fungal planet description sheets: 1042–1111. Persoonia 44(1): 301–459. https://doi.org/10.3767/persoonia.2020.44.11

Dissanayake LS, Maharachchikumbura SSN, Mortimer PE, Hyde KD, Kang JC (2021) *Acrocordiella yunnanensis* sp. nov. (Requienellaceae, Xylariales) from Yunnan, China. Phytotaxa 487(2): 103–113. https://doi.org/10.11646/phytotaxa.487.2.1

Du T, Hyde KD, Mapook A, Mortimer PE, Xu JC, Karunarathna SC, Tibpromma S (2021) Morphology and phylogenetic analyses reveal *Montagnula puerensis* sp. nov. (Didymosphaeriaceae, Pleosporales) from southwest China. Phytotaxa 514(1): 1–25. https://doi.org/10.11646/phytotaxa.514.1.1

Eriksson OE (1992) The Non-Lichenized Pyrenomycetes of Sweden. Btjtryck Lund, Sweden, 208 pp.

Fakirova VI (2004) New record of Bulgarian ascomycetes. Mycologia Balcanica 1: 41–43.

Felsenstein J (1985) Confidence limits on phylogenies: An approach using the bootstrap. Evolution; International Journal of Organic Evolution 39(4): 783–791. https://doi.org/10.2307/2408678

French AM (1989) California Plant Disease Host Index. California Department of Food and Agriculture, Sacramento, 394 pp.

Gao Y, Monkai J, Gentekaki E, Ren G-C, Wanasinghe DN, Xu J, Gui H (2021) *Dothidea kunmingensis*, a novel asexual species of Dothideaceae on *Jasminum nudiflorum* (winter jasmine) from Southwestern China. Phytotaxa 529(1): 43–56. https://doi.org/10.11646/phytotaxa.529.1.3

Gui H, Breed M, Li Y, Xu Q, Yang J, Wanasinghe DN, Li Y, Xu J, Mortimer PM (2023) Continental-scale insights into the soil microbial co-occurrence networks of Australia and their environmental drivers. Soil Biology & Biochemistry 186: e109177. https://doi.org/10.1016/j.soilbio.2023.109177

Hall TA (1999) BioEdit: A user-friendly biological sequence alignment editor and analysis program for Windows 95/98/NT. Nucleic Acids Symposium Series 41: 95–98.

Hijmans R (2023) raster: Geographic Data Analysis and Modeling. R package version 3.6–26. https://CRAN.R-project.org/package=raster

Holm L, Holm K (1993) The genus *Pleospora* s.1. from Svalbard. Sydowia 45: 167–187.

Holm L, Holm K (1994) Svalbard Pyrenomycetes. An annotated checklist. Karstenia 34(2): 65–78. https://doi.org/10.29203/ka.1994.308

Hongsanan S, Hyde KD, Bahkali AH, Camporesi E, Chomnunti P, Ekanayaka H, Gomes AAM, Hofstetter V, Jones EBG, Pinho DB, Pereira OL, Tian Q, Wanasinghe DN, Xu J-C, Buyck B (2015) Fungal biodiversity profiles 11–20. Cryptogamie. Mycologie 36(3): 355–380. https://doi.org/10.7872/crym/v36.iss3.2015.355

Huhndorf SM (1992) Studies in *Leptosphaeria*. Transfer of *Leptosphaeria opuntiae* to *Montagnula* (Ascomycetes). Brittonia 44(2): 208–212. https://doi.org/10.2307/2806834

Hyde KD, Aptroot A, Frohlich J, Taylor JE (1999) Fungi from palms. XLII. *Didymosphaeria* and similar ascomycetes from palms. Nova Hedwigia 69(3–4): 449–471. https://doi.org/10.1127/nova.hedwigia/69/1999/449

Hyde KD, Hongsanan S, Jeewon R, Bhat DJ, McKenzie EHC, Jones EBG, Phookamsak R, Ariyawansa HA, Boonmee S, Zhao Q, Abdel-Aziz FA, Abdel-Wahab MA, Banmai S, Chomnunti P, Cui BK, Daranagama DA, Das K, Dayarathne MC, de Silva NI, Dissanayake AJ, Doilom M, Ekanayaka AH, Gibertoni TB, Go'es-Neto A, Huang SK, Jayasiri SC, Jayawardena RS, Konta S, Lee HB, Li WJ, Lin CG, Liu JK, Lu YZ, Luo ZL, Manawasinghe IS, Manimohan P, Mapook A, Niskanen T, Norphanphoun C, Papizadeh M, Perera RH, Phukhamsakda C, Richter C, de Santiago ALCMA, Drechsler-Santos ER, Senanayake IC, Tanaka K, Tennakoon TMDS, Thambugala KM, Tian Q, Tibpromma S, Thongbai B, Vizzini A, Wanasinghe DN, Wijayawardene NN, Wu HX, Yang J, Zeng XY, Zhang H, Zhang JF, Bulgakov TS, Camporesi E, Bahkali AH, Amoozegar AM, Araujo-Neta LS, Ammirati JF, Baghela A, Bhatt RP, Bojantchev S, Buyck B, da Silva GA, de Lima CLF, de Oliveira RJV, de Souza CAF, Dai YC, Dima B, Duong TT, Ercole E, Mafalda-Freire F, Ghosh A, Hashimoto A, Kamolhan S, Kang JC, Karunarathna SC, Kirk PM, Kyto¨vuori I, Lantieri A, Liimatainen K, Liu ZY, Liu XZ, Lu¨cking R, Medardi G, Mortimer PE, Nguyen TTT, Promputtha I, Raj KNA, Reck MA, Lumyong S, Shahzadeh-Fazeli SA, Stadler M, Soudi MR, Su HY, Takahashi T, Tangthirasunun N, Uniyal P, Wang Y, Wen TC, Xu JC, Zhang ZK, Zhao YC, Zhou JZ, Zhu L (2016) Fungal diversity notes 367–490: Taxonomic and phylogenetic contributions to fungal taxa. Fungal Diversity 80: 1–270. https://doi.org/10.1007/s13225-016-0373-x

Hyde KD, Dong Y, Phookamsak R, Jeewon R, Bhat DJ, Jones EBG, Liu NG, Abeywickrama PD, Mapook A, Wei D, Perera RH, Manawasinghe IS, Pem D, Bundhun D, Karunarathna A, Ekanayaka AH, Bao DF, Li JF, Samarakoon MC, Chaiwan N, Lin CG, Phutthacharoen K, Zhang SN, Senanayake IC, Goonasekara ID, Thambugala KM, Phukhamsakda C, Tennakoon DS, Jiang HB, Yang J, Zeng M, Huanraluek N, Liu JK, Wijesinghe SN,

Tian Q, Tibpromma S, Brahmanage RS, Boonmee S, Huang SK, Thiyagaraja V, Lu YZ, Jayawardena RS, Dong W, Yang EF, Singh SK, Singh SM, Rana S, Lad SS, Anand G, Devadatha B, Niranjan M, Sarma VV, Liimatainen K, Hudson BA, Niskanen T, Overall A, Alvarenga RLM, Gibertoni TB, Pfliegler WP, Horváth E, Imre A, Alves AL, da Silva Santos AC, Tiago PV, Bulgakov TS, Wanasinghe DN, Bahkali AH, Doilom M, Elgorban AM, Maharachchikumbura SSN, Rajeshkumar KC, Haelewaters D, Mortimer PE, Zhao Q, Lumyong S, Xu JC, Sheng J (2020) Fungal diversity notes 1151–1276: Taxonomic and phylogenetic contributions on genera and species of fungal taxa. Fungal Diversity 100(1): 5–277. https://doi.org/10.1007/s13225-020-00439-5

Hyde KD, Norphanphoun C, Ma J, Yang HD, Zhang JY, Du TY, Gao Y, Gomes de Farias AR, He SC, He YK, Li CJY, Li JY, Liu XF, Lu L, Su HL, Tang X, Tian XG, Wang SY, Wei DP, Xu RF, Xu RJ, Yang YY, Zhang F, Zhang Q, Bahkali AH, Boonmee S, Chethana KWT, Jayawardena RS, Lu YZ, Karunarathna SC, Tibpromma S, Wang Y, Zhao Q (2023) Mycosphere notes 387–412 – novel species of fungal taxa from around the world. Mycosphere : Journal of Fungal Biology 14(1): 663–744. https://doi.org/10.5943/mycosphere/14/1/8

Katoh K, Rozewicki J, Yamada KD (2019) MAFFT online service: Multiple sequence alignment, interactive sequence choice and visualization. Briefings in Bioinformatics 20(4): 1160–1166. https://doi.org/10.1093/bib/bbx108

Leuchtmann A (1984) Uber *Phaeosphaeria* Miyake und andere bitunicate Ascomyceten mit mehrfach querseptierten Ascosporen. Sydowia 37: 75–194.

Li WL, Liang RR, Dissanayake AJ, Liu JK (2023) Mycosphere Notes 413–448: Dothideomycetes associated with woody oil plants in China. Mycosphere: Journal of Fungal Biology 14(1): 1436–1529. https://doi.org/10.5943/mycosphere/14/1/16

Liu YJ, Whelen S, Hall BD (1999) Phylogenetic relationships among ascomycetes: Evidence from an RNA polymerse II subunit. Molecular Biology and Evolution 16(12): 1799–1808. https://doi.org/10.1093/oxfordjournals.molbev.a026092

Liu JK, Hyde KD, Gareth EBG, Ariyawansa HA, Bhat DJ, Boonmee S, Maharachchikumbura SS, Mckenzie EH, Phookamsak R, Phukhamsakda C, Shenoy BD, AbdelWahab MA, Buyck B, Chen J, Chethana KWT, Singtripop C, Dai DQ, Dai YC, Daranagama DA, Dissanayake AJ, Doilom M, D'souza MJ, Fan XL, Goonasekara ID, Hirayama K, Hongsanan S, Jayasiri SC, Jayawardena RS, Karunarathna SC, Li WJ, Mapook A, Norphanphoun C, Pang KL, Perera RH, Peršoh D, Pinruan U, Senanayake IC, Somrithipol S, Suetrong S, Tanaka K, Thambugala KM, Tian Q, Tibpromma S, Udayanga D, Wijayawardene NN, Wanasinghe D, Wisitrassameewong K, Zeng XY, Abdel-Aziz FA, Adamcík S, Bahkali AH, Boonyuen N, Bulgakov T, Callac P, Chomnunti P, Greiner K, Hashimoto A, Hofstetter V, Kang JC, Xing DL, Li H, Liu XZ, Liu ZY, Matsumura M, Mortimer PE, Rambold G, Randrianjohany E, Sato G, Sri-Indrasutdhi V, Tian CM, Verbeken A, Brackel W, Wang Y, Wen TC, Xu JC, Yan JY, Zhao RL, Camporesi E (2015) Fungal diversity notes 1–110: Taxonomic and phylogenetic contributions to fungal species. Fungal Diversity 72(1): 1–197. https://doi.org/10.1007/s13225-015-0324-y

Lu B, Hyde KD, Ho WH, Tsui KM, Taylor JE, Wong KM Yanna, Zhou D (2000) Checklist of Hong Kong Fungi. Fungal Diversity Press, Hong Kong, 207 pp.

Lu L, Karunarathna SC, Dai D-Q, Xiong Y-R, Suwannarach N, Stephenson SL, Elgorban AM, Al-Rejaie S, Jayawardena RS, Tibpromma S (2022) Description of four novel species in Pleosporales associated with coffee in Yunnan, China. Journal of Fungi 8(10): e1113. https://doi.org/10.3390/jof8101113

Luis P, Saint-Genis G, Vallon L, Bourgeois C, Bruto M, Marchand C, Record E, Hugoni M (2019) Contrasted ecological niches shape fungal and prokaryotic community

structure in mangroves sediments. Environmental Microbiology 21(4): 1407–1424. https://doi.org/10.1111/1462-2920.14571

Maharachchikumbura SSN, Chen Y, Ariyawansa HA, Hyde KD, Haelewaters D, Perera RH, Samarakoon MC, Wanasinghe DN, Bustamante DE, Liu J-K, Lawrence DP, Cheewangkoon R, Stadler M (2021a) Integrative approaches for species delimitation in Ascomycota. Fungal Diversity 109(1): 155–179. https://doi.org/10.1007/s13225-021-00486-6

Maharachchikumbura SSN, Wanasinghe DN, Cheewangkoon R, Al-Sadi AM (2021b) Uncovering the hidden taxonomic diversity of fungi in Oman. Fungal Diversity 106(1): 229–268. https://doi.org/10.1007/s13225-020-00467-1

Maharachchikumbura SSN, Wanasinghe DN, Elgorban AM, Al-Rejaie SS, Kazerooni EA, Cheewangkoon R (2022) *Brunneosporopsis yunnanensis* gen. et sp. nov. and *Allocryptovalsa xishuangbanica* sp. nov., new terrestrial Sordariomycetes from Southwest China. Life 12(5): e635. https://doi.org/10.3390/life12050635

Mapook A, Hyde KD, McKenzie EHC, Gareth Jones EB, Bhat DJ, Jeewon R, Stadler M, Samarakoon MC, Malaithong M, Tanunchai B, Buscot F, Wubet T, Purahong W (2020) Taxonomic and phylogenetic contributions to fungi associated with the invasive weed *Chromolaena odorata* (Siam weed). Fungal Diversity 101(1): 1–175. https://doi.org/10.1007/s13225-020-00444-8

Miller MA, Pfeiffer W, Schwartz T (2010) Creating the CIPRES Science Gateway for Inference of large Phylogenetic Trees. Proceedings of the Gateway Computing Environments Workshop (GCE). New Orleans, 8 pp. https://doi.org/10.1109/GCE.2010.5676129

Monkai J, Wanasinghe DN, Jeewon R, Promputtha I, Phookamsak R (2021) Morphological and phylogenetic characterization of fungi within Bambusicolaceae: Introducing two new species from the Greater Mekong Subregion. Mycological Progress 20(5): 721–732. https://doi.org/10.1007/s11557-021-01694-9

Mortimer PE, Jeewon R, Xu JC, Lumyong S, Wanasinghe DN (2021) Morpho-phylo taxonomy of novel dothideomycetous fungi associated with dead woody twigs in Yunnan Province, China. Frontiers in Microbiology 12: e654683. https://doi.org/10.3389/fmicb.2021.654683

Mulenko W, Majewski T, Ruszkiewicz-Michalska M (2008) A preliminary checklist of Micromycetes in Poland. W. Szafer Institute of Botany Polish Academy of Sciences 9: e752.

Niranjan M, Sarma VV (2018) Twelve new species of ascomycetous from Andaman Islands, India. Kavaka 50: 84–97.

Pebesma E, Bivand R (2023) Spatial Data Science: With Applications in R. Chapman and Hall/CRC, 352 pp. https://doi.org/10.1201/9780429459016

Phookamsak R, Wanasinghe DN, Hongsanan S, Phukhamsakda C, Huang S, Tennakoon DS, Norphanphoun C, Camporesi E, Bulgakov TS, Promputtha I, Mortimer PE, Xu J, Hyde KD (2017) Towards a natural classification of *Ophiobolus* and ophiobolus-like taxa; introducing three novel genera *Ophiobolopsis*, *Paraophiobolus* and *Pseudoophiobolus* in Phaeosphaeriaceae (Pleosporales). Fungal Diversity 87(1): 299–339. https://doi.org/10.1007/s13225-017-0393-1

Pitt WM, Úrbez-Torres JR, Trouillas FP (2014) *Munkovalsaria donacina* from grapevines and Desert Ash in Australia. Mycosphere 5(5): 656–661. https://doi.org/10.5943/mycosphere/5/5/6

R Core Team (2022) R: A language and environment for statistical computing. R Foundation for Statistical Computing, Vienna. https://www.R-project.org/

Ramaley AW, Barr ME (1995) New dictyosporous species from leaves of Agavaceae. Mycotaxon 54: 75–90.

Rambaut A (2012) FigTree version 1.4.0. http://tree.bio.ed.ac.uk/software/figtree

Rehner SA, Buckley E (2005) A Beauveria phylogeny inferred from nuclear ITS and EF1-α sequences: Evidence for cryptic diversification and links to *Cordyceps teleomorphs*. Mycologia 97(1): 84–98. https://doi.org/10.3852/mycologia.97.1.84

Rehner SA, Samuels GJ (1994) Taxonomy and phylogeny of *Gliocladium* analysed from nuclear large subunit ribosomal DNA sequences. Mycological Research 98(6): 625–634. https://doi.org/10.1016/S0953-7562(09)80409-7

Ren GC, Wanasinghe DN, Monkai J, Mortimer PE, Hyde KD, Xu J-C, Pang A, Gui H (2021a) Novel saprobic *Hermatomyces* species (Hermatomycetaceae, Pleosporales) from China (Yunnan Province) and Thailand. MycoKeys 82: 57–79. https://doi.org/10.3897/mycokeys.82.67973

Ren GC, Wanasinghe DN, Monkai J, Hyde KD, Mortimer PE, Xu J, Pang A, Gui H (2021b) Introduction of *Neolophiotrema xiaokongense* gen. et sp. nov. to the poorly represented Anteagloniaceae (Pleosporales, Dothideomycetes). Phytotaxa 482(1): 25–35. https://doi.org/10.11646/phytotaxa.482.1.3

Ren GC, Wanasinghe DN, De Farias ARG, Hyde KD, Yasanthika E, Xu JC, Balasuriya A, Chethana KWT, Gui H (2022a) Taxonomic novelties of woody litter fungi (Didymosphaeriaceae, Pleosporales) from the Greater Mekong Subregion. Biology 11(11): e1660. https://doi.org/10.3390/biology11111660

Ren GC, Wanasinghe DN, Jeewon R, Monkai J, Mortimer PE, Hyde KD, Xu J-C, Gui H (2022b) Taxonomy and phylogeny of the novel rhytidhysteron-like collections in the Greater Mekong Subregion. MycoKeys 86: 65–85. https://doi.org/10.3897/mycokeys.86.70668

Ronquist F, Huelsenbeck J, Teslenko M (2011) MrBayes Version 3.2 Manual: Tutorials and Model Summaries. https://brahms.biology.rochester.edu/software.html [Accessed on 10 June 2023]

Scheuer C (1988) Ascomyceten auf Cyperaceen und Juncaceen im Ostalpenraum. Bibliotheca Mycologica 123: 1–274.

Senwanna C, Mapook A, Samarakoon MC, Karunarathna A, Wang Y, Tang AMC, Haituk S, Suwannarach N, Hyde KD, Cheewangkoon R (2021) Ascomycetes on Para rubber (*Hevea brasiliensis*). Mycosphere 12(1): 1334–1512. https://doi.org/10.5943/mycosphere/12/1/18

Shoemaker RA, Babcock CE (1989) Phaeosphaeria. Canadian Journal of Botany 67(5): 1500–1599. https://doi.org/10.1139/b89-199

Stamatakis A (2014) RAxML Version 8: A tool for Phylogenetic Analysis and Post-Analysis of Large Phylogenies. Bioinformatics 30(9): 1312–1313. https://doi.org/10.1093/bioinformatics/btu033

Sun Y-R, Zhang J-Y, Hyde KD, Wang Y, Jayawardena RS (2023) Morphology and phylogeny reveal three *Montagnula* species from China and Thailand. Plants 12(4): e738. https://doi.org/10.3390/plants12040738

Sung GH, Sung JM, Hywel-Jones NL, Spatafora JW (2007) A multi-gene phylogeny of Clavicipitaceae (Ascomycota, Fungi): Identification of localized incongruence using a combinational bootstrap approach. Molecular Phylogenetics and Evolution 44(3): 1204–1223. https://doi.org/10.1016/j.ympev.2007.03.011

Tedersoo L, Bahram M, Põlme S, Kõljalg U, Yorou NS, Wijesundera R, Villarreal Ruiz L, Vasco-Palacios AM, Thu PQ, Suija A, Smith ME, Sharp C, Saluveer E, Saitta A, Rosas M, Riit T, Ratkowsky D, Pritsch K, Põldmaa K, Piepenbring M, Phosri C, Peterson M, Parts K, Pärtel K, Otsing E, Nouhra E, Njouonkou AL, Nilsson RH, Morgado LN, Mayor J, May TW, Majuakim L, Lodge DJ, Lee SS, Larsson KH, Kohout P, Hosaka K, Hiiesalu I, Henkel TW, Harend H, Guo LD, Greslebin A, Grelet G, Geml J, Gates G, Dunstan W, Dunk C, Drenkhan

R, Dearnaley J, De Kesel A, Dang T, Chen X, Buegger F, Brearley FQ, Bonito G, Anslan S, Abell S, Abarenkov K (2014) Fungal biogeography. Global diversity and geography of soil fungi. Science 346(6213): e1256688. https://doi.org/10.1126/science.1256688

Tennakoon DS, Hyde KD, Wanasinghe DN, Bahkali AH, Camporesi E, Khan S, Phookamsak R (2016) Taxonomy and phylogenetic appraisal of *Montagnula jonesii* sp. nov. (Didymosphaeriaceae, Pleosporales). Mycosphere 7(9): 1346–1356. https://doi.org/10.5943/mycosphere/7/9/8

Tennakoon DS, Thambugala KM, de Silva NI, Suwannarach N, Lumyong S (2022) A taxonomic assessment of novel and remarkable fungal species in Didymosphaeriaceae (Pleosporales, Dothideomycetes) from plant litter. Frontiers in Microbiology 13: e1016285. https://doi.org/10.3389/fmicb.2022.1016285

Thaung MM (2008) Pathologic and taxonomic analysis of leaf spot and tar spot diseases in a tropical dry to wet monsoon ecosystem of lowland Burma. Australasian Plant Pathology 37(2): 180–197. https://doi.org/10.1071/AP08007

Thiyagaraja V, Senanayake IC, Wanasinghe DN, Karunarathna SC, Worthy FR, To-anun C (2019) Phylogenetic and morphological appraisal of *Diatrype lijiangensis* sp. nov. (Diatrypaceae, Xylariales) from China. Asian Journal of Mycology 2(1): 198–208. https://doi.org/10.5943/ajom/2/1/10

Thiyagaraja V, Hyde KD, Wanasinghe DN, Worthy FR, Karunarathna SC (2020) Addition to Melanommataceae: A new geographical record of *Alpinaria rhododendri* from Shangri La, China. Asian Journal of Mycology 3(1): 335–344. https://doi.org/10.5943/ajom/3/1/8

Thiyagaraja V, Wanasinghe DN, Karunarathna SC, Tennakoon DS, Hyde KD, To-Anun C, Cheewangkoon R (2021) *Alloleptosphaeria shangrilana* sp. nov. and first report of the genus (Leptosphaeriaceae, Dothideomycetes) from China. Phytotaxa 491(1): 12–22. https://doi.org/10.11646/phytotaxa.491.1.2

Tibpromma S, Hyde KD, McKenzie EH, Bhat DJ, Phillips AJ, Wanasinghe DN, Samarakoon MC, Jayawardena RS, Dissanayake AJ, Tennakoon DS, Doilom M, Phookamsak R, Tang AM, Xu J, Mortimer PE, Promputtha I, Maharachchikumbura SSN, Khan S, Karunarathna SC (2018) Fungal diversity notes 840–928: Micro-fungi associated with Pandanaceae. Fungal Diversity 93(1): 1–160. https://doi.org/10.1007/s13225-018-0408-6

Trifinopoulos J, Nguyen LT, von Haeseler A, Minh BQ (2016) W-IQ-TREE: A fast online phylogenetic tool for maximum likelihood analysis. Nucleic Acids Research 44(W1): W232–W235. https://doi.org/10.1093/nar/gkw256

Turner BL, Zemunik G, Laliberté E, Drake JJ, Jones FA, Saltonstall K (2019) Contrasting patterns of plant and microbial diversity during long-term ecosystem development. Journal of Ecology 107(2): 606–621. https://doi.org/10.1111/1365-2745.13127

Větrovský T, Morais D, Kohout P, Lepinay C, Algora C, Awokunle Hollá S, Bahnmann BD, Bílohnědá K, Brabcová V, D'Alò F, Human ZR, Jomura M, Kolařík M, Kvasničková J, Lladó S, López-Mondéjar R, Martinović T, Mašínová T, Meszárošová L, Michalčíková L, Michalová T, Mundra S, Navrátilová D, Odriozola I, Piché-Choquette S, Štursová M, Švec K, Tláskal V, Urbanová M, Vlk L, Voříšková J, Žifčáková L, Baldrian P (2020) GlobalFungi, a global database of fungal occurrences from high-throughput-sequencing metabarcoding studies. Scientific Data 7(1): e228. https://doi.org/10.1038/s41597-020-0567-7

Vilgalys R, Hester M (1990) Rapid genetic identification and mapping of enzymatically amplified ribosomal DNA from several *Cryptococcus* species. Journal of Bacteriology 172(8): 4238–4246. https://doi.org/10.1128/jb.172.8.4238-4246.1990

Wanasinghe DN, Mortimer PE (2022) Taxonomic and phylogenetic insights into novel Ascomycota from forest woody litter. Biology 11(6): e889. https://doi.org/10.3390/biology11060889

Wanasinghe DN, Jones EB, Camporesi E, Dissanayake AJ, Kamolhan S, Mortimer PE, Xu J, Abd-Elsalam KA, Hyde KD (2016) Taxonomy and phylogeny of *Laburnicola* gen. nov. and *Paramassariosphaeria* gen. nov. (Didymosphaeriaceae, Massarineae, Pleosporales). Fungal Biology 120(11): 1354–1373. https://doi.org/10.1016/j.funbio.2016.06.006

Wanasinghe DN, Jeewon R, Tibpromma S, Jones EBG, Hyde KD (2017) Saprobic Dothideomycetes in Thailand: *Muritestudina* gen. et sp. nov. (Testudinaceae) a new terrestrial pleosporalean ascomycete, with hyaline and muriform ascospores. Studies in Fungi 2(1): 219–234. https://doi.org/10.5943/sif/2/1/26

Wanasinghe DN, Jeewon R, Peršoh D, Jones EBG, Camporesi E, Bulgakov TS, Gafforov YS, Hyde KD (2018a) Taxonomic circumscription and phylogenetics of novel didymellaceous taxa with brown muriform spores. Studies in Fungi 3(1): 152–175. https://doi.org/10.5943/sif/3/1/17

Wanasinghe DN, Phukhamsakda C, Hyde KD, Jeewon R, Lee HB, Jones EBG, Tibpromma S, Tennakoon DS, Dissanayake AJ, Jayasiri SC, Gafforov Y, Camporesi E, Bulgakov TS, Ekanayake AH, Perera RH, Samarakoon MC, Goonasekara ID, Mapook A, Li W, Senanayake IC, Li J, Norphanphoun C, Doilom M, Bahkali AH, Xu J, Mortimer PE, Tibell L, Tibell S, Karunarathna SC (2018b) Fungal diversity notes 709–839: Taxonomic and phylogenetic contributions to fungal taxa with an emphasis on fungi on Rosaceae. Fungal Diversity 89(1): 1–236. https://doi.org/10.1007/s13225-018-0395-7

Wanasinghe DN, Wijayawardene NN, Xu J, Cheewangkoon R, Mortimer PE (2020) Taxonomic novelties in *Magnolia*-associated pleosporalean fungi in the Kunming Botanical Gardens (Yunnan, China). PLOS ONE 15(7): e0235855. https://doi.org/10.1371/journal.pone.0235855

Wanasinghe DN, Mortimer PE, Xu J (2021) Insight into the systematics of microfungi colonizing dead woody twigs of *Dodonaea viscosa* in Honghe (China). Journal of Fungi 7(3): e180. https://doi.org/10.3390/jof7030180

Wanasinghe DN, Mortimer PE, Bezerra JDP (2022a) Editorial: Fungal Systematics and Biogeography. Frontiers in Microbiology 12: e827725. https://doi.org/10.3389/fmicb.2021.827725

Wanasinghe DN, Ren GC, Xu JC, Cheewangkoon R, Mortimer PE (2022b) Insight into the taxonomic resolution of the pleosporalean species associated with dead woody litter in natural forests from Yunnan, China. Journal of Fungi 8(4): e375. https://doi.org/10.3390/jof8040375

Wanasinghe DN, Bezerra JDP, Xu J, Mortimer PE (2023) *Honghemyces pterolobii*, gen. et sp. nov. (Bezerromycetaceae, Tubeufiales), a new ascomycetous fungus from *Pterolobium macropterum* in Honghe, China. Sydowia 75: 13–21. https://doi.org/10.12905/0380.sydowia75-2022-0013

Wang YZ, Aptroot A, Hyde KD (2004) Revision of the Ascomycete Genus *Amphisphaeria*. Fungal Diversity Press, Hong Kong, 168 pp.

White TJ, Bruns T, Lee S, Taylor JW (1990) Amplification and Direct Sequencing of Fungal Ribosomal RNA Genes for Phylogenetics. PCR Protocols: A Guide to Methods and Applications. Academic Press, San Diego, 315–322. https://doi.org/10.1016/B978-0-12-372180-8.50042-1

Wickham H (2011) ggplot2. Wiley Interdisciplinary Reviews: Computational Statistics 3(2): 180–185. https://doi.org/10.1002/wics.147

Wijayawardene NN, Phillips AJL, Pereira DS, Dai DQ, Aptroot A, Monteiro JS, Druzhinina IS, Cai F, Fan X, Selbmann L, Coleine C, Castañeda-Ruiz RF, Kukwa M, Flakus A, Fiuza PO, Kirk PM, Kumar KCR, Arachchi ISL, Suwannarach N, Tang LZ, Boekhout T, Tan

CS, Jayasinghe RPPK, Thines M (2022) Forecasting the number of species of asexually reproducing fungi (Ascomycota and Basidiomycota). Fungal Diversity 114(1): 463–490. https://doi.org/10.1007/s13225-022-00500-5

Yasanthika E, Dissanayake LS, Wanasinghe DN, Karunarathna SC, Mortimer PE, Samarakoon BC, Monkai J, Hyde KD (2020) *Lonicericola fuyuanensis* (Parabambusicolaceae) a new terrestrial pleosporalean ascomycete from Yunnan Province China. Phytotaxa 449(2): 103–113. https://doi.org/10.11646/phytotaxa.446.2.3

Zhao ZZ, Zhao K, Chen HP, Bai X, Zhang L, Liu JK (2018) Terpenoids from the mushroom-associated fungus *Montagnula donacina*. Phytochemistry 147: 21–29. https://doi.org/10.1016/j.phytochem.2017.12.015

Zhuang W-Y (2001) Higher Fungi of Tropical China. Mycotaxon Ltd, Ithaca, 485 pp.

Supplementary material 1

The biogeography, substrate and habitat affinity of *Montagnula* inferred from the GlobalFungi database

Authors: Dhanushka N. Wanasinghe, Thilina S. Nimalrathna, Li Qin Xian, Turki KH. Faraj, Jianchu Xu, Peter E. Mortimer

Data type: xlsx

Link: https://doi.org/10.3897/mycokeys.101.113259.suppl1

Two new species of *Rhizoplaca* (Lecanoraceae) from Southwest China

Yanyun Zhang[1,2] , Yujiao Yin[1], Lun Wang[1], Christian Printzen[3] , Lisong Wang[2,4], Xinyu Wang[2,4]

1 *College of Life Sciences, Anhui Normal University, 241000, Wuhu, China*
2 *Yunnan Key Laboratory for Fungal Diversity and Green Development, Kunming Institute of Botany, Chinese Academy of Sciences, 650201, Kunming, China*
3 *Senckenberg Research Institute and Natural History Museum, 60325, Frankfurt am Main, Germany*
4 *Key Laboratory for Plant Diversity and Biogeography of East Asia, Kunming Institute of Botany, Chinese Academy of Sciences, 650201, Kunming, China*
Corresponding authors: Lisong Wang (*wanglisong@mail.kib.ac.cn*); Xinyu Wang (*wangxinyu@mail.kib.ac.cn*)

Abstract

In this study, two new species, *Rhizoplaca adpressa* Y. Y. Zhang & Li S. Wang and *R. auriculata* Y. Y. Zhang, Li S. Wang & Printzen, are described from Southwest China, based on their morphology, phylogeny and chemistry. In phylogeny, the two new species are monophyletic, and sister to each other within *Rhizoplaca chrysoleuca*-complex. *Rhizoplaca adpressa* is characterized by its placodioid and closely adnate thallus, pale green and heavily pruinose upper surface, narrow (ca. 1 mm) and white free margin on the lower surface of marginal squamules, the absence of a lower cortex, and its basally non-constricted apothecia with orange discs that turn reddish-brown at maturity. *Rhizoplaca auriculata* is characterized by its squamulose to placodioid thallus, yellowish green and marginally pruinose squamules, wide (1–3 mm) and bluish-black free margin on the lower surface of marginal squamules, the absence of a lower cortex, and its basally constricted apothecia with persistently orange discs. *Rhizoplaca adpressa* and *R. auriculata* share the same secondary metabolites of usnic and placodiolic acids.

Key words: new taxa, *Rhizoplaca chrysoleuca*-complex, *R. melanophthalma*-complex, saxicolous lichen

Citation: Zhang Y, Yin Y, Wang L, Printzen C, Wang L, Wang X (2024) Two new species of *Rhizoplaca* (Lecanoraceae) from Southwest China. MycoKeys 101: 233–248. https://doi.org/10.3897/mycokeys.101.115678

Introduction

Rhizoplaca was established by Zopf (1905), solely to accommodate the type species, *R. opaca* (Ach.) Zopf. This species has since been synonymized to *R. melanophthalma* (Ram.) Leuckert et Poelt according to the priorities established by Nomenclature Codes (Leuckert et al. 1977). The genus *Rhizoplaca* was delimited as possessing an umbilicate thallus, with a distinct upper cortex, rather loose medulla, and thick lower cortex (Arup and Grube 2000; Leuckert et al. 1977). However, one umbilicate species, *R. peltata* (DC.) Leuckert & Poelt, was transferred to *Protoparmeliopsis* M. Chiosy, and several placodioid species, including *Lecanora opiniconensis* Brodo, *L. phadrophthalma* Poelt, *L. novomexicana* H. Magn. were included in *Rhizoplaca* based on molecular phylogenetic results (Zhao et al. 2016). Therefore, the genus circumscription of *Rhizoplaca* requires further investigation.

To date, the genus *Rhizoplaca* includes ca. 25 species that have a worldwide distribution, with the exception of Australia, for which records are lacking (Leuckert et al. 1977; Leavitt et al. 2013a; Zhao et al. 2016; Zhang et al. 2020; Brinker et al. 2022). Recent studies uncovered extensive cryptic species diversity among the cosmopolitan species of *Rhizoplaca*, including *R. chrysoleuca* (Sm.) Zopf, *R. melanophthalma*, *R. phaedrophthalma* and *R. subdiscrepans* (Nyl.) R. Sant (Zhou et al. 2006; Leavitt et al. 2011, 2013a, 2016; Szczepańska et al. 2020). Five new species were described in the *R. melanophthalma*-complex, based on molecular phylogenetic results (Leavitt et al. 2013b). However, the species delimitation of the *R. chrysoleuca*-complex, *R. phaedrophthalma*-complex and *R. subdiscrepans*-complex remains largely unresolved. Our previous study on the genus *Squamarina* verified that the type species of *S.* section *Petroplaca* Poelt, *Squamarina callichroa* (Zahlbr.) Poelt (Poelt 1958), belongs to *Rhizoplaca chrysoleuca*-complex, on the basis of their orange apothecial disc, *Lecanora*-type ascus and the phylogenetic evidence (Zhang et al. 2020). After our extensive field investigations, many similar specimens were collected in Southwest China. A detailed morphological, phylogenetic and chemical study of these materials proved that they are distinct from *R. callichroa* (Zahlbr.) Y. Y. Zhang and represented two species new to science.

Materials and methods

Morphological and chemical analyses

Seventy-one specimens from the *Rhizoplaca chrysoleuca*-complex and related species were examined in this study. All the specimens were deposited in the Lichen Herbarium of Kunming Institute of Botany (KUN-L) unless stated otherwise. A dissecting microscope, Nikon SMZ745T, was used to observe the morphological features. Apothecia and thalli were sectioned by hand with a razor blade and their microscopic traits were observed and measured using a Nikon Eclipse Ci-S microscope. The macro- and micro- photographs were taken by Nikon digital camera head DS-Fi2, and Nikon D850 camera, respectively. Lugol's iodine (I) was used to examine the apical structure of asci and 10% potassium hydroxide (KOH) (K) to test whether the granules in the apothecia and thalli dissolved. Lactophenol cotton blue (LCB) was used to dye the hyphae in the microscopic study. Saturated aqueous solution of sodium hypochlorite (NaClO) (C) and 1,4-Phenylenediamine in ethanol solution (P) were applied for spot tests. We sampled ca. 1 mm^2 apex of the thallus of each dry or fresh specimen for the purpose of thin layer chromatography (TLC) analysis using the solvent systems of A, B and C (Orange et al. 2001).

DNA extraction, amplification and sequencing

We took a ca. 1 mm^2 fragment of the thallus apex from each fresh or dry specimen to extract genomic DNA, following the instructions of the AxyPrep Multisource Genomic DNA Miniprep Kit 50-prep (Qiagen). Polymerase chain reactions (PCR) were performed in an automatic thermocycler (C 1000TM). Five markers, nrITS, nrLSU, RPB1, RPB2 and mtSSU, were chosen for our phylogenetic studies using the primers of ITS1f (Gardes and Bruns 1993) and ITS4a

(Larena et al. 1999), LR0R (Rehner and Samuels 1994) and LR5 (Vilgalys and Hester 1990), gRPB1a (Stiller and Hall 1997) and fRPB1c (Matheny et al. 2002), RPB2-6f and RPB2-7cr (Liu et al. 1999), mrSSU1 mrSSU3R (Zoller et al. 1999), respectively. Amplifications were performed with a total volume of 25 µl, containing 12.5 µl 2× MasterMix [TaqDNA Polymerase (0.1 units/µl), 0.4 mM MgCl$_2$, 0.4 nM dNTPs] (Aidlab Biotechnologies Co. Ltd.), 0.5 µl of each primer, 10 µl ddH$_2$O and 1 µl of DNA. The PCR settings per locus are provided in Table 1. PCR products were sequenced by TsingKe Biological Technology using the same primers which had been used for amplification (Kunming, China).

Phylogenetic analyses

The raw sequences were initially checked with the BLAST tool on the NCBI online service (https://blast.ncbi.nlm.nih.gov/Blast.cgi) to make sure that they belonged to lichenized fungi. According to previous studies, we selected two species of the genus *Protoparmeliopsis* and two species of *Polyozosia* A. Massal. as the outgroup for the genus *Rhizoplaca* (Medeiros et al. 2021; Zhao et al. 2016; Zhang et al. 2020). Geneious R8 was used to assemble the raw sequences and generate one matrix per locus. The matrices were individually aligned with MAFFT using the web service (https://mafft.cbrc.jp/alignment/server/index.html) (Katoh et al. 2019; Kuraku et al. 2013). For alignment, we used the G-INS-1 strategy and default parameters, with the exception of the offset value, which was set as 0.2. Because of the possible incongruence between nuclear genes and mitochondrial genes, we concatenated only the nrITS, nrLSU, RPB1 and RPB2 regions as a 4-loci dataset using the program SequenceMatrix v. 1.7.8 to reconstruct the phylogenetic tree of *Rhizoplaca*. PartitionFinder 2 (Lanfear et al. 2017) was used to estimate the best schemes and nucleotide substitution models for maximum likelihood (ML) and Bayesian inference (BI) analyses. The best schemes and selected models are shown in Table 2.

Bayesian reconstruction of phylogeny based on the 4-loci dataset was performed with MrBayes v. 3.1.2 (Huelsenbeck and Ronquist 2001), using four Markov chains running for one hundred million generations with two runs. Trees were sampled every 1000 generations. The first 25% of runs were discarded as burn-in. Subset rates were modelled as fixed and equal. We used the default distributions for priors. We considered the sampling of the posterior distribution

Table 1. The PCR settings used for each marker.

Program	nrITS & nrLSU	RPB1 & RPB2	mtSSU
Initial denaturation	95 °C 5 min	94 °C 5 min	94 °C 5 min
Phase 1	10 cycles	34 cycles	4 cycles
	95 °C 30 s	94 °C 45 s	94 °C 30 s
	66 °C 30 s	52 °C 50 s	54 °C 30 s
	72 °C 1 min 30 s	72 °C 1 min	72 °C 1 min
Phase 2	34 cycles		30 cycles
	95 °C 30 s		94 °C 30 s
	56 °C 30 s		50 °C 30 s
	72 °C 1 min 30 s		72 °C 1 min
Final extension	72 °C 10 min	72 °C 10 min	72 °C 10 min

Table 2. The best schemes and nucleotide substitution models selected by Partition-Finder, based on the 4-loci dataset.

Partition scheme	Model
Subset1 (nrITS1, nrITS2)	GTR+G
Subset2 (5.8S)	K80+I
Subset3 (nrLSU)	TRNEF+I
Subset4 (RPB1-B codon1, RPB1-C codon1, RPB2-7 codon1)	TRN+G
Subset5 (RPB1-C codon2, RPB1-B codon2, RPB2-7 codon2)	F81+I
Subset6 (intron of RPB1, RPB1-B codon3, RPB1-C codon3, RPB2-7 codon3)	K80+G

to be adequate when the average standard deviation of split frequencies was < 0.01. Tracer v. 1.6 (Rambaut and Drummond 2003) was used to assess the chain convergence by checking the effective sampling size (ESS > 200). ML analyses were performed with RaxmlHPC, using the General Time Reversible model of nucleotide substitution (GTR). Support values were inferred from the 70% majority-rule tree of all saved trees obtained from 1000 non-parametric bootstrap replicates. Trees were visualized in Mega 7 and edited in PowerPoint.

Results and discussion

153 new sequences from eight species of the genera *Rhizoplaca* and *Protoparmeliopsis* were obtained in this study (Table 3). Phylogenetic trees were reconstructed based on a 4-loci dataset including 103 samples of 26 species (Fig 1). Our results were in accordance with the results of previous studies that species of *Rhizoplaca* are split into two main clades (Zhao et al. 2016; Szczepańska et al. 2020; Zhang et al. 2020; Brinker et al. 2022). Clade I (ML = 99; BI = 1.00) included a placodioid species, *Rhizoplaca novomexicana*, two vagrant species, *R. idahoensis* and *R. haydenii*, and the *R. melanophthalma*-complex. The species delimitation of *R. melanophthalma*-complex are largely dependent on the molecular data (Leavitt et al. 2013b). Species in Clade I are characterized by the bluish-black, rarely yellowish discs and mainly distributed in North America (Ryan and Nash 1991; Leavitt et al. 2011). Clade II (ML = 79; BI = 1.00) consisted of *R. chrysoleuca*-complex, *R. subdiscrepans*-complex, *R. phaedrophthalma*-complex and several other species lineages, including *R. pachyphylla*, *R. marginalis*, *R. pseudomellea* and *R. ouimetensis*.

The two new species, *Rhizoplaca adpressa* (ML = 100; BI = 1.00) and *R. auriculata* (ML = 100; BI = 1.00), formed highly supported monophyletic clade, and were grouped together as sister clades within the *R. chrysoleuca*-complex. The large genetic variation within the *R. chrysoleuca*-complex has been shown in multiple previous studies (Cansaran et al. 2006; Zhou et al. 2006; Zheng et al. 2007). Leavitt et al. (2016) delimited six species-level clades within this complex, provisionally called *Rhizoplaca chrysoleuca* 'A', 'B', 'C', 'D', 'E' and 'F'. Our phylogenetic trees showed that *R. chrysoleuca* 'B', 'E' and 'F' were also present in China. To some extent, these clades are morphologically different. Thallus of *R. chrysoleuca* 'B' is placodioid, whereas *R. chrysoleuca* 'E' and *R. chrysoleuca* 'F' are umbilicate that usually contain a conspicuous umbilicus on the lower surface. *R. chrysoleuca* 'E' differs from *R. chrysoleuca* 'F' in its yellowish thalline margins. However, the species delimitation of *R. chrysoleuca*

Table 3. Sequences used in this study; newly obtained sequences are shown in boldface.

Species	Locality*	Voucher specimens	Accession number*				
			nrITS	nrLSU	RPB1	RPB2	mtSSU
Polyozosia contractula	NA	AFTOL-ID 877	HQ650604	DQ986746	DQ986817	DQ992428	DQ986898
P. dispersa	USA	Leavitt 12-002	KT453733	NA	KT453888	KT453921	NA
Protoparmeliopsis muralis	Austria: Salzburg	ZYY120 (KUN-L)	**OR669100**	**OR669126**	**OR712769**	**OR712777**	**OR681862**
Protoparmeliopsis sp.	China: Qinghai	18-59148 (KUN-L)	**OR669101**	**OR669127**	**OR712770**	**OR712778**	**OR681863**
Rhizoplaca adpressa	China: Yunnan	17-56961 (KUN-L)	**OR669102**	NA	NA	**OR712779**	NA
R. adpressa	China: Yunnan	17-56981 (KUN-L)	**OR669103**	**OR669128**	NA	**OR712780**	NA
	China: Yunnan	17-56973 (KUN-L)	**OR669104**	**OR669129**	NA	**OR712781**	NA
	China: Yunnan	19-66393 (KUN-L)	**OR669105**	NA	NA	**OR712782**	NA
	China: Yunnan	18-59008 (KUN-L)	**OR669106**	NA	NA	NA	NA
	China: Yunnan	18-59001 (KUN-L)	**OR669107**	NA	NA	NA	NA
R. auriculata	China: Yunnan	18-60355 (KUN-L)	**OR669108**	**OR669130**	**OR712771**	**OR712783**	NA
	China: Yunnan	15-49794 (KUN-L)	**OR669109**	**OR669131**	**OR712772**	**OR712784**	NA
	China: Yunnan	15-49796 (KUN-L)	**OR669110**	**OR669132**	**OR712773**	**OR712785**	NA
R. callichroa	China: Sichuan	14-43348 (KUN-L)	MK778045	NA	NA	NA	NA
	China: Sichuan	14-43357 (KUN-L)	MK778046	NA	NA	NA	NA
	China: Sichuan	14-43359 (KUN-L)	MK778043	NA	NA	NA	NA
	China: Yunnan	14-43308 (KUN-L)	MK778044	NA	NA	NA	NA
	China: Sichuan	19-63066 (KUN-L)	**OR669111**	NA	NA	NA	NA
	China: Sichuan	19-63072 (KUN-L)	**OR669112**	NA	NA	NA	NA
	China: Sichuan	19-62900 (KUN-L)	**OR669113**	NA	NA	NA	NA
R. chrysoleuca 'A'	USA: Wisconsin	Leavitt 12-006 (F)	KU934562	NA	NA	KU935053	NA
	Russia: Altaysky	Vondrak 10125 (PRA)	KU934565	NA	KU935314	KU935056	NA
	Russia: Altaysky	Vondrak 10040 (PRA)	KU934567	NA	KU935316	KU935058	NA
R. chrysoleuca 'B'	China: Qinghai	18-59134 (KUN-L)	**OR995297**	**OR995320**	**PP049801**	**PP054345**	**PP001783**
	China: Qinghai	18-59122 (KUN-L)	**OR995298**	**OR995321**	**PP049802**	**PP054346**	**PP001784**
	China: Qinghai	18-59114 (KUN-L)	**OR995299**	**OR995322**	**PP049803**	**PP054347**	**PP001785**
	China: Qinghai	18-59142 (KUN-L)	**OR995300**	**OR995323**	**PP049804**	**PP054348**	**PP001786**
	China: Xizang	19-65470 (KUN-L)	**OR995301**	**OR995324**	NA	NA	**PP001787**
	Russia: Altaysky	Vondrak 9981 (PRA)	KU934568	NA	KU935317	KU935059	NA
	Russia: Altaysky	Vondrak 10023 (PRA)	KU934570	NA	NA	KU935061	NA
	Russia: Altaysky	Vondrak 10051 (PRA)	KU934571	NA	NA	KU935062	NA
R. chrysoleuca 'C'	Russia: Altaysky	Vondrak 10017 (PRA)	KU934573	NA	KU935318	KU935064	NA
R. chrysoleuca 'D'	USA: Utah	55019 (BRY-C)	HM577254	NA	KU935319	KU935065	NA
	USA: Colorado	Leavitt 2013-CO-CP-8640A (F)	KU934575	NA	KU935320	KU935067	NA
	USA: Colorado	Leavitt 2013-CO-RM-8655A (F)	KU934577	NA	KU935321	KU935069	NA
R. chrysoleuca 'E'	USA: Utah	55013 (BRY-C)	HM577248	NA	KU935325	KU935073	NA
	Iran: East Azarb aijan	MS014636 (hb. Sohrabi)	KT453731	NA	KU935322	KU935070	NA
	Russia: Altaysky	Vondrak 10053 (PRA)	KU934582	NA	KU935330	KU935078	NA
	China: Shaanxi	14-45108 (KUN-L)	**OR995302**	**OR995325**	NA	NA	NA
	China: Shaanxi	14-45163 (KUN-L)	**OR995303**	**OR995326**	NA	NA	**PP001788**
	Austria	0220110 (FR)	**OR995304**	NA	NA	NA	NA
	USA: Utah	St. Clair 15773 (GZU)	**OR995305**	NA	NA	NA	NA
	China: Qinghai	18-59092 (KUN-L)	**OR995306**	**OR995327**	**PP049805**	**PP054349**	**PP001789**
	China: Sichuan	16-51653 (KUN-L)	**OR995307**	**OR995328**	**PP049806**	NA	NA

Species	Locality*	Voucher specimens	Accession number*				
			nrITS	nrLSU	RPB1	RPB2	mtSSU
R. chrysoleuca 'F'	China: Xizang	16-53440 (KUN-L)	**OR995308**	**OR995329**	NA	**PP054350**	**PP001790**
	China: Xizang	16-53296 (KUN-L)	**OR995309**	**OR995330**	**PP049807**	**PP054351**	NA
	Russia: Altaysky	Davydov E. A. 6377 (M)	**OR995310**	NA	NA	NA	NA
	Turkey: Anatolia	Hafellner J. 65691 (GZU)	**OR995311**	NA	NA	NA	NA
	Italy: Trentino-Alto	Hafellner J. 61276 (GZU)	**OR995312**	NA	NA	NA	NA
	Austria: Tyrol	Mayrhofer H. 20293 (GZU)	**OR995313**	NA	NA	NA	NA
	China: Xizang	16-54163 (KUN-L)	**OR995314**	**OR995331**	NA	**PP054352**	**PP001791**
	China: Xizang	19-66093 (KUN-L)	**OR995315**	**OR995332**	**PP049808**	NA	NA
	China: Xizang	16-50956 (KUN-L)	**OR995316**	**OR995333**	NA	**PP054353**	**PP001792**
	China: Qinghai	18-59125 (KUN-L)	**OR995317**	**OR995334**	NA	**PP054354**	NA
	China: Qinghai	18-59131 (KUN-L)	**OR995318**	**OR995335**	**PP049809**	**PP054355**	**PP001793**
	China: Qinghai	17-57088 (KUN-L)	**OR995319**	**OR995336**	**PP049810**	**PP054356**	**PP001794**
	USA: Utah	55000 (BRY-C)	HM577233	NA	KU935335	KU935084	NA
	Russia: Chelyabinsk	Vondrak 9418 (PRA)	KU934593	NA	KU935344	KU935093	NA
	Spain: Teruel	226604 (MAF)	KU934596	NA	NA	NA	NA
	Turkey: Giresun	Vondrak 9739 (PRA)	KU934597	NA	KU935347	KU935096	NA
	Russia: Altaysky	Vondrak 10134 (PRA)	KU934608	NA	KU935349	KU935098	NA
R. cylindrica	USA	U305 (GZU)	AF159941	NA	NA	NA	NA
R. haydenii	USA	55029 (BRY-C)	HM577298	NA	KU935352	KU935102	NA
	USA: Idaho	Leavitt 727 (BRY-C)	NA		KT453902	KT453932	NA
R. huashanensis	China: Shaanxi	Wei18357 (HMAS-L)	AY530885	NA	NA	NA	NA
R. idahoensis	USA	55036 (BRY-C)	HM577297	NA	KU935367	KU935116	NA
R. marginalis	USA: California	Leavitt 739 (BRY-C)	KT453732	NA	KT453901	KT453936	NA
	USA	0020826b (BRY-L)	KU934655	NA	KU935370	KU935123	NA
R. melanophthalma	USA	55049 (BRY-C)	HM577270	NA	JX948324	JX948362	NA
	Iran	MS014628 (H)	JX948271	NA	JX948317	JX948355	NA
R. novomexicana	USA	55026 (BRY-C)	HM577257	NA	KU935390	KU935136	NA
	USA	Leavitt 8684A (F)	KU934708	NA	KU935391	KU935137	NA
R. occulta	USA	55076 (BRY-C)	HM577307	NA	JX948344	JX948383	NA
R. opiniconensis	NA	U217	AF159928	NA	NA	NA	NA
	China: Xizang	19-64228 (KUN-L)	**OR669116**	**OR669135**	NA	NA	NA
	China: Qinghai	19-66383 (KUN-L)	**OR669117**	**OR669136**	NA	NA	NA
	China: Xizang	18-61026 (KUN-L)	**OR669118**	NA	NA	NA	NA
	China: Qinghai	18-59112 (KUN-L)	**OR669119**	**OR669137**	**OR712775**	**OR712788**	**OR681865**
R. ouimetensis	Canada	229203 (O-L)	ON943161	NA	NA	NA	NA
	Canada	229204 (O-L)	ON943160	NA	NA	NA	NA
R. pachyphylla	China: Gansu	18-59466 (KUN-L)	MK778048	NA	MK766417	MK766436	MN192152
	China: Gansu	18-59446 (KUN-L)	MK778047	NA	MK766416	MK766435	MN192151
	China: Gansu	18-59482 (KUN-L)	MK778049	NA	MK766418	MK766437	MN192153
	China: Gansu	18-59561 (KUN-L)	MK778050	NA	MK766419	MK766438	MN192154
R. parilis	Kyrgyzstan	9203313 (H)	JX948193	NA	KU935392	KU935138	NA
	USA	55088 (BRY-C)	HM577319	NA	JX948313	JX948352	NA
R. phaedrophthalma	NA	U291	AF159938	NA	NA	NA	NA
	China: Xizang	14-46591 (KUN-L)	**OR669120**	**OR669138**	NA	NA	**OR681866**
	China: Qinghai	18-59223 (KUN-L)	**OR669121**	**OR669139**	NA	**OR712789**	**OR681867**
	China: Qinghai	18-59140 (KUN-L)	**OR669122**	**OR669140**	NA	**OR712790**	**OR681868**

Species	Locality*	Voucher specimens	Accession number*				
			nrITS	nrLSU	RPB1	RPB2	mtSSU
R. phaedrophthalma	China: Qinghai	18-59209 (KUN-L)	**OR669123**	**OR669141**	NA	**OR712791**	**OR681869**
	China: Gansu	18-59747 (KUN-L)	**OR669124**	**OR669142**	NA	**OR712792**	**OR681870**
	China: Xizang	16-50725 (KUN-L)	**OR669125**	**OR669143**	**OR712776**	**OR712793**	**OR681871**
R. polymorpha	USA	55095 (BRY-C)	HM577326	NA	KU935411	KU935159	NA
	USA	Leavitt 11-026 (F)	JX948194	NA	JX948328	JX948366	NA
R. porterii	USA	55149 (BRY-C)	HM577380	NA	JX948341	JX948380	NA
	USA	55145 (BRY-C)	HM577376	NA	JX948340	JX948379	NA
R. pseudomellea	USA	Wetmore 95084 (MIN)	MN931737	NA	NA	NA	NA
	USA	Ryan 28456 (ASU)	MN931733	NA	NA	NA	NA
R. shushanii	USA	55065 (BRY-C)	HM577286	NA	JX948334	JX948372	NA
	USA	55067 (BRY-C)	HM577288	NA	JX948335	JX948373	NA
R. subdiscrepans	Russia	9412 (PRA)	KU934899	NA	NA	NA	NA
	Russia	9420b (PRA)	KU934901	NA	NA	NA	NA

*NA = not available.

s. str. and above clades still needs future studies, including the check of type specimen, secondary metabolites and the detailed morphological features. The species, *R. callichroa*, *R. huashanensis*, together with the two new species, *R. adpressa* and *R. auriculata*, formed a monophyletic clade that forms a sister group to *R. chrysoleuca* 'C'. However, these species differ from *R. chrysoleuca* by their broadly ellipsoid to subfusiformis ascospores (Wei 1984; Zhang et al. 2020). *Rhizoplaca huashanensis* is the basal species of this clade and differs in its black apothecial disc, the presence of a lower cortex, and its restricted distribution in Northwest China (Wei 1984). *Rhizoplaca callichroa* formed a sister clade to *R. adpressa* and *R. auriculata* but was distinguished by the pale brown lower surface (Zhang et al. 2020).

To date, ten species of Clade II in *Rhizoplaca* have been reported from China: *R. adpressa*, *R. auriculata*, *R. callichroa*, *R. chrysoleuca* (representing multiple lineages), *R. fumida*, *R. huashanensis*, *R. pachyphylla*, *R. subdiscrepans*, *R. opiniconensis* and *R. phaedrophthalma* (Gao 1987; Zhao et al. 2016; Lü et al. 2020; Wei 2020; Zhang et al. 2020). The species *R. fumida* has been synonymized to *R. chrysoleuca* based on morphological and phylogenetic analyses (Wei and Wei 2005). According to a revised circumscription of *R. subdiscrepans* s. str. (Szczepańska et al. 2020), the records of this species in China need more investigation. We provided a key to only the eight species of *Rhizoplaca* Clade II which have been confirmed as present in China. This key should effectively distinguish between these species.

Taxonomy

Rhizoplaca adpressa Y. Y. Zhang & Li S. Wang, sp. nov.
MycoBank No: 851059
Fig. 2

Type. CHINA. Yunnan Prov.: Kunming Ci., Shilin Co., 24°41'N, 103°22'E, 1883 m, on calcareous rock, 25 October 2017, Li S. Wang et al. 17-56973 (KUN-L0066051).
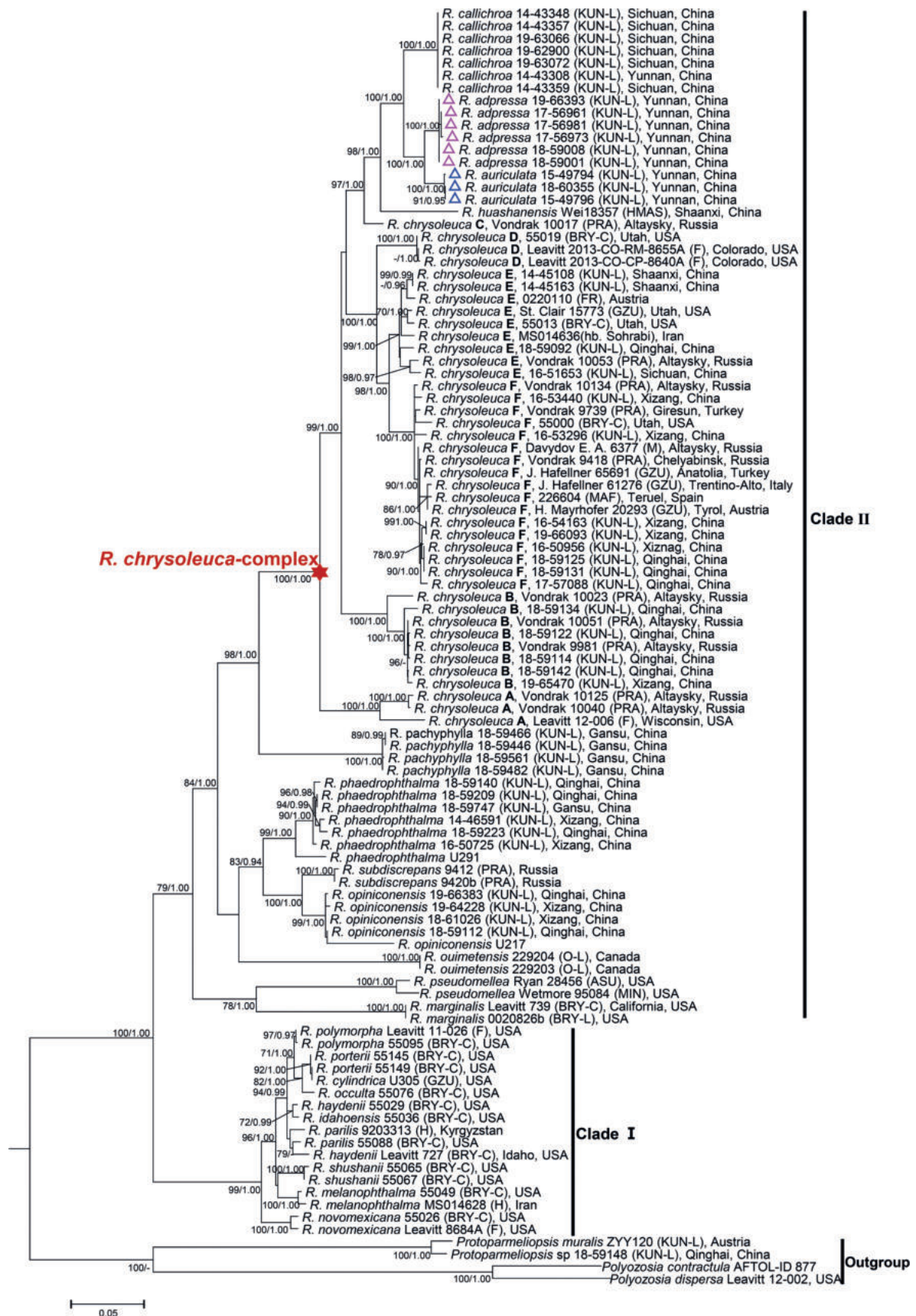
Figure 1. Maximum Likelihood tree for the genus *Rhizoplaca*, based on a 4-loci (nrITS, nrLSU, RPB1 and RPB2) concatenated dataset. Maximum Likelihood bootstrap values ≥ 70 and posterior probabilities ≥ 0.90 are displayed on adjacent branches. The two new species are marked by triangles.

Diagnosis. The species *Rhizoplaca adpressa* is characterized by its placodioid and closely adnate thallus, pale green and heavily pruinose upper surface, lower surface of marginal squamules with a white and narrow free margin, the absence of lower cortex, and the basally non-constricted apothecia with orange disc that turn reddish-brown at maturity.

Etymology. The epithet refers to the thallus, which is closely adnate to the substratum.

Description. Thallus placodioid, umbilicate at least when young, rosulate, 1–3.5 cm across, centrally areolate, areoles continuous, plane, ca. 0.5 mm in diam., marginally squamulose, squamules radiating, 1–2.5 mm across. Upper surface pale green, heavily pruinose, smooth, rarely cracked, matt, lower surface with a white and narrow (ca. 1 mm) free margin, without tomentum. Upper cortex 13–20 µm thick, filled with pale brown (soluble in K) and brown (insoluble in K) granules, consisting of thin-walled and short-celled hyphae, 1.5–2.5 µm in diam., length of cell 3–7 µm, epinecral 10–16 µm thick, filled with brown granules, partly soluble in K, algal layer continuous, filled with black substance, insoluble in K, 67–75 µm thick, algae 8.5–12 µm in diam., medulla filled with black substance, insoluble in K, lower cortex lacking.

Apothecia common, laminal, scattered to slightly grouped, lecanorine, originally at same level with thallus, without thalline margin, then adnate, not constricted at base, 0.5–1 mm in diam. Apothecial disc orange, reddish-brown with age, pruinose, plane to slightly convex, thalline margin entire, thinner than 0.1 mm, concolorous with thallus. Hymenium filled with orangish and gray granules, insoluble in K, 58–70 µm high, epihymenium non-gelatinized, filled with brown (soluble in K) and orange granules (insoluble in K), weakly interspersed, 12–16 µm thick, parathecium extremely reduced, subhymenium with orangish gray granules, insoluble in K, 12.5–20 µm, hypothecium colorless, with orange and brown granules, insoluble in K, 50–180 µm, algae under hypothecium not continuous, irregularly grouped, cortex of thalline margin same as upper cortex, even, ca. 25 µm thick, paraphyses simple, ca. 3 µm in diam., septate, length of cell 10–13 µm, asci clavate, 50–55 × 15–22 µm, ascospores broadly ellipsoid to subfusiformis, hyaline, 9.5–13 × 6.5–9 µm. Pycnidia rare, conidia filiform, 16–25 × ca. 0.7 µm.

Chemistry. K+ pale yellow, C-, P-; usnic and placodiolic acids were detected in TLC.

Distribution and ecology. The new species only grows on exposed hard calcareous rock in karst landform at elevations of 1883–2623 m in Yunnan Province, China.

Notes. *Rhizoplaca callichroa* is similar to this new species but differs in its yellowish green upper surface, the apothecia constricted at base when mature, and the persistently orange apothecial disc (Zhang et al. 2020). *Rhizoplaca huashanensis* is similar to *R. adpressa* but differs in its black lower surface that contains a lower cortex, and its restricted distribution in Shaanxi (Northwest China) (Wei 1984). *Rhizoplaca chrysoleuca* differs from *R. adpressa* in its larger apothecia (0.5–6 mm in diam.) and marginal lobes (2–5 mm long, 1–3 mm wide), a wide and bluish-black free margin on lower surface, the presence of gelatinized lower cortex, and the persistently orange apothecia with constricted base. *Rhizoplaca phaedrophthalma* also has reddish-brown apothecial disc when mature, but differs in the lobate thallus with yellowish and epruinose
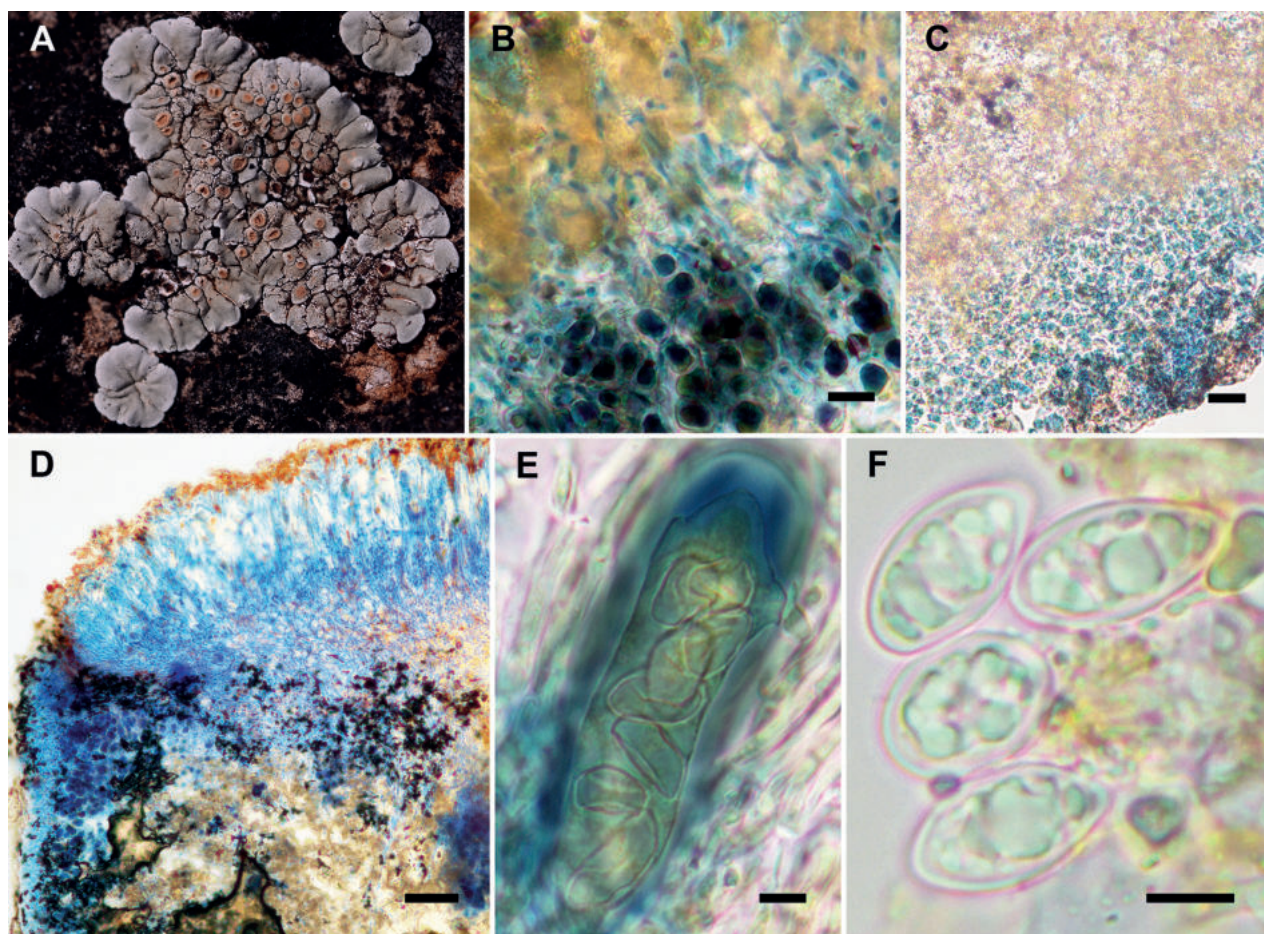
Figure 2. *Rhizoplaca adpressa* (KUN-L0066051) **A** holotype **B** hyphae of upper cortex (LCB) **C** lower surface lacks lower cortex (LCB) **D** section of apothecia (LCB) **E** ascus (Lugol's solution) **F** ascospores (water). Scale bars: 10 μm (**B**); 20 μm (**C**); 50 μm(**D**); 5 μm (**E, F**).

upper surface, the strongly convex disc, and the smaller ascospores, 7–10 × 4.5–7 μm (Lü et al. 2020; Poelt 1958).

Additional specimens examined. CHINA. Yunnan Prov.: Dali, Heqing Co., Songgui Town, 26°18'N, 100°10'E, 2229 m, on calcareous rock, 20 June 2018, Li S. Wang et al. 18-58987 (KUN-L0065133), 18-58988 (KUN-L0065134), 18-59991 (KUN-L0065137), 18-58997 (KUN-L0065143), 18-59001 (KUN-L0065147), 18-59008 (KUN-L0065154), 18-59935 (KUN-L0063742), 18-59937 (KUN-L0063744), 18-59940 (KUN-L0063747), same location, 26°18'N, 100°10'E, 2260 m, on calcareous rock, 29 August 2005, Li S. Wang, D. L. Niu & H. Luo 05-25135 (KUN-L0040473); Kunming Ci., Shilin Co., 24°41'N, 103°22'E, 1883 m, on calcareous rock, 25 October 2017, Li S. Wang et al. 17-56961 (KUN-L0066046), 17-56965 (KUN-L0062405), 17-67966 (KUN-L0062443), 17-56981 (KUN-L0076202), 17-57054 (KUN-L0062534), same location, 24°42'N, 103°21'E, 1890 m, on calcareous rock, 19 September 2003, Li S. Wang 03-22617 (KUN-L0040472), same location, 1910 m, on calcareous rock, 11 May 2008, Li S. Wang 08-29555 (KUN-L0040474), same location, 1900 m, on calcareous rock, 19 February 2010, Li S. Wang 10-31345 (KUN-L0048845); Lijiang Ci., Ning lang Co., Yongning Vil., 27°43'N, 100°40'E, 2675 m, on calcareous rock, 27 July 2020, Li S. Wang et al. 20-66488 (KUN-L0076274); Yulong Co., Mt. Yulong, 26°56'N, 100°12'E, 2623 m, on calcareous rock, 31 December 2019, Li S. Wang & Y. Y. Zhang 19-66393 (KUN-L0076201).

Rhizoplaca auriculata Y. Y. Zhang, Li S. Wang & Printzen, sp. nov.

MycoBank No: 851060

Fig. 3

Type. CHINA. Yunnan Prov.: Deqin Co., Benzilan Vil., besides Jinsha River, 28°11'N, 99°21'E, 2099 m, on chloritoid schist, 19 August 2018, Li S. Wang et al. 18-60139 (KUN-L0065413).

Diagnosis. The species is characterized by the yellowish green upper surface, ear-like marginal squamules containing a bluish-black and wide, free lower margin, the lack of lower cortex, and the persistently orange apothecia with constricted base.

Etymology. The epithet refers to the ear-like margins of marginal squamules.

Description. Thallus squamulose to placodioid, umbilicate at least when young, rosulate or not, 2–5 cm across, centrally squamulose, squamules continuous to irregularly overlapped, slightly convex, 1–2.5 mm across, marginal squamules radiating or not, larger than the center, 2–4 mm across, with ear-like margins. Upper surface yellowish green, epruinose to only pruinose at margins of squamules, smooth to rugose, lower surface with a bluish-black free margin, 1–3 mm wide, no tomentum. Upper cortex 16–22 μm thick, filled with pale brown granules, soluble in K, upper part with scattered brown granules, insoluble in K, consisting of thin-walled and short-celled hyphae, 2–3 μm in diam., length of cell 3–7 μm, epinecral 10–25 μm thick, filled with brown granules, soluble in K, algal layer continuous, 67–80 μm thick, filled with black substance, insoluble in K, algae 8.5–12 μm in diam., medulla filled with black substance, insoluble in K, lower cortex lacking.

Apothecia common, laminal, scattered to slightly grouped, lecanorine, sessile, constricted at base, 0.5–2 (3) mm in diam., disc orange, pruinose, plane to slightly convex, thalline margin entire, 0.1–0.2 mm wide, concolorous with thallus, pruinose. Hymenium filled with orange and gray granules, insoluble in K, 75–87 μm high, epihymenium non-gelatinized, filled with brown (soluble in K) and orange granules (insoluble in K), not interspersed, 12.5–19 μm thick, parathecium extremely reduced, subhymenium with gray granules, insoluble in K, 17–30 μm, hypothecium colorless, with grouped brown granules, insoluble in K, 60–100 μm, algae under hypothecium continuous to irregularly grouped, cortex of thalline margin same as upper cortex, even, 25–30 μm thick, paraphyses simple to slightly branched, ca. 3 μm in diam., septate, length of cell 9–14 μm, tips slightly thickened, asci clavate, 62–75 × 15–21 μm, ascospores broadly ellipsoid to subfusiformis, hyaline, 10–16 × 6.5–9.5 μm. Pycnidia immersed in the thallus, ostioles not seen, conidia filiform, straight to curved, 22.5–37.5 × 0.7 μm.

Chemistry. K+ pale yellow, C-, P-; usnic and placodiolic acids detected in TLC.

Distribution and ecology. The new species only grows on dry and exposed calcareous chloritoid schist at elevation of 2000–2108 m beside the Jinsha River in Sichuan and Yunnan Provinces, China.

Notes. *Rhizoplaca callichroa* is similar to this new species in thallus and apothecia size but differs by its pale brown, lower free margins (Zhang et al. 2020) and the substratum of hard calcareous rock in karst landform. *R. huashanensis* shares yellowish green upper surface and black lower surface with *R. auriculata*, but differs in the presence of a lower cortex, black apothecial discs, smaller ascospores (11.55–12.32 × 6.93–7.70 μm), and the absence
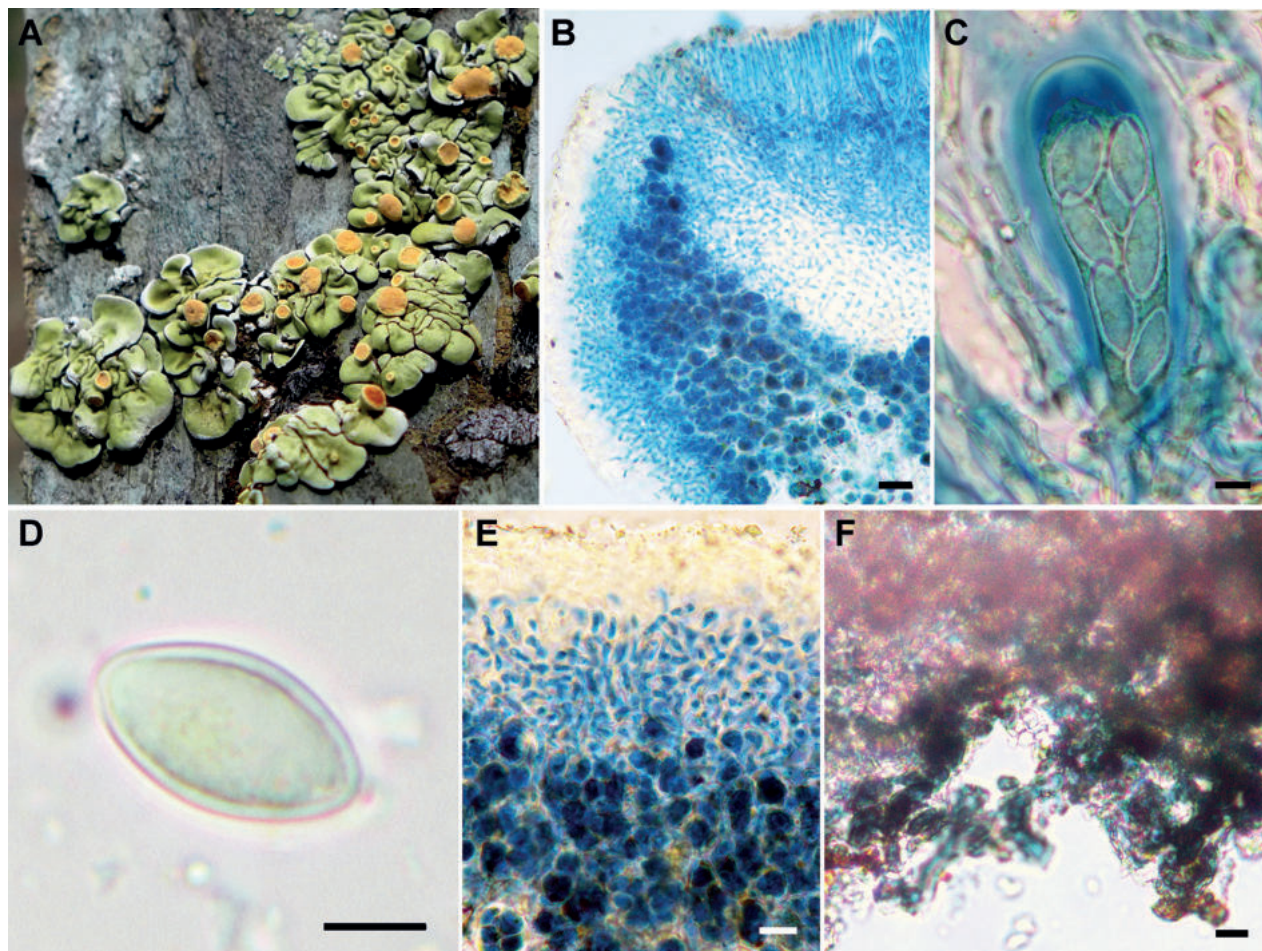
Figure 3. *Rhizoplaca auriculata* (KUN-L0065413) **A** holotype **B** section of apothecia (K and LCB) **C** asci and ascospores (Lugol's solution) **D** ascospore (water) **E** upper cortex and epinecral (K and LCB) **F** lower surface with bluish-black hyphae lacks lower cortex (LCB). Scale bars: 20 μm (**B**); 5 μm (**C, D**); 10 μm (**E, F**).

of placodiolic acid (Wei 1984). *R. chrysoleuca* differs from *R. auriculata* in its thallus with gelatinized lower cortex and the smaller ascospores (7.5–11.5 × 4–5.8 μm). *R. adpressa* differs from *R. auriculata* in its thallus with areolate center and squamulose margins, pale green upper surface with white heavy pruina, the lower surface with white free margins, and the adnate apothecia with orange to reddish-brown discs.

Additional specimens examined. Chɪɴᴀ. Sichuan Prov.: Derong Co., Benzilan Vi., besides Jinsha River, 28°12'N, 99°20'E, 1960 m, on chloritoid schist, 4 October 2009, Li S. Wang & J. Wang 09-31121 (KUN-L0048841). Yunnan Prov.: Deqin Co., Benzilan Vi., besides Jinsha River, 28°11'N, 99°21'E, 2099 m, on chloritoid schist, 19 August 2018, Li S. Wang et al. 18-60136 (KUN-L0065415), 18-60336 (KUN-L0065496), same location, 2108 m, on chloritoid schist, 19 August 2018, Li S. Wang et al. 18-60352 (KUN-L0065512), 18-60355 (KUN-L0065515), same location, 28°23'N, 99°01'E, 2000 m, on chloritoid schist, 31 October 2015, Li S. Wang, Y. Y. Zhang & M. X. Yang 15-49794 (KUN-L0040537), 15-49796 (KUN-L0040538), same location, 28°10'N, 99°23'E, 2115 m, on chloritoid schist, 27 August 2006, Li S. Wang, Oh Soon-OK & D. L. Niu 06-26670 (KUN-L0040471), 06-26684 (KUN-L0040575), same location, 28°10'N, 99°31'E, 2110 m, on rock, 27 August 2006, H. Harada 23764 (KUN-L0051510).

Key to the species of *Rhizoplaca chrysoleuca*-complex and related species in China

1   lower cortex absent...**2**
–   lower cortex present **5**
2   apothecial disc black ....***R. pachyphylla***
–   apothecial disc orange to reddish-brown **3**
3   lower surface contains bluish-black free margin ....***R. auriculata***
–   lower surface contains white or pale brown free margin **4**
4   thallus closely adnate to the substratum, centrally areolate, areoles ca. 0.5 mm in diam., apothecia adnate, not constricted at base, apothecial disc orange when young, reddish-brown when mature .... ***R. adpressa***
–   thallus relatively loosely adnate to the substratum, centrally squamulose, squamules 1–2 mm in diam., apothecia constricted at base when mature, apothecial disc persistently orange .... ***R. callichroa***
5   thallus umbilicate, apothecial disc pruinose **6**
–   thallus placodioid, apothecial disc epruinose **7**
6   apothecial disc orange....***R. chrysoleuca* (representing multiple lineages)**
–   apothecial disc black .... ***R. huashanensis***
7   apothecial disc reddish-brown, upper surface completely yellowish-green .... ***R. phaedrophthalma***
–   apothecial disc yellowish-brown, upper surface yellowish-green with marginal lobes having an orange pigmented apex................. ***R. opiniconensis***

Additional information

Conflict of interest

The authors have declared that no competing interests exist.

Ethical statement

No ethical statement was reported.

Author contributions

Yanyun Zhang performed the specimen collection, experimental work, data analysis and the draft writing; Yujiao Yin and Lun Wang conducted part of the molecular and chemical experiments. Christian Printzen, Lisong Wang and Xinyu Wang designed the project and supervised this research, revised the manuscript, and provided funding.

Author ORCIDs

Yanyun Zhang ⬤ https://orcid.org/0000-0002-0902-5066
Christian Printzen ⬤ https://orcid.org/0000-0002-0871-0803
Xinyu Wang ⬤ https://orcid.org/0000-0003-2166-6111

Data availability

All of the data that support the findings of this study are available in the main text.

References

Arup U, Grube M (2000) Is *Rhizoplaca* (Lecanorales, lichenized Ascomycota) a monophyletic genus? Canadian Journal of Botany 78(3): 318–327. https://doi.org/10.1139/b00-006

Brinker S, Evankow AM, Timdal E (2022) *Rhizoplaca ouimetensis* sp. nov. (Lecanoraceae) from Ontario, the first sorediate species in the genus. The Bryologist 125(4): 513–523. https://doi.org/10.1639/0007-2745-125.4.513

Cansaran D, Aras S, Kandemir İ, Halıcı MG (2006) Phylogenetic relations of *Rhizoplaca* Zopf. from Anatolia inferred from ITS sequence data. Zeitschrift für Naturforschung. C, A Journal of Biosciences 61c(5–6): 405–412. https://doi.org/10.1515/znc-2006-5-617

Gao XQ (1987) A new species of *Rhizoplaca*. Acta Mycologica Sinica 6(4): 233–235.

Gardes M, Bruns TD (1993) ITS primers with enhanced specificity for basidiomycetes-application for the identification of mycorrhizae and rusts. Molecular Ecology 2(2): 113–118. https://doi.org/10.1111/j.1365-294X.1993.tb00005.x

Huelsenbeck JP, Ronquist F (2001) MRBAYES: Bayesian inference of phylogenetic trees. Bioinformatics 17(8): 754–755. https://doi.org/10.1093/bioinformatics/17.8.754

Katoh K, Rozewicki J, Yamada KD (2019) MAFFT online service: Multiple sequence alignment, interactive sequence choice and visualization. Briefings in Bioinformatics 20(4): 1160–1166. https://doi.org/10.1093/bib/bbx108

Kuraku S, Zmasek CM, Nishimura O, Katoh K (2013) aLeaves facilitates on-demand exploration of metazoan gene family trees on MAFFT sequence alignment server with enhanced interactivity. Nucleic Acids Research 41(W1): W22–W28. https://doi.org/10.1093/nar/gkt389

Lanfear R, Frandsen PB, Wright AM, Senfeld T, Calcott B (2017) PartitionFinder 2: New methods for selecting partitioned models of evolution for molecular and morphological phylogenetic analyses. Molecular Biology and Evolution 34: 772–773. https://doi.org/10.1093/molbev/msw260

Larena I, Salazar O, González V, Julián MC, Rubio V (1999) Design of a primer for ribosomal DNA internal transcribed spacer with enhanced specificity for Ascomycetes. Journal of Biotechnology 75(2–3): 187–194. https://doi.org/10.1016/S0168-1656(99)00154-6

Leavitt SD, Fankhauser JD, Leavitt SH, Porter LD, Johnson LA, Clair LLS (2011) Complex patterns of speciation in cosmopolitan "rock posy" lichens – Discovering and delimiting cryptic fungal species in the lichen-forming *Rhizoplaca melanophthalma* species-complex (Lecanoraceae, Ascomycota). Molecular Phylogenetics and Evolution 59: 587–602. https://doi.org/10.1016/j.ympev.2011.03.020

Leavitt SD, Fernández-Mendoza F, Pérez-Ortega S, Sohrabi M, Divakar PK, Vondrák J, Lumbsch HT, Clair LLS (2013a) Local representation of global diversity in a cosmopolitan lichen-forming fungal species complex (*Rhizoplaca*, Ascomycota). Journal of Biogeography 40(9): 1792–1806. https://doi.org/10.1111/jbi.12118

Leavitt SD, Fernández-Mendoza F, Pérez-Ortega S, Sohrabi M, Divakar P, Lumbsch T, Clair LLS (2013b) DNA barcode identification of lichen-forming fungal species in the *Rhizoplaca melanophthalma* species-complex (Lecanorales, Lecanoraceae), including five new species. MycoKeys 7: 1–22. https://doi.org/10.3897/mycokeys.7.4508

Leavitt SD, Kraichak E, Vondrak J, Nelsen MP, Sohrabi M, Pérez-Ortega S, Clair LLS, Lumbsch HT (2016) Cryptic diversity and symbiont interactions in rock-posy lichens. Molecular Phylogenetics and Evolution 99: 261–274. https://doi.org/10.1016/j.ympev.2016.03.030

Leuckert C, Poelt J, Hahnel G (1977) Zur Chemotaxonomie der eurasischen Arten der Flechtengattung *Rhizoplaca*. Nova Hedwigia 28: 71–129.

Liu YJ, Whelen S, Hall BD (1999) Phylogenetic relationships among ascomycetes: Evidence from an RNA polymerse II subunit. Molecular Biology and Evolution 12(12): 1799–1808. https://doi.org/10.1093/oxfordjournals.molbev.a026092

Lü L, Yang YH, He JX (2020) Three placodioid species of Lecanoraceae new for China. Mycotaxon 135(4): 869–876. https://doi.org/10.5248/135.869

Matheny PB, Liu YJ, Ammirati JF, Hall BD (2002) Using RPB1 sequences to improve phylogenetic inference among mushrooms (*Inocybe*, Agaricales). American Journal of Botany 89(4): 688–698. https://doi.org/10.3732/ajb.89.4.688

Medeiros ID, Mazur E, Miadlikowska J, Flakus A, Rodriguez-Flakus P, Pardo-De la Hoz CJ, Cieślak E, Śliwa L, Lutzoni F (2021) Turnover of lecanoroid mycobionts and their *Trebouxia* photobionts along an elevation gradient in Bolivia highlights the role of environment in structuring the lichen symbiosis. Frontiers in Microbiology 12: e774839. https://doi.org/10.3389/fmicb.2021.774839

Orange A, James PW, White FJ (2001) Microchemical Methods for the Identification of Lichens. British Lichen Society, London.

Poelt J (1958) Die lobaten Arten der Flechtengattung Lecanora Ach. sensu ampl. in der Holarktis. Mitteilungen der Botanischen Staatssammlung Müchen 2(19–20): 411–589.

Rambaut A, Drummond AJ (2003) Tracer v. 1.6. http://tree.bio.ed.ac.uk/software/tracer/

Rehner SA, Samuels GJ (1994) Taxonomy and phylogeny of *Gliocladium* analysed from nuclear large subunit ribosomal DNA sequences. Mycological Research 98(6): 625–634. https://doi.org/10.1016/S0953-7562(09)80409-7

Ryan BD, Nash TH (1991) *Lecanora* sect. *Petrasterion* (lichenized Ascomycotina) in North America: Notes on the *L. novomexicana* complex (subsect. *Pseudocorticatae*). Mycotaxon 41(1): 57–65.

Stiller JW, Hall BD (1997) The origin of red algae: Implications for plastid evolution. Proceedings of the National Academy of Sciences of the United States of America 94(9): 4520–4525. https://doi.org/10.1073/pnas.94.9.4520

Szczepańska K, Urbaniak J, Śliwa L (2020) Taxonomic recognition of some species-level lineages circumscribed in nominal *Rhizoplaca subdiscrepans* s. lat. (Lecanoraceae, Ascomycota). PeerJ 8: e9555. https://doi.org/10.7717/peerj.9555

Vilgalys R, Hester M (1990) Rapid genetic identification and mapping of enzymatically amplified ribosomal DNA from several *Cryptococcus* species. Journal of Bacteriology 172(8): 4238–4246. https://doi.org/10.1128/jb.172.8.4238-4246.1990

Wei JC (1984) A preliminary study of the lichen genus *Rhizoplaca* from China. Acta Mycologica Sinica 3(4): 207–213.

Wei JC (2020) The Enumeration of Lichenized Fungi in China. China Forestry Publishing House, Beijing, 207–208.

Wei XL, Wei JC (2005) A study on delimitation of *Rhizoplaca chrysoleuca* group based on comprehensive data. Junwu Xuebao 24: 24–28.

Zhang YY, Wang XY, Li LJ, Printzen C, Timdal E, Niu DL, Yin AC, Wang SQ, Wang LS (2020) *Squamarina* (lichenised fungi) species described from China belong to at least three unrelated genera. MycoKeys 66: 135–157. https://doi.org/10.3897/mycokeys.66.39057

Zhao X, Leavitt SD, Zhao ZT, Zhang LL, Arup U, Grube M, Pérez-Ortega S, Printzen C, Śliwa L, Kraichak E, Divakar PK, Crespo A, Lumbsch TH (2016) Towards a revised generic classification of lecanoroid lichens (Lecanoraceae, Ascomycota) based on molecular, morphological and chemical evidence. Fungal Diversity 78(1): 293–304. https://doi.org/10.1007/s13225-015-0354-5

Zheng XL, Sheng HM, An LZ (2007) Phylogenetic analysis of lichen-forming fungi *Rhizoplaca* Zopf from China based on ITS data and morphology. Zeitschrift für Naturforschung. C, A Journal of Biosciences 62c(9–10): 757–764. https://doi.org/10.1515/znc-2007-9-1020

Zhou QM, Guo SY, Huang MR, Wei JC (2006) A study in the genetic variability of *Rhizoplaca chrysoleuca* using DNA sequences and secondary metabolic substances. Mycologia 98(1): 57–67. https://doi.org/10.1080/15572536.2006.11832713

Zoller S, Scheidegger C, Sperisen C (1999) PCR primers for the amplification of mitochondrial small subunit ribosomal DNA of lichen-forming Ascomycete. Lichenologist 31(5): 511–516. https://doi.org/10.1006/lich.1999.0220

Zopf W (1905) Zur Kenntnis der Flechtenstoffe. 14. Mitteilung. Justus Liebigs Annalen der Chemie 340(3): 276–309. https://doi.org/10.1002/jlac.19053400303

MycoKeys

Research Article

Two novel freshwater hyphomycetes, in *Acrogenospora* (Minutisphaerales, Dothideomycetes) and *Conioscypha* (Conioscyphales, Sordariomycetes) from Southwestern China

Lu Li[1,2,3*], Hong-Zhi Du[1,2,4*], Vinodhini Thiyagaraja[3], Darbhe Jayarama Bhat[5,6], Rungtiwa Phookamsak[3,7], Ratchadawan Cheewangkoon[1,2]

1 Department of Entomology and Plant Pathology, Faculty of Agriculture, Chiang Mai University, Chiang Mai 50200, Thailand
2 Innovative Agriculture Research Centre, Faculty of Agriculture, Chiang Mai University, Chiang Mai 50200, Thailand
3 Key Laboratory for Plant Diversity and Biogeography of East Asia, Kunming Institute of Botany, Chinese Academy of Sciences, Kunming 650201, Yunnan Province, China
4 School of Pharmacy, Guizhou University of Traditional Chinese Medicine, Guiyang 550025, Guizhou Province, China
5 Department of Botany and Microbiology, College of Science, King Saud University, P.O. Box 2455, Riyadh 11451, Saudi Arabia
6 Vishnugupta Vishwavidyapeetam, Ashoke, Gokarna 581326, India
7 Honghe Center for Mountain Futures, Kunming Institute of Botany, Chinese Academy of Sciences, Honghe County 654400, Yunnan, China
Corresponding author: Ratchadawan Cheewangkoon (ratchadawan.c@cmu.ac.th)

Abstract

Freshwater fungi are highly diverse in China and frequently reported from submerged wood, freshwater insects, herbaceous substrates, sediments, leaves, foams, and living plants. In this study, we investigated two freshwater species that were collected from Yunnan and Guizhou provinces in China. Detailed morphological analysis complemented by multi-gene phylogenetic analyses based on LSU, SSU, ITS, *RPB2* and *TEF1-α* sequences data revealed them to be two new saprobic species, namely *Acrogenospora alangii* **sp. nov.** and *Conioscypha yunnanensis* **sp. nov.** in their asexual morphs. Additionally, *Acrogenospora alangii* **sp. nov.** is reported for the first time as a freshwater ascomycete associated with the medicinal plant *Alangium chinense* (Alangiaceae). Detailed morphological descriptions, illustrations and updated phylogenetic relationships of the new taxa are provided herein.

Key words: Acrogenosporaceae, Conioscyphaceae, freshwater fungi, new taxa, taxonomy

Introduction

The freshwater fungi in China are taxonomically highly diverse which include members of Dothideomycetes, Eurotiomycetes, Laboulbeniomycetes, Leotiomycetes, Orbiliomycete, Pezizomycetes and Sordariomycetes (Hu et al. 2013; Calabon et al. 2022). The freshwater fungi are ecologically diverse, occurring on various substrates, including submerged wood, freshwater foams, herbaceous substrates, insects, leaves, sediments and other organic matter, and living plants (Hu et al. 2013; Shen et al. 2022; Calabon et al. 2023). Most species are well-known as saprobes and they play an important role in ecological func-

---

* These authors contributed equally to this work.

tioning as decomposers but also can be pathogens as well as symbionts on humans and plants (Su et al. 2015; Su et al. 2016; Dong et al. 2020).

The order Minutisphaerales (Dothideomycetes) is known as the order for freshwater fungi and comprises two families, viz. Acrogenosporaceae and Minutisphaeraceae (Wijayawardene et al. 2022). Acrogenosporaceae was introduced by Jayasiri et al. (2018) to accommodate *Acrogenospora* based on morpho-molecular evidence. The genus *Acrogenospora* was introduced by Ellis (1971) for two species namely *A. sphaerocephala* (the type species), and *A. carmichaeliana* (as *Farlowiella carmichaeliana*; asexual morph). A year later, Ellis (1972) added another new species, *A. setiformis*. While Goh et al. (1998) revised the genus and accepted eight species, Bao et al. (2020) re-investigated *Acrogenospora* and added seven new species that were reported from freshwater habitat. Subsequently, two new species *A. guizhouensis* and *A. stellata* were introduced in asexual and sexual states, respectively (Tan et al. 2022; Hyde et al. 2023). Presently, there are 23 epithets for *Acrogenospora* in Index Fungorum (http://indexfungorum.org/Names/Names.asp; accessed on 20 Nov. 2023).

Acrogenospora was considered as the asexual morph of *Farlowiella* which was further supported by the morpho-molecular analyses conducted by Jayasiri et al. (2018) and the pleomorphic status of these two genera was confirmed by Rossman et al. (2015) who recommended protecting the name *Acrogenospora* over *Farlowiella* based on the wider use and fewer name changes. The sexual morph of this genus is characterized by hysterothecial, thick-walled, apparently solitary to gregarious, but remaining erect and elevated and presenting an almost stipitate ascomata with a prominent sunken slit, 8-spored, cylindric-clavate, short pedicellate asci and 1–2-celled, hyaline or moderately pigmented ascospores (Sivanesan 1984; Boehm et al. 2009). The asexual morph is characterized by macronematous, mononematous, simple, brown, sometimes percurrently proliferating conidiophores; monoblastic, terminal or intercalary conidiogenous cells with globose, ellipsoid or obovoid, olivaceous to dark brown conidia (Hughes et al. 1978; Goh et al. 1998). The members of *Acrogenospora* mostly show similar morphology, but mainly distinguished by degree of pigmentation of the conidiophores, and conidial shape, size, color, guttules and basal cells (Hughes et al. 1978; Bao et al. 2020).

Conioscyphales (Sordariomycetes), a largely freshwater order, was introduced by Réblová et al. (2016) to accommodate a single family Conioscyphaceae and a genus *Conioscypha*. The order was placed within Hypocreomycetidae (Réblová et al. 2016). However, Conioscyphales clustered within the newly introduced subclass Savoryellomycetidae in the phylogenetic analyses conducted by Hongsanan et al. (2017). Höhnel (1904) had introduced *Conioscypha* with *C. lignicola* as the type species and the genus currently accommodates 18 species (Höhnel 1904; Matsushima 1975, 1993, 1996; Shearer 1973; Shearer and Motta 1973; Udagawa and Toyazaki 1983; Kirk 1984; Chen and Tzean 2000; Réblová and Seifert 2004; Crous et al. 2014, 2018; Zelski et al. 2015; Chuaseeharonnachai et al. 2017; Hernández et al. 2017; Feng and Yang 2018; Turland et al. 2018; Liu et al. 2019; Luo et al. 2019; Hyde et al. 2020; Jiang et al. 2022). Réblová and Seifert (2004) established *Conioscyphascus* based on *C. varius* which is the sexual morph of *Conioscypha varia* and the sexual-asexual linkage was further confirmed by culture studies and molecular data (Réblová and

Seifert 2004; Zelski et al. 2015). According to the nomenclatural priority, *Conioscyphascus* is synonymized under *Conioscypha* (Turland et al. 2018).

Species of *Conioscypha* are mostly reported from freshwater and terrestrial habitats and primarily recorded in their asexual morph. Only few species are reported in sexual morph (Shearer 1973; Shearer and Motta 1973; Kirk 1984; Zelski et al. 2015). The asexual morph is characterized by the enteroblastic percurrent conidiogenesis in distinct conidiogenous cells that retain successive wall layers at the same level as multi-collaretted as each conidium ruptures through the apex with dematiaceous aseptate conidia of various shapes (Shearer 1973; Shearer and Motta 1973; Kirk 1984; Zelski et al. 2015). The sexual morph is characterized by perithecial ascomata that are immersed to superficial, globose to subglobose, cylindrical-clavate asci with a pronounced non-amyloid apical annulus, transversely multi-septate and hyaline ascospores (Luo et al. 2019).

Guizhou and Yunnan provinces are mostly referred as part of the Southwestern China (Feng and Yang 2018; Jiang et al. 2022). This region is a center of biodiversity for freshwater fungi (Shen et al. 2022). Many new freshwater fungi have been reported in Yunnan and Guizhou provinces in recent years (Su et al. 2016; Wang et al. 2016; Li et al. 2017, 2020; Luo et al. 2018a, b, 2019; Zhao et al. 2018; Dong et al. 2020; Wan et al. 2021; Shen et al. 2022). In particular, Yunnan province stands out as a hotspot for freshwater fungal research (Luo et al. 2019; Dong et al. 2020; Shen et al. 2022). The diversity of freshwater fungi in streams and rivers in northwestern Yunnan has been intensely studied, resulting in the discovery of a large number of new species and new records in some highly diverse genera e.g. *Acrogenospora*, *Dictyosporium*, *Distoseptispora*, *Pleurotheciella*, *Sporidesmium* and *Sporoschisma* (Su et al. 2016; Wang et al. 2016; Li et al. 2017, 2020; Luo et al. 2018a, b, 2019; Zhao et al. 2018; Bao et al. 2020; Wan et al. 2021; Shen et al. 2022).

In this study, two collections were obtained from decaying submerged wood and dead branches of *Alangium chinense* in freshwater habitat in Southwestern China. Multi-gene phylogenetic analyses based on Maximum likelihood (ML) and Bayesian analyses along with morphological characters support the establishment of the new species. We also provided a comparative synoptic table for *Conioscypha*. This study adds new data to our knowledge on fungal diversity of freshwater streams in Southwestern China.

Materials and methods

Sample collection, isolation and morphological studies

Submerged decaying wood and branches were collected from Guizhou and Yunnan provinces, China. Fresh specimens were studied following the methods described by Luo et al. (2018b). The samples were incubated in plastic boxes at room temperature for one week. Micromorphological characters were observed using a stereomicroscope (SteREO Discovery.V12, Carl Zeiss Microscopy GmBH, Germany) and photographed using a Nikon ECLIPSE 80i compound microscope fitted with a NikonDS-Ri2 digital camera. Microscopic structures were measured using Tarosoft (R) Image Frame Work program and the photo-

micrographs were processed using Adobe Photoshop CS6 version 10.0 software (Adobe Systems, USA).

Single spore isolation was performed following the method described by Luo et al. (2018b). The germinated conidia were transferred to fresh PDA plates and incubated at room temperature. The specimens were dried under natural light, wrapped in absorbent paper, and placed in a Ziplock bag with mothballs. Herbarium specimens were deposited in the Herbarium of Cryptogams, Kunming Institute of Botany Academia Sinica (**KUN-HKAS**), Kunming, China, and Herbarium, University of Electronic Science and Technology (**HUEST**), Chengdu, China. The cultures were deposited in Kunming Institute of Botany, Chinese Academy of Sciences (**KUNCC**), Kunming, Yunnan, China and the University of Electronic Science and Technology Culture Collection (**UESTCC**), Chengdu, China. The novel species were registered in Faceoffungi (Jayasiri et al. 2015) and MycoBank databases (https://www.mycobank.org/mycobank-deposit; accessed on 22 September 2023).

DNA extraction, PCR amplification and sequencing

Fresh mycelia were scraped from colonies grown on potato dextrose agar (PDA) medium. DNA extraction was carried out using DNA extraction kit following the manufacturer's instructions (TOLOBIO Plant Genomic DNA Extraction Kit, Tsingke Company, Beijing, P.R. China). PCR amplification was performed using primers pairs LR0R/LR5 (Vilgalys and Hester 1990) for the nuclear ribosomal large subunit 28S rDNA gene (LSU); NS1/NS4 (White et al. 1990) for the nuclear ribosomal small subunit 18S rDNA gene (SSU); ITS5/ITS4 (White et al. 1990) for the internal transcribed spacer rDNA region (ITS); fRPB2-5F/fRPB2-7cR (Liu et al. 1999) for the RNA polymerase second largest subunit (*RPB2*); and EF1-983F/EF1-2218R (Rehner and Buckley 2005) for the translation elongation factor 1-alpha (*TEF1-α*). The PCR amplification was carried out in a 25 μL reaction volume containing 12.5 μL of 2× Power Taq PCR Master Mix, 1 μL of each forward and reward primer (10 μM), 1 μL of genomic DNA template (30–50 ng/μL) and 9.5 μL of sterilized double-distilled water. Amplifications were carried out using the BioTeke GT9612 thermocycler (Tsingke Company, Beijing, P.R. China). The PCR amplification conditions for ITS, LSU, and SSU consisted of initial denaturation at 98 °C for 3 minutes, followed by 35 cycles of denaturation at 98 °C for 20 seconds, annealing at 53 °C for 10 seconds, an extension at 72 °C for 20 seconds, and a final extension at 72 °C for 5 minutes. The PCR amplification condition for *RPB2* consisted of initial denaturation at 95 °C for 5 minutes, followed by 40 cycles of denaturation at 95 °C for 1 minute, annealing at 52 °C for 2 minutes, an extension at 72 °C for 90 seconds, and a final extension at 72 °C for 10 minutes. The amplification condition for *TEF1-α* consisted of initial denaturation at 94 °C for 3 minutes, followed by 35 cycles of 45 seconds at 94 °C, 50 seconds at 55 °C and 1 minute at 72 °C, and a final extension period of 10 minutes at 72 °C. Quality of PCR products were checked using 1% agarose gel electrophoresis and distinct bands were visualized in gel documentation system (Compact Desktop UV Transilluminator analyzer GL-3120). The PCR products were purified and obtained Sanger sequences by Tsingke Company, Beijing, P.R. China.

Sequence alignments and phylogenetic analyses

The newly generated sequences were subjected to the nucleotide BLAST search via NCBI (https://blast.ncbi.nlm.nih.gov/Blast.cgi; accessed on 1 September 2023) for searching the closely related taxa and confirming the correctness of the sequences. The closely related taxa of the novel species were retrieved from GenBank based on nucleotide BLAST (www.ncbi.nlm.nih.gov/blast/) searches and recent publications (Liu et al. 2019; Bao et al. 2020). Outgroups were selected based on recently published data (Liu et al. 2019; Bao et al. 2020) (Tables 1, 2). Multiple sequence alignments were aligned with MAFFT v.7 (http://mafft.cbrc.jp/alignment/server/index.html; accessed on 2 September 2023) and automatically trimmed using TrimAl (http://phylemon.bioinfo.cipf.es/utilities.html; accessed on 2 September 2023). A combined sequence dataset was performed with SquenceMatrix v.1.7.8 (Capella et al. 2009; Vaidya

Table 1. Taxon names, strain numbers and GenBank accession numbers of the ITS, LSU, SSU, *RPB2* and *TEF1-α* sequences used in the phylogenetic analyses. Newly generated sequences are highlighted in black bold font. The ex-type strains are indicated by superscript T. "−" stands for no sequence data in GenBank.

Taxon	Voucher/Culture	GenBank accession number				
		ITS	LSU	SSU	*RPB2*	*TEF1-α*
Acrogenospora alangii	**KUNCC 23–14553[T]**	**OR557426**	**OR553807**	**OR553806**	**OR575924**	**OR575926**
	UESTCC 23.0140	**OR578817**	**OR574254**	**OR574239**	**OR575925**	**OR575927**
Acrogenospora aquatic	MFLUCC 16–0949	–	MT340732	–	MT367160	MT367152
	MFLUCC 20–0097[T]	–	–	MT340743	MT367159	MT367151
Acrogenospora basalicellularispora	MFLUCC 16–0992[T]	–	MT340729	–	–	–
Acrogenospora carmichaeliana	CBS 206.36	–	MH867287	AY541482	–	–
	CBS 179.73	–	–	GU296148	–	–
	CBS 164.76	–	GU301791	GU296129	GU371748	GU349059
	FMR11021	HF677172	HF677191	–	–	–
Acrogenospora guttulatispora	MFLUCC 17–1674[T]	–	MT340730	–	MT367157	–
Acrogenospora obovoidspora	MFLUCC 18–1622[T]	–	MT340736	MT340747	MT367163	MT367155
Acrogenospora olivaceospora	MFLUCC 20–0096[T]	–	MT340731	MT340742	MT367158	MT367150
Acrogenospora sphaerocephala	MFLUCC 16–0179	MH606233	MH606222	–	MH626448	–
Acrogenospora submerse	MFLUCC 18–1324[T]	–	MT340735	MT340746	MT367162	MT367154
Acrogenospora subprolata	MFLUCC 18–1314	–	MT340739	MT340750	–	–
Acrogenospora stellate	AMI-SPL 1243	OP439740	OP439739	–	–	–
Acrogenospora terricola	PS3565	ON176299	ON176305	ON176286	–	–
	PS3417	ON176288	–	–	–	–
	PS3610 [T]	ON176304	ON176306	ON176287	–	–
Acrogenospora thailandica	MFLUCC 17–2396[T]	MH606234	MH606223	MH606221	MH626449	–
Acrogenospora verrucispora	MFLUCC 20–0098	–	MT340737	MT340748	–	–
	MFLUCC 18–1617	–	MT340738	MT340749	MT367164	MT367156
Acrogenospora yunnanensis	MFLUCC 20–0099	–	MT340734	MT340745	MT367161	MT367153
	MFLUCC 18–1611[T]	–	MT340733	MT340744	–	–
Minutisphaera aspera	DSM 29478[T]	NR_154621	NG_060319	NG_065059	–	–
Minutisphaera japonica	HHUF30098[T]	NR_119419	NG_042338	NG_064840	–	–

Table 2. Taxon names, strain numbers and GenBank accession numbers of the LSU, ITS, SSU and *RPB2* sequences used in the phylogenetic analyses. The newly generated sequences are highlighted in black bold font. The ex-type strains are indicated by superscript T. "−" stands for no sequence data in GenBank.

Taxon	Voucher/Culture	Gene accession numbers			
		LSU	ITS	SSU	*RPB2*
Conioscypha aquatic	MFLUCC 18−1333[T]	MK835857	MK878383	–	MN194030
Conioscypha bambusicola	JCM 7245[T]	NG059037	NR154660	–	–
Conioscypha boutwelliae	CBS 144928[T]	LR025183	LR025182	–	–
Conioscypha hoehnelii	FMR 11592	KY853497	KY853437	HF937348	–
Conioscypha japonica	CBS 387.84[T]	AY484514	–	JQ437438	JQ429259
Conioscypha lignicola	CBS 335.93	AY484513	–	JQ437439	JQ429260
Conioscypha minutispora	FMR 11245[T]	KF924559	NR137847	HF937347	–
Conioscypha nakagirii	BCC77658[T]	KU509985	KY859266	KU509984	KU513952
	BCC77659	KU509987	KY859267	KU509986	KU513952
Conioscypha peruviana	CBS 137657[T]	NG058867	–	–	–
Conioscypha pleiomorpha	FMR 13134[T]	KY853498	KY853438	–	–
Conioscypha submerse	MFLU 18−1639[T]	MK835856	MK878382	–	–
Conioscypha tenebrosa	MFLU 19−0688[T]	MK804508	MK804506	MK804510	MK828514
	MFLU 19−0687	MK804509	MK804507	MK804511	MK828515
Conioscypha varia	CBS 602.70	MH871654	MH859868	–	–
	CBS 436.70	MH871548	MH859785	–	–
	CBS 604.70	MH871656	MH859869	–	–
	CBS 603.70	MH871655	–	–	–
Conioscypha verrucosa	MFLUCC 18-0419[T]	MN061364	MN061350	MN061352	MN061668
Conioscypha yunnanensis	**KUNCC23−13319[T]**	**OR478379**	**OR234669**	**OR478381**	**OR487158**
	KUNCC23−13172	**OR478380**	**OR478183**	**OR478382**	**OR487157**
Parafuscosporella garethii	BCC79986[T]	KX958430	OK135602	KX958428	–
Parafuscosporella moniliformis	MFLUCC 15−0626[T]	KX550895	NR152557	NG063614	–

Abbreviation: AMI-SPL: Collection of A. Mateos & S. De la Peña, Azores, Terceira, Portugal; **BCC:** BIOTEC Culture Collection, Thailand; **CBS:** CBS-KNAW Fungal Biodiversity Centre, Utrecht, The Netherlands; **DSM:** Leibniz Institute DSMZ-German Collection of Microorganisms and Cell Cultures GmbH, Braunschweig, Science Campus Braunschweig-Süd, Germany; **FMR:** Facultat de Medicina i Ciencies de la Salut, Reus, Spain; **JCM:** Japan Collection of Microorganism, RIKEN BioResource Center, Japan; **HHUF:** Herbarium of Hirosaki University, Japan; **KUNCC:** Kunming Institute of Botany, Chinese Academy of Sciences Culture Collection, Kunming, Yunnan, China; **MFLU:** the herbarium of Mae Fah Luang University, Chiang Rai, Thailand; **MFLUCC:** Mae Fah Luang University Culture Collection, Chiang Rai, Thailand; **PS:** the R. L. Gilbertson Mycological Herbarium at the University of Arizona (MYCO-ARIZ); **UESTCC:** University of Electronic Science and Technology Culture Collection, Chengdu, China.

et al. 2011; Katoh and Standley 2013). Phylogenetic relationships of the new species were performed based on Maximum likelihood (ML) and Bayesian inference (BI) analyses.

Maximum likelihood (ML) was performed by RAxML-HPC2 v.8.2.12 on the XSEDE (8.2.12) tool via the CIPRES Science Gateway (http://www.phylo.org/portal2; accessed on 4 September 2023) (Stamatakis 2006; Miller et al. 2015) following the default setting but adjusted by setting 1,000 bootstrap replications and GTRGAMMA model of nucleotide substitution.

The evolution model for the Bayesian inference (BI) analyses was performed using MrModeltest v2.3 (Ronquist et al. 2012). GTR+I+G was selected as the best-fit model for LSU, SSU, ITS, *RPB2* and *TEF1-α* dataset. Markov Chain Monte Carlo sampling (MCMC) was computed to estimate Bayesian posterior probabilities (BPP) using MrBayes v.3.2.7 (Ronquist et al. 2012). Six simultaneous Markov chains were run for random trees for 1,000,000 generations and trees

were sampled every 200th generation. The first 10% of the total trees were set as burn-in and were discarded. The remaining trees were used to calculate Bayesian posterior probabilities (BPP) in the majority rule consensus tree (when the final average standard deviation of split frequencies reached below 0.01). Phylograms were visualized using FigTree v1.4.0 (Rambaut 2006) and rearranged in Adobe Photoshop CS6 software (Adobe Systems, USA).

The newly generated sequences were deposited in GenBank (Tables 1, 2). The final alignment and phylogenetic tree was registered in TreeBASE (http://www.treebase.org/) under the submission ID: 30847 (*Acrogenospora*) and ID:30689 (*Conioscypha*).

Results

Phylogenetic analyses

Two phylogenetic analyses were conducted to resolve the phylogenetic affinities of the two new freshwater species, one each, within the genera *Acrogenospora* (Acrogenosporaceae/ Minutisphaerales/ Dothideomycetes; Analysis 1), and the other within *Conioscypha* (Conioscyphaceae/ Conioscyphales/ Sordariomycetes; Analysis 2), as follows:

Analysis 1: The phylogram generated from ML analysis based on combined LSU, SSU, ITS, *RPB2* and *TEF1-α* sequences data was selected to represent the relationship between the new species and other known species in *Acrogenospora*. Twenty-six strains were included in the combined dataset which comprised 4,527 characters (LSU: 987 bp, SSU: 1007 bp, ITS: 535 bp, *RRB2*: 1044 bp, *TEF1-α*: 954 bp) after alignment (including gaps). *Minutisphaera aspera* (DSM29478) and *M. japonica* (HHUF30098) were selected as the outgroup taxa. The best RAxML tree with a final likelihood value of -15211.062629 is presented in Fig. 1. RAxML analysis yielded 1,028 distinct alignment patterns and 43.09% of undetermined characters or gaps. Estimated base frequencies were as follows: A = 0.260065, C = 0.232516, G = 0.268900, T = 0.238519, with substitution rates AC = 1.050467, AG = 3.191516, AT = 1.485302, CG = 1.086194, CT = 7.658416, GT = 1.000000; gamma distribution shape parameter alpha = 0.180026. The final average standard deviation of split frequencies at the end of total MCMC generations for BI analysis was 0.009674 (the critical value for the topological convergence diagnostic is below 0.01).

Phylogenetic analyses retrieved from ML and BI analyses were not significantly different and showed similar topologies. Phylogenetic analyses showed that our new collection (KUNCC23−14553 and UESTCC 23.0140) formed an independent subclade with strong statistical support (100% MLBS/ 1.00 BPP) and shared the same clade with *Acrogenospora. terricola* and *A. thailandica* with moderate statistical support (71% MLBS/ 0.95 BPP; Fig. 1).

Analysis 2: The phylogram generated from ML analysis based on combined LSU, ITS, SSU and *RPB2* sequences data was selected to represent the relationship between the new species and other known species in *Conioscypha*. Twenty-three strains were included in the combined dataset which comprised 3,679 characters (LSU: 904 bp, ITS: 696 bp, SSU: 1026 bp, *RPB2*: 1053 bp) after alignment (including gaps). *Parafuscosporella garethii* (BCC79986) and *P. moniliformis* (MFLUCC 15−0626) were selected as the outgroup taxa. The
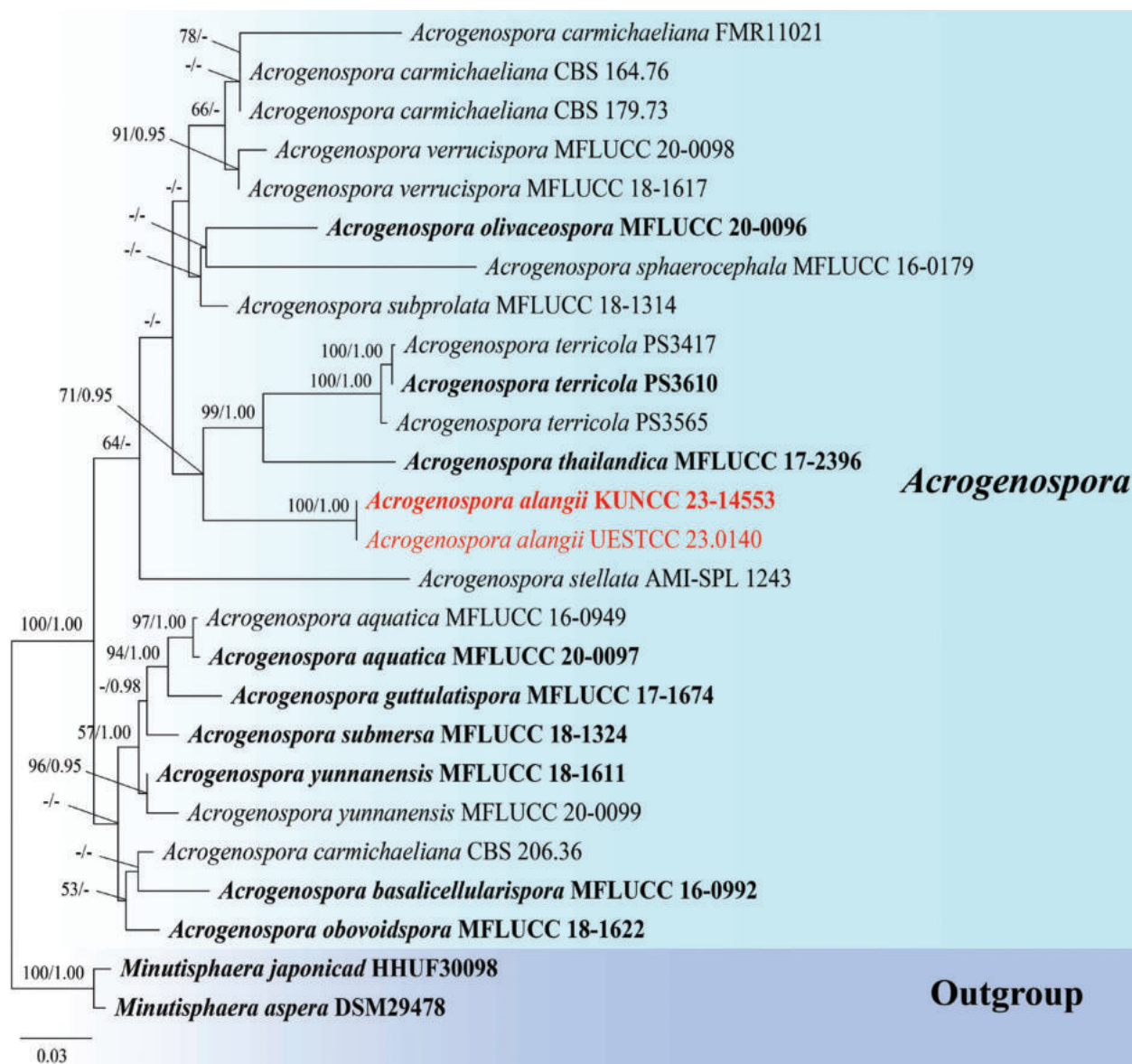
Figure 1. Phylogenetic tree constructed from RAxML analysis of LSU, SSU, ITS, *RPB2* and *TEF1-α* sequences data. Bootstrap support values for ML equal or greater than 50% and Bayesian posterior probabilities greater than 0.95 BPP are indicated at the nodes. The tree is rooted to *Minutisphaera aspera* (DSM29478) and *Minutisphaera japonica* (HHUF30098). The new isolates are in red bold.

best RAxML tree with a final likelihood value of -14285.072957 is presented in Fig. 2. RAxML analysis yielded 1,112 distinct alignment patterns and 40.07% of undetermined characters or gaps. Estimated base frequencies were as follows: A = 0.236438, C = 0.267389, G = 0.295788, T = 0.200385, with substitution rates AC = 1.738303, AG = 2.933990, AT = 1.389088, CG = 1.593182, CT = 7.181256, GT = 1.000000; gamma distribution shape parameter alpha = 0.453781. The final average standard deviation of split frequencies at the end of total MCMC generations for BI analysis was 0.003901 (the critical value for the topological convergence diagnostic is below 0.01).

Phylogenetic analyses retrieved from ML and BI analyses were not significantly different and showed similar topologies. Phylogenetic analyses showed that our new collections (KUNCC 23−13319 and KUNCC 23−13172) formed an
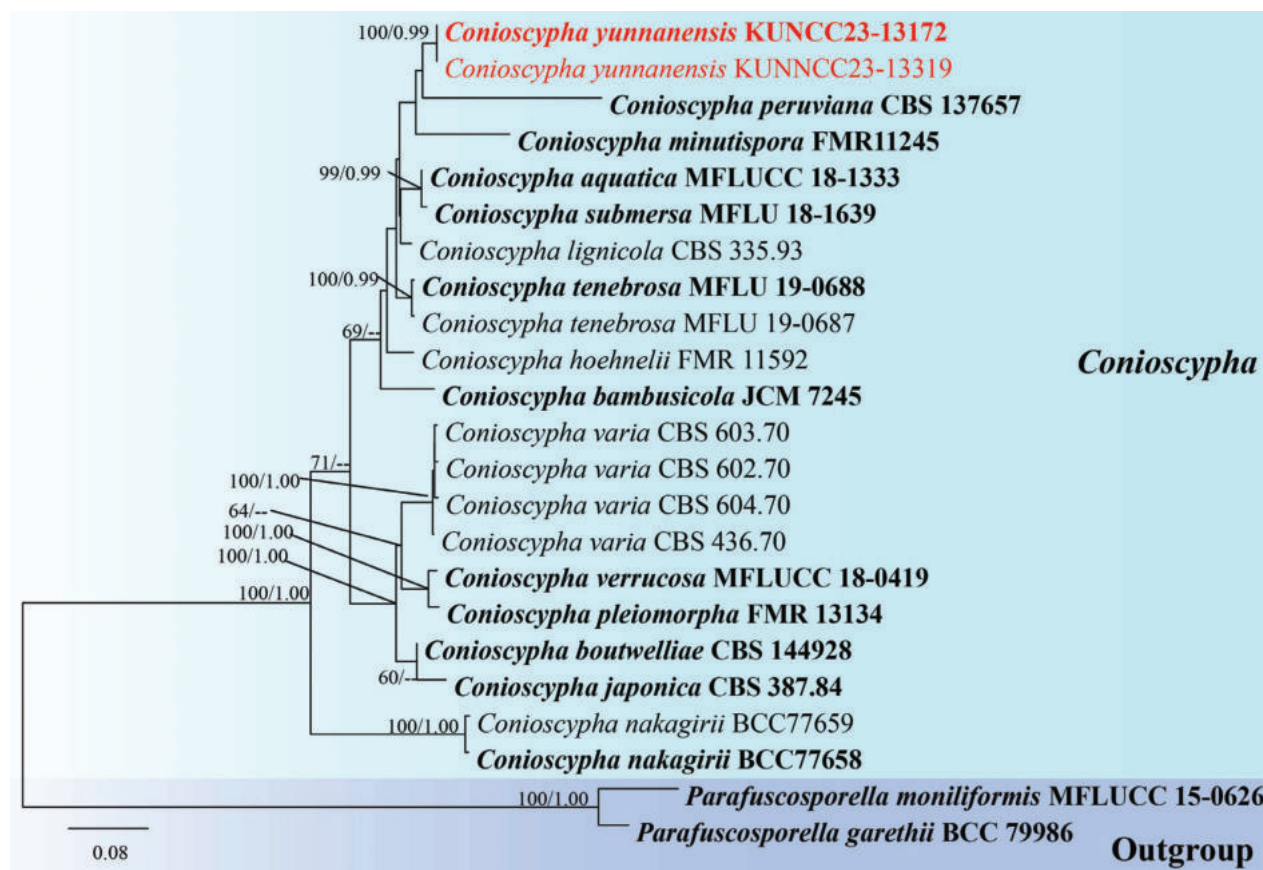
Figure 2. Phylogenetic tree constructed from RAxML analysis of LSU, ITS, SSU and *RPB2* sequences data. Bootstrap support values for ML equal or greater than 50% and Bayesian posterior probabilities greater than 0.95 BPP are indicated at the nodes. The tree is rooted to *Parafuscosporella moniliformis* (MFLUCC 15−0626) and *P. garethii* (BCC79986). The new isolates are in red bold.

independent subclade with strong statistical support (100% MLBS/ 0.99 BPP) and clustered with *Conioscypha peruviana* and *C. minutispora*. In this study, *C. aquatica* (MFLUCC 18−1333) shared the same branch length with *C. submersa* (MFLU 18-1636) with high statistic support (99% MLBS/ 0.99 BPP). Simultaneously, *C. pleiomorpha* (FMR 13134) shares the same branch length with *C. verrucosa* (MFLUCC 18−0419) with high support (100% MLBS/ 1.00 BPP). While *C. boutwelliae* (CBS 144928) also shares the same branch length with *C. japonica* (CBS 387.84), it exhibits low statistical support in both ML and BI analyses. Therefore, the conspecific status of these species is questionable.

Taxonomy

***Acrogenospora alangii* H.Z. Du & Cheewangkoon, sp. nov.**
MycoBank No: 850015
Facesoffungi Number: FoF15041
Fig. 3

Etymology. The epithet '*alangii*' refers to the host genus *Alangium* on which the holotype was collected.
    Holotype. KUN-HKAS 130312.

Description. *Saprobic* on submerged decaying branches of *Alangium chinense* (Alangiaceae). *Asexual morph*: Hyphomycetous. *Colonies* on natural substrate, effuse, hairy, black, glistening. *Mycelium* partly semi-immersed, composed of septate, brown to dark brown, branched, smooth hyphae. *Conidiophores* 179−687 × 2.7−5.5 μm ($\bar{x}$ = 485 × 4.2 μm, n = 20), mononematous, macronematous, solitary, erect, straight or slightly flexuous, cylindrical, unbranched, brown to dark brown, paler toward apex, septate, proliferating percurrently, smooth. *Conidiogenous cells* monoblastic, integrated, initially terminal, later becoming intercalary, cylindrical, smooth, pale brown. *Conidia* 15−22 × 15−23 μm ($\bar{x}$ = 19.5 × 19 μm, n = 30) acrogenous, solitary, spherical or subspherical, truncate at base, aseptate, with apical appendages, hyaline and pale gray when young, pale to dark brown when mature, smooth. *Sexual morph*: Undetermined.

Culture characteristics. Conidia germinating on PDA within 24 h and germ tubes produced from the conidial base. Colonies reaching 16 mm diam at the room temperature in natural light for one month. Colonies on PDA medium dense, irregular in shape, slightly raised to umbonate or convex, surface rough, radially striated with lobate edge, fairy fluffy to floccose, white at the center, white-gray to gray sparse towards the margin; in reverse, white to white-gray at the center, with dark gray to brown-gray in the middle, white to pale yellowish at the edge, radiating outwards with irregular ring; no pigmentation on PDA.

Material examined. CHINA, Guizhou Province, Guiyang City, Wudang District, Xiangzhigou scenic spot, (26°46'7"N, 106°54'55"E), on dead branches of medicinal plant *Alangium chinense* (Alangiaceae) from freshwater stream, 25 February 2022, H.Z. Du, S136 (KUN-HKAS 130312, **holotype**), ex-holotype living culture = KUNCC 23−14553; ibid., S136A (HUEST 23.0140, isotype), ex-isotype living culture = UESTCC 23.0140.

Notes. In the combined multi-locus phylogenetic analyses, *Acrogenospora alangii* formed a distinct clade with *A. terricola* and *A. thailandica* with significant support (71% MLBS/ 0.95 BPP; Fig. 1). The nucleotide base pair comparison between *A. alangii* (KUNCC 23−14553) and *A. terricola* (PS 3610) revealed the differences as 25/829 bp (3.0%) of LSU and 5/1006 bp (0.50%) of SSU. While the differences between *A. alangii* (KUNCC 23−14553) and *A. thailandica* (MFLUCC 17−2396) showed 30/834 bp (3.6%) of LSU and 2/1029 bp (0.2%) of SSU and 131/1045 bp (12.5%) of *RPB2*. *Acrogenospora alangii* can be distinguished from *A. terricola* in having conidia that are hyaline to pale gray when young, becoming pale brown to dark brown when mature, while *A. terricola* has olive green to dark brown conidia. Additionally, *A. thailandica* differs from *A. alangii* in having deep brown to black conidia (Hyde et al. 2019; Harrington et al. 2022). Furthermore, *A. alangii* also differs from the type species *A. sphaerocephala* in conidial color which is dark reddish brown, or pale to mid brown in *A. sphaerocephala* (Hughes 1978). Both *A. alangii* and *A. guizhouensis* were collected from Guizhou Province. However, morphological comparison of *A. alangii* with *A. guizhouensis* shows their differences in conidial color (hyaline, to pale gray, becoming pale brown to dark brown vs. brown) and position of conidial development (acropleurogenous vs. acrogenous) (Hyde et al. 2023).

Figure 3. *Acrogenospora alangii* (KUN-HKAS 130312, holotype) **a** hostplant growing near water body **b, c** colonies on host substrate **d−h** conidiophores, conidiogenous cells and conidia **i** germinating conidium **j, k** colony on PDA (up-front, down-reverse) **l, n** conidia with apical appendages **l−p** conidia. Scale bars: 100 μm (**d, e**), 40 μm (**f−i**), 20 μm (**l−p**).

Conioscypha yunnanensis L. Li, Bhat & Phookamsak, sp. nov.

MycoBank No: 849830

Facesoffungi Number: FoF14746

Fig. 4

Etymology. The specific epithet "*yunnanensis*" refers to the name of the region, Yunnan Province (China), from where the holotype was collected.

Holotype. KUN-HKAS 129616.

Description. *Saprobic* on submerged wood and unidentified twigs from freshwater habitat. *Asexual morph*: Hyphomycetous. *Colonies* on natural substrates effuse, black, glistening. *Conidiophores* reduced to conidiogenous cells. *Conidiogenous cells* phialidic, integrated, terminal, globose to subglobose, cup-shaped, percurrently proliferating in the same level, becoming multi-layered, multi-collaretted with outwardly curved edge, hyaline, smooth-walled. *Conidia* 18−26 × 17−22 μm ($\bar{x}$ = 22 × 20 μm, n = 20), acrogenous, brown to dark brown, globose to subglobose, smooth-walled, aseptate, rounded at apex, subtruncate at base. *Sexual morph*: Undetermined.

Culture characteristics. Conidia germinating on PDA within 48 h and germ tubes produced from the conidial base. Colonies reaching 4.3 mm diam at room temperature in natural light for three months. Colonies on PDA medium dense to dense, circular, white and gray in the center, with packed mycelium, becoming black mycelial patch in the middle, white to cream at the margin, slightly radiating with irregular edge, radially furrowed aspect; in reverse, dark brown to black at the center, radiated with pale yellowish and dark greenish furrowed ring, white to cream at the margin with furrows aspects; no pigmentation on PDA.

Material examined. CHINA, Yunnan Province, Xishuangbanna (21°10'−22°40'N, 99°55'−101°50'E), on decaying submerged wood in a freshwater stream, 9 September 2022, L. Li, LILU-117-1 (KUN-HKAS 129616, *holotype*), ex-type living culture = KUNCC 23−13319; Dujuanhu Lake (22°29'−25°30'N, 100°16'−103°16'E), on unidentified twigs, 26 August 2022, LILU-109-1 (KUN-HKAS 129617, paratype), living culture KUNCC = 23−13172.

Notes. *Conioscypha yunnanensis* has close phylogenetic relationships with *C. peruviana* and *C. minutispora*. The nucleotide base pair comparison between *C. yunnanensis* (KUNCC 23−13319) and *C. peruviana* (CBS 137657) revealed 95/828 bp (11.2%) of LSU differences. The nucleotide base pair comparison between *C. yunnanensis* (KUNCC 23−13319) and *C. minutispora* (FMR 11245) revealed 57/623 bp (9.2%) of LSU, 118/554 bp (22%) of ITS and 10/937 (1.1%) of SSU differences. The new taxon shares similar morphology with *C. peruviana* in having cup-like phialidic conidiogenous cells, and brown conidia but differing by varied shapes (globose to subglobose vs. ellipsoidal to allantoid or fabiform), the size (18−26 × 17−22 μm vs. 13.5−18 × 5−8.5 μm) and absence of lipid droplets (Zelski et al. 2015). *Conioscypha yunnanensis* also resembles *C. minutispora* in having subglobose conidia but differs in the size measurement (18−26 × 17−22 μm vs. 6−9 × 5−6 μm) (Crous et al. 2014). Furthermore, *C. yunnanensis* shares similar morphology to the type species *C. lignicola* in having micronematous conidiophores and globose to subglobose conidia that are brown. However, *C. yunnanensis* differs by the absence of dark brown ring
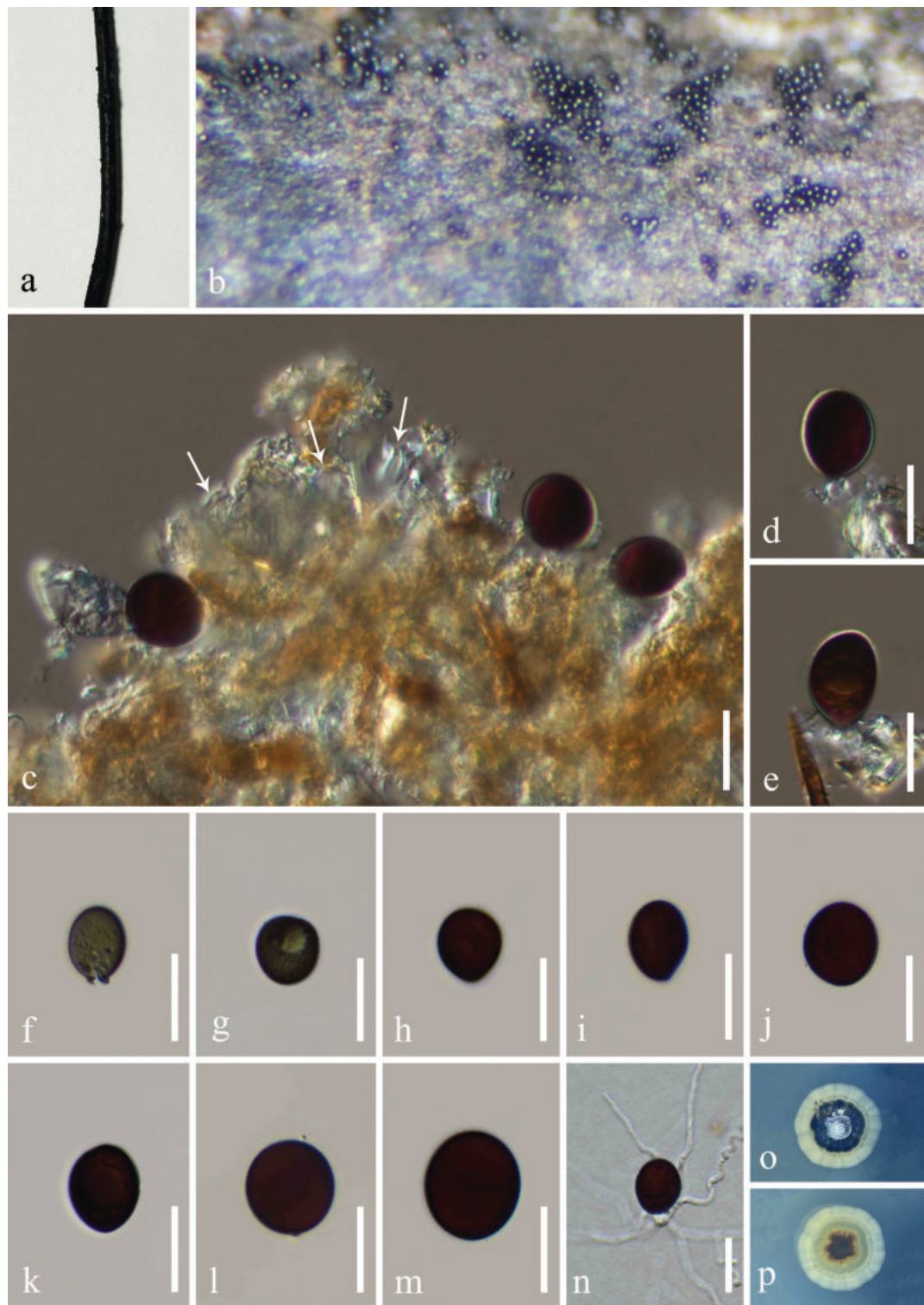
Figure 4. *Conioscypha yunnanensis* (KUN-HKAS 129616, holotype) **a** host specimen **b** colonies on submerged wood **c** conidiogenous cells bearing conidia (note: arrow points = cupulate conidionenous cells) **d, e** conidiogenous cell attached with conidia **f–m** conidia **n** germinated conidium **o, p** colony on PDA (**o** = up-front, **p** = down-reverse). Scale bars: 20 µm (**c–n**).

surrounded in the conidia and presence of guttules periphery of conidia (Shearer 1973). The morphological comparison with other *Conioscypha* species is also provided in Table 3.

Table 3. Synopsis and distribution of *Conioscypha* species. The new species is indicated by black bold.

Species	Conidiophores	Conidiogenous cells	Conidia	Hosts / Habitats / Distribution	References
Conioscypha aquatica	–	–	Globose to subglobose, dark brown to black, 19–23 × 17–21 µm	Submerged wood / Freshwater / China	Luo et al. 2019
C. bambusicola	Semi-macronematous to micronematous, mononematous	Percurrent, cuneiform, 1.6–8.0 × 2.3–4.8 µm	Ovoid or broadly obclavate, base truncate, apex apiculate, dark brown, 11–16 × 6–10 µm	Bamboo / Terrestrial / Japan	Matsushima 1975
C. boutwelliae	Reduced to conidiogenous cells	Monoblastic, endogenous, 11.5–20.5 × 8–15 µm	Ellipsoidal, obovoid or subglobose, base truncate with a central pore of 1–1.5 µm diam, brown, pitted-wall, 10.5–21 × 8–13.5 µm	Soil / Terrestrial / Netherlands	Crous et al. 2018
C. dimorpha	–	–	Macroconidia: oblong to cylindrical, apex round, base truncate, olivaceous to brown, 8–18 × 4–6.5 µm	Decayed leaves	Matsushima 1996
			Microconidia: subglobose to oblong, apex round, base truncate, pale brown, 2.0–3.0 × 2.0–2.5 µm	Terrestrial / South Africa	
C. fabiformis	–	–	Oblong or round, slightly curved, olivaceous, black in mass, 10–16 × 4.5–6.6 µm	Decayed leaves / Terrestrial / Peru	Matsushima 1993
C. gracilis	–	–	Ellipsoidal to flammiform, base truncate, slightly tapering towards apex, reddish brown, 8.5–9.5 × 5.5–7 µm, L/W 1.6:1	Decayed wood / Terrestrial and Freshwater / Denmark and Japan	Zelski et al. 2015
C. hoehnelii	Semi-macronematous to micronematous, mononematous	Cuneiform, cylindrical, often with a conspicuous cup-shaped, multi-collarette at the apex	Globose to subglobose or sometimes irregular, with a central pore in the inconspicuous scar at the base, brown to dark brown, 12–17 × 11–15 µm	Bark of *Eucalyptus* sp., leaf of *Phormium tenax* and unidentified wood / Terrestrial / UK and China	Kirk 1984; Chen and Tzean 2000
C. japonica	Micronematous to semi-macronematous, mononematous	Percurrent, with a multi-layered, cup-like, collarette at the apex, 4.0–17.6 × 3.2–3.8 µm	Obpyriform or subglobose, sometimes elongate, base truncate, broadly rounded at apex, smooth but with irregular pigments deposited at the periphery of the wall to give the appearance of roughness, with a pore at the point of attachment to the conidiogenous cell, entirely covered by a thin gelatinous sheath, dark brown, 9–14 × 4.5–10 µm	Scraping and hair of male dog and rotten herbaceous stem / Terrestrial / Japan and China	Udagawa and Toyazaki 1983; Chen and Tzean 2000
C. lignicola	Micronematous to semi-macronematous, mononematous	Mostly cuneiform, doliiform, percurrent, often with a cup-shaped multi-collarette, up to 16.0 µm wide at the apex, 1.6–4.8 × 2.8–6.8 µm	Obovate or sometimes subglobose, truncate at the base, with reduced lumina, smooth but dark dots deposited at the periphery, at the base with a central pore, surrounded by a dark brown ring, 11–21.6 × 10.6–16.8 µm	Balsa wood and rotten leaf of *Phyllostachys pubescens* / Freshwater and terrestrial / USA and China	Shearer and Motta 1973; Shearer 1973; Chen and Tzean 2000
C. minutispora	Reduced to conidiogenous cells	Cuneiform, percurrent, with a cup-like collarette, up to 4.0 µm wide at the apex, 7–10 × 4–5 µm	Ellipsoidal, obovoid or subglobose, apex rounded, base truncate with a central pore, dark brown, 6–9 × 5–6 µm	Submerged wood / Freshwater / Spain	Crous et al. 2014
C. nakagirii	Micronematous to semi-macronematous, mononematous	Cuneiform, cylindrical, percurrent, with a cup-shaped multi-collarette, up to 50 µm wide at the apex, 7.5–15 × 5–7.5 µm	Turbinate to pyriform, rounded at apex, truncate with a basal pore	Submerged wood / Freshwater / Thailand	Chuaseeharonnachai et al. 2017
C. peruviana	–	–	Ellipsoidal to allantoid or fabiform, containing lipid droplets, brown, 13.5–18 × 5–8.5 µm	Submerged wood / Freshwater / Peru	Zelski et al. 2015
C. pleiomorpha	Micronematous, reduced to conidiogenous cells	Monoblastic, cupulate, endogenous, multilayer-cupulate collarette after several percurrent, enteroblastic, tiny elongations, 9–12 × 13–16 µm, up to 14.0 µm	Ellipsoidal, obovoid or subglobose, base truncate with a central pore, brown, 13–18 × 12–14 µm	Dead wood / Unknown habitat / Spain	Hernández-Restrepo et al. 2017

Species	Conidiophores	Conidiogenous cells	Conidia	Hosts / Habitats / Distribution	References
C. submersa	Reduced to conidiogenous cells	–	Globose to subglobose or ovoid, pale brown, guttulate, when young, dark brown to black when mature, 17–19 × 15–17 μm	Submerged wood / Freshwater / China	Luo et al. 2019
C. tenebrosa	Micronematous, mononematous, often reduced to conidiogenous cells	Phialidic, integrated, sessile or on short conidiophores, subcylindrical, percurrently proliferating, with cup-shaped multi-collarette	Globose to subglobose, obovoid, olivaceous, aseptate, broadly rounded at apex, base subtruncate, dark brown to black when mature, 18–25 × 14–20 μm	Submerged wood / Freshwater / China	Liu et al. 2019
C. taiwaniana	Micronematous to semi-macronematous, mononematous	Cuneiform, percurrent, smooth, hyaline, with a multilayered cup-like collarette, up to 25.0 μm wide at the apex, 2.8–6.4 × 4.0–7.2 μm	Ovoid or broadly obclavate, truncate at the base, often tapering towards a point at the apex, olive brown to yellowish brown or dark brown, 14.1–20.0 × 6.4–8.0 μm	Decaying stem / Terrestrial / China	Hyde et al. 2020
C. varia	–	–	Ovoid, flammiform, naviculiform, or subellipsoid, dark brown, 8.4–15 × 5.6–8.5 μm	Balsa wood / Freshwater / USA	Shearer and Motta 1973; Shearer 1973
C. verrucosa	Macronematous, mononematous, sometimes reduced to conidiogenous cells	Monoblastic, integrated, terminal, globose to ellipsoidal, 5.5–13 × 5–11.5 μm	Globose, subglobose, ellipsoidal or obovoid, aseptate, verrucose, guttulate, dark olivaceous to with a central basal pore, dark olivaceous to dark brown, 12.5–23 × 10.5–20 μm	Submerged wood / Freshwater / China	Hyde et al. 2020
C. yunnanensis	**Reduced to conidiogenous cells**	**Monoblastic, phialidic, integrated, terminal, globose to subglobose, cup-shaped, percurrently proliferating to the same level, multi-collarette with outwardly curved edge, hyaline, smooth-walled**	**Globose, subglobose, smooth-walled, aseptate, rounded at apex, subtruncate at base, brown to dark brown, 18–26 × 17–22 μm**	**Submerged wood / Freshwater / China**	**This study**

Discussion

Dothideomycetes and Sordariomycetes are the two largest classes of lignicolous freshwater fungi (Luo et al. 2019; Calabon et al. 2022; Shen et al. 2022). In this study, two new freshwater species belonging to Dothideomycetes and Sordariomycetes were introduced which add to the fundamental knowledge on the diversity of freshwater fungi in Southwestern China. Furthermore, an updated phylogenetic information was provided and thus we attempted to resolve the taxonomic ambiguities of the genus *Acrogenospora* (Acrogenosporaceae, Minutisphaerales, Dothideomycetes) and *Conioscypha* (Conioscyphaceae, Conioscyphales, Sordariomycetes). The study will provide a better understanding of the taxonomic boundaries of these two genera with the illustration of two new species.

Acrogenospora species are mostly reported from freshwater habitats (Bao et al. 2020; Hyde et al. 2023). Recent studies have revealed that more than half of the new and interesting *Acrogenospora* species were observed from freshwater habitats in China, including *A. alangii* (in this study), *A. aquatica*, *A. basalicellularispora*, *A. ellipsoidea*, *A. guizhouensis*, *A. guttulatispora*, *A. hainanensis*, *A. obovoidspora*, *A. olivaceospora*, *A. ovalia*, *A. sphaerocephala*, *A. submersa*, *A. subprolata*, *A. verrucispora* and *A. yunnanensis* (Goh et al. 1998; Ho et al. 2001; Zhu et al. 2005; Hu et al. 2010; Bao et al. 2020; Hyde et al. 2023). Previous studies revealed that the highest number of *Acrogenospora* species were reported from Yunnan Province whereas a few species have been reported from Guizhou, Hainan, Hongkong, and Xizang. This suggests a high diversity of freshwater fungi in Yunnan Province, especially of the genus *Acrogenospora*. Simultaneously, Guizhou Province is located in southwestern China that shares

similar biogeographical environments with Yunnan Province and therefore, the province may also offer a potential diversity of *Acrogenospora*.

Morphologically, species of *Acrogenospora* are distinguished from each other with difficulty and previous studies made efforts to segregate them based on shape, size, and color of the conidia and the degree of pigmentation of the conidiophores (Hughes 1978; Bao et al. 2020). A comprehensive study of *Acrogenospora* was carried out by Bao et al. (2020) who provided an updated taxonomic treatment of *Acrogenospora* and introduced seven new *Acrogenospora* species from Yunnan, China. Bao et al. (2020) and Hughes (1978) also provided a synoptic table of morphological comparison for all known *Acrogenospora* species. No significant morphological differences have been observed among known *Acrogenospora* species according to the species delineation provided by Bao et al. (2020). However, phylogenetic evidence and nucleotide pairwise comparison provide adequate justification for our species novelty following the recommendation of Jeewon and Hyde (2016).

The host association of freshwater fungi is difficult to identify. Besides, *Acrogenospora* species were mostly reported on submerged wood. Interestingly, the host associations of some *Acrogenospora* species (e.g., *A. altissima*, *A. gigantospora*, *A. sphaerocephala*, and *A. verrucispora*) have been identified. In this study, we reported *A. alangii* from freshwater habitat and associated with the medicinal plant *Alangium chinense* for the first time.

Preliminary phylogenetic analyses of a combined LSU, SSU, ITS, *RPB2* and *TEF1-α* sequence dataset based on Maximum likelihood (ML) (Suppl. material 1: fig. S1) showed that *Acrogenospora* sp. (JX 43) [as *Farlowiella carmichaeliana*] is sister to *A. submersa* (MFLUCC 18–1324) with low support in this study. Hyde et al. (2019) identified *Acrogenospora* sp. (JX 43) as *A. thalandica* based on phylogenetic evidence of a combined LSU, SSU and ITS sequence dataset. However, we have rechecked the sequences of *Acrogenospora* sp. (JX 43) via NCBI nucleotide BLAST search. The nucleotide BLAST search of LSU (KF836062) showed the similarity of this strain to *Chaetomium globosum* (CBS 828.73) with 100% similarity (Identities: 894/894 bp with no gap), of SSU (KF836061) showed 100% similarity to *A. thailandica* (MFLUCC 17–2396) (Identities: 1025/1025 bp with no gap), and of ITS (KF836060) showed 96.31% similarity to *Camposporium cambrense* (CBS 132486) (Identities: 496/515 bp with 5 gaps). As the nucleotide BLAST results showed three different genes of *Acrogenospora* sp. (JX 43) aligning in different genera, we excluded this strain from our analysis to avoid misidentification.

Present phylogenetic analyses also showed that *Acrogenospora carmichaeliana* (CBS 206.36) formed a separated clade with other strains of *A. carmichaeliana* (CBS 164.76, CBS 179.73, FMR 11021). *Acrogenospora carmichaeliana* (CBS 206.36) was identified as *Farlowiella carmichaeliana* (sexual morph) by E.W. Mason (https://wi.knaw.nl/fungal_table; accessed on 17 October 2023). While strain CBS 164.76 was priorly identified as *Acrogenospora sphaerocephala* (on decaying wood in Belgium), strain CBS 179.73 was identified as *Farlowiella carmichaeliana* (on decaying wood in Germany) and FMR 11021 was identified as *Farlowiella carmichaeliana* (unknown source). Hyde et al. (2019) introduced a new species *A. thailandica* and designated the reference specimen for the type species of *Acrogenospora*, *A. sphaerocephala*. Based on their phylogenetic analyses, these four unpublished strains were identified as *A. carmichaeliana*. However, the molecular data from the ex-type strain of *A. carmi-*

chaeliana is unavailable. Therefore, the phylogenetic affinity of *A. carmichaeli-ana* remains uncertain, pending further study.

According to current reports, the species of *Conioscypha* are distributed worldwide, including Africa (*C. dimorpha*) (Matsushima 1996), United States of America (*C. lignicola*, *C. fabiformis*, *C. peruviana* and *C. varia*) (Matsushima 1993; Shearer 1973; Shearer and Motta 1973; Chen and Tzean 2000; Zelski et al. 2015), Asia (*C. aquatica*, *C. bambusicola*, *C. gracilis*, *C. hoehnelii*, *C. japonica*, *C. lignicola*, *C. nakagirii*, *C. submersa*, *C. tenebrosa*, *C. taiwaniana*, *C. verruco-sa* and *C. yunnanensis*) (Shearer 1973; Shearer and Motta 1973; Matsushima 1975; Udagawa and Toyazaki 1983; Kirk 1984; Chen and Tzean 2000; Zelski et al. 2015; Chuaseeharonnachai et al. 2017; Liu et al. 2019; Luo et al. 2019; Hyde et al. 2020) and Europe (*C. gracilis*, *C. boutwelliae*, *C. hoehnelii*, *C. minutis-pora* and *C. pleiomorpha*)(Kirk 1984; Chen and Tzean 2000; Crous et al. 2014, 2018; Zelski et al. 2015; Hernández et al. 2017). In China, so far nine species have been reported including *C. aquatica*, *C. hoehnelii*, *C. japonica*, *C. lignico-la*, *C. submersa*, *C. taiwaniana*, *C. tenebrosa* and *C. verrucosa* (Shearer 1973; Shearer and Motta 1973; Udagawa and Toyazaki 1983; Kirk 1984; Chen and Tzean 2000; Liu et al. 2019; Luo et al. 2019; Hyde et al. 2020).

Through our research on *Conioscypha yunnanensis*, it has been observed that the species of *Conioscypha* are largely indistinguishable in morphology. Hence, it has become necessary to use the potential of phylogenetic mark-ers for clarifying their phylogenetic relationships. In this study, the single gene trees of *Conioscypha* (ITS, LSU, SSU, *RPB2*) and combined sequence datasets (LSU-ITS, LSU-ITS-SSU, and LSU-ITS-*RPB2*) were priorly conducted for com-paring the reliable phylogenetic markers (Suppl. material 1: figs S2–S8). The results of these prior analyses demonstrated that the addition of *RPB2* gene could provide a better phylogenetic resolution of *Conioscypha*. Therefore, *RPB2* gene is recommended as a genetic marker for resolving phylogenetic relation-ships among species in *Conioscypha*.

Present phylogenetic analyses indicated that our new species formed a stable subclade independently and clustered with *Conioscypha peruviana* (CBS 137657, ex-type strain) and *C. minutispora* (FMR 11245, ex-type strain). However, the phy-logenetic relationships of these three species are not well-resolved in the pres-ent study. This may be due to the available sequence data wherein only LSU gene is available for *C. peruviana* while ITS, LSU, and SSU sequences are available for *C. minutispora*. Due to the recommendation of using *RPB2* gene for delineating species of *Conioscypha*, more sequence data of *C. peruviana* and *C. minutispora* are required for providing a better phylogenetic resolution on *Conioscypha*.

Meanwhile, *Conioscypha aquatica* and *C. submersa*, introduced by Luo et al. (2019), were shown to be conspecific in the present phylogenetic analyses. Com-parison of nucleotide pairwise of ITS and *TEF1-α* also demonstrated that these two species were not significantly different (7/530 bp (1.32%) of ITS and 10/801 bp (1.24%) of *TEF1-α*). However, *C. submersa* lacks *RPB2* gene that could separate these two species. Therefore, we tentatively instate these two species as a distinct species until the reliable gene (*RPB2*) is analyzed for resolving their conspecific status. Simultaneously, *C. pleiomorpha* and *C. verrucosa* have also been shown to be conspecific in the present phylogenetic analyses. However, a comparison of nucleotide pairwise of ITS and LSU demonstrated that these two species are different in 24/515 bp (4.66%) of ITS and 7/852 bp (0.82%) of LSU which is ade-

quate to justify the species' novelty. Similarly, there are only ITS and LSU sequence data of *C. pleiomorpha* currently available. These two genes may be inadequate to resolve the phylogenetic relationship of *C. pleiomorpha* and *C. verrucosa*.

The phylogenetic relationship of *Conioscypha boutwelliae* and *C. japonica* is not well-resolved in the present study. This also may be affected by the available genes used in the analyses. There are only ITS and LSU sequences available for *C. boutwelliae* whereas LSU, SSU, and *RPB2* are available for *C. japonica*. Unfortunately, the nucleotide pairwise comparison between *C. boutwelliae* and *C. japonica* could not be done due to the LSU sequence of *C. japonica* is too short (531 bp) and lacking needful genetic information compared with *C. boutwelliae* (1,053 bp). Notably, *C. boutwelliae* was introduced by Crous et al. (2018). The species was isolated from soil in the Netherlands (holotype CBS H-23743, cultures ex-type CBS 144928 = JW203008, GenBank no. LR025182 (ITS) and LR025183 (LSU), MycoBank: MB828023). The search results of LR025182 (ITS) and LR025183 (LSU) via NCBI nucleotide search brought us to the species *C. pleiomorpha*. We have rechecked the detailed source information of LR025182 (ITS) and LR025183 (LSU) and resolved that the source information belongs to *C. boutwelliae*, resulting that the sequence name of *C. boutwelliae* is incorrect in NCBI database and the name "*C. boutwelliae*" should instead be referred to as "*C. pleiomorpha*" for the GenBank no. LR025182 (ITS) and LR025183 (LSU).

Acknowledgments

Additional information

Conflict of interest

The authors have declared that no competing interests exist.

Ethical statement

No ethical statement was reported.

Funding

Author contributions

Conceptualization: LL, HZD. Data curation: LL, HZD, RP. Formal analysis: LL, HZD, RP, VT. Funding acquisition: LL, RC. Investigation: LL, HZD. Methodology: LL, HZD, DJB, VT. Project administration: LL, RC. Supervision: RP, RC. Writing – original draft: LL

Author ORCIDs

Lu Li ⬤ https://orcid.org/0000-0003-4695-2528
Hong-Zhi Du ⬤ https://orcid.org/0000-0003-0350-4530
Vinodhini Thiyagaraja ⬤ https://orcid.org/0000-0002-8091-4579
Darbhe Jayarama Bhat ⬤ https://orcid.org/0000-0002-3800-5910
Rungtiwa Phookamsak ⬤ https://orcid.org/0000-0002-6321-8416
Ratchadawan Cheewangkoon ⬤ https://orcid.org/0000-0001-8576-3696

Data availability

All of the data that support the findings of this study are available in the main text or Supplementary Information.

References

Bao DF, McKenzie EHC, Bhat DJ, Hyde KD, Luo ZL, Shen H-W, Su H-Y (2020) *Acrogeno-spora* (Acrogenosporaceae, Minutisphaerales) appears to be a very diverse genus. Frontiers in Microbiology 11: e1606. https://doi.org/10.3389/fmicb.2020.01606

Boehm EW, Mugambi GK, Miller AN, Huhndorf SM, Marincowitz S, Spatafora JW, Schoch CL (2009) A molecular phylogenetic reappraisal of the Hysteriaceae, Mytilinidiaceae and Gloniaceae (Pleosporomycetidae, Dothideomycetes) with keys to world species. Studies in Mycology 64: 49–83. https://doi.org/10.3114/sim.2009.64.03

Calabon MS, Hyde KD, Jones EBG, Luo ZL, Dong W, Hurdeal V, Gentekaki E, Rossi W, Leonardi M, Thiyagaraja V, Lestari A, Shen HW, Bao DF, Boonyuen N, Zeng M (2022) Freshwater fungal numbers. Fungal Diversity 114(1): 3–235. https://doi.org/10.1007/s13225-022-00503-2

Calabon MS, Hyde KD, Jones EBG, Bao DF, Bhunjun CS, Phukhamsakda C, Shen HW, Gentekaki E, Al Sharie AH, Barros J, Chandrasiri KSU, Hu DM, Hurdeal VG, Rossi W, Valle LG, Zhang H, Figueroa M, Raja HA, Seena S, Song HY, Dong W, El-Elimat T, Leonardi M, Li Y, Li YJ, Luo ZL, Ritter CD, Strongman DB, Wei Mj, Balasuriya A (2023) Freshwater fungal biology. Mycosphere 14(1): 195–413. https://doi.org/10.5943/mycosphere/14/1/4

Capella GS, Silla MJM, Gabaldón T (2009) trimAl: A tool for automated alignment trimming in large-scale phylogenetic analyses. Bioinformatics 25(15): 1972–1973. https://doi.org/10.1093/bioinformatics/btp348

Chen JL, Tzean SS (2000) *Conioscypha taiwaniana* sp. nov. and several new records of the genus from Taiwan. Botanical Bulletin of Academia Sinica 41: 315–322.

Chuaseeharonnachai C, Somrithipol S, Suetrong S, Klaysuban A, Pornputtapong N, Jones EBG, Boonyuen N (2017) *Conioscypha nakagirii*, a new species from naturally submerged wood in Thailand based on morphological and molecular data. Mycoscience 58(6): 424–431. https://doi.org/10.1016/j.myc.2017.06.003

Crous PW, Shivas RG, Quaedvlieg W, Bank M, Zhang Y, Summerell BA, Guarro J, Wingfield MJ, Wood AR, Alfenas AC, Braun U, Cano-Lira JF, García D, Marin-Felix Y, Alvarado P, Andrade JP, Armengol J, Assefa A, Breeÿen A, Camele I, Cheewangkoon R, De Souza JT, Duong TA, Esteve-Raventós F, Fournier J, Frisullo S, García-Jiménez J, Gardiennet A, Gené J, Hernández-Restrepo M, Hirooka Y, Hospenthal DR, King A, Lechat C, Lombard L, Mang SM, Marbach PAS, Marincowitz S, Marin-Felix Y, Montaño-Mata NJ, Moreno G, Perez CA, Pérez Sierra AM, Robertson JL, Roux J, Rubio E, Schumacher RK, Stchigel AM, Sutton DA, Tan YP, Thompson EH, Linde E, Walker AK, Walker DM, Wickes BL, Wong PTW, Groenewald JZ (2014) Fungal Planet description sheets: 2142–2180. Persoonia 32(1): 184–306. https://doi.org/10.3767/003158514X682395

Crous PW, Luangsa-Ard JJ, Wingfield MJ, Carnegie AJ, Hernández-Restrepo M, Lombard L, Roux J, Barreto RW, Baseia IG, Cano-Lira JF, Martín MP, Morozova OV, Stchigel AM, Summerell BA, Brandrud TE, Dima B, García D, Giraldo A, Guarro J, Gusmão LFP, Khamsuntorn P, Noordeloos ME, Nuankaew S, Pinruan U, Rodríguez-Andrade E, Souza-Motta CM, Thangavel R, van Iperen AL, Abreu VP, Accioly T, Alves JL, Andrade JP, Bahram M, Baral HO, Barbier E, Barnes CW, Bendiksen E, Bernard E, Bezerra JDP, Bezerra JL, Bizio E, Blair JE, Bulyonkova TM, Cabral TS, Caiafa MV, Cantillo T, Colmán AA, Conceição LB, Cruz S, Cunha AOB, Darveaux BA, da Silva AL, da Silva GA, da Silva GM, da Silva RMF, de Oliveira RJV, Oliveira RL, De Souza JT, Dueñas M, Evans HC, Epifani F, Felipe MTC, Fernández-López J, Ferreira BW, Figueiredo CN, Filippova NV, Flores JA, Gené J, Ghorbani G, Gibertoni TB, Glushakova AM, Healy R, Huhndorf SM, Iturrieta-González I, Javan-Nikkhah M, Juciano RF, Jurjević Ž, Kachalkin AV, Keochanpheng K, Krisai-Greilhuber I, Li YC, Lima AA, Machado AR, Madrid H, Magalhães OMC, Marbach PAS, Melanda GCS, Miller AN, Mongkolsamrit S, Nascimento RP, Oliveira TGL, Ordoñez ME, Orzes R, Palma MA, Pearce CJ, Pereira OL, Perrone G, Peterson SW, Pham THG, Piontelli E, Pordel A, Quijada L, Raja HA, Rosas de Paz E, Ryvarden L, Saitta A, Salcedo SS, Sandoval-Denis M, Santos TAB, Seifert KA, Silva BDB, Smith ME, Soares AM, Sommai S, Sousa JO, Suetrong S, Susca A, Tedersoo L, Telleria MT, Thanakitpipattana D, Valenzuela-Lopez N, Visagie CM, Zapata M, Groenewald JZ (2018) Fungal Planet description sheets: 785–867. Persoonia 41(1): 238–417. https://doi.org/10.3767/persoonia.2018.41.12

Dong W, Wang B, Hyde KD, McKenzie EHC, Raja HA, Tanaka K, Abdel-Wahab MA, Abdel-Aziz FA, Doilom M, Phookamsak R, Hongsanan S, Wanasinghe DN, Yu XD, Wang GN, Yang H, Yang J, Thambugala KM, Tian Q, Luo ZL, Yang JB, Miller AN, Fournier J, Boonmee S, Hu DM, Nalumpang S, Zhang H (2020) Freshwater Dothideomycetes. Fungal Diversity 105(1): 319–575. https://doi.org/10.1007/s13225-020-00463-5

Ellis MB (1971) *Dematiaceous Hyphomycetes*. Commonwealth Mycological Institute, Kew, 114–115. https://doi.org/10.1079/9780851986180.0000

Ellis MB (1972) *Dematiaceous hyphomycetes*. XI. Mycological Papers 131: 1–25. https://doi.org/10.1079/9780851986180.0000

Feng B, Yang ZL (2018) Studies on diversity of higher fungi in Yunnan, southwestern China: A review. Plant Diversity 40(4): 165–171. https://doi.org/10.1016/j.pld.2018.07.001.

Goh TK, Hyde KD, Tsui KM (1998) The hyphomycete genus *Acrogenospora*, with two new species and two new combinations. Mycological Research 102(11): 1309–1315. https://doi.org/10.1017/S0953756298006790

Harrington AH, Sarmiento C, Zalamea PC, Dalling JW, Davis AS, Arnold AE (2022) *Acrogenospora terricola* sp. nov., a fungal species associated with seeds of pioneer trees in the soil seed bank of a lowland forest in Panama. International Journal of Systematic and Evolutionary Microbiology 72(10): e005558. https://doi.org/10.1099/ijsem.0.005558

Hernández RM, Gené J, Castañeda RRF, Mena PJ, Crous PW, Guarro J (2017) Phylogeny of saprobic microfungi from Southern Europe. Studies in Mycology 86: 53–97. https://doi.org/10.1016/j.simyco.2017.05.002

Ho WH, Hyde KD, Hodgkiss IJ (2001) Fungal communities on submerged wood from streams in Brunei, Hong Kong, and Malaysia. Mycological Research 105(12): 1492–1501. https://doi.org/10.1017/S095375620100507X

Höhnel FXR von (1904) Mycologische Fragmente. (Fortsetzung) [XLII–LXIX]. Annales mycologici 2(1): 38–60.

Hongsanan S, Maharachchikumbura SSN, Hyde KD, Samarakoon MC, Jeewon R, Zhao Q, Al-Sadi AM, Bahkali AH (2017) An updated phylogeny of Sordariomycetes based on

phylogenetic and molecular clock evidence. Fungal Diversity 84(1): 25–41. https://doi.org/10.1007/s13225-017-0384-2

Hu DM, Cai L, Chen H, Bahkali AH, Hyde KD (2010) Four new freshwater fungi associated with submerged wood from Southwest Asia. Sydowia 62: 191–203.

Hu DM, Liu F, Cai L (2013) Biodiversity of aquatic fungi in China. Mycology 4(3): 125–168. https://doi.org/10.1080/21501203.2013.835752

Hughes SJ (1978) New Zealand Fungi 25. Miscellaneous species. New Zealand Journal of Botany 16(3): 311–370. https://doi.org/10.1080/0028825X.1978.10425143

Hyde KD, Tennakoon DS, Jeewon R, Bhat DJ, Maharachchikumbura SSN, Rossi W, Leonardi M, Lee HB, Mun HY, Houbraken J, Nguyen TTT, Jeon SJ, Frisvad JC, Wanasinghe DN, Lűcking R, Aptroot A, Cáceres MES, Karunarathna SC, Hongsanan S, Phookamsak R, Silva NI, Thambugala KM, Jayawardena RS, Senanayake IC, Boonmee S, Chen J, Luo ZL, Phukhamsakda C, Pereira OL, Abreu VP, Rosado AWC, Bart B, Randrianjohany E, Hofstetter V, Gibertoni TB, Soares AMS, Plautz Jr HL, Sotão HMP, Xavier WKS, Bezerra JDP, Oliveira TGL, Souza-Motta CM, Magalhães OMC, Bundhun D, Harishchandra D, Manawasinghe IS, Dong W, Zhang SN, Bao DF, Samarakoon MC, Pem D, Karunarathna A, Lin CG, Yang J, Perera RH, Kumar V, Huang SK, Dayarathne MC, Ekanayaka AH, Jayasiri SC, Xiao Y, Konta S, Niskanen T, Liimatainen K, Dai YC, Ji XH, Tian XM, Mešić A, Singh SK, Phutthacharoen K, Cai L, Sorvongxay T, Thiyagaraja V, Norphanphoun C, Chaiwan N, Lu YZ, Jiang HB, Zhang JF, Abeywickrama PD, Aluthmuhandiram JVS, Brahmanage RS, Zeng M, Chethana T, Wei D, Réblová M, Fournier J, Nekvindová J, Barbosa RN, Santos JEF, Oliveira NT, Li GJ, Ertz D, Shang QJ, Phillips AJL, Kuo CH, Camporesi E, Bulgakov TS, Lumyong S, Jones EBG, Chomnunti P, Gentekaki E, Bungartz F, Zeng XY, Fryar S, Tkalčec Z, Liang J, Li G, Wen TC, Singh PN, Gafforov Y, Promputtha I, Yasanthika E, Goonasekara ID, Zhao RL, Zhao Q, Kirk PM, Liu JK, Yan JY, Mortimer PE, Xu J, Doilom M (2019) Fungal diversity notes 1036−1150: Taxonomic and phylogenetic contributions on genera and species of fungal taxa. Fungal Diversity 96(1): 1−242. https://doi.org/10.1007/s13225-019-00429-2

Hyde KD, Dong Y, Phookamsak R, Jeewon R, Bhat DJ, Jones EBG, Liu NG, Abeywickrama PD, Mapook A, Wei D, Perera RH, Manawasinghe IS, Pem D, Bundhun D, Karunarathna A, Ekanayaka AH, Bao DF, Li JF, Samarakoon MC, Chaiwan N, Lin CG, Phutthacharoen K, Zhang SN, Senanayake IC, Goonasekara ID, Thambugala KM, Phukhamsakda C, Tennakoon DS, Jiang HB, Yang J, Zeng M, Huanraluek N, Liu JK, Wijesinghe SN, Tian Q, Tibpromma S, Brahmanage RS, Boonmee S, Huang SK, Thiyagaraja V, Lu YZ, Jayawardena RS, Dong W, Yang EF, Singh SK, Singh SM, Rana S, Lad SS, Anand G, Devadatha B, Niranjan M, Sarma VV, Liimatainen K, Aguirre-Hudson B, Niskanen T, Overall A, Alvarenga RLM, Gibertoni TB, Pfiegler WP, Horváth E, Imre A, Alves AL, Santos ACS, Tiago PV, Bulgakov TS, Wanasinghe DN, Bahkali AH, Doilom M, Elgorban AM, Maharachchikumbura SSN, Rajeshkumar KC, Haelewaters D, Mortimer PE, Zhao Q, Lumyong S, Xu J, Sheng J (2020) Fungal diversity notes 1151−1276: Taxonomic and phylogenetic contributions on genera and species of fungal taxa. Fungal Diversity 100(1): 5−277. https://doi.org/10.1007/s13225-020-00439-5

Hyde KD, Norphanphoun C, Ma J, Yang HD, Zhang JY, Du TY, Gao Y, Gomes de Farias AR, Gui H, He SC, He YK, Li CJY, Liu XF, Lu L, Su HL, Tang X, Tian XG, Wang SY, Wei DP, Xu RF, Xu RJ, Yang Q, Yang YY, Zhang F, Zhang Q, Bahkali AH, Boonmee S, Chethana KWT, Jayawardena RS, Lu YZ, Karunarathna SC, Tibpromma S, Wang Y, Zhao Q (2023) Mycosphere notes 387−412 – novel species of fungal taxa from around the world. Mycosphere 14(1): 663−744. https://doi.org/10.5943/mycosphere/14/1/8

Jayasiri SC, Hyde KD, Ariyawansa HA, Bhat DJ, Buyck B, Cai L, Dai YC, Abd-Elsalam KA, Ertz D, Hidayat I, Jeewon R, Jone EBG, Bahkal AH, Karunarathna SC (2015) The faces

of fungi database: Fungal names linked with morphology, phylogeny and human impacts. Fungal Diversity 74(1): 3–18. https://doi.org/10.1007/s13225-015-0351-8

Jayasiri SC, Hyde KD, Jones EBG, Persoh D (2018) Taxonomic novelties of hysteriform Dothideomycetes. Mycosphere 9(4): 803–837. https://doi.org/10.5943/mycosphere/9/4/8

Jeewon R, Hyde KD (2016) Establishing species boundaries and new taxa among fungi: Recommendations to resolve taxonomic ambiguities. Mycosphere 7(11): 1669–1677. https://doi.org/10.5943/mycosphere/7/11/4

Jiang HB, Phookamsak R, Hongsanan S, Bhat DJ, Mortimer PE, Suwannarach N, Kakumyan P, Xu JC (2022) A review of bambusicolous Ascomycota in China with an emphasis on species richness in southwest China. Studies in Fungi 7(1): 1–20. https://doi.org/10.48130/SIF-2022-0020

Katoh K, Standley DM (2013) MAFFT multiple sequence alignment software version 7: Improvements in performance and usability. Molecular Biology and Evolution 30(4): 772–780. https://doi.org/10.1093/molbev/mst010

Kirk PM (1984) New or interesting microfungi XII. A new species of *Conioscypha* (Hyphomycetes). Transactions of the British Mycological Society 82(1): 177–178. https://doi.org/10.1016/S0007-1536(84)80230-2

Li WL, Luo ZL, Liu JK, Bhat D, Bao DF, Su HY, Hyde KD (2017) Lignicolous freshwater fungi from China I: *Aquadictyospora lignicola* gen. et sp. nov. and new record of *Pseudodictyosporium wauense* from northwestern Yunnan Province. Mycosphere 8(10): 1587–1597. https://doi.org/10.5943/mycosphere/8/10/1

Li WL, Bao DF, Bhat DJ, Su HY (2020) *Tetraploa aquatica* (Tetraplosphaeriaceae), a new freshwater fungal species from Yunnan Province, China. Phytotaxa 459(2): 181–189. https://doi.org/10.11646/phytotaxa.459.2.8

Liu YJ, Whelen S, Hall BD (1999) Phylogenetic relationships among ascomycetes: Evidence from an RNA polymerase II subunit. Molecular Biology and Evolution 16(12): 1799–1808. https://doi.org/10.1093/oxfordjournals.molbev.a026092

Liu NG, Bhat DJ, Hyde KD, Liu JK (2019) *Conioscypha tenebrosa* sp. nov. (Conioscyphaceae) from China and notes on *Conioscypha* species. Phytotaxa 413(2): 159–171. https://doi.org/10.11646/phytotaxa.413.2.5

Luo ZL, Hyde KD, Bhat DJ, Jeewon R, Maharachchikumbura SSN, Bao DF, Li WL, Su XJ, Yang XY, Su HY (2018a) Morphological and molecular taxonomy of novel species Pleurotheciaceae from freshwater habitats in Yunnan, China. Mycological Progress 17(5): 511–530. https://doi.org/10.1007/s11557-018-1377-6

Luo ZL, Hyde KD, Liu JK, Bhat DJ, Bao DF, Li WL, Su HY (2018b) Lignicolous freshwater fungi from China II: Novel *Distoseptispora* (Distoseptisporaceae) species from northwestern Yunnan Province and a suggested unified method for studying lignicolous freshwater fungi. Mycosphere 9(3): 444–461. https://doi.org/10.5943/mycosphere/9/3/2

Luo ZL, Hyde KD, Liu JK, Maharachchikumbura SSN, Jeewon R, Bao DF, Bhat DJ, Lin CG, Li WL, Yang J, Liu NG, Lu YZ, Jayawardena RS, Li JF, Su HY (2019) Freshwater Sordariomycetes. Fungal Diversity 99(1): 451–660. https://doi.org/10.1007/s13225-019-00438-1

Matsushima T (1975) Icones microfungorum a Matsushima lectorum. Matsushima book, 209 pp.

Matsushima T (1993) Matsushima Mycological Memoirs. No. 7. Published by the author, Kobe, Japan, 131 pp.

Matsushima T (1996) Matsushima Mycological Memoirs. No. 9. Matsushima Fungus collection, Kobe, Japan, 120 pp.

Miller MA, Schwartz T, Pickett BE, He S, Klem EB, Scheuermann RH, Passarotti M, Kaufman S, O'Leary MAA (2015) Restful API for access to phylogenetic tools via the CIPRES science gateway. Evolutionary Bioinformatics Online 11: 43–48. https://doi.org/10.4137/EBO.S21501

Rambaut A (2006) FigTree. Tree figure drawing tool version 1.3.1. Institute of Evolutionary Biology, University of Edinburgh, UK.

Réblová M, Seifert KA (2004) *Conioscyphascus*, a new ascomycetous genus for holomorphs with *Conioscypha* anamorphs. Studies in Mycology 50: 95–108.

Réblová M, Seifert KA, Fournier J, Štěpánek V (2016) Newly recognised lineages of perithecial ascomycetes: The new orders Conioscyphales and Pleurotheciales. Persoonia 37(1): 57–81. https://doi.org/10.3767/003158516X689819

Rehner SA, Buckley EA (2005) Phylogeny inferred from nuclear ITS and *EF1-a* sequences evidence for cryptic diversification and links to *Cordyceps* teleomorphs. Mycologia 97(1): 84–98. https://doi.org/10.3852/mycologia.97.1.84

Ronquist F, Teslenko M, Van Der Mark P, Ayres DL, Darling A, Höhna S, Larget B, Liu L, Suchard MA, Huelsenbeck JP (2012) MrBayes 3.2: Efficient Bayesian phylogenetic inference and model choice across a large model space. Systematic Biology 61(3): 539–542. https://doi.org/10.1093/sysbio/sys029

Rossman AY, Crous PW, Hyde KD, Hawksworth DL, Aptroot A, Bezerra JL, Bhat JD, Boehm E, Braun U, Boonmee S, Camporesi E, Chomnunti P, Dai DQ, D'souza MJ, Dissanayake A, Gareth Jones EB, Groenewald JZ, Hernández-Restrepo M, Hongsanan S, Jaklitsch WM, Jayawardena R, Jing LW, Kirk PM, Lawrey JD, Mapook A, McKenzie EH, Monkai J, Phillips AJ, Phookamsak R, Raja HA, Seifert KA, Senanayake I, Slippers B, Suetrong S, Taylor JE, Thambugala KM, Tian Q, Tibpromma S, Wanasinghe DN, Wijayawardene NN, Wikee S, Woudenberg JH, Wu HX, Yan J, Yang T, Zhang Y (2015) Recommended names for pleomorphic genera in Dothideomycetes. IMA Fungus 6(2): 507–523. https://doi.org/10.5598/imafungus.2015.06.02.14

Shearer CA (1973) Fungi of the Chesapeake Bay and its tributaries II. The genus *Conioscypha*. Mycologia 65(1): 128–136. https://doi.org/10.1080/00275514.1973.12019411

Shearer CA, Motta JJ (1973) Ultrastructure and conidiogenesis in *Conioscypha* (Hyphomycetes). Canadian Journal of Botany 51(10): 1747–1751. https://doi.org/10.1139/b73-226

Shen HW, Bao DF, Bhat DJ, Su HY, Luo ZL (2022) Lignicolous freshwater fungi in Yunnan Province, China: An overview. Mycology 13(2): 119–132. https://doi.org/10.1080/21501203.2022.2058638

Sivanesan A (1984) The Bitunicate Ascomycetes and their anamorphs. Strauss and Cramer GmbH. Hirschberg, 280–282.

Stamatakis A (2006) RAxML-VI-HPC: Maximum likelihood-based phylogenetic analyses with thousands of taxa and mixed models. Bioinformatics 22(21): 2688–2690. https://doi.org/10.1093/bioinformatics/btl446

Su HY, Udayanga D, Luo ZL, Manamgoda DS, Zhao YC, Yang J, Liu XY, McKenzie EHC, Zhou DQ, Hyde KD (2015) Hyphomycetes from aquatic habitats in Southern China: species of *Curvularia* (Pleosporaceae) and *Phragmocephala* (Melannomataceae). Phytotaxa 226(3): 201–216. https://doi.org/10.11646/phytotaxa.226.3.1

Su HY, Hyde KD, Maharachchikumbura SSN, Ariyawansa HA, Luo ZL, Promputtha I, Tian Q, Lin CG, Shang QJ, Zhao YC, Chai HM, Liu XY, Bahkali A, Bhat JD, McKenzie E, Zhou DQ (2016) The families Distoseptisporaceae fam. nov., Kirschsteiniotheliaceae, Sporormiaceae and Torulaceae, with new species from freshwater in Yunnan Province, China. Fungal Diversity 80(1): 375–409. https://doi.org/10.1007/s13225-016-0362-0

Tan YP, Bishop HSL, Shivas RG, Cowan DA (2022) Fungal Planet description sheets: 1436–1477. Persoonia 49: 261–350. https://doi.org/10.3767/persoonia.2022.49.08

Turland NJ, Wiersema JH, Barrie FR, Greuter W, Hawksworth DL, Herendeen PS, Knapp S, Kusber WH, Li DZ, Marhold K, May TW, Mcneill J, Monro AM, Prado J, Price MJ, Smith GF (2018) International Code of Nomenclature for algae, fungi, and plants (Shenzhen Code) adopted by the Nineteenth International Botanical Congress Shenzhen, China, July 2017. Regnum Vegetabile 159. Koeltz Botanical Books, Glashütten. https://doi.org/10.12705/Code.2018

Udagawa S, Toyazaki N (1983) A new species of *Conioscypha*. Mycotaxon 18: 131–137.

Vaidya G, Lohman DJ, Meier R (2011) SequenceMatrix: Concatenation software for the fast assembly of multi-gene datasets with character set and codon information. Cladistics 27(2): 171–180. https://doi.org/10.1111/j.1096-0031.2010.00329.x

Vilgalys R, Hester M (1990) Rapid genetic identification and mapping of enzymatically amplified ribosomal DNA from several *Cryptococcus* species. Journal of Bacteriology 172(8): 4238–4246. https://doi.org/10.1128/jb.172.8.4238-4246.1990

Wan YL, Bao DF, Luo ZL, Bhat DJ, Xu YX, Su HY, Hao YE (2021) Two new species of *Minimelanolocus* (Herpotrichiellaceae, Chaetothyriales) from submerged wood in Yunnan, China. Phytotaxa 480(1): 45–56. https://doi.org/10.11646/phytotaxa.480.1.4

Wang RX, Luo ZL, Hyde KD, Bhat DJ, Su XJ, Su HY (2016) New species and records of *Dictyocheirospora* from submerged wood in north-western Yunnan, China. Mycosphere: Journal of Fungal Biology 7(9): 1357–1367. https://doi.org/10.5943/mycosphere/7/9/9

White TJ, Bruns T, Lee S, Taylor J (1990) Amplification and direct sequencing of fungal ribosomal RNA genes for phylogenetics. In: Innis M, Gelfand D, Shinsky J, White T (Eds) PCR Protocols: A Guide to Methods and Applications. Academic Press, New York, 315–322. https://doi.org/10.1016/B978-0-12-372180-8.50042-1

Wijayawardene NN, Hyde KD, Dai DQ, Sánchez-García M, Goto BT, Saxena RK, Erdoğdu M, Selçuk F, Rajeshkumar KC, Aptroot A, Błaszkowski J, Boonyuen N, da Silva GA, de Souza FA, Dong W, Ertz D, Haelewaters D, Jones EBG, Karunarathna SC, Kirk PM, Kukwa M, Kumla J, Leontyev DV, Lumbsch HT, Maharachchikumbura SSN, Marguno F, Martínez-Rodríguez P, Mešić A, Monteiro JS, Oehl F, Pawłowska J, Pem D, Pfliegler WP, Phillips AJL, Pošta A, He MQ, Li JX, Raza M, Sruthi OP, Suetrong S, Suwannarach N, Tedersoo L, Thiyagaraja V, Tibpromma S, Tkalčec Z, Tokarev YS, Wanasinghe DN, Wijesundara DSA, Wimalaseana SDMK, Madrid H, Zhang GQ, Gao Y, Sánchez-Castro I, Tang LZ, Stadler M, Yurkov A, Thines M (2022) Outline of Fungi and fungus-like taxa-2021. Mycosphere 13(1): 53–453. https://doi.org/10.5943/mycosphere/13/1/2

Zelski SE, Raja HA, Miller AN, Shearer CA (2015) *Conioscypha peruviana* sp. nov., its phylogenetic placement based on 28S rRNA gene, and a report of *Conioscypha gracilis* comb. nov. from Peru. Mycoscience 56(3): 319–325. https://doi.org/10.1016/j.myc.2014.09.002

Zhao N, Luo ZL, Hyde KD, Su HY, Bhat DJ, Liu JK, Bao DF, Hao YE (2018) *Helminthosporium submersum* sp. nov. (Massarinaceae) from submerged wood in north-western Yunnan Province, China. Phytotaxa 348(4): 269–278. https://doi.org/10.11646/phytotaxa.348.4.3

Zhu H, Cai L, Hyde KD, Zhang KQ (2005) A new species of *Acrogenospora* from submerged Bamboo in Yunnan, China. Mycotaxon 92: 383–386.

Supplementary material 1

Supplementary document

Authors: Lu Li, Hong-Zhi Du, Vinodhini Thiyagaraja, Darbhe Jayarama Bhat, Rungtiwa Phookamsak, Ratchadawan Cheewangkoon

Data type: docx

Link: https://doi.org/10.3897/mycokeys.101.115209.suppl1

MycoKeys

Hidden diversity of *Pestalotiopsis* and *Neopestalotiopsis* (Amphisphaeriales, Sporocadaceae) species allied with the stromata of entomopathogenic fungi in Taiwan

Sheng-Yu Hsu[1]*, Yuan-Cheng Xu[1]*, Yu-Chen Lin[1], Wei-Yu Chuang[1], Shiou-Ruei Lin[2], Marc Stadler[3], Narumon Tangthirasunun[4], Ratchadawan Cheewangkoon[5], Hind A. AL-Shwaiman[6], Abdallah M. Elgorban[6], Hiran A. Ariyawansa[1]

1 Department of Plant Pathology and Microbiology, National Taiwan University, Taipei 106319, Taiwan
2 Section of Tea Agronomy, Tea Research and Extension Station, Council of Agriculture, Taoyuan City 326011, Taiwan
3 Department Microbial Drugs, Helmholtz Centre for Infection Research GmbH (HZI), Inhoffenstrasse 7, 38124, Braunschweig, Germany
4 Department of Biology, School of Science, King Mongkut's Institute of Technology Ladkrabang (KMITL), Bangkok, 10520, Thailand
5 Department of Entomology and Plant Pathology, Faculty of Agriculture, Chiang Mai University, Chiang Mai, 50200, Thailand
6 Department of Botany and Microbiology, College of Sciences, King Saud University, P.O. Box 2455, Riyadh, 11451, Saudi Arabia
Corresponding authors: Narumon Tangthirasunun (narumon.ta@kmitl.ac.th); Hiran A. Ariyawansa (ariyawansa44@ntu.edu.tw)

OPEN ACCESS

Abstract

Pestalotiopsis sensu lato, commonly referred to as pestalotiopsis-like fungi, exhibit a broad distribution and are frequently found as endophytes, saprobes and pathogens across various plant hosts. The taxa within pestalotiopsis-like fungi are classified into three genera viz. *Pestalotiopsis*, *Pseudopestalotiopsis* and *Neopestalotiopsis*, based on the conidial colour of their median cells and multi-locus molecular phylogenies. In the course of a biodiversity investigation focusing on pestalotiopsis-like fungi, a total of 12 fungal strains were identified. These strains were found to be associated with stromata of *Beauveria*, *Ophiocordyceps* and *Tolypocladium* in various regions of Taiwan from 2018 to 2021. These strains were evaluated morphologically and multi-locus phylogenetic analyses of the ITS (internal transcribed spacer), *tef1-α* (translation elongation factor 1-α) and *tub2* (beta-tubulin) gene regions were conducted for genotyping. The results revealed seven well-classified taxa and one tentative clade in *Pestalotiopsis* and *Neopestalotiopsis*. One novel species, *Pestalotiopsis manyueyuanani* and four new records, *N. camelliae-oleiferae*, *N. haikouensis*, *P. chamaeropis* and *P. hispanica*, were reported for the first time in Taiwan. In addition, *P. formosana* and an unclassified strain of *Neopestalotiopsis* were identified, based on similarities of phylogeny and morphology. However, the data obtained in the present study suggest that the currently recommended loci for species delimitation of pestalotiopsis-like fungi do not deliver reliable or adequate resolution of tree topologies. The *in-vitro* mycelial growth rates of selected strains from these taxa had an optimum temperature of 25 °C, but growth ceased at 5 °C and 35 °C, while all the strains grew faster under alkaline than acidic or neutral pH conditions. This study provides the first assessment of pestalotiopsis-like fungi, associated with entomopathogenic taxa.

Key words: DNA sequence data, new species, *Pestalotiopsis sensu lato*, taxonomy

---

* These authors contributed equally to this work.

Introduction

Fungi are ubiquitous and essential components of all ecosystems on Earth and are more significant to human lives than people assume. Fungi interact with various organisms, including different groups of fungi, to acquire nutrients to successfully complete their life cycle (Ariyawansa et al. 2018b; Tsai et al. 2018; Sun et al. 2019; Tsai et al. 2021; Hsu et al. 2022). In recent years, various kinds of fungi have been identified in different ecological niches, but their ecological roles are largely unknown (Grossart et al. 2019).

Sordariomycetes is one of the largest classes of Ascomycota with members occupying the most varied habitats and niches. The genus *Pestalotiopsis* was initially identified by Steyaert (1949) to accommodate taxa with 5-celled conidia (Liu et al. 2019). Members of this fungal group were traditionally identified, based on the colour density of median conidial cells, apical appendages and conidiogenous cells (Guba 1961; Maharachchikumbura et al. 2014). However, Maharachchikumbura et al. (2014) divided *Pestalotiopsis* into three genera viz. *Pestalotiopsis*, *Pseudopestalotiopsis* and *Neopestalotiopsis*, based on the results of multi-locus phylogenies inferred using the internal transcribed spacer (ITS), β-tubulin (*tub2*) and partial translation elongation factor 1-α (*tef1-α*) gene regions, coupled with morphological features and regarded it as *Pestalotiopsis sensu lato* (also known as pestalotiopsis-like fungi). These species are widely distributed in tropical and temperate regions (Maharachchikumbura et al. 2014). Pestalotiopsis-like fungi commonly occur on living plants as pathogens and endophytes or are saprobic on dead plant materials (Maharachchikumbura et al. 2011). Some species of pestalotiopsis-like fungi have been reported as mycoparasites (Xie et al. 2014; Li et al. 2017), while several taxa have been identified as human and insect pathogens (Lv et al. 2011; Monden et al. 2013).

Taiwan is an island in the western Pacific Ocean. The rich diversity of fungal taxa (over 6,670 fungal species) in Taiwan has been frequently reported (Chen et al. 2021; Chen et al. 2022; Hsiao et al. 2022; Huang and Chien 2022). We have been studying pestalotiopsis-like fungi in Taiwan with the aim of providing a natural classification and determining their ecological roles (Ariyawansa et al. 2018b; Tsai et al. 2018; Sun et al. 2019; Tsai et al. 2021; Hsu et al. 2022). However, no published studies have investigated species of pestalotiopsis-like fungi allied with entomogenous fungi. During our investigation of the biodiversity of pestalotiopsis-like fungi in Taiwan, we identified a total of 12 fungal conidia with morphology similar to pestalotiopsis-like fungi. These were found associated with stromata of entomopathogenic fungi. Therefore, the primary objective of this study was to determine the identification and placement of these fungi in *Pestalotiopsis sensu lato*, based on DNA sequence-based phylogeny coupled with morphological data. Furthermore, to gain a better understanding of their biology, experiments were conducted to determine the optimal temperature and pH conditions required for mycelial growth of the isolated fungal strains under laboratory conditions.

Materials and methods

Sample collection, fungal isolation and morphological examination

During an exploration of pestalotiopsis-like fungi between 2018 and 2021 in Taiwan (including Hsinchu County, New Taipei City, Pingtung County, Taichung

City, Taoyuan City and Yilan County), fungal spores that are morphologically similar to pestalotiopsis-like fungi were observed on stromata of entomopathogenic fungal species (Fig. 1J, K). The stromata of entomopathogenic fungal species with spores of pestalotiopsis-like fungi were initially mounted in distilled water and separated spores were isolated using the single spore isolation technique as detailed in Choi et al. (1999).

To further study the morphological features of the isolated pestalotiopsis-like fungi, strains were first inoculated on carnation-leaf agar (CLA) (sterile carnation leaf placed on 2% water agar) and incubated at 25 °C with blue light exposure to induce sporulation (Strobel et al. 1996). The conidiomata were placed on a slide and observed through an optical microscope (Olympus DP27) with a digital camera (Olympus BX51). Conidia were imaged and measured with cellSense Standard software (Olympus); 30 measurements were performed for each structure and are shown in Suppl. material 1: table S1.

DNA extraction, PCR and sequencing

Isolates were inoculated on potato dextrose agar (PDA) media and incubated at 25 °C in the dark for seven days. Fresh mycelia were harvested and the genomic DNA were extracted from fresh mycelium using EasyPure Genomic DNA Spin Kit (Bioman), following the manufacturer's protocol (Bioman Scientific Co., Ltd).

PCR amplification was carried out in a 25 µl reaction containing 12.5 µl of 2× Taq Mix-RED (Bioman), 9.5 µl of ddH$_2$O, 1 µl of each forward and reverse primer and 1 µl of fungal DNA. Three DNA loci used previously for characterisation of pestalotiopsis-like fungi were selected: ITS, *tub2* and *tef1-α*. Primer sets and touchdown PCR conditions used to amplify ITS, *tub2* and *tef1-α* gene loci are listed in Suppl. material 1: table S4.

Strain selection, sequence alignment and phylogenetic analyses

Newly-generated sequence data in this study were observed and manually adjusted via BioEdit version 7.2.5 (Hall et al. 2011; http://bioedit.software.informer.com/) to check the quality of the sequences. Additional related sequences of pestalotiopsis-like fungi were downloaded from GenBank (https://www.ncbi.nlm.nih.gov/nuccore) based on recent publications (Solarte et al. 2018; Fiorenza et al. 2022; Jiang et al. 2022a, 2022b; Peng et al. 2022; Tian et al. 2022; Xiong et al. 2022; Zhang et al. 2022; Guterres et al. 2023; Sun et al. 2023) and are listed in Suppl. material 1: tables S2, S3. Multiple sequence alignments were carried out using MAFFT version 7 (http://mafft.cbrc.jp/alignment/server/index.html) with default settings. To identify closely-associated taxa, single gene phylogenies were inferred for ITS, *tub2* and *tef1-α*, then sequences of these loci were concatenated to conduct a multi-locus analysis including Maximum Likelihood (ML), Maximum Parsimony (MP) and Bayesian Inference (BI) methods.

For the ML analysis, the best-fit substitution models (Suppl. material 1: table S5) were executed for each gene region under the Akaike Information Criterion (AIC) with the nexus-formed partition file from the Model Selection of the IQ-TREE web server (Trifinopoulos et al. 2016; http://iqtree.cibiv.univie.ac.at/). ML trees were inferred with 1,000 bootstrap tests using the ultrafast algorithm
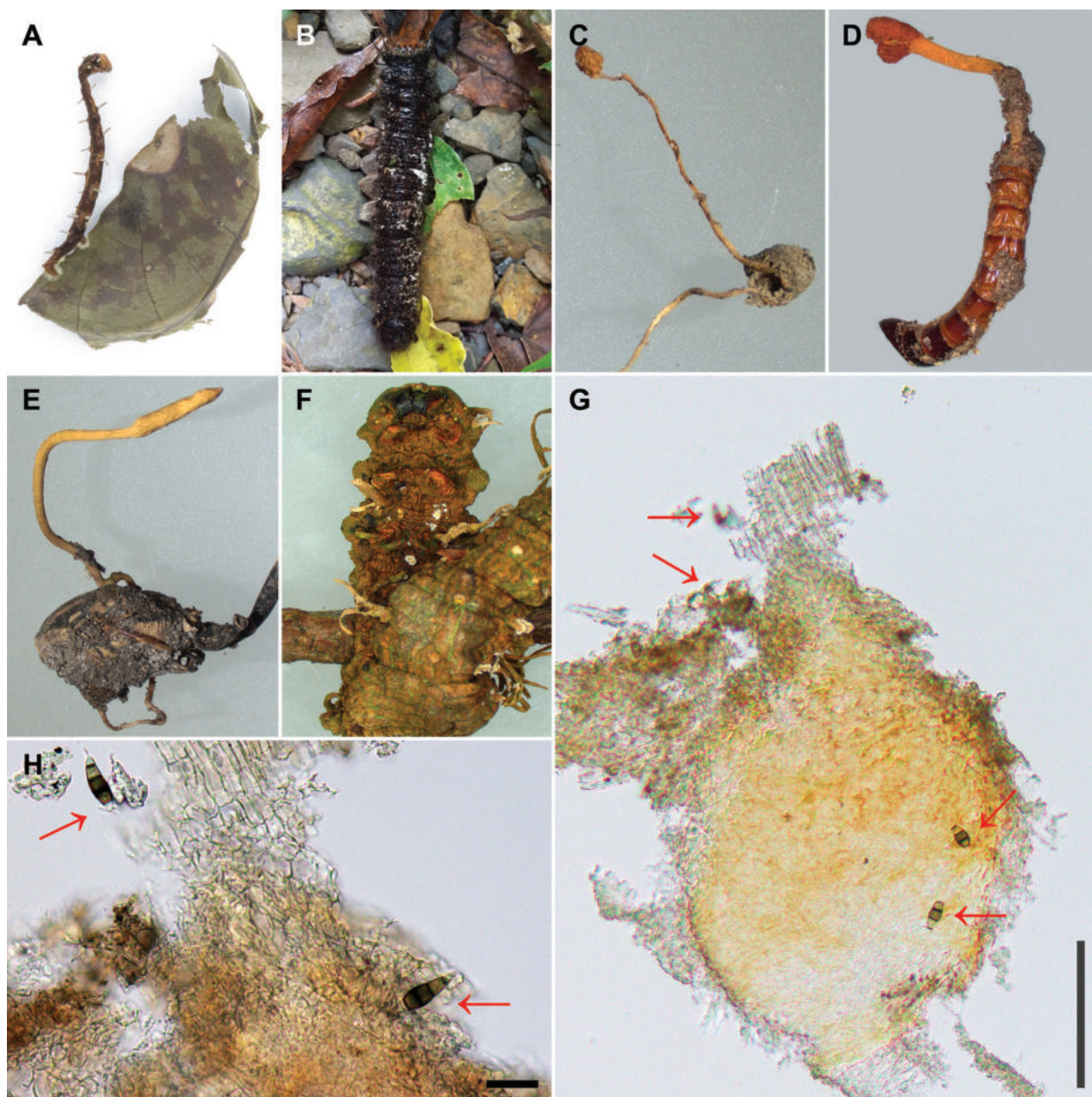
Figure 1. The habitat of *Pestalotiopsis* and *Neopestalotiopsis* species, situated on the stromata of entomopathogenic fungi. Specimens **A** *Ophiocordyceps* sp. NTUPPMH 18-160 **B** *Beauveria* sp. NTUPPMH 18-161 **C** *Tolypocladium* sp. NTUPPMH 21-055 **D** *Ophiocordyceps* sp. NTUPPMH 21-054 **E** *Ophiocordyceps* sp. NTUPPMH 21-053 **F** *Ophiocordyceps* sp. NTUPPMH 18-164 **G, H** the section of conidioma of *Ophiocordyceps* sp. showing the location of conidia of pestalotiopsis-like fungi (red arrow). Scale bars: 100 µm (**G**); 20 µm (**H**).

in the IQ-TREE and Maximum Likelihood bootstrap (MLB) values ≥ 70% were indicated at each node. MP phylogenetic trees were inferred using the heuristic search option with 1,000 random sequence additions via PAUP version 4.0a169 (Swofford 2003) and Maximum Parsimony bootstrap (MPB) values ≥ 70% were indicated at each node of the final tree obtained from MP analysis.

For the BI analyses, the best evolutionary model was decided under the AIC via MrModelTest version 2.3 (Nylander 2004) and shown in Suppl. material 1: table S5. MrBayes version 3.2.5 (Ronquist et al. 2012) was used to generate Bayesian phylogenetic trees under optimal criteria per partition and posterior

probabilities (PP) were determined by Markov Chain Monte Carlo (MCMC) sampling methods. MCMC analysis settings followed previous studies (Tsai et al. 2018, 2021) and four simultaneous Markov chains were initially run for 100,000,000 generations and for every 1000th generation, a tree was sampled (critical value for the topological convergence diagnostic set to 0.01, options of "Bstoprule = yes" and "Bstopval = 0.01"); the MCMC heated chain was set with a "temperature" value of 0.15. The distribution of log-likelihood scores was examined using the Tracer 1.7 programme to determine the stationary phase for each search and to decide whether extra runs were required to achieve convergence (Rambaut et al. 2018). All sampled topologies beneath the asymptote (20%) were discarded as part of a burn-in procedure and the remaining trees were used to calculate PPs in the majority rule consensus tree. All phylogenetic trees and related data files were examined and visualised using FigTree version 1.4.4 (http://tree.bio.ed.ac.uk/software/figtree) and modified using Adobe Illustrator version cc 2022 (https://www.adobe.com/tw/products/illustrator.html).

Species delimitation analyses

To determine species delimitations in pestalotiopsis-like fungi, Genealogical Concordance Phylogenetic Species Recognition (GCPSR) was applied (Dettman et al. 2003). Based on the GCPSR principle, species should be recognised when they satisfy one criterion of genealogical concordance or genealogical non-discordance (Dettman et al. 2003; Tsai et al. 2018, 2021). Genealogical concordance was determined if phylogenetic clades were present within at least some gene trees; non-discordance was acknowledged if phylogenetic clades had strong statistical support (MLB ≥ 70%; MPB ≥ 70%; PP ≥ 0.95) in a single locus without conflict at or above this supportive level in any other single-gene trees (Tsai et al. 2018, 2021).

To infer recombination within novel pestalotiopsis-like fungi, the pairwise homoplasy index test (PHI, Φ_w) (Bruen 2005) and phylogenetic network analysis (Hilário et al. 2021a, 2021b) were employed. The PHI test was used to select hypothesised "species"/populations to infer the occurrence of sexual recombination, based on the standard of incongruence amongst individual single-gene lineages to deduce the recombination level within the complex and between every pair of clades via SplitsTree version 4.16.1 (Huson and Bryant 2006; Hilário et al. 2021b). Results of the PHI index were considered to demonstrate significant recombination occurring with a threshold below 0.05 (Φ_w < 0.05). Phylogenetic network analyses were implemented using the LogDet transformation and the NeighborNet algorithm options in SplitsTree software to visualise the relationships between closely-related taxa (Hilário et al. 2021a, 2021b).

Mycelial growth test

In total, eight strains representing eight taxa identified in this study were selected to determine the growth rate of mycelia. A 4 mm-diam. mycelial disc was aseptically excised from the edge of the culture and placed at the centre of a PDA media (12 ml in a 9 mm diam. Petri dish). After incubation at 25 °C in the dark for seven days, the diameter of the cultures was measured and two independent tests were conducted with five replicates per trial.

Temperature and pH effects on mycelial growth

The same fungal strains, inoculation method and measurement standards used in the mycelial growth test were also used to evaluate the effects of temperature and pH on fungal growth.

Further details for each assessment are described below. The effect of temperature on radial mycelial growth was measured on the seventh day after inoculation at 5, 10, 15, 20, 25, 30, 35 and 40 °C in the dark. All single inoculations were conducted on Petri dishes of 12 ml PDA media. The test was performed twice with five replicates per trial.

The optimal pH for mycelial growth was tested at pH 3, 5, 7, 9 and 11. The PDA plates were heated prior to sterilisation and the pH values were adjusted with 1 M hydrochloric acid (HCl) and 1 M sodium hydroxide (NaOH) solutions. The tested cultures were incubated at 25 °C in the dark for seven days and colony sizes were measured. The test was conducted twice with five replicates per trial.

Statistical analysis

Data were processed using Microsoft Excel 2021 to compute the mean and standard deviation. Data analysis was performed with SAS University Edition (version 3.8), utilising one-way analysis of variance (ANOVA) and the mean values were compared using Tukey's HSD (honestly significant difference) test ($\alpha = 0.05$) following Tsai et al. (2021).

Results

Fungal observation and isolation

In total, 12 strains of pestalotiopsis-like fungi associated with the stromata of the entomopathogenic fungi were successfully isolated (Suppl. material 1: table S1 and Fig. 1). Pure cultures of these strains were used in subsequent experiments to understand their molecular taxonomy, biology and diversity.

Phylogenetic analysis

ITS sequence data were used for initial identification of the genera of pestalotiopsis-like fungal strains in the present study. Based on the ITS sequence results, 12 strains identified in this study were categorised into two pestalotiopsis-like fungal genera: *Pestalotiopsis* and *Neopestalotiopsis*. Subsequently, to determine the phylogenetic placement of these strains, two different datasets were prepared using the concatenated data matrices of ITS, *tub2* and *tef1-α* gene regions to separately represent the phylogenies.

Figs 2, 3 are the phylogenetic trees obtained in different analyses (ML, MP and BI) using concatenated data matrices. In the multi-locus phylogenies, the topologies of the trees inferred for the individual genes were checked visually to confirm that the general tree topologies of the single-gene datasets (Suppl. material 2: figs S5–S10) were similar to each other and resembled the trees obtained from the combined gene dataset alignments.
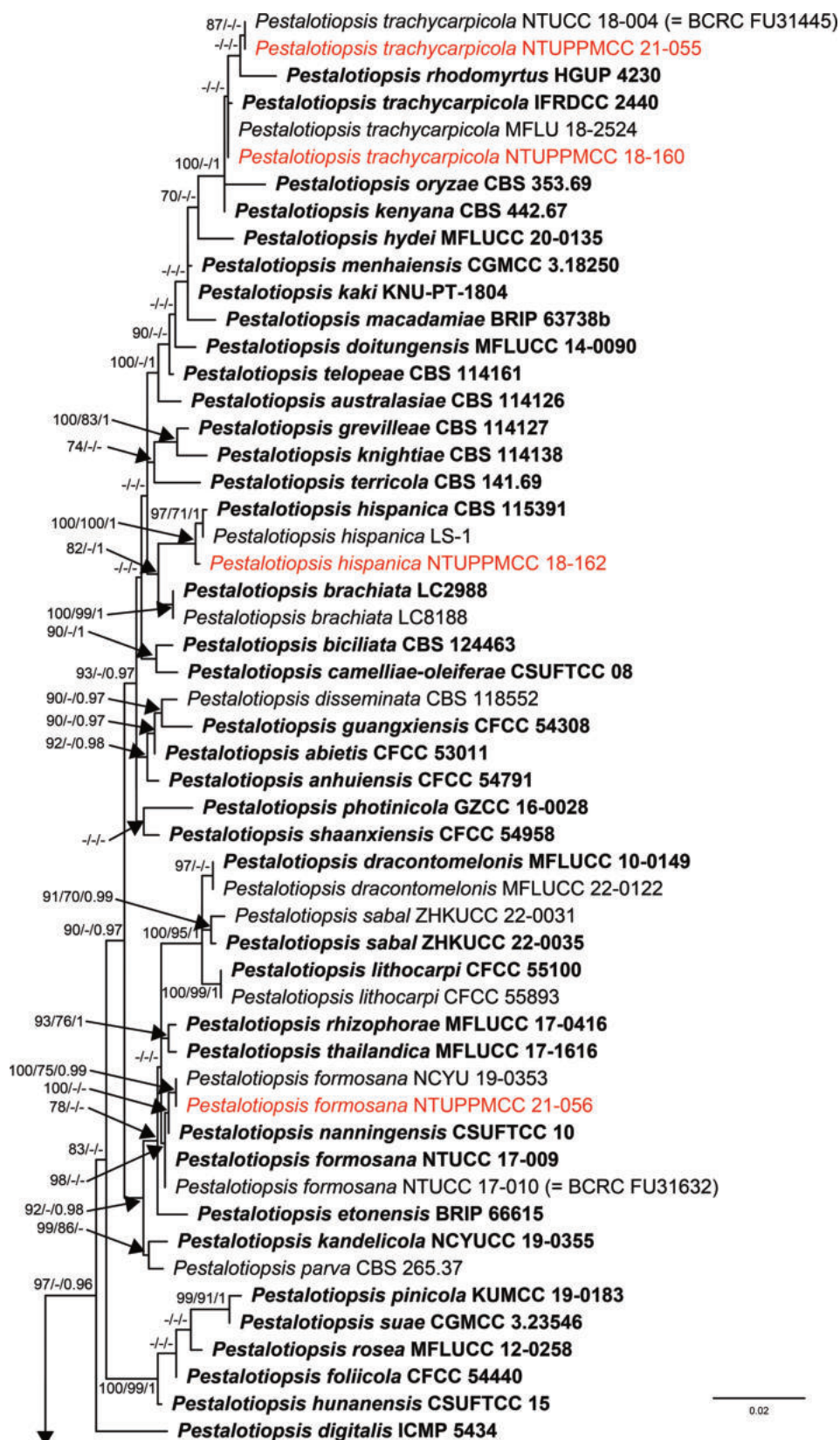
Figure 2. ML phylogenetic tree of *Pestalotiopsis* obtained from the concatenated DNA sequence data of ITS, *tub2* and *tef1-α* genes implemented in IQ-TREE. ML bootstrap values (MLB) ≥ 70%, Maximum Parsimony bootstrap (MPB) values ≥ 70% and Bayesian Posterior Probabilities (PP) ≥ 0.95 are given at the nodes. The scale-bar shows the number of estimated substitutions per site. *Neopestalotiopsis protearum* (CBS 114178) was used as an outgroup. The new isolates are in red and taxa representing ex-type cultures are in bold.
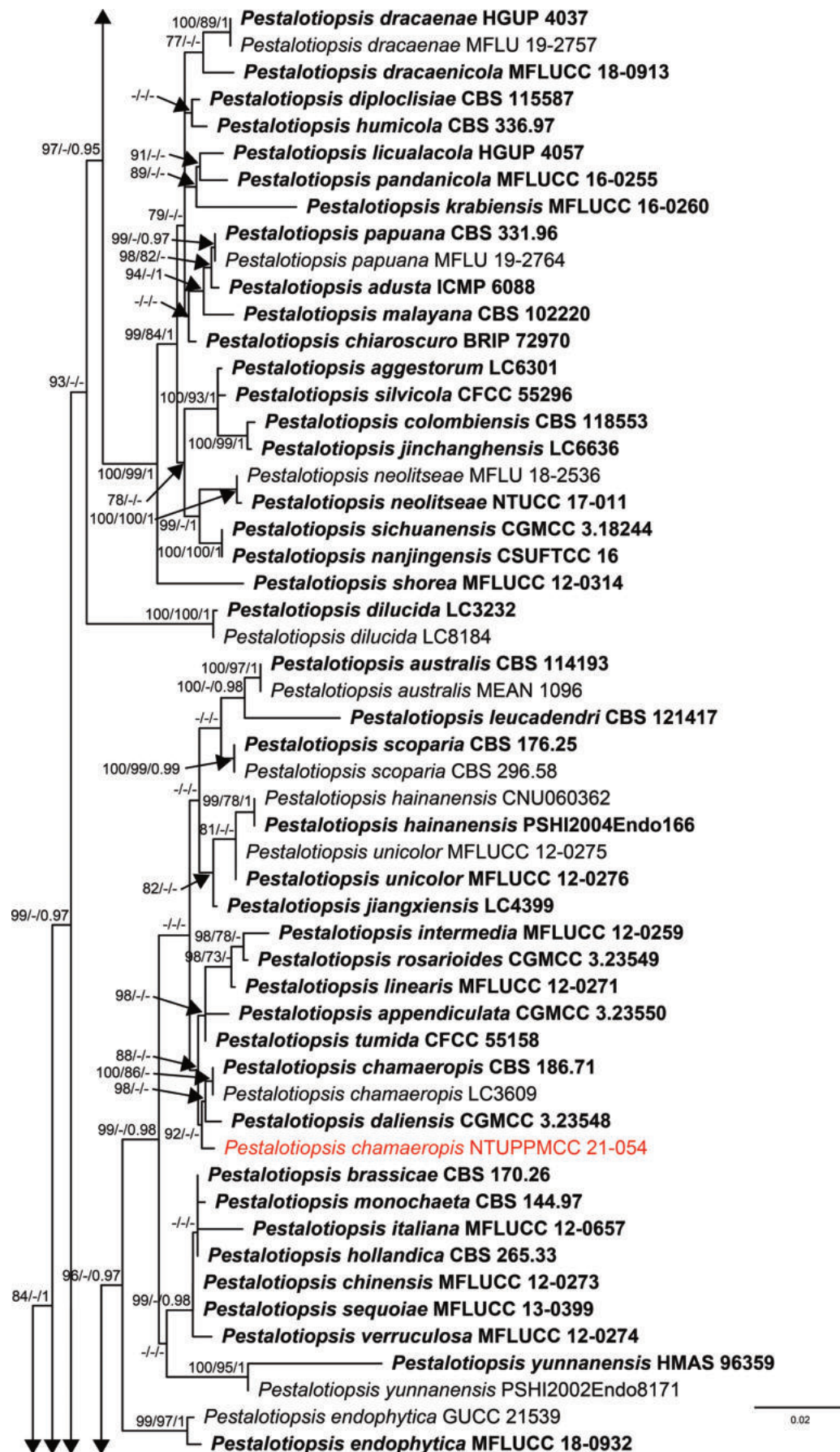
Figure 2. Continued.
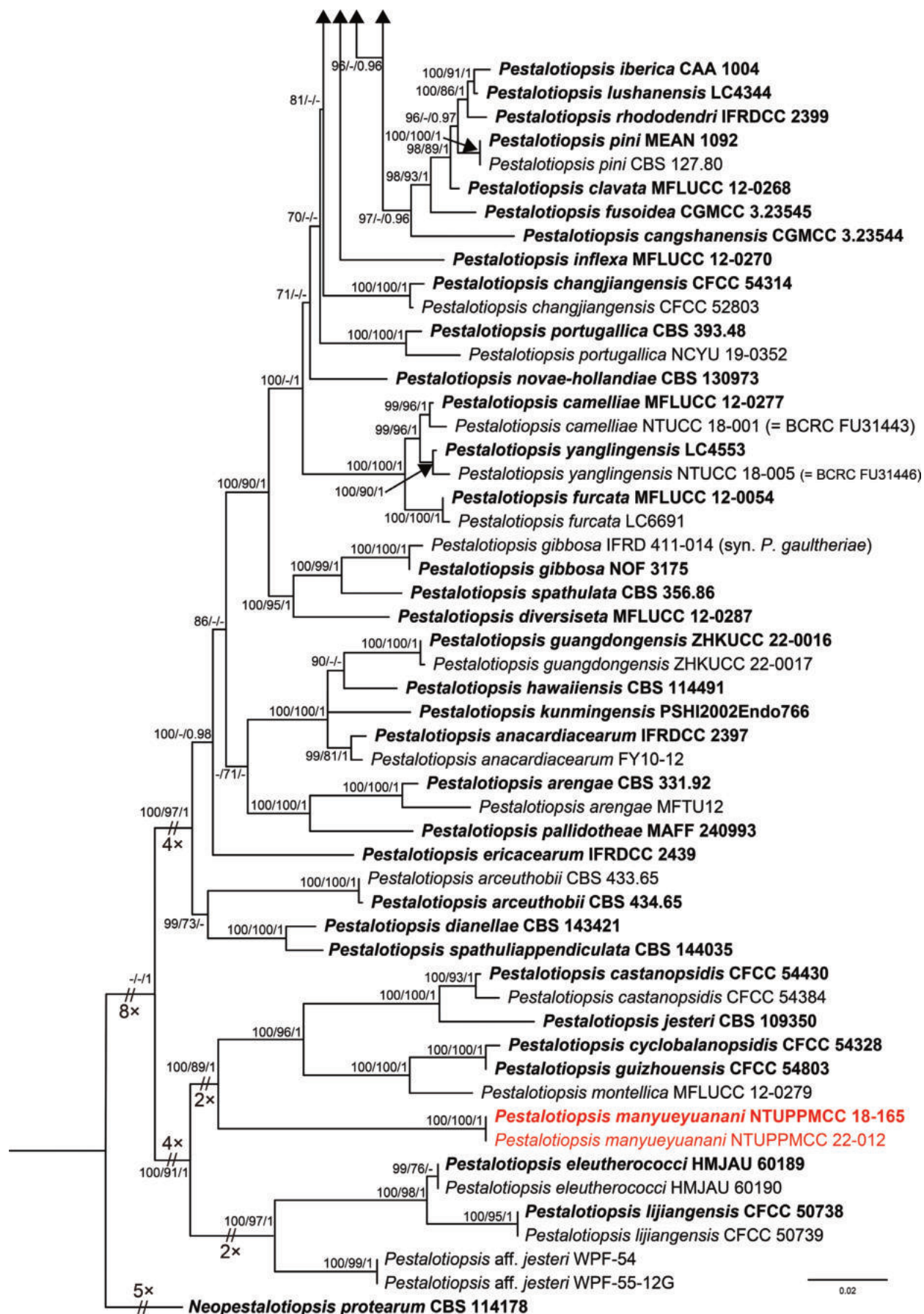
Figure 2. Continued.
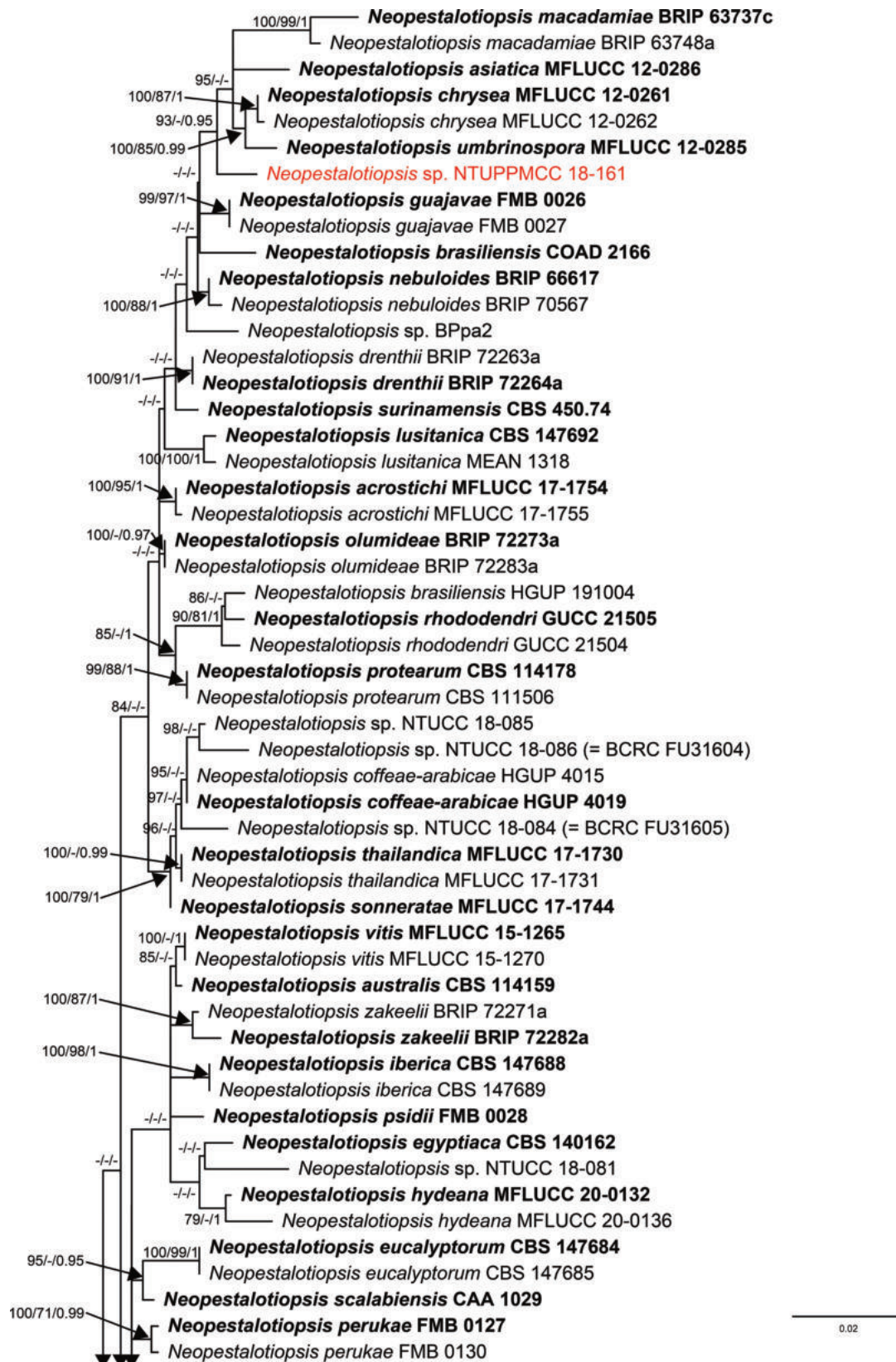
Figure 3. ML Phylogenetic tree of genus *Neopestalotiopsis* attained from the concatenated DNA sequence data of ITS, *tub2* and *tef1-α* loci implemented via IQ-TREE. ML bootstrap values (MLB) ≥ 70%, Maximum Parsimony bootstrap (MPB) values ≥ 70% and Bayesian Posterior Probabilities (PP) ≥ 0.95 are given at the nodes. The scale-bar shows the number of estimated substitutions per site. *Pseudopestalotiopsis theae* (MFLUCC 12-0055) was used as an outgroup. The new isolates are in red and taxa representing ex-type cultures are in bold.
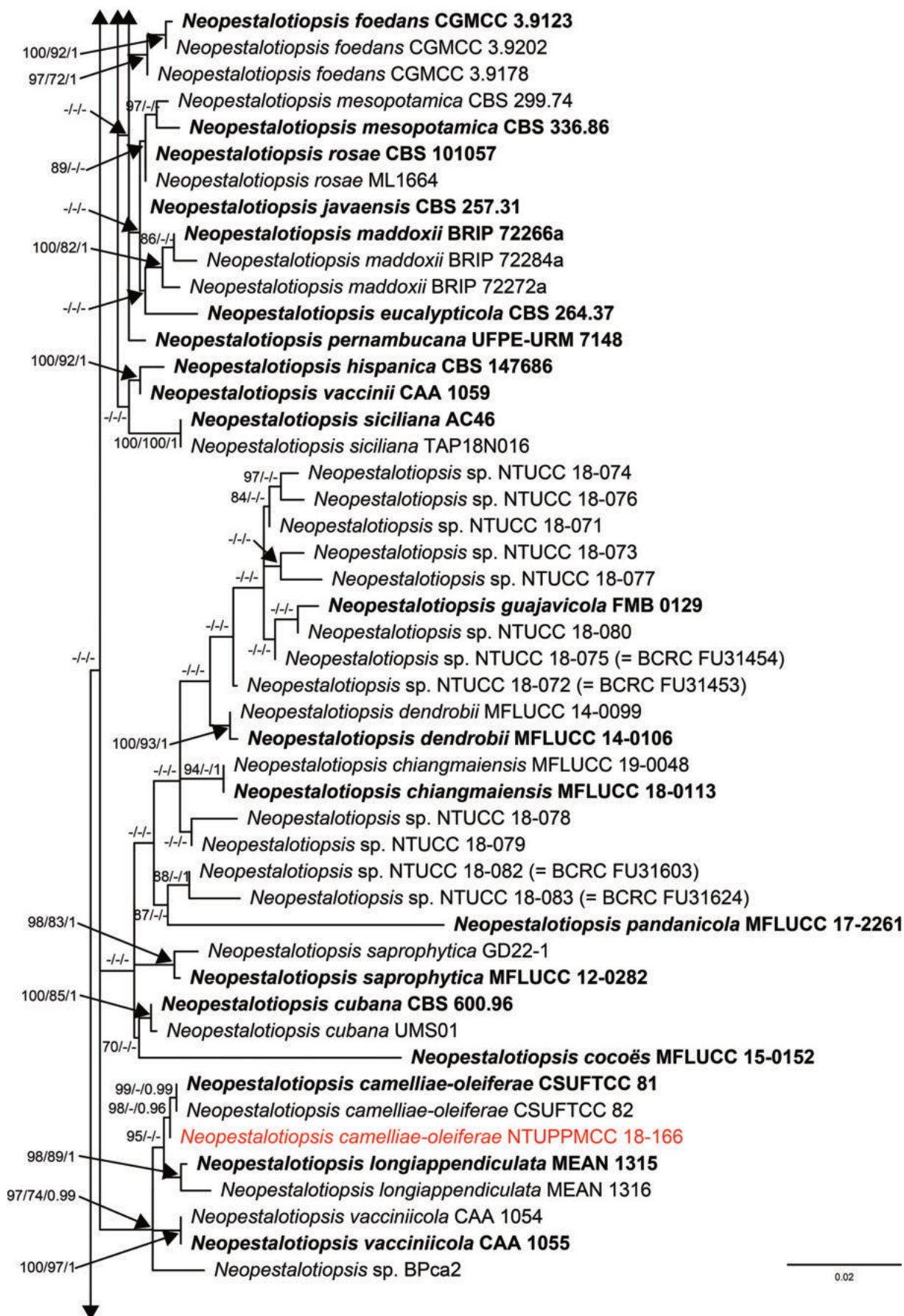
Figure 3. Continued.
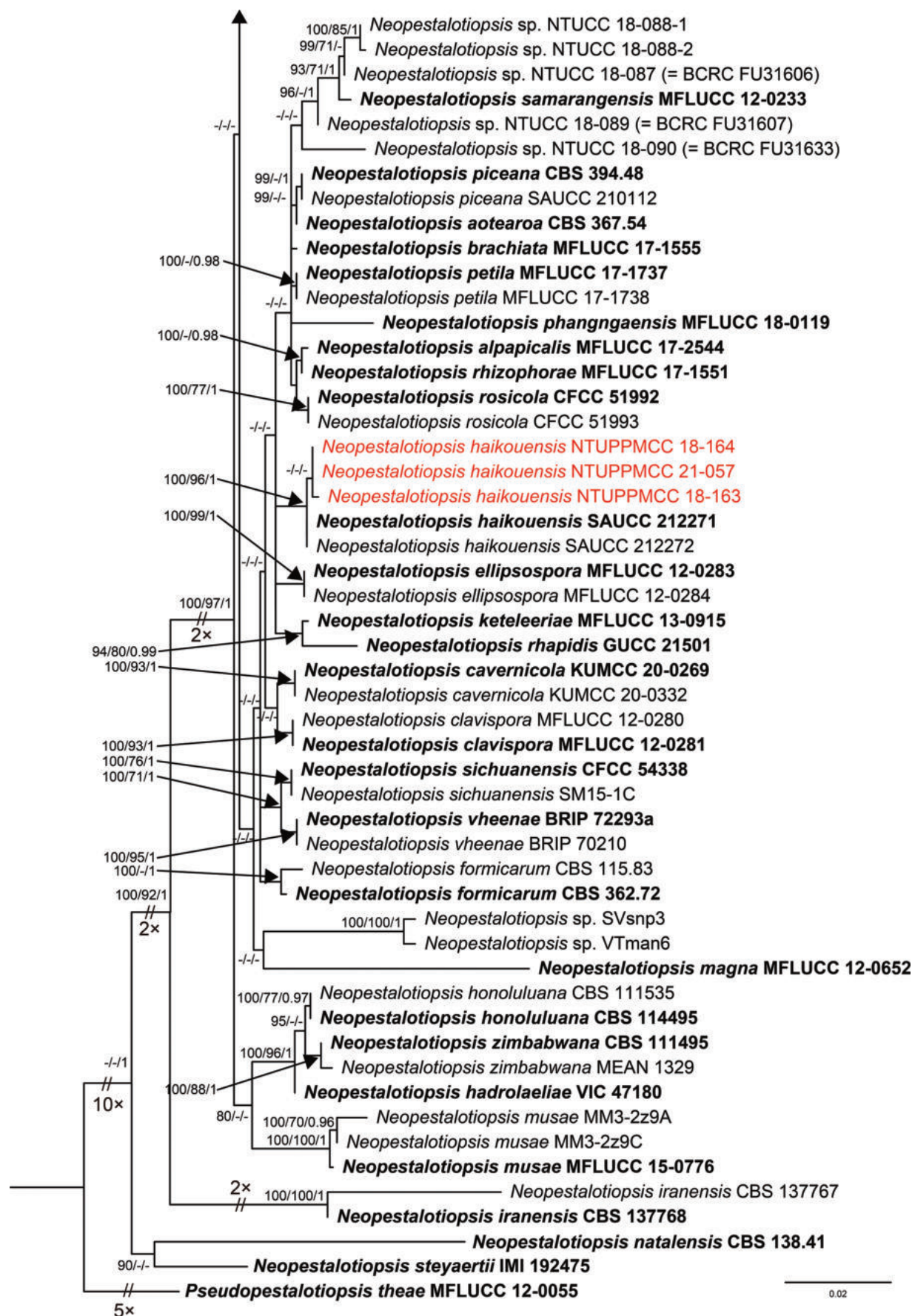
Figure 3. Continued.

Phylogeny of *Pestalotiopsis*

A total of 160 strains representing 118 accepted species and one unclassified taxon were comprised in the final alignment matrix of *Pestalotiopsis*. *Neopestalotiopsis protearum* CBS 114178 was assigned as the outgroup taxon (Xiong et al. 2022; Sun et al. 2023). The final dataset was comprised of 1,458 characters (ITS: 550; *tub2*: 457; *tef1-α*: 451), of which 885 characters were constant, 129 variable characters were parsimony-uninformative and 444 were parsimony-informative characters. A best-scoring ML tree resulted in a final ML optimisation value of likelihood of −12523.681; MLB values are presented in Fig. 2. The parsimony analysis of the data matrix resulted in two equally parsimonious trees and the support values of the first tree (tree length, TL = 1,954 steps; consistency index, CI = 0.442; retention index, RI = 0.817; rescaled consistency index, RC = 0.361; homoplasy index, HI = 0.558) and MPB values are presented in Fig. 2. The Bayesian analysis resulted in 69,660 trees after 6,966,000 generations of topological convergence. The first 13,932 trees were discarded, as the burn-in phase of the analyses, whereas the remaining trees were used for computing Bayesian PPs in the majority rule consensus tree, which are shown in Fig. 2. All methods achieved almost the same topology at the species level in compliance with previous studies based on ML, MP and BI (Maharachchikumbura et al. 2014; Tsai et al. 2021; Sun et al. 2023).

Remarkably, two newly-isolated strains in this study (NTUPPMCC 18-165 and 22-012) formed a distinct clade basal to species clades of *P. castanopsidis*, *P. cyclobalanopsidis*, *P. guizhouensis*, *P. jesteri* and *P. montellica* with high statistical support in the single-locus and concatenated data matrices. Thus, the new lineage is introduced as *Pestalotiopsis manyueyuanani* (Fig. 2). A single strain, NTUPPMCC 18-162, was resolved in the clade including the type strain *P. hispanica* (CBS 115391), while one isolate (NTUPPMCC 21-056) clustered within the species clade *P. formosana* (NTUCC 17-009, NTUCC 17-010 and NCYU 19-0353) with high statistical support. Furthermore, the isolate NTUPPMCC 21-054, used in the present study, formed a clade basal to the clade containing the ex-type strains of *P. chamaeropis* (CBS 186.71) and *P. daliensis* (CGMCC 3.23548) with high statistical support in the phylogenetic tree, based on concatenated dataset. The two new isolates (NTUPPMCC 18-160 and NTUPPMCC 21-055), produced in this study, clustered with the strains containing the ex-type strain of *P. trachycarpicola* (IFRDCC 2440) and several representative strains of the species (MFLU 18-2524 and NTUCC 18-004) plus ex-type strains of *P. kenyana* (CBS 442.67), *P. oryzae* (CBS 353.69) and *P. rhodomyrtus* (HGUP 4230) in ITS, *tub2* and multi-locus phylogenies.

Phylogeny of *Neopestalotiopsis*

In total, 152 strains representing 74 accepted *Neopestalotiopsis* species constituted the final DNA alignment matrix of *Neopestalotiopsis*. *Pseudopestalotiopsis theae* MFLUCC 12-0055 was used as the outgroup taxon following a recent publication (Guterres et al. 2023). The dataset had 1,440 characters (ITS: 507; *tub2*: 407; *tef1-α*: 523), of which 1,011 characters were constant, 173 variable characters were parsimony-uninformative and 256 were parsimony-informa-

tive characters. A best-scoring ML tree resulted in a final ML optimisation value of likelihood of −8052.524 and the final ML tree with MLB values were given in Fig. 3. Parsimony analysis of the data matrix resulted in two equally parsimonious trees and the support values belong to the first tree (TL = 990 steps; CI = 0.547; RI = 0.759; RC = 0.415; HI = 0.453) and the MPB values are shown in Fig. 3. The Bayesian analysis obtained 1,000,000 trees after 100,000,000 generations following topological convergence. The burn-in phase of the analyses showed that the first 20% of trees were discarded and the remaining trees were used for calculating PP in the majority rule consensus tree and the final PP values are plotted in Fig. 3.

However, as mentioned in previous studies and as observed in the present study, the topologies of the *Neopestalotiopsis* phylogenetic trees obtained from all analyses (ML, MP and BI) were unstable and had low statistical support and short branch lengths (Maharachchikumbura et al. 2014; Solarte et al. 2018; Tsai et al. 2021; Fiorenza et al. 2022; Peng et al. 2022; Santos et al. 2022; Zhang et al. 2022). Nevertheless, most of the strains generated in this study formed several consistent clades in both single- and multi-locus analysis. A single isolate (NTUPPMCC 18-166) included in the present study formed a well-supported clade with the ex-type strain of *N. camelliae-oleiferae* CSUFTCC 81, while three isolates (NTUPPMCC 18-163, NTUPPMCC 18-164 and NTUP-PMCC 21-057) clustered with the ex-type strain of *N. haikouensis* SAUCC 212271 with robust statistical support. In addition, one isolate (NTUPPMCC 18-161) formed a distinct clade basal to the clades containing ex-type strains of *N. asiatica* (MFLUCC 12-0286), *N. chrysea* (MFLUCC 12-0261), *N. macadamiae* (BRIP 63737c) and *N. umbrinospora* (MFLUCC 12-0285) in multi-locus phylogenetic trees obtained from all analyses (ML, MP and BI). However, the NTUPPMCC 18-161 strain did not consistently form clades in most of the single-locus trees when compared with the results of multi-locus analysis (Suppl. material 2: figs S8−S10). Due to the uncertainty of phylogenetic placement, *Neopestalotiopsis* strain NTUPPMCC 18-161, isolated in this study, was not classified to species level.

Taxonomy

Pestalotiopsis chamaeropis Maharachch., K.D. Hyde & Crous, 2014
Fig. 4

Description. On carnation leaves (*Dianthus caryophyllus*) supplanted on WA (NTUPPMCC 21-054). Sexual morph was not observed in culture. Asexual morph: ***Conidiomata*** acervular, globose, semi-immersed, solitary or gregarious, 200−350 µm diam.; oozing globose, black conidial masses. ***Conidiophores*** obclavate to subcylindrical, 1−3-septate, branched, hyaline, smooth, sometimes merged to conidiogenous cells. ***Conidiogenous cells*** oval to cylindrical or fusiform, hyaline, smooth, (4.8−)5.1−5.7(−5.9) × (20−)21.3−23.9(−25.5) µm, $\bar{x}$ ± SD = 5.4 ± 0.3 × 22.6 ± 1.3 µm. ***Conidia*** fusoid, straight or slightly curved, 4-septate, smooth, (2.4−)3.2−5(−5.4) × (4.6−)6.2−10.5(−12.4) µm, $\bar{x}$ ± SD = 4.1 ± 0.9 × 8.4 ± 2.2 µm, bearing appendages; basal cell obconic with a truncate base, hyaline, thin-walled, (3.7−)4.2−5.4(−6.2) µm long, $\bar{x}$ ± SD = 4.8 ± 0.6 µm; three median cells subcylindrical, pale brown, concolourous, thick-
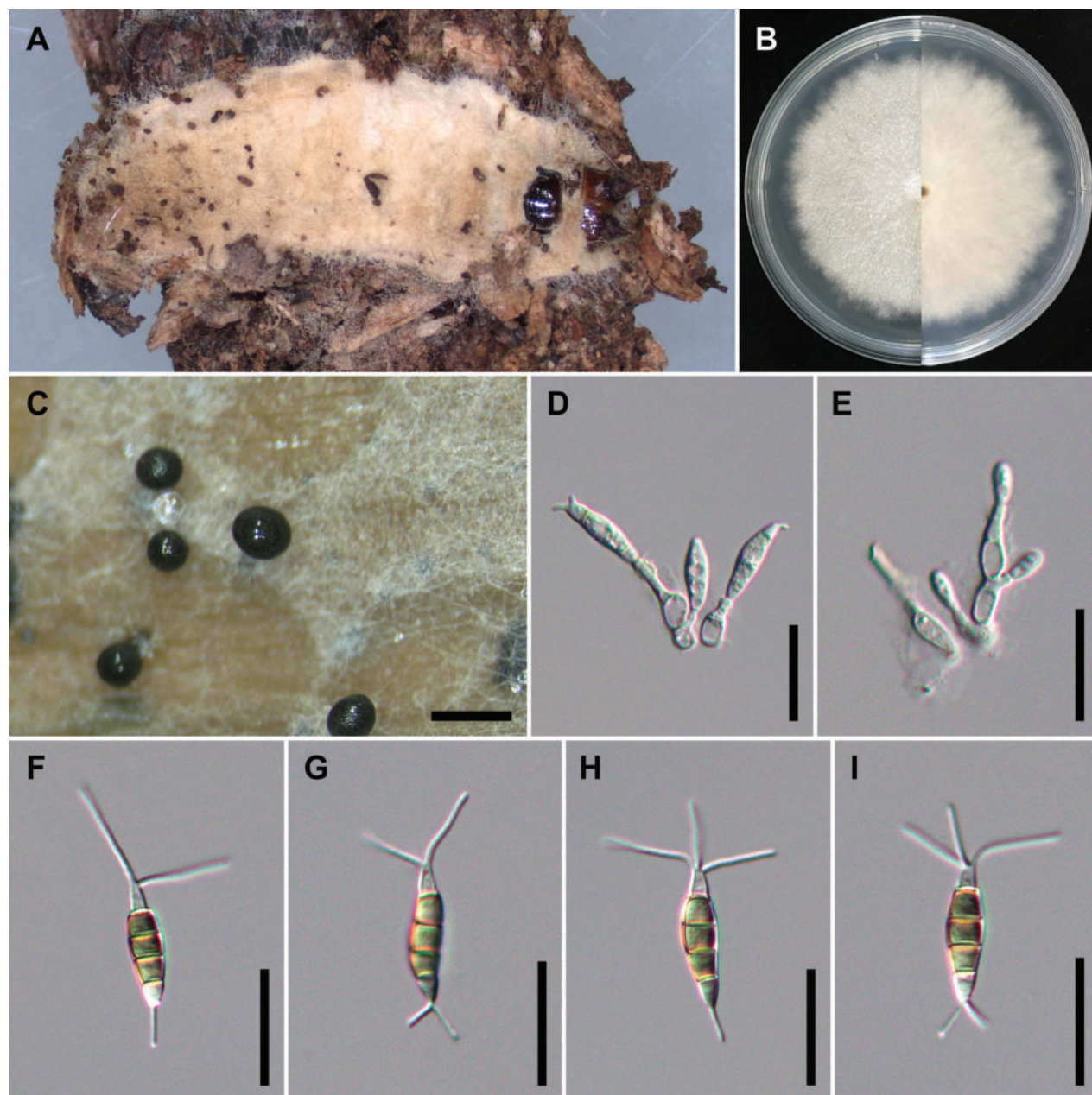
Figure 4. *Pestalotiopsis chamaeropis* (NTUPPMCC 21-054 = CD09) **A** the original habitat of *Pestalotiopsis chamaeropis*; the stroma of *Ophiocordyceps* sp. **B** top view (left) and bottom view (right) of the colony on potato dextrose agar (PDA) after incubation for seven days **C** conidiomata on carnation leaf **D, E** conidiogenous cells and immature conidia **F−I** conidia. Scale bars: 250 μm (**C**); 20 μm (**D−I**).

walled, the first median cell from base (3.8−)4.1−4.7(−5) μm long ($\bar{x}$ ± SD = 4.4 ± 0.3 μm), the second median cell (4−)4.2−4.8(−5.3) μm long ($\bar{x}$ ± SD = 4.5 ± 0.3 μm), the third median cell (3.9−)4.3−5(−5.2) μm long ($\bar{x}$ ± SD = 4.6 ± 0.3 μm), together (12−)12.8−14.2(−15.1) μm long ($\bar{x}$ ± SD = 13.5 ± 0.7 μm); apical cell conical to subcylindrical with a truncate or acute apex, hyaline, thick-walled, (3.6−)4−4.7(−5.1) μm long ($\bar{x}$ ± SD = 4.3 ± 0.4 μm). ***Appendages*** tubular, hyaline, straight or slightly bent, apical appendage 2−3 (mostly 3), unbranched, (8.8−)10.8−17.2(−23.9) μm long ($\bar{x}$ ± SD = 14.0 ± 3.2 μm), basal appendage 1−2 (mostly single), centric, unbranched, (2.9−)4.5−7.7(−10.0) μm long ($\bar{x}$ ± SD = 6.1 ± 1.6 μm).

Culture characteristics. Colonies on PDA reaching 71.3 mm diam. on average after culturing at 25 °C in the dark for seven days, flat with smooth edge, aerial mycelium dense, white; reverse similar in colour.

Materials examined. Taiwan, Taichung City, Heping District, Yuanzui Mountain, on stroma of *Ophiocordyceps* sp. parasitic on a cocoon (Lepidoptera), 6 July 2021, Ming-Syun Wu, living culture NTUPPMCC 21-054 (= CD09).

Notes. For ML, MP and BI with both single locus and concatenated datasets used in the present study, isolate NTUPPMCC 21-054 formed a clade sister to the clade containing the ex-type strains of *P. chamaeropis* (CBS 186.71) and *P. daliensis* (CGMCC 3.23548) with high statistical support. However, we did not find clear morphological support to consider our isolate as a separate species because NTUPPMCC 21-054 showed overlapping morphologies with both *P. chamaeropis* (CBS 186.71) and *P. daliensis* (CGMCC 3.23548) (Suppl. material 1: table S6). Therefore, giving priority to the oldest name between *P. chamaeropis* and *P. daliensis*, we tentatively named NTUPPMCC 21-054 as *P. chamaeropis* rather than introducing it as a new species. To the best of our knowledge, this is the first report of *P. chamaeropis* in Taiwan.

Pestalotiopsis formosana H.A. Ariyaw. & K.D. Hyde, 2018
Fig. 10

Description. See Suppl. material 1: table S1.

Materials examined. Taiwan, Hsinchu County, Jianshi Township, Ptlaman Mountain, on stroma of *Ophiocordyceps* sp. parasitic on an insect (Coleoptera), 28 July 2021, Li-Hong Chen, living culture NTUPPMCC 21-056 (= CD11).

Notes. Morphological features of *Pestalotiopsis formosana* (NTUPPMCC 21-056), obtained in this study, overlap with the original taxonomic description of *P. formosana* in Ariyawansa and Hyde (2018). Hence, considering both the phylogeny, based on DNA sequence data and morphological characterisation, NTUPPMCC 21-056 was recognised as *Pestalotiopsis formosana*.

Pestalotiopsis hispanica F. Liu, L. Cai & Crous
Fig. 5

Description. On carnation leaves (*Dianthus caryophyllus*) supplanted on WA (NTUPPMCC 18-162). Sexual morph was not observed in culture. Asexual morph: ***Conidiomata*** acervular, globose, solitary or gregarious, semi-immersed, 100–500 µm diam.; oozing globose to clavate, black conidial masses. ***Conidiophores*** subcylindrical, hyaline, smooth, annelidic, indistinct and frequently merged to conidiogenous cells. ***Conidiogenous cells*** long pyriform to cylindrical, hyaline, smooth, (1.8–)2.0–3.7(–5.6) × (6.3–)9.7–17.2(–23.2) µm, $\bar{x}$ ± SD = 2.9 ± 0.8 × 13.5 ± 3.8 µm. ***Conidia*** fusoid, straight or slightly curved, 4-septate, smooth, (4.7–)5.5–6.5(–7.5) × (21.1–)22.4–25.4(–27.4) µm, $\bar{x}$ ± SD = 6.0 ± 0.5 × 23.9 ± 1.5 µm, bearing appendages; basal cell obconic with a truncate base, hyaline or pale brown, thin-walled, (0.8–)4.0–6.1(–6.6) µm long, $\bar{x}$ ± SD = 5.0 ± 1.0 µm; three median cells long doliiform to subcylindrical, pale brown, concolourous, thick-walled, the first median cell
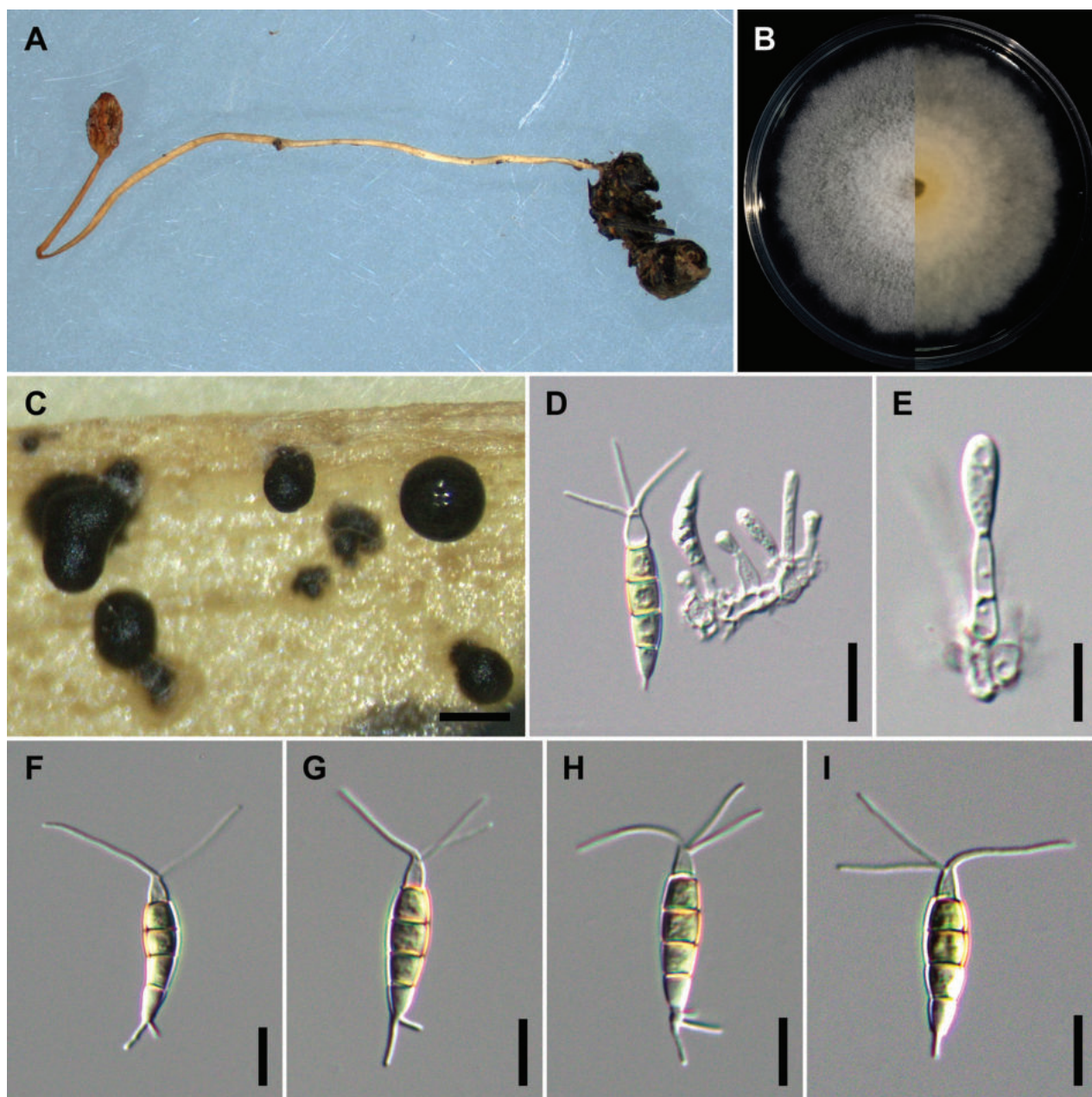
Figure 5. *Pestalotiopsis hispanica* (NTUPPMCC 18-162 = CD03) **A** the original habitat of *Pestalotiopsis hispanica*; the stroma of *Ophiocordyceps* sp. **B** top view (left) and bottom view (right) of the colony on potato dextrose agar (PDA) after incubation for seven days **C** conidiomata on carnation leaf **D, E** conidiogenous cells and immature conidia **F−I** conidia. Scale bars: 250 μm (**C**); 10 μm (**D−I**).

from base (4.1−)4.5−5.3(−5.8) μm long (x̄ ± SD = 4.9 ± 0.4 μm), the second median cell (3.8−)4.3−5.0(−5.3) μm long (x̄± SD = 4.6 ± 0.3 μm), the third median cell (4.3−)4.6−5.4(−6.3) μm long (x̄ ± SD = 5.0 ± 0.4 μm), together (12.7−)13.7−15.2 (−16.0) μm long (x̄ ± SD = 14.5 ± 0.8 μm); apical cell conical to subcylindrical with a truncate or acute apex, hyaline, thick-walled, (3.5−)3.8−4.7(−5.2) μm long (x̄ ± SD = 4.3 ± 0.5 μm). ***Appendages*** tubular, hyaline, straight or slightly bent, apical appendage 2−3, unbranched, (8.5−)12.1−18.7(−24.9) μm long (x̄ ± SD = 15.4 ± 3.3 μm), basal appendage 1−3 (mostly single), centric, unbranched (rarely branched), (2.5−)3.2−6.1(−8.8) μm long (x̄ ± SD = 4.7 ± 1.4 μm).

Culture characteristics. Colonies on PDA reaching 71.9 mm diam. on average after culturing at 25 °C in the dark for seven days, circular, flat with slightly undulate edge, aerial mycelium dense, white; reverse yellowish.

Materials examined. Taiwan, Taoyuan City, Dongyanshan, on the stroma of *Ophiocordyceps* sp. parasitic on an insect (Hymenoptera), 7 October 2018, Wei-Yu Chuang, living culture NTUPPMCC 18-162 (= CD03).

Notes. Multi-locus phylogenetic analysis indicated that strain NTUPPMCC 18-162 was clustered in the same clade with the ex-type strain of *P. hispanica* CBS 115391 with absolute statistical support (MLB = 100%, MPB = 100%, PP = 1.00). Even though the DNA sequences of ITS (100%), *tub2* (99.22%) and *tef1-α* (100%) genes of NTUPPMCC 18-162 were very similar to the ex-type strain of *P. hispanica* (CBS 115391), the morphology of our strain is somewhat different from the original description of *P. hispanica* (holotype CBS H-23554) published by Liu et al. (2019). For instance, NTUPPMCC 18-162 has longer apical appendages (12−18 µm versus 2−14 µm) and contains higher numbers of basal appendages (0−1 versus 0−3) (Suppl. material 1: table S7) compared to the *P. hispanica* holotype CBS H-23554. However, *P. hispanica* was originally isolated from *Protea* cv. 'Susara' (Proteaceae) and collected in Spain, while NTUPPMCC 18-162 was isolated from the stroma of *Ophiocordyceps* sp. in Taiwan. Different locations, nutrition modes and natural habitats might have affected the morphology of these two strains. Therefore, considering the identity of the DNA sequences data, we classify NTUPPMCC 18-162 as *P. hispanica* and, to the best of our knowledge, this is the first report of *P. hispanica* in Taiwan.

Pestalotiopsis manyueyuanani S.Y. Hsu, Y.C. Xu, W.Y. Chuang & Ariyawansa, sp. nov.

MycoBank No: 849030
Fig. 6

Etymology. The specific epithet '*manyueyuanani*' is based on the place the fungus was originally collected.

Typification. Taiwan, New Taipei City, Manyueyuan National Forest Recreation Area, on stroma of *Ophiocordyceps* sp. parasitic on an insect (*Cletus* sp., Hemiptera), 25 May 2018, Wei-Yu Chuang, holotype, NTUPPMH 18-165 (permanently preserved in a metabolically inactive state), ex-holotype NTUPPMCC 18-165 (= CD07). *ibid*., ex-isotype NTUPPMCC 22-012.

Description. Based on the morphology of ex-holotype 18-165 growing on carnation leaves (*Dianthus caryophyllus*) supplanted on WA. Sexual morph was not observed on culture. Asexual morph: **Conidiomata** acervular, globose, scattered, solitary, semi-immersed, black, < 30−100 µm diam.; oozing globose to subcylindrical, black conidial masses. **Conidiophores** pyriform to subcylindrical, hyaline, smooth, indistinct and frequently merged to conidiogenous cells. **Conidiogenous cells** ampulliform to spherical, hyaline, smooth, (2.8−)3.8−5.3(−6.0) × (6.8−)8.2−12.4(−14.7) µm, $\bar{x}$ ± SD = 4.6 ± 0.7 × 10.3 ± 2.1 µm. **Conidia** fusoid, straight or slightly curved, 4-septate, smooth, slightly constricted at the septa, (6.7−)7.4−9.2(−10.4) × (22.5−)24.6−30.0(−32.7) µm, $\bar{x}$ ± SD = 8.3 ± 0.9 × 27.3 ± 2.7 µm, bearing
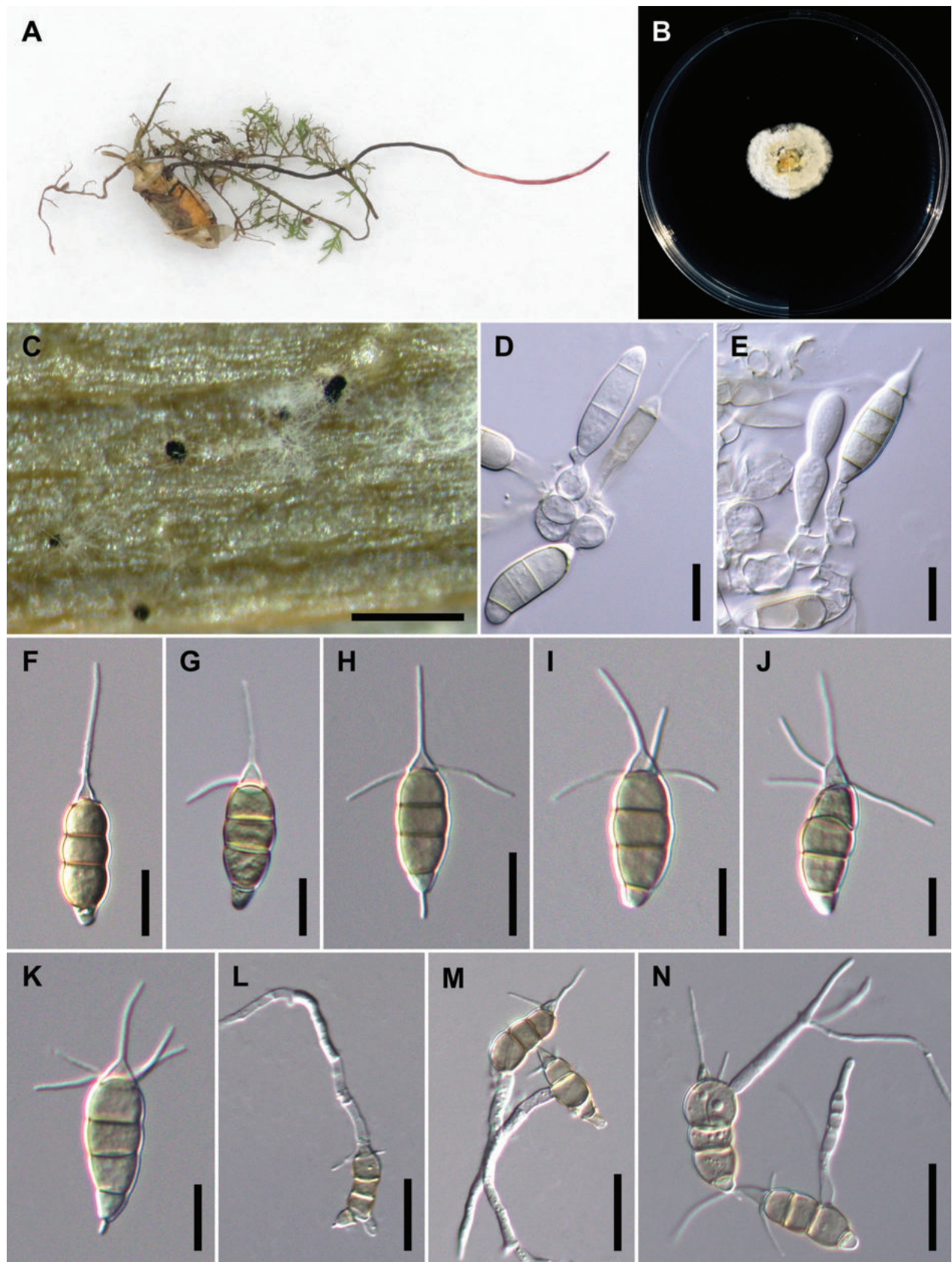
Figure 6. The morphology of *Pestalotiopsis manyueyuanani* **A** the original habitat of conidia of *Pestalotiopsis manyueyua-nani*; stroma of *Ophiocordyceps* sp. **B** top view (left) and bottom view (right) of the colony on potato dextrose agar (PDA) after incubation for seven days **C** formation of conidiomata on carnation leaf **D, E** conidiogenous cells and immature conidia **F−K** conidia **L−N** germinated conidia. Scale bars: 250 μm (**C**); 10 μm (**D−K**); 20 μm (**L−N**).

appendages; basal cell obconic with a truncate base, hyaline or pale brown, thin-walled, (2.9−)3.5−4.7(−5.3) µm long, $\overline{x}$ ± SD = 4.1 ± 0.6 µm; three median cells doliiform to subcylindrical, pale brown to brown, concolourous, thick-walled, the first median cell from base (5.3−)5.8−7.9(−9.2) µm long ($\overline{x}$ ± SD = 6.9 ± 1.0 µm), the second median cell (4.1−)4.9−6.6(−7.8) µm long ($\overline{x}$ ± SD = 5.7 ± 0.9 µm), the third median cell (4.3−)5.5−7.3(−8.6) µm long ($\overline{x}$ ± SD = 6.4 ± 0.9 µm), together (15.1−)16.7−21.2 (−24.5) µm long ($\overline{x}$ ± SD = 18.9 ± 2.3 µm); apical cell conical with an acute apex, hyaline, thick-walled, (2.2−)3.3−5.1(−5.8) µm long ($\overline{x}$ ± SD = 4.2 ± 0.9 µm). ***Appendages*** tubular, hyaline, unbranched, straight or slightly bent, apical appendage single (rarely two), (3.9−)8.7−16.8(−19.1) µm long ($\overline{x}$ ± SD = 12.8 ± 4.0 µm), lateral appendages 1−4 (mostly 2, occasionally absent), forming from apical cell, arising above the septum dividing the apical cell and the third median cell, (5.4−)7.3−13.4(−15.4) µm long ($\overline{x}$ ± SD = 10.3 ± 3.0 µm), basal appendage single (occasionally absent), centric, (1.8−)2.7−5.5(−6.5) µm long ($\overline{x}$ ± SD = 4.1 ± 1.4 µm). Germinating conidia pattern, solitary or multiple, forming from inflated apical cell or median cells.

Culture characteristics. Colonies on PDA reaching 18−24 mm diam. after culturing at 25 °C in the dark for seven days, circular, flat with entire to slightly undulate edge, aerial mycelium sparse, yellowish to orange in the centre, whitish at the margin; reverse similar in colour.

Notes. *Pestalotiopsis manyueyuanani* sp. nov. is a representative of *Pestalotiopsis* in having pale brown to brown, concolourous median cells without knobbed apical appendages. In both single and concatenated gene analysis, two isolates of *P. manyueyuanani* clustered in a distinct clade with strong statistical support basal to the clade comprising *P. castanopsidis* CFCC 54384 and CFCC 54430, *P. cyclobalanopsidis* CFCC 54328, *P. guizhouensis* CFCC 54803, *P. jesteri* CBS 109350 and *P. montellica* MFLUCC 12-0279 (Fig. 2 and Suppl. material 2: figs S5−S7). However, *P. manyueyuanani* has overlapping conidial morphologies with *P. castanopsidis*, *P. cyclobalanopsidis*, *P. eleutherococci*, *P. guizhouensis*, *P. jesteri*, *P. lijiangensis* and *P. montellica*, showing that these taxa are cryptic species as shown in Suppl. material 1: table S8. At present, the species limitations of cryptic taxa are widely determined by phylogenies, based on single/multi-locus sequence data together with ecology (including host range and pathogenicity), distribution or physiology (Crous et al. 2015; Tsai et al. 2018). Apart from the unique placement in phylogenetic inference, *P. manyueyuanani* differs from other taxa clustered as mentioned above, by host and distribution (Suppl. material 1: table S2). In addition, to further support our hypothesis, we also implemented PHI tests to determine if there are any occurrences of sexual recombination between *P. manyueyuanani* and its closely-related taxa (*P. castanopsidis*, *P. cyclobalanopsidis*, *P. eleutherococci*, *P. guizhouensis*, *P. jesteri*, *P. lijiangensis* and *P. montellica*). The PHI tests indicated that there were no significant recombinations detected within tested groups (Fig. 7, ITS: Φ_w = 0.5665; *tub2*: Φ_w = 0.7653; *tef1-α*: Φ_w = 0.6276), supporting reproductive isolation within the phylogenetically closely-related groups. Therefore, based on these observations, we introduce *P. manyueyuanani* (NTUPPMCC 18-165 and NTUPPMCC 22-012) as a novel species in the genus *Pestalotiopsis*.
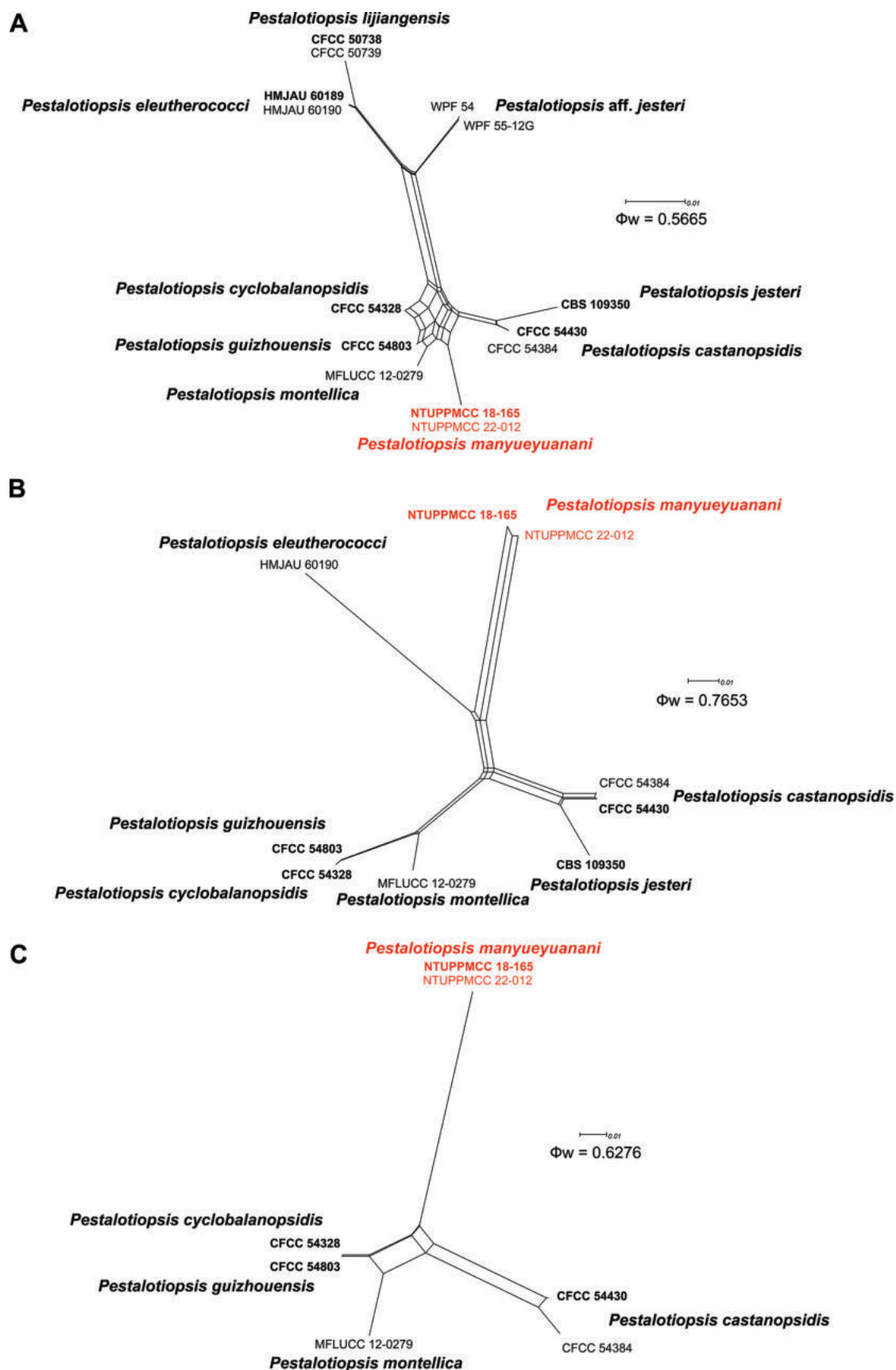
Figure 7. Split graphs showing the results of PHI tests for three gene regions (**A** ITS **B** *tub2* **C** *tef1-a*) of *Pestalotiopsis manyueyuanani* with their phylogenetically closely -related species using LogDet transformation and splits decomposition options. The new taxon in each graph is shown in red and taxa representing ex-type strains are in bold.

Pestalotiopsis trachycarpicola Yan M. Zhang & K.D. Hyde, 2012
Fig. 10

Description: See Suppl. material 1: table S1.

Materials examined. Taiwan, Yilan County, Yuanshan Township, on stroma of *Ophiocordyceps* sp. parasitic on an insect (Lepidoptera), 15 June 2018, Wei-Yu Chuang, living culture NTUPPMCC 18-160 (= CD01). Taiwan, Taichung City, Heping District, Yuanzui Mountain, on stroma of *Ophiocordyceps* sp. parasitic on an ootheca (Mantodea), 14 July 2021, Ming-Syun Wu, living culture NTUP-PMCC 21-055 (= CD10).

Notes. The two new strains NTUPPMCC 18-160 and NTUPPMCC 21-055, used in the present study, clustered within a clade containing ex-type strains of four *Pestalotiopsis* taxa, namely *P. kenyana* (CBS 442.67), *P. oryzae* (CBS 353.69), *P. rhodomyrtus* (HGUP 4230) and *P. trachycarpicola* (IFRDCC 2440) in both single- and multi-locus phylogenies with poor statistical support and short branch lengths. Furthermore, a comparison of the morphological features of these four species and the two strains used in the present study revealed overlapping characteristics, as shown in Suppl. material 1: table S9. However, two strains, included in the present study, tentatively named as *P. trachycarpicola* (Zhang et al. 2012) giving the priority for the oldest species name amongst these four *Pestalotiopsis* species. Nevertheless, further studies of *P. trachycarpicola* (IFRDCC 2440), *P. rhodomyrtus* (HGUP 4230), *P. oryzae* (CBS 353.69) and *P. kenyana* (CBS 442.67) are essential to determine whether these species belong to a single population or if the few informative loci used in the present and previous studies (Liu et al. 2017; Tsai et al. 2021) lead to the poorly-resolved phylogram.

Neopestalotiopsis camelliae-oleiferae Qin Yang & He Li, 2021
Fig. 8

Description. On carnation leaves (*Dianthus caryophyllus*) supplanted on WA (NTUPPMCC 18-166). Sexual morph was not observed in culture. Asexual morph: **Conidiomata** acervular, globose, semi-immersed, solitary or gregarious, 50−250 µm diam.; oozing globose, black conidial masses. **Conidiophores** obclavate to subcylindrical, hyaline, smooth, annelidic, indistinct and frequently merged to conidiogenous cells. **Conidiogenous cells** ampulliform to fusiform, hyaline or sometimes pale brown, smooth, (2.1−)2.9−4.5(−5.2) × (3.8−)5.5−8.7(−10.8) µm, $\bar{x}$ ± SD = 3.7 ± 0.8 × 7.1 ± 1.6 µm. **Conidia** fusoid, straight or slightly curved, 4-septate, smooth, (5.5−)6.3−7.3(−7.8) × (22.1−)23.5−27.4(−29.4) µm, $\bar{x}$ ± SD = 6.8 ± 0.5 × 25.4 ± 2 µm, bearing appendages; basal cell obconic with a truncate base, hyaline, thin-walled, (3.6−)4.6−5.8(−6.6) µm long, $\bar{x}$ ± SD = 5.2 ± 0.6 µm; three median cells doliiform to subcylindrical, versicoloured, septa darker than the rest of the cell, thick-walled, the first median cell from base pale brown, (4.1−)4.4−5.7(−6.1) µm long ($\bar{x}$ ± SD = 5.1 ± 0.6 µm), the second median cell medium to dark brown, (4.1−)4.7−5.9(−6.4) µm long ($\bar{x}$ ± SD = 5.3 ± 0.6 µm), the third median cell medium to dark brown, (2.9−)4.6−6.1(−6.6) µm long ($\bar{x}$ ± SD = 5.3 ± 0.7 µm), together (13.2−)14.4−17(−18.1) µm long ($\bar{x}$ ± SD = 15.7 ± 1.3 µm); apical cell conical to subcylindrical with a truncate or acute apex, hyaline, thick-walled, (3.5−)4.1−5(−5.4) µm long ($\bar{x}$ ± SD = 4.5 ± 0.4 µm). **Appendages** tubular,
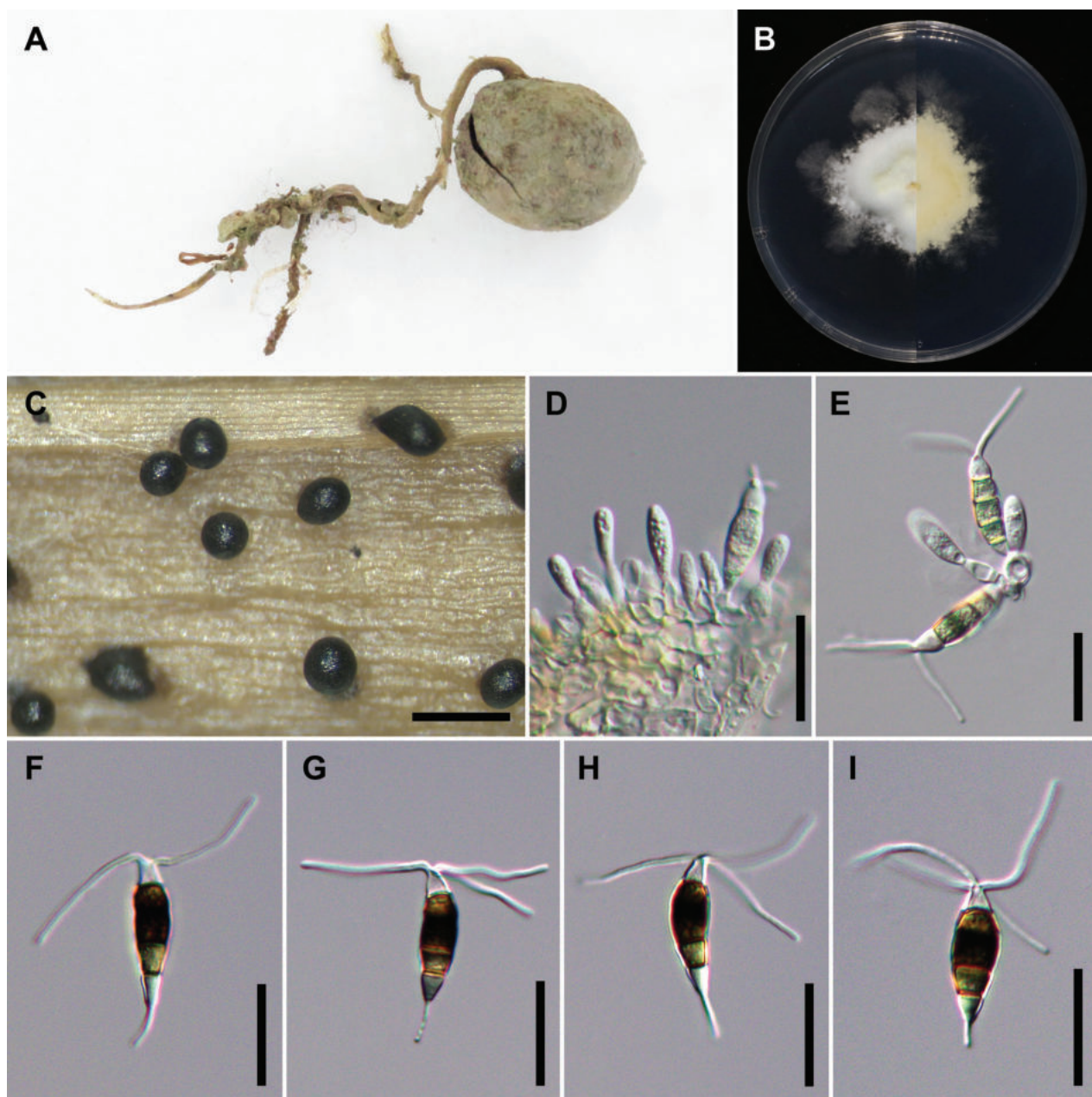
Figure 8. *Neopestalotiopsis camelliae-oleiferae* (NTUPPMCC 18-166 = CD08) **A** the original habitat of *Neopestalotiopsis camelliae-oleiferae*; the stroma of *Tolypocladium* sp. hyperparasitic on an ascocarps of *Elaphomyces* sp. (Ascomycota) **B** top view (left) and bottom view (right) of the colony on potato dextrose agar (PDA) after incubation for seven days **C** conidiomata on carnation leaf **D, E** conidiogenous cells and immature conidia **F–I** conidia. Scale bars: 250 μm (**C**); 20 μm (**D–I**).

hyaline, straight or slightly bent, apical appendage 2–4 (mostly 3), unbranched, (16.3–)21.0–27.0(–30.1) μm long ($\overline{x}$ ± SD = 24.0 ± 3.0 μm), basal appendage single, centric, unbranched, (4–)6.5–9.6(–10.3) μm long ($\overline{x}$ ± SD = 8.1 ± 1.5 μm).

Culture characteristics. Colonies on PDA reaching 46.25 mm diam. on average after culturing at 25 °C in the dark for seven days, filamentous to circular, with slightly undulate edge, aerial mycelium dense, white to yellowish; reverse yellowish.

Materials examined. Taiwan, New Taipei City, Sanxia District, Manyueyuan National Forest Recreation Area, on stroma of *Tolypocladium* sp. hyperparasitic on an ascocarps of *Elaphomyces* sp. (Ascomycota), 25 May 2018, Wei-Yu Chuang, living culture NTUPPMCC 18-166 (= CD08).

Notes. *Neopestalotiopsis camelliae-oleiferae* was originally documented by Li et al. (2021) and the isolate NTUPPMCC 18-166, used in the present study, share comparable morphological features with the illustration of holotype material (CSUFT 081). As a result, the present study recognised NTUPPMCC 18-166 as *N. camelliae-oleiferae*. Additionally, this marks the first report of *N. camelliae-oleiferae* in Taiwan.

Neopestalotiopsis haikouensis Z.X. Zhang, J.W. Xia & X.G. Zhang, 2022
Fig. 9

Description. On carnation leaves (*Dianthus caryophyllus*) supplanted on WA (NTUPPMCC 18-163). Sexual morph was not observed in culture. Asexual morph: ***Conidiomata*** acervular, globose, semi-immersed, solitary or gregarious, 50−250 µm diam.; oozing globose, dark brown to black conidial masses. ***Conidiophores*** obclavate to subcylindrical, hyaline, smooth, annelidic, indistinct and frequently merged to conidiogenous cells. ***Conidiogenous cells*** ampulliform to subcylindrical, hyaline to pale brown, smooth, (2−)2.3−3.6(−5.2) × (5.4−)6.4−9(−10.1) µm, $\bar{x}$ ± SD = 2.9 ± 0.7 × 7.7 ± 1.3 µm. ***Conidia*** fusoid to oval, straight or slightly curved, 4-septate, smooth, (4.7−)4.8−5.6(−6.4) × (22.6−)23.7−26.4(−28.5) µm, $\bar{x}$ ± SD = 5.2 ± 0.4 × 25 ± 1.3 µm, bearing appendages; basal cell obconic with a truncate base, hyaline, thin-walled, (2.9−)4.3−5.5(−5.9) µm long, $\bar{x}$ ± SD = 4.9 ± 0.6 µm; three median cells doliiform to subcylindrical, versicoloured, septa darker than the rest of the cell, thick-walled, the first median cell from base pale brown, (4.4−)4.6−5.4(−6.3) µm long ($\bar{x}$ ± SD = 5 ± 0.4), the second median cell honey-brown to brown, (4.1−)4.4−5.2(−5.6) µm long ($\bar{x}$ ± SD = 4.8 ± 0.4 µm), the third median cell brown, (4.6−)4.8−5.5(−5.9) µm long ($\bar{x}$ ± SD = 5.2 ± 0.4 µm), together (13.4−)14.1−15.9(−17.5) µm long ($\bar{x}$ ± SD = 15 ± 0.9 µm); apical cell conical to subcylindrical with a truncate or acute apex, hyaline, thick-walled, (3.5−)4.6−5.6(−6) µm long ($\bar{x}$ ± SD = 5.1 ± 0.5 µm). ***Appendages*** tubular, hyaline, straight or slightly bent, apical appendage 2−3 (mostly 3), unbranched, (15.5−)17.7−25.5(−33.4) µm long ($\bar{x}$ ± SD = 21.6 ± 3.9 µm), basal appendage single, centric, unbranched, (3.2−)4−6.3(−8.2) µm long ($\bar{x}$ ± SD = 5.1 ± 1.2 µm).

Culture characteristics. Colonies on PDA reaching 45.65 mm diam. on average after culturing at 25 °C in the dark for seven days, filamentous to circular, flat with undulate edge, aerial mycelium moderate dense, white to grey white; reverse similar in colour.

Materials examined. Taiwan, New Taipei City, Sanxia District, Manyueyuan National Forest Recreation Area, on stroma of *Ophiocordyceps* sp. parasitic on an insect (Hymenoptera), 1 August 2018, Wei-Yu Chuang, living culture NTUPPMCC 18-163 (= CD04). Taiwan, Yilan County, Fushan Botanical Garden, on stroma of *Ophiocordyceps* sp. parasitic on an insect (Hymenoptera), 19 July 2018, Wei-Yu Chuang, living culture NTUPPMCC 18-164 (= CD05). Taiwan, New Taipei City, Sanxia District, Manyueyuan National Forest Recreation Area, on stroma of *Tolypocladium* sp. hyperparasitic on an ascocarps of *Elaphomyces* sp. (Ascomycota), 15 July 2021, Yu-Chen Lin, living culture NTUPPMCC 21-057 (= CD12).

Notes. Multi-locus phylogenetic analysis revealed that three newly-identified strains (NTUPPMCC 18-163, NTUPPMCC 18-164 and NTUPPMCC 21-057) form a clade closely associated with the ex-type strain of *N. haikouensis*
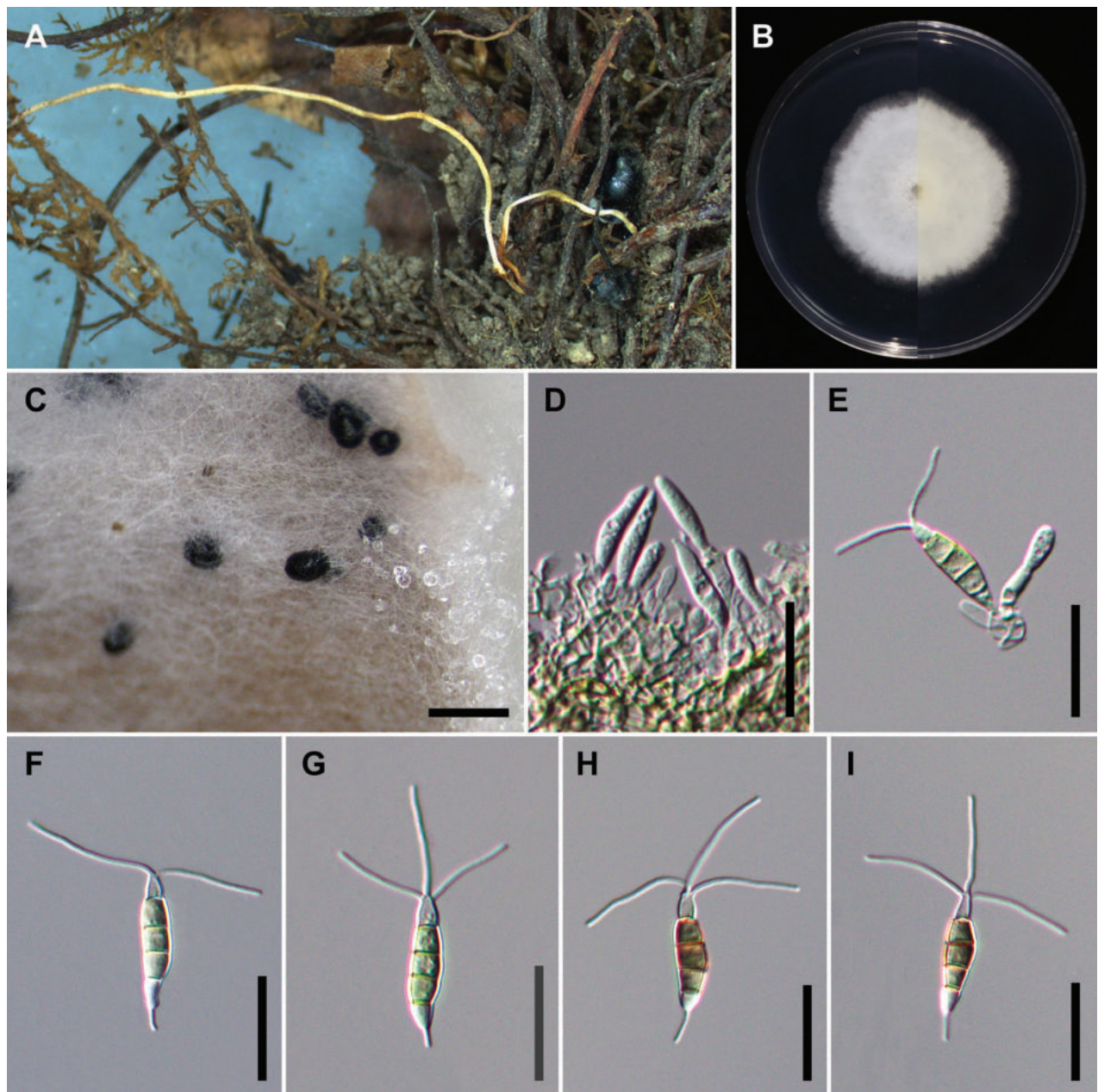
Figure 9. *Neopestalotiopsis haikouensis* (NTUPPMCC 18-163 = CD04) **A** the original habitat of *Neopestalotiopsis haikouensis*; the stroma of *Ophiocordyceps* sp. **B** top view (left) and bottom view (right) of the colony on potato dextrose agar (PDA) after incubation for seven days **C** conidiomata on carnation leaf **D, E** conidiogenous cells and immature conidia **F–I** conidia. Scale bars: 250 μm (**C**); 20 μm (**D–I**).

SAUCC 212271, with robust statistical support (MLB = 100%, MPB = 96%, PP = 1.00). Additionally, the DNA sequences of ITS (100%), *tub2* (99.73%) and *tef1-α* (99.77%) genes of NTUPPMCC 18-163 closely resemble those of the ex-type strain of *N. haikouensis* (SAUCC 212271) and the morphological features of NTUPPMCC 18-163 align with the original taxonomic description in Zhang et al. (2022). Hence, based on both the phylogenetic analysis utilising DNA sequence data and morphological characteristics, strains NTUPPMCC 18-163, NTUPPMCC 18-164 and NTUPPMCC 21-057 were identified as *Neopestalotiopsis haikouensis*. To the best of our knowledge, this study marks the first report of *N. haikouensis* in Taiwan.

Neopestalotiopsis sp.
Fig. 10

Description. See Suppl. material 1: table S1.

Materials examined. Taiwan, Pingtung County, Chunri Township, Tahan Forest Road, on stroma of *Beauveria* sp. parasitic on an insect (Lepidoptera), 7 October 2018, Wei-Yu Chuang, living culture NTUPPMCC 18-161 (= CD02).

Notes. As mentioned earlier in this manuscript, even though the new strain NTUPPMCC 18-161 formed a distinct clade basal to *N. asiatica*, *N. chrysea*, *N. macadamiae* and *N. umbrinospora* in all ML, MP and BI phylogenetic trees, based on the concatenated DNA sequence data matrix, it did not consistently form clades in most of single-locus trees. For instance, in the ITS phylogeny (Suppl. material 2: fig. S8), NTUPPMCC 18-161 clustered with *N. acrostichi* (MFLUCC 17-1755) and the clade containing the ex-type strain (MFLUCC 15-0776) of *N. musae*, along with two representative strains (MM3-2z9A and MM3-2z9C). Conversely, in the phylogenetic tree, based on *tub2* (Suppl. material 2: fig. S9), NTUPPMCC 18-161 formed a well-supported clade with the clade containing the ex-type strain of *N. asiatica* (MFLUCC 12-0286), *N. chrysea* (MFLUCC 12-0261), *N. coffeae-arabicae* (HGUP 4019), *N. macadamiae* (BRIP 63737c), *N. sonneratae* (MFLUCC 17-1744), *N. thailandica* (MFLUCC 17-1730) and *N. umbrinospora* (MFLUCC 12-0285). Meanwhile, it formed a separate sister clade to *N. guajavae*, *N. pandanicola* and *N. psidii* in the *tef1-α* phylogeny (Suppl. material 2: fig. S10) with poor branch and statistical support. When comparing the morphological features of strain NTUPPMCC 18-161 with its phylogenetically closelyrelated species, it becomes evident that our strain exhibits overlapping morphological features, particularly in the number of appendages and sizes of the conidial features (Suppl. material 1: table S10). Therefore, owing to the uncertainty in both phylogenetic placement and morphological data, we tentatively identify NTUPPMCC 18-161 as an unclassified *Neopestalotiopsis* strain. However, additional strains and information are required to clarify the correct placement of this strain.

Growth rate

Based on the results of the phylogenetic analysis, single strains representing each species were selected to test the growth rate. In total, eight strains were selected and grown on PDA media at 25 °C in the dark for seven days. The diameters of colonies were measured (mm) and the means were calculated and are shown in Fig. 11. Isolate NTUPPMCC 18-161 (*Neopestalotiopsis* sp.) and isolate NTUPPMCC 21-054 (*P. chamaeropis*) showed the widest diameter colonies (71.9 and 71.3 mm on average, respectively) and displayed significantly faster growth after seven days of incubation. In contrast, strain NTUPPMCC 18-165 (*P. manyueyuanani*) had the lowest colony diameter (17.15 mm on average) exhibiting significantly low growth compared to all the other isolates.

Temperature effects

Fungal mycelial growth was detected for all the tested isolates between 5 to 40 °C and measured as colony diameter. The results of the effect of temperatures on the mycelium growth of tested strains are presented in Fig. 11 and
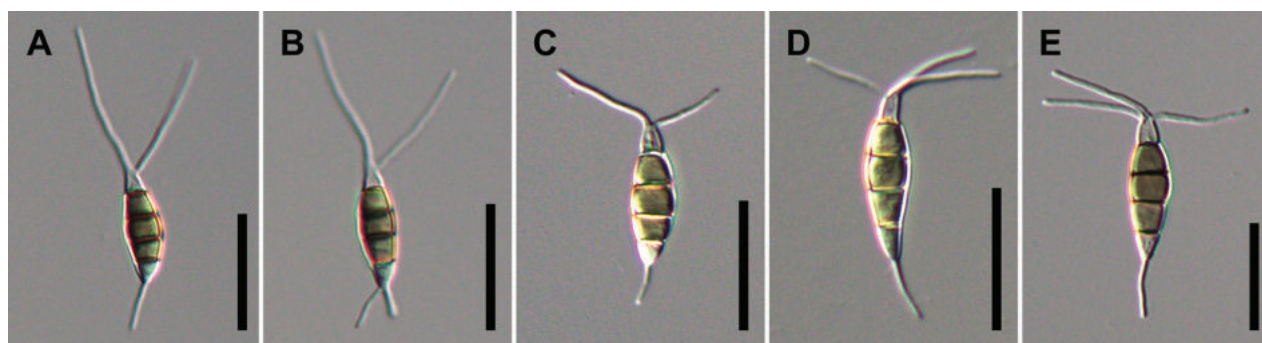
Figure 10. Conidial morphology of *Pestalotiopsis formosana* (**A, B** NTUPPMCC 21-056), *Pestalotiopsis trachycarpicola* (**C** NTUPPMCC 18-160 **D** NTUPPMCC 21-055) and *Neopestalotiopsis* sp. (**E** NTUPPMCC 18-161), isolated from entomopathogenic fungi in this study. Scale bars: 20 μm (**A–E**).
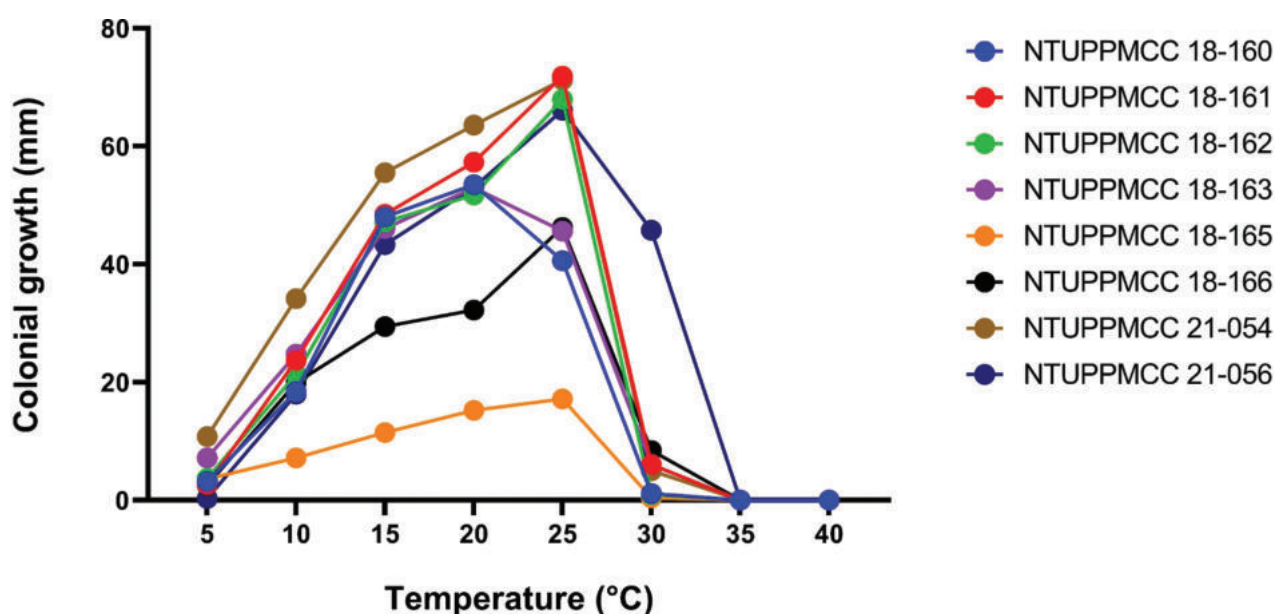
Figure 11. Temperature effect on mycelial growth according to the comparison of colonial growth (mm) of different species at each temperature, based on the mean values presented in Table S11. Colours represent different taxa: NTUPPMCC 18-160, *Pestalotiopsis trachycarpicola*; NTUPPMCC 18-161, *Neopestalotiopsis* sp.; NTUPPMCC 18-162, *Pestalotiopsis hispanica*; NTUPPMCC 18-163, *Neopestalotiopsis haikouensis*; NTUPPMCC 18-165, *Pestalotiopsis manyueyuanani.*; NTUPPMCC 18-166, *Neopestalotiopsis camelliae-oleiferae*; NTUPPMCC 21-054, *Pestalotiopsis chamaeropis*; NTUPPMCC 21-056, *Pestalotiopsis formosana*.

Suppl. material 1: table S11. The results showed that the temperature regimes intensely mediate the growth of tested fungal strains ($p \leq 0.05$); the maximum growth was determined at 25 °C for most of the strains, except for NTUPPMCC 18-160 (*P. trachycarpicola*) and NTUPPMCC 18-163 (*N. haikouensis*) where it showed the highest growth at 20 °C (mean 53.5 mm and 52.95 mm). The results of comparison of the mycelium growth rates for all the representative strains at 25 °C were shown in Fig. 12. In addition, strain NTUPPMCC 19-165 (*P. manyueyuanani*) had no significant difference in mycelium growth between 20 °C and 25 °C, but both were significantly higher than other tested temperatures. However, for all the isolates (Fig. 11 and Suppl. material 1: table S11), the minimum or a lack of growth was observed at 35–40 °C.
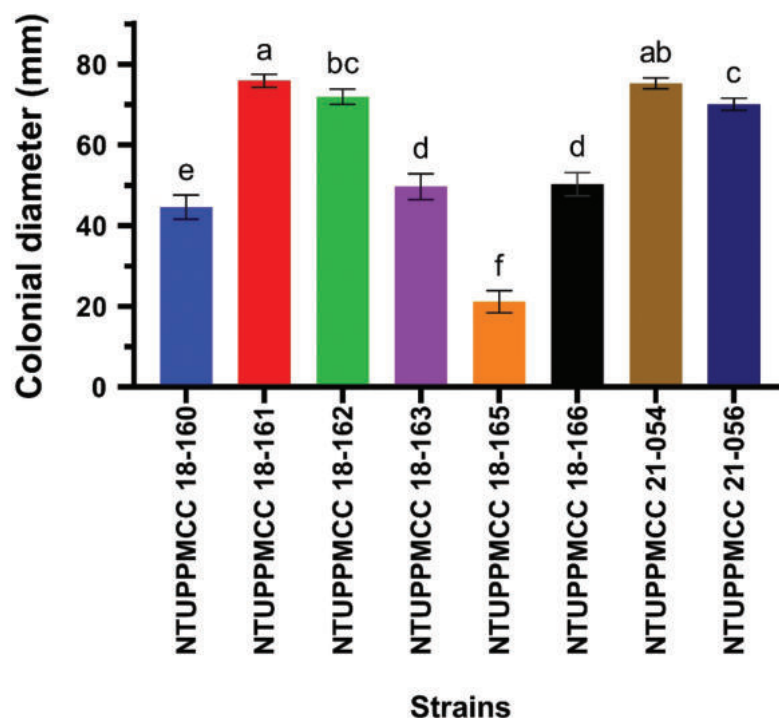
Figure 12. Comparison of the mycelium growth rates of eight pestalotiopsis-like fungal strains at 25 °C. According to Tukey's range test, data (mean ± standard deviation) with the same letters are not significantly different. Colours represent different taxa: NTUPPMCC 18-160, *Pestalotiopsis trachycarpicola*; NTUPPMCC 18-161, *Neopestalotiopsis* sp.; NTUPPMCC 18-162, *Pestalotiopsis hispanica*; NTUPPMCC 18-163, *Neopestalotiopsis haikouensis*; NTUPPMCC 18-165, *Pestalotiopsis manyueyuanani*.; NTUPPMCC 18-166, *Neopestalotiopsis camelliae-oleiferae*; NTUPPMCC 21-054, *Pestalotiopsis chamaeropis*; NTUPPMCC 21-056, *Pestalotiopsis formosana*.

Optimal pH

The effect of pH on the mycelium growth of tested strains is shown in Fig. 13 and Suppl. material 1: table S12. Our results indicated that, generally, most of the strains used in this study grow better in alkaline medium (pH 7–11) compared with slightly acidic to neutral medium (pH 3–7). Except for isolate NTUPPMCC 21-056 (*P. formosana*), the maximum growth rates of isolates were at pH 5 and pH 9. Isolate NTUPPMCC 18-165 (*P. manyueyuanani*) showed relatively slow growth under all the tested pH upon mycelial growth compared with the other strains.

Discussion

Species of *Pestalotiopsis sensu lato* comprise a ubiquitous group of fungi that have been reported from various ecological niches. They have been identified as plant pathogens (Tsai et al. 2018, 2021; Fiorenza et al. 2022; Xiong et al. 2022; Zhang et al. 2022; Sun et al. 2023), human pathogens (Monden et al. 2013), saprobes (Ariyawansa and Hyde 2018; Sun et al. 2023) and endophytes (Maharachchikumbura et al. 2011; Sun et al. 2023). *Neopestalotiopsis* species have recently been identified as a group of emerging plant pathogens, causing severe diseases on economically important crops and fruits, such as strawberry (Baggio et al. 2021), guava (Solarte et al. 2018; Bhogal et al. 2022), grape (Huanaluek et al. 2021), mangosteen (Huanaluek et al. 2021), avocado (Fiorenza et
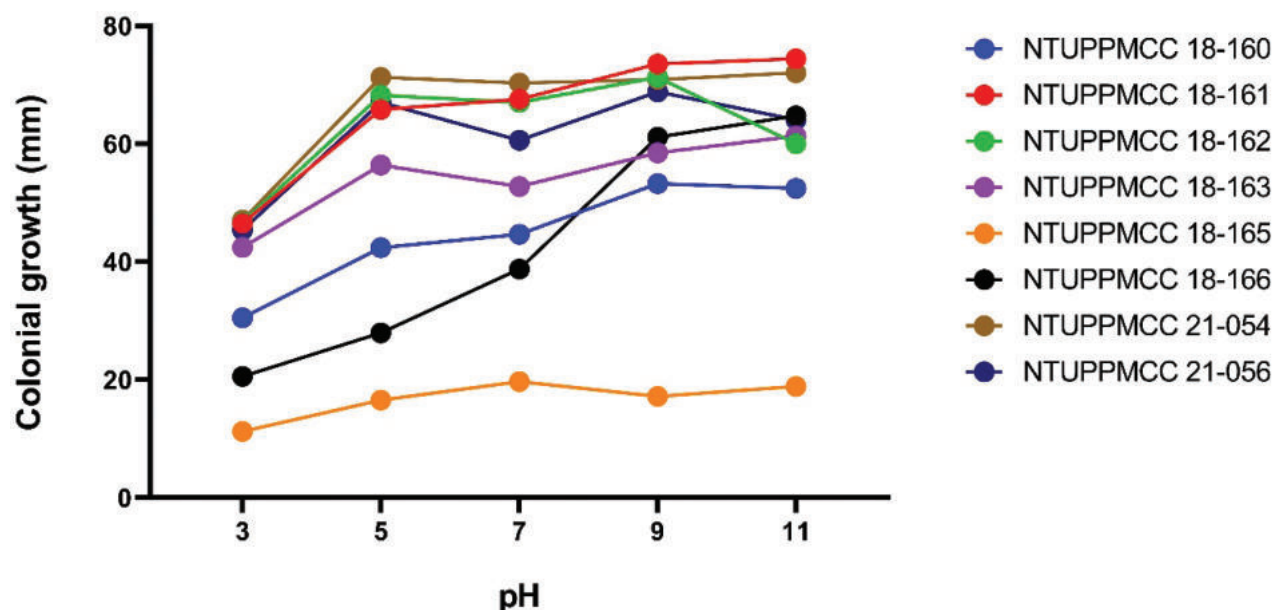
Figure 13. Optimal pH for mycelial growth of each species according to the comparison of colonial growth (mm) of different species at each pH, based on the mean values presented in Table S12. Colours represent different taxa: NTUP-PMCC 18-160, *Pestalotiopsis trachycarpicola*; NTUPPMCC 18-161, *Neopestalotiopsis* sp.; NTUPPMCC 18-162, *Pestalotiopsis hispanica*; NTUPPMCC 18-163, *Neopestalotiopsis haikouensis*; NTUPPMCC 18-165, *Pestalotiopsis manyueyuanani*.; NTUPPMCC 18-166, *Neopestalotiopsis camelliae-oleiferae*; NTUPPMCC 21-054, *Pestalotiopsis chamaeropis*; NTUPPMCC 21-056, *Pestalotiopsis formosana*.

al. 2022), blueberry (Santos et al. 2022), jabuticaba (Lin et al. 2022) and persimmon (Qin et al. 2023). Apart from that, many pestalotiopsis-like fungal species have been identified as promising in terms of producing novel biologically active compounds (Xie et al. 2014; Deshmukh et al. 2017). The highest diversity of pestalotiopsis-like fungi is recorded in tropical and subtropical countries (Jiang et al. 2022a; Peng et al. 2022; Xiong et al. 2022; Seifollahi et al. 2023; Sun et al. 2023). While most pestalotiopsis-like taxa are associated with plants (Maharachchikumbura et al. 2011), investigations regarding their biodiversity and occurrence in unusual habitats are rare (Liu et al. 2021; Rajulu et al. 2022).

In the present study, we identified several strains of *Pestalotiopsis sensu lato*. The species grouped in *Pestalotiopsis* and *Neopestalotiopsis* were associated with the stromata of entomopathogenic fungal species, based on morphology coupled with evolutionary relationships obtained from multi-locus phylogeny. Classification of pestalotiopsis-like fungal species mainly relies on morphological features together with evolutionary relationships, based on the multi-locus phylogeny of ITS, *tub2* and *tef1-α* genes. Even though many species have been introduced in recent years using this criterion, we observed several inconsistencies in the species' evolutionary relationships based on phylogeny. For example, the two strains. identified as *P. trachycarpicola* (NTUPPMCC 18-160 and NTUP-PMCC 21-055) in the present study and the ex-type strains of *P. kenyana*, *P. oryzae* and *P. rhodomyrtus*, were clustered within the same clade of *P. trachycarpicola* containing the ex-type strain plus several representative strains (MFLU 18-2524 and NTUCC 18-004) included in ITS, *tub2* and multi-locus phylogenies (Fig. 2 and Suppl. material 2: figs S5–S7). A similar scenario was observed in the clade where one of the strains identified as *P. chamaeropis* (NTUPPMCC 21-056) in

this study and the type strains *P. chamaeropis* (CBS 186.71) and *P. daliensis* (CGMCC 3.23548) clustered within the same clade in single gene and multi-locus phylogenies. In both scenarios, the trees have significantly short branch lengths and poor statistical support in BI, ML and MP analysis (Fig. 2, Suppl. material 2: figs S1–S2). Similar circumstances were detected in the topology of the *Neopestalotiopsis* phylogenetic tree. In the present study, both concatenated gene and single gene trees of *Neopestalotiopsis* resolved unstable topologies with poor branch lengths and low bootstrap support (Fig. 3, Suppl. material 2: figs S3, S4, S8–S10), consistent with previous studies (Maharachchikumbura et al. 2014; Liu et al. 2017; Liu et al. 2019; Tsai et al. 2021). Hence, it is essential to conduct further investigations to ascertain whether the limited informative loci result in an unambiguously resolved phylogram or if the poorly-resolved branches signify populations rather than distinct species.

We also implemented Genealogical Concordance Phylogenetic Species Recognition (GCPSR) to understand the species limits of *Pestalotiopsis* and *Neopestalotiopsis* taxa. This approach has been applied to delineate species in several fungal groups (Dettman et al. 2003; Tsai et al. 2018, 2021; Hilário et al. 2021a, 2021b). However, lacking DNA sequence data of some gene regions of ex-type strains, such as *P. brassicae*, *P. chinensis*, *P. dianellae*, *P. digitalis*, *P. dracontomelonis*, *P. eleutherococci*, *P. endophytica*, *P. hainanensis*, *P. kunmingensis*, *P. sequoiae*, *P. unicolor*, *P. verruculosa* and *P. yunnanensis*, plus the absence of type strains for some important species, such as *P. disseminata* and *P. longiseta* (Maharachchikumbura et al. 2012), meant that this approach was not useful to delimit species. Thus, future studies are essential to provide the correct natural classification of these taxa by providing missing sequence data and applying recently proposed DNA-based delimitation techniques, such as Generalised Mixed Yule Coalescent (GMYC) (Fujisawa and Barraclough 2013) or Poisson Tree Processes (PTP) (Zhang et al. 2013).

Environmental factors including temperature and pH are the most important components mediating fungal growth and helping researchers understand the biology of fungal taxa. In general, pestalotiopsis-like fungi show optimal growth at 20–30 °C (Liu 1995; Tsukamoto and Hino 1956; Hopkins and McQuilken 2000; Liu et al. 2021). Most of the known pestalotiopsis-like fungi typically have a wide pH optimum, regularly covering 5–9 pH units without substantial inhibition of their growth (Wheeler et al. 1991; Nevarez et al. 2009; Das et al. 2010). In the present study, all strains used in the *in-vitro* mycelial growth rate test under different temperatures demonstrated high radial mycelia growth at 25 °C, consistent with previous studies (Tsukamoto and Hino 1956; Liu 1995). Conversely, most of the strains used in the present study showed optimal mycelial growth under alkaline conditions (pH 7–11). These observations somewhat differ from previous findings (pH 5–7) regarding the species in *Pestalotiopsis sensu lato* (Tsukamoto and Hino 1956; Hopkins and McQuilken 2000; Liu et al. 2021).

In recent years, various studies have illustrated novel and promising taxa associated with stromata of entomopathogenic fungi, such as *Cordyceps* and *Ophiocordyceps*. For instance, Ariyawansa et al. (2018a) introduced a new pleosporalean family Tzeananiaceae typified by the genus *Tzeanania* and the species *T. taiwanensis* to accommodate a strain isolated from mycelium growing on the stroma of an *Ophiocordyceps* species. In addition, Sun et al. (2016) illustrated a novel pathogenic taxon, which causes significant quality and yield losses, from

the stromata of *Cordyceps militaris* and named *Calcarisporium cordycipiticola*. Although in the present study a single conidia culture of pestalotiopsis-like fungi was obtained from the stromata of entomopathogenic fungal taxa and their morphological features were observed, based on the spore-bearing structures formed on CLA, single spore isolation of their hosts, entomopathogenic fungal strains, were not successful. Therefore, we could not elucidate the potential nutritional mode of these pestalotiopsis-like fungal isolates or interactions with their entomopathogenic fungal hosts. Hence, further investigations are vital to understanding the interaction between these unusual fungal strains and their hosts.

Conclusions

The present study introduced a novel species, *Pestalotiopsis manyueyuanani* and reported four new records *N. camelliae-oleiferae*, *N. haikouensis*, *P. chamaeropis* and *P. hispanica* in Taiwan for the first time. The optimal temperature for *in-vitro* mycelial growth in selected strains from these taxa was found to be 25 °C. Growth was observed to cease at both 5 °C and 35 °C. Furthermore, all strains exhibited faster growth under alkaline conditions when compared to acidic or neutral pH environments. This study expands our knowledge of the diversity of pestalotiopsis-like fungi in Taiwan. Additionally, it represents the first assessment of pestalotiopsis-like fungi associated with the stromata of entomopathogenic fungal taxa. However, since none of the entomopathogenic fungi in this study was successfully isolated and cultured, interactions between these pestalotiopsis-like fungi and entomopathogenic fungi are still unknown.

Acknowledgements

Additional information

Conflict of interest

The authors have declared that no competing interests exist.

Ethical statement

No ethical statement was reported.

Funding

Author contributions

Conceptualisation, HA; methodology SYH, YCX and HA; software, SYH, YCX, HA and YCL; validation, SYH, YCX, NT, MS and HA; formal analysis, SYH, YCX and HA; investigation, WYC and YCL; resources, HA, HAA, AME, NT, MS; data curation, SYH, YCX, HA and YCL; writing-original draft preparation, SYH, YCX, NT, MS and HA; writing-review and editing, SYH, YCX, NT, MS, RC, HAA, AME, HA and SRL; visualisation, HAA, AME, SYH and YCX; supervision, project administration, HA and NT; funding acquisition, SRL, NT, RC and HA. All authors have read and agreed to the published version of the manuscript.

Author ORCIDs

Sheng-Yu Hsu https://orcid.org/0000-0001-6227-0936
Yuan-Cheng Xu https://orcid.org/0000-0002-3885-498X
Yu-Chen Lin https://orcid.org/0000-0002-2319-0869
Marc Stadler https://orcid.org/0000-0002-7284-8671
Narumon Tangthirasunun https://orcid.org/0000-0001-7619-9464
Ratchadawan Cheewangkoon https://orcid.org/0000-0001-8576-3696
Hind A. AL-Shwaiman https://orcid.org/0009-0002-5872-9083
Abdallah M. Elgorban https://orcid.org/0000-0003-3664-7853
Hiran A. Ariyawansa https://orcid.org/0000-0001-8526-7721

Data availability

All of the data that support the findings of this study are available in the main text or Supplementary Information.

References

Ariyawansa HA, Hyde KD (2018) Additions to *Pestalotiopsis* in Taiwan. Mycosphere 9(5): 999–1013. https://doi.org/10.5943/mycosphere/9/5/4

Ariyawansa HA, Phillips AJ, Chuang WY, Tsai I (2018a) Tzeananiaceae, a new pleosporalean family associated with *Ophiocordyceps macroacicularis* fruiting bodies in Taiwan. MycoKeys 37: 1–17. https://doi.org/10.3897/mycokeys.37.27265

Ariyawansa HA, Tsai I, Jones EG (2018b) A new cryptic species of *Pseudopestalotiopsis* from Taiwan. Phytotaxa 357(2): 133–140. https://doi.org/10.11646/phytotaxa.357.2.6

Baggio JS, Forcelini BB, Wang NY, Ruschel RG, Mertely JC, Peres NA (2021) Outbreak of leaf spot and fruit rot in Florida strawberry caused by *Neopestalotiopsis* spp. Plant Disease 105(2): 305–315. https://doi.org/10.1094/PDIS-06-20-1290-RE

Bhogal S, Jarial K, Jarial RS, Banyal SK (2022) Cultural analysis and growth kinetics of *Pestalotiopsis psidii* (Pat.) Mordue causing scabby fruit canker in guava (*Psidium guajava* L.). Indian Phytopathology 75(3): 691–701. https://doi.org/10.1007/s42360-022-00501-z

Bruen T (2005) PhiPack: PHI test and other tests of recombination. McGill University, Montreal Quebec, 1–8.

Chen YC, Wang CT, Chen CY, Xu YC, Hsiao WW (2021) Investigation of macrofungi in the proposed Taiwan Red Cypress Ecological Conservation Area of the Experimental Forest, National Taiwan University. Journal of the Experimental Forest of National Taiwan University 35(4): 265–276. https://doi.org/10.6542/EFNTU.202112_35(4).0003

Chen CY, Xu YC, Hsiao WW (2022) Investigation of macrofungi in the proposed Luona Taiwania Ecological Conservation Area. Journal of the Experimental Forest

of National Taiwan University 36(3): 221–235. https://doi.org/10.6542/EFN-TU.202209_36(3).0005

Choi YW, Hyde KD, Ho WH (1999) Single spore isolation of fungi. Fungal Diversity 3: 29–38.

Crous PV, Hawksworth DL, Wingfield MJ (2015) Identifying and naming plant-pathogenic fungi: Past, present and future. Annual Review of Phytopathology 53(1): 247–267. https://doi.org/10.1146/annurev-phyto-080614-120245

Das R, Chutia M, Das K, Jha DK (2010) Factors affecting sporulation of *Pestalotiopsis disseminata* causing grey blight disease of *Persea bombycina* Kost., the primary food plant of muga silkworm. Crop Protection (Guildford, Surrey) 29(9): 963–968. https://doi.org/10.1016/j.cropro.2010.05.012

Deshmukh SK, Prakash V, Ranjan N (2017) Recent advances in the discovery of bioactive metabolites from *Pestalotiopsis*. Phytochemistry Reviews 16(5): 883–920. https://doi.org/10.1007/s11101-017-9495-3

Dettman JR, Jacobson DJ, Turner E, Pringle A, Taylor JW (2003) Reproductive isolation and phylogenetic divergence in *Neurospora*: Comparing methods of species recognition in a model eukaryote. Evolution; International Journal of Organic Evolution 57(12): 2721–2741. https://doi.org/10.1111/j.0014-3820.2003.tb01515.x

Fiorenza A, Gusella G, Aiello D, Polizzi G, Voglmayr H (2022) *Neopestalotiopsis siciliana* sp. nov. and *N. rosae* causing stem lesion and dieback on avocado plants in Italy. Journal of Fungi (Basel, Switzerland) 8(6): 562. https://doi.org/10.3390/jof8060562

Fujisawa T, Barraclough TG (2013) Delimiting species using single-locus data and the Generalized Mixed Yule Coalescent approach: a revised method and evaluation on simulated data sets. Systematic Biology 62: 707–724. https://doi.org/10.1093/sysbio/syt033

Grossart HP, van den Wyngaert S, Kagami M, Wurzbacher C, Cunliffe M, Rojas-Jimenez K (2019) Fungi in aquatic ecosystems. Nature Reviews. Microbiology 17(6): 339–354. https://doi.org/10.1038/s41579-019-0175-8

Guba EF (1961) Monograph of *Pestalotia* and *Monochaetia*. Harvard University Press., 342 pp.

Guterres DC, Silva MA, Martins MD, Azevedo DMQ, Lisboa DO, Pinho DB, Furtado GQ (2023) Leaf spot caused by *Neopestalotiopsis* species on Arecaceae in Brazil. Australasian Plant Pathology 52(1): 47–62. https://doi.org/10.1007/s13313-022-00893-6

Hall T, Biosciences I, Carlsbad C (2011) BioEdit: An important software for molecular biology. GERF Bulletin of Biosciences 2: 60–61.

Hilário S, Gonçalves MF, Alves A (2021a) Using genealogical concordance and coalescent-based species delimitation to assess species boundaries in the *Diaporthe eres* complex. Journal of Fungi (Basel, Switzerland) 7(7): 507. https://doi.org/10.3390/jof7070507

Hilário S, Santos L, Alves A (2021b) *Diaporthe amygdali*, a species complex or a complex species? Fungal Biology 125(7): 505–518. https://doi.org/10.1016/j.funbio.2021.01.006

Hopkins KE, McQuilken MP (2000) Characteristics of *Pestalotiopsis* associated with hardy ornamental plants in the UK. European Journal of Plant Pathology 106(1): 77–85. https://doi.org/10.1023/A:1008776611306

Hsiao HY, Ariyawansa HA, Hsu CC, Wang CJ, Shen YM (2022) New records of powdery mildews from Taiwan: *Erysiphe ipomoeae* comb. nov., *E.* aff. *betae* on Buckwheat, and *E. neolycopersici* comb. nov. on *Cardiospermum halicacabum*. Diversity 14(3): 204. https://doi.org/10.3390/d14030204

Hsu SY, Lin YC, Xu YC, Chang HX, Chung PC, Ariyawansa HA (2022) High-quality genome assembly of *Neopestalotiopsis rosae* ML1664, the pathogen causing strawberry leaf blight and crown rot. Molecular Plant-Microbe Interactions 35(10): 949–953. https://doi.org/10.1094/MPMI-04-22-0077-A

Huanaluek N, Jayawardena RS, Maharachchikumbura SS, Harishchandra DL (2021) Additions to pestalotioid fungi in Thailand: *Neopestalotiopsis hydeana* sp. nov. and *Pestalotiopsis hydei* sp. nov. Phytotaxa 479(1): 23–43. https://doi.org/10.11646/phytotaxa.479.1.2

Huang YL, Chien IT (2022) *Pezicula neosporulosa*, a fungal endophyte from *Chamaecyparis formosensis* (Cupressaceae) newly recorded in Taiwan. Fungal Science 37: 9–20.

Huson DH, Bryant D (2006) Application of phylogenetic networks in evolutionary studies. Molecular Biology and Evolution 23(2): 254–267. https://doi.org/10.1093/molbev/msj030

Jiang N, Dou Z, Xue H, Piao C, Li Y (2022a) Identification of *Pestalotiopsis* species based on morphology and molecular phylogeny. Terrestrial Ecosystem and Conservation. 2: 39–53. https://doi.org/10.12356/j.2096-8884.2022-0007

Jiang N, Voglmayr H, Xue H, Piao CG, Li Y (2022b) Morphology and Phylogeny of *Pestalotiopsis* (Sporocadaceae, Amphisphaeriales) from Fagaceae leaves in China. Microbiology Spectrum 10(6): e03272–e22. https://doi.org/10.1128/spectrum.03272-22

Li J, Xie J, Li XN, Zhou ZF, Liu FL, Chen YH (2017) Isolation, identification and antimicrobial activity of mycoparasites (*Pestalotiopsis*) from *Aecidium pourthiaea*. Biotechnology Bulletin 33: 122. https://doi.org/10.13560/j.cnki.biotech.bull.1985.2017.03.018

Li L, Yang Q, Li H (2021) Morphology, phylogeny, and pathogenicity of pestalotioid species on *Camellia oleifera* in China. Journal of Fungi (Basel, Switzerland) 7(12): 1080. https://doi.org/10.3390/jof7121080

Lin YZ, Chang TD, Wen CJ, Tsai SH, Lin YH (2022) First report of leaf brown blight caused by *Neopestalotiopsis formicarum* on jabuticaba in Taiwan. Plant Disease 106(9): 2527. https://doi.org/10.1094/PDIS-07-21-1414-PDN

Liu TD (1995) The occurrence of *Pestalotiopsis eriobotryicola* in loquat and effects on yield and quality of fruits. Bulletin of Taichung District Agricultural Research and Extension Station 47: 59–66.

Liu F, Hou L, Raza M, Cai L (2017) *Pestalotiopsis* and allied genera from *Camellia*, with description of 11 new species from China. Scientific Reports 7(1): 1–19. https://doi.org/10.1038/s41598-017-00972-5

Liu F, Bonthond G, Groenewald JZ, Cai L, Crous PW (2019) Sporocadaceae, a family of coelomycetous fungi with appendage-bearing conidia. Studies in Mycology 92(1): 287–415. https://doi.org/10.1016/j.simyco.2018.11.001

Liu X, Tibpromma S, Zhang F, Xu J, Chethana KWT, Karunarathna SC, Mortimer PE (2021) *Neopestalotiopsis cavernicola* sp. nov. from Gem Cave in Yunnan Province, China. Phytotaxa 512(1): 1–27. https://doi.org/10.11646/phytotaxa.512.1.1

Lv C, Huang B, Qiao M, Wei J, Ding B (2011) Entomopathogenic fungi on *Hemiberlesia pitysophila*. PLOS ONE 6(8): e23649. https://doi.org/10.1371/journal.pone.0023649

Maharachchikumbura SS, Guo LD, Chukeatirote E, Bahkali AH, Hyde KD (2011) *Pestalotiopsis*-Morphology, phylogeny, biochemistry and diversity. Fungal Diversity 50(1): 167–187. https://doi.org/10.1007/s13225-011-0125-x

Maharachchikumbura SS, Guo LD, Cai L, Chukeatirote E, Wu WP, Sun X, Crous PW, Bhat DJ, McKenzie EHC, Hyde KD (2012) A multi-locus backbone tree for *Pestalotiopsis*,

with a polyphasic characterization of 14 new species. Fungal Diversity 56(1): 95–129. https://doi.org/10.1007/s13225-012-0198-1

Maharachchikumbura SS, Hyde KD, Groenewald JZ, Xu J, Crous PW (2014) *Pestalotiopsis* revisited. Studies in Mycology 79(1): 121–186. https://doi.org/10.1016/j.simyco.2014.09.005

Monden Y, Yamamoto S, Yamakawa R, Sunada A, Asari S, Makimura K, Inoue Y (2013) First case of fungal keratitis caused by *Pestalotiopsis clavispora*. Clinical Ophthalmology (Auckland, N.Z.) 7: 2261–2264. https://doi.org/10.2147/OPTH.S48732

Nevarez L, Vasseur V, Le Madec L, Le Bras L, Coroller L, Leguérinel I, Barbier G (2009) Physiological traits of *Penicillium glabrum* strain LCP 08.5568, a filamentous fungus isolated from bottled aromatised mineral water. International Journal of Food Microbiology 130(3): 166–171. https://doi.org/10.1016/j.ijfoodmicro.2009.01.013

Nylander J (2004) MrModeltest version 2. Program distributed by the author. Evolutionary Biology Centre, Uppsala University, Uppsala, Sweden.

Peng C, Crous PW, Jiang N, Fan XL, Liang YM, Tian CM (2022) Diversity of Sporocadaceae (pestalotioid fungi) from *Rosa* in China. Persoonia 49(1): 201–260. https://doi.org/10.3767/persoonia.2022.49.07

Qin R, Li Q, Huang S, Chen X, Mo J, Guo T, Huang H, Tang L, Yu Z (2023) Fruit rot on persimmon caused by *Neopestalotiopsis saprophytica* and *Neopestalotiopsis ellipsospora* in Guangxi, China. Plant Disease 107(8): 2531. https://doi.org/10.1094/PDIS-05-22-1168-PDN

Rajulu MG, Rajamani T, Murali TS, Suryanarayanan TS, Minj D (2022) The fungal endobiome of seaweeds of the Andaman Islands, India. Current Science 123(12): 1508. https://doi.org/10.18520/cs/v123/i12/1508-1514

Rambaut A, Drummond AJ, Xie D, Baele G, Suchard MA (2018) Posterior summarization in Bayesian phylogenetics using Tracer 1.7. Systematic Biology 67(5): 901–904. https://doi.org/10.1093/sysbio/syy032

Ronquist F, Teslenko M, van der Mark P, Ayres DL, Darling A, Höhna S, Larget B, Liu L, Suchard MA, Huelsenbeck JP (2012) MrBayes 3.2: Efficient Bayesian phylogenetic inference and model choice across a large model space. Systematic Biology 61(3): 539–542. https://doi.org/10.1093/sysbio/sys029

Santos J, Hilário S, Pinto G, Alves A (2022) Diversity and pathogenicity of pestalotioid fungi associated with blueberry plants in Portugal, with description of three novel species of *Neopestalotiopsis*. European Journal of Plant Pathology 162(3): 539–555. https://doi.org/10.1007/s10658-021-02419-0

Seifollahi E, de Farias ARG, Jayawardena RS, Hyde KD (2023) Taxonomic Advances from fungal flora associated with ferns and fern-like hosts in Northern Thailand. Plants 12(3): 683. https://doi.org/10.3390/plants12030683

Solarte F, Muñoz CG, Maharachchikumbura SS, Álvarez E (2018) Diversity of *Neopestalotiopsis* and *Pestalotiopsis* spp., causal agents of guava scab in Colombia. Plant Disease 102(1): 49–59. https://doi.org/10.1094/PDIS-01-17-0068-RE

Steyaert RL (1949) Contribution à l'étude monographique de *Pestalotia* de Not. et *Monochaetia* Sacc. (*Truncatella* gen. nov. et *Pestalotiopsis* gen. nov.). Bulletin du Jardin botanique de l'Etat, Bruxelles/Bulletin van den Rijksplantentuin, Brussel, 285–347. https://doi.org/10.2307/3666710

Strobel G, Yang X, Sears J, Kramer R, Sidhu RS, Hess WM (1996) Taxol from *Pestalotiopsis microspora*, an endophytic fungus of *Taxus wallachiana*. Microbiology (Reading, England) 142(2): 435–440. https://doi.org/10.1099/13500872-142-2-435

Sun JZ, Dong CH, Liu XZ, Liu JK, Hyde KD (2016) *Calcarisporium cordycipiticola* sp. nov., an important fungal pathogen of *Cordyceps militaris*. Phytotaxa 268(2): 135–144. https://doi.org/10.11646/phytotaxa.268.2.4

Sun JZ, Liu XZ, McKenzie EH, Jeewon R, Liu JK, Zhang XL, Zhao Q, Hyde KD (2019) Fungicolous fungi: Terminology, diversity, distribution, evolution, and species checklist. Fungal Diversity 95(1): 337–430. https://doi.org/10.1007/s13225-019-00422-9

Sun YR, Jayawardena RS, Sun JE, Wang Y (2023) Pestalotioid species associated with medicinal plants in southwest China and Thailand. Microbiology Spectrum 11(1): e03987–e22. https://doi.org/10.1128/spectrum.03987-22

Swofford D (2003) PAUP*. Phylogenetic analysis using parsimony (*and other methods). Version 4.0. Sinauer associates. Sunderland, Massachusetts.

Tian S, Xu R, Bhunjun CS, Su W, Hyde KD, Li Y, Fu YP, Phukhamsakda C (2022) Combination of morphological and molecular data support *Pestalotiopsis eleutherococci* (Sporocadaceae) as a new species. Phytotaxa 566(1): 105–120. https://doi.org/10.11646/phytotaxa.566.1.6

Trifinopoulos J, Nguyen LT, von Haeseler A, Minh BQ (2016) W-IQ-TREE: A fast online phylogenetic tool for maximum likelihood analysis. Nucleic Acids Research 44(W1): W232–W235. https://doi.org/10.1093/nar/gkw256

Tsai I, Maharachchikumbura SS, Hyde KD, Ariyawansa HA (2018) Molecular phylogeny, morphology and pathogenicity of *Pseudopestalotiopsis* species on *Ixora* in Taiwan. Mycological Progress 17(8): 941–952. https://doi.org/10.1007/s11557-018-1404-7

Tsai I, Chung CL, Lin SR, Hung TH, Shen TL, Hu CY, Hozzein WN, Ariyawansa HA (2021) Cryptic diversity, molecular systematics, and pathogenicity of genus *Pestalotiopsis* and allied genera causing gray blight disease of tea in Taiwan, with a description of a new *Pseudopestalotiopsis* species. Plant Disease 105(2): 425–443. https://doi.org/10.1094/PDIS-05-20-1134-RE

Tsukamoto E, Hino T (1956) On the twig blight of the tree peony and its causal fungus *Pestalotia paeoniicola* sp. nov. Annals of the Phytopathological Society of Japan 21(4): 181–184. https://doi.org/10.3186/jjphytopath.21.181

Wheeler KA, Hurdman BF, Pitt JI (1991) Influence of pH on the growth of some toxigenic species of *Aspergillus*, *Penicillium* and *Fusarium*. International Journal of Food Microbiology 12(2-3): 141–150. https://doi.org/10.1016/0168-1605(91)90063-U

Xie J, Li J, Yang YH, Chen YH, Zhao PJ (2014) Two new ambuic acid analogs from *Pestalotiopsis* sp. cr013. Phytochemistry Letters 10: 291–294. https://doi.org/10.1016/j.phytol.2014.10.002

Xiong YR, Manawasinghe IS, Maharachchikumbura SSN, Lu L, Dong ZY, Xiang M, Xu B (2022) Pestalotioid species associated with palm species from south China. Current Research in Environmental & Applied Mycology 12(1): 285–321. https://doi.org/10.5943/cream/12/1/18

Zhang Y, Maharachchikumbura SSN, McKenzie E, Hyde KD (2012) A novel species of Pestalotiopsis causing leaf spots of *Trachycarpus fortunei*. Cryptogamie. Mycologie 33(3): 311–318. https://doi.org/10.7872/crym.v33.iss3.2012.311

Zhang J, Kapli P, Pavlidis P, Stamatakis A (2013) A general species delimitation method with applications to phylogenetic placements. Bioinformatics 29: 2869e2876. https://doi.org/10.1093/bioinformatics/btt499

Zhang Z, Liu R, Liu S, Mu T, Zhang X, Xia J (2022) Morphological and phylogenetic analyses reveal two new species of Sporocadaceae from Hainan, China. MycoKeys 88: 171–192. https://doi.org/10.3897/mycokeys.88.82229

Supplementary material 1

The morphological features of *Pestalotiopsis sensu lato* fungi and GenBank accession numbers

Authors: Sheng-Yu Hsu, Yuan-Cheng Xu, Yu-Chen Lin, Wei-Yu Chuang, Shiou-Ruei Lin, Marc Stadler, Narumon Tangthirasunun, Ratchadawan Cheewangkoon, Hind A. AL-Shwaiman, Abdallah M. Elgorban, Hiran A. Ariyawansa

Data type: xlsx

Explanation note: **table S1.** The morphological features of pestalotiopsis-like fungi isolated in this study; **table S2.** GenBank accession numbers of *Pestalotiopsis* isolates included in the phylogenetic analysis; **table S3.** GenBank accession numbers of *Neopestalotiopsis* isolates included in the phylogenetic analysis; **table S4.** Primers and PCR conditions used to amplify ITS, *tub2* and *tef1-α* gene regions; **table S5.** Nucleotide substitution models used in the phylogenetic analyses; **table S6.** Morphological comparison of *Pestalotiopsis chamaeropis* and its closely-related taxa; **table S7.** Morphological comparison of *Pestalotiopsis hispanica* and its closely-related taxa; **table S8.** Morphological comparison of *Pestalotiopsis manyueyuanani* and its closely-related taxa; **table S9.** Morphological comparison of *Pestalotiopsis trachycarpicola* and its closely-related taxa; **table S10.** The morphological comparison of *Neopestalotiopsis* strain NTUPPMCC 18-161 and its closely-related taxa; **table S11**. Mycelium growth of individual isolate of pestalotiopsis-like fungi at each temperature in this study; **table S12.** Mycelium growth of individual isolates of pestalotiopsis-like fungi at each pH in this study.

Link: https://doi.org/10.3897/mycokeys.101.113090.suppl1

Supplementary material 2

Phylogenetic trees generated by maximum parsimony analysis of single and combined ITS, *tub2* and *tef1-α* sequence data

Authors: Sheng-Yu Hsu, Yuan-Cheng Xu, Yu-Chen Lin, Wei-Yu Chuang, Shiou-Ruei Lin, Marc Stadler, Narumon Tangthirasunun, Ratchadawan Cheewangkoon, Hind A. AL-Shwaiman, Abdallah M. Elgorban, Hiran A. Ariyawansa

Data type: pdf

Explanation note: **fig. S1.** Phylogenetic tree generated by maximum parsimony analysis of combined ITS, *tub2* and *tef1-α* sequence data of *Pestalotiopsis*. MPB values ≥ 70% are given at the nodes. The scale-bar represents the number of nucleotide substitutions per site. *Neopestalotiopsis protearum* CBS 114178 was used as an outgroup to rooting the tree. New isolates are in red and taxa representing ex-type cultures are in bold; **fig. S2.** Phylogenetic tree obtained through Bayesian Inference for the dataset of ITS, *tub2* and *tef1-α* loci of *Pestalotiopsis*. PP ≥ 0.95 are given at the nodes. The scale-bar represents the number of nucleotide substitutions per site. *Neopestalotiopsis protearum* CBS 114178 was used as an outgroup for rooting the tree. New isolates are in red and taxa representing ex-type cultures are in bold;

fig. S3. Phylogenetic tree generated by maximum parsimony analysis of combined ITS, *tub2* and *tef1-α* sequence data of *Neopestalotiopsis*. MPB values ≥ 70% are given at the nodes. The scale-bar represents the number of nucleotide substitutions per site. *Pseudopestalotiopsis theae* MFLUCC 12-0055 was used as an outgroup for rooting the tree. New isolates are in red and taxa representing ex-type cultures are in bold; **fig. S4.** Phylogenetic tree obtained through Bayesian inference for the dataset of ITS, *tub2* and *tef1-α* loci of *Neopestalotiopsis*. PP ≥ 0.95 are given at the nodes. The scale-bar represents the number of nucleotide substitutions per site. *Pseudopestalotiopsis theae* MFLUCC 12-0055 was used as an outgroup for rooting the tree. New isolates are in red and taxa representing ex-type cultures are in bold; **fig. S5.** Phylogenetic tree generated by Maximum Likelihood analysis of ITS sequence data of *Pestalotiopsis*. MLB values ≥ 70% are given at the nodes. The scale-bar shows the number of estimated substitutions per site. *Neopestalotiopsis protearum* (CBS 114178) was used as an outgroup for rooting the tree. New isolates are in red and taxa representing ex-type cultures are in bold; **fig. S6.** Phylogenetic tree generated by Maximum Likelihood analysis of *tub2* sequence data of *Pestalotiopsis*. MLB values ≥ 70% are given at the nodes. The scale-bar shows the number of estimated substitutions per site. *Neopestalotiopsis protearum* (CBS 114178) was used as an outgroup for rooting the tree. New isolates are in red, and taxa representing ex-type cultures are in bold; **fig. S7.** Phylogenetic tree generated by Maximum Likelihood analysis of *tef1-α* sequence data of *Pestalotiopsis*. MLB values ≥ 70% are given at the nodes. The scale-bar shows the number of estimated substitutions per site. *Neopestalotiopsis protearum* (CBS 114178) was used as an outgroup for rooting the tree. New isolates are in red and taxa representing ex-type cultures are in bold; **fig. S8.** Phylogenetic tree generated by Maximum Likelihood analysis of ITS sequence data of *Neopestalotiopsis*. MLB values ≥ 70% are given at the nodes. The scale-bar shows the number of estimated substitutions per site. *Pseudopestalotiopsis theae* MFLUCC 12-0055 was used as an outgroup for rooting the tree. New isolates are in red and taxa representing ex-type cultures are in bold; **fig. S9.** Phylogenetic tree generated by Maximum Likelihood analysis of *tub2* sequence data of *Neopestalotiopsis*. MLB values ≥ 70% are given at the nodes. The scale-bar shows the number of estimated substitutions per site. *Pseudopestalotiopsis theae* MFLUCC 12-0055 was used as an outgroup for rooting the tree. New isolates are in red and taxa representing ex-type cultures are in bold; **fig. S10.** Phylogenetic tree generated by Maximum Likelihood analysis of *tef1-α* sequence data of *Neopestalotiopsis*. MLB values ≥ 70% are given at the nodes. The scale-bar shows the number of estimated substitutions per site. *Pseudopestalotiopsis theae* MFLUCC 12-0055 was used as an outgroup for rooting the tree. New isolates are in red and taxa representing ex-type cultures are in bold.

Link: https://doi.org/10.3897/mycokeys.101.113090.suppl2

MycoKeys

Three new *Dioszegia* species (Bulleribasidiaceae, Tremellales) discovered in the phylloplane in China

Ya-Zhuo Qiao[1], Shan Liu[1], Qiu-Hong Niu[1,2], Feng-Li Hui[1,2]

1   *School of Life Science and Agricultural Engineering, Nanyang Normal University, Nanyang 473061, China*
2   *Research Center of Henan Provincial Agricultural Biomass Resource Engineering and Technology, Nanyang Normal University, Nanyang 473061, China*
Corresponding authors: Qiu-Hong Niu (*qiuhongniu723@163.com*); Feng-Li Hui (*fenglihui@yeah.net*)

Abstract

The genus *Dioszegia* is comprised of anamorphic basidiomycetous yeasts and is classified in the family Bulleribasidiaceae of the order Tremellales. Currently, 24 species have been described and accepted as members of the genus, although its diversity and global distribution have not been thoroughly investigated. In this study, yeasts were isolated from plant leaves collected in the Guizhou and Henan Provinces of China and identified through a combination of morphological and molecular methods. Phylogenetic analyses of the combined ITS and LSU sequences coupled with morphological studies revealed three novel species, *D. guizhouensis* **sp. nov.**, *D. foliicola* **sp. nov.**, and *D. aurantia* **sp. nov.**, proposed here. Additionally, our phylogenetic analyses suggest that the recently discovered species *D. terrae* is a synonym of *D. maotaiensis*. This study presents detailed descriptions and illustrations of three new *Dioszegia* species and highlights distinctions between them and their close relatives. The findings of this study contribute to our knowledge of the biodiversity of *Dioszegia*, offering a foundation for future research.

Key words: Basidiomycota, leaf, phylogenetic analysis, taxonomy, Tremellomycetes

OPEN ACCESS

Introduction

The genus *Dioszegia* encompasses a group of epiphytic basidiomycetes that inhabit the phylloplane. It was first proposed by Zsolt (1957) based on the single species *Dioszegia hungarica*. Roughly a decade later, the presence of sterigmata or 'neck-likeconnections' and lack of ballistoconidia in the species led to its reclassification as a member of the genus *Cryptococcus* (Phaff and Fell 1970). This was later disputed based on new molecular phylogenetic analyses which indicated a great distance between the species and other members of *Cryptococcus* (Takashima and Nakase 1999). In 2001, *Dioszegia* was reinstated and confirmed as a distinct genus based on phylogenetic analysis of the small subunit (SSU) rRNA genes. This finding allowed *D. hungarica* to re-join the genus along with two new combinations, *D. aurantiaca* and *D. crocea* (Takashima et al. 2001). Since then, the genus has expanded and now accommodates a total of 24 described species (Bai et al. 2002; Wang et al. 2003, 2008; Inácio et al. 2005; Connell et al. 2010; Takashima and Nakase 2011; Takashima et al. 2011; Trochine et al. 2017; Li et al. 2020; Maeng et al. 2022). A multi-gene

phylogeny placed the genus *Dioszegia* within the newly proposed family Bulleribasidiaceae of the order Tremellales (Liu et al. 2015).

Members of the genus *Dioszegia* share several characteristics that are helpful for phenotypic identification. They exhibit orange or orange-red colonies, polar budding, a non-fermentative nature, and possess co-enzyme Q-10 (Takashima et al. 2001; Takashima and Nakase 2011). Additionally, all known species have thus far only been documented in an asexual stage (Takashima et al. 2001; Wang et al. 2008; Takashima and Nakase 2011). Some species may also form ballistoconidia, hyphae, and poorly developed pseudohyphae (Connell et al. 2010; Li et al. 2020).

Members of *Dioszegia* have been increasingly studied for a wide array of biotechnological applications. The carotenoid-producing abilities of species such as *D. patagonica* and *D. takashimae* offer commercial potential for products such as pigments, nutritional supplements, and pharmaceuticals (Mannazzu et al. 2015). At low temperatures, *D. fristingensis* and *D. patagonica* can secrete extracellular enzymes such as amylase, esterase, pectinase, cellulase, and lipase, making them potential sources of industrially relevant cold-active enzymes (Carrasco et al. 2012; Trochine et al. 2017)

In the past two decades, there has been a flurry of taxonomic research elucidating the diversity of *Dioszegia* species in China. At present, 18 of the 24 accepted *Dioszegia* species have been reported in China, 10 of which were initially described in the country (*D. athyri*, *D. butyracea*, *D. changbaiensis*, *D. heilongjiangensis*, *D. kandeliae*, *D. maotaiensis*, *D. milinica*, *D. ovata*, *D. xingshanensis*, and *D. zsoltii*). The remaining eight species were first documented in other countries (*D. thyrium*, *D. aurantiaca*, *D. butyracea*, *D. cream*, *D. fristingensis*, *D. hungarica*, *D. statzelliae*, *D. takashimae*, and *D. zsoltii*) (Bai et al. 2002; Wang et al. 2003, 2008; Li et al. 2020). There is still much to learn about the *Dioszegia* diversity and distribution in China and beyond. Our recent investigations revealed three new species over two years. This paper aims to employ an integrative taxonomic approach for the delimitation and description of these new taxa, providing a foundation for future investigations of *Dioszegia*.

Materials and methods

Sample collection and yeast isolation

Leaf samples were collected in the Guiyang Medicinal Botanical Garden (26°53'72"N, 106°70'52"E) and Baotianman Nature Reserve (33°30'44"N, 111°55'47"E) in China. The Guiyang Medicinal Botanical Garden is located in the city of Guiyang in the Yunnan Province of southwest China. With more than 1200 kinds of medicinal plants, it is known as the natural medicine valley. The local climate in this botanical garden is warm winters and fresh and cool summers, with annual mean temperatures around 15.3 °C. The Baotianman Nature Reserve, located in the Henan Province of central China, measures 4,285 ha. With a forest coverage rate of 98%, it is classified as World Biosphere Reserve by the United Nations Educational, Scientific and Cultural Organization (UNESCO). The reserve encompasses a virgin forest with more than 2000 species of vascular plants. The local climate is typical of a transitional climate from northern subtropical zone to warm temperate zone, with cold dry winters, and fresh rainy summers. The annual mean temperature is 15.1 °C.

Yeast strains were isolated from leaf surfaces using the improved ballisto-spore-fall method as described by Nakase and Takashima (1993). In brief, vaseline was employed to affix fresh and healthy leaves to the inside lids of Petri dishes containing yeast extract-malt extract (YM) agar (0.3% yeast extract, 0.3% malt extract, 0.5% peptone, 1% glucose, and 2% agar). Plates were then incubated at 20 °C until visible colonies had formed. Colonies with different morphotypes were selected and streaked onto additional YM agar plates for purification. After purification, strains were suspended in YM broth supplemented with 20% (v/v) glycerol and stored at −80 °C for future use. All obtained isolates were preserved at the Microbiology Lab, Nanyang Normal University, Henan, China.

Morphological and physiological characterization

Phenotypic and physiological characteristics of each yeast isolate were examined using the methods established by Kurtzman et al. (2011). Cell morphology was examined using a Leica DM2500 microscope (Leica Microsystems GmbH, Wetzlar, Germany) equipped with a Leica DFC295 digital microscope color camera under bright field, phase contrast, and differential interference contrast (DIC) conditions. Sexual cycles were investigated for both individual and paired strains on potato dextrose agar (PDA) (20% potato infusion, 2% glucose, and 1.5% agar), corn meal (CM) agar, and yeast carbon base plus 0.01% ammonium sulphate (YCBS) agar for two months and observed at weekly intervals (Li et al. 2020). Ballistoconidium-forming activity was investigated using the inverted-plate method (do Carmo-Sousa and Phaff 1962) after two weeks of incubation on CM agar at 20 °C. Glucose fermentation was observed using Durham fermentation tubes with a liquid medium. Carbon and nitrogen assimilation tests were conducted in a liquid medium, with starved inoculum employed for the latter (Kurtzman et al. 2011). Growth at various temperatures (15, 20, 25, 30, 35, and 37 °C) was determined by cultivation on YM agar. All novel taxonomic descriptions and proposed names were deposited in the MycoBank database (Robert et al. 2013).

DNA extraction, PCR amplification, and sequencing

Genomic DNA was extracted from each yeast strain using the Ezup Column Yeast Genomic DNA Purification Kit according to the manufacturer's instructions (Sangon Biotech Co., Shanghai, China). The ITS region and the D1/D2 domain of the LSU rRNA gene were amplified using primer sets ITS1/ITS4 (White et al. 1990) and NL1/NL4 (Kurtzman and Robnett 1998), respectively. Amplifications were performed in a 25 μL reaction- tube containing 9.5 μL ddH$_2$O, 12.5 μL 2× Taq PCR Master Mix with blue dye (Sangon Biotech Co., Shanghai, China), 1 μL DNA template, and 1 μL of each primer. Amplifications were conducted with the following parameters: initial denaturation at 95 °C for 2 min, followed by 35 cycles of 95 ° for C 30 s, 51 °C for 30 s, 72 °C for 40 s, and a final extension at 72 °C for 10 min (Wang et al. 2014). PCR products were purified and sequenced using the same primers by Sangon Biotech Co., Ltd (Shanghai, China). The identity and accuracy of the newly obtained sequences were determined by comparison to GenBank (Sayers et al. 2022) entries. Sequence assembly was conducted using BioEdit v. 7.1.3.0 (Hall 1999). All generated sequences were submitted to GenBank and their corresponding accession numbers are listed in Table 1.

Table 1. Taxon names, strain numbers, and GenBank accession numbers used for phylogenetic analyses. Entries in bold were newly generated for this study.

Taxa name	Strain number	GenBank accession numbers	
		ITS	LSU D1/D2
Bulleribasidium begoniae	CBS 10762[T]	NR_154878	NG_058707
Bulleribasidium foliicola	CBS 11407[T]	KY101801	NG_058708
Bulleribasidium hainanense	CBS 11409[T]	NR_154879	NG_058709
Bulleribasidium oberjochense	CBS 9110[T]	NR_121467	NG_042388
Bulleribasidium panici	CBS 9932[T]	NR_121293	NG_058710
Bulleribasidium pseudovariabile	CBS 9609[T]	NR_111085	NG_042393
Bulleribasidium sanyaense	CBS 11408[T]	NR_159742	GQ438831
Bulleribasidium setariae	CBS 10763[T]	NR_154880	NG_058610
Bulleribasidium siamensis	CBS 9933[T]	NR_144773	AY188388
Bulleribasidium variabile	CBS 7347[T]	NR_111058	AF189855
Bulleribasidium wuzhishanense	CBS 11411[T]	NR_153643	GQ438830
***Dioszegia aurantia* sp. nov.**	**NYNU 229189[T]**	**OP566892**	**OP566893**
Dioszegia aurantia sp. nov.	G.M. 2006-09-03.6 951	OP419710	OP419710
Dioszegia anctarctica	CBS 10920 [T]	NR_159813	FJ640575
Dioszegia athyri	CBS 10119[T]	EU070926	EU070931
Dioszegia aurantiaca	CBS 6980 [T]	NR_155060	NG_059153
Dioszegia buhagiarii	CBS 10054[T]	NR_073346	NG_059154
Dioszegia butyracea	CBS 10122 [T]	KY103348	KY107637
Dioszegia catarinonii	CBS 10051[T]	NR_155061	NG_059155
Dioszegia changbaiensis	CBS 9608[T]	NR_136964	NG_059069
Dioszegia crocea	CBS 6714[T]	NR_155062	KY107640
Dioszegia cryoxerica	CBS 10919[T]	FJ640565	FJ640562
Dioszegia dumuzii	CBS 12501[T]	LT548261	LT548261
***Dioszegia foliicola* sp. nov.**	**NYUN 229182[T]**	**OP566887**	**OP566888**
***Dioszegia foliicola* sp. nov.**	**NYNU 229188**	**OP566890**	**OP566889**
***Dioszegia foliicola* sp. nov.**	**NYNU 2211140**	**OR863956**	**OR863957**
Dioszegia fristingensis	CBS 10052 [T]	NR_136970	NG_070549
***Dioszegia guizhouensis* sp. nov.**	**NYNU 22985[T]**	**OP566883**	**OP566880**
***Dioszegia guizhouensis* sp. nov.**	**NYUN 229195**	**OP566896**	**OP581919**
Dioszegia heilongjiangensis	CGMCC 2.5674[T]	NR_174736	MK050291
Dioszegia hungarica	CBS 4214[T]	NR_073227	NG_042350
Dioszegia kandeliae	CGMCC 2.5658[T]	NR_174739	MK050296
Dioszegia maotaiensis	CGMCC 2.4537[T]	NR_174738	MK050295
Dioszegia milinica	CGMCC2.5628[T]	MK050290	NR_174735
Dioszegia ovata	CGMCC 2.3625[T]	NR_174737	MK050294
Dioszegia patagonica	CBS 14901[T]	NR_158412	NG_088008
Dioszegia rishiriensis	CBS 11844[T]	NR_157461	NG_059156
Dioszegia statzelliae	CBS 8925[T]	AY029342	AY029341
Dioszegia takashimae	CBS 10053 [T]	NR_136971	AY562149
Dioszegia terrae	KCTC 27998 [T]	MZ734406	MZ734403
Dioszegia xingshanensis	CBS 10120[T]	KY103359	KY107649

Taxa name	Strain number	GenBank accession numbers	
		ITS	LSU D1/D2
Dioszegia zsoltii var. *yunnanensis*	CBS 9128[T]	NR_156190	NG_070550
Dioszegia zsoltii var. *zsoltii*	CBS 9127[T]	AF385445	NG_059157
Nielozyma formosana	CBS 10306 [T]	NR_154221	NG_058356
Nielozyma melastomae	CBS 10305[T]	NR_154221	AB119464
Sugitazyma miyagiana	CBS 7526[T]	NR_073237	AF189858

CBS, CBS-KNAW Collections, Westerdijk Fungal Biodiversity Institute, Utrecht, The Netherlands; CG-MCC, China General Microbiological Culture Collection Center, Beijing, China; KCTC, Korea Collection for Type Cultures, KRIBB, Korea; NYNU, Microbiology Lab, Nanyang Normal University, Henan, China; [T,] type strain. Species obtained in this study are in bold.

Phylogenetic analysis

Phylogenetic analyses employed a total of 92 nucleotide sequences, including 12 novel sequences generated in this study. The remaining sequences were obtained from previous studies (Li et al. 2020; Maeng et al. 2022) and GenBank (Table 1). *Sugitazyma miyagiana* CBS 7526[T] was used as the outgroup. Phylogenetic relationships between the new *Dioszegia* species and their close relatives were determined using a combined ITS and LSU sequence dataset. Sequences of individual markers were aligned with either Clustal X v. 1.83 (Thompson et al. 1997) or MAFFT v. 7.110 (Katoh and Standley 2013) using default settings. Aligned sequences of the different markers were concatenated with PhyloSuite v. 1.2.2 (Zhang et al. 2020). Alignments were improved through manual gap adjustments. Ambiguously aligned regions were excluded prior to analysis.

Phylogenetic analyses were conducted employing both maximum likelihood (ML) and Bayesian inference (BI). ML was determined with 1,000 searches on RAxML v. 8.2.3 (Stamatakis 2014) and ML bootstrap values (MLBS) were assessed through 1,000 rapid bootstrap replicates using the GTRCAT model. For BI, ModelFinder (Kalyaanamoorthy et al. 2017) was used to determine the optimal substitution model to fit the DNA evolution. BI data was analysed with MrBayes v. 3.2.7a (Ronquist et al. 2012) through the CIPRES Science Gateway version 3.3. Best-fit evolution models for the ITS and LSU partitions were GTR+I+G. Six simultaneous Markov chains were run for 50 million generations with trees being sampled every 1,000[th] generation. The first 25% of created sample trees were discarded as the burn-in phase of analysis. The remaining trees were used to infer Bayesian posterior probabilities (BPP) for the clades.

The resulting trees were viewed in FigTree v. 1.4.3 (Andrew 2016) and processed with Adobe Illustrator CS5. Branches that received MLBS ≥ 50% and BPP ≥ 0.95 were considered significantly supported.

Results

Molecular phylogeny

This study presents the discovery of three novel *Dioszegia* species represented by six strains isolated from leaf samples in the provinces of Guizhou and Henan (Table 2). The combined ITS and LSU sequence data was utilized to elucidate the phylogenetic positions of the new species. 120 aligned positions

Table 2. Strains representing the novel species described in this study and relevant information associated to them.

Strain	Source	Location
Dioszegia guizhouensis sp. nov.		
NYNU 22985[T]	Leaf of *Schisandra* sp.	Guiyang Medicinal Botanical Garden, Guiyang, Guizhou Province, China
NYUN 229195	Leaf of *Mussaendae* sp.	Guiyang Medicinal Botanical Garden, Guiyang, Guizhou Province, China
Dioszegia foliicola sp. nov.		
NYUN 229182[T]	Leaf of *Salvia* sp.	Guiyang Medicinal Botanical Garden, Guiyang, Guizhou Province, China
NYNU 229188	Leaf of *Broussonetia papyrifera*	Guiyang Medicinal Botanical Garden, Guiyang, Guizhou Province, China
NYNU 2211140	Leaf from an unidentified tree	Baotianman Nature Reserve, Nanyang, Henan Province, China
Dioszegia aurantia sp. nov.		
NYNU 229189[T]	Leaf of *Cornus officinalis*	Guiyang Medicinal Botanical Garden, Guiyang, Guizhou Province, China

were excluded from the alignment due to problematic homology assessment. This final dataset consisted of 997 characters, 588 from ITS and 409 from LSU. Among these, 604 were constant and 393 were variable, out of which 292 were parsimony-informative. Finally, 101 were singletons. The topology of the ML and Bayesian trees was consistent with each other, and only the ML tree is shown (Fig. 1). The five strains isolated in this study formed three strongly supported groups (100% MLBS/1 BPP), distinct from other known species of *Dioszegia*.

The strains NYUN 22985 and NYUN 229195 had similar sequences with only one nt difference in the ITS region, suggesting that they belong to the same species. Two strains in the NYUN 22985 group formed a separate branch on the phylogenetic tree (Fig. 1), forming a clade with *D. hungarica*, the *Dioszegia* type species, and 15 other known species with strong support (100 MLBS/1 BPP). BLASTn searches of the D1/D2 and ITS sequences indicated that *D. hungarica* is the closet relative, differing by four nt (~0.7%) substitutions in the D1D2 domain and 14−15 nt (~2.9−3.1%) mismatches in the ITS region. The NYUN 22985 group is considered a distinct *Dioszegia* species based on the basidiomycetous yeast species threshold (Fell et al. 2000; Vu et al. 2016), which suggests that strains differing by two or more nucleotide substitutions in the D1/D2 domains or exhibiting 1−2% nucleotide differences in the ITS regions may represent different taxa. Therefore, *D. guizhouensis* sp. nov. is proposed as a novel *Dioszegia* species to accommodate the strains.

Three strains, viz. NYNU 229182, NYNU 229188, and 2211140, possessed mutually similar sequences with three nt differences in the D1/D2 region and one in the ITS region, indicating conspecificity. Additionally, the NYNU 229182 group shared similar D1/D2 sequences (one to two nt differences) with the GenBank isolate WOct07D (2)-Y3 (GQ352531) identified as '*Dioszegia zsoltii*', suggesting another conspecific relationship. BLASTn searches of the D1/D2 sequences indicated that this group was most closely related to *D. maotaiensis* and *D. terrae*, differing by 10−11 nt (~1.7−1.8%) substitutions in the D1/D2 domain and more than 27 nt (5.4%) mismatches in ITS region. Thus, the group represents a novel *Dioszegia* species, for which the name *D. foliicola* sp. nov. is proposed.

Strain NYNU 229189 grouped with G.M.2006-09-03.6951 (OP419710), an unpublished strain obtained from the bark of rotting branches collected in
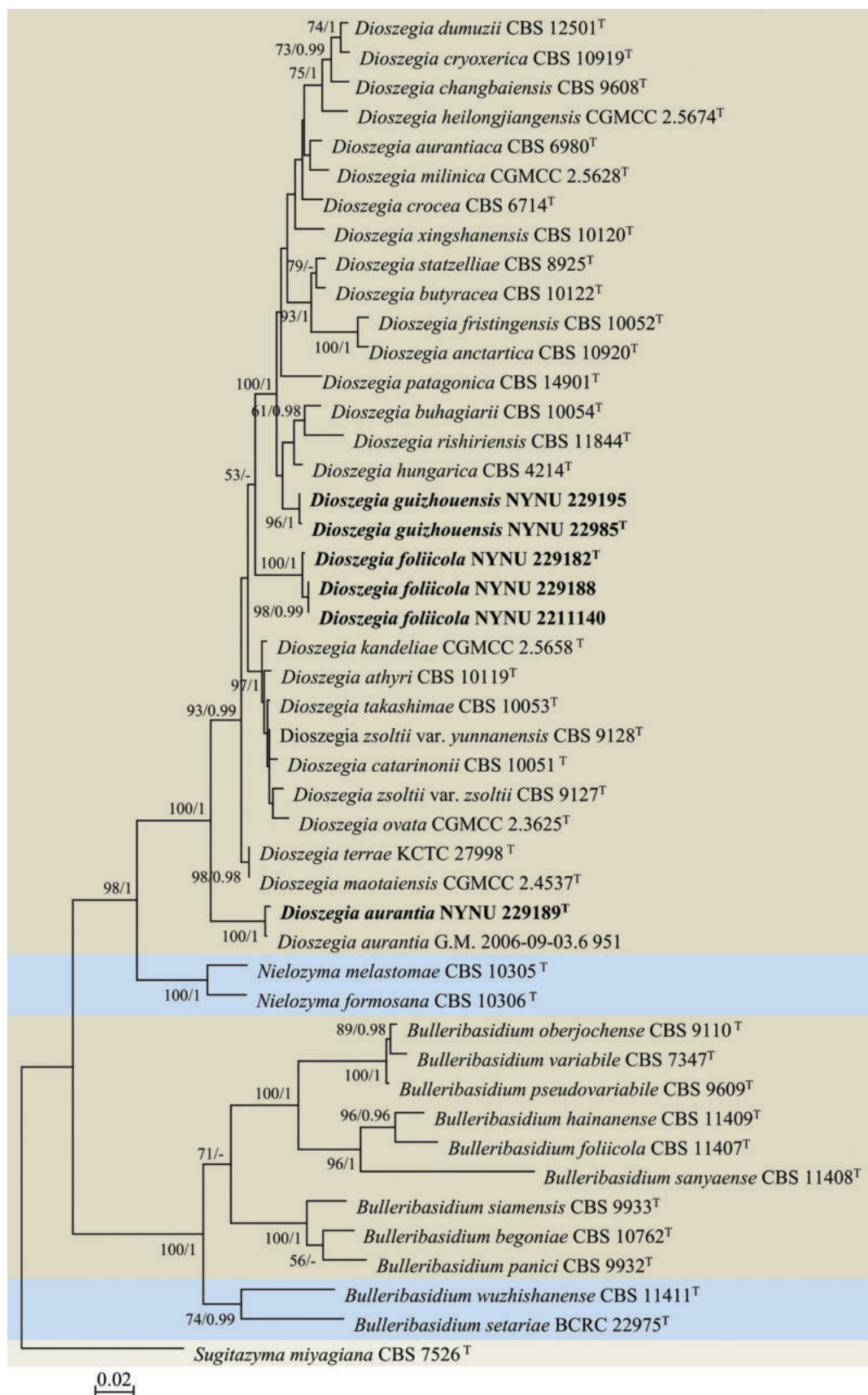
Figure 1. Maximum likelihood (ML) phylogram of *Dioszegia* species and close relatives based on combined ITS and LSU sequence data. *Sugitazyma miyagiana* CBS 7526[T] serves as the outgroup. Branches are labelled with MLBS ≥ 50% and BPP ≥ 0.95. Novel strains are highlighted in bold.

Australia, which jointly were placed as a separate branch as the sister clade to the remaining part of of *Dioszegia* (Fig. 1). The two strains differed by only two and four nt differences in the D1/D2 and ITS region, respectively, suggesting conspecificity. NYNU 229189 is closely related to *D. maotaiensis* and *D. terrae*, differing from the latter two by 16 nt (~2.7%) substitutions in the D1/D2 domain and more than 23 nt (~5.7%) mismatches in the ITS region. This suggests that NYNU 229189 represents a new *Dioszegia* species, for which the name *D. aurantia* sp. nov. is proposed.

Taxonomy

Dioszegia guizhouensis Y.Z. Qiao & F.L. Hui, sp. nov.
MycoBank No: 851291
Fig. 2A

Etymology. The specific epithet *guizhouensis* refers to the geographic origin of the type strain, Guizhou province.

Typus. China, Guizhou Province, Guiyang City, Guiyang Botanical Garden, in the phylloplane of *Schisandra* sp., September 2022, L. Zhang and F.L. Hui, NYUN 22985 (holotype GDMCC 2.311^T preserved as a metabolically inactive state, culture ex-type PYCC 9938).

Description. On YM agar, after 7 days at 20 °C, the streak culture is pink to orange, butyrous, smooth. The margin is entire. On YM agar, after 7 days at 20 °C, cells are ovoid and ellipsoidal, 2.8−4.6 × 4.1−6.8 µm and single, budding is polar. After 1 month at 20 °C, a ring and sediment are present. In Dalmau plate culture on corn meal agar, hyphae and pseudohyphae are not formed. Sexual structures are not observed for individual strains and strain pairs on PDA, CM agar, and YCBS agar for two months. Ballistoconidia are not produced on CM agar after two weeks at 20 °C. Glucose fermentation is absent. Glucose, sucrose, raffinose, melibiose, galactose, trehalose, maltose, melezitose, cellobiose, salicin, L-sorbose (delayed), L-rhamnose, D-xylose, L-arabinose, D-arabinose, 5-keto-D-gluconate (weak), D-ribose, galactitol, D-mannitol, D-glucitol, succinate (weak), citrate, D-gluconate, N-acetyl-D-glucosamine, 2-keto-D-gluconate, D-glucuronate, and glucono-1,5-lactone are assimilated as carbon sources. Inulin, lactose, methyl-α-D-glucoside, methanol, ethanol, glycerol, erythritol, ribitol, myo-inositol, DL-lactate, and D-glucosamine are not assimilated. Nitrite is assimilated as the sole nitrogen source. Nitrate, ethylamine, L-lysine, and cadaverine are not assimilated. Maximum growth temperature is 30 °C. Growth in vitamin-free medium is positive. Starch-like substances are produced. Urease activity is positive. Diazonium Blue B reaction is positive.

Additional strain examined. China, Guizhou Province, Guiyang City, Guiyang Botanical Garden, in the phylloplane of *Mussaendae* sp., September 2022, L. Zhang and F.L. Hui, NYUN 229195.

GenBank accession numbers. Holotype NYUN 22985^T (ITS: OP566883, D1/D2: OP566880); additional strain 229195 (ITS: OP566896, D1/D2: OP581919).

Note. *Dioszegia guizhouensis* sp. nov. can be physiologically differentiated from its closest known species *D. hungarica* (Takashima and Nakase 2011) by its inability to assimilate D-glucosamine, its ability to assimilate melibiose and L-sorbose, and its capacity to grow in vitamin-free medium and at 30 °C.

Dioszegia foliicola Y.Z. Qiao & F.L. Hui, sp. nov.

MycoBank No: 851294

Fig. 2B

Etymology. The specific epithet *foliicola* refers to the type strain isolated from a leaf.

Typus. CHINA, Guizhou Province, Guiyang City, Guiyang Botanical Garden, in the phylloplane of *Salvia* sp., September 2022, L. Zhang and F.L. Hui, NYUN 229182 (holotype GDMCC 2.316^T preserved as a metabolically inactive state, culture ex-type PYCC 9939 and CICC 33571).

Description. On YM agar, after 7 days at 20 °C, the streak culture is orange, butyrous, smooth. The margin is entire. On YM agar, after 7 days at 20 °C, cells are ovoid and ellipsoidal, 3.9–4.8 × 4.8–7.9 μm and single, budding is polar. After 1 month at 20 °C, a ring and sediment are present. In Dalmau plate culture on corn meal agar, hyphae and pseudohyphae are not formed. Sexual structures are not observed for individual strains and strain pairs on PDA, CM agar and YCBS agar for two months. Ballistoconidia are not produced on CM agar after two weeks at 20 °C. Glucose fermentation is absent. Glucose, sucrose, raffinose, melibiose, galactose, trehalose, maltose, melezitose, methyl-α-D-glucoside, cellobiose, salicin, L-sorbose, L-rhamnose, D-xylose, L-arabinose, D-arabinose, 5-keto-D-gluconate, D-ribose, galactitol, D-mannitol, succinate, D-gluconate, N-acetyl-D-glucosamine, 2-keto-D-gluconate and D-glucuronate are assimilated as carbon sources. Inulin, lactose, methanol, ethanol, glycerol, erythritol, ribitol, D-glucitol, myo-inositol, DL-lactate, citrate, D-glucosamine, and glucono-1,5-lactone are not assimilated. Nitrite and L-lysine are assimilated as nitrogen sources. Nitrate, ethylamine, and cadaverine are not assimilated. Maximum growth temperature is 30 °C. Growth in vitamin-free medium is positive. Starch-like substances are produced. Urease activity is positive. Diazonium Blue B reaction is positive.

Additional strain examined. CHINA, Guizhou Province, Guiyang City, Guiyang Botanical Garden, in the phylloplane of *Broussonetia papyrifera*, September 2022, L. Zhang and F.L. Hui, NYUN 229188 and China, Henan Province, Nanyang City, Baotianman Nature Reserve, in the phylloplane from an unidentified tree, October 2022, J.Z. Li, NYUN 2211140.

GenBank accession numbers. Holotype GDMCC 2.316^T (ITS: OP566887, D1/D2: OP566888); additional strains NYUN 229188 (ITS: OP566890, D1/D2: OP566889) and NYUN 2211140 (ITS: OR863956, D1/D2: OR863957).

Note. *Dioszegia foliicola* sp. nov. can be physiologically differentiated from its closest known species *D. maotaiensis* (Li et al. 2020) by its inability to assimilate inulin and citrate, its ability to assimilate methyl-α-D-glucoside, salicin, L-sorbose, D-ribose, galactitol, and D-mannitol, and its capacity to grow at 30 °C.

Dioszegia aurantia Y.Z. Qiao & F.L. Hui, sp. nov.

MycoBank No: 851296

Fig. 2C

Etymology. The specific epithet *aurantia* refers to the *aurantiaca* colony morphology.

Typus. CHINA, Guizhou Province, Guiyang City, Guiyang Botanical Garden, in the phylloplane of *Cornus officinalis*, September 2022, L. Zhang and F.L. Hui,
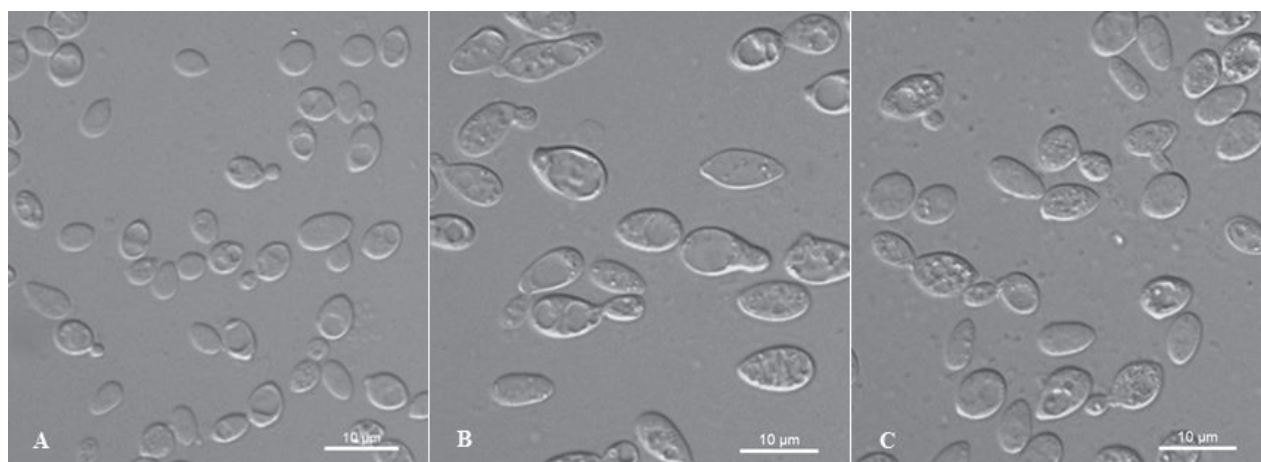
Figure 2. Vegetative cells of *Dioszegia guizhouensis* sp. nov. NYNU 22985^T (**A**), *Dioszegia foliicola* sp. nov. NYUN 229182^T (**B**), and *Dioszegia aurantia* sp. nov. NYNU 229189^T (**C**) following growth in YM broth for 7 days at 20 °C. Scale bars: 10 μm.

NYUN 229189 (holotype GDMCC 2.335^T preserved as a metabolically inactive state, culture ex-type PYCC 9937 and CICC 33572).

Description. On YM agar, after 7 days at 20 °C, the streak culture is orange, butyrous, smooth. The margin is entire. On YM agar, after 7 days at 20 °C, cells are ovoid and ellipsoidal, 4.6–5.0 × 5.0–8.2 μm and single, budding is polar. After 1 month at 20 °C, a ring and sediment are present. In Dalmau plate culture on corn meal agar, hyphae and pseudohyphae are not formed. Sexual structures are not observed for individual strains and strain pairs on PDA, CM agar, and YCBS agar for two months. Ballistoconidia are not produced on CM agar after two weeks at 20 °C. Glucose fermentation is absent. Glucose, inulin, sucrose, raffinose, melibiose, galactose, trehalose, maltose, melezitose, methyl-α-D-glucoside (delayed), cellobiose, salicin (weak), L-sorbose (delayed), L-rhamnose (delayed and weak), D-xylose, L-arabinose, D-arabinose (weak), 5-keto-D-gluconate, D-ribose, galactitol, D-mannitol, D-glucitol, succinate (weak), N-acetyl-D-glucosamine, 2-keto-D-gluconate (delayed and weak), and D-glucuronate are assimilated as carbon sources. Lactose, methanol, ethanol, glycerol, erythritol, ribitol, myo-inositol, DL-lactate, citrate, D-gluconate, D-glucosamine, and glucono-1,5-lactone are not assimilated. Nitrite (delayed) and L-lysine (delayed and weak) are assimilated as nitrogen sources. Nitrate, ethylamine, and cadaverine are not assimilated. Maximum growth temperature is 25 °C. Growth in vitamin-free medium is negative. Starch-like substances are produced. Urease activity is positive. Diazonium Blue B reaction is positive.

GenBank accession numbers. Holotype GDMCC 2.335^T (ITS: OP566892, D1/D2: OP566893).

Note. *Dioszegia aurantia* sp. nov. can be physiologically differentiated from its closest known species *D. maotaiensis* (Li et al. 2020) by its inability to assimilate citrate, its ability to assimilate methyl-α-D-glucoside, salicin, L-sorbose, D-ribose, D-mannitol, D-glucitol, and N-acetyl-D-glucosamine, and its capacity to grow in vitamin-free medium and at 30 °C.

Discussion

In this study, we present three novel *Dioszegia* species discovered in China: *D. guizhouensis* sp. nov., *D. foliicola* sp. nov., and *D. aurantia* sp. nov. This work

provides a comprehensive description of each species based on molecular analyses and morphological examinations. Moreover, our phylogenetic analyses illustrate clear distinctions between each new species and other members of *Dioszegia*, which was confirmed as a monophyletic genus in a strongly supported clade (Fig. 1). Pairwise sequence comparisons of the D1/D2 domain and the ITS region of the novel species and their close relatives support species differentiation based on the common threshold applied to basidiomycetous yeasts (Fell et al. 2000; Vu et al. 2016). The new species were highly similar in cell shape, colony morphology, and color, but differed from closely related species in terms of physiological and biochemical characteristics. Therefore, the results of our molecular phylogenetic analyses and phenotypic examinations support the description of three new *Dioszegia* species.

Several new species have been added to *Dioszegia* recently (Li et al. 2020; Maeng et al. 2022). Notably, our phylogenetic analyses revealed that the recently described species *D. terrae* clustered with *D. maotaiensis* in a well-supported clade within *Dioszegia* (Fig. 1). *D. maotaiensis* was described first and the description of *D. terrae* seminly overlooked the previously validly described species *D. maotaiensis*. These two species had only one nt difference in the ITS region, suggesting that *D. terrae* is a synonym of *D. maotaiensis*. Consequently, 26 species, including three new species described in the present study, are currently included in the genus *Dioszegia*.

Members of the genus *Dioszegia* are widely distributed across a variety of habitats. Although isolates are commonly obtained as epiphytic phylloplane fungi in temperate and subtropical climate regions (Inácio et al. 2005; Wang et al. 2008; Li et al. 2020), previous studies have also collected samples from roots (Renker et al. 2004) and soil (Takashima et al. 2011; Maeng et al. 2022). Additionally, isolates have also been collected from cold substrates such as snow (Trochine et al. 2017), glacial melt (de García et al. 2007; Trochine et al. 2017), and polar desert soil (Connell et al. 2010). In this study, six strains of three new *Dioszegia* species share with most other species in the genus association with plant leaves. The results further confirm that the natural distribution of *Dioszegia* species in the phylloplane is common. Furthermore, strain WOct07D (2)-Y3 (GQ352531), identified as '*Dioszegia zsoltii*' from USA, is conspecific with *D. foliicola* sp. nov., while strain G.M.2006-09-03.6951 (OP419710) from Australia is conspecific with *D. aurantia* sp. nov. These observations suggests that the two new species *D. foliicola* sp. nov. and *D. aurantia* sp. nov. may be broadly distributed outside of China. Indeed, further large-scale studies are needed to explore the diversity and distribution of *Dioszegia* species worldwide. *D. fristingensis* is a versatile extremophilic species that has been frequently found in plants inhabiting hyper-arid, alkaline, and hypersaline environments (Abu-Ghosh et al. 2014; Wei et al. 2022), implying that this species may help plants survive in dry areas. We also isolated six strains of three novel *Dioszegia* species—*D. guizhouensis* sp. nov., *D. foliicola* sp. nov., and *D. aurantia* sp. nov.—from plant leaves, and it is possible that these species provide similar ecological functions benefits to their hosts as does *D. fristingensis*.

Many *Dioszegia* species have adapted to tolerate challenges presented by their environments. Notably, more than 10 *Dioszegia* species are known to accumulate mycosporin-glutamine-glucoside (MGG), a UVB-absorbing molecule that acts in response to photostimulation (Trochine et al. 2017). *D. patagonica*

even contains higher levels of MGG than *Phaffia rhodozyma*, which is recognized for its ability to endure UV-B radiation (Madhour et al. 2005; Libkind et al. 2009). Further exploration of *Dioszegia* diversity is necessary to determine whether MGG is associated with other taxonomic traits or influences UV radiation tolerance (Libkind et al. 2009).

Acknowledgments

Additional information

Conflict of interest

The authors have declared that no competing interests exist.

Ethical statement

No ethical statement was reported.

Funding

Author contributions

Data curation: YZQ. Methodology: YZQ, SL. Molecular phylogeny: YZQ, QHN. Writing – original draft: YZQ. Writing – review and editing: QHN, FLH. All authors read and approved the final manuscript.

Author ORCIDs

Ya-Zhuo Qiao https://orcid.org/0009-0000-9074-2443
Shan Liu https://orcid.org/0009-0003-2845-1495
Qiu-Hong Niu https://orcid.org/0000-0003-1695-7117
Feng-Li Hui https://orcid.org/0000-0001-7928-3055

Data availability

All of the data that support the findings of this study are available in the main text or Supplementary Information.

References

Abu-Ghosh S, Droby S, Korine C (2014) Seasonal and plant-dependent variations in diversity, abundance and stress tolerance of epiphytic yeasts in desert habitats. Environmental Microbiology Reports 6(4): 373–382. https://doi.org/10.1111/1758-2229.12161

Andrew R (2016) FigTree: Tree figure drawing tool Version 1.4.3. Institute of Evolutionary Biology, University of Edinburgh Press, United Kingdom.

Bai FY, Takashima M, Jia JH, Nakase T (2002) *Dioszegia zsoltii* sp. nov., a new ballistoco-nidium-forming yeast species with two varieties. The Journal of General and Applied Microbiology 48(1): 17–23. https://doi.org/10.2323/jgam.48.17

Carrasco M, Rozas JM, Barahona S, Alcaíno J, Cifuentes V, Baeza M (2012) Diversity and extracellular enzymatic activities of yeasts isolated from King George Island, the sub-Antarctic region. BMC Microbiology 12(1): e251. https://doi.org/10.1186/1471-2180-12-251

Connell LB, Redman R, Rodriguez R, Barrett A, Iszard M, Fonseca A (2010) *Dioszegia antarctica* sp. nov. and *Dioszegia cryoxerica* sp. nov., psychrophilic basidiomycetous yeasts from polar desert soils in Antarctica. International Journal of Systematic and Evolutionary Microbiology 60(Pt 6): 1466–1472. https://doi.org/10.1099/ijs.0.015412-0

de García V, Brizzio S, Libkind D, Buzzini P, van Broock M (2007) Biodiversity of cold-adapted yeasts from glacial meltwater rivers in Patagonia, Argentina. FEMS Microbiology Ecology 59(2): 331–241. https://doi.org/10.1111/j.1574-6941.2006.00239.x

do Carmo-Sousa L, Phaff HJ (1962) An improved method for the detection of spore discharge in the Sporobolomycetaceae. Journal of Bacteriology 83(2): 434–435. https://doi.org/10.1128/jb.83.2.434-435.1962

Fell JW, Boekhout T, Fonseca A, Scorzetti G, Statzell-Tallman A (2000) Biodiversity and systematics of basidiomycetous yeasts as determined by large-subunit rDNA D1/D2 domain sequence analysis. International Journal of Systematic and Evolutionary Microbiology 50(Pt 3): 1351–1371. https://doi.org/10.1099/00207713-50-3-1351

Hall TA (1999) Bioedit: A user-friendly biological sequence alignment editor and analysis program for Windows 95/98/NT. Nucleic Acids Symposium Series 41: 95–98.

Inácio J, Portugal L, Spencer-Martins I, Fonseca A (2005) Phylloplane yeasts from Portugal: Seven novel anamorphic species in the Tremellales lineage of the Hymenomycetes (Basidiomycota) producing orange-coloured colonies. FEMS Yeast Research 5(12): 1167–1183. https://doi.org/10.1016/j.femsyr.2005.05.007

Kalyaanamoorthy S, Minh BQ, Wong TKF, Von Haeseler A, Jermiin LS (2017) Modelfinder: Fast model selection for accurate phylogenetic estimates. Nature Methods 14(6): 587–589. https://doi.org/10.1038/nmeth.4285

Katoh K, Standley DM (2013) MAFFT multiple sequence alignment software version 7: Improvements in performance and usability. Molecular Biology and Evolution 30(4): 772–780. https://doi.org/10.1093/molbev/mst010

Kurtzman CP, Robnett CJ (1998) Identification and phylogeny of ascomycetous yeasts from analysis of nuclear large subunit (26S) ribosomal DNA partial sequences. Antonie van Leeuwenhoek 73(4): 331–371. https://doi.org/10.1023/A:1001761008817

Kurtzman CP, Fell JW, Boekhout T (2011). Methods for isolation, phenotypic characterization and maintenance of yeasts. In: Kurtzman CP, Fell JW, Boekhout T (Eds) The Yeasts – A Taxonomic Study (5th edn., Vol. 2). Amsterdam, Elsevier, 87–110. https://doi.org/10.1016/B978-0-444-52149-1.00007-0

Li AH, Yuan FX, Groenewald M, Bensch K, Yurkov AM, Li K, Han PJ, Guo LD, Aime MC, Sampaio JP, Jindamorakot S, Turchetti B, Inacio J, Fungsin B, Wang QM, Bai FY (2020) Diversity and phylogeny of basidiomycetous yeasts from plant leaves and soil: Proposal of two new orders, three new families, eight new genera and one hundred and seven new species. Studies in Mycology 96: 17–140. https://doi.org/10.1016/j.simyco.2020.01.002

Libkind D, Moliné M, Sampaio JP, van Broock M (2009) Yeasts from high-altitude lakes: Influence of UV radiation. FEMS Microbiology Ecology 69(3): 353–362. https://doi.org/10.1111/j.1574-6941.2009.00728.x

Liu XZ, Wang QM, Theelen B, Groenewald M, Bai FY, Boekhout T (2015) Phylogeny of tremellomycetous yeasts and related dimorphic and filamentous basidiomycetes reconstructed from multiple gene sequence analyses. Studies in Mycology 81(1): 1–26. https://doi.org/10.1016/j.simyco.2015.08.001

Madhour A, Anke H, Mucci A, Davoli P, Weber RW (2005) Biosynthesis of the xanthophyll plectaniaxanthin as a stress response in the red yeast *Dioszegia* (Tremellales, Heterobasidiomycetes, Fungi). Phytochemistry 66(22): 617–626. https://doi.org/10.1016/j.phytochem.2005.09.010

Maeng S, Park Y, Sung GH, Lee HB, Kim MK, Srinivasan S (2022) Description of *Vishniacozyma terrae* sp. nov. and *Dioszegia terrae* sp. nov., two novel basidiomycetous yeast species isolated from soil in Korea. Mycobiology 50(6): 439–447. https://doi.org/10.1080/12298093.2022.2147135

Mannazzu I, Landolfo S, da Silva TL, Buzzini P (2015) Red yeasts and carotenoid production: Outlining a future for nonconventional yeasts of biotechnological interest. World Journal of Microbiology & Biotechnology 31(11): 1665–1673. https://doi.org/10.1007/s11274-015-1927-x

Nakase T, Takashima M (1993) A simple procedure for the high frequency isolation of new taxa of ballistosporous yeasts living on the surfaces of plants. RIKEN Review 3: 33–34.

Phaff HJ, Fell JW (1970) *Cryptococcus* Kutzing emend. Phaff et Spencer. In: Lodder J (Ed.) The Yeasts, A Taxonomic Study (2nd edn.). North-Holland, Amsterdam, 1088–1145.

Renker C, Blanke V, Börstler B, Heinrichs J, Buscot F (2004) Diversity of *Cryptococcus* and *Dioszegia* yeasts (Basidiomycota) inhabiting arbuscular mycorrhizal roots or spores. FEMS Yeast Research 4(6): 597–603. https://doi.org/10.1016/j.femsyr.2004.01.001

Robert V, Vu D, Amor AB, van de Wiele N, Brouwer C, Jabas B, Szoke S, Dridi A, Triki M, Ben Daoud S, Chouchen O, Vaas L, de Cock A, Stalpers JA, Stalpers D, Verkley GJ, Groenewald M, Dos Santos FB, Stegehuis G, Li W, Wu L, Zhang R, Ma J, Zhou M, Gorjón SP, Eurwilaichitr L, Ingsriswang S, Hansen K, Schoch C, Robbertse B, Irinyi L, Meyer W, Cardinali G, Hawksworth DL, Taylor JW, Crous PW (2013) MycoBank gearing up for new horizons. IMA Fungus 4(2): 371–379. https://doi.org/10.5598/imafungus.2013.04.02.16

Ronquist F, Teslenko M, van der Mark P, Ayres DL, Darling A, Höhna S, Larget B, Liu L, Suchard MA, Huelsenbeck JP (2012) MrBayes 3.2: Efficient Bayesian phylogenetic inference and model choice, across a large model space. Systematic Biology 61(3): 539–542. https://doi.org/10.1093/sysbio/sys029

Sayers EW, O'Sullivan C, Karsch-Mizrachi I (2022) Using GenBank and SRA. Methods in Molecular Biology (Clifton, N.J.) 2443: 1–25. https://doi.org/10.1007/978-1-0716-2067-0_1

Stamatakis A (2014) RAxML Version 8: A tool for phylogenetic analyses and post analyses of large phylogenies. Bioinformatics 30(9): 1312–1313. https://doi.org/10.1093/bioinformatics/btu033

Takashima M, Nakase T (1999) Molecular phylogeny of the genus *Cryptococcus* and related species based on the sequences of 18S rDNA and internal transcribed spacer regions. Microbiology and Culture Collections 15: 35–47.

Takashima M, Nakase T (2011) *Dioszegia* Zsolt emend. Takashima, Deák & Nakase (2001). In: Kurtzman CP, Fell JW, Boekhout T (Eds) The Yeasts – A Taxonomic Study

(5th edn., Vol. 2). Elsevier, Amsterdam, 1747–1757. https://doi.org/10.1016/B978-0-444-52149-1.00141-5

Takashima M, Deak T, Nakase T (2001) Emendation of *Dioszegia* with redescription of *Dioszegia hungarica* and two new combinations, *Dioszegia aurantiaca* and *Dioszegia crocea*. The Journal of General and Applied Microbiology 47(2): 75–84. https://doi.org/10.2323/jgam.47.75

Takashima M, Van BH, An KD, Ohkuma M (2011) *Dioszegia rishiriensis* sp. nov., a novel yeast species from soil collected on Rishiri Island, Hokkaido, Japan. International Journal of Systematic and Evolutionary Microbiology 61(Pt 7): 1736–1739. https://doi.org/10.1099/ijs.0.025254-0

Thompson JD, Gibson TJ, Plewniak F, Jeanmougin F, Higgins DG (1997) The CLUSTAL_X windows interface: Flexible strategies for multiple sequence alignment aided by quality analysis tools. Nucleic Acids Research 25(24): 4876–4882. https://doi.org/10.1093/nar/25.24.4876

Trochine A, Turchetti B, Vaz ABM, Brandao L, Rosa LH, Buzzini P, Rosa C, Libkind D (2017) Description of *Dioszegia patagonica* sp. nov., a novel carotenogenic yeast isolated from cold environments. International Journal of Systematic and Evolutionary Microbiology 67(Pt 11): 4332–4339. https://doi.org/10.1099/ijsem.0.002211

Vu D, Groenewald M, Szöke S, Cardinali G, Eberhardt U, Stielow B, de Vries M, Verkleij GJ, Crous PW, Boekhout T, Robert V (2016) DNA barcoding analysis of more than 9 000 yeast isolates contributes to quantitative thresholds for yeast species and genera delimitation. Studies in Mycology 85(1): 91–105. https://doi.org/10.1016/j.simyco.2016.11.007

Wang QM, Bai FY, Zhao JH, Jia JH (2003) *Dioszegia changbaiensis* sp. nov., a basidiomycetous yeast species isolated from northeast China. The Journal of General and Applied Microbiology 49(5): 295–299. https://doi.org/10.2323/jgam.49.295

Wang QM, Jia JH, Bai FY (2008) Diversity of basidiomycetous phylloplane yeasts belonging to the genus *Dioszegia* (Tremellales) and description of *Dioszegia athyri* sp. nov., *Dioszegia butyracea* sp. nov. and *Dioszegia xingshanensis* sp. nov. Antonie van Leeuwenhoek International Journal of General and Molecular Microbiology 93(4): 391–399. https://doi.org/10.1007/s10482-007-9216-9

Wang QM, Theelen B, Groenewald M, Bai FY, Boekhout T (2014) Moniliellomycetes and Malasseziomycetes, two new classes in Ustilaginomycotina. Persoonia 33(1): 41–47. https://doi.org/10.3767/003158514X682313

Wei XY, Zhu HY, Song L, Zhang RP, Li AH, Niu QH, Liu XZ, Bai FY (2022) Yeast diversity in the Qaidam Basin Desert in China with the description of five new yeast species. Journal of Fungi 8(8): e858. https://doi.org/10.3390/jof8080858

White TJ, Bruns T, Lee S, Taylor J (1990) Amplification and direct sequencing of fungal ribosomal RNA genes for phylogenetics. In: Innis MA, Gelfand DH, Sninsky JJ, White TJ (Eds) PCR Protocols: A Guide to Methods and Applications. Academic Press, New York, 315–322. https://doi.org/10.1016/B978-0-12-372180-8.50042-1

Zhang D, Gao F, Jakovlić I, Zou H, Zhang J, Li WX, Wang GT (2020) Phylosuite: An integrated and scalable desktop platform for streamlined molecular sequence data management and evolutionary phylogenetics studies. Molecular Ecology Resources 20(1): 348–355. https://doi.org/10.1111/1755-0998.13096

Zsolt J (1957) Egy új élesztö: *Dioszegia hungarica* nov. gen. et sp. Botanikai Közlemények 47(1–2): 63–66.

Supplementary material 1

Molecular data

Authors: Ya-Zhuo Qiao, Shan Liu, Qiu-Hong Niu, Feng-Li Hui

Data type: fas

Explanation note: A dataset of ITS and LSU for Fig. 1.

Copyright notice: This dataset is made available under the Open Database License (http://opendatacommons.org/licenses/odbl/1.0/). The Open Database License (ODbL) is a license agreement intended to allow users to freely share, modify, and use this Dataset while maintaining this same freedom for others, provided that the original source and author(s) are credited.

Link: https://doi.org/10.3897/mycokeys.101.117174.suppl1

MycoKeys

Morphology and multigene phylogeny reveal three new species of *Samsoniella* (Cordycipitaceae, Hypocreales) from spiders in China

Ting Wang[1,2] , Jun Li[1] , Xiaoyun Chang[1] , Zengzhi Li[1,3] , Nigel L. Hywel-Jones[3] ,
Bo Huang[1] , Mingjun Chen[1]

1   Anhui Provincial Key Laboratory for Microbial Pest Control, Anhui Agricultural University, Hefei 230036, China
2   Natural Resources and Planning Bureau of Bengbu City, Bengbu, Anhui 233000, China
3   Zhejiang BioAsia Institute of Life Sciences, 1938 Xinqun Road, Economic and Technological Development Zone, Pinghu, Zhejiang 314200, China
Corresponding authors: Bo Huang (bhuang@ahau.edu.cn); Mingjun Chen (mjchen@ahau.edu.cn)

Abstract

The genus *Samsoniella* was erected based on orange cylindrical to clavate stromata, superficial perithecia and conidiophores with *Isaria*-like phialides and to segregate them from the *Akanthomyces* group. In this study, based on morphological features and multigene (SSU, LSU, *TEF*, *RPB1* and *RPB2*) phylogenetic analysis six *Samsoniella* species parasitizing spiders were collected in China. Three of them belong to known species *S. alpina*, *S. erucae* and *S. hepiali*. Three new species *S. anhuiensis* **sp. nov.**, *S. aranea* **sp. nov.** and *S. fusiformispora* **sp. nov.** are illustrated and described. They are clearly distinct from other species in *Samsoniella* occurring in independent subclades. Furthermore, among the four insect-pathogenic fungi specimens collected from similar sites, three of them were identified as the new species described below. Our study significantly broadens the host range of *Samsoniella* from Insecta to Arachnida, marking a noteworthy expansion in understanding the ecological associations of these fungi. Additionally, the identification of both mononematous and synnematous conidiophores in our study not only expands the knowledge of *Samsoniella* species but also provides a basis for future research by comparing the ecological significance between these conidiophore types. In conclusion, our study enhances the understanding of *Samsoniella* diversity, presenting a refined phylogenetic framework and shedding light on the ecological roles of these fungi in spider parasitism.

Key words: Araneogenous fungi, *Isaria*-like, *Samsoniella*, taxonomy

Introduction

The genus *Isaria* Pers. was established by Persoon (1794) with *I. farinosa* (Pers.) Fr. as the type species (Hodge et al. 2005). *Isaria* is characterized by the formation of branched synnemata that give rise to flask-shaped phialides produced in whorls. For a considerable period, *Isaria* has been considered the asexual morph of *Cordyceps sensu stricto*, a classification within the family Cordycipitaceae, which encompasses numerous species featuring pallid or brightly pigmented, fleshy stromata (Sung et al. 2007; Maharachchikumbura et al. 2015). Samson (1974) transferred some species including *I. farinosa* to *Paecilomyces* Bainer

(1907). However, Hodge et al. (2005), based on morphological and molecular phylogenetic studies, moved *Paecilomyces farinosa* back to *Isaria* re-establishing the type as *Isaria farinosa* (Holmsk.) Fr. Most of the insect-pathogenic mesophilic *Paecilomyces* species in sect. *Isarioidea* of Samson (1974) were transferred to *Isaria* (Luangsa-ard et al. 2004, 2005; Gams et al. 2005). Nonetheless, Kepler et al. (2017) proposed the rejection of the genus *Isaria* due to the polyphyletic distribution of *Isaria* species. Recently, molecular phylogenetic analysis, has shown that some *Isaria*-like fungi are distributed in the genus *Akanthomyces* of the family Cordycipitaceae, forming monophyletic branches and are closely related to the genus *Akanthomyces*. Mongkolsamrit et al. (2018) established this phylogenetic branch as a new genus *Samsoniella* Mongkols., Noisrip., Thanakitp., Spatafora & Luangsa-ard. They accommodated three species of Lepidoptera entomopathogenic fungi in the genus; *S. alboaurantia* (G. Sm.) Mongkolsamrit, *S. aurantia* Mongkolsamrit and *S. inthanonensis* Mongkolsamrit. The three species have orange cylindrical to clavate stromata, superficial perithecia and orange conidiophores with *Isaria*-like phialides and hyaline conidia.

Over the past seven years, there has been extensive research on the species diversity within the genus *Samsoniella*, possibly driven by the significant medical and ecological value associated with certain species in the genus. In a follow-up study, Wang et al. (2020a) documented nine new species within the genus *Samsoniella*. Specifically, *Paecilomyces hepiali* Chen, formerly misconstrued as the asexual counterpart of *Ophiocordyceps sinensis*, demonstrated the ability to produce *Isaria*-like phialides. The perplexing taxonomic status of *P. hepiali* prompted taxonomists to reconsider its classification. Wang et al. (2020a) determined that the most suitable systematic position for *P. hepiali* is within the genus *Samsoniella*. Consequently, they proposed the new taxonomic combination *S. hepiali* for this species. Subsequently, Chen et al. (2020) described three additional species of *Samsoniella*. Furthermore, phylogenetic analysis led to the repositioning of strains previously identified as *I. farinosa*. Notably, strains CBS 240.32 and CBS 262.58 were integrated into the genus *Samsoniella* and redesignated as *S. alboaurantia* (Mongkolsamrit et al. 2018; Chen et al. 2021). Similarly, strains OSC 111005 and OSC 111006 were reassigned to *S. farinosa* Wang (Wang et al. 2020b). More recently, Chen et al. (2021, 2022, 2023), Wang et al. (2022), Wang et al. (2023) and Crous et al. (2023) contributed descriptions of fifteen additional novel *Samsoniella* species. Consequently, the genus *Samsoniella* now comprises a total of thirty-one recognized species.

We carried out a series of surveys for spider pathogenic fungi in China. A total of seven spider cadavers infected by *Samsoniella* were collected and isolated. Based on morphological and molecular phylogenetic analyses, three were identified as *S. alpina*, *S. erucae*, and *S. hepiali*. However, the other four strains represented four new species, which are described here as *S. anhuiensis* sp. nov., *S. aranea* sp. nov. and *S. fusiformispora* sp. nov. Among the four insect-pathogenic fungi specimens collected from the same sites, three of them were identified as the new species described below. Our study enhances the understanding of *Samsoniella* diversity, presenting a refined phylogenetic framework and shedding light on the ecological roles of these fungi in spider parasitism.

Materials and methods

Sample collection, isolation and morphological observations

The majority of spider specimens infected by fungi were collected from all over China. Four specimens were collected from the Jingting Mountains National Forest Park, Anhui Province, southeastern China. Four specimens were collected from the Jinggang Mountains National Nature Reserve, Jiangxi Province, southeastern China. One specimen was collected from the Maiji National Forest Park, Gansu Province, northwestern China. One specimen was collected from the Yaoluoping National Forest Park, Anhui Province, southeastern China, and one specimen was collected from the Wanfo Mountains, Anhui Province, southeastern China. Several insect specimens infected by fungi were collected from sites similar to those where spider specimens were collected. The collections were noted and photographed in the field, then carefully deposited in plastic boxes and returned to the laboratory. Fungal cultures were isolated from fresh conidia or mycelia from spider cadavers. Pure cultures were established and incubated on fresh potato dextrose agar (PDA) plates and grown at 25 °C for 2 weeks. The fresh structures of specimens and isolated strains were mounted in water for measurements and lactophenol cotton blue solution for microphotography following Wang et al. (2020a). Features such as size and shape of conidia, colony color in culture, were made from squash mounts and sections made from fresh specimen and culture grown on oatmeal agar (OA, Difco), PDA and one quarter strength SDAY (SDAY/4, Difco) (Bischoff et al. 2009). The color of the cultures was characterized using the Naturalist's Color Guide (Smith 1975). Microscopic observations were made from squash mounts and sections made from fresh material using a ZEISS Axiolab 5 microscope. All samples and strains studied here were deposited in the Research Center for Entomogenous Fungi (RCEF) of Anhui Agricultural University.

DNA extraction, PCR amplification and sequencing

Total genomic DNA was extracted from cultured mycelia with CTAB method (Liu et al. 2001), then stored in -20 °C. Two gene regions, namely the small subunit ribosomal RNA (SSU) and large subunit ribosomal RNA (LSU) were sequenced from the cell nuclei, and three protein coding genes, translation elongation factor-1a (*TEF*) and the largest and second largest subunits of RNA polymerase II (*RPB1* and *RPB2*) were used in this study. The SSU and LSU were amplified with NS1/NS4 (White et al. 1990) and LROR (Vilgalys and Hester 1990)/LR7(Hopple 1994). The *TEF* with 983F/2218R (Rehner and Buckley 2005), *RPB1* with CRPB1/RPB1−Cr (Castlebury et al. 2004) and *RPB2* with fRPB2−7CR /fRPB2−5F (Liu et al. 1999) were amplified. PCR reactions of the five nuclear loci were carried out in 25 μL reaction mixture containing 12.5 μL 2× Taq Plus MasterMix (CoWin Biosciences, Beijing, China), 1 μL of each primer (10 μM), 1.5 μL of template DNA (1−2 ng) and 9 μL of sterile water. PCR cycle conditions were as previously described (Sung et al. 2007). PCR products were purified and sequenced by Sangon Company (Shanghai, China). The resulting sequences were checked manually, then submitted to GenBank.

Sequence alignment and phylogenetic analyses

The sequences in this study were uploaded to BLAST and searched in the GenBank database to determine probable taxa. DNA sequences generated in this study were assembled and edited using version 6.0. DNASTAR. Generated SSU, LSU, *TEF*, *RPB1* and *RPB2* sequences were aligned with those published by Chen et al. (2020) and Wang et al. (2020a) and others downloaded from Gen-Bank were used as a dataset of taxa in *Samsoniella* and closely related *Samsoniella* groups (Table 1). Sequences of the genus *Akanthomyces* (*A. aculeatus* HUA772 and HUA 186145) were chosen as the outgroup. Multiple sequence alignment was conducted with MAFFT 7.3.13 (Katoh and Standley 2013). The final sequence alignment of the combined dataset was used for analyses using Maximum Likelihood (ML) and Bayesian Inference (BI) to infer their phylogenetic relationships.

Phylogenetic inference was done according to Maximum Likelihood (ML) using RAxML version 8 (Stamatakis 2014) and Bayesian Inference (BI) using MrBayes v.3.2 (Ronquist et al. 2012). For the ML analysis, we used the GTR-CAT model for all partitions, in accordance with recommendations in the RAx-ML manual against the use of invariant sites and 1000 rapid bootstrap replicates. The GTR+I+G model was selected by MrModeltest 2.2 (Darriba et al. 2012) as the best nucleotide substitution model for the Bayesian analysis. Four MCMC chains were executed simultaneously for 2000,000 generations, sampling every 100 generations. Finally, phylogenetic trees were visualized using the Interactive Tree of Life (iTOL) (https://itol.embl.de) online tool (Letunic and Bork 2016).

Table 1. Species, strain numbers, accession numbers and origins of *Samsoniella* and related taxa used in this study, new sequences were shown in bold.

Species	Strain No.	GenBank accession No.				
		SSU	LSU	*TEF*	*RPB1*	*RPB2*
Akanthomyces aculeatus	HUA772	KC519368	KC519370	–	–	–
A. aculeatus	HUA186145[T]	MF416572	MF416520	MF416465	–	–
A. cf. *coccidioperitheciatus*	NHJ 5112	EU369109	EU369043	EU369026	EU369066	–
A. coccidioperitheciatus	NHJ 6709	EU369110	EU369042	EU369025	EU369067	EU369086
A. farinosa	CBS541.81	MF416606	MF416553	–	MF416655	–
A. lecanii	CBS101247	AF339604	AF339555	DQ522359	DQ522407	DQ522466
A. muscarius	CBS 143.62	KM283774	KM283798	KM283821	KM283841	KM283863
Beauveria bassiana	ARSEF1564[T]	–	–	HQ880974	HQ880833	HQ880905
B. brongniartii	ARSEF 617[T]	–	–	HQ880991	HQ880854	HQ880926
	BCC 16585	–	JF415967	JF416009	JN049885	JF415991
B. staphylinidicola	ARSEF 5718	EF468981	EF468836	EF468776	EF468881	–
Cordyceps farinosa	CBS111113	AY526474	MF416554	GQ250022	MF416656	GU979973
C. militaris	OSC 93623	AY184977	AY184966	DQ522332	DQ522377	AY545732
Isaria sp.	spat 09-050	MF416613	MF416559	MF416506	MF416663	MF416457
	spat 09-051	MF416614	MF416560	MF416507	MF416664	MF416458
Samsoniella alboaurantium	CBS 240.32	JF415958	JF415979	JF416019	JN049895	JF415999
	CBS 262.58	–	–	MF416497	MF416654	MF416448

Species	Strain No.	GenBank accession No.				
		SSU	LSU	*TEF*	*RPB1*	*RPB2*
S. alpina	YFCC 5818	MN576753	MN576809	MN576979	MN576869	MN576923
	YFCC 5831	MN576754	MN576810	MN576980	MN576870	MN576924
S. alpina	**RCEF0643**	–	–	**OM482385**	–	–
S. anhuiensis	**RCEF2830**	**OM268843**	**OM268848**	**OM483864**	**OM751889**	–
	RCEF2590	**OR978313**	**OR978316**	**OR966516**	**OR989964**	–
S. antleroides	YFCC 6016	MN576747	MN576803	MN576973	MN576863	MN576917
	YFCC 6113	MN576748	MN576804	MN576974	MN576864	MN576918
S. aranea	**RCEF2831**	**OM268844**	**OM268849**	**OM483865**	**OM751882**	**OM802500**
	RCEF2868	**OM268845**	**OM268850**	**OM483866**	**OM751883**	**OM802501**
	RCEF2870	**OR978314**	**OR978317**	**OR966517**	**OR989965**	**OR989966**
S. aurantia	TBRC 7271ᵀ	–	MF140728	MF140846	MF140791	MF140818
	TBRC 7273	–	–	MF140844	–	MF140816
S. cardinalis	YFCC5830	MN576732	MN576788	MN576958	MN576848	MN576902
	YFCC 6144	MN576730	MN576786	MN576956	MN576846	MN576900
S. cristata	YFCC6021	MN576735	MN576791	MN576961	MN576851	MN576905
	YFCC6023	MN576736	MN576792	MN576962	MN576852	MN576906
S. coccinellidicola	YFCC8772	ON563166	ON621670	ON676514	ON676502	ON568685
	YFCC8773	ON563167	ON621671	ON676515	ON676503	ON568686
S. coleopterorum	A19502	–	–	MT642602	MT642603	MN101587
S. duyunensis	DY09162	–	OQ363114	OQ398146	–	–
	DY07501	–	OR263307	OR282780	OR282773	OR282776
	DY07502	–	OR263427	OR282781	–	OR282777
S. erucae	KY11121	–	ON502835	ON525425	–	ON525424
	KY11122	–	ON502822	ON525427	–	ON525426
S. erucae	**RCEF2595**	**OM268842**	**OM268847**	**OM483863**	**OM751888**	–
	RCEF2592	–	–	**OR966518**	–	–
S. farinosa	OSC111005	DQ522558	DQ518773	DQ522348	DQ522394	–
	OSC111006	EF469127	EF469080	EF469065	EF469094	–
S. farinospora	YFCC8774	ON563168	ON621672	ON676516	ON676504	ON568687
	YFCC9051	ON563169	ON621673	ON676517	ON676505	ON568688
S. fusiformispora	**RCEF5406**	**OM268846**	**OM268851**	**OM483867**	**OM751890**	–
	RCEF2588	**OR978312**	**OR978315**	**OR966515**	–	–
S. guizhouensis	KY11161	–	ON502830	ON525429	–	ON525428
	KY11162	–	ON502846	ON525431	–	ON525430
S. haniana	YFCC8769	ON563170	ON621674	ON676518	ON676506	ON568689
	YFCC8770	ON563171	ON621675	ON676519	ON676507	ON568690
	YFCC8771	ON563172	ON621676	ON676520	ON676508	ON568691
S. hepiali	YFCC 5823	MN576745	MN576801	MN576971	MN576861	MN576915
	YFCC 5828	MN576744	MN576800	MN576970	MN576860	MN576914
S. hepiali	**RCEF1481**	**OL854202**	–	**OM482386**	–	–
S. hymenopterorum	A19521	–	–	MN101588	MT642603	MT642604
	A19522	–	–	MN101591	MN101589	MN101590
S. inthanonensis	TBRC 7915	–	MF140725	MF140849	MF140790	MF140815
S. kunmingensis	YHH16002	MN576746	MN576802	MN576972	MN576862	MN576916
S. lanmaoa	YFCC6148ᵀ	MN576733	MN576789	MN576959	MN576849	MN576903
	YFCC6193	MN576734	MN576790	MN576960	MN576850	MN576904

Species	Strain No.	GenBank accession No.				
		SSU	LSU	*TEF*	*RPB1*	*RPB2*
S. lepidopterorum	DL10071	–	–	MN101594	MN101592	MN101593
	DL10072	–	–	MT642606	–	MT642605
S. neopupicola	KY11321	–	ON502839	ON525433	–	ON525432
	KY11322	–	ON502833	ON525435	–	ON525434
S. pseudogunnii	GY407201	–	MZ827010	–	–	–
	GY407202	–	MZ831865	–	–	–
S. pseudotortricidae	YFCC9052	ON563173	ON621677	ON676521	ON676509	ON568692
	YFCC9053	ON563174	ON621678	ON676522	ON676510	ON568693
S. pupicola	DY101681	–	MZ827009	MZ855231	–	MZ855237
	DY101682	–	MZ827635	MZ855232	–	MZ855238
S. ramosa	YFCC6020^T	MN576749	MN576805	MN576975	MN576865	MN576919
S. sinensis	YFCC8766	ON563175	ON621679	ON676523	ON676511	ON568694
	YFCC8767	ON563176	ON621680	ON676524	ON676512	ON568695
	YFCC8768	ON563177	ON621681	ON676525	ON676513	ON568696
S. tiankengensis	KY11741	–	ON502838	ON525437	–	ON525436
	KY11742	–	ON502841	ON525439	–	ON525438
S. tortricidae	YFCC6013	MN576751	MN576807	MN576977	MN576867	MN576921
	YFCC6131	MN576750	MN576806	MN576976	MN576866	MN576920
S. vallis	DY07241	–	OR263306	OR282778	OR282772	OR282774
	DY07242	–	OR263308	OR282779	–	OR282775
	DY091091	–	OR263428	OR282782	–	–
	DY091092	–	OR263431	OR282783	–	–
S. winandae	TBRC17511	–	OM491231	OM687896	OM687901	OM687899
S. winande	TBRC17512	–	OM491232	OM687897	OM687902	OM687900
S. yunnanensis	YFCC 1527	MN576756	MN576812	MN576982	MN576872	MN576926
	YFCC 1824	MN576757	MN576813	MN576983	MN576873	MN576927

Boldface: data generated in this study.

Results

Phylogenetic analysis

To determine the phylogenetic relationship between these fungi and allied species from NCBI we constructed a phylogenetic tree based on Maximum Likelihood (ML) and Bayesian analysis, based on concatenated sequences of five genes included 89 taxa, comprising 4491 characters (SSU: 1047bp, LSU: 849 bp, *TEF*: 945bp, *RPB1*: 717 bp, *RPB2*: 933bp). The multi-gene phylogenetic tree consisted of four genera belonging to the family Cordycipitaceae, including *Akanthomyces*, *Beauveria*, *Cordyceps* and *Samsoniella*, with strong support (100%). Statistical support (≥75%/0.75) is shown at the nodes for ML bootstrap support/BI posterior probabilities and the strains' numbers are noted after each species' name (Fig. 1).

In the phylogenetic tree, *Samsoniella* species clustered in a clade easily distinguished from species of *Akanthomyces sensu stricto*, *Beauveria* and *Cordyceps*. Within the *Samsoniella* clade, the majority of *Samsoniella* species grouped together, while only two strains, named as *S. lepidopterorum*, formed a separate branch with a relatively far genetic distance. Furthermore, the
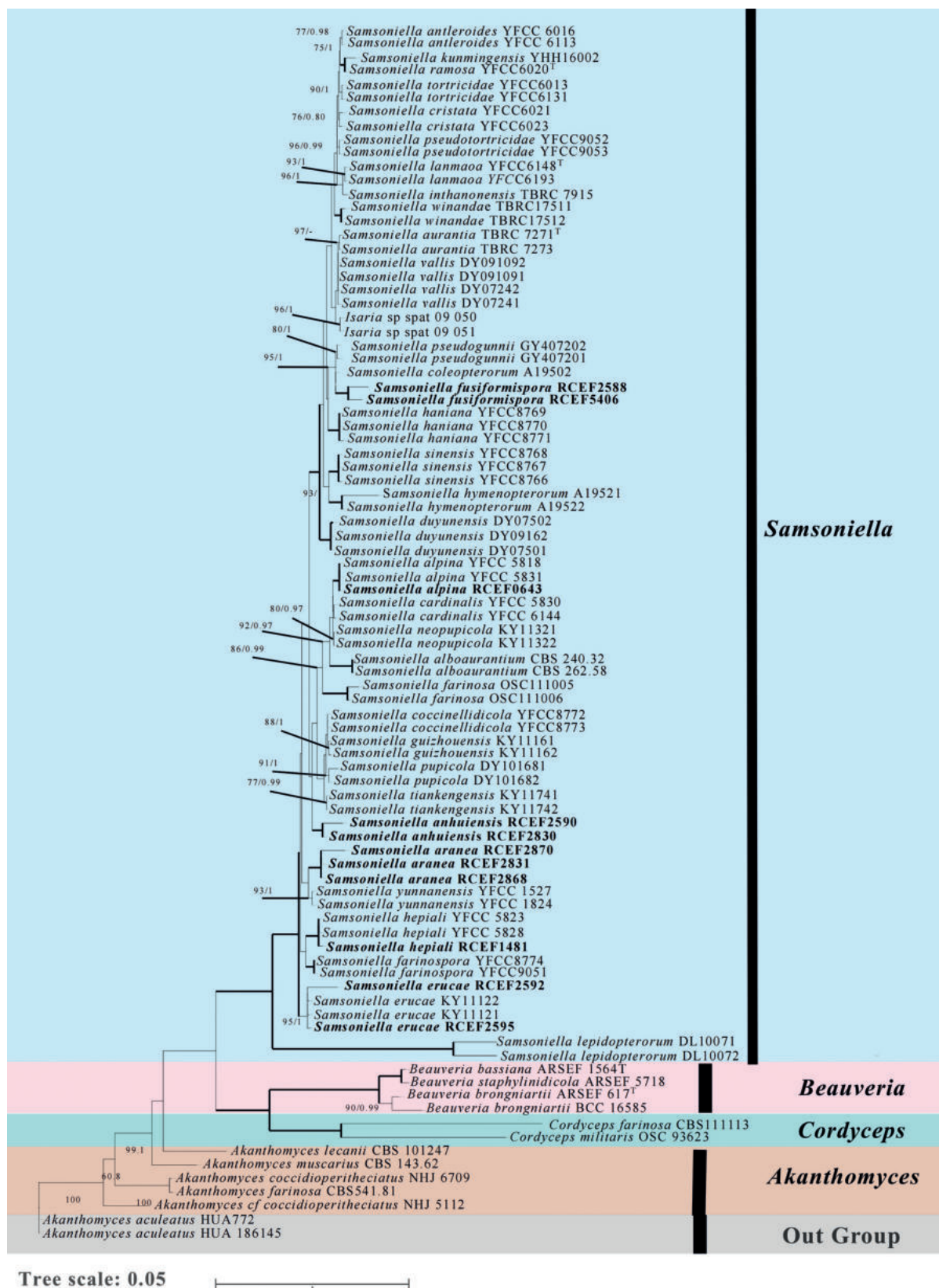
Figure 1. Phylogenetic relationships between the genus *Samsoniella* and closely-related species, based on multigene dataset (SSU, LSU, *TEF*, *RPB1* and *RPB2*) for maximum likelihood/ Bayesian method. Note: The ML tree presented here, and the node support rate of the two methods is displayed on the branches. The maximum likelihood support values / Bayesian posterior probabilities value (≥75%/0.75) are shown, and bold lines mean support for the two analyses were 98%. The typical strain of the species is marked with the superscript "T"

seven spider- pathogenic strains (RCEF 0643, RCEF 1481, RCEF 2831, RCEF 2868, RCEF 2588, RCEF 2830, RCEF 2595) and four insect- pathogenic strains (RCEF2590, RCEF 2592, RCEF 2870, RCEF 5406) in this study are located on different branches of the *Samsoniella* clade. Strains RCEF 0643 and *S. alpina* were clustered in the same branch (MLBP=98, PP=1.00). Strain RCEF 2592 and RCEF 2595 were grouped with *S. erucae* clade (MLBP=95,PP=1.00). Strain RCEF 1481 was clustered in the same clade with *S. hepiali* (MLBP=100,PP=1.00). However, another seven strains formed three independent branches. *S. fusiformispora* (RCEF 5406 and RCEF 2588) formed a monophyletic group which closely clustered with *S. hymenopterorum* and *S. farinosa* with high bootstrap values. *S. aranea* (RCEF 2831 RCEF 2868, and RCEF 2870) clustered in an independent branch, which was phylogenetically close to *S. yunnanensis* (MLBP=100,PP=1.00). *S. anhuiensis* (RCEF 2830 and RCEF 2590) formed an independent sister branch with high support(MLBP=97, PP=0.97). Five-gene phylogenetic analyses suggested that RCEF 0643, RCEF 1481, RCEF 2592, and RCEF 2595 were known species. However, the other seven strains were three new species in *Samsoniella*.

Taxonomy

Samsoniella anhuiensis T. Wang, Ming J. Chen & B. Huang, sp. nov.
MycoBank No: 849801
Fig. 2

Etymology. Named after the location Anhui Province where the species was originally collected.

Typification. CHINA. Anhui Province: Xuancheng City, the Jingting Mountains National Forest Park, on a spider attached to a leaf, 15 March 2006, Mingjun Chen & Xueqiu Zhao, holotype XC20060315-06. Sequences from strain RCEF2830 and RCEF2590 have been submitted to GenBank with accession numbers. RCEF2830: SSU = OM268844; LSU = OM268849; *TEF* = OM483865; *RPB1* = OM751889. RCEF2590: SSU = OR978313; LSU = OR978316; *TEF* = OR966516; *RPB1* = OR989964.

Description. *Sexual morph*: Undetermined. *Asexual morph*: *Isaria*-like. Synnemata arising from the whole body of spider, white, flexuous, multiple, fleshy, up to 12 mm long, with terminal branched, white conidia produced from the branches of synnemata, powdery and floccose (Fig. 2A). Conidiophores arising from the aerial and prostrate hyphae, solitary and verticillate. Phialides in whorls of 2–5, 5.0–15.2 × 1.5–2.3 µm, smooth-walled, with basal portion swollen to ellipsoidal, tapering into a distinct neck, 1.8–5.2 × 0.8–1.2 µm. Conidia in chains, spherical to elliptical, aseptate, hyaline, 2.1–3.2 × 1.3–2.2 µm.

Culture characteristics. Colonies on 1/4 SDAY, attaining a diam 38–42 mm in 14 d at 25 °C. Colonies white, with smooth and neat edge, with high mycelial density at the centrum (Fig. 2B). Reverse pale yellow to yellowish, appears flesh pink at 30 d. Hyphae smooth, septate, hyaline, 1.5–2.3 µm width. Erect conidiophores usually arising from aerial hyphae, with phialides in whorls of two to three or occasionally with solitary phialides along the hyphae. Phialides basal portion cylindrical, tapering to a distinct neck, 4.8–16.0 µm long, 1.4–2.0 µm
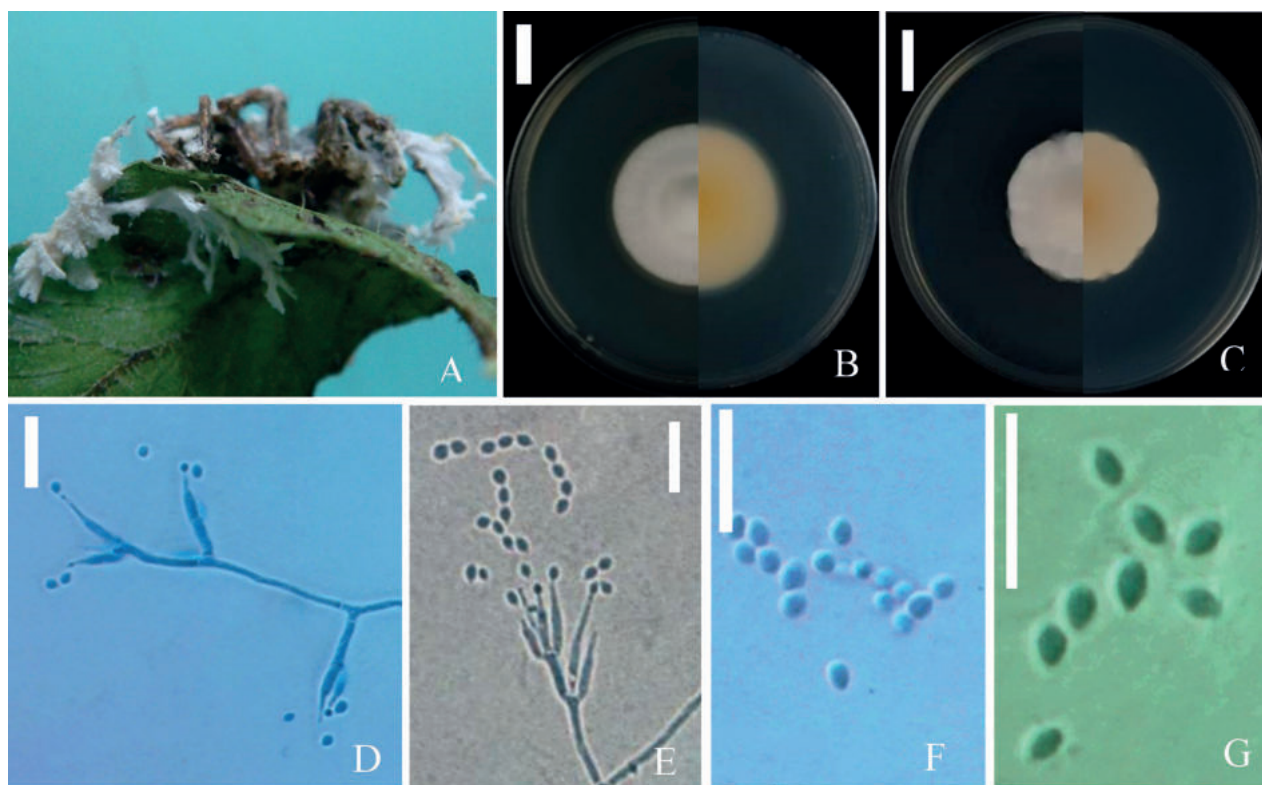
Figure 2. *Samsoniella anhuiensis* **A** fungus on spider **B** colony on SDAY/4 **C** colony on PDA **D, F** conidiophores structure and conidia on SDAY/4 **E, G** conidiophores structure and conidia on PDA. Scale bars: 15 mm (**B, C**); 10 µm (**D–G**).

basal width and 0.6–1.0 µm distinct neck width. Conidia in (Fig. 2D), smooth-walled, hyaline, spherical to elliptical, ovoid, occasionally pointed at both ends, 2.4–3.2 × 1.5–2.1 µm (Fig. 2F). Chlamydospores and synnemata not observed.

Colonies on PDA, 39–41mm diameter in 14 d at 25 °C, white. The central part of the colony is raised and appears light yellowish (Fig. 2C). Reverse yellowish in the center. Hyphae smooth, septate, hyaline, with septum and branches, 1.5–2.8 µm width, with phialides in whorls of two to five. Phialides basal portion cylindrical, tapering to a distinct neck, (7-)8–11.5(-13) µm long, 1.3–2.2 µm basal width and 0.5–0.8 µm distinct neck width (Fig. 2E). Conidia in chains, 1-celled, smooth-walled, hyaline, fusiform, elliptical, to obovate, 2–3(-3.5) × 1–2.5 µm (Fig. 2G).

Habitat. Occurring on spider attached to the upperside of tree leaf.

Notes. *Samsoniella anhuiensis* was easily identified as belonging to *Samsoniella* based on the phylogenetic analyses (Fig. 1). Based on the combined multigene dataset, *S. anhuiensis* has an independent branch and has a close relationship with *S. tiankengensis*. However, colonies of *S. tiankengensis* exhibit a faster growth rate on PDA compared to *S. anhuiensis*, displaying white to light pink colonies with a light yellowish reverse. In contrast, colonies of *S. anhuiensis* appear light yellowish and take on a flesh-pink hue at 30 days on 1/4 SDAY, with a yellowish center in reverse. Notably, *S. anhuiensis* distinguishes itself from S. tiankengensis through the presence of larger spherical, elliptical to ovoid conidia (Table 2).

Table 2. Morphological comparison of three new species with other related *Samsoniella* species (Wang et al. 2022).

Species	Synnemata (mm)	Conidiophores (µm)	Colony growth rate (mm)(14d, 25 °C)	Phialide	Phialides size (µm)	Conidia (µm)	Hosts/ substrates	Reference
				Morphological characteristics				
S. anhuiensis	white, flexuous, multiple, fleshy, up to 12, with terminal branched	-	39−41	verticillate, in whorls of 2 to 5	8.0−11.5 × 1.3−2.2, wide (apex) 0.5−0.8, basal portion cylindrical to narrowly lageniform	Fusiform, spherical, to obovate 2.0−3.5 × 1.0−2.5	spider	this study
S. alpina	irregularly branched, 3−20 long, cylindrical or clavate stipes with white powdery heads	3.1−6.5 × 1.6−2.8	up to 40	verticillate on conidiophores, solitary or verticillate on hyphae	4.7−9.5 × 1.9−3.1, wide (apex) 0.5−1.1, basal portion cylindrical to narrowly lageniform	fusiform or oval 2.0−3.1 × 1.3−2.1	larvae of *Hepialus baimaensis*	Wang et al. 2020a
S. aranea	Synnemata not observed	-	34.5−36	verticillate, in whorls of 2 to 4	6.9−11.2 × 1.4−1.9, wide (apex) 0.5−0.9, basal portion cylindrical to narrowly lageniform	elliptical, fusiform 1.9−3.4 × 1.2−2.4	spider	this study
S. coleopterorum	Synnemata not observed	-	36−40	verticillate, in whorls of 2 to 4	5.4−9.7 × 1.2−1.8, a cylindrical to ellipsoidal basal portion	fusiform, ellipsoidal or subglobose 1.7−2.5 × 1.2−1.8	Snout beetle Curculionidae	Chen et al. 2020
S. erucae	branched or unbranched, fleshy	-	46−48	solitary or in groups of three	6.8−13.7 × 1.1−1.5 with a cylindrical or ellipsoidal basal portion and tapered into a short, distinct neck	fusiform to ellipsoidal 2.3−2.9 × 1.1−1.5	caterpillar Lepidoptera	Chen et al. 2022
S. fusiformispora	multiple, unbranched, 2−3 long	-	36.5−39	verticillate, in whorls of 2 to 5	7.4−16.0 × 1.3−1.9, wide (apex) 0.5−1.0, basal portion cylindrical to narrowly lageniform	fusiform 1.9−3.4 × 1.2−2.4	spider	this study
S. hepiali	branched or unbranched, 5−41long	4.0−7.6 × 1.4−2.2	50−55	verticillate, in whorls of 2 to 5, solitary or opposite on hyphae	3.5−13.6 × 1.3−2.1, wide (apex) 0.5−1.0, basal portion cylindrical to narrowly lageniform	fusiform or oval 1.8−3.3 × 1.4−2.2	larvae of *Hepialus armoricanus*	Wang et al. 2020a
S. tiankengensis	branched or unbranched, fleshy	-	53−56	solitary or in groups of four	5.4−10.4 × 1.3−2.2, cylindrical or subellipsoidal basal portion and tapered into a short, distinct neck	ellipsoidal 2.3−2.8 × 1.6−1.8	pupa of Lepidoptera	Chen et al. 2022
S. yunnanensis	gregarious, flexuous, fleshy, 4.0−18.0 long, with terminal branches of 3−7 × 1.0−2.0	4.2−23.5 × 1.4−2.3	48−50	verticillate, in whorls of 2 to 7, usually solitary on hyphae	4.5−11.6 × 1.2−2.4, wide (apex) 0.6−1.0, basal portion cylindrical to narrowly lageniform	fusiform or oval 2.0−3.3 × 1.1−2.2	pupa of Limacodidae	Wang et al. 2020a

Samsoniella aranea T. Wang, Ming J. Chen & B. Huang, sp. nov.

MycoBank No: 849800

Fig. 3

Etymology. Referring to its host, spider, family Araneae.

Typification. China. Anhui Province: Xuancheng City, the Jingting Mountains National Forest Park, on spiders, in the litter layer, 15 March 2006 and 27 April 2006, Mingjun Chen & Xueqiu Zhao, holotype XC20060427-06, ex-holotype XC20060315-12. Sequences from strains RCEF2868, RCEF2831 and RCEF 2870 have been submitted to GenBank with accession numbers: RCEF2868: SSU = OM268846; LSU = OM268851; *TEF* = OM483867; *RPB1* = OM751883; *RPB2* = OM802501. RCEF2831: SSU = OM268845; LSU = OM268850; *TEF* = OM483866; *RPB1* = OM751882; *RPB2* = OM802500. RCEF 2870: SSU = OR978314; LSU = O978317; *TEF* = OR966517; *RPB1* = OR989965; *RPB2* = OR989966.

Description. *Sexual morph*: Undetermined. ***Asexual morph*:** *Isaria*-like. Mycellium on the spider consisting of white, smooth, branched, septate, 1.6−2.5 µm diam hyphae (Fig. 3A). Conidiophores solitary, arising from superficial hyphae, smooth, cylindrical, flexuous. Phialides verticillate, in whorl of 2−4, 5.0−12.6 × 1.2−2.3 µm, with basal portion swollen to ellipsoidal, tapering into a distinct neck, 4.0−6.0 × 0.8−1.0µm. Conidia in chains, fusiform, aseptate, hyaline, 2.1−3.6 × 1.5−2.4 µm.

Culture characteristics. Colonies on 1/4 SDAY, attaining a diam of 34.5−41.0 mm in 14 d at 25 °C, floccose, colonies white to cream-yellowish, with white smooth and neat edge (Fig. 3B), reverse light yellowish, sporulating abundantly. Hyphae smooth-walled, branched, hyaline, septate, 1.5−2.3 µm wide. Conidiophores smooth-walled, cylindrical, verticillate, 4.8−16.0 × 1.4−2.0 µm. Phialides in whorls of two to four, usually solitary on hyphae, basal portion cylindrical, tapering to a distinct neck; 5.1−16.9 µm long, 1.3−2.1 µm wide at the base, and 0.5−1.0 µm wide at the apex (Fig. 3D). Conidia in chains, smooth-walled, hyaline, elliptical, occasionally fusiform, 1.9−3.5 × 1.4−2.6 µm (Fig. 3G). Chlamydospores and synnemata not observed.

Colonies on PDA, attaining a diam of 34.5−36 mm in 14 d at 25 °C, floccose, colonies white to cream-yellowish, with a white smooth and neat edge, forming radial folds from the center outwards (Fig. 3C). Reverse yolk yellowish, sporulating abundantly. Hyphae smooth walled, branched, hyaline, septate, 1.5−2.6 µm wide. Conidiophores smooth − walled, cylindrical, verticillate. Phialides in whorls of two to four, usually solitary on hyphae, basal portion cylindrical, tapering to a distinct neck; 6.9−11.2 µm long, 1.4−1.9 µm wide at the base, and 0.5−0.9µm wide at the apex (Fig. 3E). Conidia 1-celled, in chains, smooth-walled, hyaline, elliptical, occasionally fusiform, 1.9−3.4 × 1.2−2.4 µm (Fig. 3F).

Habitat. Occurring on spiders in the litter layer.

Notes. *Samsoniella aranea* was readily classified within the genus *Samsoniella* through phylogenetic analyses (Fig. 1). Analysis of the combined multigene dataset unveiled that *S. aranea* forms an independent branch and shares a close relationship with *S. yunnanensis*. However, notable distinctions were observed between the two species. Unlike *S. yunnanensis*, where synnemata arise from insect cocoons, synnemata of *S. aranea* were not observed. Additionally, distinct growth characteristics were noted, with colonies of *S. yunnanensis* exhibiting a faster growth rate on PDA compared to *S. aranea*.
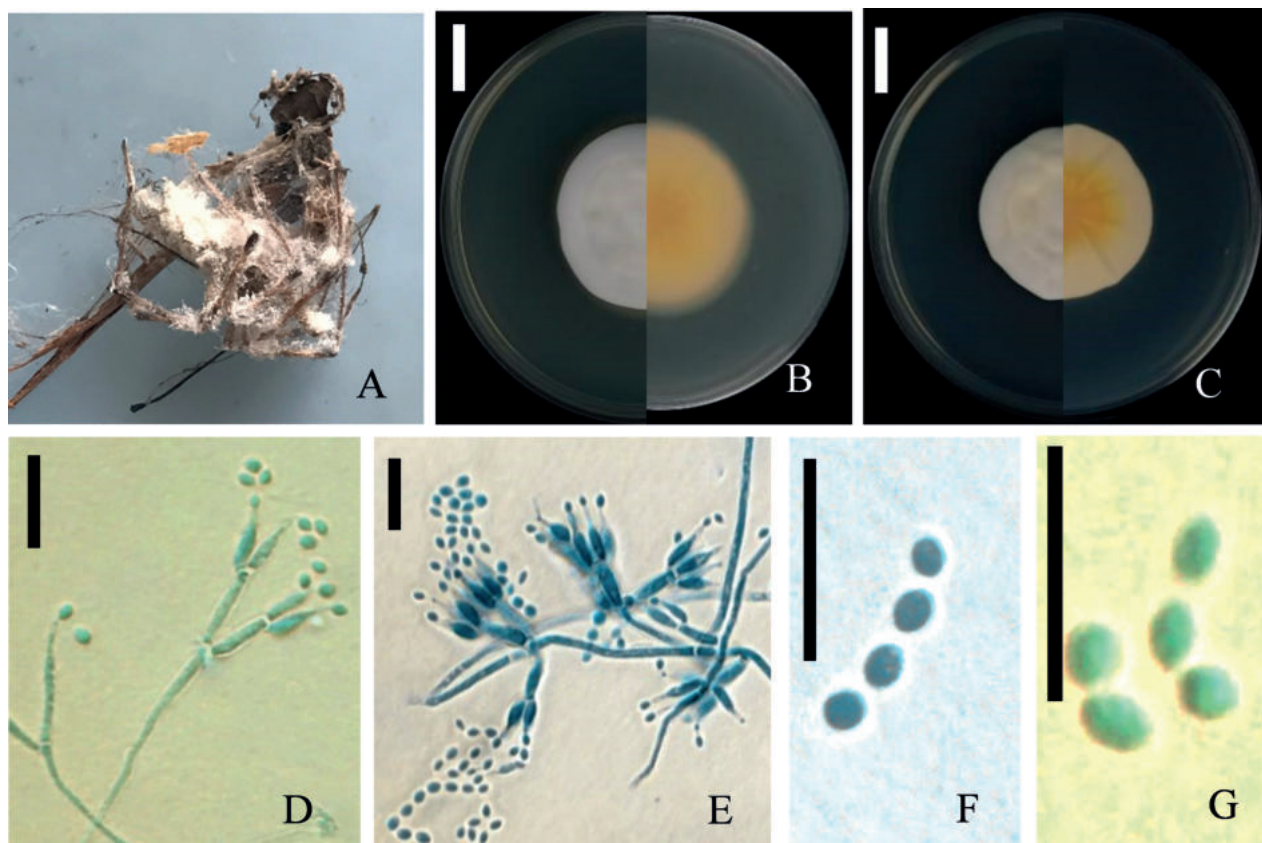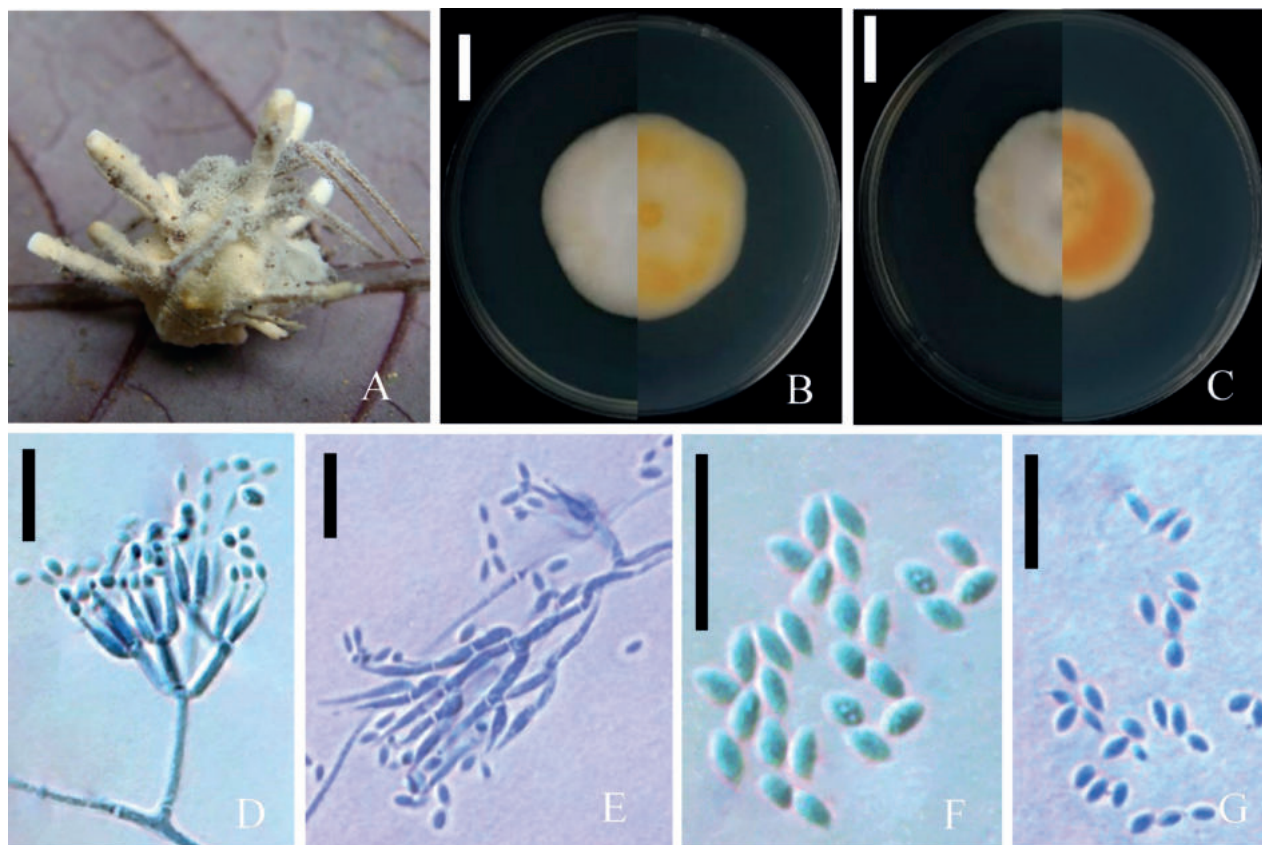
Figure 3. *Samsoniella aranea* **A** fungus on spider **B** colony on SDAY/4 **C** colony on PDA **D, G** conidiophores structure and conidia on SDAY/4 **E, F** conidiophores structure and conidia on PDA. Scale bars: 15 mm (**B, C**); 10 μm (**D–G**).

Morphological differences were evident in the colonies on PDA, with *S. aranea* colonies being floccose, white to cream-yellowish, and having a yolk-yellowish reverse. On the other hand, colonies of *S. yunnanensis* were described as loose and hairy, appearing white with a reddish-brown reverse.

***Samsoniella fusiformispora* T. Wang, Ming J. Chen & B. Huang, sp. nov.**
MycoBank No: 849799
Fig. 4

Etymology. Referring to the typical fusiform conidia.

Typification. CHINA. Gansu Province: Tianshui City, Maiji National Forest Park, on a spider, underside of tree leaf, 22 September 2010, Wang Liming, holotype MJS20100922-21. Sequences from strain RCEF5406 and RCEF2588 submitted to GenBank with accession numbers. RCEF5406: SSU = OM268843; LSU = OM268848; *TEF* = OM483864; *RPB1* = OM751890. RCEF2588: SSU = OR978312; LSU = OR978315; *TEF* = OR966515.

Description. *Sexual morph*: Undetermined. ***Asexual morph*:** *Isaria*-like. Synnemata multiple, unbranched, arising from the whole body of spider, 3–6 mm long, Stipes cylindrical or clavate, 0.5–1.0 mm wide, pale yellowish, white conidia produced from the synnemaya and hyphal layer (Fig. 4A). Phialides verticillate, in whorl of 2–5, 5.0–12.0 × 1.9–2.8 μm, with basal portion swollen

Figure 4. *Samsoniella fusiformispora* **A** fungus on spider **B** colony on SDAY/4 **C** colony on PDA **D, F** conidiophores structure and conidia on SDAY/4 **E, G** conidiophores structure and conidia on PDA. Scale bars: 15 mm (**B, C**); 10 µm (**D−G**).

to ellipsoidal, tapering into a distinct neck, 2.3 -3.8 × 0.5−1.2 µm. Conidia in chains, fusiform, aseptate, hyaline, 2.1−3.5 × 1.6−2.2 µm.

Culture characteristics. Colonies on 1/4 SDAY fast-growing, 39.5−44 mm diameter in 14 d at 25 °C, colonies white edge to yellowish center, cottony (Fig. 4B), reverse yellow to orange-yellow, hyphae smooth − walled, branched, hyaline, septate, 1.7−2.6 µm wide. Conidiophores smooth-walled, cylindrical, verticillate. Phialides in whorls of three to five, usually solitary on hyphae, basal portion cylindrical, tapering to a distinct neck; 7.6−15 µm long, 1.9−2.6 µm wide at the base, and 0.7−1.2 µm wide at the apex (Fig. 4D). Conidia in chains, smooth-walled, hyaline, fusiform, 2.1−3.6(-4.4) × 1.8−2.2 µm (Fig. 4F). Chlamydospores and synnemata not observed. Size and shape of phialides and conidia similar in culture. Sexual state not observed.

Colonies on PDA, attaining a diam of 36.5−39 mm in 14 d at 25 °C, floccose, colonies white to yellowish, with high mycelial density at the centrum (Fig. 4C). Reverse pale yellowish edge to orang center. Hyphae smooth- walled, branched, hyaline, septate, 1.5−2.5 µm wide. Conidiophores smooth − walled, cylindrical, verticillate. Phialides in whorls of two to five, usually solitary on hyphae, basal portion cylindrical, tapering to a distinct neck; 7.4−16(−26) µm long, 1.3−1.9(−2.4) µm wide at the base, and 0.5−1.0 µm wide at the apex (Fig. 4E). Conidia 1-celled, in chains, smooth-walled, hyaline, fusiform, 1.9−3.4 × 1.2−2.4 µm (Fig. 4G).

Habitat. Occurring on spider attached to the underside of tree leaf.

Notes. *Samsoniella fusiformispora* was unequivocally identified as a member of the Samsoniella genus through phylogenetic analyses (Fig. 1) and was found to share a close relationship with *S. coleopterorum*. However, upon further investigation and comparison of the morphological characteristics of the three new species with other related *Samsoniella* species (Table 2), distinct differences emerged. Colonies of *S. fusiformispora* were noted to be white to yellowish, with a pale yellowish edge transitioning to an orange center in reverse. In contrast, colonies of *S. coleopterorum* were observed to be white, with a yellowish reverse.

Discussion

The typical characteristics of *Samsoniella* were oval to fusiform conidia, bright red-orange stromata of the sexual morphs and synnemata of the asexual morphs (Chen et al. 2020). In this study, we present a phylogenetic investigation of cordycipitaceous *Isaria*-like fungi pathogenic on spiders. Combined with microscopic characteristics and phylogenetic analysis based on multi-locus sequence data, *S. fusiformispora*, *S. aranea* and *S. anhuiensis* were described and illustrated as new species in *Samsoniella*. It was found that the hosts of most reported *Samsoniella* species are Lepidoptera larvae or pupae, while the host of *S. coleopterorum* is a snout beetle (Curculionidae), and the host of *S. hymenopterorum* is a bee (Mongkolsamrit et al. 2018; Chen et al. 2020; Wang et al. 2020a). However, it should be noted that Wang et al. (2020a) described the host of *S. hymenopterorum* as being "Bee, family Vespidae". The family Vespidae are wasps, not bees. Our study has expanded the hosts of *Samsoniella* from Insecta to Arachnida.

Generally, the phialides of *S. fusiformispora* were longer and thinner than those of the closely-related *S. coleopterorum* while they also had bigger typical fusiform conidia with greater length to width ratio. In the ML and BI phylogenetic trees, *S. aranea* was inferred as a phylogenetic sister of *S. yunnanensis* with strong support (93%/1.00) and distinct from other related species in *Samsoniella*. The synnemata of *S. aranea* was not observed, but *S. yunnanensis* has gregarious, flexuous and fleshy synnemata arising from the limacodid cocoons (Wang et al. 2020a). Furthermore *S. yunnanensis* has smaller fusiform to oval conidia than *S. aranea* and the colonies on PDA grow faster than *S. aranea*. Similarly, *S. anhuiensis* was easily separated by the phylogenetic analyses with independent branches in the phylogenetic tree.

Kepler et al. (2017) found that sequences of *Isaria* sp. spat 09-050 and *Isaria* sp. spat 09-051 were firstly obtained, and two strains were clustered as the phylogenetic sister of *Isaria* spp. with 100 bootstrap proportion in the weighted parsimony (WP) analytic tree based on five genes (SSU, LSU, TEF, *RPB1* and *RPB2*), which was classified as *Akanthomyces* group. Then Wang et al. (2020a) constructed the multigene phylogenetic tree studied the new taxa of the family Cordycipitaceae and the new systematic position of the Chinese cordycipitoid fungus *Paecilomyces hepiali*. In this multigene phylogenetic tree, *Isaria* sp. spat 09-050 and *Isaria* sp. spat 09-051 were clustered in genus *Samsoniella* as sister group of *S. vallis* but in two independent branches. In this study, we obtained the same results. We convinced that *Isaria* sp. spat 09-050 and *Isaria* sp. spat

09-051 is an unpublished new species of the *Samsoniella*, should be revised to *Samsoniella* sp. spat 09-050 and *Samsoniella* sp. spat 09-051.

In this study, based on morphological characteristics and five loci phylogenetic analysis, *S. anhuiensis*, *S. aranea* and *S. fusiformispora* were separated from other *Samsoniella* species, which are described here as new species. The strain RCEF0643 was identified as *S. alpina*, the strain RCEF1481 was named as *S. hepiali*, and the strains RCEF2592 and RCEF 2590 was identified as *S. erucae*. Furthermore, our study significantly broadens the host range of *Samsoniella* from Insecta to Arachnida, marking a noteworthy expansion in understanding the ecological associations of these fungi. Additionally, the identification of both mononematous and synnematous conidiophores in our study not only expands the knowledge of *Samsoniella* species but also provides a basis for future research by comparing the ecological significance between these conidiophore types.

Additional information

Conflict of interest

The authors have declared that no competing interests exist.

Ethical statement

No ethical statement was reported.

Funding

Author contributions

MC and BH conceived and designed the study. TW and MC wrote the manuscript, conducted the experiments, and analyzed the data. JL, and XC did a part of the experiments. Zl and NH edited the manuscript. MC and BH edited the manuscript and supervised the project.

Author ORCIDs

Ting Wang https://orcid.org/0000-0002-9296-7280
Jun Li https://orcid.org/0009-0009-3183-2604
Xiaoyun Chang https://orcid.org/0000-0002-0093-9582
Zengzhi Li https://orcid.org/0000-0002-9606-5030
Nigel L. Hywel-Jones https://orcid.org/0009-0004-8219-3682
Bo Huang https://orcid.org/0000-0001-6032-7396
Mingjun Chen https://orcid.org/0000-0002-1439-7796

Data availability

All of the data that support the findings of this study are available in the main text.

References

Bainer G (1907) Mycotheque del' École de Pharmacie XI. *Paecilomyces*, genre noveau de Mucédinées. Bulletin de la Société Mycologique de France 23: 26–27.

Bischoff JF, Rehner SA, Humber RA (2009) A multilocus phylogeny of the *Metarhizium anisopliae* lineage. Mycologia 101(4): 512–530. https://doi.org/10.3852/07-202

Castlebury LA, Rossman AY, Sung GH, Hyten AS, Spatafora JW (2004) Multigene phylogeny reveals new lineage for *Stachybotrys chartarum*, the indoor air fungus. Mycological Research 108(8): 864–872. https://doi.org/10.1017/S0953756204000607

Chen WH, Han YF, Liang JD, Tian WY, Liang ZQ (2020) Morphological and phylogenetic characterisations reveal three new species of *Samsoniella* (Cordycipitaceae, Hypocreales) from Guizhou, China. MycoKeys 2020(74): 1–15. https://doi.org/10.3897/mycokeys.74.56655

Chen WH, Liang JD, Ren XX, Zhan JH, Han YF, Liang ZQ (2021) Cryptic diversity of *Isaria*-like species in Guizhou, China. Life 11(10): e1093. https://doi.org/10.3390/life11101093

Chen WH, Liang JD, Ren XX, Zhao JH, Han YF, Liang ZQ (2022) Species Diversity of *Cordyceps*-Like Fungi in the Tiankeng Karst Region of China. Microbiology Spectrum 10(5): e0197522. https://doi.org/10.1128/spectrum.01975-22

Chen WH, Liang JD, Ren XX, Zhao JH, Han YF (2023) Two new species of *Samsoniella* (Cordycipitaceae, Hypocreales) from the Mayao River Valley, Guizhou, China. MycoKeys 99: 209–226. https://doi.org/10.3897/mycokeys.99.109961

Crous PW, Osieck ER, Shivas RG, Tan YP, Bishop-Hurley SL, Esteve-Raventós F, Larsson E, Luangsa-ard JJ, Pancorbo F, Balashov S, Baseia IG, Boekhout T, Chandranayaka S, Cowan DA, Cruz RHSF, Czachura P, De la Peña-Lastra S, Dovana F, Drury B, Fell J, Flakus A, Fotedar R, Jurjević Ž, Kolecka A, Mack J, Maggs-Kölling G, Mahadevakumar S, Mateos A, Mongkolsamrit S, Noisripoom W, Plaza M, Overy DP, Piątek M, Sandoval Denis M, Vauras J, Wingfield MJ, Abell SE, Ahmadpour A, Akulov A, Alavi F, Alavi Z, Altes A, Alvarado P, Anand G, Ashtekar N, Assyov B, Banc-Prandi G, Barbosa KD, Barreto GG, Bellanger JM, Bezerra JL, Bhat DJ, Bilanski P, Bose T, Bozok F, Chaves J, Costa-Rezende DH, Danteswari C, Darmostuk V, Delgado G, Denman S, Eichmeier A, Etayo J, Eyssartier G, Faulwetter S, Ganga KGG, Ghosta Y, Goh J, Góis JS, Gramaje D, Granit L, Groenewald M, Gulden G, Gusmão LFP, Hammerbacher A, Heidarian Z, Hywel-Jones N, Jankowiak R, Kaliyaperumal M, Kaygusuz O, Kezo K, Khonsanit A, Kumar S, Kuo CH, Læssøe T, Latha KPD, Loizides M, Luo SM, Maciá-Vicente JG, Manimohan P, Marbach PAS, Marinho P, Marney TS, Marques G, Martín MP, Mille AN, Mondello F, Moreno G, Mufeeda KT, Mun HY, Nau T, Nkomo T, Okrasińska A, Oliveira JPAF, Oliveira RL, Ortiz DA, Pawłowska J, Pérez-De-Gregorio MÀ, Podile AR, Portugal A, Privitera N, Rajeshkumar KC, Rauf I, Rian B, Rigueiro-Rodríguez A, Rivas-Torres GF, Rodriguez-Flakus P, Romero-Gordillo M, Saar I, Saba M, Santos CD, Sarma PVSRN, Siquier JL, Sleiman S, Spetik M, Sridhar KR, Stryjak-Bogacka M, Szczepańska K, Taşkın H, Tennakoon DS, Thanakitpipattana D, Trovao J, Türkekul İ, van Iperen AL, van't Hof P, Vasquez G, Visagie CM, Wingfield BD, Wong PTW, Yang WX, Yarar M, Yarden O, Yilmaz N, Zhang N, Zhu YN, Groenewald JZ (2023) Fungal Planet description sheets: 1478–1549. Persoonia 50(1): 158–310. https://doi.org/10.3767/persoonia.2023.50.05

Darriba D, Taboada GL, Doallo R, Posada D (2012) jModelTest 2: More models, new heuristics and parallel computing. Nature Methods 9(8): 772–772. https://doi.org/10.1038/nmeth.2109

Gams W, Hodge KT, Samson RA, Korf RP, Seifert KA (2005) Proposal to conserve the name *Isaria* (anamorphic fungi) with a conserved type. Taxon 54(2): e537. https://doi.org/10.2307/25065390

Hodge KT, Gams W, Samson RA, Korf RP, Seifert KA (2005) Lectotypification and status of *Isaria* Pers. Taxon 54(2): 485–489. https://doi.org/10.2307/25065379

Hopple JS (1994) Phylogenetic Investigations in the Genus Coprinus Based on Morphological and Molecular Characters. Ph.D. Dissertation, Duke University, Durham, USA.

Katoh K, Standley DM (2013) MAFFT multiple sequence alignment software version 7: Improvements in performance and usability. Molecular Biology and Evolution 30(4): 772–780. https://doi.org/10.1093/molbev/mst010

Kepler RM, Luangsa-ard JJ, Hywel-Jones NL, Quandt CA, Sung GH, Rehner SA, Aime MC, Henkel TW, Sanjuan T, Zare R, Chen MJ, Li ZZ, Rossman AY, Spatafora JW, Shrestha B (2017) A phylogenetically -based nomenclature for Cordycipitaceae (Hypocreales). IMA Fungus 8(2): 335–353. https://doi.org/10.5598/imafungus.2017.08.02.08

Letunic I, Bork P (2016) Interactive tree of life (iTOL) v3: An online tool for the display and annotation of phylogenetic and other trees. Nucleic Acids Research 44(W1): W242–W245. https://doi.org/10.1093/nar/gkw290

Liu YJ, Whelen S, Hall BD (1999) Phylogenetic relationships among ascomycetes: Evidence from an RNA polymerse II subunit. Molecular Biology and Evolution 16(12): 1799–1808. https://doi.org/10.1093/oxfordjournals.molbev.a026092

Liu ZY, Liang ZQ, Whalley AJS, Yao YJ, Liu AY (2001) *Cordyceps brittlebankisoides*, a new pathogen of grubs and its anamorph, *Metarhizium anisopliae* var. *majus*. Journal of Invertebrate Pathology 78(3): 178–182. https://doi.org/10.1006/jipa.2001.5039

Luangsa-ard JJ, Hywel-Jones NL, Samson RA (2004) The order level polyphyletic nature of *Paecilomyces* sensu lato as revealed through 18S-generated rRNA phylogeny. Mycologia 96: 773–780. https://doi.org/10.1080/15572536.2005.11832925

Luangsa-ard JJ, Hywel-Jones NL, Manoch L, Samson RA (2005) On the relationships of *Paecilomyces* sect. *Isarioidea* species. Mycological Research 109(5): 581–589. https://doi.org/10.1017/S0953756205002741

Maharachchikumbura SSN, Hyde KD, Jones EBG, McKenzie EHC, Huang SK, Abdel-Wahab MA, Daranagama DA, Dayarathne M, D'souza MJ, Goonasekara ID, Hongsanan S, Jayawardena RS, Kirk PM, Konta S, Liu JK, Liu ZY, Norphanphoun C, Pang KL, Perera RH, Senanayake IC, Shang QJ, Shenoy BD, Xiao YP, Bahkali AH, Kang JC, Somrothipol S, Suetrong S, Wen TC, Xu JC (2015) Towards a natural classification and backbone tree for Sordariomycetes. Fungal Diversity 72(1): 199–301. https://doi.org/10.1007/s13225-015-0331-z

Mongkolsamrit S, Noisripoom W, Thanakitpipattana D, Wutikhun T, Spatafora JW, Luangsa-ard JJ (2018) Disentangling cryptic species with *Isaria*-like morphs in Cordycipitaceae. Mycologia 110(1): 230–257. https://doi.org/10.1080/00275514.2018.1446651

Persoon CH (1794) Dispositio methodica fungorum. Neues Magazin für die Botanik 1: 81–128.

Rehner SA, Buckley E (2005) A *Beauveria* phylogeny inferred from nuclear ITS and EF1-α sequences: Evidence for cryptic diversification and links to *Cordyceps* teleomorphs. Mycologia 97(1): 84–98. https://doi.org/10.3852/mycologia.97.1.84

Ronquist F, Teslenko M, van der Mark P, Ayres DL, Darling A, Höhna S, Larget B, Liu L, Suchard MA, Huelsenbeck JP (2012) MrBayes 3.2: Efficient Bayesian phylogenetic inference and model choice across a large model space. Systematic Biology 61(3): 539–542. https://doi.org/10.1093/sysbio/sys029

Samson RA (1974) *Paecilomyces* and some allied hyphomycetes. Studies in Mycology 6: 1–119.

Smith FB (1975) Naturalist's Color Guide. America Museum Natural History, New York, 22 pp.

Stamatakis A (2014) RAxML version 8: A tool for phylogenetic analysis and post-analysis of large phylogenies. Bioinformatics 30(9): 1312–1313. https://doi.org/10.1093/bioinformatics/btu033

Sung GH, Hywel-Jones NL, Sung JM, Luangsa-ard JJ, Shrestha B, Spatafora JW (2007) Phylogenetic classification of *Cordyceps* and the clavicipitaceous fungi. Studies in Mycology 57(1): 5–59. https://doi.org/10.3114/sim.2007.57.01

Vilgalys R, Hester M (1990) Rapid genetic identification and mapping of enzymatically amplified ribosomal DNA from several *Cryptococcus* species. Journal of Bacteriology 172(8): 4238–4246. https://doi.org/10.1128/jb.172.8.4238-4246.1990

Wang YB, Wang Y, Fan Q, Duan DE, Zhang GD, Dai RQ, Dai YD, Zeng WB, Chen ZH, Li DD, Tang DX, Xu ZH, Sun T, Nguyen TT, Tran NL, Dao VM, Zhang CM, Huang LD, Liu YJ, Zhang XM, Yang DR, Sanjuan T, Liu XZ, Yang ZL, Yu H (2020a) Multigene phylogeny of the family Cordycipitaceae (Hypocreales): New taxa and the new systematic position of the Chinese cordycipitoid fungus *Paecilomyces hepiali*. Fungal Diversity 103(1): 1–46. https://doi.org/10.1007/s13225-020-00457-3

Wang Y, Tang DX, Duan DE, Wang YB, Yu H (2020b) Morphology, molecular characterization, and virulence of *Beauveria pseudobassiana* isolated from different hosts. Journal of Invertebrate Pathology 172: e107333. https://doi.org/10.1016/j.jip.2020.107333

Wang Z, Wang Y, Dong Q, Fan Q, Dao VM, Yu H (2022) Morphological and phylogenetic characterization reveals five new species of *Samsoniella* (Cordycipitaceae, Hypocreales). Journal of Fungi 8(7): e747. https://doi.org/10.3390/jof8070747

Wang Y, Wang ZQ, Thanarut C, Dao VM, Wang YB, Hong Y (2023) Phylogeny and species delimitations in the economically, medically, and ecologically important genus *Samsoniella* (Cordycipitaceae, Hypocreales). MycoKeys 99: 227–250. https://doi.org/10.3897/mycokeys.99.106474

White TJ, Bruns T, Lee S, Taylor J (1990) Amplification and direct sequencing of fungal ribosomal RNA genes for phylogenetics. PCR protocols: a guide to methods and applications 18(1): 315–322. https://doi.org/10.1016/B978-0-12-372180-8.50042-1

Three novel species and new records of *Kirschsteiniothelia* (Kirschsteiniotheliales) from northern Thailand

Antonio Roberto Gomes de Farias[1], Naghmeh Afshari[1,2], Veenavee S. Hittanadurage Silva[1,3], Johnny Louangphan[1,3], Omid Karimi[1,3], Saranyaphat Boonmee[1,3]

1 *Center of Excellence in Fungal Research, Mae Fah Luang University, Chiang Rai, 57100, Thailand*

2 *Department of Biology, Faculty of Sciences, Chiang Mai University, Chiang Mai 50200, Thailand*

3 *School of Science, Mae Fah Luang University, Chiang Rai 57100, Thailand*

Corresponding author: Antonio Roberto Gomes de Farias (rfariasagro@gmail.com)

Abstract

Kirschsteiniothelia (Kirschsteiniotheliales, Pleosporomycetidae) includes 39 saprobic species recorded from dead or decaying wood in terrestrial and freshwater habitats. This study focuses on exploring *Kirschsteiniothelia* diversity in woody litter in Thailand. Wood samples were collected from forest areas in Chiang Rai and Chiang Mai Provinces in Thailand and examined for fungal fructifications. Fungal isolates were obtained and their morphological and sequence data were characterised. Micromorphology associated with multilocus phylogeny of ITS, LSU and SSU sequence data identified three isolates as novel species (*Kirschsteiniothelia inthanonensis*, *K. saprophytica* and *K. zizyphifolii*) besides new host records for *K. tectonae* and *K. xishuangbannaensis*. The placement of the new taxa and records are supported by morphological illustrations, descriptions and molecular phylogenies and the implications of these findings are discussed. Our findings provide information for understanding *Kirschsteiniothelia* diversity and ecology.

Key words: Multilocus phylogeny, new host records, saprobic fungi, three new species, woody litter

Introduction

Since its introduction by Hawksworth (1985), the taxonomic placement of *Kirschsteiniothelia* (Kirschsteiniotheliaceae, Pleosporales, Pleosporomycetidae) has undergone several revisions. It was introduced in Pleosporaceae, with *Kirschsteiniothelia aethiops* as the type species. However, Barr (1993) moved it to Pleomassariaceae based on morphology and, based on molecular phylogenetic analyses, Schoch et al. (2006) demonstrated that *K. aethiops* does not belong to Pleosporaceae and should be placed in a new family. Kirschsteiniotheliaceae was established by Boonmee et al. (2012) to accommodate the holomorphic genus *Kirschsteiniothelia*. This was due to the fact that *K. elaterascus* and *K. maritima* clustered into Morosphaeriaceae and Mytilinidiales, respectively (Schoch et al. 2009; Suetrong et al. 2009; Boonmee et al. 2012). Later, Hernández-Restrepo et al. (2017) assigned it

to the newly-proposed order Kirschsteiniotheliales (Dothideomycetes) due to its phylogenetic significance. Boonmee et al. (2012) also synonymised *Dendryphiopsis atra* under *K. atra* (Corda) D. Hawksw. due to their phylogenetic and asexual morph similarity (Boonmee et al. 2012; Schoch et al. 2009). The placement of *Kirschsteiniothelia* in the latest Outline of fungi and fungus-like taxa (Wijayawardene et al. 2022) is Kirschsteiniotheliaceae, Kirschsteiniotheliales, Dothideomycetes order incertae sedis, Dothideomycetes, Ascomycota.

Kirschsteiniothelia sexual morphs essentially have superficial to semi-immersed, subglobose to globose, dark brown to black ascomata; cylindrical clavate, bitunicate, 8-spored asci; and brown to dark brown, ellipsoidal, septate ascospores with or without a mucilaginous sheath (Hawksworth 1985; Boonmee et al. 2012; Hyde et al. 2013). However, its asexual morphs include dendryphiopsis-like and sporidesmium-like structures, with *Dendryphiopsis* taxa confirmed to be linked to *Kirschsteiniothelia*, based on morphology and molecular evidence (Schoch et al. 2009; Boonmee et al. 2012).

Kirschsteiniothelia species are mostly saprobes on dead or decaying wood in freshwater and terrestrial habitats (Boonmee et al. 2012; Hyde et al. 2013; Su et al. 2016; Mehrabi et al. 2017; Bao et al. 2018; Dong et al. 2020; Sun et al. 2021; Liu et al. 2023). These taxa play a crucial role in nutrient cycling and decomposition processes, contributing to the breakdown of organic matter in their respective ecosystems (Bucher et al. 2004). Their ability to colonise wood in freshwater habitats further emphasises their ecological significance (Su et al. 2016). In addition, Nishi et al. (2018) reported *Kirschsteiniothelia* associated with ankle bursitis in a Japanese patient and Guegan et al. (2021) with foot chromoblastomycosis in an immunosuppressed patient. Besides, Poch et al. (1992) discovered new compounds in *Kirschsteiniothelia* species, including kirschsteinin, which showed antimicrobial activity and Bugni and Ireland (2004) reported antibacterial activity from *K. maritima*.

This study focuses on exploring *Kirschsteiniothelia* diversity in woody litter in Thailand. We introduce three new species viz. *K. inthanonensis*, *K. saprophytica* and *K. zizyphifolii*, along with two new host records of *Kirschsteiniothelia*, based on a morpho-molecular approach, expanding our knowledge of the diversity in Pleosporomycetidae.

Material and methods

Sample collection, fungal isolation and microscopic characterisation

Wood litter samples were collected from forest areas in Chiang Rai and Chiang Mai, Thailand. Morphological studies were performed following the methods described by Senanayake et al. (2020). The fungal structures were examined using a Leica EZ4 stereomicroscope. The micro-morphological features were observed and photographed using a Nikon ECLIPSE Ni compound microscope with a Canon 600 D digital camera. The Tarosoft Image Frame Work programme was used to measure specimen structures, and photo plates were prepared using the open-source Inkscape v.1.3 (https://inkscape.org/).

Pure cultures were obtained through single spore isolation on Difco potato dextrose agar (PDA) using the spore suspension method (Choi et al. 1999). Germinating spores were transferred to a new PDA plate and incubated at room temperature for seven days. Ex-type pure living cultures were deposited in the Mae Fah Luang University Culture Collection (MFLUCC) and herbarium material was deposited in the Mae Fah Luang University Fungarium (MFLU), Chiang Rai, Thailand. Faces of fungi numbers (FoF) (Jayasiri et al. 2015) and Index Fungorum numbers (Index Fungorum 2023) were obtained as instructed and the data were uploaded to the Greater Mekong Subregion in the GMS database (Chaiwan et al. 2021).

DNA extraction, PCR amplification and sequencing

Genomic DNA was extracted from fresh mycelium scrapings using the EE.Z.N.A. Tissue DNA Kit from Omega Bio-tek, Inc., following the manufacturer's instructions. PCR amplifications were performed in a 50 µl reaction volume containing 10× PCR Master Mix, forward and reverse primers, DNA template and double sterilised H_2O. Amplified DNA of the ITS, LSU and SSU were obtained through a polymerase chain reaction (PCR) using the pairs of primers ITS4/ITS5 (White et al. 1990), LROR/LR5 (Vilgalys and Hester 1990) and NS1/NS4 (White et al. 1990), correspondingly. The quality of the PCR products was visualised on a 1% agarose gel and sequenced by Biogenomed Co., Ltd (South Korea).

Alignments and phylogenetic analyses

The reads were assembled using the Staden Package (Staden et al. 2003) and compared against the NCBI non-redundant GenBank database (Sayers et al. 2020) and related reference sequences downloaded (Table 1). Except for concatenation and visualisation, all the steps of phylogenetic analysis were conducted in a Windows Subsystem for Linux (Microsoft, USA). The individual datasets were aligned using MAFFT with the --*auto* flag and automatically trimmed using TrimAl v.1.3 with the -*gt* (0.3) option (Capella-Gutierrez et al. 2009). The best-fit model was selected using ModelTest-NG v.0.1.7 with the --*template mrbayes* option for DNA 3 schemes matrices (Darriba et al. 2020). The alignments were concatenated using SequenceMatrix and subjected to Maximum Likelihood (ML) and Bayesian Inference (BI) analyses.

Maximum Likelihood (ML) trees were generated using RAxML-HPC2 on XSEDE (8.2.8) (Stamatakis 2014) in the CIPRES Science Gateway platform (Miller et al. 2010), using 1,000 bootstraps replications and applying a partitioned model of evolution calculated by ModelTest-NG. Bayesian Inference was performed using MrBayes (Ronquist et al. 2012), with four simultaneous Markov Chain Monte Carlo (MCMC) chains and four runs for 3,000,000 million generations, sampling trees every 300th generation. The first 25% of trees were discarded as burn-in and posterior probabilities (PP) were calculated from the remaining trees. The consensus phylograms were visualised using FigTree (Rambaut 2012) and edited using the open-source Inkscape v.1.3 (https://inkscape.org/).

Table 1. Names, strain numbers, and corresponding GenBank accession numbers of *Kirschsteiniotheliales* taxa used in the phylogenetic analyses.

Taxa	Strains	Accession numbers		
		ITS	LSU	SSU
Acrospermum adeanum	M133	EU940180	EU940104	EU940031
Acrospermum compressum	M151	EU940161	EU940084	EU940012
Acrospermum gramineum	M152	EU940162	EU940085	EU940013
Aliquandostipite crystallinus	R 76–1	–	EF175651	EF175630
Aliquandostipite khaoyaiensis	CBS 118232[T]	–	GU301796	–
Anisomeridium ubianum	MPN94	–	GU327709	JN887379
Dyfrolomyces rhizophorae	JK5456A	–	GU479799	GU479766
Dyfrolomyces tiomanensis	NTOU3636	–	KC692156	KC692155
Flavobathelium epiphyllum	MPN67	–	GU327717	JN887382
Halokirschsteiniothelia maritima	CBS 221.60	–	AY849943	AF053726
Helicomyces roseus	CBS 283.51	AY916464	AY856881	AY856928
	MFLUCC 15–0343	KY320523	KY320540	–
Homortomyces combreti	CPC 19808[T]	JX517281	JX517291	–
Homortomyces tamaricis	MFLUCC 13–0280	KU752184	KU561874	KU870905
	MFLUCC 14–0167	KU934190	KU561875	–
	MFLUCC 13–0441[T]	NR_155161	NG_059495	–
Jahnula bipileata	F49–1 [T]	JN942353	EF175657	EF175635
Jahnula sangamonensis	A402–1B	JN942349	EF175661	EF175639
Jahnula seychellensis	SS 2113.2	–	EF175664	EF175643
Kirschsteiniothelia acutispora	MFLU 21–0127[T]	OP120780	ON980758	ON980754
Kirschsteiniothelia aquatica	MFLUCC 16–1685[T]	MH182587	MH182594	MH182618
Kirschsteiniothelia arasbaranica	IRAN 2509C	KX621986	KX621987	KX621988
	IRAN 2508C[T]	KX621983	KX621984	KX621985
Kirschsteiniothelia atra	DEN	MG602687	–	–
	CBS 109.53	–	AY016361	AY016344
	MFLUCC 16–1104	MH182583	MH182589	MH182615
	S–783	MH182586	MH182595	MH182617
	MFLUCC 15–0424	KU500571	KU500578	KU500585
Kirschsteiniothelia cangshanensis	GZCC19–0515	–	MW133829	MW134609
	MFLUCC 16–1350[T]	MH182584	MH182592	–
	MFLU 23–0358[T]	OR575473	OR575474	OR575475
Kirschsteiniothelia crustaceum	MFLU 21–0129[T]	MW851849	MW851854	–
Kirschsteiniothelia dushanensis	GZCC 19–0415	OP377845	MW133830	MW134610
Kirschsteiniothelia ebriosa	CBS H–23379	–	LT985885	–
Kirschsteiniothelia emarceis	MFLU 10–0037[T]	NR_138375	NG_059454	–
Kirschsteiniothelia extensum	MFLU 21–0130[T]	MW851850	MW851855	–
Kirschsteiniothelia fluminicola	MFLUCC 16–1263[T]	MH182582	MH182588	–
Kirschsteiniothelia inthanonensis	**MFLUCC 23–0277[T]**	**OR762773**	**OR762781**	**OR764784**
Kirschsteiniothelia lignicola	MFLUCC 10–0036[T]	HQ441567	HQ441568	HQ441569
Kirschsteiniothelia nabanheensis	HJAUP C2006	OQ023274	OQ023275	OQ023037
	HJAUP C2004[T]	OQ023197	OQ023273	OQ023038

Taxa	Strains	Accession numbers		
		ITS	LSU	SSU
Kirschsteiniothelia phoenicis	MFLU 18−0153	NR_158532	NG_064508	−
	MFLUCC 18−0216[T]	MG859978	MG860484	MG859979
Kirschsteiniothelia puerensis	ZHKUCC 22−0272	OP450978	OP451018	OP451021
	ZHKUCC 22−0271[T]	OP450977	OP451017	OP451020
Kirschsteiniothelia rostrata	MFLUCC 15−0619[T]	KY697280	KY697276	KY697278
Kirschsteiniothelia septemseptatum	MFLU 21−0126[T]	OP120779	ON980757	ON980752
Kirschsteiniothelia saprophytica	**MFLUCC 23−0275[T]**	**OR762774**	**OR762783**	**−**
	MFLUCC 23−0276	**OR762775**	**OR762782**	**−**
Kirschsteiniothelia spatiosum	MFLU 21−0128[T]	−	OP077294	ON980753
Kirschsteiniothelia submersa	S−481	−	MH182591	MH182616
	S−601	MH182585	MH182593	−
	MFLUCC 15−0427[T]	KU500570	KU500577	KU500584
Kirschsteiniothelia tectonae	MFLUCC 12−0050	KU144916	KU764707	−
	MFLUCC 13−0470	KU144924	−	−
Kirschsteiniothelia tectonae	**MFLUCC 23−0271**	**OR762771**	**OR762779**	**OR764782**
	MFLUCC 23−0272	**OR762772**	**OR762780**	**OR764783**
Kirschsteiniothelia thailandica	MFLUCC 20−0116[T]	MT985633	MT984443	MT984280
Kirschsteiniothelia thujina	JF13210	KM982716	KM982718	KM982717
Kirschsteiniothelia vinigena	CBS H−23378[T]	−	NG_075229	−
Kirschsteiniothelia xishuangbannaensis	ZHKUCC 22−0221	OP289563	OP289565	OP303182
	ZHKUCC 22−0220[T]	OP289566	OP289564	OP303181
Kirschsteiniothelia xishuangbannaensis	**MFLUCC 23−0273**	**OR762770**	**OR762778**	**OR764781**
	MFLUCC 23−0274	**OR762769**	**OR762777**	**OR764780**
Kirschsteiniothelia zizyphifolii	**MFLUCC 23−027[T]**	**OR762768**	**OR762776**	**OR764779**
Megalotremis verrucosa	MPN104	−	GU327718	JN887383
Phyllobathelium anomalum	MPN 242	−	GU327722	JN887386
Stemphylium vesicarium	CBS 191.86	MH861935	GU238160	GU238232
	MFLUCC 14−0920	KY659560	KY659563	KY659567
Tubeufia helicomyces	CBS 271.52	AY916461	AY856887	AY856933
Tubeufia javanica	MFLUCC 12−0545[T]	KJ880034	KJ880036	KJ880035
Acrospermum adeanum	M133	EU940180	EU940104	EU940031
Acrospermum compressum	M151	EU940161	EU940084	EU940012

The newly-generated sequences are indicated in bold. "[T]" refers to holotype or ex-type strains and "−" shows unavailable data in GenBank.

Results

Phylogenetic analyses

The concatenated nucleotide alignment of the ITS, LSU and SSU datasets comprised 69 *Kirschsteiniotheliales* strains, including the outgroups (*S. vesicarium* MFLUCC 14−0920 and CBS191.86) and included 2,640 sites (ITS = 1−561; LSU = 562−1596; SSU = 1597−2640), of which 1,550 comprised of distinct alignment patterns (ITS = 427, LSU = 668 and SSU = 455), with of 32.01% undetermined characters or gaps. The final GAMMA-based score of the best tree

was -24775.722822. Maximum Likelihood phylogeny and Bayesian analyses of single- and multi-loci had similar topologies and are combined in Fig. 1. Parameters for the models of each amplicon were described in Table 2. The Bayesian analysis tracer of the combined runs checked at six million generations had an effective sampling size for all the parameters higher than 3,000 and convergence diagnostic (PSRF = Potential Scale Reduction Factor; Gelman and Rubin (1992) of 1.0. The run resulted in 10,001 trees, of which 7,501 were sampled after 25% of the trees were discarded as burn-in. The alignment contained 1,802
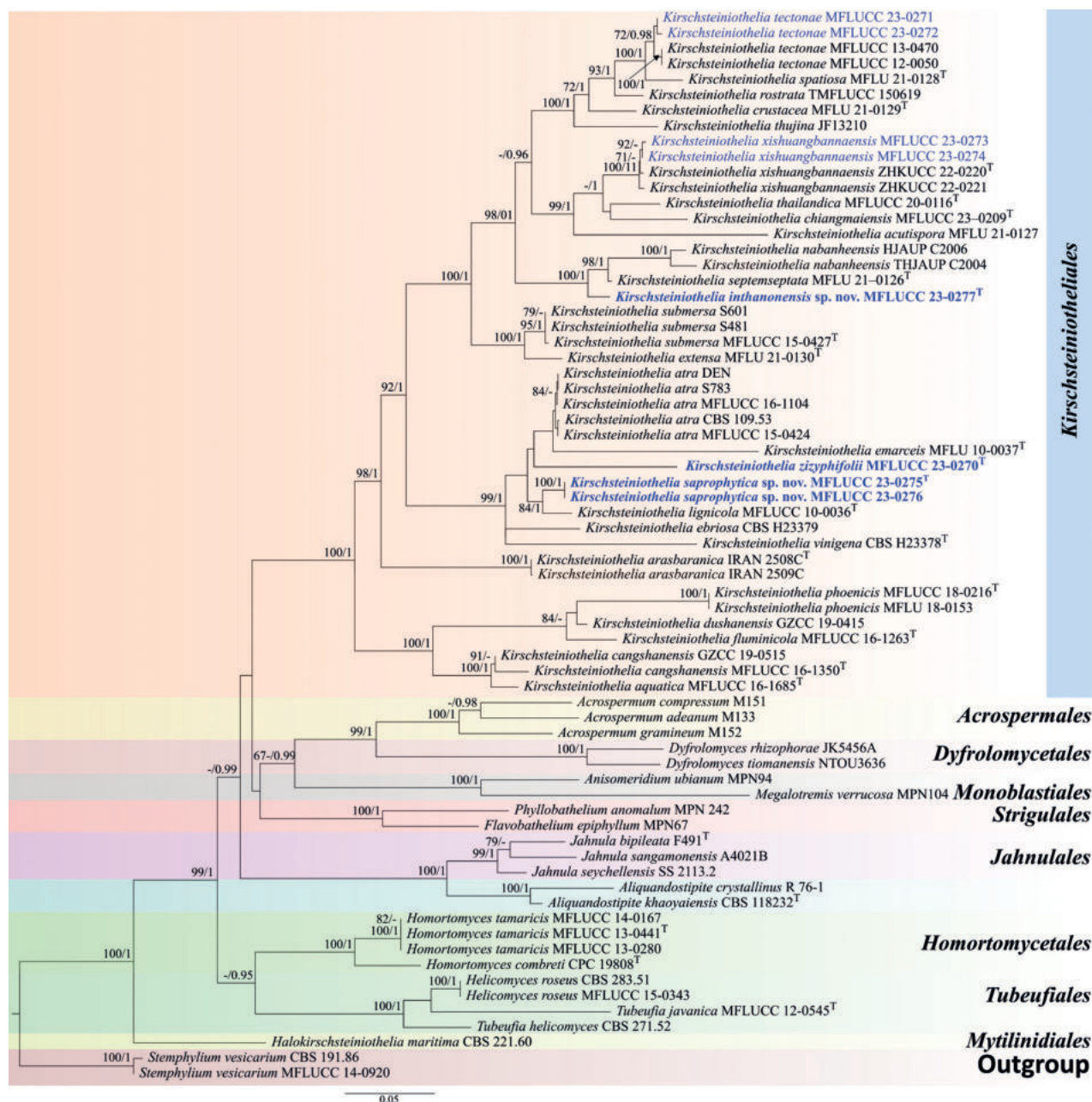
Figure 1. Maximum Likelihood phylogenetic tree generated from ITS, LSU and SSU sequence data for selected Kirschsteiniotheliales and related Dothideomycetes orders. The tree is rooted with *Stemphylium vesicarium* (CBS 191.86 and MFLUCC 14−0920). Newly-generated sequences are in blue and new species are in bold. Holotype and ex-type strains are symbolic by "ᵀ". Maximum Likelihood bootstrap (MLBS) values ≥ 70% and Bayesian posterior probabilities (BYPP) ≥ 0.95 are shown at the nodes.

Table 2. Maximum Likelihood indices of *Kirschsteiniothelia* tree.

Parameters	ITS	LSU	SSU
Evolutionary model	GTR+I+G4	GTR+G4	GTR+I+G4
Gamma distribution shape parameter α	0.267050	0.557118	0.228478
Estimated base frequencies			
A	0.199482	0.235780	0.260410
C	0.306708	0.238788	0.213687
G	0.279166	0.322010	0.267932
T	0.214644	0.203422	0.257971
Substitution rates			
AC	1.269939	0.865025	1.305091
AG	2.734587	2.259149	2.368982
AT	1.504952	1.054098	0.620257
CG	1.112253	0.931891	0.757010
CT	3.835090	5.793263	8.684577
GT	1.000000	1.000000	1.000000

unique sites (ITS = 427, LSU = 782, SSU = 593). The ML and BI analyses showed similar tree topologies.

Four strains (MFLUCC 23−0277, MFLUCC 23−0270 and MFLUCC 23−0275 and MFLUCC 23−0276) clustered in three independent lineages (Fig. 1). MFLUCC 23−0277 clustered sister to *K. septemseptata* (MFLU 21−0126) with 100% Maximum Likelihood bootstrap support (MLBS) and 1.00 Bayesian posterior probabilities (BYPP) support, while MFLUCC 23−0270 grouped as a sister of *K. emarceis* MFLU 10−0037, but with only 16% MLBS, 0.63 BYPP support, while MFLUCC 23−0275 and MFLUCC 23−0276 clustered with *K. lignicola* MFLUCC 10−0036 with 84% MLBS, 1.00 BYPP support. The other strains clustered with the known species *K. tectonae* (MFLUCC 23−0272 and MFLUCC 23−0271) and *K. xishuangbannaensis* (MFLUCC 23−0273 and MFLUCC 23−0274) with 71% MLBS and 72 MLBS/0.98 BYPP support, respectively. Based on the result of morphological evidence (Figs 2−7), three new species (*K. zizyphifolii*, *K. inthanonensis* and *K. saprophytica*) are proposed, along with the two new host records for *K. xishuangbannaensis* and *K. tectonae*.

Taxonomy

Kirschsteiniothelia inthanonensis J. Louangphan & Gomes de Farias, sp. nov.
Index Fungorum number: IF901384
Facesoffungi Number: FoF14982
Fig. 3

Etymology. The name refers to the location "Doi Inthanon" where the holotype was collected.

Holotype. MFLU 23−0420

Description. Saprobic on decaying wood. **Sexual morph:** Not observed. **Asexual morph:** Hyphomycetes. Colonies on the host substrate are superficial, effuse, long hairy, fascicular, scattered, dark brown to black. Mycelium super-
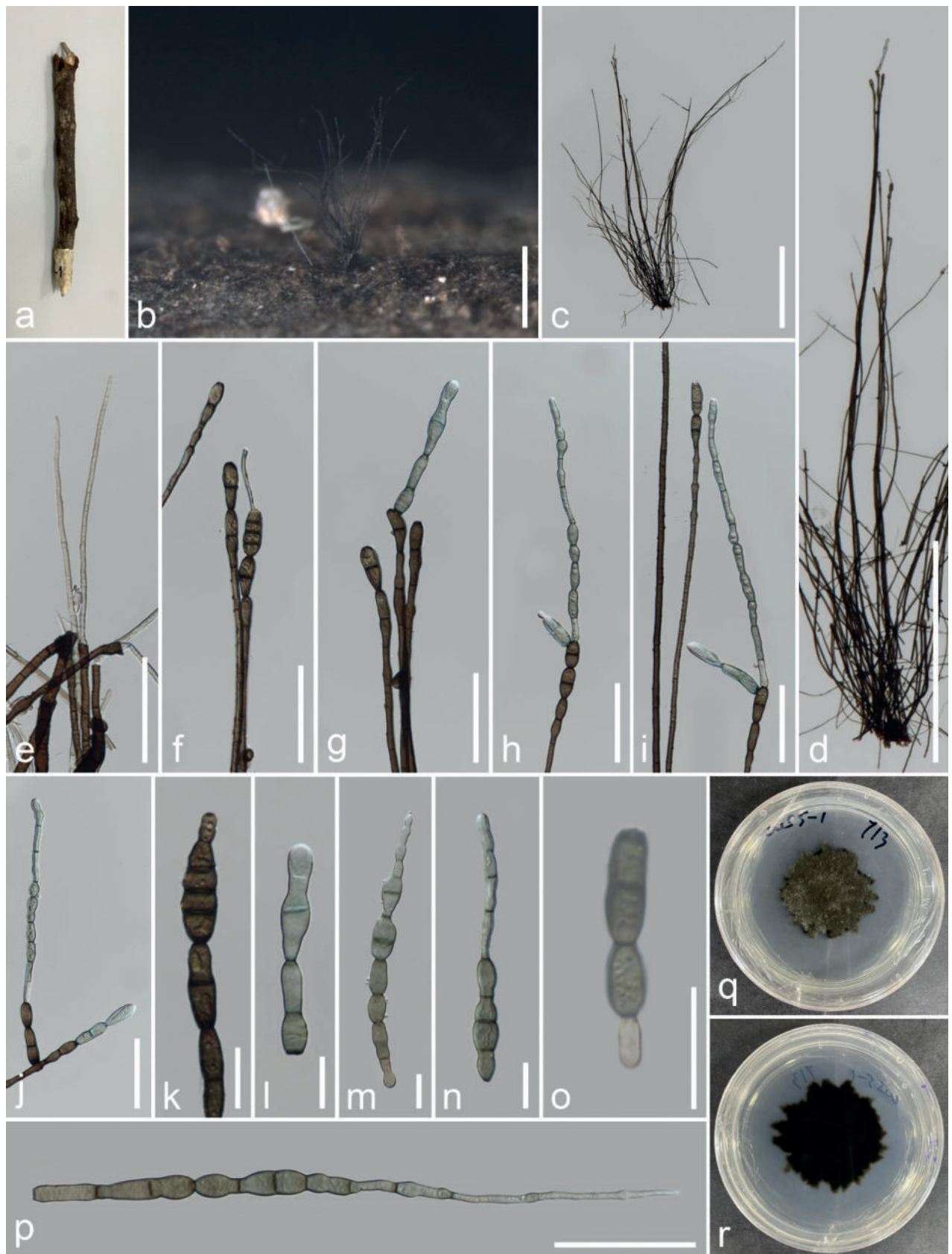
Figure 2. *Kirschsteiniothelia inthanonensis* (MFLU 23−0420, holotype) **a, b** colonies on the host **c, d** conidiophores and conidia **e** regeneration of conidiophores **f−j** conidiogenous cells and conidia **l−o** conidia **p** germinating conidium **q, r** colony on PDA (front and reverse). Scale bars: 500 μm (**b−d**); 50 μm (**e−j**); 20 μm (**k−p**).

ficial and immersed, composed of branched, septate, pale brown and smooth hyphae. Conidiophores 611−1549 × 2.5−6.6 µm ($\bar{x}$ = 1070 × 4.1 µm, n = 20), macronematous, synnematous, compact fasciculate, straight to flexuous, brown to dark brown, branched at the apex, multi-septate, thick and smooth-walled. Conidiogenous cells 15−45 × 6.7−10.4 µm ($\bar{x}$ = 24.3 × 8 µm, n = 20), monotretic to polytretic, calyciform, integrated, discrete, terminal, darkened at the apex, proliferating portion, brown, 2−4 septate. Conidia 24−230 × 5.7−14.3 µm ($\bar{x}$ = 101 × 9 µm, n = 15), acrogenous, solitary, obclavate, rostrate, straight or curved, truncate at base, grey to brown, pale at apex, partly tapering towards and rounded at the apex, 2−10− euseptate, smooth-walled.

Culture characteristics. Conidia germinated on PDA within 48 hours. Germ tubes germinated from end cell. Colony, reaching 30−35 mm diam. after one month at room temperature, circular form, flat, undulate edges, dense velvety surface, dark green on the surface, white mycelium on the tip, dark in reverse with dark green margin.

Material examined. Thailand, Chiang Mai, Chom Thong, Doi Inthanon National Park, on twigs of *Quercus oleoides*, 30 November 2022, Veenavee Silva, DIFWS5-01 (MFLU 23−0420, holotype), ex-type living culture MFLUCC 23−0277.

Notes. *Kirschsteiniothelia inthanonensis* (MFLUCC 23−0277) resembles *K. septemseptatum* and *K. nabanheensis* in having septate, cylindrical conidiophores with branches near apex, integrated, terminal conidiogenous cells and solitary, obclavate, septate conidia without mucilaginous sheaths. However, *K. inthanonensis* MFLUCC 23−0277 has longer and smaller conidiophores than *K. septemseptatum* and *K. nabanheensis* (611−1549 µm vs. 250−580 µm and 320−588 µm) and (2.5−6.6 µm vs. 6.5−14.5 µm and 8−12 µm), respectively and elongated conidia (Jayawardena et al. 2022; Liu et al. 2023). In addition, our phylogenetic analyses show that *K. inthanonensis* forms an independent branch with 100% MLBS and 1.00 BYPP support. BLASTn base pair comparisons between *K. inthanonensis* (MFLUCC 23−0277) and *K. septemseptatum* (MFLU 21−0126) show 95% similarity of ITS (479/504, 6 gaps), 99% similarity of LSU (844/853, no gaps) and 99% similarity of SSU (787/789, 2 gaps). *Kirschsteiniothelia nabanheensis* (HJAUP C2004) shows 94% similarity of ITS (483/513, 7 gaps), 99% similarity of LSU (540/547, no gaps) and 98% similarity of SSU (864/883, no gaps). Based on these data, we introduce *K. inthanonensis* as a new species.

Kirschsteiniothelia saprophytica O. Karimi, V. Silva & Gomes de Farias, sp. nov.
Index Fungorum number: IF561030
Facesoffungi Number: FoF14983
Figs 4, 5

Etymology. The species epithet refers to the saprobic life mode of the fungus.

Holotype. MFLU 23−0419

Description. Saprobic on dead wood of undetermined host. ***Sexual morph*:** Ascomata 146.7−72.26 µm diam., superficial, solitary, globose to subglobose, dark brown to black. Pseudoparaphyses 1.2−2.7 µm wide ($\bar{x}$ = 1.9, n = 20), hyaline, branched, filiform, abounded. Asci 68−125 × 18−23 µm ($\bar{x}$ = 101 × 20 µm, n = 10), bitunicate, 8-spored, cylindrical-claviform, sessile or short pedicellate.
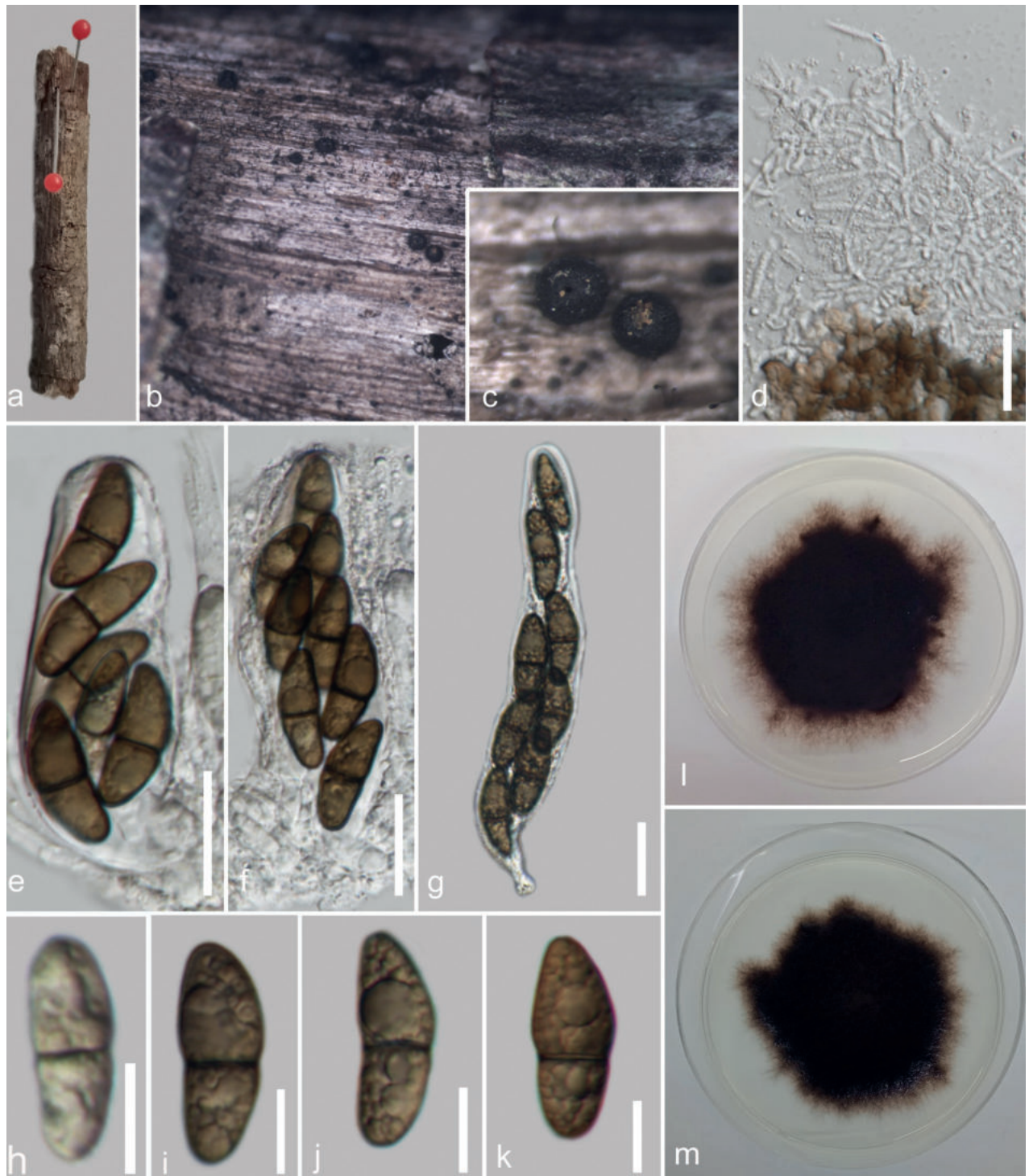
Figure 3. *Kirschsteiniothelia saprophytica* (MFLU 23−0419, holotype) **a** host **b, c** appearance of ascomata on host surface **d** paraphyses **e−g** asci **h−k** ascospores **l, m** culture on PDA (front and reverse). Scale bars: 20 μm (**d−g**); 10 μm (**h−k**).

Ascospores 13−25 (−40) × 7−11 (−14) μm ($\bar{x}$= 24 × 9.8 μm, n = 25), ellipsoid, upper cell broader than lower cell, pale brown to dark brown, 1-septate, guttulate, smooth-walled. ***Asexual morph*:** Hyphomycetous. Colonies on host gregarious. Conidiophores 90−216 × 8−12 μm ($\bar{x}$ = 165 × 10.6 μm, n = 10), macronematous, mononematous, cylindrical, straight to flexuous, branched, dark brown, multi-septate, constricted at the septa. Conidiogenous cells 6.7−35 × 5−15 μm

Figure 4. *Kirschsteiniothelia saprophytica* (MFLUCC 23−0276) **a** host **b** colonies on the host, associated with asexual morph **c** conidiophore with conidiogenous cell and conidiospore **d, e** conidiophore (**e** − from the culture) **f−j** conidiospore from culture **k** germinating spore **m, n** culture on PDA (front and reverse). Scale bars: 50 μm (**c−e**); 20 μm (**f−k**).

($\bar{x}$ = 17 × 10 μm, n = 10), holoblastic, monoblastic, terminal, cylindrical, brown to dark brown. Conidia 36−69 × 19−35 μm ($\bar{x}$ = 55 × 27 μm, n = 15), cylindrical rounded at ends, 2−3-septa, dark brown to black, smooth-walled.

Culture characteristics. Ascospores germinating on PDA within 24 hours. Colonies growing on PDA 16.8 mm diam. at room temperature after 38 days and on MEA 24 mm after 12 days. Mycelium on PDA superficial to immerse, dark olivaceous to dark brown on the top, reverse dark brown to black. Conidia germinating on PDA within 48 h. Colonies growing on PDA 17 mm diam. at room temperature after 16 days. Mycelium superficial to immerse, dark olivaceous to dark brown on the top, reverse dark brown to black.

Material examined. THAILAND, Mae Fah Luang University, Chiang Rai, on dead wood of unidentified host, 20 October 2022, V. Silva, V020 (MFLU 23−0419, holotype), ex-type living culture MFLUCC 23−0275 and MFLUCC 23−0276.

Notes. Our collection (MFLUCC 23−0275) shares similar general characteristics to the type strain *Kirschsteiniothelia lignicola* (MFLUCC 10−0105), such as spherical and dark pigmented ascomata, cylindrical to claviform asci, ellipsoidal septate ascospores and cylindrical with brown conidia (Boonmee et al. 2012). However, our collection differs from *K. lignicola* in having shorter asci (68−125 × 18−23 vs. 107−163.3 × 19−28.5 μm), with shorter pedicels (5−6 vs. 14.5−24 μm), shorter conidiophores (90−216 × 8−12 vs. 287−406 × 11−13 μm) and 2−3 transverse septa. Phylogenetically, our isolate clustered with *K. lignicola* with 84% MLBS, 1.00 BYPP. The pairwise base comparisons of the ITS and LSU sequences between *K. saprophytica* and *K. lignicola* showed identities of 93.08% (484/520, 10 gaps) and 91.18% (806/884, 4 gaps), respectively. Based on these differences, we introduce *K. saprophytica* as a new species.

Kirschsteiniothelia zizyphifolii N. Afshari & Gomes de Farias, sp. nov.

Index Fungorum number: IF901382
Facesoffungi Number: FoF14981
Fig. 2

Etymology. "*zizyphifolii*" refers to the host species on which the fungus was found.

Holotype. MFLU 23−0415

Description. Saprobic on *Nayariophyton zizyphifolium* (Malvaceae) woody litter in terrestrial habitat. *Sexual morph*: Not observed. *Asexual morph*: Hyphomycetes. Colonies on the substratum are superficial, effuse, dark brown to black and hairy. Mycelia superficial, composed of septate, branched, smooth-walled, dark brown hyphae. Conidiophores 287−444.5 × 10.3 −17 (−19.7) μm ($\bar{x}$ = 358.5 × 13.4 μm, n = 15), macronematous, mononematous, erect, with several short branches near the apex, irregular, solitary, cylindrical, flexuous, sometimes slightly straight, dark brown to black, paler towards the apex, septate, smooth-walled. Conidiogenous cells 11−20.4 × 5.8−10.6 μm ($\bar{x}$ = 14.6 × 7.6 μm, n = 25), tretic, occasionally percurrent, integrated, terminal or intercalary, cylindrical or doliiform, brown, smooth-walled. Conidia (29.5−) 37.6−46.5 × 13.5−19 μm ($\bar{x}$ = 43 × 16 μm, n = 20), acrogenous, solitary, cylindrical to rarely clavate, rounded at the apex, straight or moderately curved, brown dark to brown, 2−3-septate, constricted and pigmented at the septa, smooth-walled.

Culture characteristics. Ascospores germinating on PDA within 24 hours, reaching up to 30 mm diam. after one week at room temperature. Germ tubes

Figure 5. *Kirschsteiniothelia zizyphifolii* (MFLU 23−0415, holotype) **a** colonies on wood **b−d, g** conidiophores and conidiogenous cells **e, f** conidiophores with conidia **h−o** conidia **p** germinated conidium **q, r** cultures on PDA from the surface and reverse. Scale bars: 200 μm (**a**); 100 μm (**b−d**); 50 μm (**e, f**); 20 μm (**g−p**).

germinated from both end cells. Colony dense, circular, velvety, narrow towards the edge, from front, grey at centre, black towards edge, from reverse, black.

Material examined. THAILAND, Chiang Rai, Mae Fa Luang, Doi Tung Forest, on dead wood of *Nayariophyton zizyphifolium*, 26 March 2022, N. Afshari 1C1T2R4b (MFLU23−0415, holotype), ex-type living culture MFLUCC 23−0270.

Notes. *Kirschsteiniothelia zizyphifolii* (MFLUCC 23−0270) resembles *K. lignicola* (MFLUCC 10−0036) and *K. emarceis* (MFLU 10−0037) in having erect and branched conidiophores with apical dark brown conidia. However, it differs from *K. lignicola* in the sizes of conidiophores and conidia. Furthermore, BLASTn search of ITS and LSU sequences showed that *K. zizyphifolii* was closest to *K. emarceis* with similarity values of 90% (472/522, 12 gaps) and 84% (708/842, 22 gaps), respectively. Furthermore, our isolate (MFLUCC 23−0270) was close to *K. lignicola* (MFLUCC 10−0036) with similarity values of 89% (ITS = 474/532, 19 gaps), 99% (LSU = 844/853, 2 gaps) and 99% (SSU = 643/648, 2 gaps). Based on these phylogenetic data, we introduce *K. zizyphifolii* as a new species.

Kirschsteiniothelia tectonae Doilom, Bhat & K.D. Hyde, 2016

Index Fungorum number: IF551992
Facesoffungi Number: FoF01883
Fig. 6

Description. Saprobic on *Microcos paniculata* (Malvaceae) woody litter in terrestrial habitats. **Sexual morph:** Not observed. **Asexual morph:** Hyphomycetes. Colonies on the substrate, hairy, superficial, dark brown, scattered, partially grouped. Conidiophores 59−90 × 8.6−12 μm ($\bar{x}$ = 75 × 10.7 μm, n = 10), superficial, simple, macronematous, mononematous, cylindrical, straight to slightly curved, branched or unbranched, septate, dark brown to black. Conidiogenous cells 7−9.4 × 6−7.3 μm ($\bar{x}$ = 8 × 6.7 μm, n = 5), monoblastic, determinate, integrated, terminal. Conidia 62.5− 133 × 11 − 18.5(−21) μm ($\bar{x}$ = 94 × 16 μm, n = 30), cylindrical-obclavate, elongate, straight to slightly curved, rounded being slightly paler at the apex, obconically truncate at the base, 7−12−septa, olivaceous green to brown, smooth−walled.

Culture characteristics. Conidia germinating on PDA within 24 hours, reaching up to 15−20 mm diam. after one week at room temperature. Germ tubes generated from basal cells. Colony on PDA, dense, circular, flat or effuse, velvety, from front brown at the centre and black at the edge, from reverse, dark brown.

Material examined. THAILAND, Chiang Rai, Mae Fa Luang, Doi Tung, on dead wood of *Microcos paniculata*, 6 June 2022, N. Afshari 3C2T3R5 (MFLU 23−0416), living culture MFLUCC 23−0272. On dead wood of *Dalbergia cana*, 3 March 2022, N. Afshari 4C1T2R3 (MFLU 23−0417), living culture MFLUCC 23−0272.

Known distribution. Thailand (Li et al. 2016; this study)

Known hosts. *Tectona grandis* (Li et al. 2016), *Microcos paniculata* and *Dipterocarpus alatus* (this study)
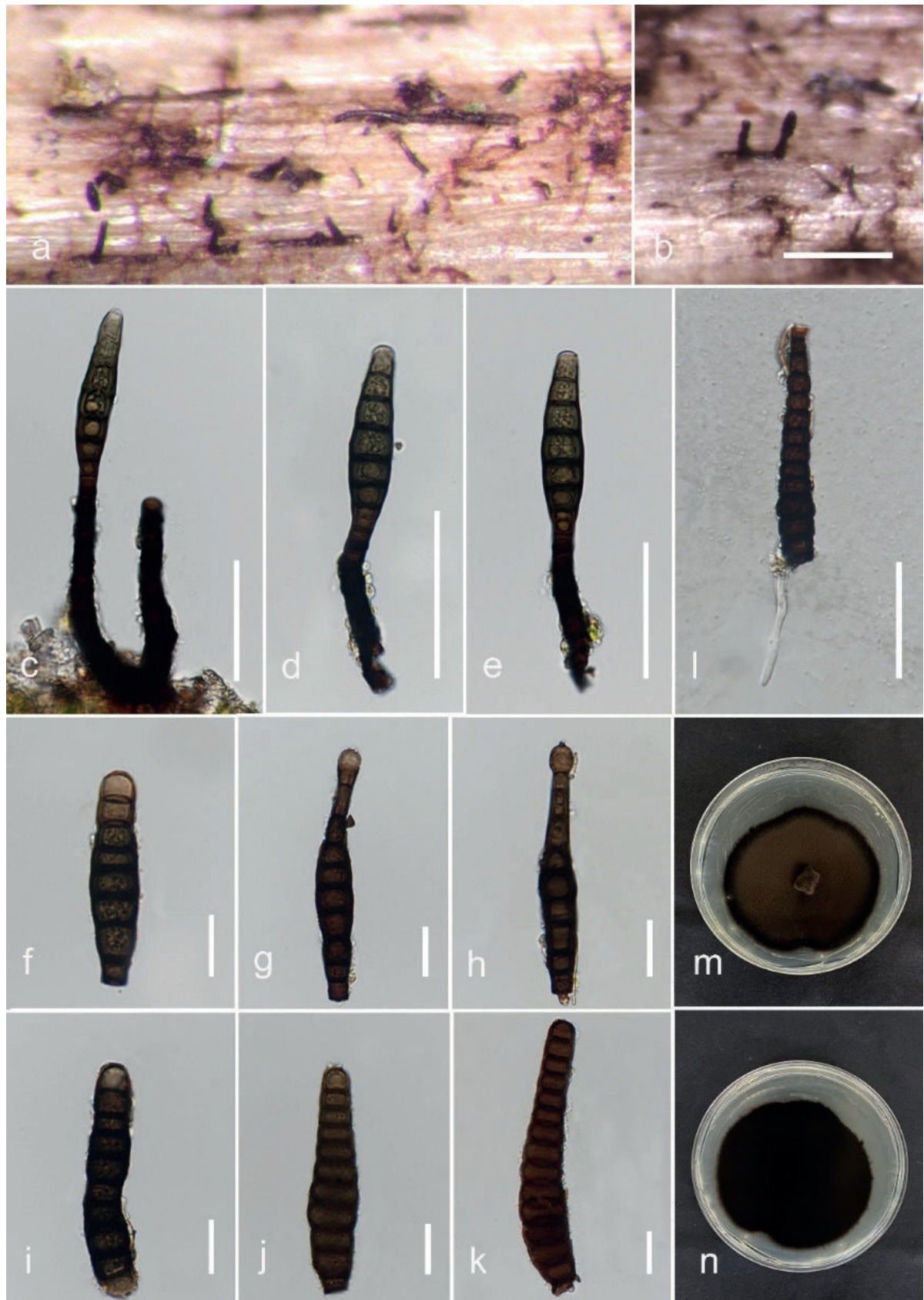
Figure 6. *Kirschsteiniothelia tectonae* (MFLUCC 23–0271, new record) **a, b** colonies on wood **c–e** conidiophores with conidia and conidiogenous cells **f–k** conidia **l** germinated conidium **m, n** culture on PDA (front and reverse). Scale bars: 100 μm (**a, b**); 50 μm (**c–e, l**); 20 μm (**f–k**).

Kirschsteiniothelia xishuangbannaensis R.F. Xu & Tibpromma

Index Fungorum number: IF559433
Facesoffungi Number: FoF12758
Fig. 7

Description. Saprobic on *Microcos paniculata* (Malvaceae) woody litter in terrestrial habitats. *Sexual morph*: Not observed. *Asexual morph*: Hyphomycetes. Colonies effuse on the substrate, hairy, solitary or scattered, dark brown. Conidiophores 135−178 × 7.7−11 µm ($\bar{x}$ = 151 × 9 µm, n = 10), macronematous, straight to curved, solitary, brown, slightly larger at base, narrowing towards apex, septate. Conidiogenous cells 14.4−27.4 × 7.8−11 µm ($\bar{x}$ = 22 × 10 µm, n = 10), holoblastic, monoblastic, integrated, smooth, terminal, determinate, cylindrical or lageniform, brown. Conidia 70−141 × 14.5−19 µm ($\bar{x}$ = 100 × 17 µm, n = 20), solitary, acrogenous, obclavate, rostrate, straight or slightly curved, truncate at the base, olivaceous green to brown, subhyaline at the apex, 5−10-septate, large guttulate.

Culture characteristics. Conidia germinating on PDA within 24 hours reaching up to 2 cm diam. after one week at room temperature. Germ tubes generated from both end cells. Colony on PDA, dense, circular, flat or effuse, velvety, from front, brown at the centre and dark brown at edge, from reverse, black to pale brown radiating.

Material examined. THAILAND, Chiang Rai, Mae Fa Luang, Doi Tung, on dead wood of *Microcos paniculata*, 6 June 2022, N. Afshari 3C2T1R1, living culture MFLUCC 23−0273. On dead wood of *Dipterocarpus alatus*, 27 September 2022, N. Afshari 2C3T1R3c (MFLU 23−0418), living culture MFLUCC 23−0274.

Known distribution. China (Xu et al. 2023), Thailand (this study).

Known hosts. *Hevea brasiliensis* (Xu et al. 2023), *Microcos paniculata* and *Dalbergia cana* (this study).

Discussion

This study introduces three new species and new host records of *Kirschsteiniothelia* from dead wood from Chiang Rai Province, Thailand, based on morphological and molecular analyses (Figs 1−7). *Kirschsteiniothelia* species have been found almost worldwide, including in the United States of America (Hawksworth 1985; Hyde 1997; Wang et al. 2004; Su et al. 2016), Iran (Mehrabi et al. 2017), Switzerland (Hawksworth 1985; Wang et al. 2004), Thailand (Boonmee et al. 2012; Li et al. 2016; Bao et al. 2018; Hyde et al. 2018; Sun et al. 2021; Jayawardena et al. 2022), South Africa (Marincowitz et al. 2008), China (Chen et al. 2006; Su et al. 2016; Bao et al. 2018; Liu et al. 2023; Yang et al. 2023; Xu et al. 2023), Canada (Hawksworth 1985), Italy (Wang et al. 2004), Spain (Rodríguez-Andrade et al. 2019) and India (Bao et al. 2018). Most of the species (*K. acutispora*, *K. chiangmaiensis*, *K. crustacea*, *K. emarceis*, *K. extensa*, *K. lignicola*, *K. phoenicis*, *K. rostrata*, *K. septemseptata*, *K. spatiosa*, *K. tectonae* and *K. thailandica*) have been reported from Thailand (Boonmee et al. 2012; Li et al. 2016; Bao et al. 2018; Hyde et al. 2018; Sun et al. 2021; Jayawardena et al. 2022), representing more than 25% of the species in this genus. Our results expand the knowledge of the diversity of this genus, especially in Thailand.

Figure 7. *Kirschsteiniothelia xishuangbannaensis* (MFLUCC 23−0273, new record) **a, b** colonies on wood **c, d** conidiophores and conidiogenous cells **e** conidiophore with conidium **f−o** conidia **p** germinated conidium **q, r** culture on PDA (front and reverse). Scale bars: 200 μm (**a**); 100 μm (**b**); 50 μm (**c, d, p**); 30 μm (**e**); 20 μm (**f−o**).

This genus is also prone to be highly speciose, given the recent introduction of ten new species (Jayawardena et al. 2022; Hyde et al. 2023; Liu et al. 2023; Louangphan et al. 2023 (under review); Xu et al. 2023). With the introductions of the present study (*K. inthanonensis*, *K. saprophytica*, *K. paniculata* and *K. zizyphifolii*), 32.5% of the species will have been introduced within two years, mainly as saprobes in woody litter. Besides, most *Kirschsteiniothelia* species have been reported from terrestrial environments, with only a few (*K. cangshanensis*, *K. fluminicola* and *K. rostrata*) reported from freshwater habitats (Bao et al. 2018). Their ecological significance also relies on their ability to infect humans (Nishi et al. 2018; Guegan et al. 2021). This demonstrates the potential for further discoveries on the diversity and lifestyles within *Kirschsteiniothelia*. Thus, exploring its diversity, especially in woody litter in protected environments and other tropical areas, will reveal the vast diversity within Kirschsteiniotheliaceae. For example, frequent incursions into fungal diversity have established Thailand as a hotspot for its diversity (Hyde et al. 2018).

Furthermore, *Kirschsteiniothelia* species appear to not have host specificity, as from our results, the same species were found associated with different hosts: *K. xishuangbannaensis*, previously reported from dead branches of *Hevea brasiliensis* (Xu et al. 2023), was recorded from *Microcos paniculata* (MFLUCC 23−0273) and *Dipterocarpus alatus* (MFLUCC 23−0274); *K. paniculata* was isolated from *Microcos paniculata* (MFLUCC 23−0271) and *Dalbergia cana* (MFLUCC 23−0272). In this regard, the host-specificity or host-recurrence of saprobic fungi has been discussed over the last two decades (Hooper et al. 2000; Zhou and Hyde 2001; Santana et al. 2005; Kodsueb et al. 2008; Tennakoon et al. 2022). However, saprotrophs seem to be less host-specific when compared with other trophic modes (Zhou and Hyde 2001). This may be because different hosts have different chemical compositions, which may affect the fungi of a particular species (Hyde et al. 2007). This hypothesis suggests that woody litter may harbour many species yet to be discovered (Kodsueb et al. 2008).

A combined approach should be employed to resolve the taxonomic placement of new species in this genus. This approach should include at least molecular phylogeny and morphological characters (Chethana et al. 2021; Maharachchikumbura et al. 2021). It should also include the linking of sexual and asexual morphologies, which are important factors in the taxonomy of Ascomycota, as pleomorphism can bias the morphological characters (Maharachchikumbura et al. 2021). However, only a few of the 39 *Kirschsteiniothelia* species, specifically *K. atra* and *K. recessa* (Hawksworth 1985) and *K. lignicola* and *K. emarceis* (Boonmee et al. 2012), are known from both their sexual and asexual morphs.

The findings of this study underscore the importance of integrating multiple types of evidence for the identification and classification of fungal species and they demonstrate the potential for further discoveries within *Kirschsteiniothelia*. The discovery of new species and host records has significant implications for our understanding of the ecological roles and interactions of this genus. In particular, identifying new host records provides valuable insights into the host range and specificity of *Kirschsteiniothelia* species, which may help elucidate the mechanisms underlying these interactions. Further research is necessary to fully explore the ecological significance of these findings and determine the potential impacts of *Kirschsteiniothelia* species on their hosts and ecosystems.

Acknowledgements

Additional information

Conflict of interest

The authors have declared that no competing interests exist.

Ethical statement

No ethical statement was reported.

Funding

Author contributions

Antonio Roberto Gomes de Farias: Conceptualization and design of the study, Funding acquisition, Writing – original draft; Naghmeh Afshari: Methodology, Writing – original draft; Veenavee S. Hittanadurage Silva: Methodology, Writing – original draft; Johnny Louangphan: Methodology, Writing – original draft; Omid Karimi: Writing – original draft; Saranyaphat Boonmee: Funding acquisition, Methodology, Supervision, Writing – revision.

Author ORCIDs

Antonio Roberto Gomes de Farias ⓘ https://orcid.org/0000-0003-4768-1547
Veenavee S. Hittanadurage Silva ⓘ https://orcid.org/0000-0001-8921-1370
Omid Karimi ⓘ https://orcid.org/0000-0001-9652-2222
Saranyaphat Boonmee ⓘ https://orcid.org/0000-0001-5202-2955

Data availability

All of the data that support the findings of this study are available in the main text.

References

Bao D, Luo Z, Liu J, Bhat D, Sarunya N, Li W, Su H, Hyde K (2018) Lignicolous freshwater fungi in China III: Three new species and a new record of *Kirschsteiniothelia* from northwestern Yunnan Province. Mycosphere: Journal of Fungal Biology 9(4): 755–768. https://doi.org/10.5943/mycosphere/9/4/4

Barr ME (1993) Notes on the Pleomassariaceae. Mycotaxon 49(1): 129–142.

Boonmee S, Ko Ko T, Chukeatirote E, Hyde K, Chen H, Cai L, Mckenzie E, Jones E, Kodsueb R, Bahkali A (2012) Two new *Kirschsteiniothelia* species with *Dendryphiopsis* anamorphs cluster in Kirschsteiniotheliaceae fam. nov. Mycologia 104(4): 698–714. https://doi.org/10.3852/11-089

Bucher VVC, Hyde KD, Pointing SB, Reddy CA (2004) Production of wood decay enzymes, loss of mass, and lignin solubilisation in wood by diverse tropical freshwater fungi. Microbial Ecology 15(3): 1–14. https://doi.org/10.1007/s00248-003-0132-x

Bugni TS, Ireland CM (2004) Marine-derived fungi: A chemically and biologically diverse group of microorganisms. Natural Product Reports 21(1): 143–163. https://doi.org/10.1039/b301926h

Capella-Gutierrez S, Silla-Martínez J, Gabaldón T (2009) TrimAl: A tool for automated alignment trimming in large-scale phylogenetic analyses. Bioinformatics 25(15): 1972–1973. https://doi.org/10.1093/bioinformatics/btp348

Chaiwan N, Gomdola D, Wang S, Monkai J, Tibpromma S, Doilom M, Wanasinghe DN, Mortimer PE, Lumyong S, Hyde KD (2021) An online database providing updated information of microfungi in the Greater Mekong Subregion. Mycosphere: Journal of Fungal Biology 12(1): 1513–1526. https://gmsmicrofungi.org. https://doi.org/10.5943/mycosphere/12/1/19

Chen CY, Wang CL, Huang JW (2006) Two new species of *Kirschsteiniothelia* from Taiwan. Mycotaxon 98: 153–158.

Chethana KT, Manawasinghe IS, Hurdeal VG, Bhunjun CS, Appadoo MA, Gentekaki E, Raspé O, Promputtha I, Hyde KD (2021) What are fungal species and how to delineate them? Fungal Diversity 109(1): 1–25. https://doi.org/10.1007/s13225-021-00483-9

Choi YW, Hyde KD, Ho WH (1999) Single spore isolation of fungi. Fungal Diversity 3: 19–38.

Darriba D, Posada D, Kozlov AM, Stamatakis A, Morel B, Flouri T (2020) ModelTest-NG: A new and scalable tool for the selection of DNA and protein evolutionary models. Molecular Biology and Evolution 37(1): 291–294. https://doi.org/10.1093/molbev/msz189

Dong W, Wang B, Hyde KD, McKenzie EH, Raja HA, Tanaka K, Abdel-Wahab MA, Abdel-Aziz FA, Doilom M, Phookamsak R, Hongsanan S, Wanasinghe DN, Yu XD, Wang GN, Yang H, Yang J, Thambugala KM, Tian Q, Luo ZL, Yang JB, Miller AN, Fournier J, Boonmee S, Hu DM, Nalumpang S, Zhang H (2020) Freshwater Dothideomycetes. Fungal Diversity 105(1): 319–575. https://doi.org/10.1007/s13225-020-00463-5

Gelman A, Rubin DB (1992) Inference from iterative simulation using multiple sequences. Statistical science 7(4): 457–72. https://doi.org/10.1214/ss/1177011136

Guegan H, Cailleaux M, Le Gall F, Robert-Gangneux F, Gangneux JP (2021) chromoblastomycosis due to a never-before-seen dematiaceous fungus in a kidney transplant patient. Microorganisms 9(10): e2139. https://doi.org/10.3390/microorganisms9102139

Hawksworth DL (1985) *Kirschsteiniothelia*, a new genus for the *Microthelia incrustans*-group (Dothideales). Botanical Journal of the Linnean Society 91(1–2): 181–202. https://doi.org/10.1111/j.1095-8339.1985.tb01144.x

Hernández-Restrepo M, Gené J, Castañeda-Ruiz RF, Mena-Portales J, Crous PW, Guarro J (2017) Phylogeny of saprobic microfungi from Southern Europe. Studies in Mycology 86: 53–97. https://doi.org/10.1016/j.simyco.2017.05.002

Hooper DU, Bignell DE, Brown VK, Brussard L, Dangerfield JM, Wall DH, Wardle DA, Coleman DC, Giller KE, Lavelle P, Van Der Putten WH (2000) Interactions between aboveground and belowground biodiversity in terrestrial ecosystems: Patterns, mechanisms, and feedbacks: We assess the evidence for correlation between aboveground and belowground diversity and conclude that a variety of mechanisms could lead to positive, negative, or no relationship-depending on the strength and type of interactions among species. Bioscience 50(12): 1049–1061. https://doi.org/10.1641/0006-3568(2000)050[1049:IBAABB]2.0.CO;2

Hyde KD (1997) Ascomycetes described on Freycinetia. Sydowia 49: 1–20.

Hyde KD, Bussaban B, Paulus B, Crous PW, Lee S, Mckenzie EH, Photita W, Lumyong S (2007) Diversity of saprobic microfungi. Biodiversity and Conservation 16(1): 7–35. https://doi.org/10.1007/s10531-006-9119-5

Hyde KD, Jones EBG, Liu J-K, Ariyawansa H, Boehm E, Boonmee S, Braun U, Chomnunti P, Crous PW, Dai D-Q, Diederich P, Dissanayake A, Doilom M, Doveri F, Hongsanan S, Jayawardena R, Lawrey JD, Li Y-M, Liu Y-X, Lücking R, Monkai J, Muggia L, Nelsen MP, Pang KL, Phookamsak R, Senanayake IC, Shearer CA, Suetrong S, Tanaka K, Thambugala KM, Wijayawardene NN, Wikee S, Wu HX, Zhang Y, Aguirre-Hudson B, Alias SA, Aptroot A, Bahkali AH, Bezerra JL, Bhat DJ, Camporesi E, Chukeatirote E, Gueidan C, Hawksworth DL, Hirayama K, De Hoog S, Kang JC, Knudsen K, Li WJ, Li XH, Liu ZY, Mapook A, McKenzie EHC, Miller AN, Mortimer PE, Phillips AJL, Raja HA, Scheuer C, Schumm F, Taylor JE, Tian Q, Tibpromma S, Wanasinghe DN, Wang Y, Xu JC, Yacharoen S, Yan JY, Zhang M (2013) Families of Dothideomycetes. Fungal Diversity 63(1): 1–313. https://doi.org/10.1007/s13225-013-0263-4

Hyde KD, Chaiwan N, Norphanphoun C, Boonmee S, Camporesi E, Chethana KW, Dayarathne MC, De Silva NI, Dissanayake AJ, Ekanayaka AH, Hongsanan S, Huang SK, Jayasiri SC, Jayawardena R, Jiang HB, Karunarathna A, Lin CG, Liu JK, Liu NG, Lu YZ, Luo ZL, Maharachchimbura SSN, Manawasinghe IS, Pem D, Perera RH, Phukhamsakda C, Samarakoon MC, Senwanna C, Shang QJ, Tennakoon DS, Thambugala KM, Tibpromma S, Wanasinghe DN, Xiao YP, Yang J, Zeng XY, Zhang JF, Zhang SN, Bulgakov TS, Bhat DJ, Cheewangkoon R, Goh TK, Jones EBG, Kang JC, Jeewon R, Liu ZY, Lumyong S, Kuo CH, McKenzie EHC, Wen TC, Yan JY, Zhao Q (2018) Mycosphere notes 169–224. Mycosphere: Journal of Fungal Biology 9(2): 271–430. https://doi.org/10.5943/mycosphere/9/2/8

Index Fungorum (2023) Index Fungorum. http://www.indexfungorum.org/Names/Names.asp

Jayasiri SC, Hyde KD, Ariyawansa HA, Bhat J, Buyck B, Cai L, Dai YC, Abd-Elsalam KA, Ertz D, Hidayat I, Jeewon R, Jones EBG, Bahkali AH, Karunarathna SS, Liu JK, Luangsa-ard JJ, Lumbsch HT, Maharachchikumbura SSN, McKenzie EHC, Moncalvo JM, Ghobad-Nejhad M, Nilsson H, Pang KL, Pereira OL, Phillips AJL, Raspé O, Rollins AW, Romero AI, Etayo J, Selçuk F, Stephenson SL, Suetrong S, Taylor JE, Tsui CKM, Vizzini A, Abdel-Wahab MA, Wen TC, Boonmee S, Dai DQ, Daranagama DA, Dissanayake AJ, Ekanayaka AH, Fryar SC, Hongsanan S, Jayawardena RS, Li WJ, Perera RH, Phookamsak R, de Silva NI, Thambugala KM, Tian Q, Wijayawardene NN, Zhao RL, Zhao Q, Kang JC, Promputtha I (2015) The Faces of Fungi database: Fungal names linked with morphology, phylogeny and human impacts. Fungal Diversity 74(1): 3–18. https://doi.org/10.1007/s13225-015-0351-8

Jayawardena RS, Hyde KD, Wang S, Sun YR, Suwannarach N, Sysouphanthong P, Abdel-Wahab MA, Abdel-Aziz FA, Abeywickrama PD, Abreu VP, Armand A, Aptroot A, Bao DF, Begerow D, Bellanger JM, Bezerra JDP, Bundhun D, Calabon MS, Cao T, Cantillo T, Carvalho JLVR, Chaiwan N, Chen CC, Courtecuisse R, Cui BK, Damm U, Denchev CM, Denchev TT, Deng CY, Devadatha B, de Silva NI, dos Santos LA, Dubey NK, Dumez S, Ferdinandez HS, Firmino AL, Gafforov Y, Gajanayake AJ, Gomdola D, Gunaseelan S, He S, Htet ZH, Kaliyaperumal M, Kemler M, Kezo K, Kularathnage ND, Leonardi M, Li JP, Liao CF, Liu S, Loizides M, Luangharn T, Ma J, Madrid H, Maharachchikumbura SSN, Manamgoda DS, Martín MP, Mekala N, Moreau PA, Mu Y, Pahoua P, Pem D, Pereira OL, Phonrob W, Phukhamsakda C, Raza M, Ren GC, Rinaldi AC, Rossi W, Samarakoon BC, Samarakoon MC, Sarma VV, Senanayake IC, Singh A, Souza MF, Souza-Motta CM, Spielmann AA, Su W, Tang X, Tian XG, Thambugala KM, Thongklang N, Tennakoon DS, Wannathes N, Wei DP, Welti S, Wijesinghe SN, Yang H, Yang Y, Yuan HS, Zhang H, Zhang J, Balasuriya A, Bhunjun CS, Bulgakov TS, Cai L, Camporesi E, Chomnunti P, Deepika YS, Doilom M, Duan WJ, Han SL, Huanraluek N, Jones EBG, Lakshmidevi N, Li Y, Lumyong S, Lu ZL, Khuna S, Kumla J, Manawasinghe IS, Mapook A, Punyaboon W, Tibpromma S, Lu YZ, Yan JY, Wang Y (2022) Fungal diversity notes 1512−1610: Taxonomic and phylogenetic contributions on genera and species of fungal taxa. Fungal Diversity 117(1): 1−272. https://doi.org/10.1007/s13225-022-00513-0

Kodsueb R, McKenzie EH, Lumyong S, Hyde KD (2008) Fungal succession on woody litter of *Magnolia liliifera* (Magnoliaceae). Fungal Diversity 31: 30(5): 55−72.

Li GJ, Hyde KD, Zhao RL, Hongsanan S, Abdel-Aziz FA, Abdel-Wahab MA, Alvarado P, Alves-Silva G, Ammirati JF, Ariyawansa HA, Baghela A (2016) Fungal diversity notes 253−366: taxonomic and phylogenetic contributions to fungal taxa. Fungal diversity 78: 1−237. https://doi.org/10.1007/s13225-016-0366-9

Liu J, Hu Y, Luo X, Castañeda-Ruíz RF, Xia J, Xu Z, Cui R, Shi X, Zhang L, Ma J (2023) Molecular phylogeny and morphology reveal four novel species of *Corynespora* and *Kirschsteiniothelia* (Dothideomycetes, Ascomycota) from China: A checklist for *Corynespora* reported worldwide. Journal of Fungi 9(1): e107. https://doi.org/10.3390/jof9010107

Maharachchikumbura SS, Chen Y, Ariyawansa HA, Hyde KD, Haelewaters D, Perera RH, Samarakoon MC, Wanasinghe DN, Bustamante DE, Liu JK, Lawrence DP (2021) Integrative approaches for species delimitation in Ascomycota. Fungal Diversity 09(1): 155−179. https://doi.org/10.1007/s13225-021-00486-6

Marincowitz S, Crous PW, Groenewald JZ (2008) Microfungi occurring on Proteaceae in the fynbos. CBS Biodiversity Series 7: 1−166.

Mehrabi M, Hemmati R, Asgari B (2017) *Kirschsteiniothelia arasbaranica* sp. nov., and an emendation of the Kirschsteiniotheliaceae. Cryptogamie, Mycologie 38(1): 13−25. https://doi.org/10.7872/crym/v38.iss1.2017.13

Miller MA, Pfeiffer W, Schwartz T (2010) Creating the CIPRES Science Gateway for inference of large phylogenetic trees. Proceedings of the Gateway Computing Environments Workshop (GCE), 14 Nov 2010, New Orleans, 8 pp. https://doi.org/10.1109/GCE.2010.5676129

Nishi M, Okano I, Sawada T, Hara Y, Nakamura K, Inagaki K, Yaguchi T (2018) Chronic *Kirschsteiniothelia* infection superimposed on a pre-existing non-infectious bursitis of the ankle: the first case report of human infection. BMC Infectious Diseases 8(1): 1−5. https://doi.org/10.1186/s12879-018-3152-3

Poch GK, Gloer JB, Shearer CA (1992) New bioactive metabolites from a freshwater isolate of the fungus *Kirschsteiniothelia* sp. Journal of Natural Products 55(8): 1093−1099. https://doi.org/10.1021/np50086a010

Rodríguez-Andrade E, Stchigel AM, Guarro J, Cano-Lira JF (2019) Fungal diversity of deteriorated sparkling wine and cork stoppers in Catalonia, Spain. Microorganisms 8(1): 1–12. https://doi.org/10.3390/microorganisms8010012

Ronquist F, Teslenko M, Van Der Mark P, Ayres DL, Darling A, Höhna S, Larget B, Liu L, Suchard MA, Huelsenbeck JP (2012) MrBayes 3.2: efficient Bayesian phylogenetic inference and model choice across a large model space. Systematic biology 61(3): 539–542. https://doi.org/10.1093/sysbio/sys029

Rambaut A (2014) FigTree 1.4.2. http://tree.bio.ed.ac.uk/software/figtree [Accessed on 25 September 2023]

Santana ME, Lodge DJ, Lebow P (2005) Relationship of host recurrence in fungi to rates of tropical leaf decomposition. Pedobiologia 49(6): 549–564. https://doi.org/10.1016/j.pedobi.2005.06.009

Sayers EW, Cavanaugh M, Clark K, Ostell J, Pruitt KD, Karsch-Mizrachi I (2020) GenBank. Nucleic Acids Research 48: D84–D86. https://doi.org/10.1093/nar/gkz956

Schoch CL, Shoemaker RA, Seifert KA, Hambleton S, Spatafora JW, Crous PW (2006) A multigene phylogeny of the Dothideomycetes using four nuclear loci. Mycologia 98(6): 1041–1052. https://doi.org/10.1080/15572536.2006.11832632

Schoch CL, Crous PW, Groenewald JZ, Boehm EWA, Burgess TI, de Gruyter J, de Hoog GS, Dixon LJ, Grube M, Gueidan C, Harada Y, Hatakeyama S, Hirayama K, Hosoya T, Huhndorf SM, Hyde KD, Jones EBG, Kohlmeyer J, Kruys Å, Li YM, Lücking R, Lumbsch HT, Marvanová L, Mbatchou JS, McVay AH, Miller AN, Mugambi GK, Muggia L, Nelsen MP, Nelson P, Owensby CA, Phillips AJL, Phongpaichit S, Pointing SB, Pujade-Renaud V, Raja HA, Rivas ER, Robbertse B, Ruibal C, Sakayaroj J, Sano T, Selbmann L, Shearer CA, Shirouzu T, Slippers B, Suetrong S, Tanaka K, Volkmann-Kohlmeyer B, Wingfield MJ, Wood AR, Woudenberg JHC, Yonezawa H, Zhang Y, Spatafora JW (2009) A class-wide phylogenetic assessment of Dothideomycetes. Studies in Mycology 64: 1–15. https://doi.org/10.3114/sim.2009.64.01

Senanayake IC, Rathnayaka AR, Marasinghe DS, Calabon MS, Gentekaki E, Lee HB, Hurdeal VG, Pem D, Dissanayake LS, Wijesinghe SN, Bundhun D (2020) Morphological approaches in studying fungi: Collection, examination, isolation, sporulation and preservation. Mycosphere: Journal of Fungal Biology 11(1): 2678–2754. https://doi.org/10.5943/mycosphere/11/1/20

Staden R, Judge DP, Bonfield JK (2003) Analysing sequences using the Staden package and EMBOSS. In Introduction to Bioinformatics: A Theoretical and practical approach. Humana Press, Totowa, 393–410. https://doi.org/10.1007/978-1-59259-335-4_24

Stamatakis A (2014) RAxML version 8: A tool for phylogenetic analysis and post-analysis of large phylogenies. Bioinformatics 30(9): 1312–1313. https://doi.org/10.1093/bioinformatics/btu033

Su H, Hyde KD, Maharachchikumbura SSN, Ariyawansa HA, Luo Z, Promputtha I, Tian Q, Lin C, Shang Q, Zhao Y, Chai H, Su H, Hyde KD, Maharachchikumbura SS, Ariyawansa HA, Luo Z, Promputtha I, Tian Q, Lin C, Shang Q, Zhao Y, Chai H, Liu X, Bahkali AH, Bhat JD, McKenzie EHC, Zhou D (2016) The families Distoseptisporaceae fam. nov., Kirschsteiniotheliaceae, Sporormiaceae and Toruloceae, with new species from freshwater in Yunnan Province, China. Fungal Diversity 80(1): 375–409. https://doi.org/10.1007/s13225-016-0362-0

Suetrong S, Schoch CL, Spatafora JW, Kohlmeyer J, Volkmann-Kohlmeyer B, Sakayaroj J, Phongpaichit S, Tanaka K, Hirayama K, Jones EB (2009) Molecular systematics of the marine Dothideomycetes. Studies in Mycology 64(1): 155–173. https://doi.org/10.3114/sim.2009.64.09

Sun YR, Jayawardena RS, Hyde KD, Wang Y (2021) *Kirschsteiniothelia thailandica* sp. nov. (Kirschsteiniotheliaceae) from Thailand. Phytotaxa 490(2): 172−182. https://doi.org/10.11646/phytotaxa.490.2.3

Tennakoon DS, Kuo CH, Purahong W, Gentekaki E, Pumas C, Promputtha I, Hyde KD (2022) Fungal community succession on decomposing leaf litter across five phylogenetically related tree species in a subtropical forest. Fungal Diversity 115(1): 73−103. https://doi.org/10.1007/s13225-022-00508-x

Vilgalys R, Hester M (1990) Rapid genetic identification and mapping of enzymatically amplified ribosomal DNA from several Cryptococcus species. Journal of Bacteriology 172(8): 4238−4246. https://doi.org/10.1128/jb.172.8.4238-4246.1990

Wang YZ, Aptroot A, Hyde KD (2004) Revision of the genus *Amphisphaeria*. Fungal Diversity Research Series 13: 1−168.

White TJ, Bruns T, Lee S, Taylor J (1990) Amplification and direct sequencing of fungal ribosomal RNA genes for phylogenetics. PCR Protocols: A Guide to Methods and Applications 18: 315−322. https://doi.org/10.1016/B978-0-12-372180-8.50042-1

Wijayawardene NN, Hyde KD, Dai DQ, Sánchez-García M, Goto BT, Saxena RK, Erdoğdu M, Selçuk F, Rajeshkumar KC, Aptroot A, Błaszkowski J, Boonyuen N, da Silva GA, de Souza FA, Dong W, Ertz D, Haelewaters D, Jones EBG, Karunarathna SC, Kirk PM, Kukwa M, Kumla J, Leontyev DV, Lumbsch HT, Maharachchikumbura SSN, Marguno F, Martínez-Rodríguez P, Mešić A, Monteiro JS, Oehl F, Pawłowska J, Pem D, Pfliegler WP, Phillips AJL, Pošta A, He MQ, Li JX, Raza M, Sruthi OP, Suetrong S, Suwannarach N, Tedersoo L, Thiyagaraja V, Tibpromma S, Tkalčec Z, Tokarev YS, Wanasinghe DN, Wijesundara DSA, Wimalaseana SDMK, Madrid H, Zhang GQ, Gao Y, Sánchez-Castro I, Tang LZ, Stadler M, Yurkov A, Thines M (2022) Outline of Fungi and fungus-like taxa − 2021. Mycosphere: Journal of Fungal Biology 13(1): 53−453. https://doi.org/10.5943/mycosphere/13/1/2

Xu RF, Phukhamsakda C, Dai DQ, Karunarathna SC, Tibpromma S (2023) *Kirschsteiniothelia xishuangbannaensis* sp. nov. from pará rubber (*Hevea brasiliensis*) in Yunnan, China. Current Research in Environmental & Applied Mycology 13(1): 34−56. https://doi.org/10.5943/cream/13/1/3 [Journal of Fungal Biology]

Yang J, Liu LL, Jones EG, Hyde KD, Liu ZY, Bao DF, Liu NG, Li WL, Shen HW, Yu XD, Liu JK (2023) Freshwater fungi from karst landscapes in China and Thailand. Fungal Diversity 119(1): 1−212. https://doi.org/10.1007/s13225-023-00514-7

Zhou D, Hyde KD (2001) Host-specificity,host-exclusivity, and host-recurrence in saprobic fungi. Mycological Research 105(12): 1449−1457. https://doi.org/10.1017/S0953756201004713